A·S·P·E·N
Center for Physics

ASPEN WINTER CONFERENCE
ON
GRAVITATIONAL WAVES AND THEIR DETECTION

JANUARY 14-20, 1996

DATA ANALYSIS
LIGO RESEARCH COMMUNITY
SPACE BASED DETECTORS-LISA

PROGRAM COMMITTEE/ASPEN ORGANIZING COMMITTEE

Barry Barish ....Caltech
Karsten Danzmann ....Hanover
Sam Finn ....Northwestern
Adalberto Giazotto ....INFN Pisa
John Hall ....JILA
William Hamilton ....LSU
James Hough ....Glasgow
Sydney Meshkov ....Caltech
Charles Prescott ....SLAC
Fred Raab ....Caltech
Albrecht Ruediger ..MPI-Garching
Gary Sanders ....Caltech
Peter Saulson ....Syracuse
Bernard Schutz ....MPI-Potsdam
David Shoemaker ....MIT
Kip Thorne ....Caltech
Rainer Weiss ....MIT
Stan Whitcomb ....Caltech

EDITOR: SYDNEY MESHKOV

LIGO-G960288-00-M

PROGRAM

ASPEN WINTER CONFERENCE ON GRAVITATIONAL WAVES AND THEIR DETECTION

Aspen Center for Physics
January 14 - 20, 1996

Monday AM: Interferometers and Bars
January 15 Chair: R. Drever

8:00	S. Meshkov(Caltech) S. Mencimer(ACP)	Welcome
8:10	A. Ruediger(Garching)	Current Interferometer Projects
8.35	Discussion	
8:45	G. Pizzella(Rome)	Operation of Resonant Detectors
8:50	W. Johnson(LSU)	Status of Current Bar Experiments
9:10	Discussion	
9:20	Coffee Break	
9:35	S.Finn(Northwestern)	The Path to Data Analysis
10:00	Discussion	
10:10	D. Shoemaker(MIT)	LIGO Status Report
10:35	Discussion	

Monday PM: Interferometer Issues
January 15 Chair: J. Centrella

4:30	R. Drever(Caltech)	Advanced Interferometers
4:55	Discussion	
5:05	M. Schrempl(Hannover)	GEO 600 Status Report
~~5:30~~	~~Discussion~~	
5:40	Coffee Break	
5:55	F. Raab(Caltech)	Time-Domain Behavior of the 40m Interferometer
6:20	Discussion	
6:30	R. DeSalvo(Pisa)	Virgo Experiment and Seismic Isolation
6:55	Discussion	
7:05	E. Mizuno(Kanagawa)	Data Acquisition and Analysis for TENKO100 and TAMA300
7:30	Discussion	
7:40	R. Byer(Stanford)	A Sagnac Interferometer for Gravitational Wave Detection
7:55	Discussion	

Tuesday AM Space Based Detectors-LISA I
January 16 Chair: A. Ruediger

8:00	P. Bender(JILA)	Sources for LISA
8:25	Discussion	
8:35	H. Ward(Glasgow)	LISA Overview
9:00	Discussion	
9:10	Coffee Break	
9:25	H. Ward(Glasgow)	LISA Overview(continued)
9:50	Discussion	
10:00	D. Hils(JILA)	BH-SMBH Binaries
10:25	Discussion	

Tuesday PM   Space Based Detectors-LISA II
January 16   Chair: R. Schilling

4:30	B. Willke(Hannover)	Lasers for LISA
5:00	Discussion	
5:10	D. Robertson(Glasgow)	Spacecraft Pointing
5:40	Discussion	
5:50	R. Stebbins(JILA)	LISA Error Budgets
6:20	Discussion	
6:30	Coffee Break	
6:45	D. Robertson(Glasgow)	GEO 600 Developments
7:15	Discussion	
7:25	D. Schnier(Hannover)	Power Recycling
7:40	Discussion	

Wednesday AM   LIGO Research Community(LRC)
January 17   Chair: H. Ward

8:00	G. Sanders(Caltech)	The View From LIGO
8:20	Discussion	
8:30	Meeting of LIGO Research Community and Discussion	
1:30	Meeting of LIGO Research Community(continued)	

~~Wednesday PM   Shot Noise; Detector Improvement~~
January 17   Chair: D. Shoemaker

4:30	A. Ruediger(Garching)	History and Derivation of Shot Noise Equations
5:00	Discussion	
5:10	J. Hall(JILA)	Dynamic Light-induced Mirror Birefringence
5:40	Discussion	

Wednesday Evening: Public Lecture, Wheeler Opera House
Chair: S. Meshkov

8:00	L. Krauss (Case-Western Reserve)	The Physics of Star Trek

Thursday AM   Data Analysis I. Search for Compact Object Binaries
January 18   Chair: S. Finn(Northwestern)

8:00	C. Will(Washington U)	Compact Binary Inspiral: A Post-Newtonian Playground
8:25	Discussion	
8:35	J. Wilson(LLNL)	Neutron Star Binaries Hydrodynamics
9:00	Discussion	
9:10	A. Wiseman(Caltech)	Final Wave Forms for Binary Inspiral
9:35	Discussion	
9:45	Coffee Break	
10:00	K. Thorne(Caltech)	The Final Merger of Compact Binaries: Information Content, Waveform Computations, and Data Analysis Changes
10:25	Discussion	
10:35	R. Matzner(UT-Austin)	Grand Challenge Update
11:00	Discussion	

Thursday PM January 18	Data Analysis II. Time-Frequency Techniques and Other Issues Chair: C. Will	
4:30	B. Owen(Caltech)	Searching for Coalescing Binaries: Templates, Strategies, Computing Requirements
4:55	Discussion	
5:05	J. Centrella(Drexel)	Coalescence Wave Forms and Rotational Instabilities
5:30	Discussion	
5:40	A. Krolak(Warsaw)	Estimating Parameters of GW Signals Using Wavelet Analysis
6:05	Discussion	
6:15	Coffee Break	
6:30	A. Vecchio(Cardiff)	Why Realistic Errors in Parameter Extraction Don't Follow Cramer-Rao Bounds
6:55	Discussion	
7:05	H. Yamamoto(Caltech)	LIGO Simulation Environment
7:30	Discussion	

Friday AM January 19	Data Analysis III. Pulsar and Other Periodic Source Searches Stochastic Background Searches Chair: F. Raab	
8:00	D. Nicholson(Cardiff)	Realistic Search of One Year's Data
8:30	Discussion	
8:40	G. Jones(Cardiff)	Results of a Practical Search of a Large Patch of Sky for a Pulsar-type Signal
9:10	Discussion	
9:20	Coffee Break	
9:30	B. Allen(Milwaukee)	Stochastic Background Searches
10:00	Discussion	
10:10	R. Fakir(UBC)	The GAP Concept
10:15	Discussion	

Friday PM January 19	Data Analysis IV. Analysis of Existing and Future Data Chair: N. Robertson	
4:30	D. Nicholson(Cardiff)	Overview of Data Analysis for 100 hour Glasgow-Garching Run
5:00	Discussion	
5:10	R. Schilling(Garching)	Time Domain Analysis of 100hr Glasgow-Garching Run
5:40	Discussion	
5:50	Coffee Break	

6:05	S. Finn (Northwestern)	Data Analysis for A Network of Interferometers
6:35	Discussion	
6:45	B. Mours (LAPP-Annecy)	Plans for Organizing Data Analysis for Virgo
7:15	Discussion	

Saturday AM — Impulsive Signal Searches, Round Table
January 20 — Chair: K. Thorne

8:00	D. Nicholson (Cardiff)	Nonlinear Adaptive Filters
8:30	Discussion	
8:45	Coffee Break	
9:00	S. Finn, W. Johnson A. Krolak, B. Mours, D. Nicholson. D. Shoemaker, R. Stebbins K. Thorne	Round Table on Waveforms and Data Analysis for Stellar Core Collapse and Other Sources
11:00	Conference Adjourns	

Monday AM: Interferometers and Bars
January 15 Chair: R. Drever

8:00	S. Meshkov(Caltech)	Welcome
	S. Mencimer(ACP)	
8:10	A. Ruediger(Garching)	Current Interferometer Projects
8.35	Discussion	
8:45	G. Pizzella(Rome)	Operation of Resonant Detectors
8:50	W. Johnson(LSU)	Status of Current Bar Experiments
9:10	Discussion	
9:20	Coffee Break	
9:35	S.Finn(Northwestern)	The Path to Data Analysis
10:00	Discussion	
10:10	D. Shoemaker(MIT)	LIGO Status Report
10:35	Discussion	

Albrecht Rüdiger

1996 Aspen Winter Conference
on
Gravitational Waves and Their Detection

January 14-20, 1996

Our thanks to those who made it possible:

Aspen Center for Physics
Syd Meshkov
Sally Mencimer
Saint Peter

Three major topics selected for Conference:

1. First meeting of LIGO Research Community
2. Signal processing in GW research
3. Laser-interferometric detectors in space (LISA)

First meeting of LIGO Research Community

Historical event:

Worldwide group of GW scientists
common platform for
intensive discussions
exchange of ideas
mutual assistance and consultation

LIGO as condensation nucleus
largest project
furthest developed
most heavily funded

but perhaps change the name ?
what's in a name ?
A rose by any other name would smell as sweet

Expectation:
become truly international,
mutually fertilizing entity

LRC Executive Committee:

1. David Shoemaker
2. Sam Finn
3. Bill Hamilton
4. Harry Ward
5. Joan Centrella
6. Eric Gustafson
7. Bruce Allen

Chair: Sam Finn

Good blend of scientists active in

theory,
astrophysics,
experimentation of
  interferometric detectors,
  resonant mass detectors,
signal processing.

3a

LISA

Laser Interferometer Space Antenna
for the detection and observation of gravitational waves

A Cornerstone Project in
ESA's long term space science programme
"Horizon 2000 Plus"

Pre-Phase A Report

December 1995

Signal Processing in GW Research

in case of laser interferometry:

in recent years (decades !) emphasis on

establishing feasibility

optimizing projects

getting funded

now with construction under way:

intensify studies of signal processing

optimize strategies

interaction between different detectors

Sam Finn: overview on Signal Analysis, today

deal with signal analysis both for

interferometer detectors

resonant mass detectors

Prior to that:

lay foundations with review talks

Warren Johnson resonant mass detectors

Albrecht Rüdiger interferometer detectors

Gravitational Waves

emitted at measurable strengths only when
cosmic masses undergo **strong** accelerations

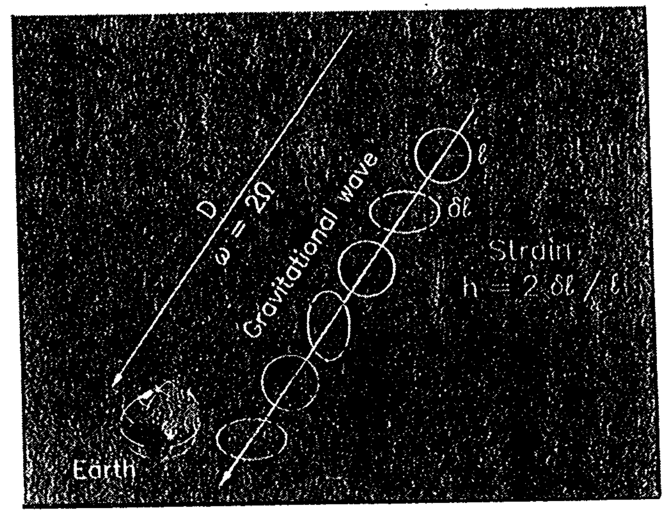

GW: transversal, quadrupole strain in space

relative change in distances: $\delta\ell\,/\,\ell$

expressed as $h := 2\,\delta\ell\,/\,\ell$

Michelson interferometer is ideally suited:

measures changes in *path difference*:

$$h = \frac{\delta\mathcal{L}}{\mathcal{L}} = \frac{\delta(\mathcal{L}_2 - \mathcal{L}_1)}{\mathcal{L}}$$

Sources of Gravitational Radiation

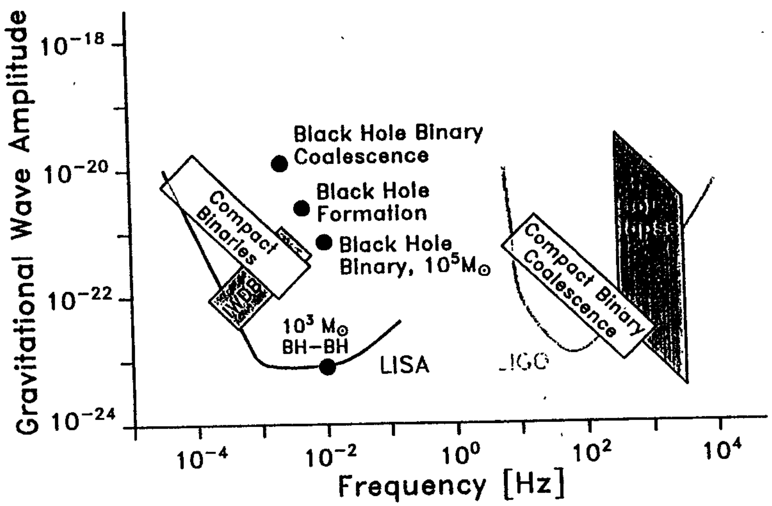

vast frequency spectrum:

from kHz (supernovae, NS coalescence)
down to sub-mHz (supermassive black holes)

Observe two clearly separate regimes:

no overlap; but ideal complementarity
from 10 Hz to several kHz (*terrestrial*)
from 10^{-4} Hz to 10^{-1} Hz (*space*)

Space project treated separately (LISA)

start out with:

ground-based **interferometric detectors**

Michelson Interferometer

Optical path $\mathcal{L} \rightarrow \frac{1}{2} \Lambda_{GW}$:

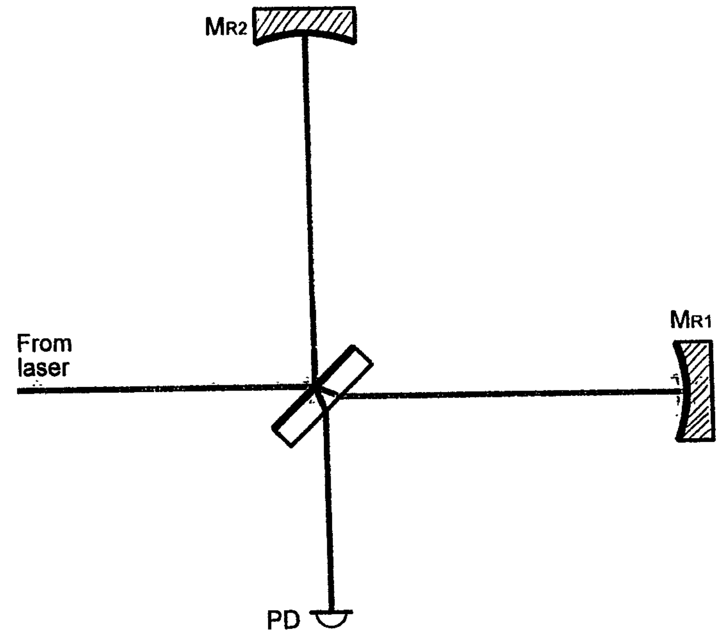

add near mirrors: DL or FP

Shot noise limit reduces as $P^{-1/2}$.

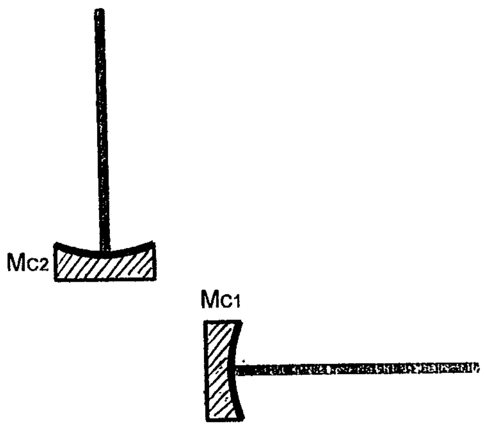

add mirror M_P: "power recycling"

If $\mathcal{L} \ll \frac{1}{2}\Lambda$ (DL, few bounces)

add mirror M_S for "signal recycling"
(increases signal, at price of bandwidth)

If $\mathcal{L} \gg \frac{1}{2}\Lambda$ (FP, excellent mirrors, high f_{GW}):
same mirror M_S can avoid cancelling:
"Resonant sideband extraction"

Laser-Interferometric GW Detectors
Past – Present – Future

ountry: / istitute:	USA MIT	USA Caltech	GER MPQ	GBR Glasgow	FRA CNRS	ITA INFN	JPN ISAS	JPN NAO	AUS Perth	AUS (all)
ototypes:										
tart:	1972	1980	1975	1977	1983	1986	1986	1991	1991	
aser:	Ar^+	Ar^+	Ar^+	Ar^+	(Ar^+)	(Ar^+)	Ar^+	YAG	YAG	YAG
rm length ℓ:	40 m		30 m	10 m	0.5 m		100 m	20 m	8 m	
train sensitivity $\tilde{h}$ [$Hz^{-\frac{1}{2}}$]:	$1 \cdot 10^{-20}$ 1995		$11 \cdot 10^{-20}$ 1986	$6 \cdot 10^{-20}$ 1992			$20 \cdot 10^{-20}$ 1994	10^{-17} 1994		
rge Interferometric Detectors:										
lanning (start):	1982	1984	1985	1986	1986	1986	1987	1994	1990	1994
rm length ℓ:	4 km 2 km	4 km	600 m		3 km		300 m		400 m	
ite (State)	Hanford (WA)	Livingston (LA)	Hannover GER		Pisa ITA		Mitaka JPN		Perth AUS	
ost (10^6 US$):	292		7		90		15		12	
roject name:	**LIGO**		GEO 600		**VIRGO**		TAMA 300		**AIGO 400**	

solicit your assistance in filling holes

Development of prototypes

Country: Institute:	USA MIT	USA Caltech	GER MPQ	GBR Glasgow	FRA CNRS	ITA INFN	JPN ISAS	JPN NAO	AUS Perth	AUS (all)	USA Stanford
Prototypes:											
Start:	1972	1980	1975	1977	1983	1986	1986	1991	1991		1994
Laser:	Ar^+	Ar^+	Ar^+	Ar^+	(Ar^+)	(Ar^+)	Ar^+	YAG	YAG	YAG	YAG
Technique:	DL	FP	DL	FP	FP	FP	DL	FP	FP	FP	FP
Arm length ℓ:	(1.5 m) 5 m	40 m	30 m	10 m	0 5 m		100 m	20 m	8 m		10 m
Strain sensitivity $\tilde{h}$ $[Hz^{-\frac{1}{2}}]$:	$(4 \cdot 10^{-17})$ (1980)	$1 \cdot 10^{-20}$ 1995	$11 \cdot 10^{-20}$ 1986	$6 \cdot 10^{-20}$ 1992			$20 \cdot 10^{-20}$ 1994	10^{-17} 1994			
Special features	pioneer, DL washing out phase sens. light power	Fabry-Perot leads in sensitivity	direct susp. mode cleaner power recycl power recycl. RSE	Fabry-Perot extern. mod. signl recycl. mode cleaner	extern. mod. power recycl. mode cleaner optical meas. simulations	extreme seism. isolation super-atten optical meas modelling	DL scheme longest prototype	first FP- -recombin. 3m prototp	seismic isol. cantilever springs		Sagnac advanced ~~technol.~~
Large Interferometric Detectors:											
Planning (start):	1982	1984	1985	1986	1986	1986	1987	1994	1990	1994	1994
Arm length ℓ:	4 km 2 km	4 km	600 m		3 km		300 m		400 m		400 m
Project name:	LIGO		GEO 600		VIRGO		TAMA 300		AIGO 400		

Technology

Work on prototypes and for
large-scale projects
has spawned technological research in:

Optics:

- substrate quality
- superpolishing
- supercoating
- modulation
- mode cleaning

revived interest in diffractive optics

Lasers:

- Nd:YAG (MISER)
- efficiency
- laser diode pumping
- lifetime
- laser stabilization
  - frequency
  - power

Mechanics:

- suspension techniques
- active seismic control
- cantilever springs
- high Q materials
- high Q bonding techniques

Vacuum:

- tube construction
- low outgassing materials
- cleaning
- heat treatment

Country: Institute:	USA MIT	USA Caltech	FRA CNRS	ITA INFN	GER MPQ	GBR Glasgow	JPN ISAS	JPN NAO	AUS Perth	AUS (all)	USA Stanford
Prototypes:											
Start:	1972	1980	1983	1986	1975	1977	1986	1991	1991		1994
Laser:	Ar^+	Ar^+	(Ar^+)	(Ar^+)	Ar^+	Ar^+	Ar^+	YAG	YAG	YAG	YAG
Armlength ℓ:	40 m		0.5 m		30 m	10 m	100 m	20 m	8 m		10 m
Strain sensitivity h [$Hz^{-\frac{1}{2}}$]:	$1 \cdot 10^{-20}$ 1995				$11 \cdot 10^{-20}$ 1986	$6 \cdot 10^{-20}$ 1992	$20 \cdot 10^{-20}$ 1994	10^{-17} 1994			
Large Interferometric Detectors:											
Planning (start):	1982	1984	1986	1986	1985	1986	1987	1994	1990	1994	1994
Arm length L:	4 km 2 km	4 km	3 km		600 m		300 m		400 m		400 m
Site (State)	Hanford (WA)	Livingston (LA)	Pisa ITA		Hannover GER		Mitaka JPN		Perth AUS		Stanford (CA)
Cost (10^6 US$):	292		90		7		15		12		
Project name:	**LIGO**		**VIRGO**		**GEO 600**		**TAMA 300**		**AIGO 400**		
special features:	autonomous: 2 + 1 interf.		super-attenuator low frequencies		advanced optics tunable		"small is beautiful" <= low cost =>		ext'ble to 3 km suspension		

Outlook

often asked question:

when will interferometers be ready ?

have to define what 'ready' means

- construction finished
- optics installed
- first interference
- first operation, at reduced level
- full sensitivity reached
- all finished for longer data-acquisition run

any answer to be taken with a grain of salt

safest statement:

by turn of millennium

leaves one year contingency (2000, 2001 ?)

still much better off than **LISA**

scheduled for **2015** if all goes well!

AVAILABLE | EXPERIMENTAL DATA

Operation of Resonant Detectors

G. Pizzella
ROG collaboration (ROME)
I and II University of Rome
University of L'Aquila
National Institute for Nuclear Physics (INFN)
National Council of Research (CNR)

1990 1991 1992 1993 1994 1995 1996

ROME
EXPLORER (ROG)

ALLEGRO (LSU)

NIOBE (UWA)

sensitivity for short bursts $h \approx 6\ 10^{-19}$

at the resonance $\tilde{h} \approx \dfrac{10^{-21}}{\sqrt{Hz}}$

It is important to make available the raw data, in order to exploit the experiments with the best possible efficiency.
One should try to consider the various apparatuses as part of one single detector, each part giving its own contribution to the study of the still unknown phenomenon of gravitational waves.
This data exchange should be done soon

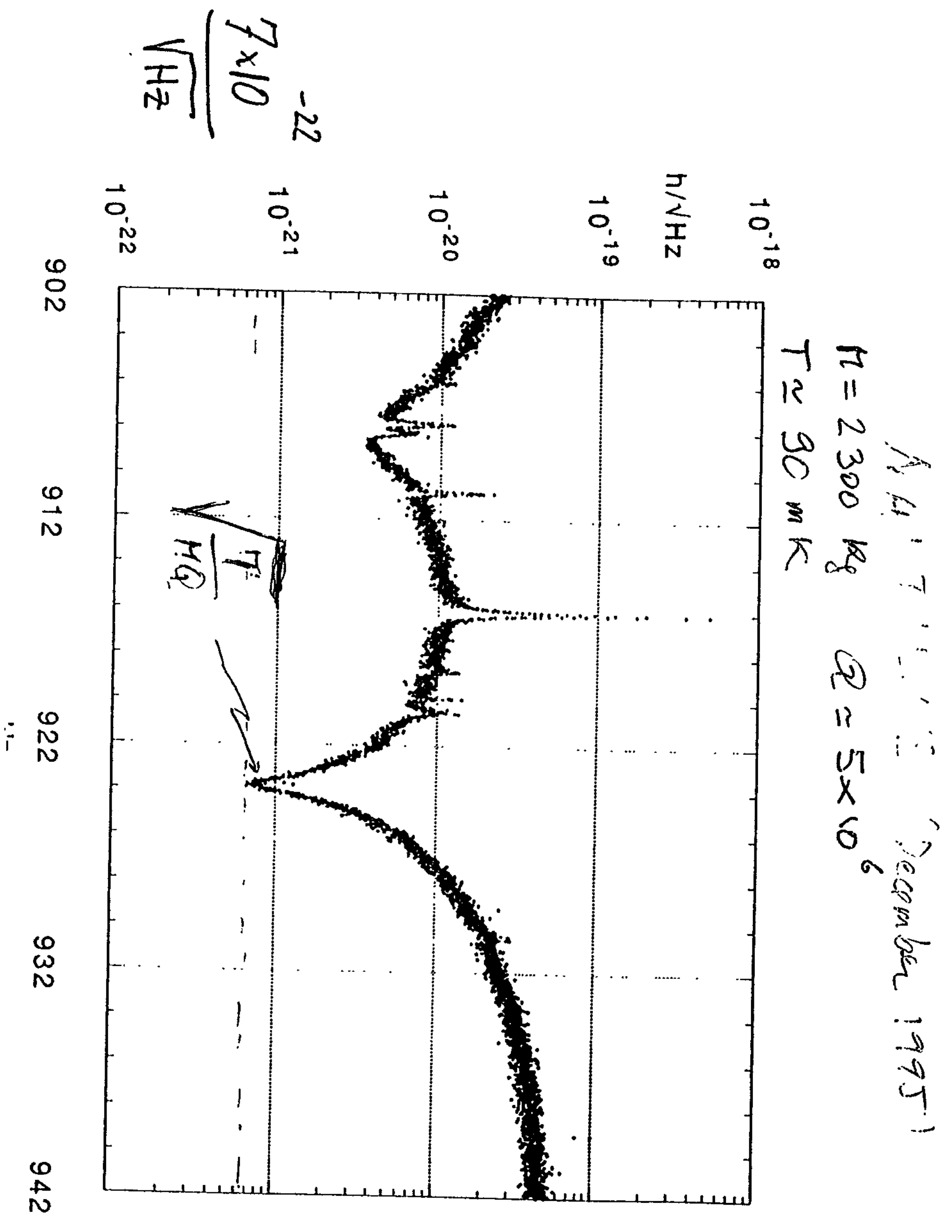

STATUS OF ~~BAR~~ DETECTORS
RESONANT CRYOGENIC

WARREN JOHNSON
LSU

1.

Observing Instruments ·
Instruments in Progress
Proposed Instruments

Search for events · Single Blind Search

NOISE BUDGET - ALLEGRO '93 1b

—— RESONATOR THERMO-MECHANICAL FORCE ("BROWNIAN")
...... ANTENNA " " "
-·-·-·- AMPLIFIER (SQUID) NOISE

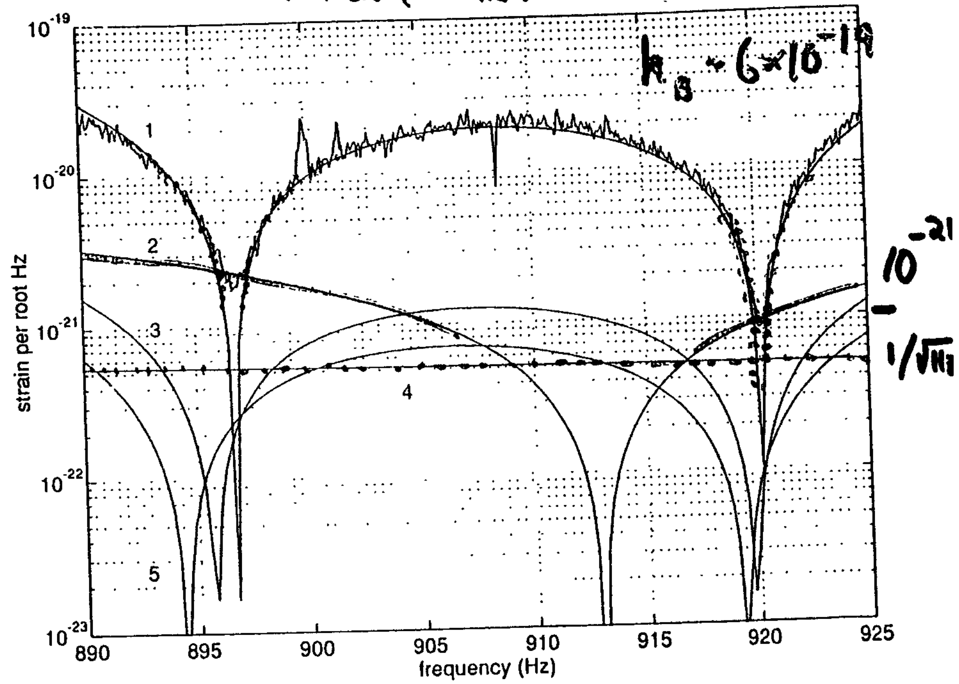

THERMO-MECHANICAL NOISE $\propto \sqrt{\frac{T}{mQ}}$

AMP NOISE $\propto$ $\frac{\text{ADDITIVE NOISE}}{\text{COUPLING STRENGTH}}$

What can be done with cryogenic techniques

Observing Instruments

(Stanford 4K - operational (early 80's) damaged '89)

Rome (EXPLORER) - operational late '80s
- to present

LSU (ALLEGRO) - operational '91 - '95
spent '95 fixing cryogenics & vacuum
1st try at improved sensitivity has failed
will probably return to observing anyway.

Australia - (NIOBE) - operational '94 - present

In Progress

(Stanford 50mK - discontinued '95)

Rome (NAUTILUS) - first truly mK antenna
shows 80mK cryogenics are possible
isolation & upconversion are problems
operational late '95

Legnaro (AURIGA) - younger sister to NAUTILUS
cryostat done, antenna under construction

4

Omni-Directional Antennas (large, spherical)

- International Efforts
- US collaboration - TIGA project
- Direction Finding-Spin of Graviton(s)

- Technology - Very Recent Progress
  - Antenna Fabrication- Explosive Bonding
  - Mechanical Q
  - Multi-stage Resonators
  - Transducers
    - Inductive
    - Optical
  - real SQUIDs
  - Modeling
- Sources ?

tiga arrangement 4 2
scale = 25:1
dimensions in cm

5

3 Multistage Mechanical Isolators:
Tube and Disk Geometery

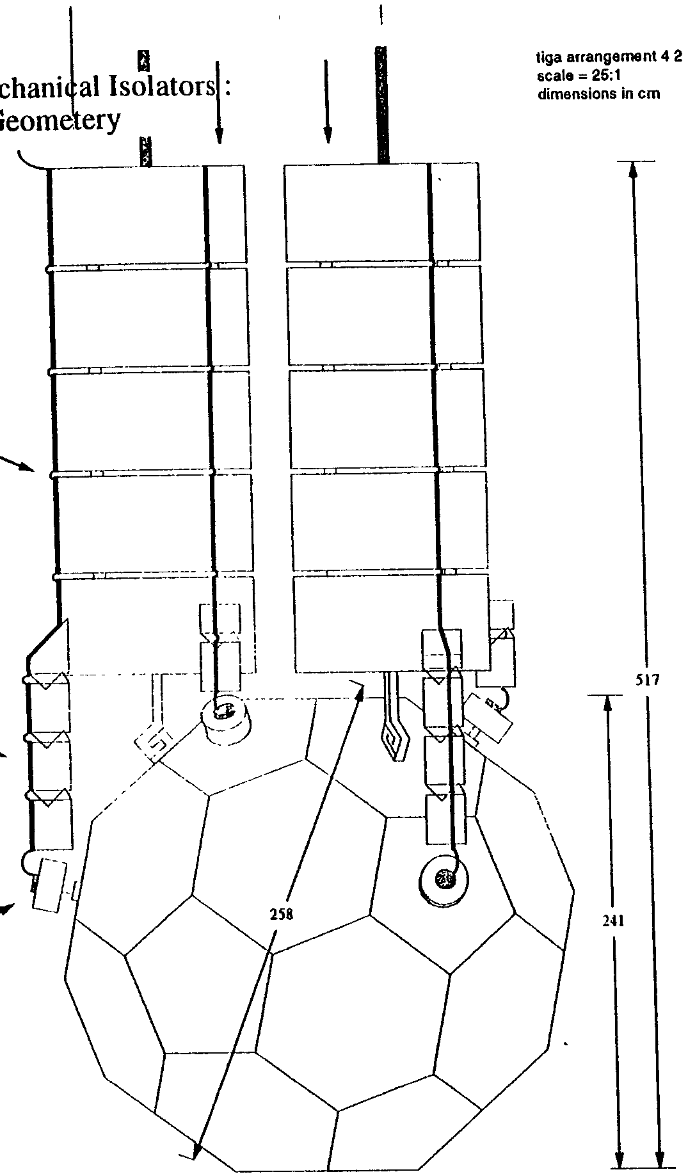

Wiring &
Thermal Links

Mechanical
Isolator

Resonator and
Transducer

Side View

Spherical Resonant GW Detector International Effort

"OMEGA"
OMnidirectional Experiments with Gravitational Antennae

<u>US</u>	<u>Italy</u>	<u>Netherlands</u>	<u>Brazil</u>
TIGA	**"NAIAO"**	**GRAIL**	**GRAVITON**
• LSU	• Rome, "Tor Vergata"	• Leiden	• INPE
• Maryland	• Rome	• Amsterdam	• Sao Paolo
• Rochester	• L'Aquila	• Twente	• Brasilia
	• Legnaro	• Eindhoven	

\+ • Barcelona
\+ • Paris "Inst. d'Aphys"
= EUROMEGA

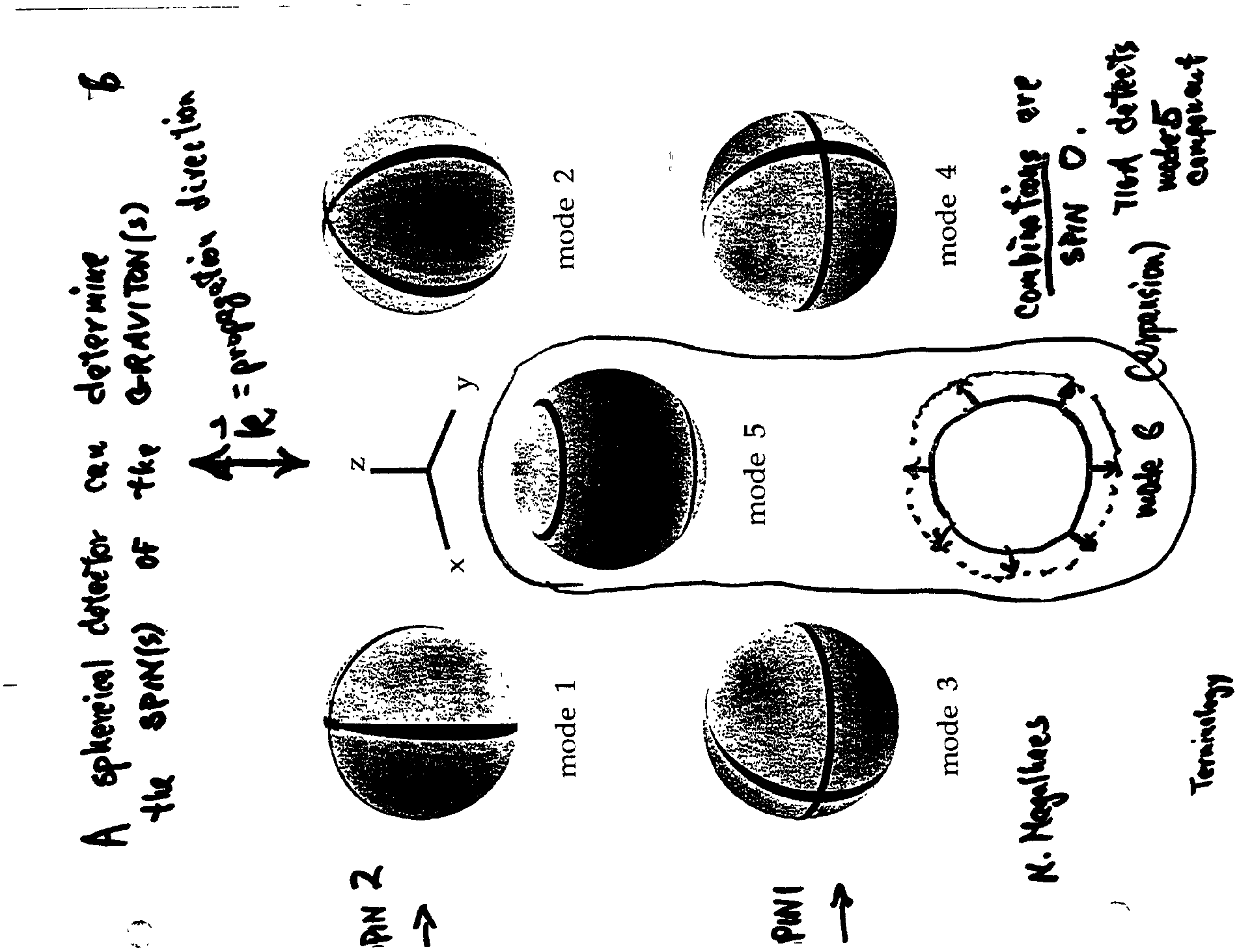

World-wide Status Report

US - TIGA **(2.6 m (1 kHz) Al sphere @ 50 mK)**

TIGA physics
Cryogenic design - prelim. eng. drawings
Transducers - inductive, optical
Materials (Al alloys)

Presently separately funded efforts
Submit joint R&D proposal 12/95
Construction proposal 1997-8

Italy

Materials (Al alloys, BeCu, CuAl)
Ultracryogenics (10 mK)
Coordinate EUROMEGA

Nautilus (100 mK 1.5 ton bar)
EUROMEGA funding
Construction proposal

Netherlands **(3 m 'sphere' - 660 Hz (100 tons) @ 10 mK)**

Materials (Al alloys, BeCu, CuAl)
Ultracryogenics (10 mK)

R&D funding - 1995
2 m prototype - 1996-1998.5
3 m sphere - operation in 2001

Brazil **(3 m 'sphere' < 100 mK)**

Materials (Bronze alloys)

Complete feasibility studies in 1995
Submit construction proposal by 1996

US collaboration (Gravity Coop)

(TIGA - Truncated Icosahedral Gravitational Antenna)

L.S.U.	- W. Hamilton, W. Johnson, K. Geng
Maryland	- H.J. Paik, T. Stevenson
	- J.P. Richard, Y. Pang
	- F. Wellstood, I. Jin
Rochester	- M. Bocko
Santa Clara	- W. Duffy

Working Groups - systematically attacking the technology

Modeling -understand tensor and multimode behavior
- guide component development

SQUIDs - design and construct devices that reach intrinsic noise

Inductive Transducer
- increase Qm and Qe
- maintain coupling
- integrate the advanced SQUIDs

Optical Transducer - develop alternate technology that is compatible with cryogenics and shot noise limited

Resonators and Antenna - increase bandwidth and coupling
- increase Qm

Cryogenics and Isolation
- operate at <60 mK with 40-50 tons
- engineered for antennadevelopment
- assure sufficent vibration isolation
- eliminate non-thermal noise

SOURCES !

10

Impulse Location

S. Merkowitz
L.S.U.

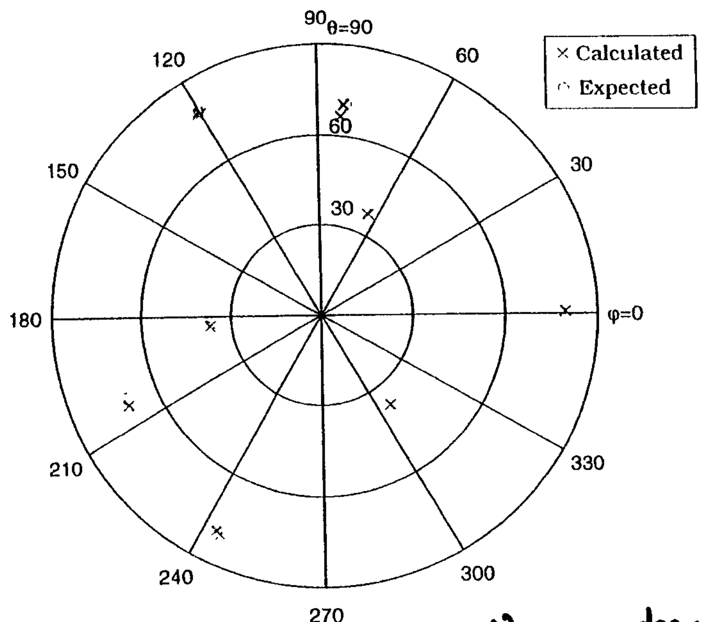

Proves we can deconvolve:
→ modes → direction

Impulse Face	θ Calculated	θ Expected	φ Calculated	φ Expected
Pent 1	36.8°	37.3°	64.6°	60.0°
Pent 2	37.0°	37.3°	- 53.4°	- 60.0°
Pent 3	36.8°	37.3°	- 175.1°	180.0°
Pent 4	79.3°	79.1°	- 116.4°	- 120.0°
Pent 5	79.4°	79.1°	0 6°	0.0°
Pent 6	78.6°	79.1°	120.2°	120.0°
Top Hex 6	70.4°	70.5°	82.9°	82.2°
Bottom Hex 6	66.5°	70.5°	83.4°	82.2°
Top Hex 8	70.6°	70.5°	- 155.6°	- 157.7°

11

Explosive Bonding - proposed by E. Coccia
'unlimited' size! if rect. + made of plates < 2" thick
layered to 3 meters seems possible

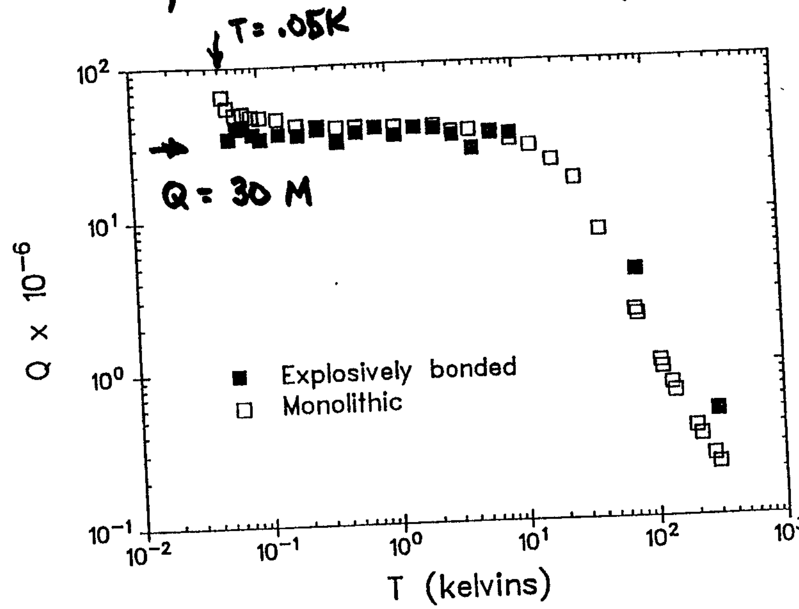

Proves Material OK. (Coccia & Frossati also)

Preprint 12/95

Cryogenics, W. Duffy, Jr. and S. Dalal, Fig. 3

NEW SQUID design Simplified Chip Diagram

I. Jin, F. Wellstood
U. Maryland

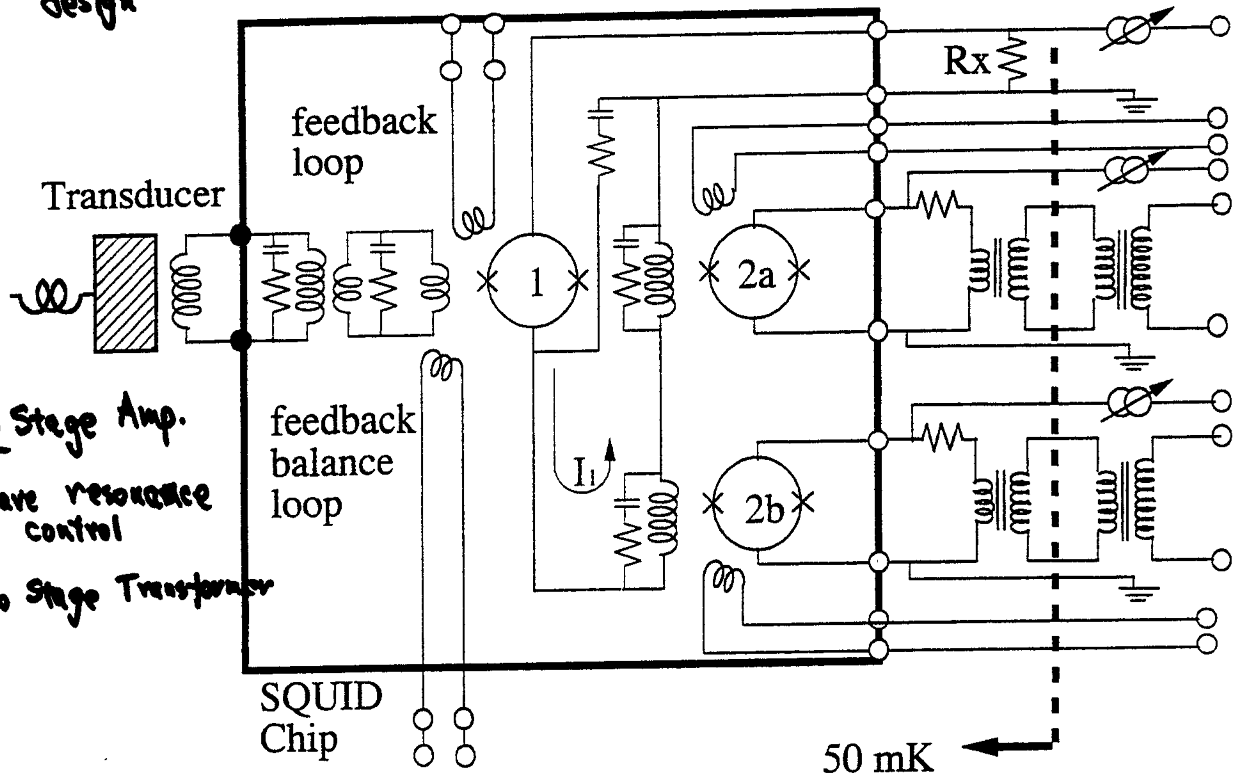

Two Stage Amp.

μWave resonance control

Two Stage Transformer

Two Mode Transducer Prototype

C. Prajna
K. Geng
N. Solomonson
LSU.

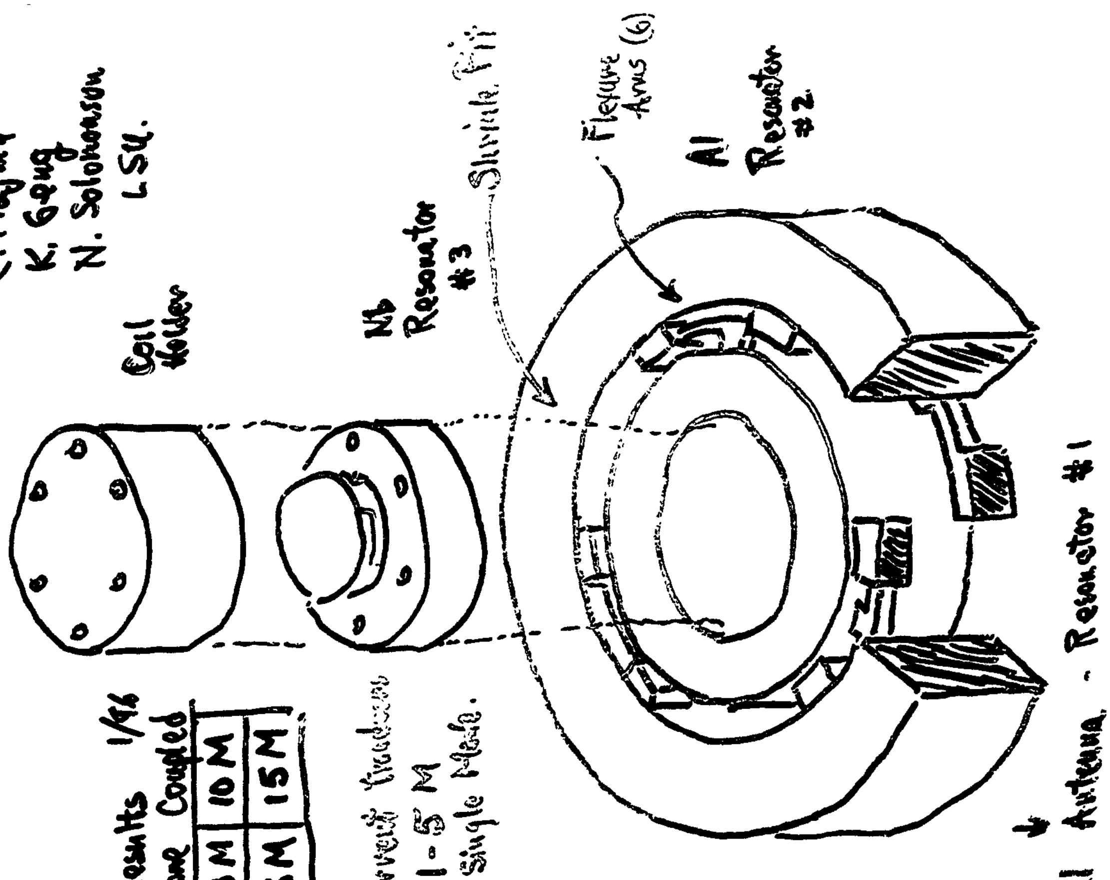

Q First Results 1/96

	Alone	Coupled
Al	13M	10M
Nb	16M	15M

Q_J: current tradeoff 1-5 M Single Mode.

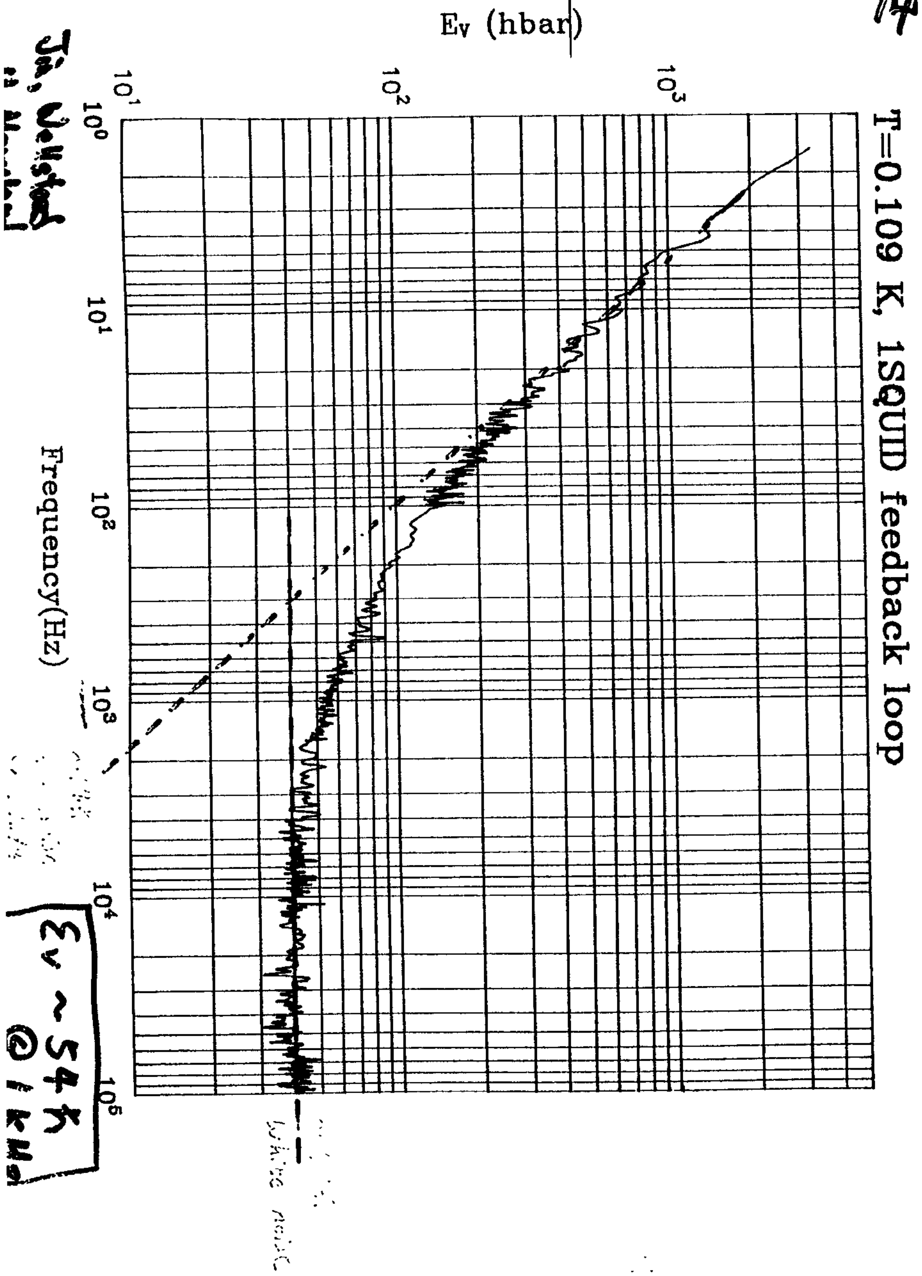

Calculated Strain Noise Advanced TIGA

Carlos Frajuca
LSU

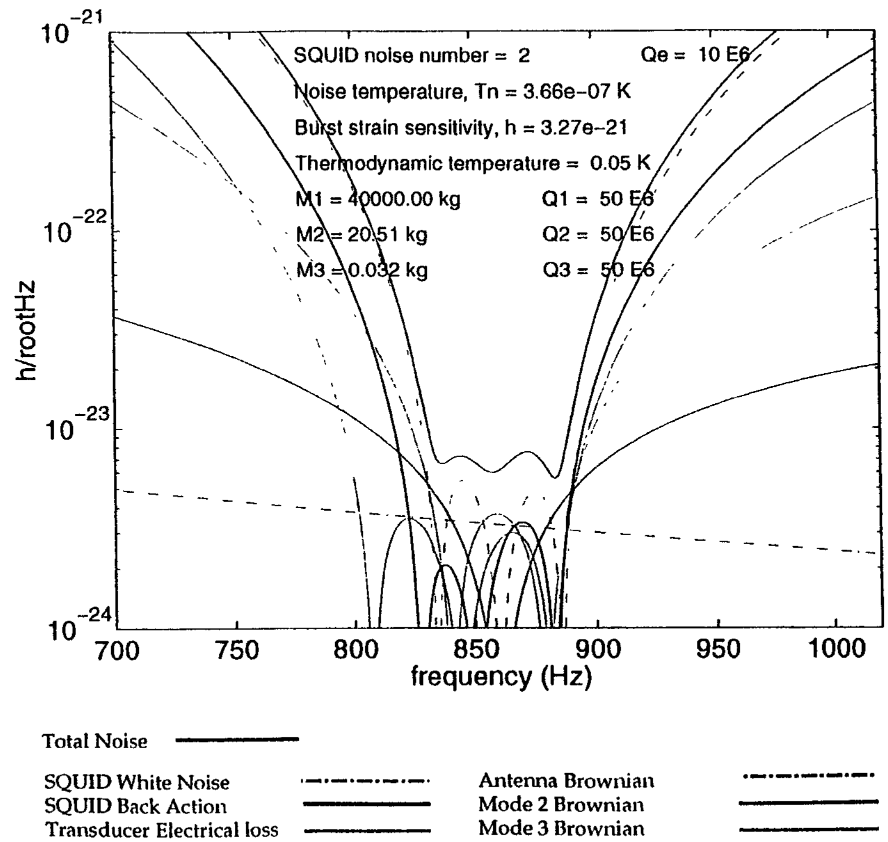

Summary & Questions

- Nearly quantum limited 'spherical' detector arrays are being developed world-wide.

But

- What are the best candidate sources for such detectors?

- Which frequency range should we try to cover first? (600 Hz to 4 kHz)

  'Guaranteed' sources may be necessary for U.S. funding

Gravitational Astronomy - Search for Impulsive Events

Filter the raw data to get Event Candidates
Eliminate bad data
Coincidence Search using data from another detector

Problems
- Background is not stationary
- Event signatures are arguable
- Difficult to correctly evaluate accidental rate
- High confidence required for discovery of new physics

A Solution? - Single Blind Multiple Search W. Johnson E. Mauceli

Search through N event lists from other detector
Compare them to [redacted] own :
- N-1 are to evaluate REAL accidentals because real list, but time-shifted
- 1 list is the real one

Blind, because searcher does not know which list is [redacted] real one.

Can the search distinguish the real from the shifted?

Is there any penalty for blind searches?

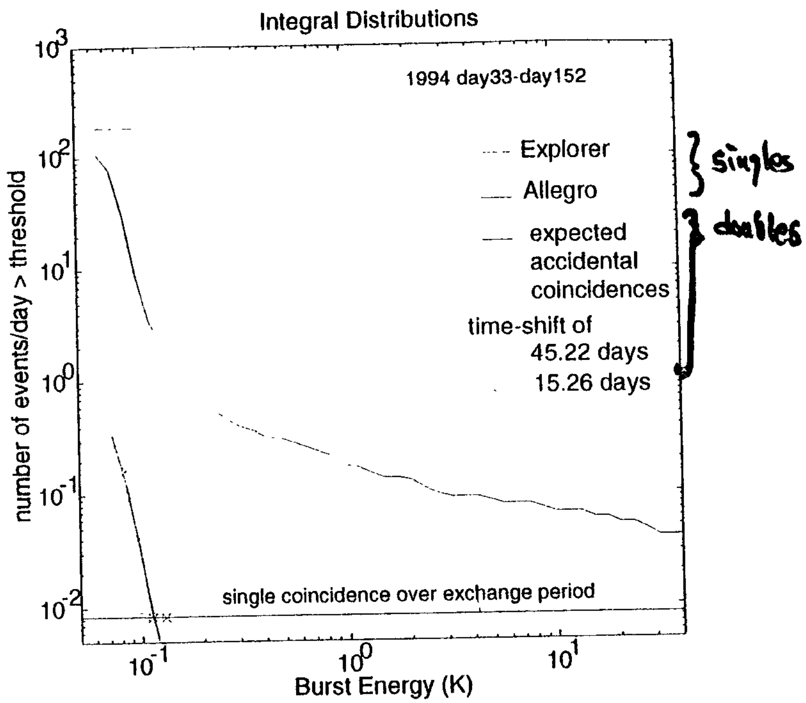

Symmetric Single Blind Coincidence Search

Data Exchange

1. Generate a list of 1000 random time-shifts.
   Pick one (≡ x), whose value is undisclosed.
2. reported event times = (real event times + x) mod L,
   where L is the length of the exchange (120 days)
3. Replace x by its "inverse" L-x in the list of time-shifts.
4. Send the list of reported times
   and the list of 1000 time-shifts to other group(s).

Coincidence Search

1. Use any reasonable selection criteria on both event lists.
2. Choose (first) time-shift from the received list (≡ y).
3. Candidate event times = (reported times + y) mod L
4. Find coincidences between candidate event times
   and own real event list.
5. Redo with next time-shift from list, until done.

(Real event times returned when y = L-x)

So 999 searchs for (guaranteed) accidental coincidences,
1 search for real coincidences

The Big Question : Does the real search stand out
from the accidentals ?

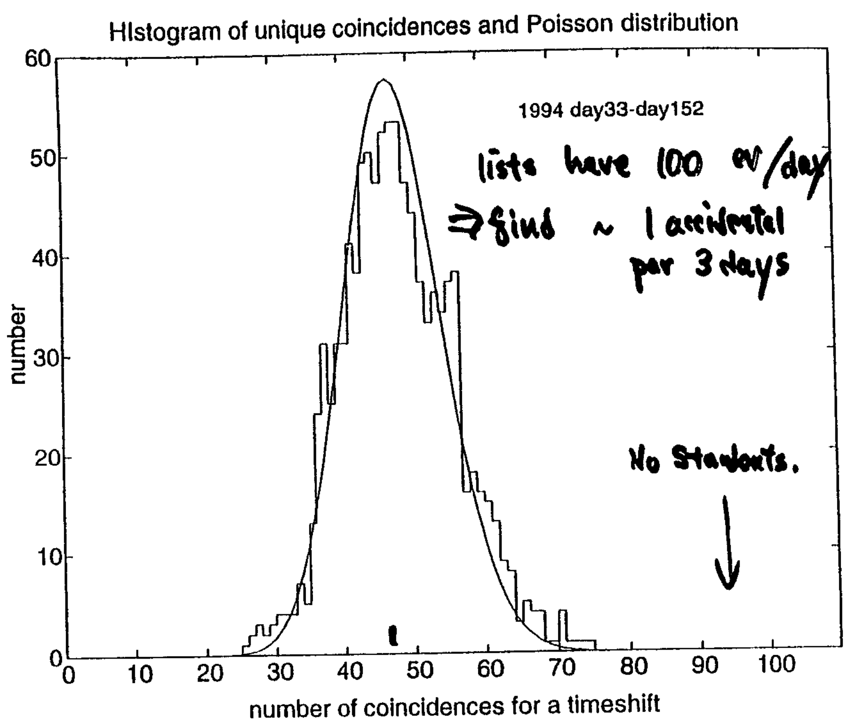
HIstogram of unique coincidences and Poisson distribution
1994 day33-day152
lists have 100 ev/day
⇒ find ~ 1 accidental
per 3 days
No Standouts.
number
number of coincidences for a timeshift

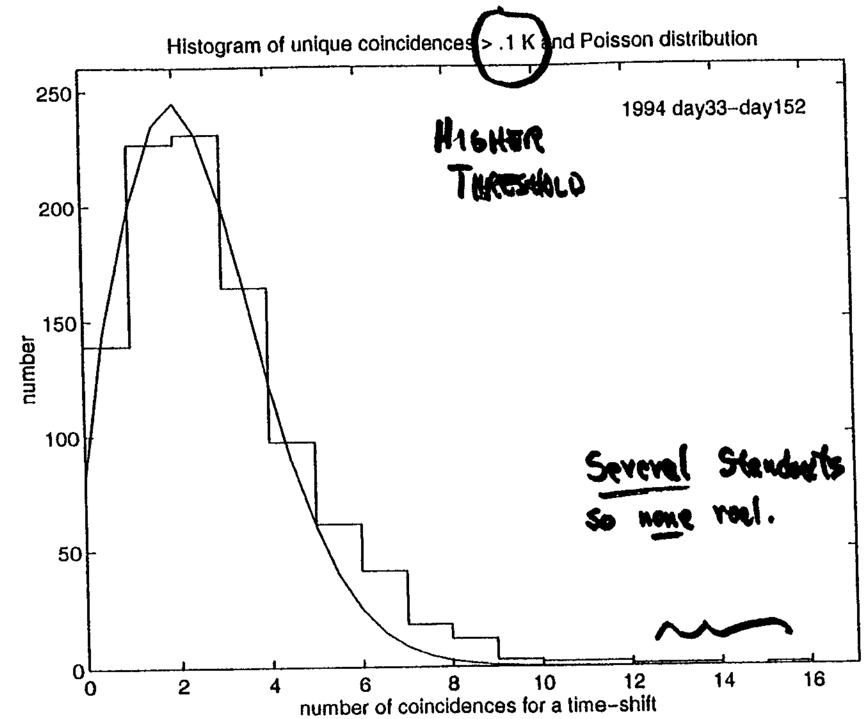
Histogram of unique coincidences > .1 K and Poisson distribution
1994 day33-day152
HIGHER THRESHOLD
Several Standouts!
so none real.
number
number of coincidences for a time-shift

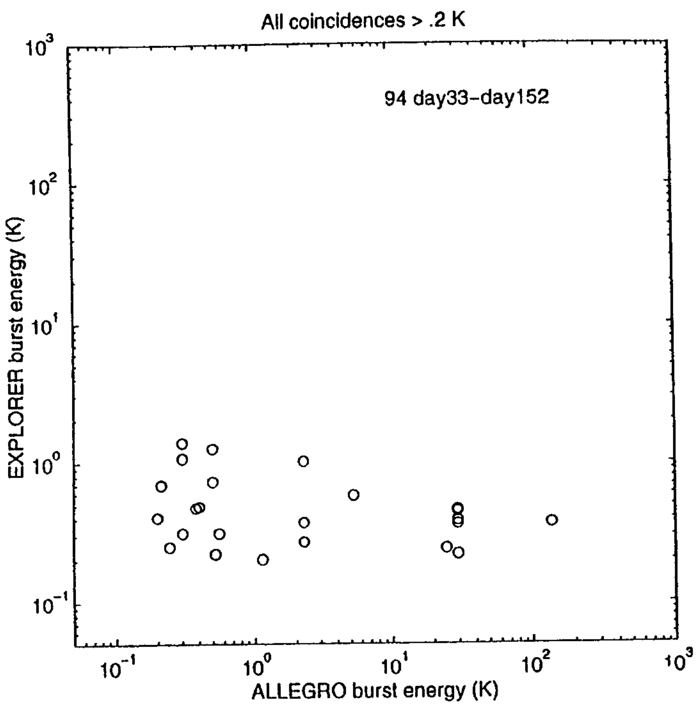

require energy
Coincidence also

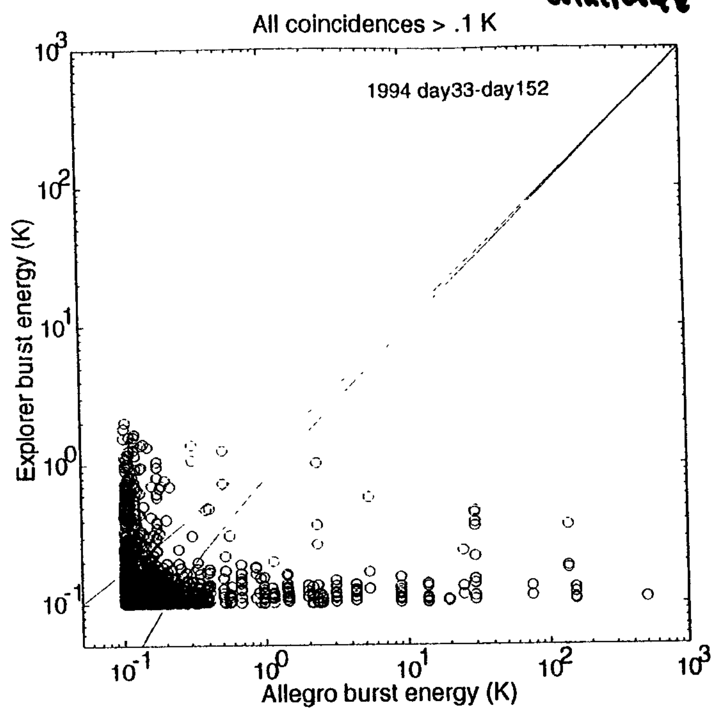

Conclusion: > 2 detectors essential unless?

Use Blind Search with 3 detectors?

The Path To Data Analysis

Sam Finn
Northwestern Univ.

Data Analysis :

Finding a needle
in a haystack.

Haystack	Data Stream
Needle	Signals
Method for separating needles from hay	Statistics

Data Stream

Integrity

- Continuity — Resolution, duty cycle
- Soundness — Calibration

Content

- Detector response
- Noise
  - Intrinsic instrument noise
  - Extrinsic environmental noise
  - Gaussian vs. non-gaussian noise
- Instrument/Environmental "Vetos"

Sources & Signals

Signal is not waveform

Stochastic vs. "deterministic" signals

Detector Response

Detector motion

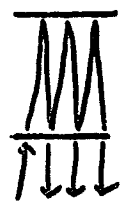

$\int_{t-T}^{t} h(t)\,dt$

Known vs. Unknown Sources

No unknown signals!

Signal Models

Particular sources

General physical principles

Signal-model Accuracy

Accurate model where signal power overlaps detector bandwidth

Example: Binary Inspiral

$$\rho \simeq 8\left(\frac{r_0}{d_L}\right)\left(\frac{\mathcal{M}}{1.2 M_\odot}\right)^{5/6} \mathrm{H}$$

$$r_0^2 \equiv \frac{5 M_\odot^2}{12\pi}\left(\frac{3}{20}\right)^{5/3} x_{7/3}$$

$$x_{7/3} \equiv \int_0^\infty \frac{df\,(\pi M_\odot)^2}{(\pi f M_\odot)^{7/3} S_n(f)}$$

$$\frac{d\rho}{df} \propto 1/f^{7/3} S_n(f)$$

$d\log(\rho)\,/\,d\log(f)$
(f_{max} large)

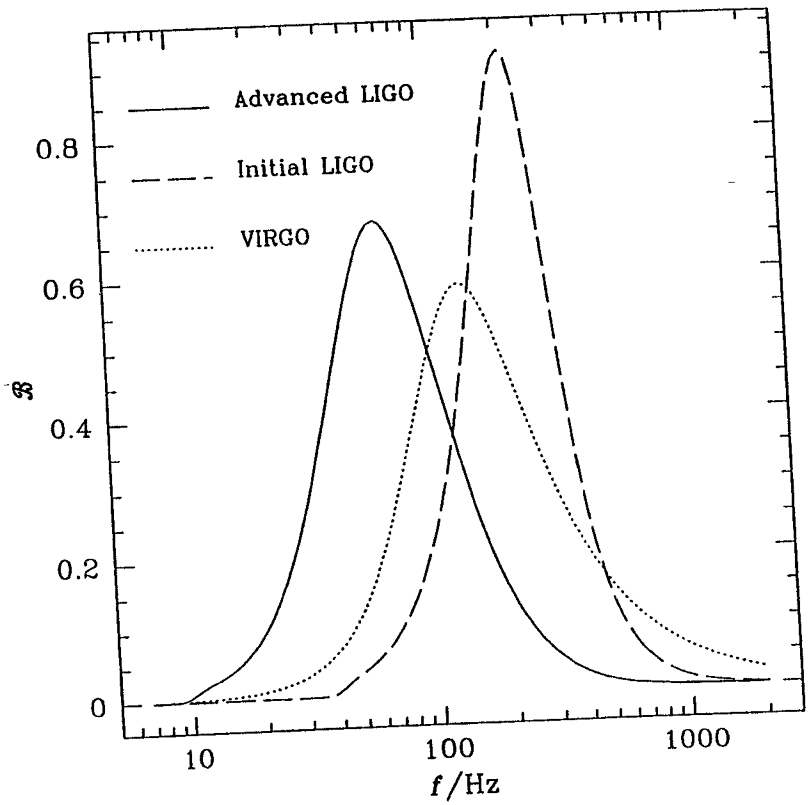

Statistics

What is signal? What is noise?

CWDBs & LISA

Supernovae & binary inspiral.

Quantifying confidence

Frequentist / Classical / Neyman-Pearson statistics

Bayesian statistics

Algorithms

Detection & Frequentist Statistics

Pick a descriptive statistic

e.g., maximum likelihood SNR ρ

Evaluate statistic distribution

Signal absent $P(\rho)$

Signal present $Q(\rho)$

Set Detection Threshold p

If ρ in $\{\rho : P(\rho) < p\}$ *say signal present*

$$\alpha \equiv \int_{\{\rho : P(\rho) < p\}} P(\rho)\,d\rho \qquad \text{False alarm prob.}$$

$$\beta \equiv \int_{\{\rho : P(\rho) > p\}} Q(\rho)\,d\rho \qquad \text{False dismissal prob.}$$

Interpretation

Probability $\longleftrightarrow$ Frequency, not likelihood
Long-run performance of statistic ρ

Measurement & Frequentist Statistics

Pick estimator e of source property

Average e over detector ensemble is source property E

Define test statistic $t \propto e - E$

$P(t)$ is distribution of t, is prob e differs from E

$I(x)$ is shortest interval of t s.t. $x = \int_{I(x)} P(t)\,dt$

$I(x)$ covers $e - E$ with probability x

Interpretation

Long run behavior of e
Not probability that E takes particular value

Frequency interpretation of probability central

Relative frequency of repeatable measurements
Not likelihood of proposition

Detection, Measurement & Bayesian Statistics

Probability: Likelihood of proposition

Bayes law: $P(A|B)\,P(B) = P(A,B) = P(B|A)\,P(A)$

signal described by param. μ

$$P(s(\mu)|g) = \frac{P(g|s(\mu))\,P(\mu|s)\,P(s)}{P(g|0)\,P(0) + P(s)\int d\mu\, P(g|s(\mu))\,P(\mu|s)}$$

detector output

$$= \frac{\Lambda(\mu)}{\Lambda + P(0)/P(s)}$$

$$\Lambda(\mu) \equiv \frac{P(g|s(\mu))}{P(g|0)}\,P(\mu|s)$$

$$\Lambda \equiv \int d\mu\, \Lambda(\mu)$$

Prior probabilities:

$P(\mu|s)$ — Expectation/prior knowledge regarding distribution of μ

$P(s)$, $P(0)$ — Expectation/prior knowledge regarding event rate

Interpretation

Conclusions

Data Analysis: Searching for a needle in a haystack

Data Stream: Haystack

Integrity, Content:
Characterizing non-gaussian noise

Signals: Needles

Detector response & Signal model accuracy
Source event rate, distribution
Signal modeling and unknown sources

Statistics: Distinguishing hay from needles

One persons signal is another's noise
Bayesian & Frequentist statistics

LIGO Status Report

David Shoemaker

LIGO Project

15 January 1996

Organization of talk: From the outside in

- sites
- beam tubes
- buildings
- vacuum equipment
- detector, supporting research
- systems
- people
- plans

LIGO Sites

Hanford, WA

- 25 km from Richland, WA
- cleared, graded, and settling
- seismic noise survey completed

Livingston, LA

- 50km from Baton Rouge, LA
- dedication 6 July 95
- cleared; rough grading started

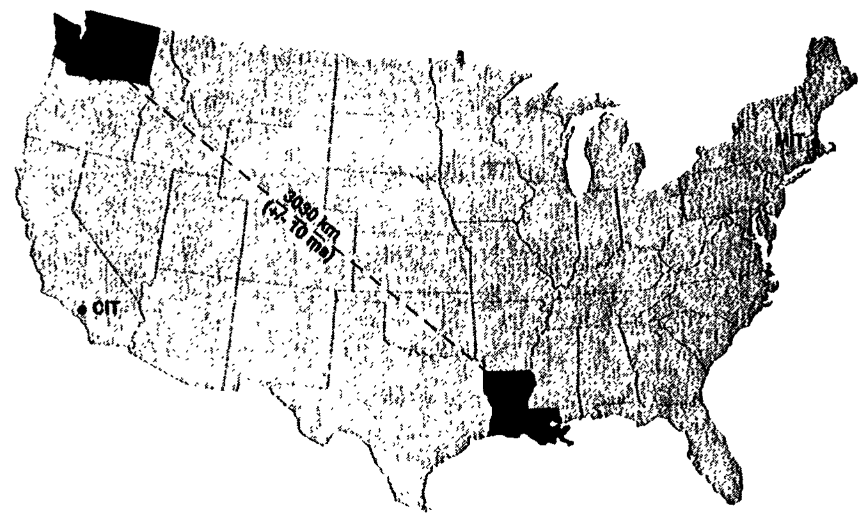

Beam Tube

Beam Tube Chicago Bridge and Iron

- total of 16 km of 1.2 m diameter high vacuum
- tests of fabrication, cleaning, vacuum performed
- baffle design chosen: black porcelain on SS

Beam Tube Enclosure RM Parsons

- supports and aligns Beam Tube, protects (from bullets!)
- final design, Oct 95

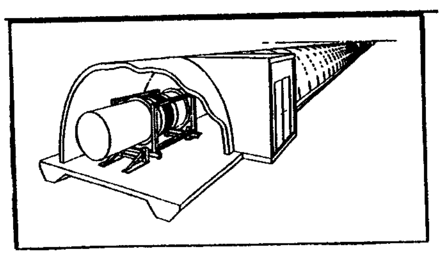

Buildings

Civil construction contract RM Parsons

- clean, quiet, temperature regulated environment
- work over requirements, realization from Dec 94 - Nov 95
- Preliminary Design Review in Nov 95

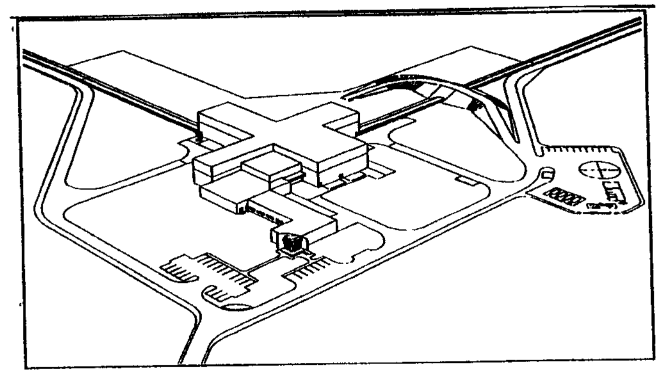

- WA: 2 full length or 1 full length, one half-length
- LA: 2 full length interferometers
- room to expand for additional interferometers

Vacuum equipment

Contractor selected

- Process Systems International
- provides flexible envelope for interferometer components
- allows isolation of elements, mechanical and electrical interface

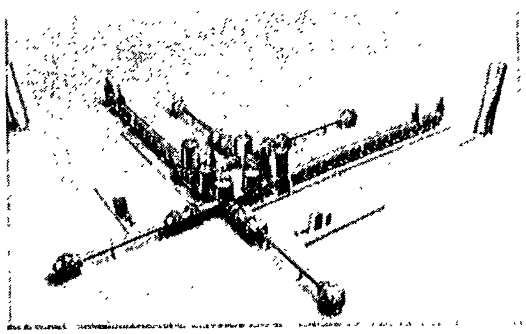

- Preliminary Design Review in October, 95
- basic design of system, components well advanced

Detector: Laser

LIGO baseline was Argon Ion laser

- workhorse since 70's
- well established control technology
- dated technology, obsolete in 2000

Solid State laser adopted as new baseline

- Nd:YAG or equivalent
- 1064 nm, near infrared wavelength

Advantages

- allows adiabatic increase in power—no mirror changes
- relaxed mirror surface requirements (longer yardstick)
- some better optical components available (modulators...)
- common with other GW efforts, industry momentum

Disadvantages

- reworking of (advanced) laser system, control design

Nd:YAG development effort

- contract for commercial development (early stages)
- internal effort to transfer technology
- incorporation into high-sensitivity instruments (5m, 40m)

Detector: Optics

Suspended Mode Cleaner

- 12m model of LIGO system
- control tests (locking, manual alignment)
- performance tests (beam jitter, passing of modulation)

LIGO Optics Pathfinder

- to find path for industrial fabrication of LIGO optics
- substrates (Corning at present)
- polishing (several contractors)
- metrology (with help from NIST)
- coating (REO)

Coating: real progress

- development of requirements (FFT and analytic modeling)
- development of implications for coating (modeling: 0.1% uniformity required over ~10cm diameter)
- development of masking techniques for coating
- comparison of transmission, AR coating reflectivity measurements
- looks feasible!

Detector: Suspensions

Refinement of single sling suspension

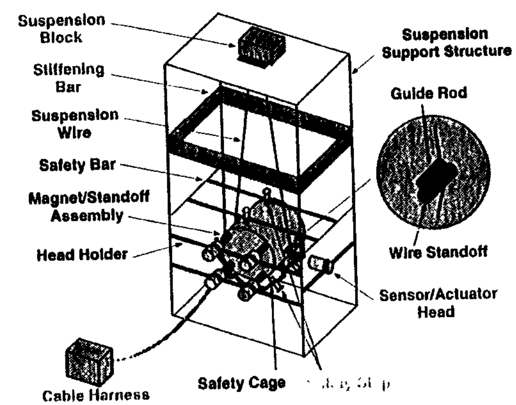

- techniques for maintaining high substrate 'Q' used
- refined versions of coil-magnet motor, LED-PD sensor
- version for 40m in preparation, soon to be installed
- designs for LIGO to follow

Measurement of *Q* for full-size mass underway

- electrostatic excitation
- study of sling, attachments
- no results yet

Detector: Isolation

Test of Commercial active vibration-isolation system

- 'beta' test of commercial system
  - active servo system, measures ground noise, feedback
  - six degrees of freedom
  - at MIT, suppresses local non-stationary noise (trucks, subways...)
  - for LIGO, can reduce controller dynamic range, up-conversion
- system functional
  - required collaborative work between Barry, Inc. and LIGO staff
  - significant reduction in noise: factor 100 in vertical, 2-30 Hz
  - still short of prediction in horizontal, but
  - makes qualitative difference in seismic environment

Barry Control Isolators: Vertical transfer function (ground to bottom table)

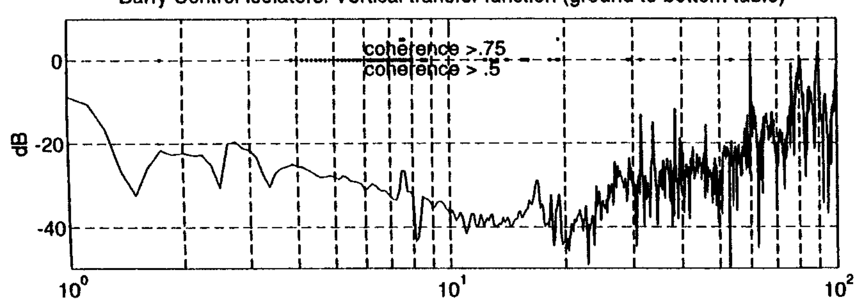

Detector: Length sensing/control

Recombined-Beam 40m interferometer configuration

- Objective: give tests of models for dynamics of length control
  - linear model (time constants similar to LIGO)
  - acquisition (pendulum suspensions, correct D.O.F.)
- Requires optical configuration of LIGO
  - recombination of beams from the two arms
  - addition of recycling mirror
- Significant construction project finished
  - modifications to in-vacuum components
  - arms asymmetrized for modulation technique
  - new modulation and control system

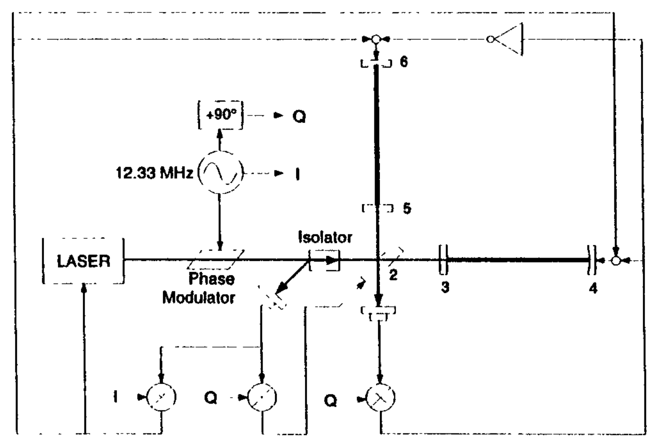

Detector: Lock Acquisition

Guided Lock Acquisition

- traditional brute-force method for acquiring 'lock' of cavity
  - system moves very quickly through resonance - non-adiabatic
  - very wide-bandwidth, high-force servo control
  - short effective duty-cycle
- better idea: reduce test-mass velocity
  - analyze signal output in time domain of unlocked system
  - calculate relative velocity of test masses
  - apply force X duration to 'brake' masses
  - THEN acquire lock
- success
  - considerably reduced locking time
  - valuable information for locking strategies
  - good technical experience for hardware/software

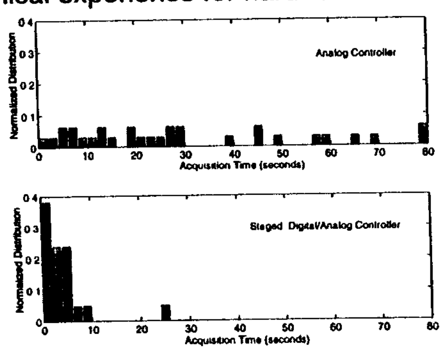

Detector: Phase Noise sensitivity

OBJECTIVES:

- demonstrate the initial LIGO phase sensitivity ($\sim 10^{-10}\,\mathrm{rad}/\sqrt{\mathrm{Hz}}$)
- develop the sensors, electronics, scattering control needed

Activity in '95 dominated by construction

- re-commissioning of vacuum system
- fabrication of seismic isolation system
- design, production of optic suspensions
- replication of the Argon pre-stabilized laser
- control and monitor systems
- recycled Michelson now being commissioned

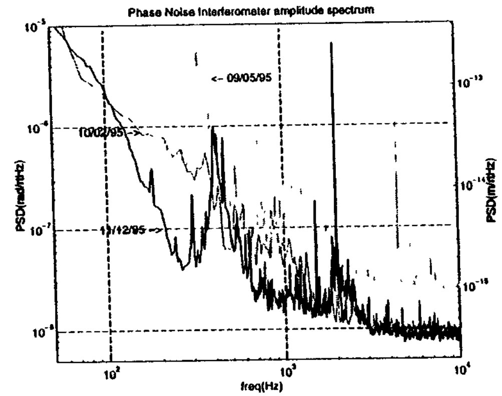

Detector: And...

Alignment research

- detailed design of wavefront sensing system
- construction of complete tabletop model
- fully digital servo and control system
- system requirements, subsystem specifications for LIGO

Modeling (and joint with System Integration, or SysInt alone)

- FFT model: optimizing, automating, propagating
- also, dual-recycling FFT model, real optics (in process)
- dynamics of coupled cavities, means to generalize
- data analysis of 40m
- end-to-end noise modeling, housekeeping

...etc.

System Integration

Interfaces, top-level requirements, and everything else

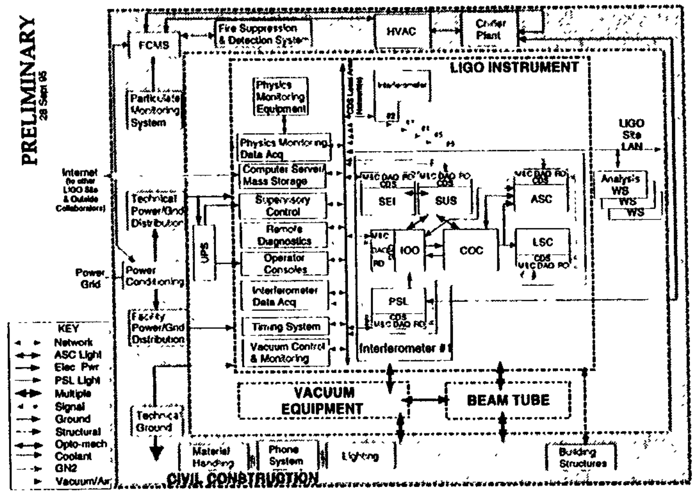

Interface Control Documents

- example: Vacuum Equipment/Beam Tube - Civil Construction

System Integration: Facility Limits

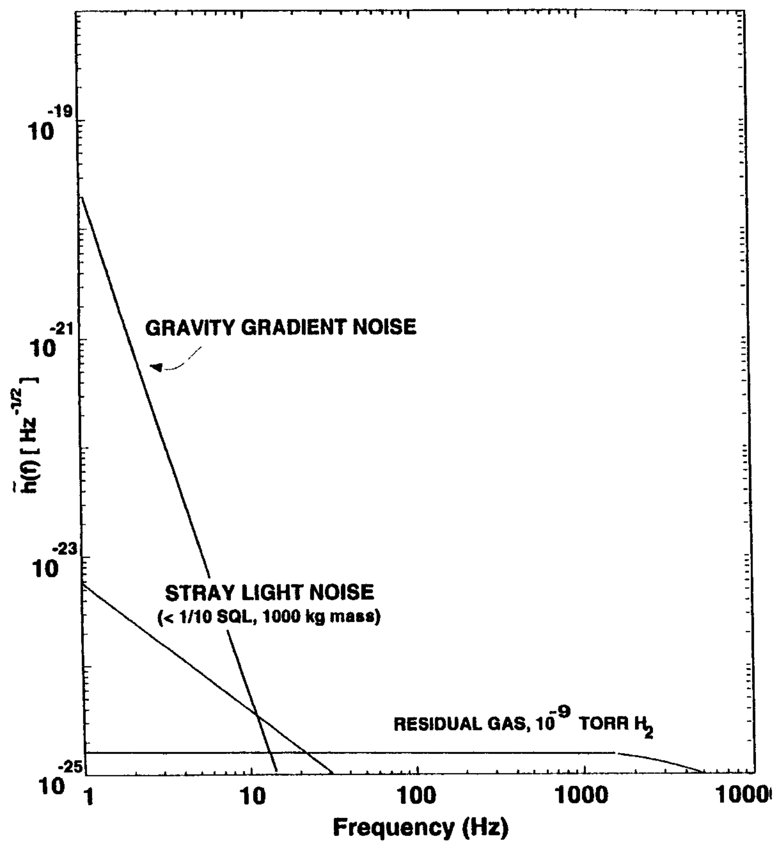

Structure of LIGO

The heart of the project: People

- 85 people, 29 new in '95
- several more in '96
- Visitors (B. Allen, D. Gustafson, P. Saulson, K. Sliwa)

Organizational

- Detector and R&D groups brought together (S. Whitcomb)
- Site directors named (F. Raab, M. Coles)
- LRC born and moved out (S. Finn)

Milestones (WA, LA)

- Initiate Beam Tube Fabrication: imminent
- Initiate building construction: 6/96, 1/97
- Accept beam tube and cover: 3/98, 9/98
- Accept buildings, became equipment: 3/98, 9/98
- Initiate interferometer installation: 7/98, 1/99
- **Begin coincidence tests: 07/00**

Monday PM: Interferometer Issues
January 15 Chair: J. Centrella

4:30	R. Drever (Caltech)	Advanced Interferometers
4:55	Discussion	
5:05	M. Schrempel (Hannover)	GEO 600 Status Report
5:30	Discussion	
5:40	Coffee Break	
5:55	F. Raab (Caltech)	Time-Domain Behavior of the 40m Interferometer
6:20	Discussion	
6:30	R. DeSalvo (Pisa)	Virgo Experiment and Seismic Isolation
6:55	Discussion	
7:05	E. Mizuno (Kanagawa)	Data Acquisition and Analysis for TENKO100 and TAMA300
7:30	Discussion	
7:40	R. Byer (Stanford)	A Sagnac Interferometer for Gravitational Wave Detection
7:55	Discussion	

SOME CONCEPTS FOR ADVANCED INTERFEROMETERS.

(ASPEN 15/1/96)

R. W. P. DREVER. (CALTECH)

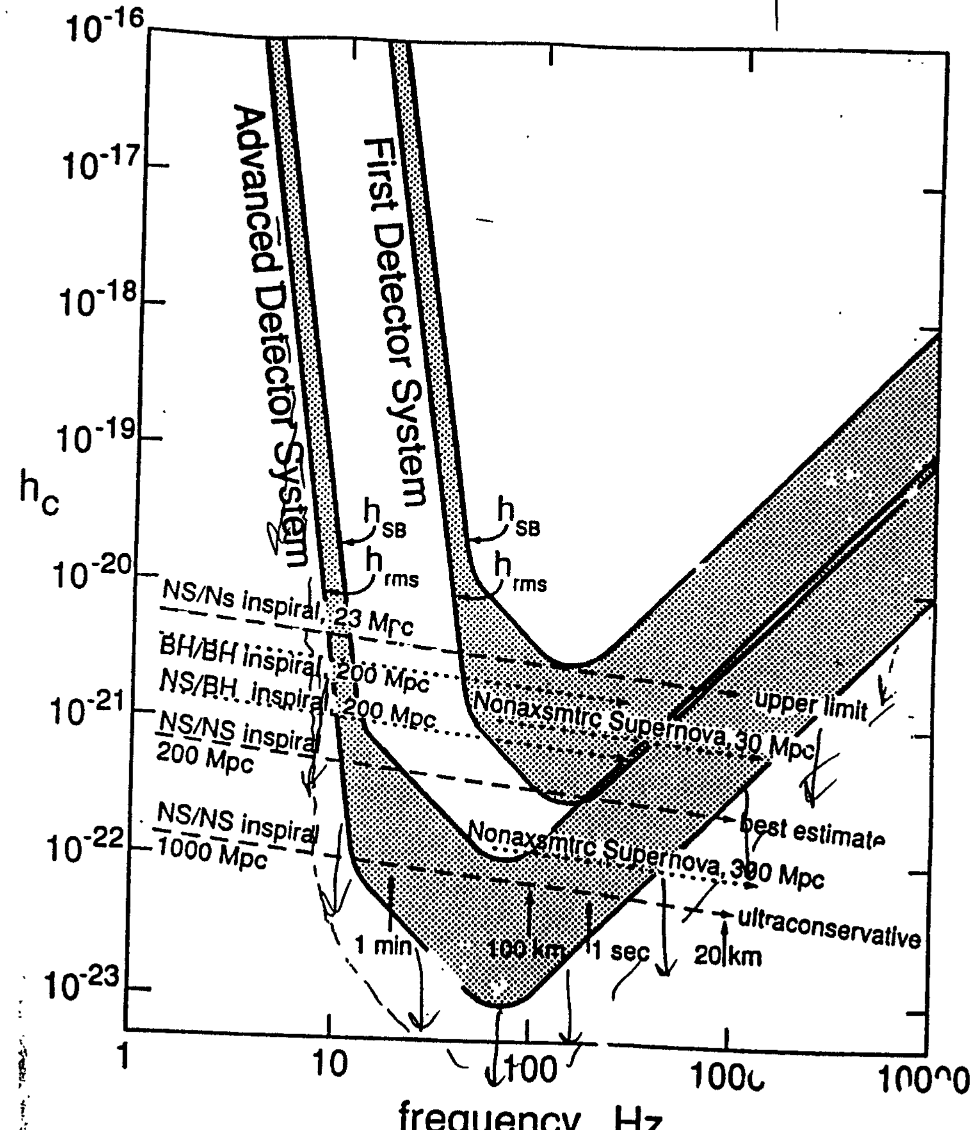

(PLOT OF K. THORNE, WITH ADDITIONS)

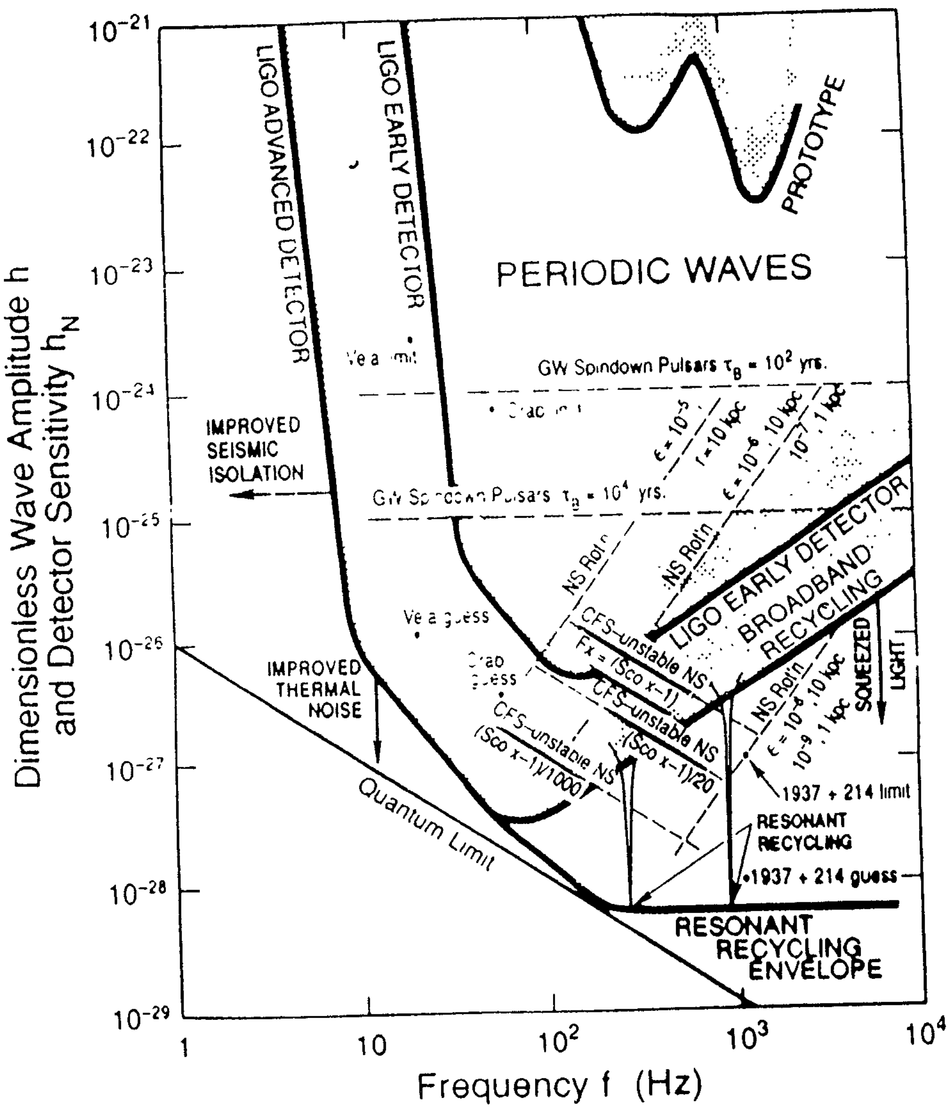

DIFFRACTION COUPLING

ONE EXAMPLE

2-OUTPUT CASE

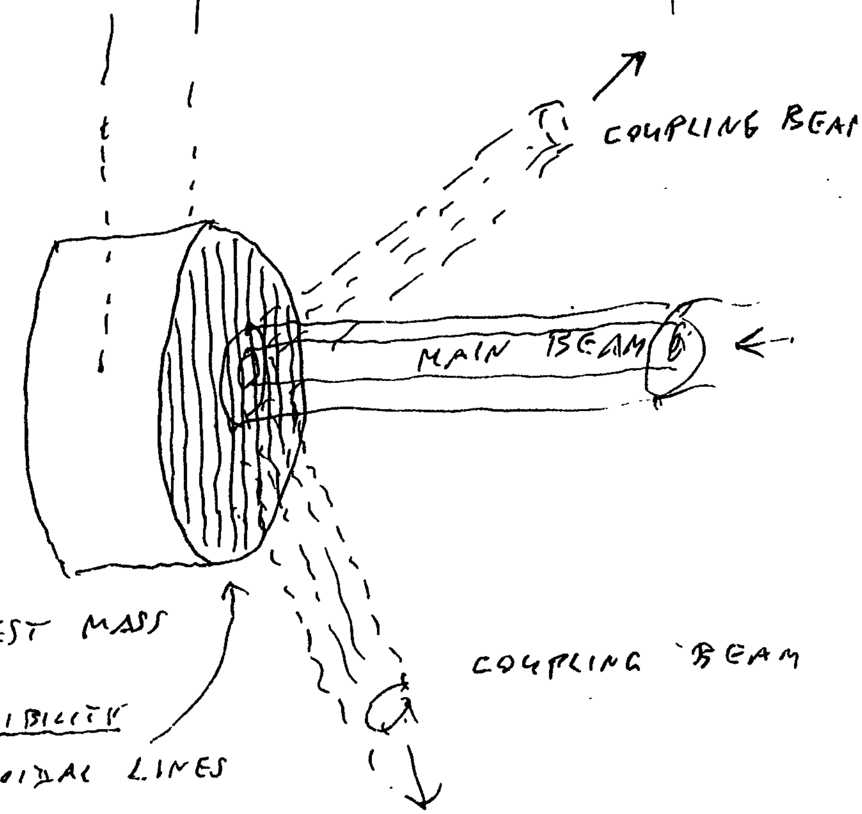

1 (?) POSSIBILITY

SINUSOIDAL LINES

$\sim 1\lambda$ SPACING

$\delta \sim \frac{1}{100}\lambda$ DEEP (FOR SMALL PICK-OFF)

2. 5/1/92

HOLOGRAPHIC (DIFFRACTION) BEAMSPLITTER — SINGLE OUTPUT

(OBLIQUE INCIDENCE)

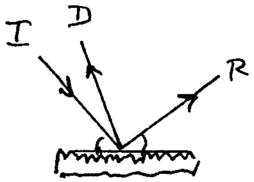

DUAL RECYCLING INTERFEROMETER

(50% GRATING)

(i.e. 50% OF BEAM TO BE DIFFRACTED)

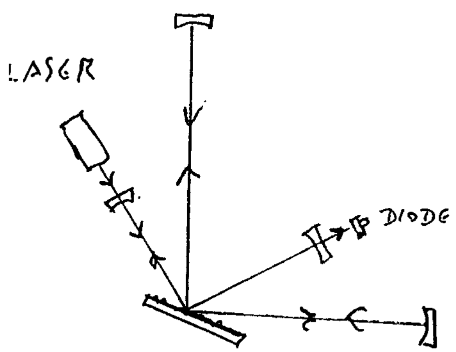

MODE CLEANING CAVITY

(SMALL COUPLING OK)

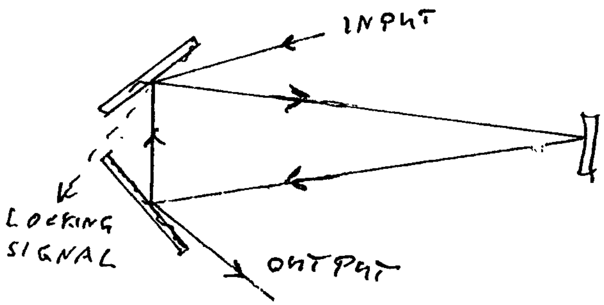

"HOLOGRAPHIC" INTERFEROMETERS

(SMALL-AMPLITUDE SURFACE PATTERN)

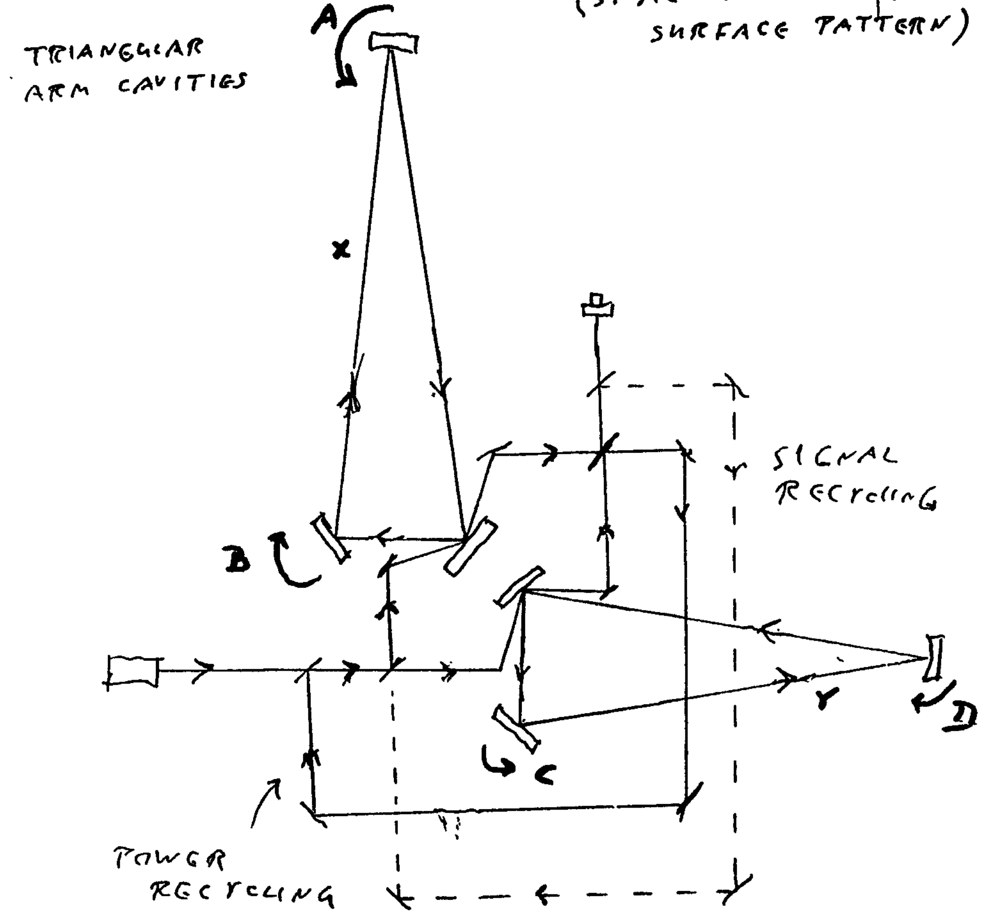

(NOTE: CAN ROTATE A, B, C, D TO ELIMINATE X, Y AND GET 2 FOLDED LINEAR CAVITIES)

INTERFEROMETER WITH TEST MASSES AT LOW TEMPERATURE

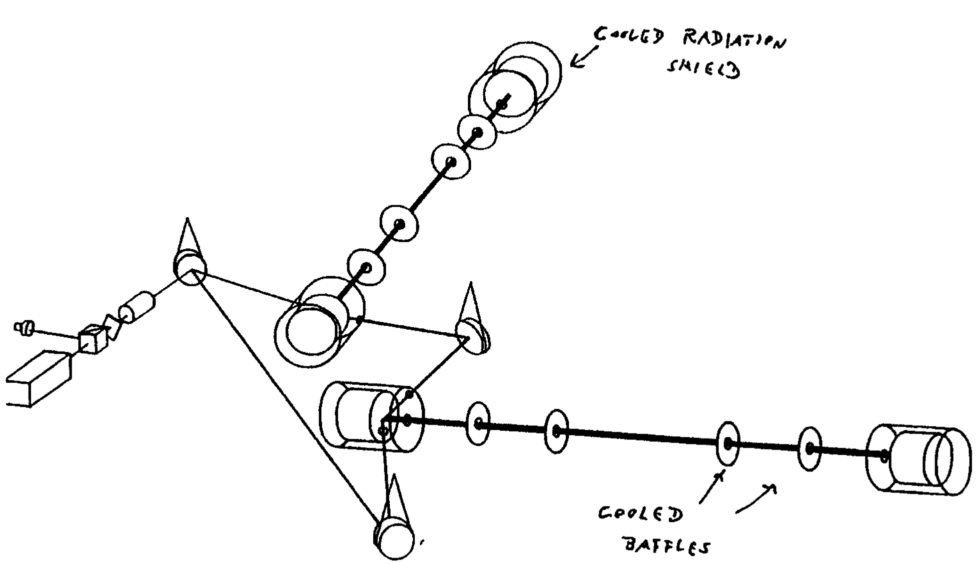

7/23/84 R
R.Drever

MAGNETIC LEVITATION GEOMETRIES BEING DEVELOPED. (CONCEPTS ONLY).

1. SIMPLE. PERIODS NOT THE LONGEST.

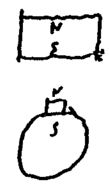

2. ADJUSTABLE FOR LARGE RANGE OF LOADS. LONG PERIODS POSSIBLE
ROTATION CAUSES INSTABILITY PROBLEM.
(~3 LEGS USED TO CONTROL THIS IN TEST EXPERIMENTS)

3. VERY LONG PERIOD POSSIBLE IN ONE DIRECTION
(PERIODS >10 SECONDS FOUND EASILY OBTAINED IN PRELIMINARY EXPERIMENTS)

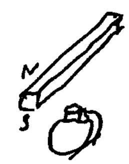

4. QUADRUPOLE – LESS COUPLING TO OUTSIDE MAG. FIELD.

CAN EXTEND TO 4, 6, 8 .... POLE SYSTEM.

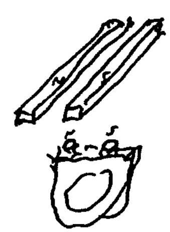

13/1/96
RD

3-LEGGED TEST RIG FOR MAGNETIC ISOLATION

STAGE (CONCEPT ONLY)

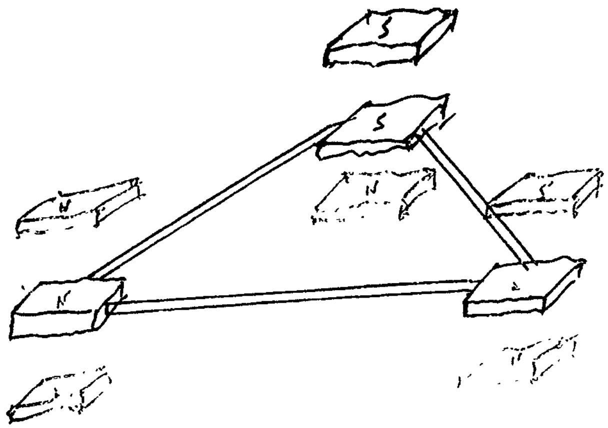

(FOR SEISMIC ISOLATION)
(PRIMARILY)

5/1/96
RD.

ONE UNIT OF 3-LEGGED TEST RIG.

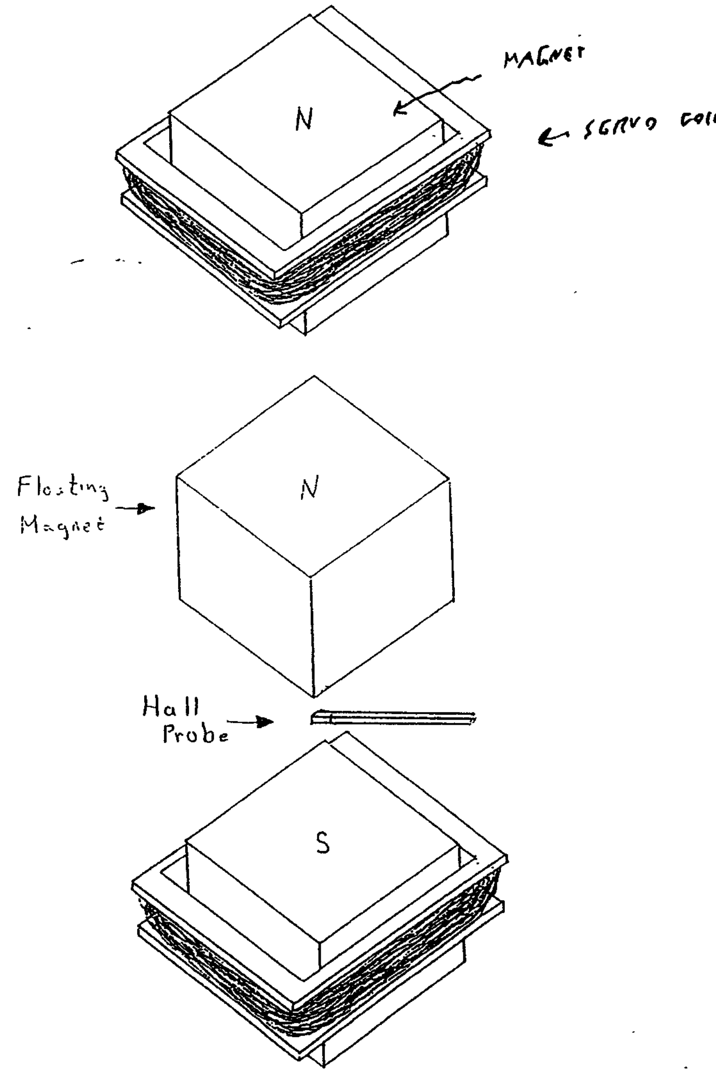

5/1/96
RD.

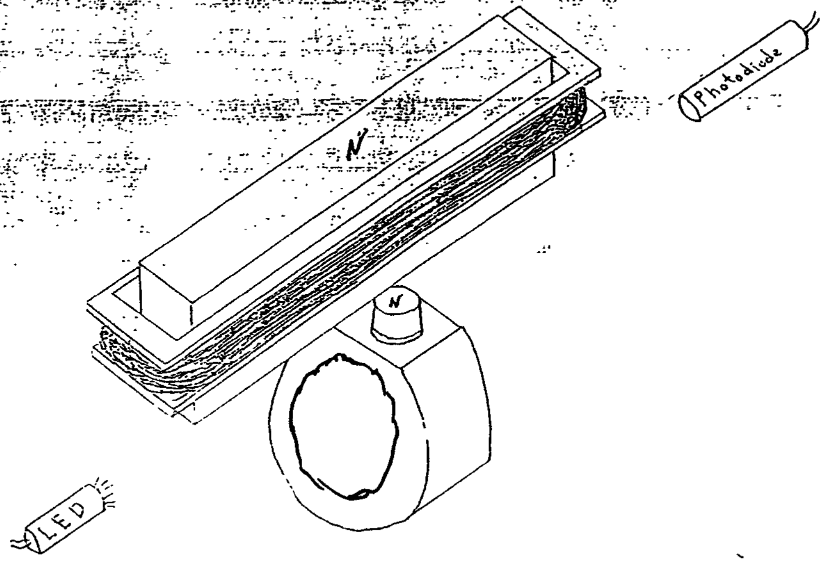

EXPERIMENTAL TEST MASS SUSPENSION

15/1/96
RD.

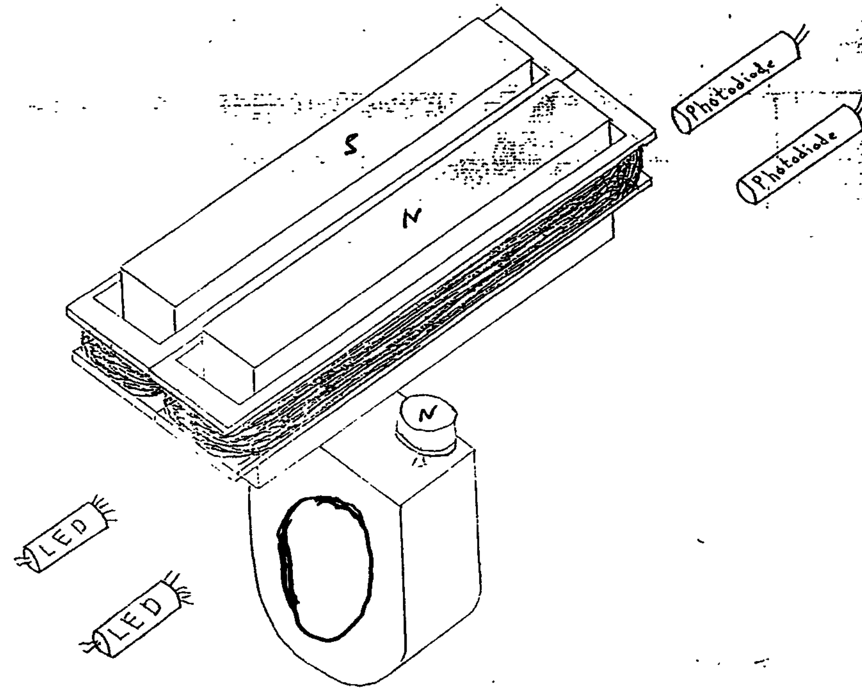

(CAN EXTEND TO MORE POLES)

15/1/96
RD.

ILT-COUPLED LOW FREQUENCY SUSPENSION

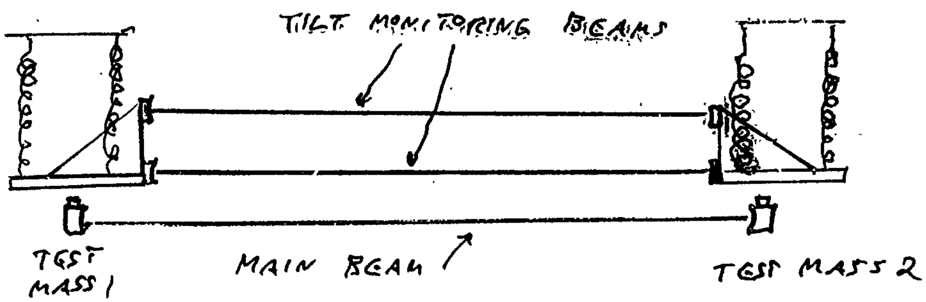

11/96
ED

GEO 600
Status Report

Mathias Schrempel
and the GEO 600 Team

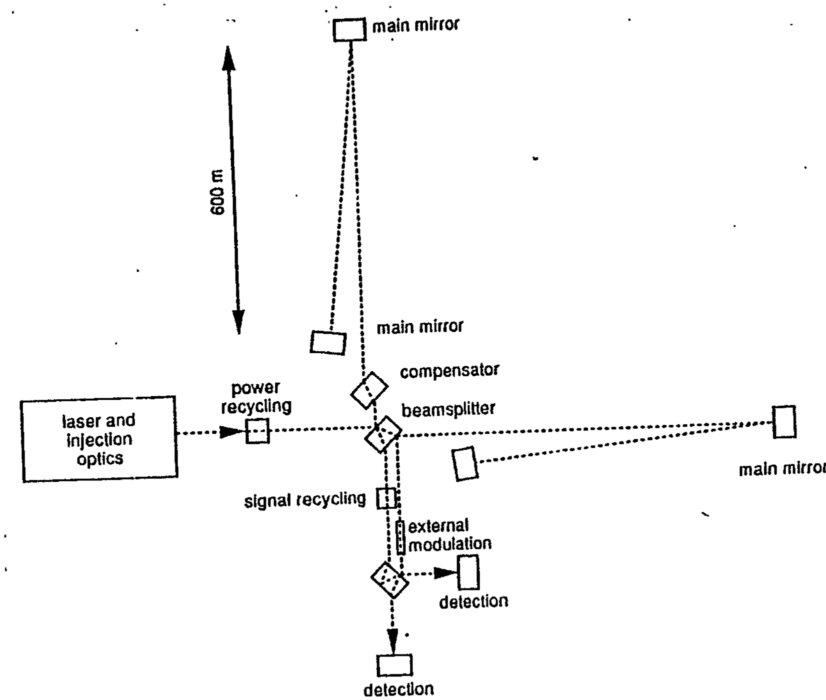

layout schematics

GEO 600 optical layout

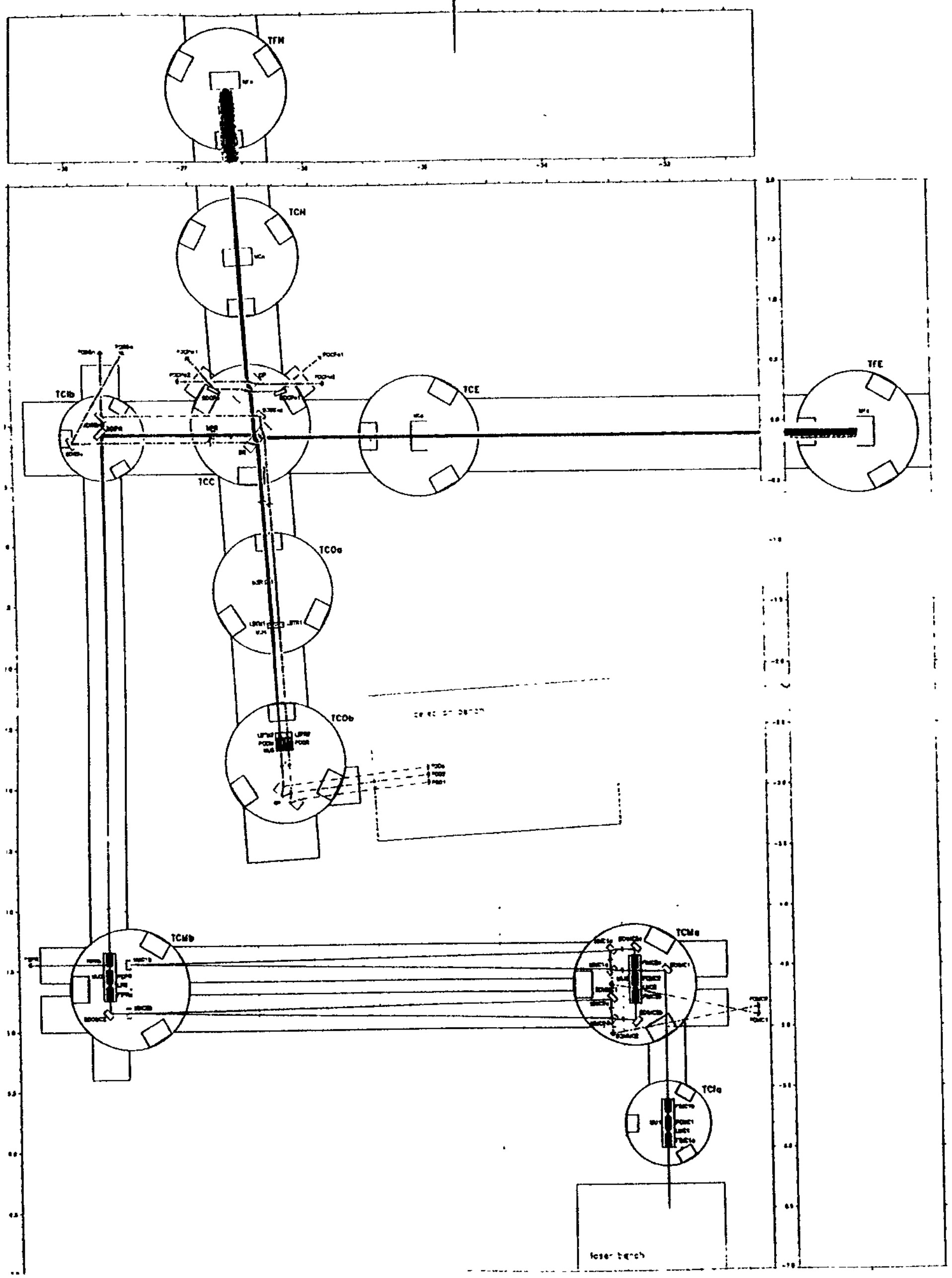

GEO 600

arm length	2 × 600 m, NNW and ENE
laser	diode pumped Nd^{3+} YAG Laser, 10W Master - Slave system
test masses	25 cm dia., 15 cm thick, OH^{-}-free fused silica, absorption ≤ 1ppm/cm
coatings	ionsputtered, absorption < 1ppm
power recycling	up to 10kW circulating power
signal recycling	150 to 1500 ~~M~~Hz bandwidth
tunability	0 to 1kHz
seismic isolation	encapsulated 4-layer stacks, active suspension optional
suspension	double pendulums, monolithic lower stage
vacuum system	60cm dia. corrugated beam tubes, hydrocarbon-free $<5\times10^{-8}$mbar for H_2, $<5\times10^{-9}$mbar for other gases
sensitivity	depending on bandwidth $h\sim10^{-22}$ to $4\times10^{-23}/\sqrt{Hz}$

Sensitivity Limits

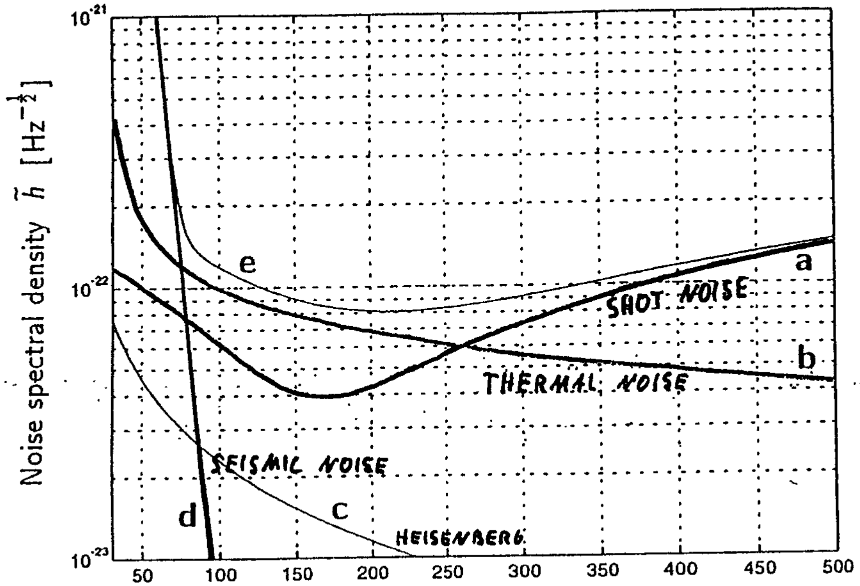

- 10kW internal power, 20ppm mirrors
- Q: 5×10^6 internal, 10^8 pendulum
- 4-layer stack, double pendulums

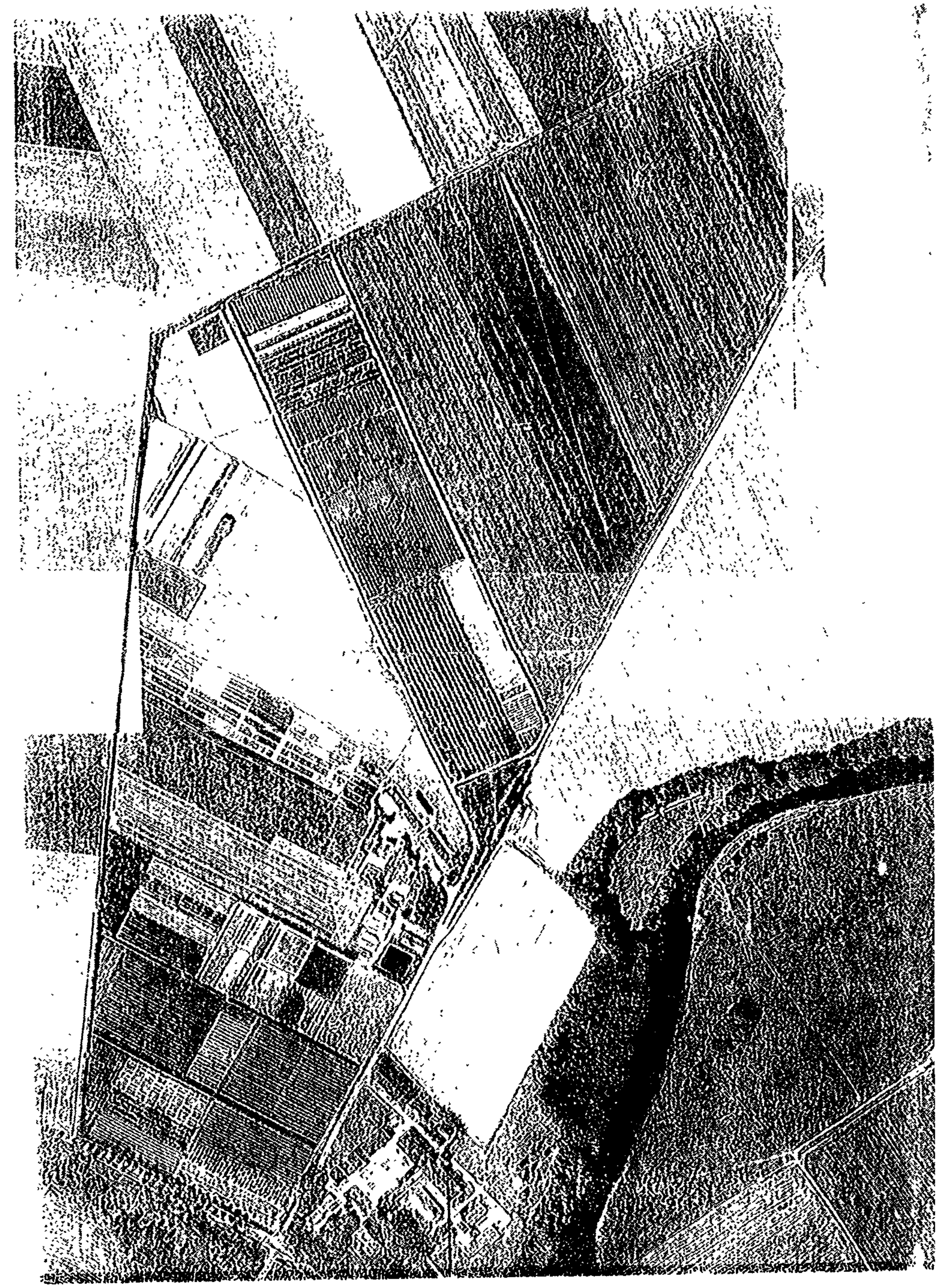

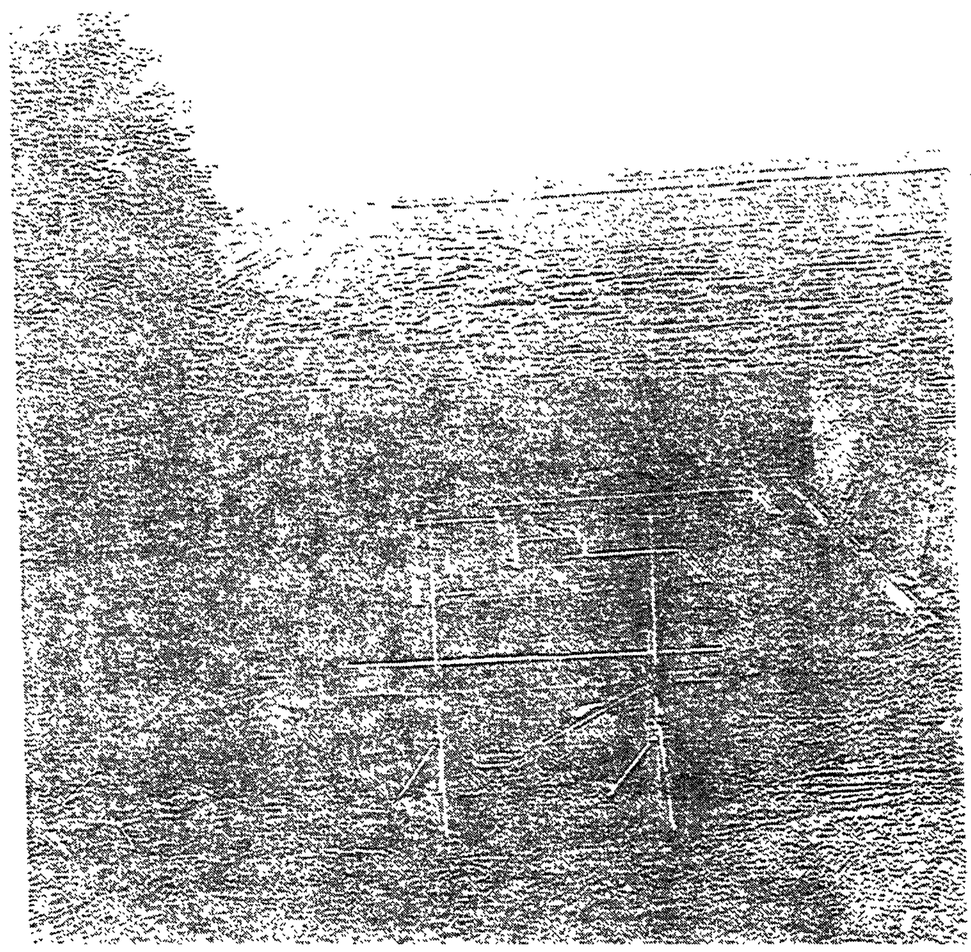

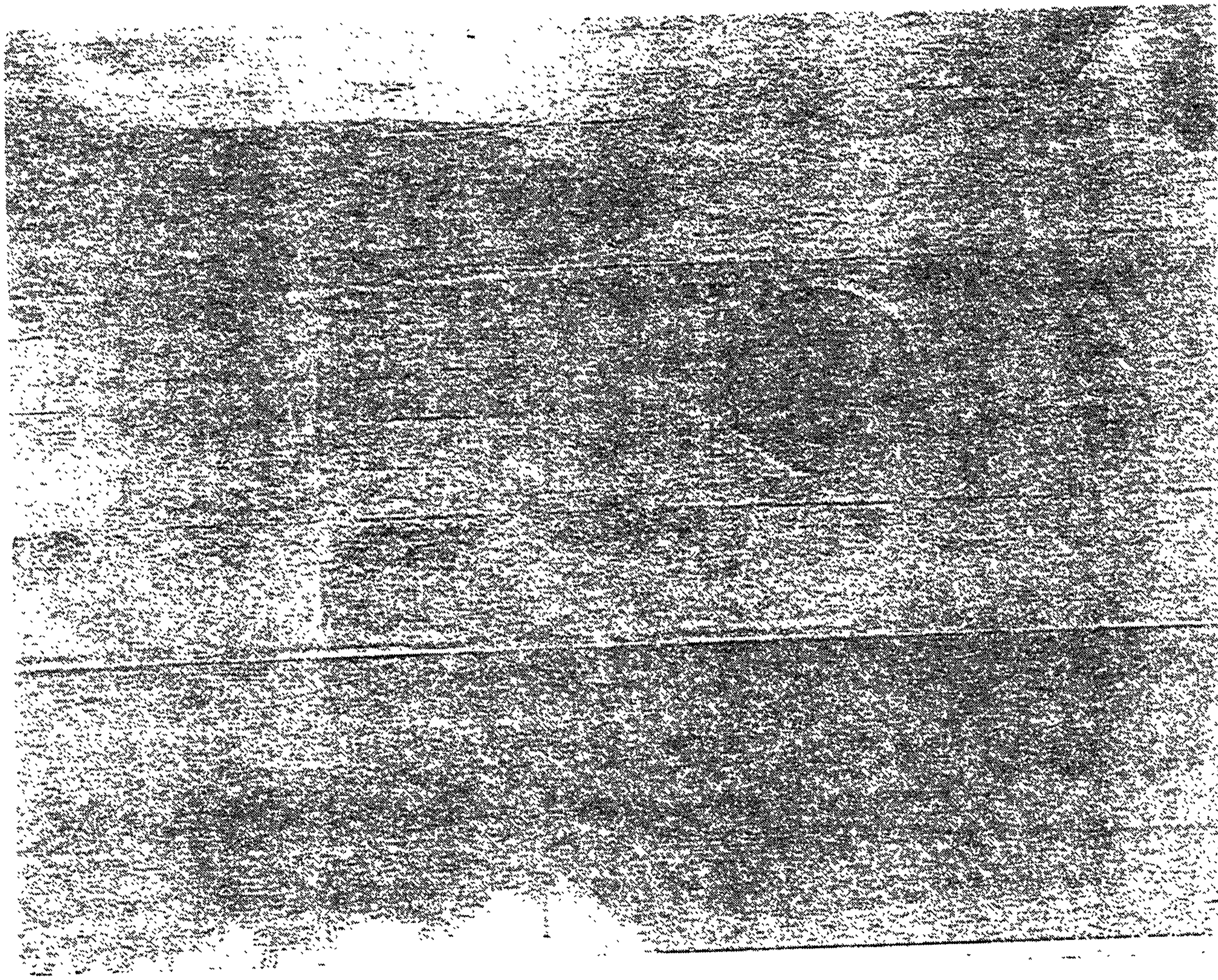

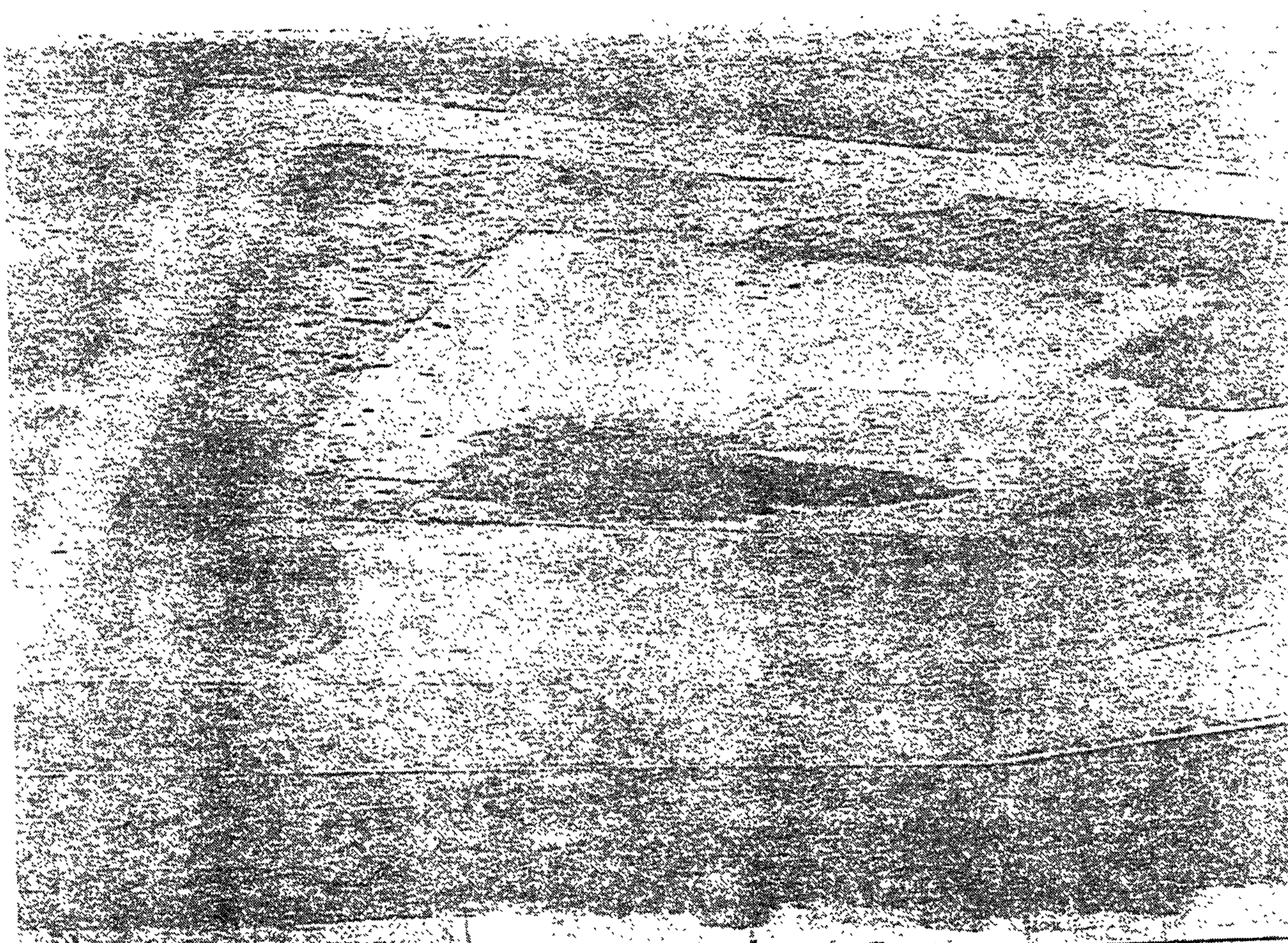

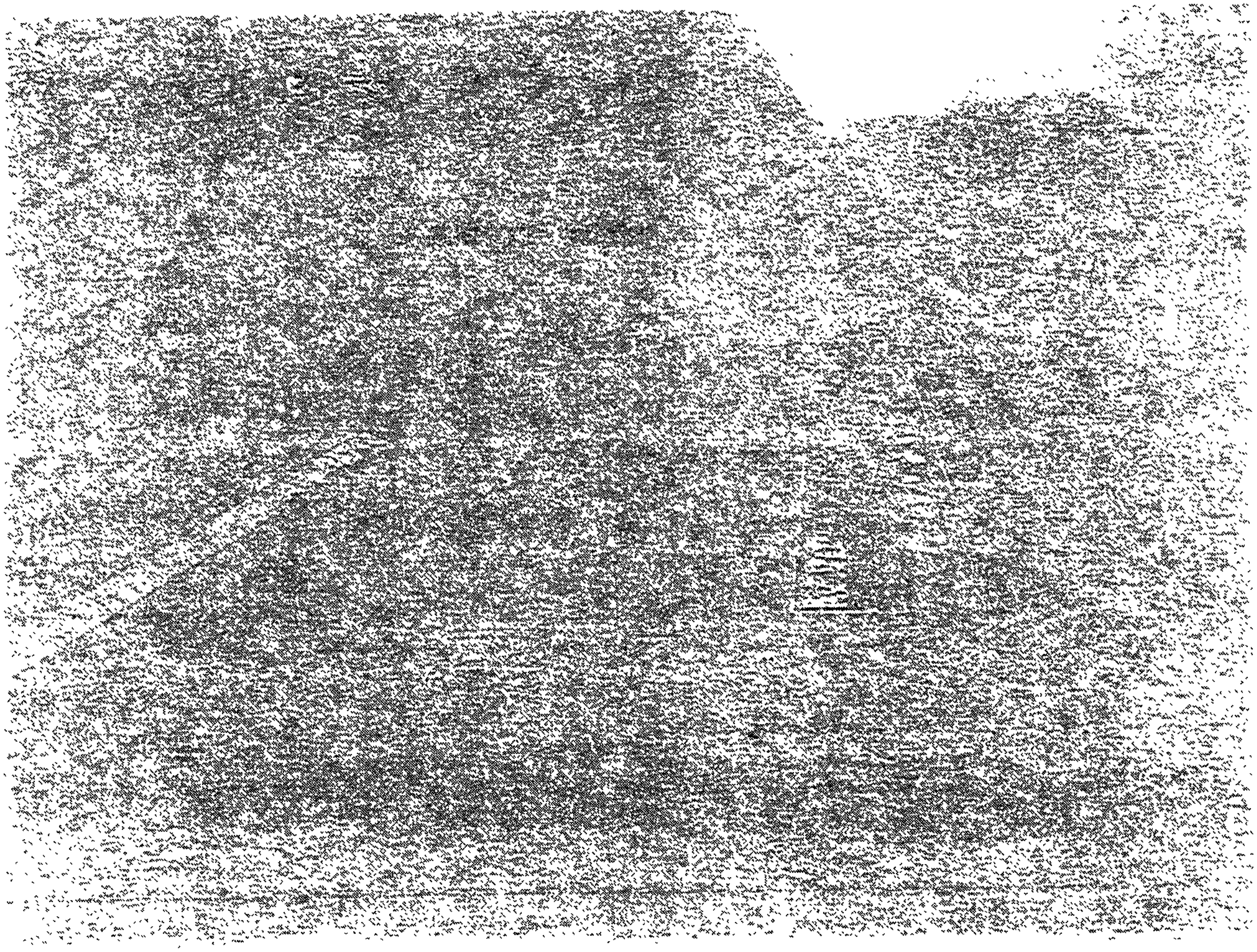

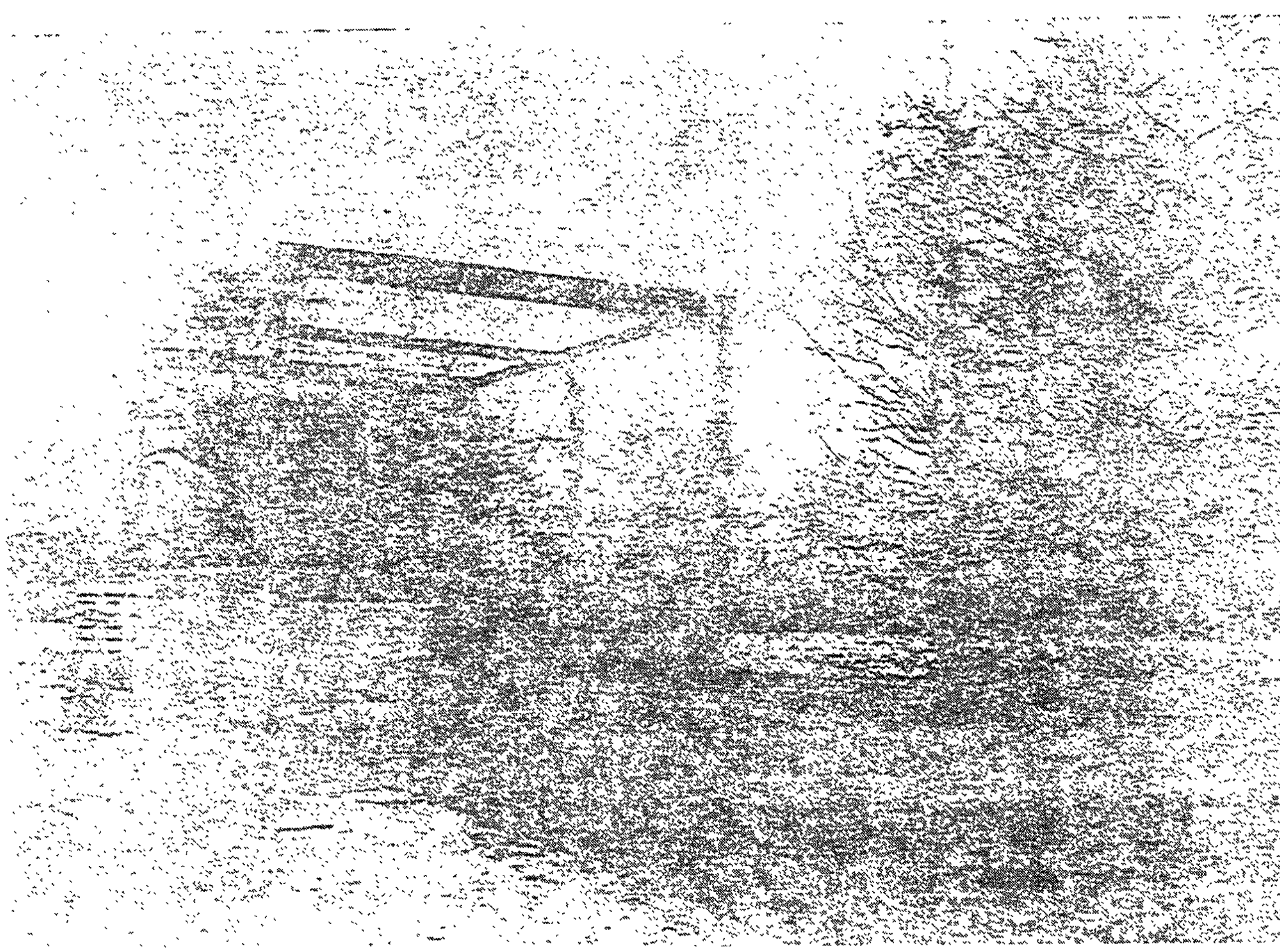

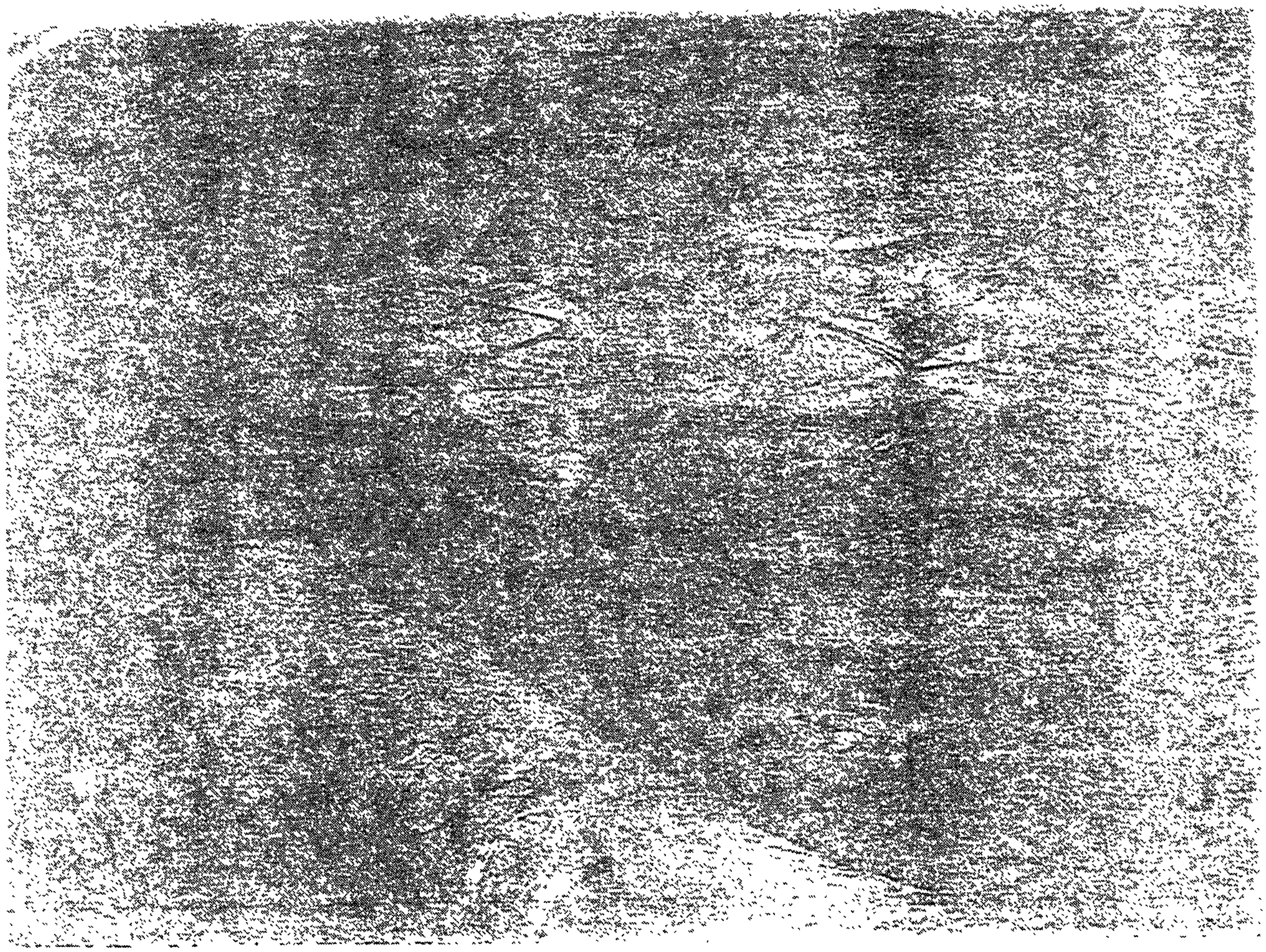

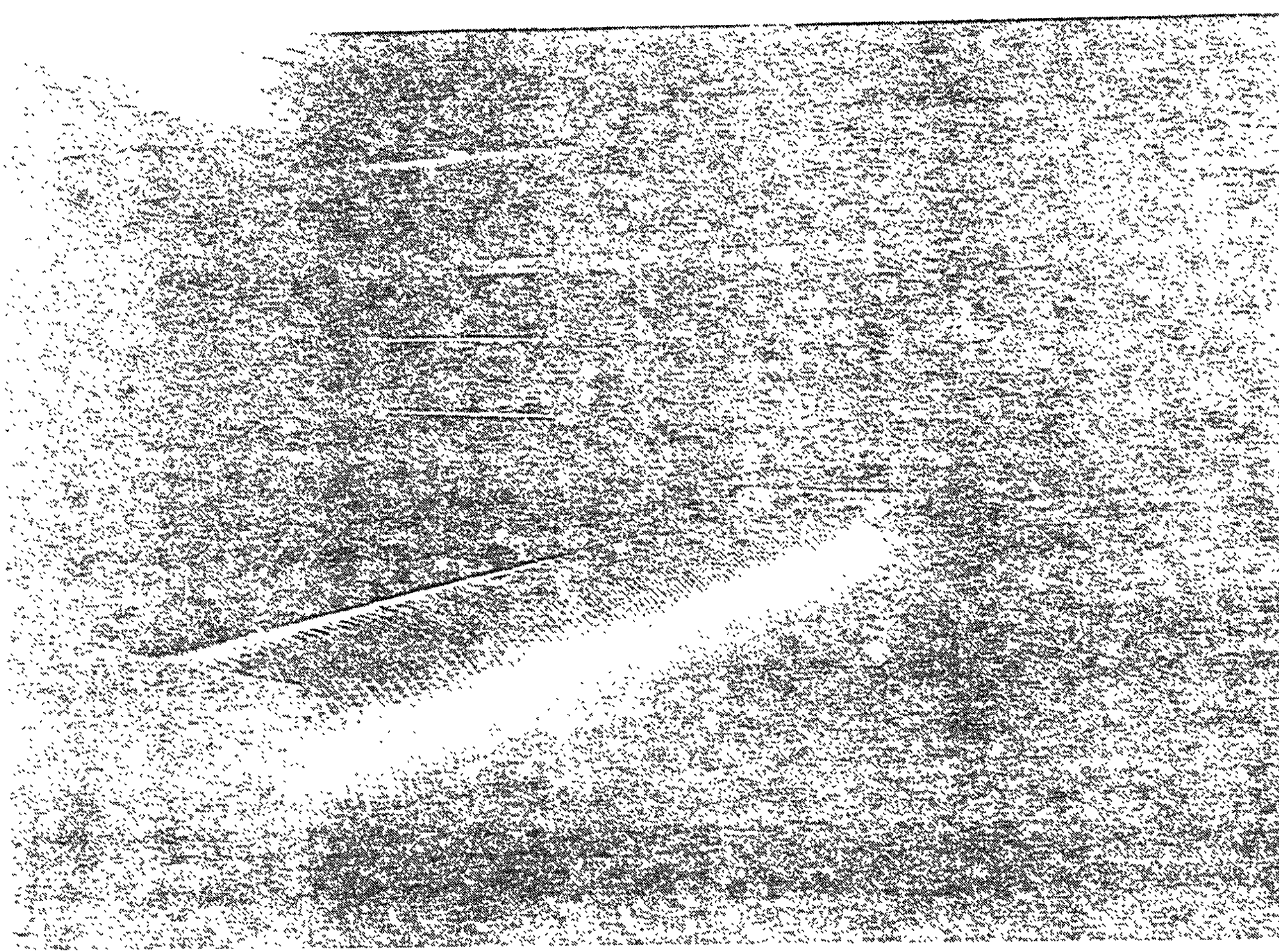

Time Table

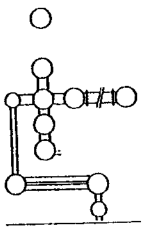

Vacuum System 6 '96

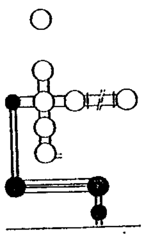

Modecleaners, Laser Bench 6 '97

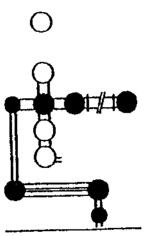

1200m Cavity 6 '98

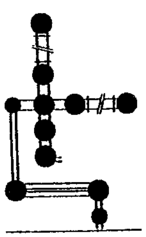

Michelson 6 '99

Final Optics 2000

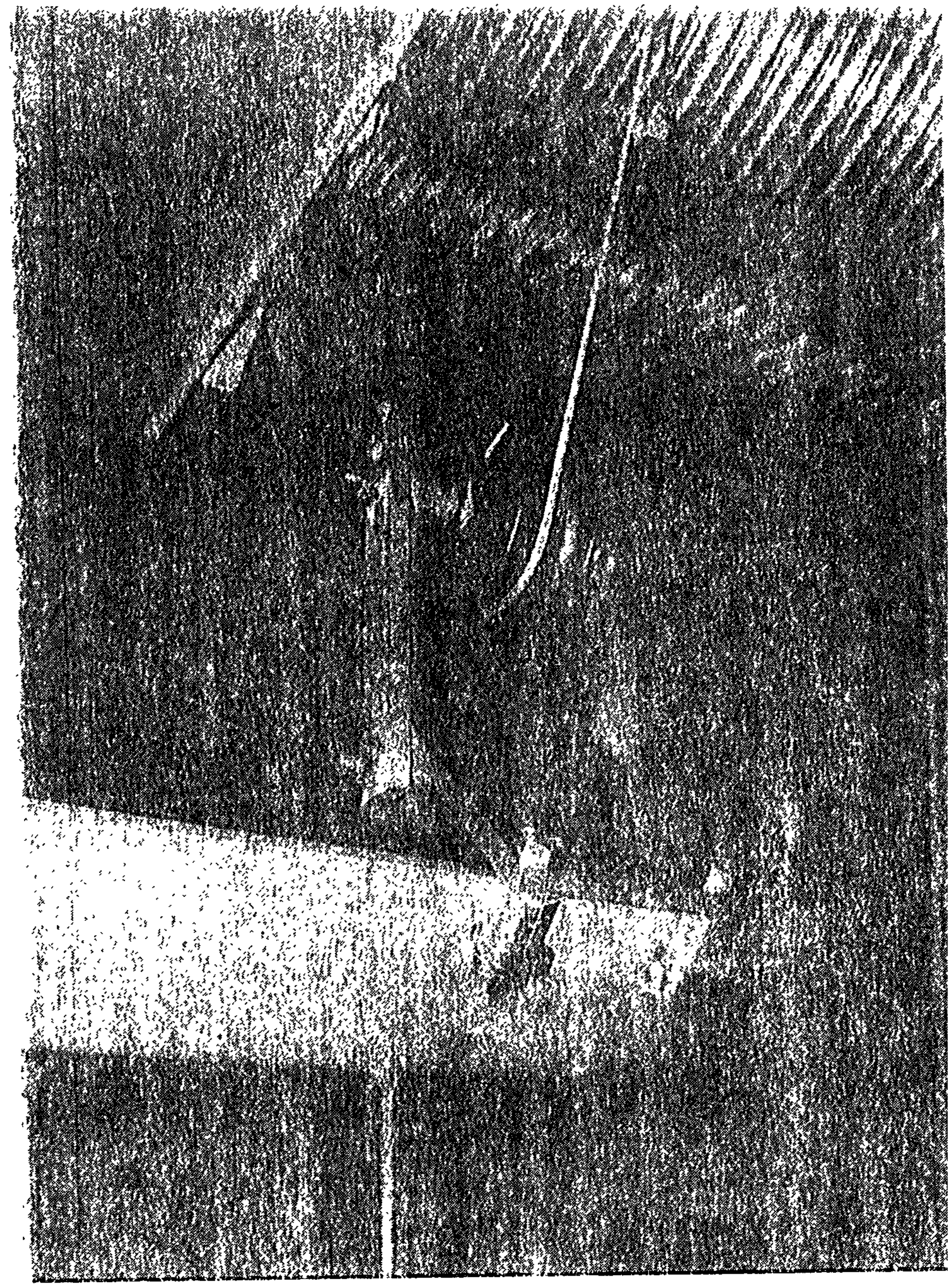

Time-Domain Behavior of the 40-Meter Interferometer

Fred Raab

January 15, 1996

A Report on Preliminary Studies and Future Plans for Work with Collaborators:

- Torrey Lyons
- Aaron Gillespie (now at NBS, Gaithersburg)
- Kent Blackburn
- Andy Kuhnert
- James Mason

Goal: Institute Regular Time-Domain Operation and Analysis.

Non-Stationary Noise in a Laser Interferometer

- Most source detectability arguments are based on smooth stationary gaussian noise spectra with $\Delta f \approx f$; is this reasonable?
- Excess (non-gaussian) noise must be vetoed through environmental monitoring and coincidence techniques.
- Coincidence strategies often assume uniform rates for non-gaussian events (i.e. stationary). For LIGO:

$$R_{TRIPLE} \approx \tau_{12}\tau_{13}R_1R_2R_3$$

where τ_{ij} refer to coincidence window widths and R_k refer to the post-veto singles rates for interferometers 1, 2 and 3.

Mark II 40–Meter Interferometer

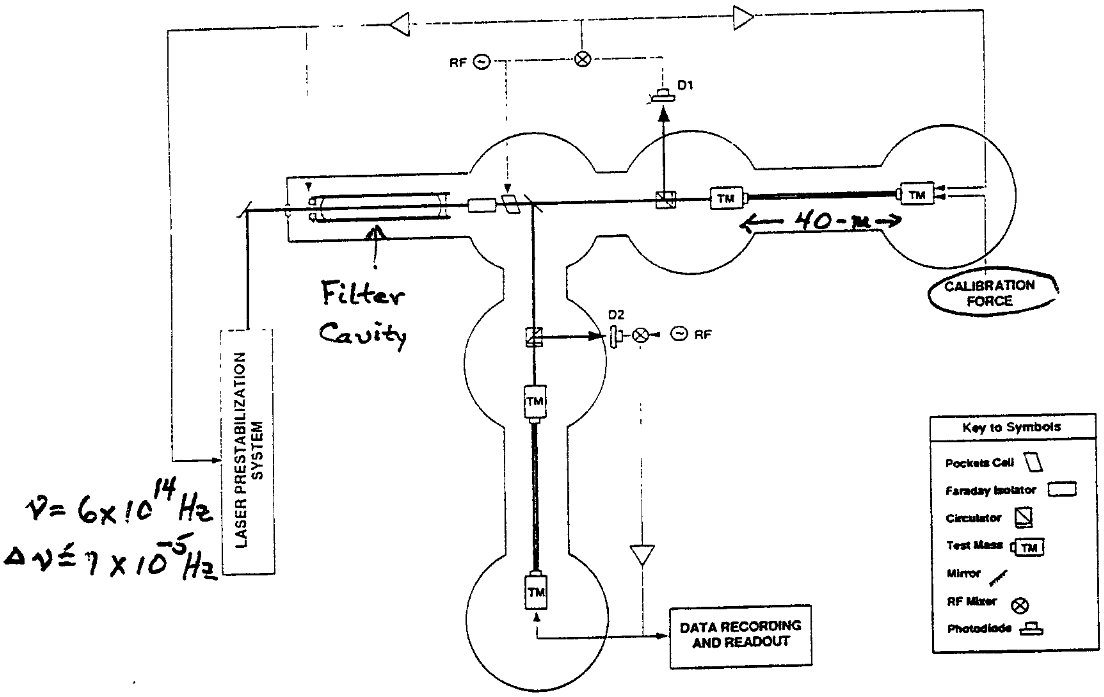

LIGO

3

40 m Displacement Sensitivity

Comparison of Estimated Noise Levels on 10/28/94

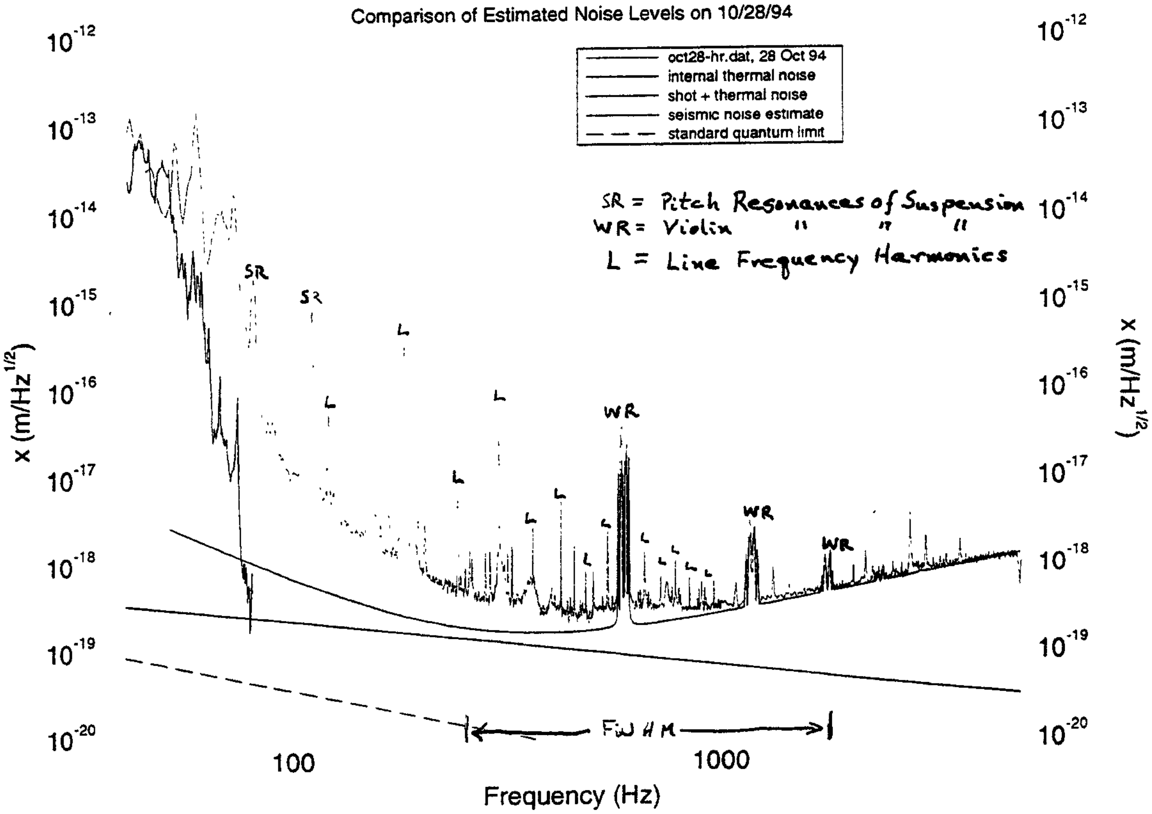

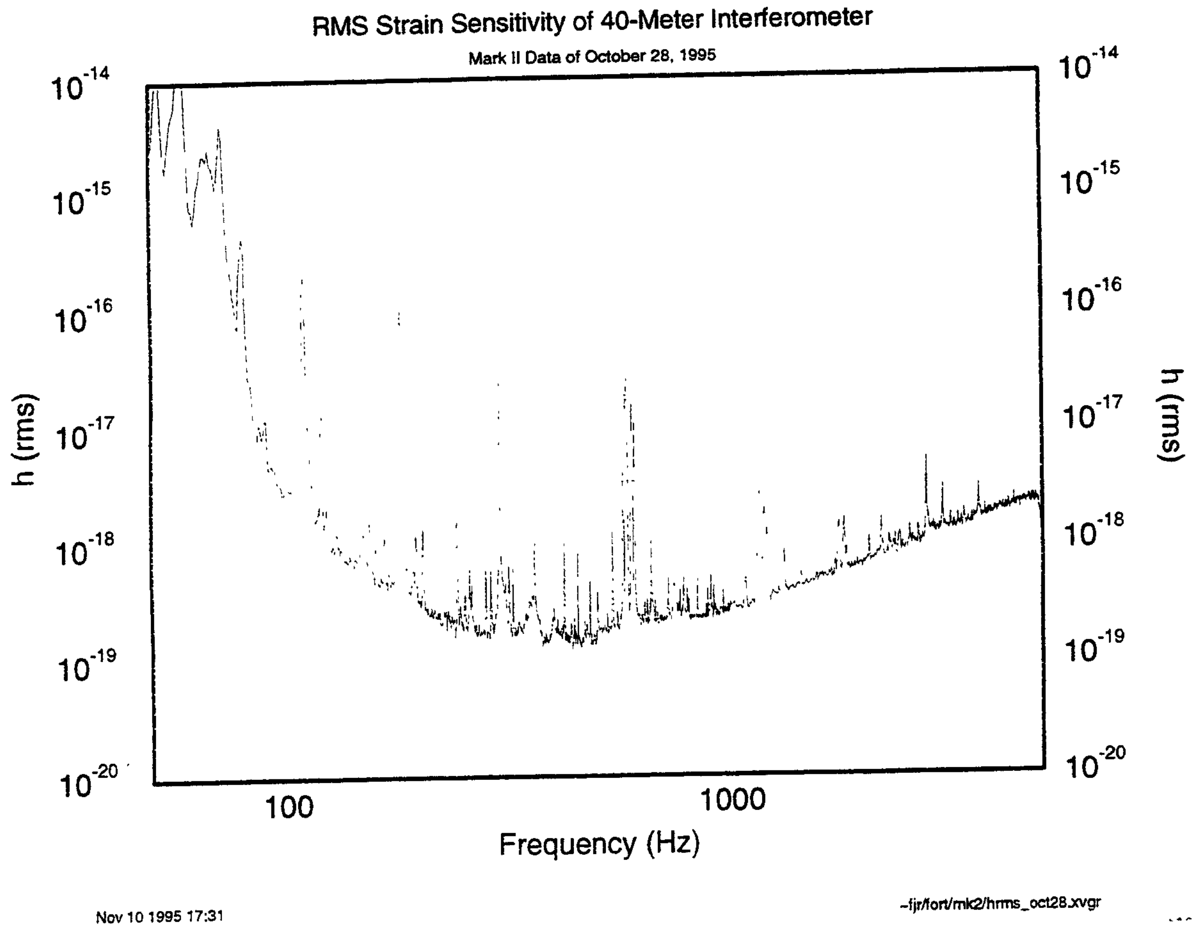

How Can Experimental Data From a Noisy Interferometer Be Characterized?

- Sample histograms from a wide-band channel are not very informative (at least not to us).
- Correlating data with templates: great for finding the expected, but surprises could get away!
- Machine artifacts need identification and characterization, but may not trigger sharply even in extensive template sets.
- Some tool kit for identifying "events" and characterizing is needed.

Utility of a Simple Event Finder Algorithm

- Threshold for event turn-on, variable dead time filter

Sample Histogram

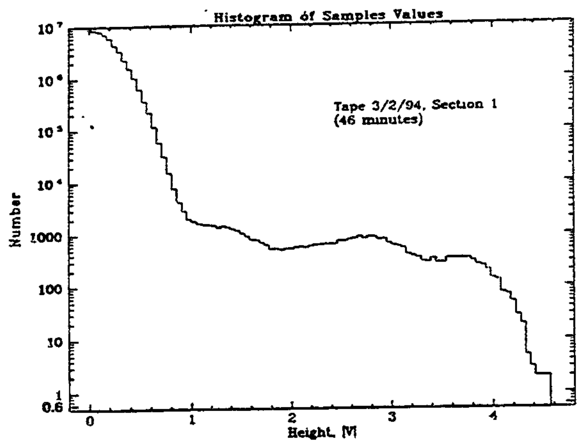

Event Histogram

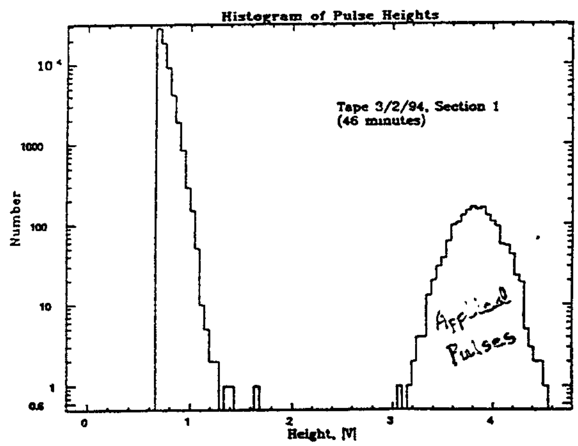

An Example of Non-Stationary Non-Gaussian Events

- Event histogram for this locked section is almost purely gaussian, except for a "minute" interval:

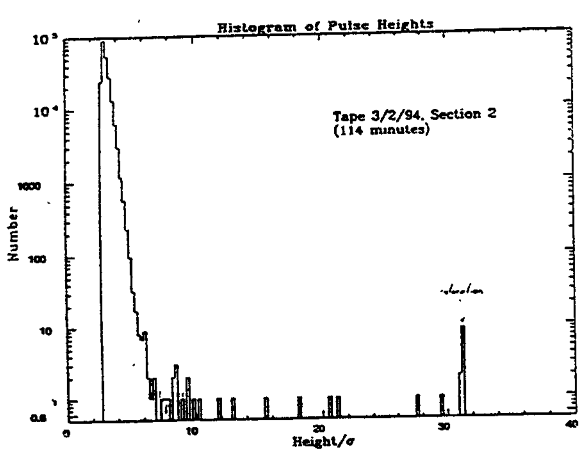

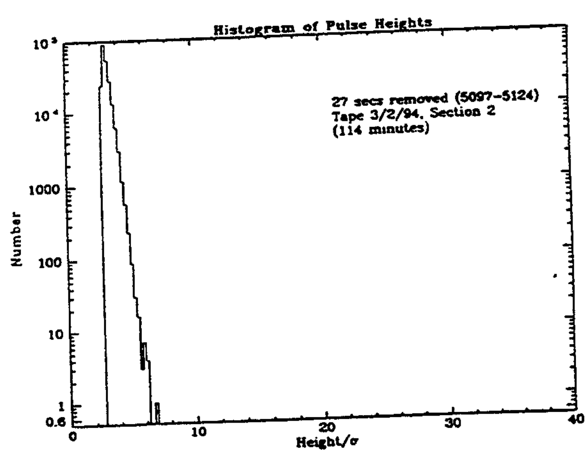

Pulse Sensitivity

(preliminary data)

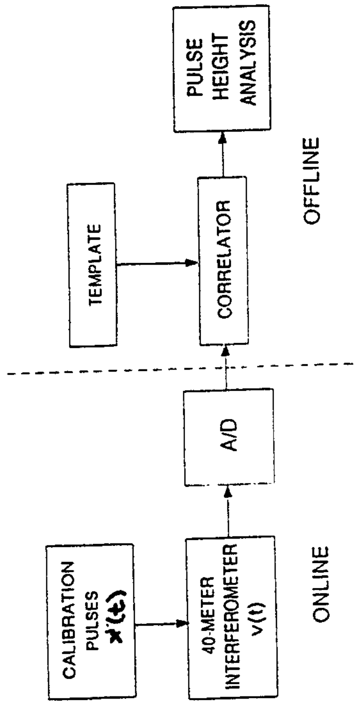

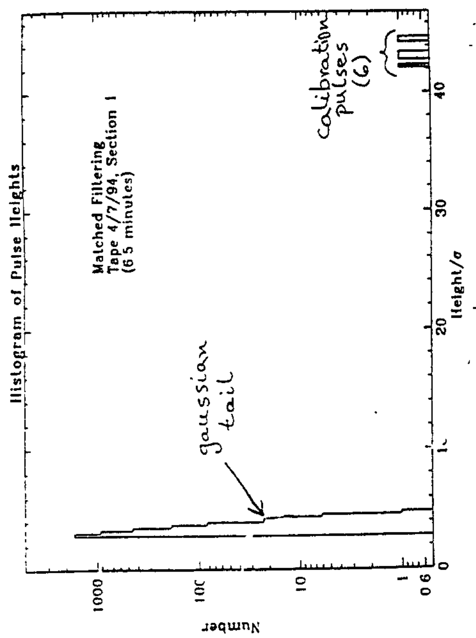

LIGO

An Example of a Non-Gaussian Event Feeding Through a Template

- Coalescing binary filter output is typical over large range of filters

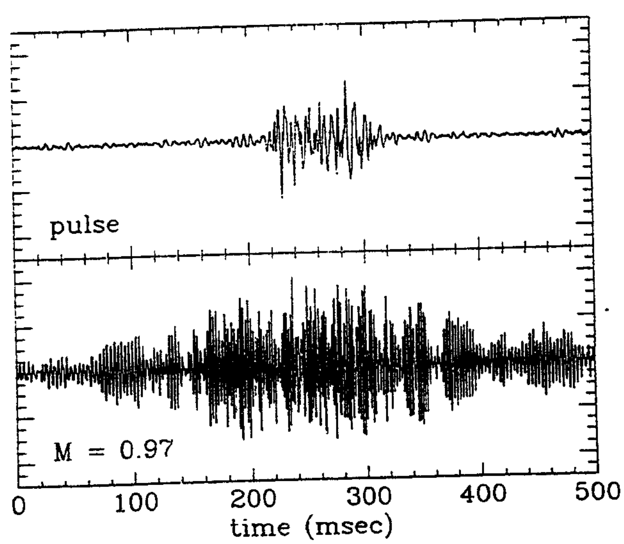

Findings From Preliminary Look at 40-Meter IFO Time-Domain Data

- Observed non-gaussian events are non-stationary
- Events vary in character: clicks, "the scraper", "the howler", "the whistler", etc.
- Causes which have been identified:

  ››higher-order transverse optical modes

  ››maladies in test-mass damping servos

  ››connector noise

  ››edge effects on photodiodes
- Promising news: event rates are sometimes very low!
- To keep rates always low will require comprehensive data on machine status

Future Plans

- Commence program of regular data runs with rapid analysis turn-around time:

  ››Increase running time with split between R&D and DATA shifts

  ››Limited manpower requires automated hardware and modest but efficient analysis

  ››Constant changes required by R&D/Detector programs means sensitivity will often be less than optimal
- Institute low-bandwidth, high-channel environmental/status monitoring system

  ››Use housekeeping statistics for cross-correlation studies of non-stationary noise

  ››Learn about drift and aging effects in machine operation

THE VIRGO PROJECT

INFN - CNRS

Experiment funded by INFN Italy (55%) and CNRS France (45%)

Presented by **Riccardo DeSalvo**

INFN Sez. Pisa
via Livornese 1291
56010 S. Piero a Grado

tel. ++ 39 50 880 349
fax ++ 39 50 880 350

The Virgo Collaboration

INFN	CNRS
LNF-Frascati	LAPP-Annecy
Napoli	IPN-Lyon
Perugia	LAL-Orsay
Pisa	ESPCI-Paris
Roma 1	

Responsibility Subdivision

Infrastructures	
Central Building	Pisa
Tunnels	Pisa
Equipments	Pisa
Clean Areas	LAPP-Annecy
Infrastructures for mirrors	IPN-Lyon
Vacuum	
Tube	Pisa
Tube	LAL-Orsay
Baffles	LAL-Orsay
Towers	LAPP-Annecy
Pumping	Pisa

Interferometer	
Optics	LAL-Orsay
Laser-Injection Bench	LAL-Orsay
Detection Bench	LAPP-Annecy
Mirrors	IPN-Lyon
Alignement	LNF-Frascati
Calibration	LAPP-Annecy
Suspensions	
Seismic Isolation	Pisa
Marionetta	Pisa
Wires and Clamps	Perugia
Local Electronics	Pisa
Electronics and Software	
Global Control	LAL-Orsay
Networks and cabling	LAL-Orsay
Data acquisition	LAPP-Annecy
Data archive	Napoli
Simulation	LAPP-Annecy

1) Generalities on the experiment

very very fast

2) Civil engineering status

fast

3) Super attenuators technical development

Interferometric detection of gravitational waves

Gravitational waves are **quadrupolar** waves

a gravitational wave of dimentionless **amplitude h**
propagating along the **Z** axis
with **polarization** along the **X** and **Y** axis
induces a change ΔLx of an arbitrary length Lx (Ly)

$\Delta Lx = h\,Lx$ $(\Delta Ly = h\,Ly)$

typical **h** values are 10^{-21}

Typical GW signal **mirror displacement**

$\Delta X = h\ 3\ Km = 3\ 10^{-18}\ m$

Typical GW signal phase shift

$\Delta\Phi = 4\pi\ \Delta X\ f_{FP} / \lambda = 4\pi\ \ 3\ 10^{-18}\ \ 50 / 10^{-6} = 15\ \ 10^{-10}$ **radians**

THE VIRGO PROJECT

INFN - CNRS

Broad Band Gravitational Wave Interferometric Antenna

10 Hz to **10 KHz** sensitivity

Main characteristics

3 + 3 Km vacuum Michelson Spectrometer

Arms made with **f=50** Fabry Perot cavities

1 μm wavelength laser light

1 KW laser power at the beam splitter

Very high degree of seismic isolation at low frequency (> 5 Hz)

EFFECTS OF A GRAVITATIONAL WAVE ON A SUSPENDED INTERFEROMETER

PHASE SHIFT $\left|\frac{4\pi h(t) L}{\lambda}\right|$

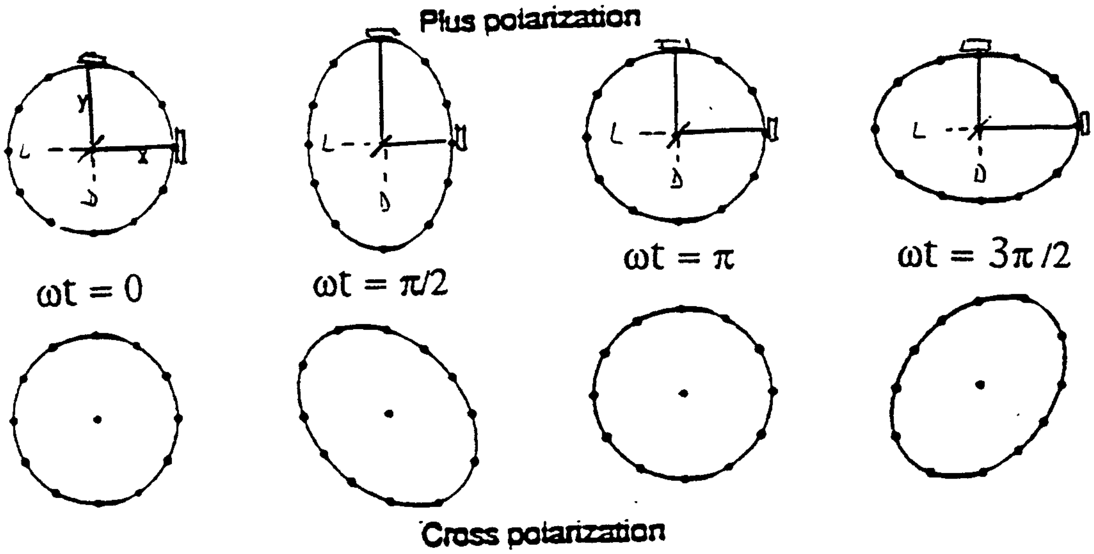

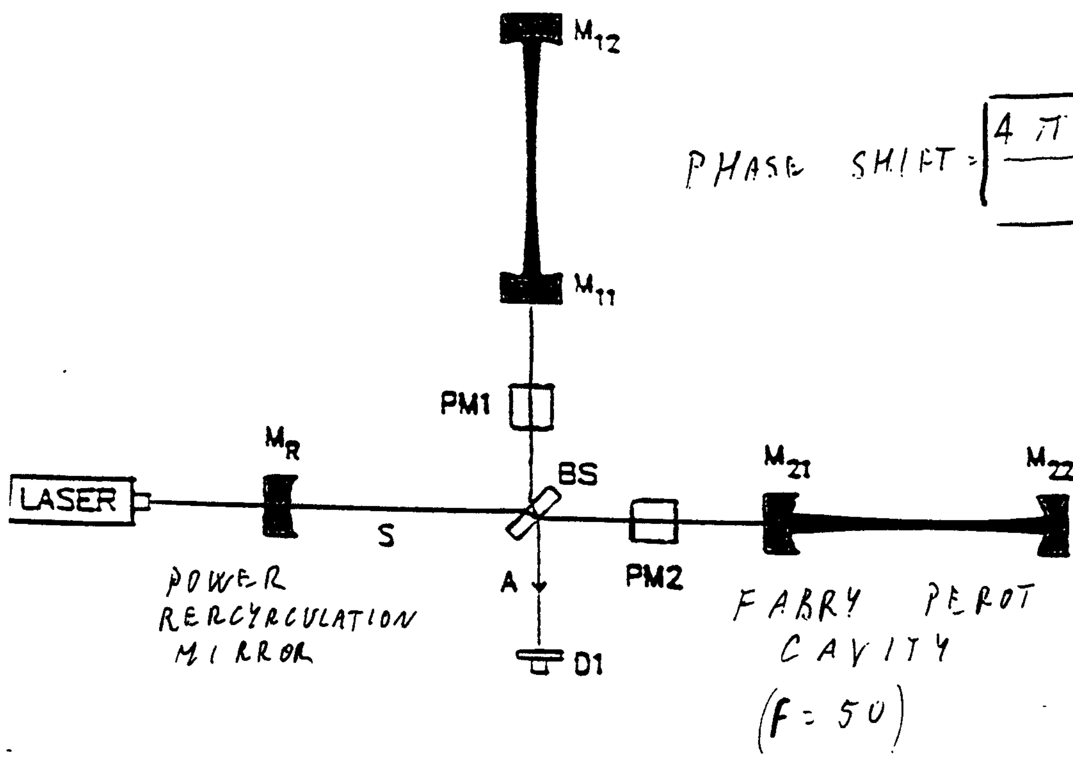

PHASE SHIFT = $\left|\frac{4\pi F\, h(t) L}{\lambda}\right|$

Signal / Noise Ratio

For detection the signal must be higher than noise

Dominating noise sources

Seismic noise 0-5 Hz attenuated
(0-50 Hz unattenuated)

Suspension thermal noise 4-40 Hz high Q suspensions
(50-200 Hz low Q suspensions)

Mirror thermal modes 40-200 Hz

Shot noise > 200 Hz
(effective power enhanced by F.P. cavities
and power recycling)

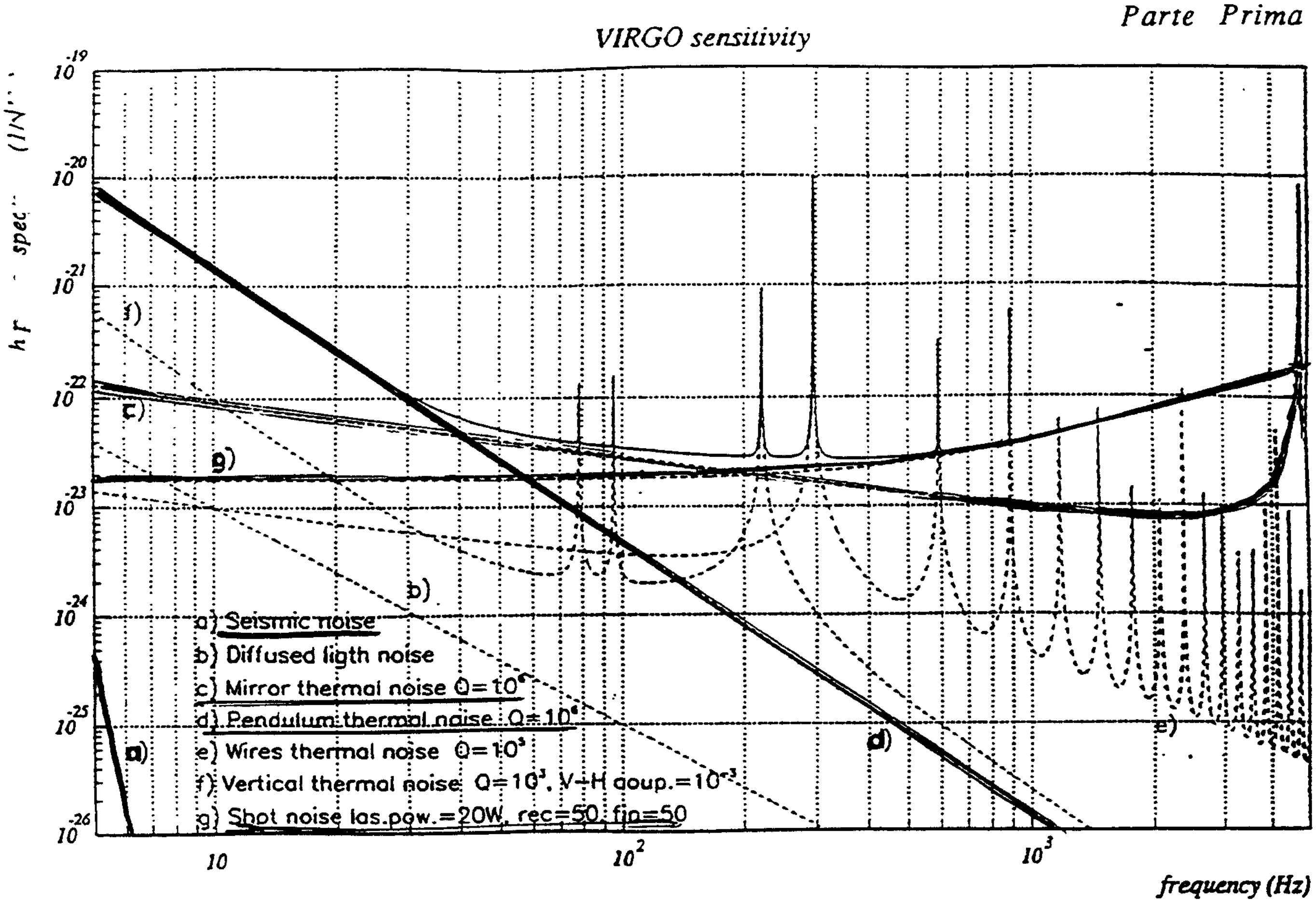

Other Noise Souces

Laser Frequency fluctuations ($10^{-6}\ Hz^{-1/2}$)

Laser Power fluctuations ($4 \quad 10^{-10}\ Hz^{-1/2}$)

Vacuum fluctuations (req.10^{-8} Torr, obt.10^{-9} Torr)

Seismic noise on light diffused in beam pipe walls (baffles)

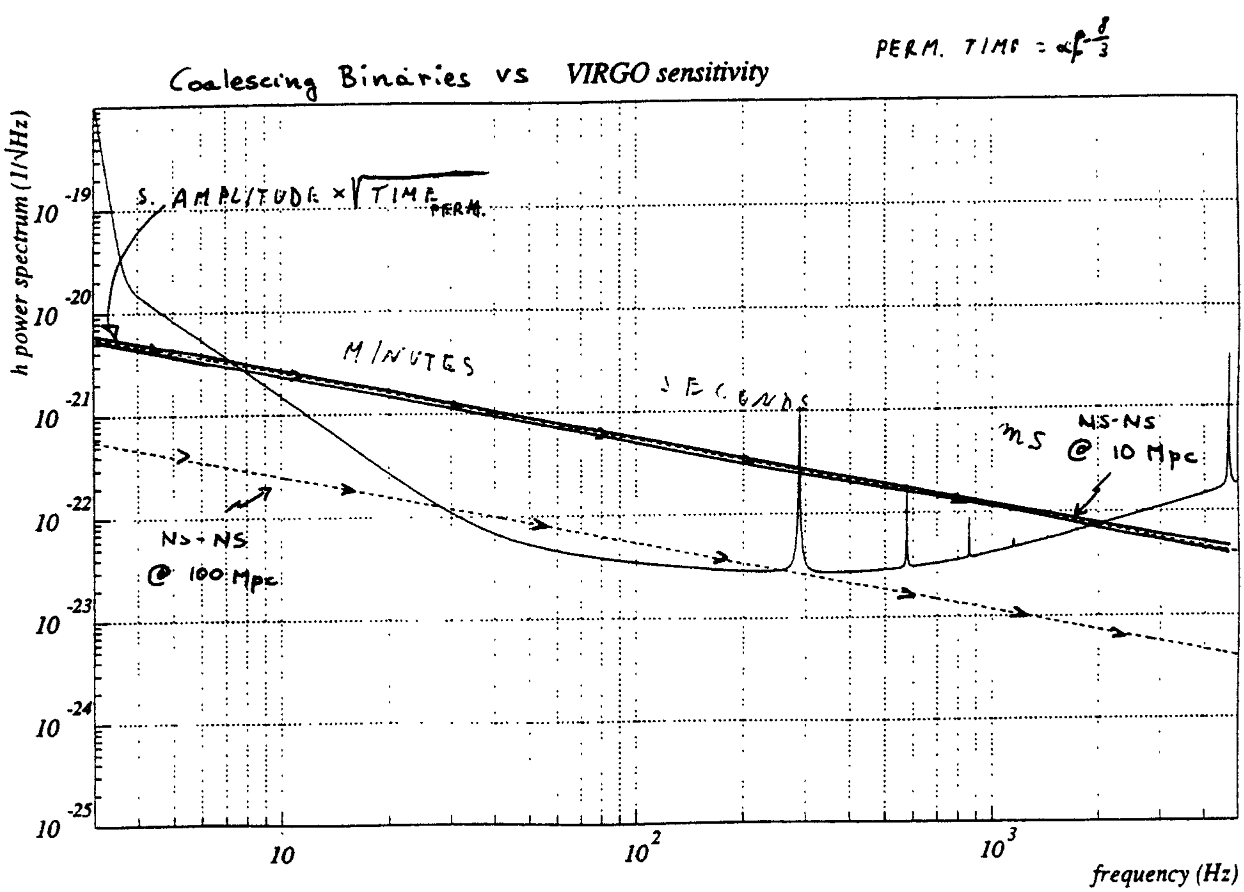

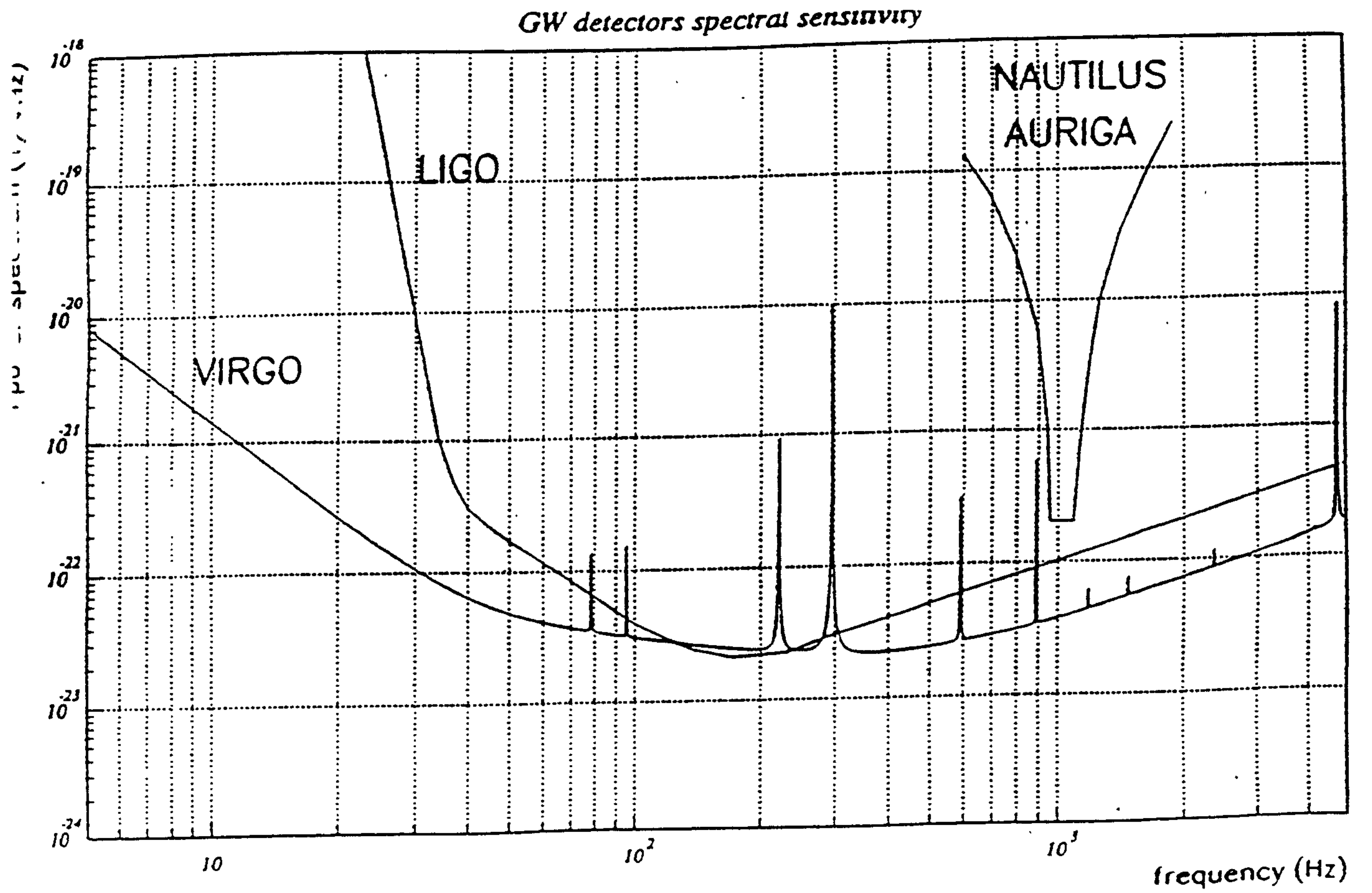

1 19

Status of the VIRGO project

Central building project adjudicated

Decree of public utility emitted

Currently mine clearing the land

Construction beginning shortly (One year construction time)

Other buildings to follow

Mechanics and tubes

Finalise R&D in some components

Bidding process in remaining components

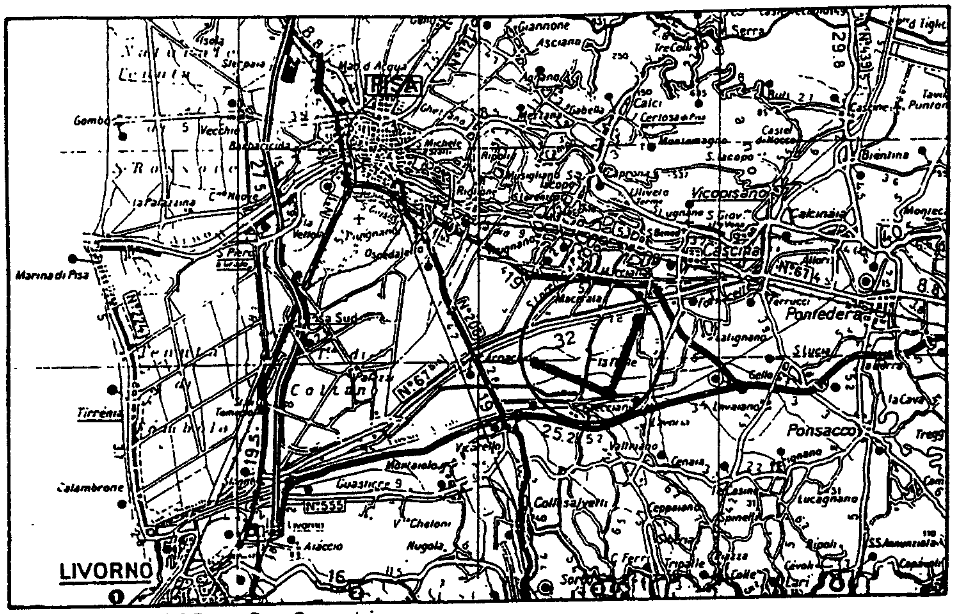

Sept. 1993 - De Carolis

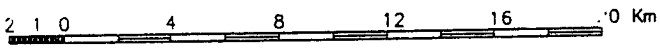

[redacted]

E = ASSEMBLY BUILDING
F = TERMINAL BUILDING

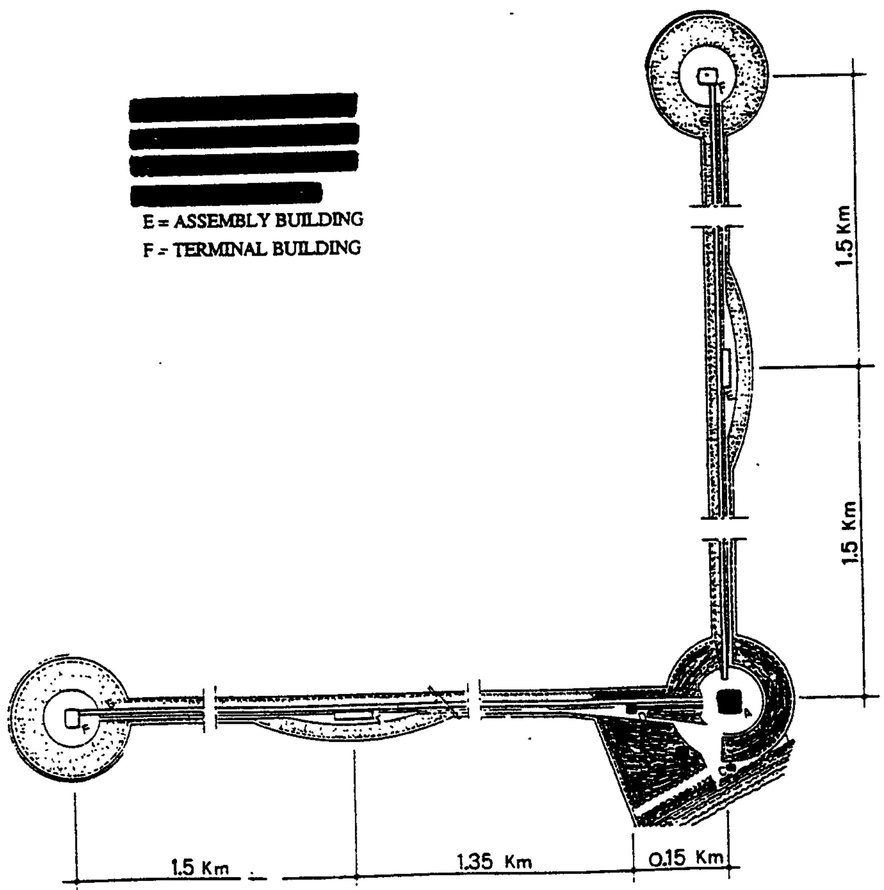

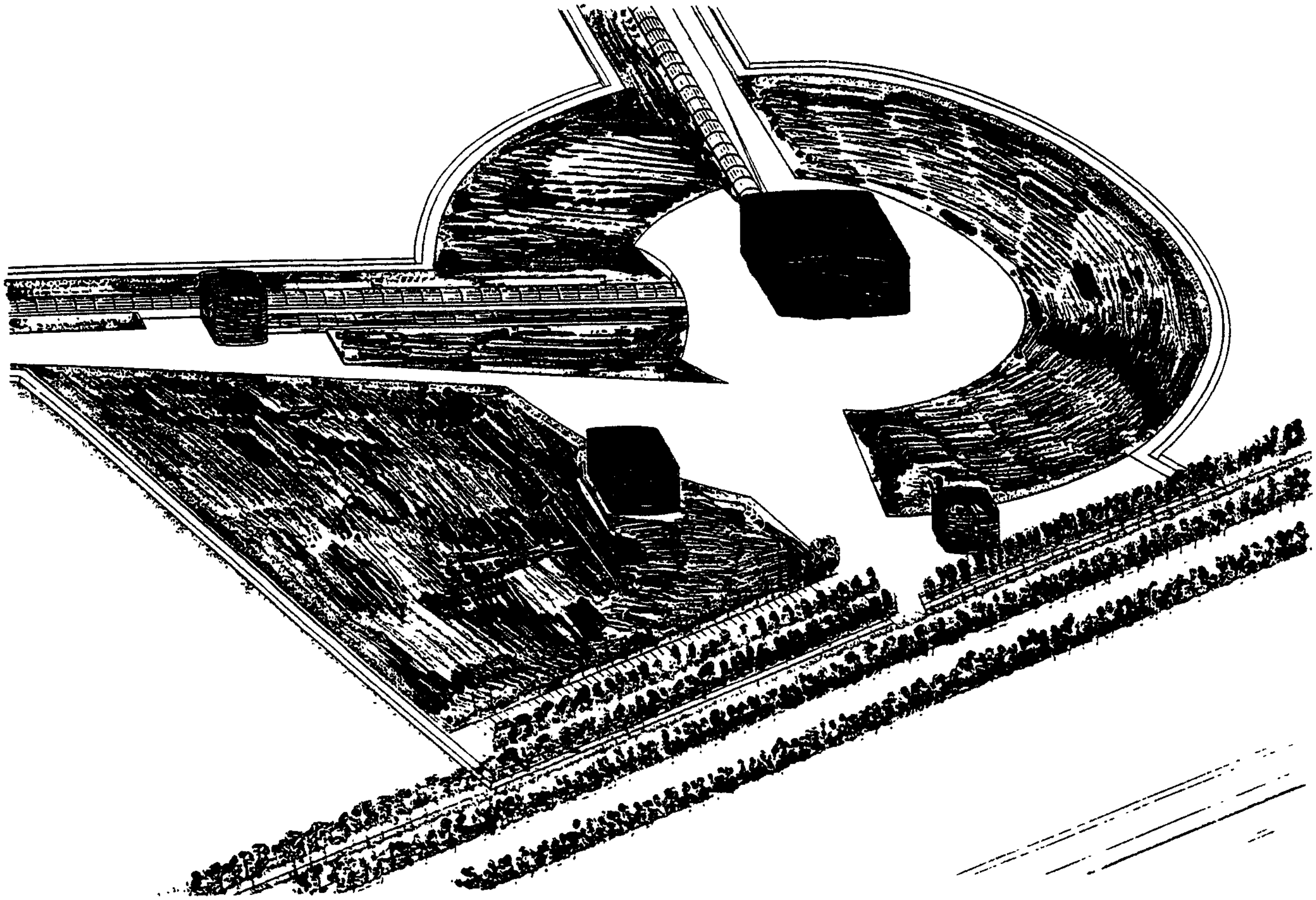

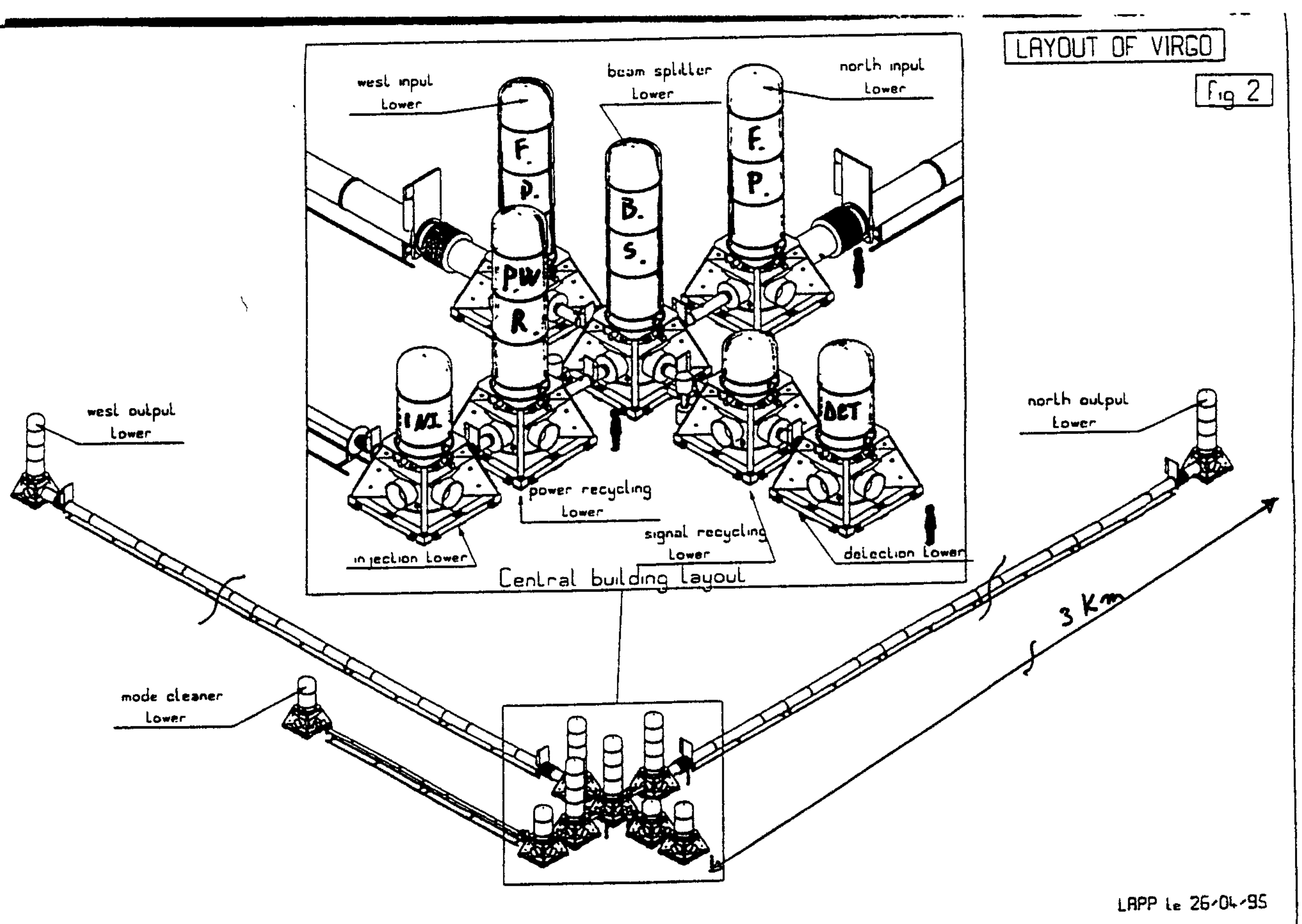
LAYOUT OF VIRGO
fig 2
west input tower
beam splitter tower
north input tower
F.
P.
B.
S.
PW
R
INJ
DET
power recycling tower
signal recycling tower
injection tower
detection tower
Central building layout
west output tower
north output tower
mode cleaner tower
3 Km
LAPP le 26-04-95

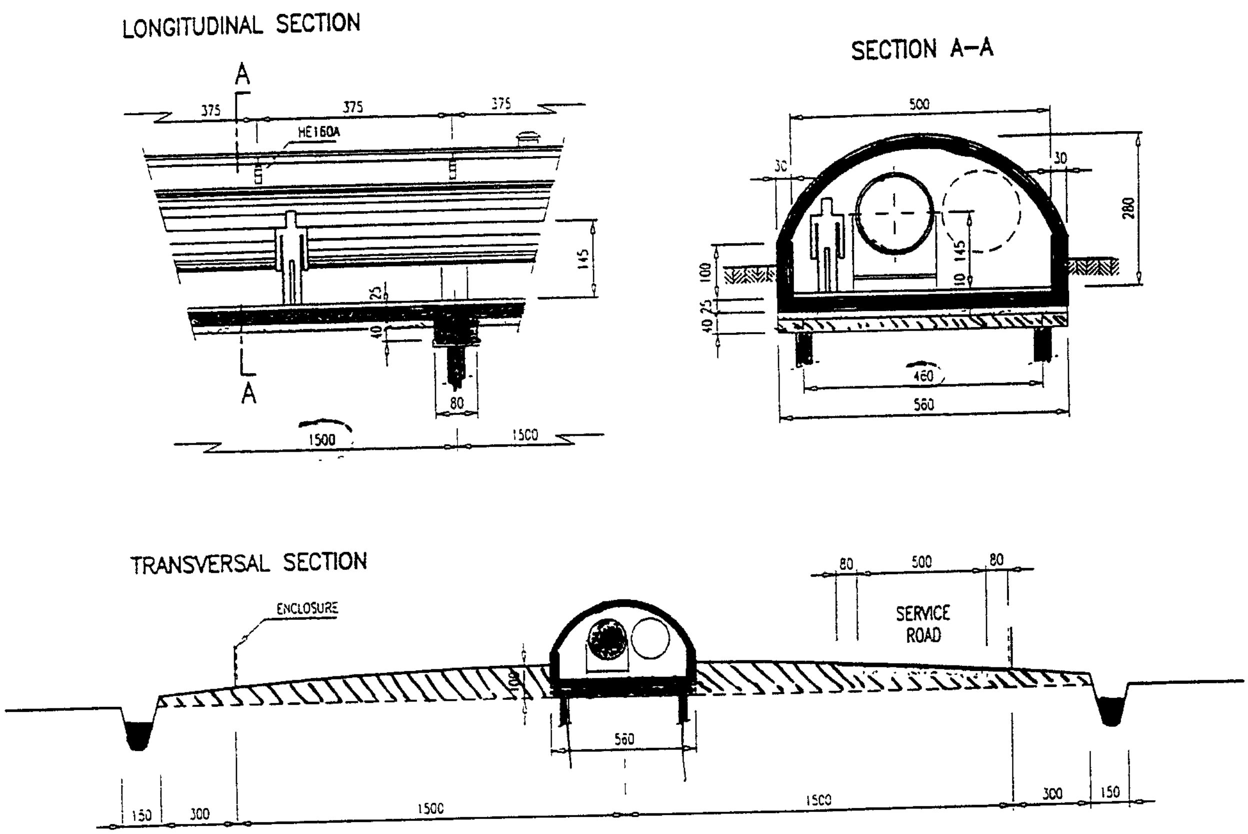
LONGITUDINAL SECTION
A
375
375
375
HE160A
145
25
40
A
80
1500
1500
SECTION A-A
500
30
30
280
145
100
10
75
40
460
560
TRANSVERSAL SECTION
ENCLOSURE
80
500
80
SERVICE
ROAD
560
150
300
1500
1500
300
150

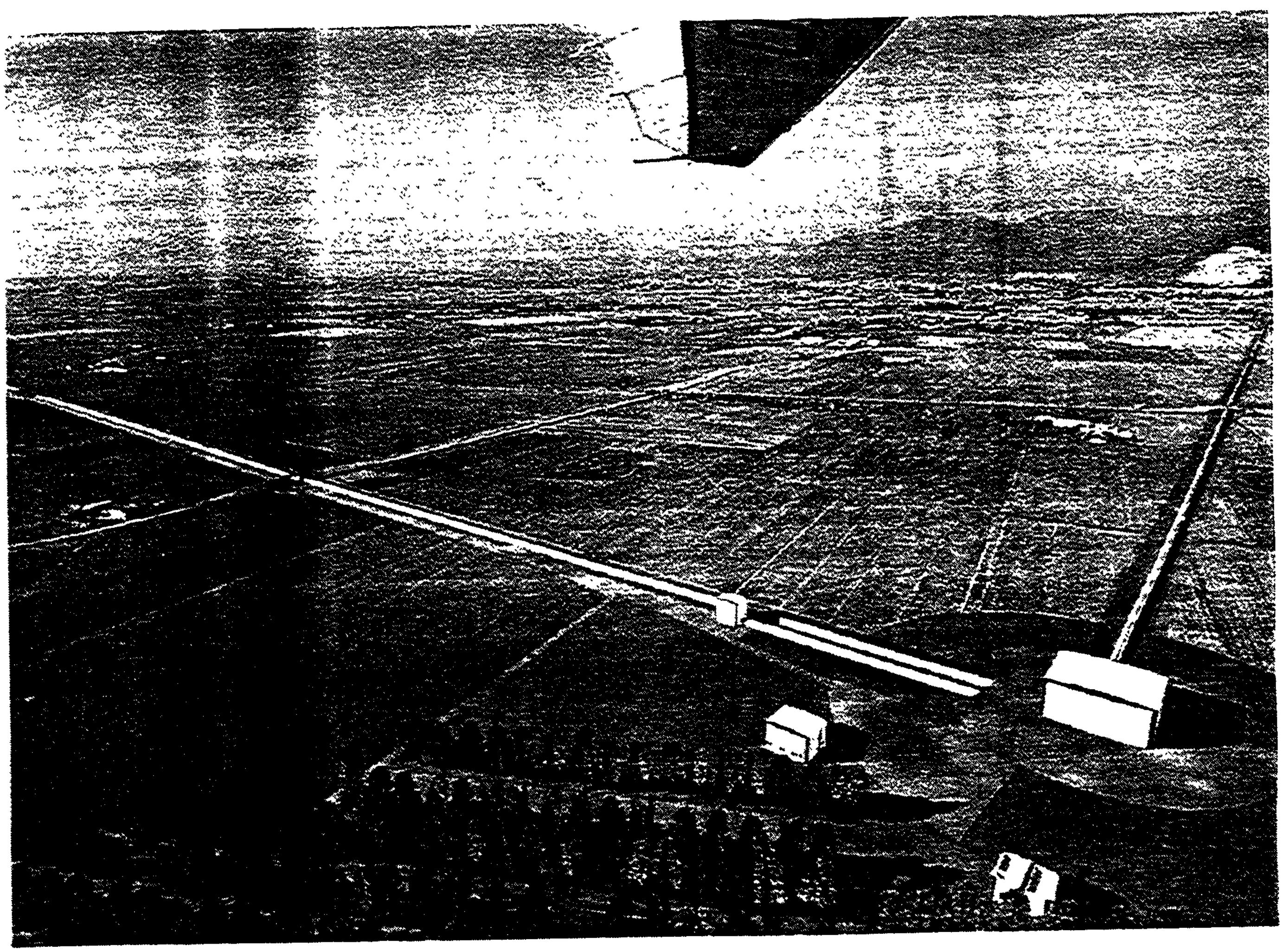

ARM TUBES OF THE ANTENNA

I. GENERAL SPECIFICATIONS

The general sketch of the antenna, limited to tubes and towers is presented in Fig.x.
The main parameters of the two 3km long vacuum tubes are summarized below:

Inner diameter	1200 mm
External pressure	1 bar (3 for the calculation)
Lenght of each arm	3000 m $\pm$ 30m
Residual pressure	10^{-9}mbar for H2
	10^{-10}mbar for other gas
Outgassing rate	$< 10^{-12}$ mbar l/s cm^2 for H_2
Temperature of reference	20°C
Temperature range	-20°c, +150°C
Working temperature range	-5°C, +40°C
Lifetime	20 years
Gate valves at end of arms	1200mm
Bake-out temperature	150°C (maximum power 1MW)
Distance between pumping groups	300 m
Distance between floor and tube axis	$\geq$ 1300m

Straightness: the tube axis has to be contained within a 50mm diamater
Presence of baffles in the tube
No elastomere gaskets for the permanent seals
Minimum amplification of the seismic noise for any frequency

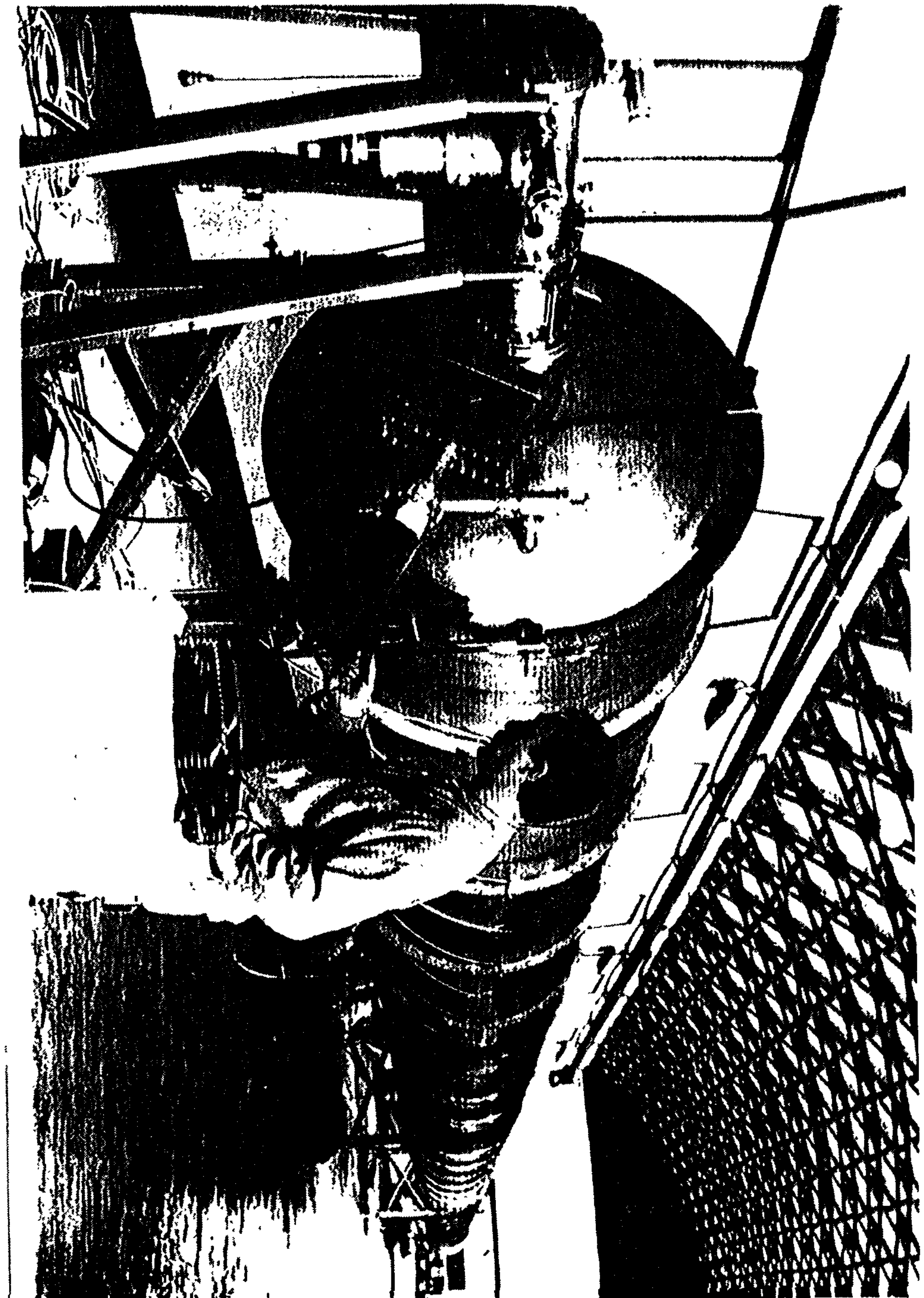

Super Attenuator Tower components

Top table movement

7 attenuation filters

(2nd filter actively cooled)

Steering marionetta

Suspended mirror and recoil mass

10 m tall tower

2 m diameter

1.1 tons suspended mass

10-6 Torr vacuum

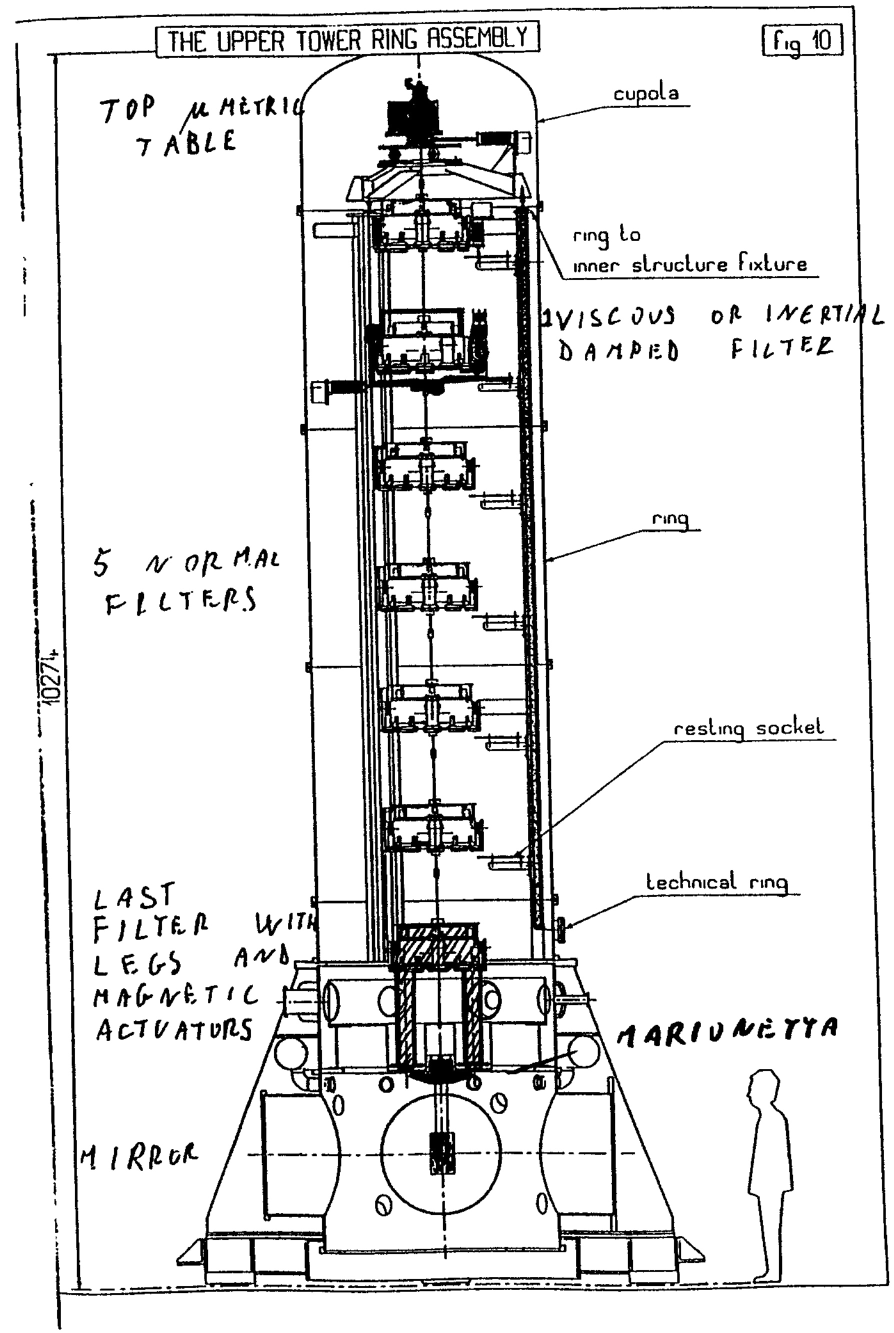

Top table movement

Main issues

Cold welds in movements under stress

1.1 tons load under vacuum

Movements in 3 dimentions + 1 rotation

smoother tha seismic vibrations (1 μm)

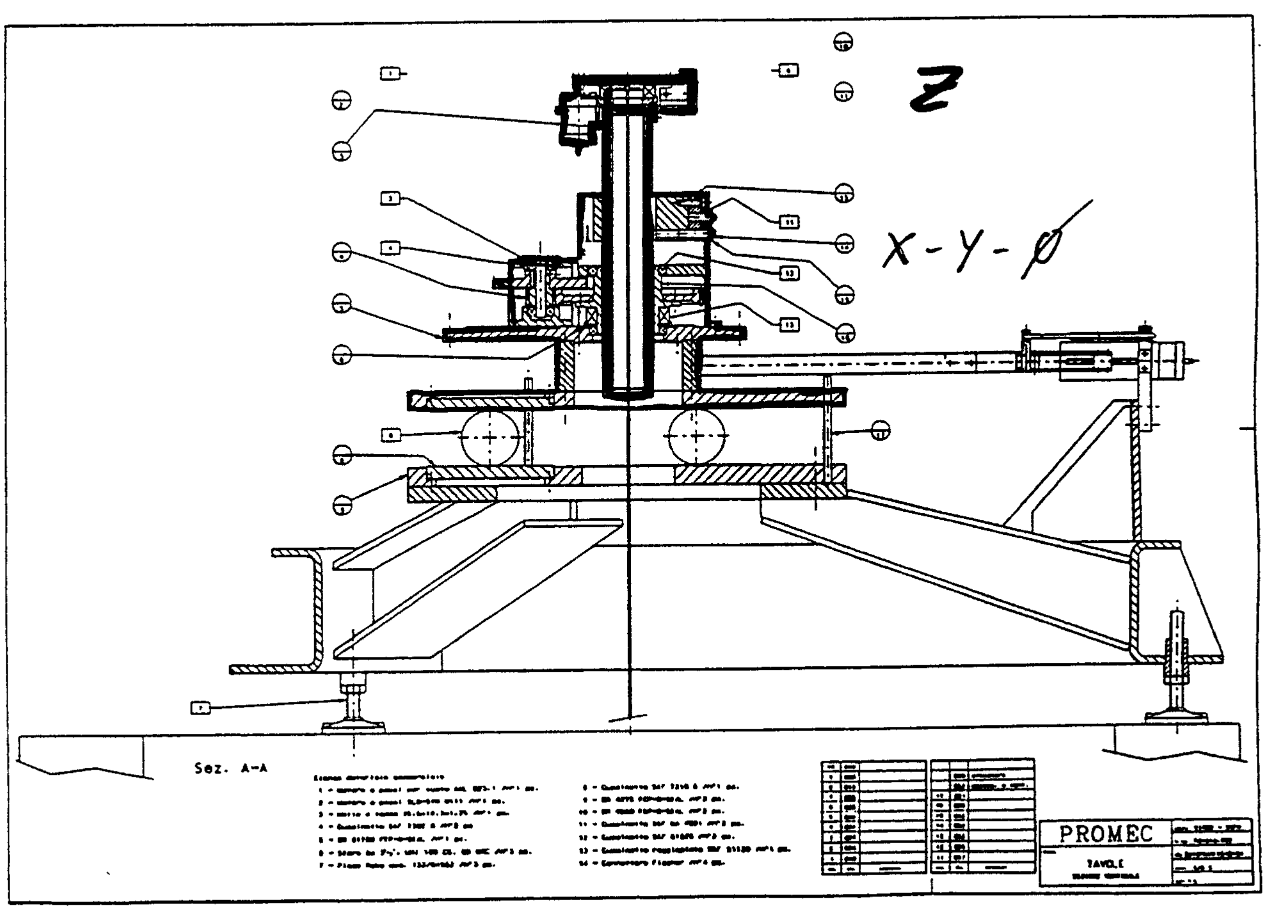

c:/dgn/tavole_2.dgn May. 15, 1995 20:47:22

FILTER 2 DAMPING

VISCOUS OR INERTIAL DAMPING IS NECESSARY
AT SOME STAGE OF THE ATTENUATION CHAIN
IN ORDER TO DAMP THE MOTION OF NORMAL MODES
WITHIN THE LOCKING SYSTEM DYMAMIC RANGE

VISCOUS DAMPING WITH RESPECT WITH THE EXTERNAL STRUCTURE

OK 0n 6 Degrees of Freedom

INERTIAL DAMPING
CAN PROVIDE ALSO SEISMIC NOISE SUPPRESSION

IN DEVELOPMENT

Inertial damping of filter 2

Principle of attenuation:

Acceleration detected with six low frequency
linear and torsional **accelerometer**

Acceleration neutralised with a feedback of **magnetic forces**

Damping of main oscillation resonances

Very complex mechanics and electronics

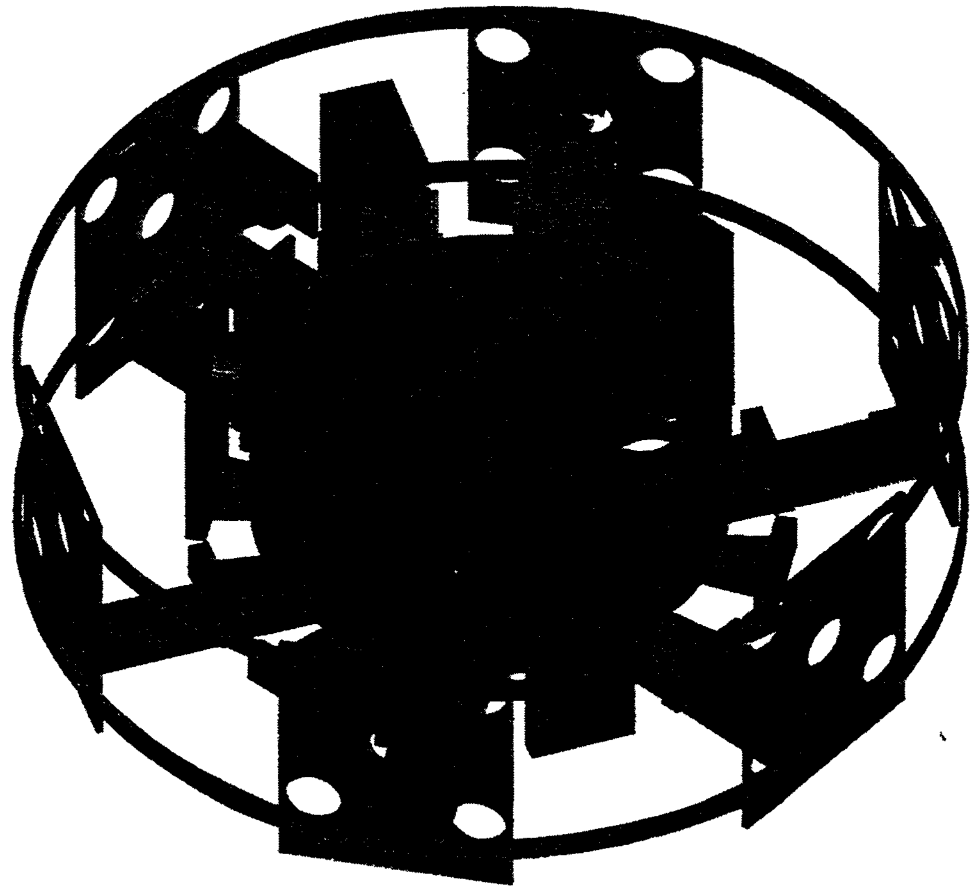

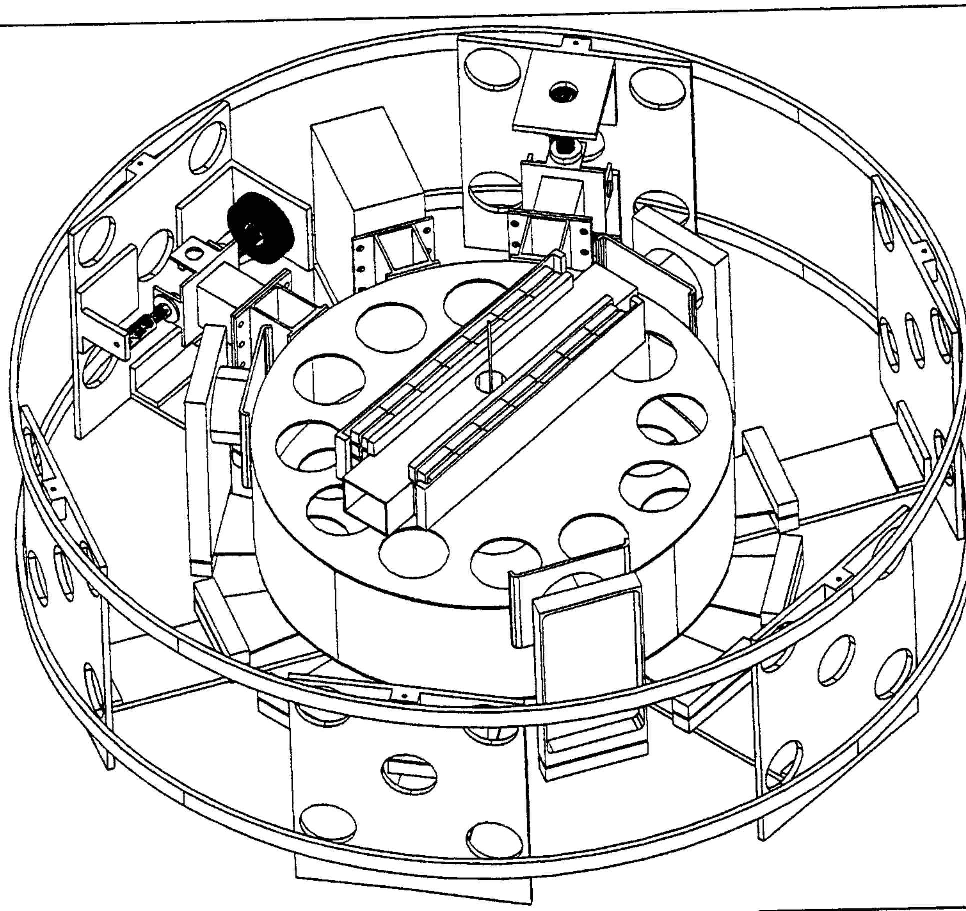

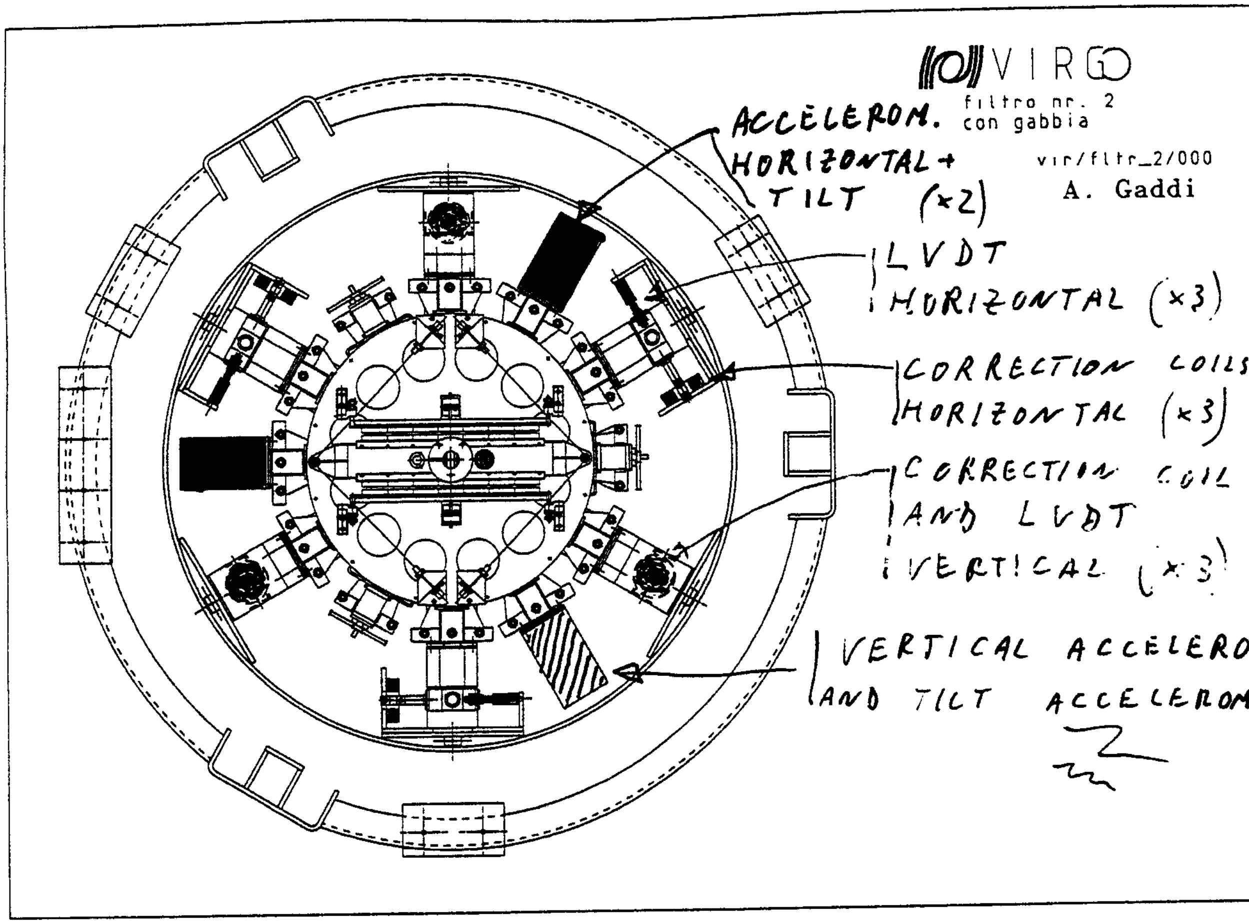

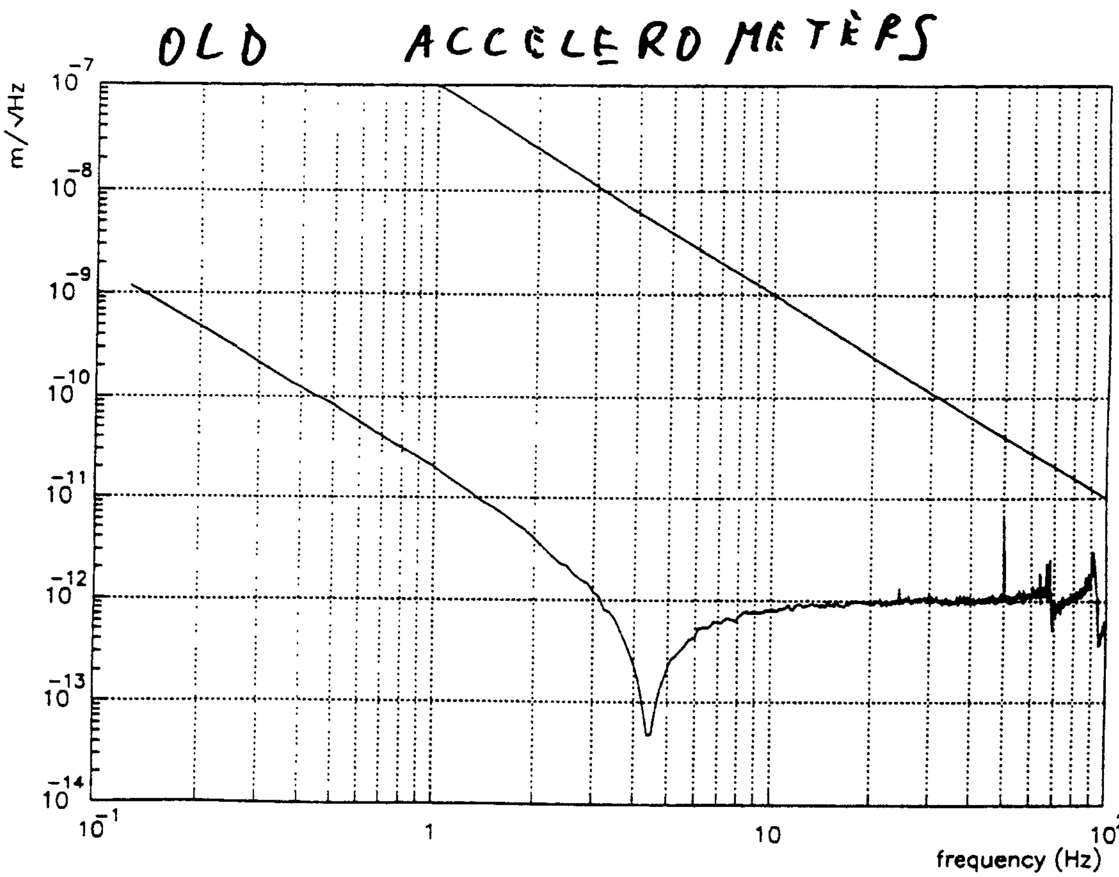

FIG. 5. Displacement spectral sensitivity function (compared with the behavior of a typical spectrum of seism: $x_{seism}(f) = 10^{-7}/f^2$ m/$\sqrt{\text{Hz}}$).

In Fig. 1 a block diagram of the electronic circuit is shown. The suspended central coil of the LVDT is driven at

(proportional integrative derivative) network, whose

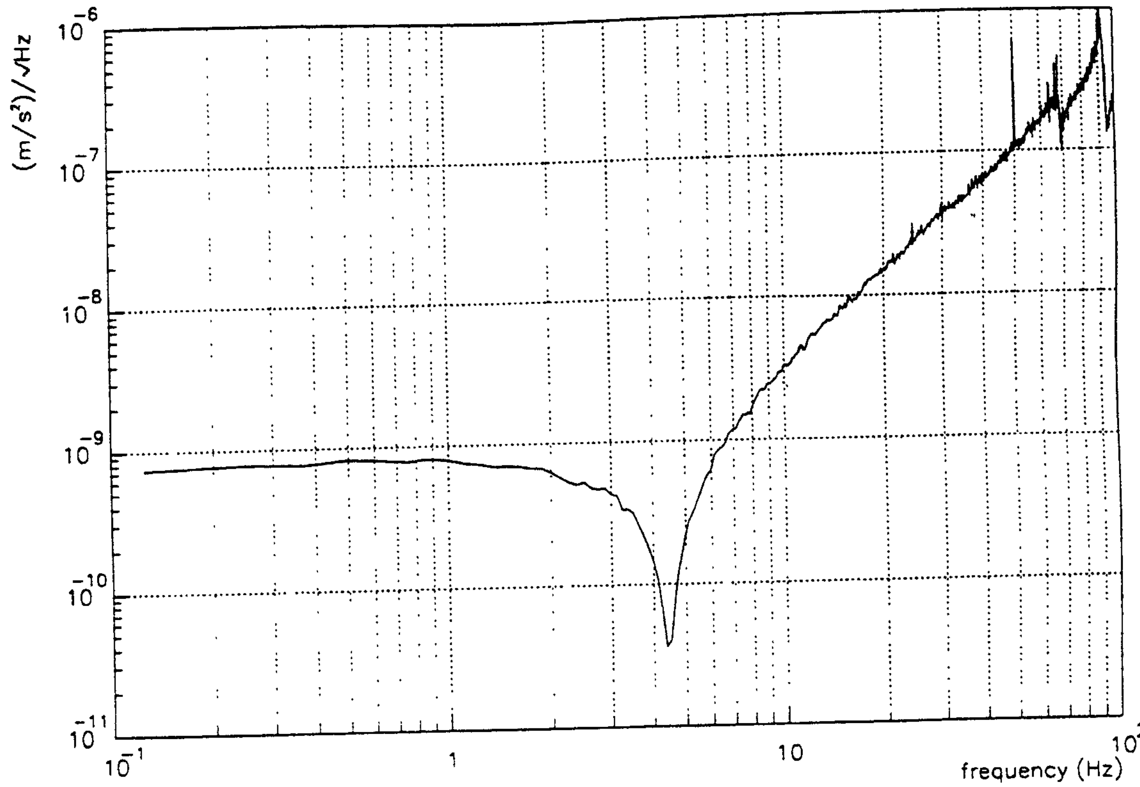

FIG. 4. Acceleration spectral sensitivity function.

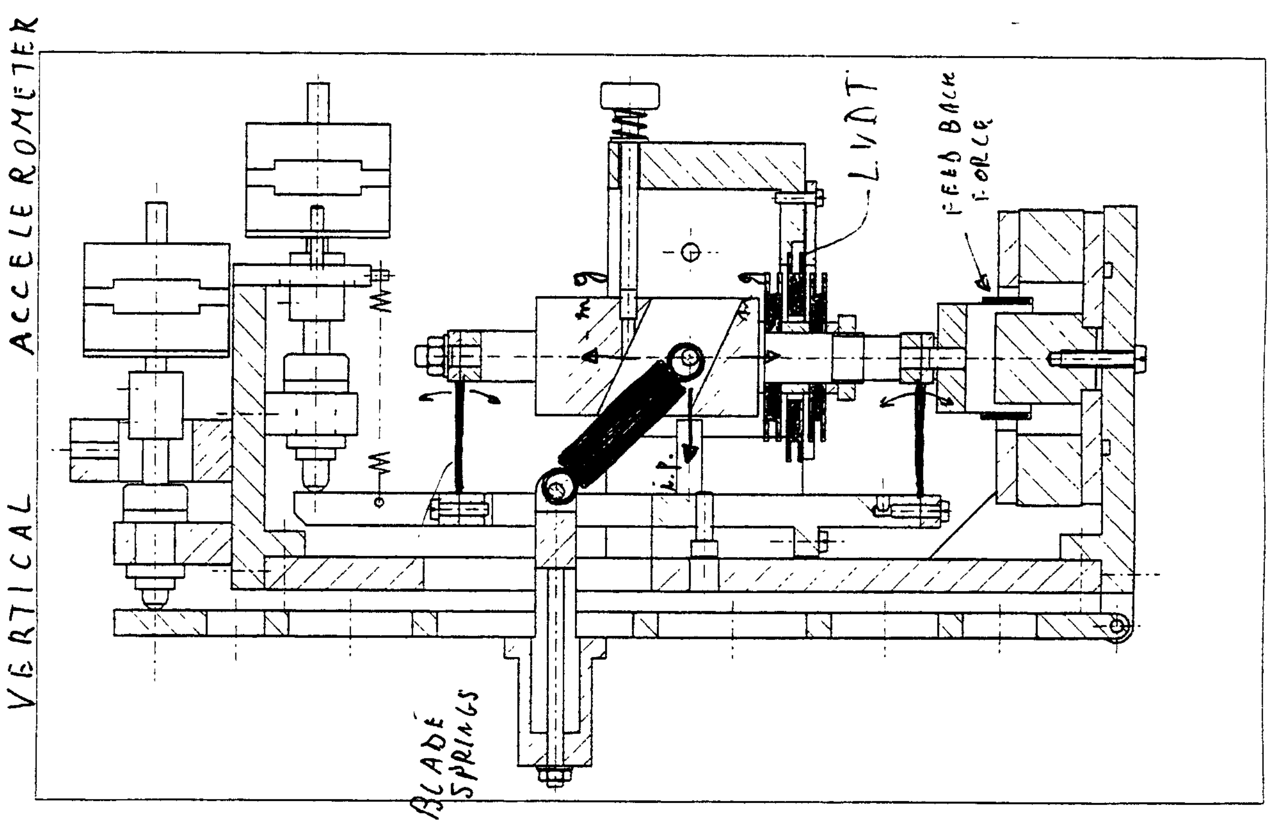

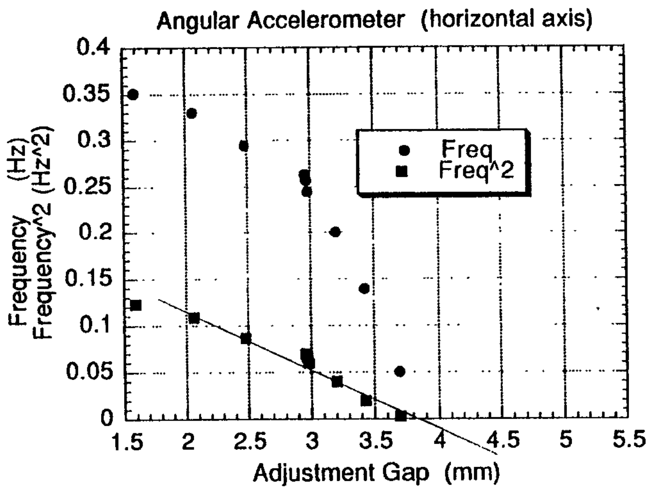

Angular Accelerometer (horizontal axis)
Frequency (Hz)
Frequency^2 (Hz^2)
Freq
Freq^2
Adjustment Gap (mm)

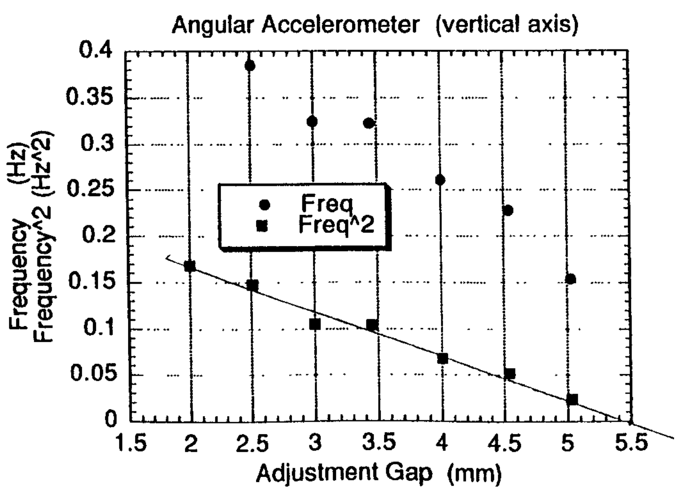

Angular Accelerometer (vertical axis)
Frequency (Hz)
Frequency^2 (Hz^2)
Freq
Freq^2
Adjustment Gap (mm)

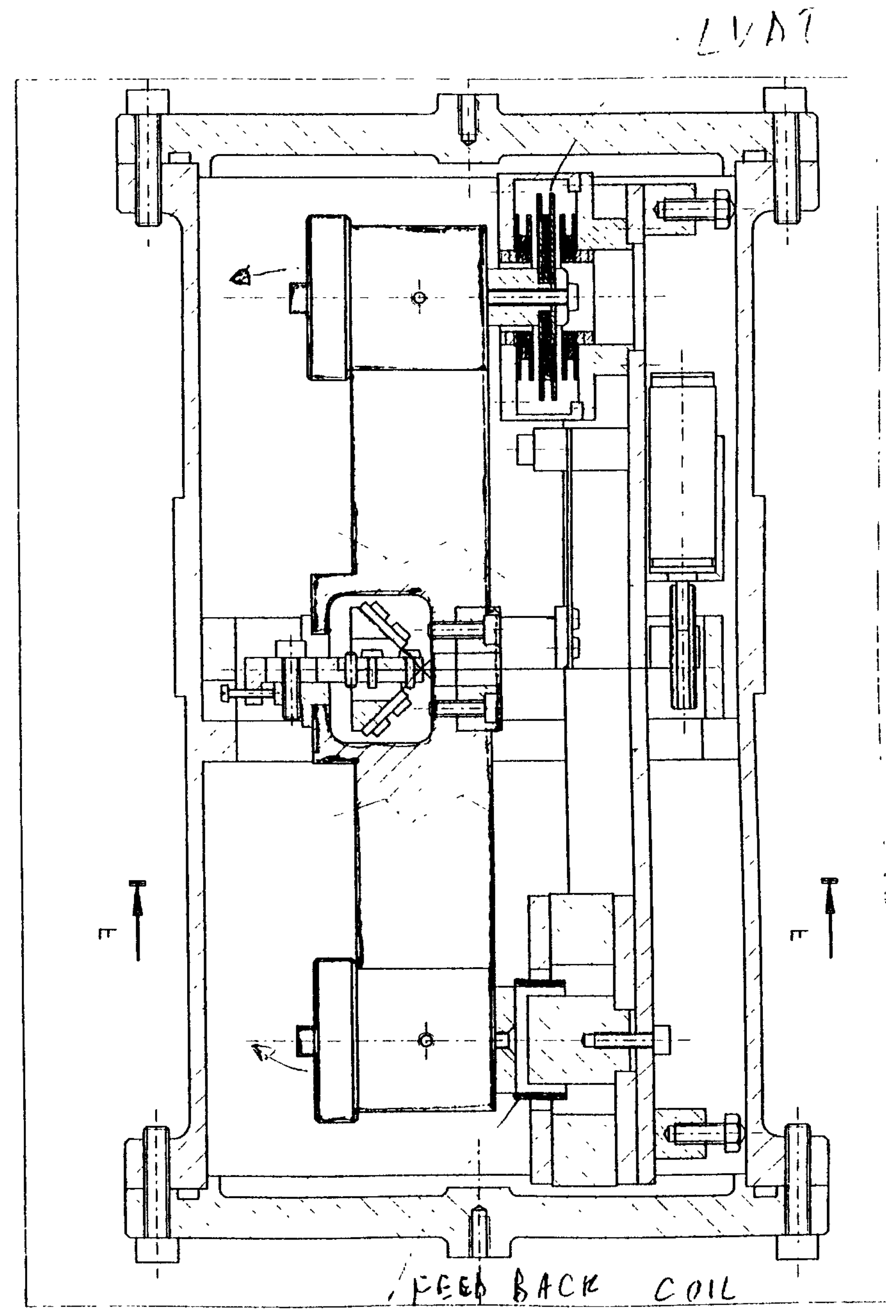

LVDT
FEED BACK COIL

Marionetta positioning

of mirror and reference mass

The **mirror** and its reference mass are

suspended from a cross shaped structure (**marionetta**).

The **marionetta** is **suspended from** the **last attenuator**

The **marionetta** is **actuated** through **magnetic coils**

mounted on the last attenuator and pushing on the cross arms

rotation, x-y tilt and **back/forward** movements are possible

Total movement 2-3 microns

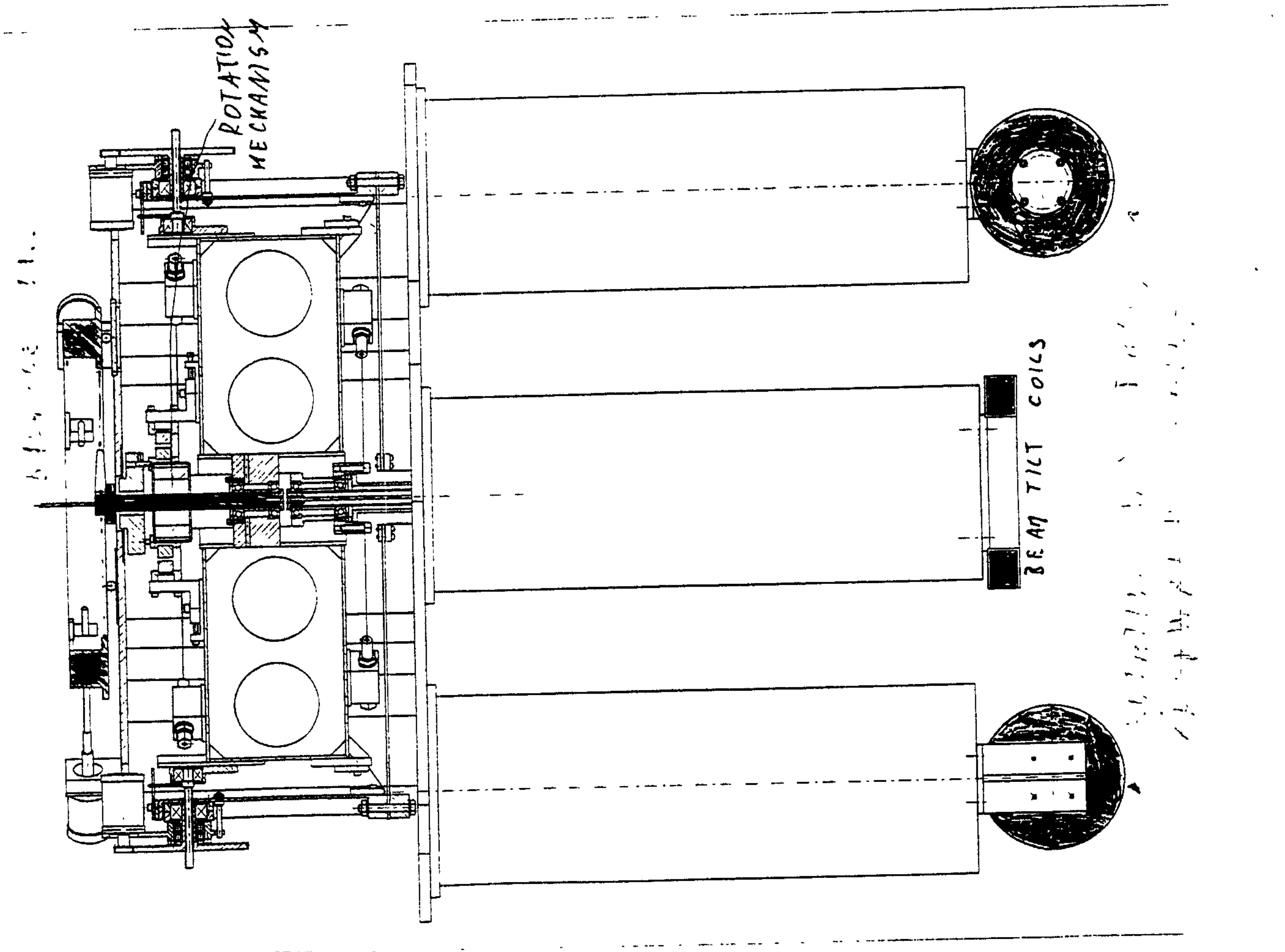

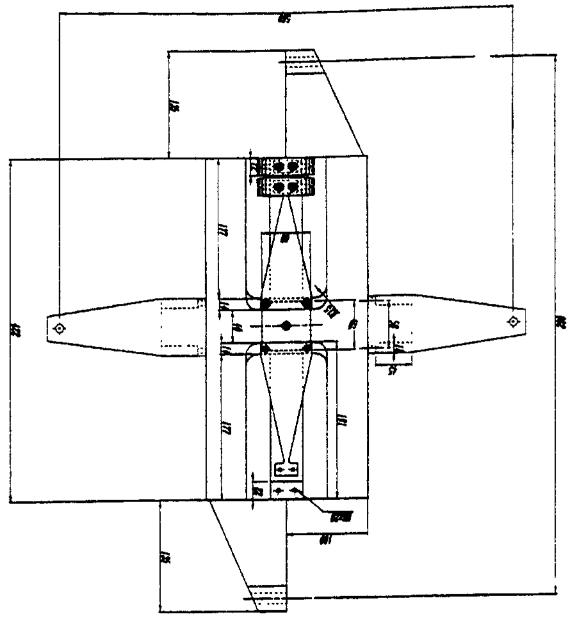

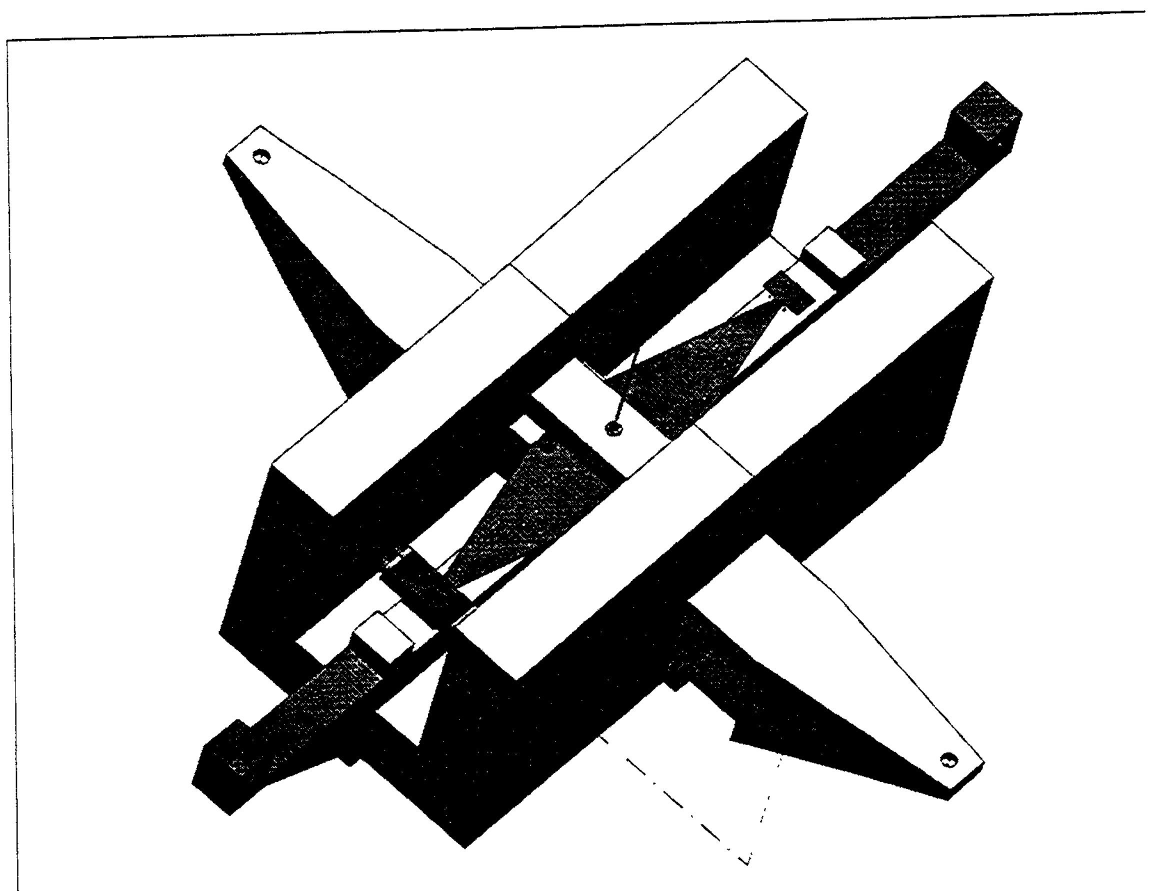

VIRGO-Infn. Sez. Roma1

Mirror positioning

The **mirror and** its **reference mass** are

independently suspended from the marionetta

The reference mass is a cup with mass equal to the mirror mass

The reference mass encases the mirror and

houses four coils acting on tiny magnets on the mirror

Mirror **tilt around the** z **and** y axis and x **movements** are possible

x positioning better than $\mathbf{10^{-18}\ m/Hz^{-1/2}}$

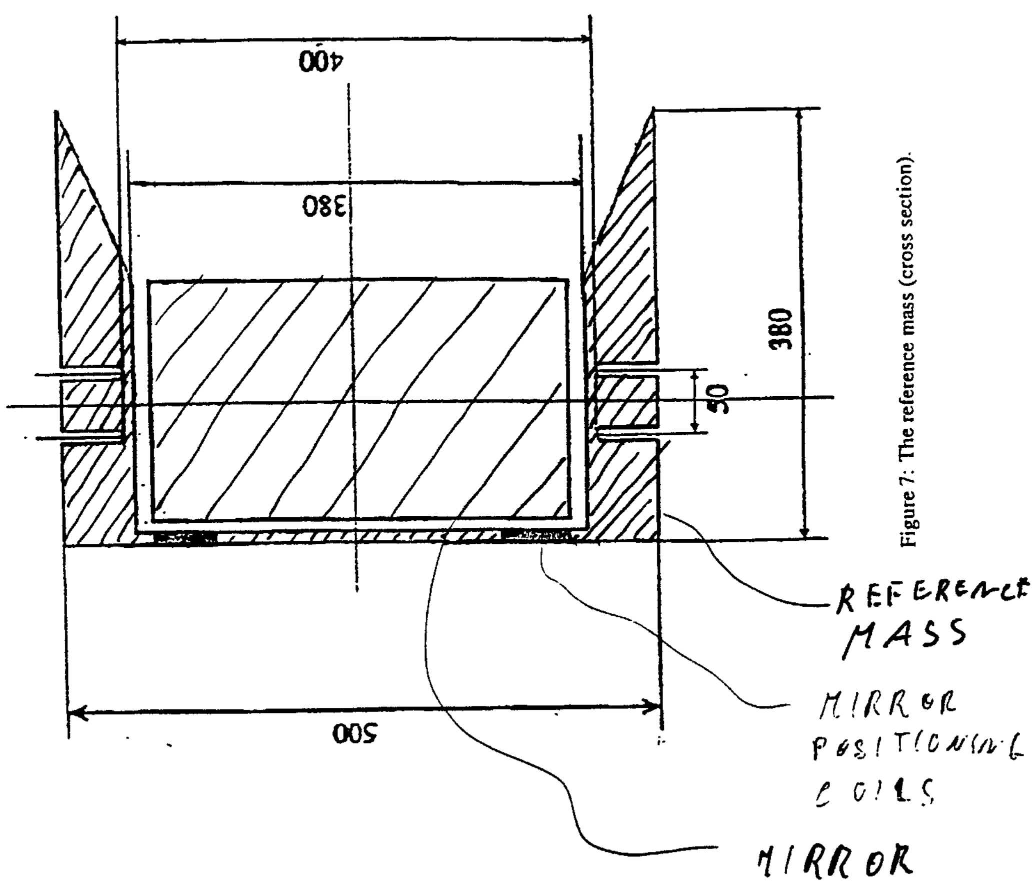

Figure 7: The reference mass (cross section).

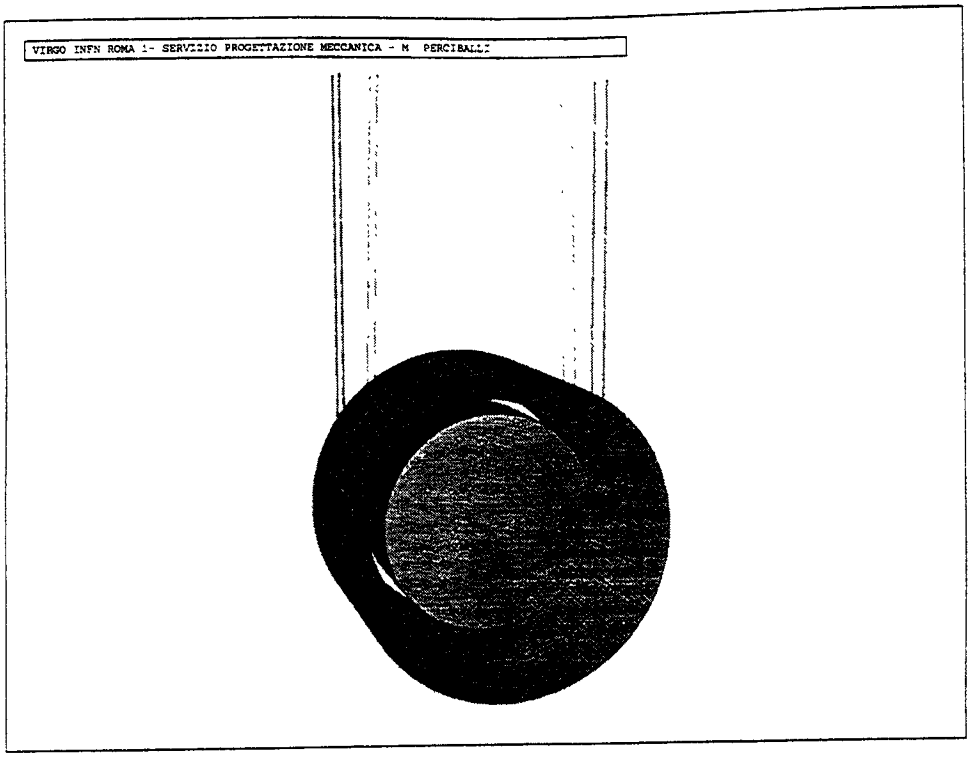
VIRGO INFN ROMA 1- SERVIZIO PROGETTAZIONE MECCANICA - M PERCIBALLI

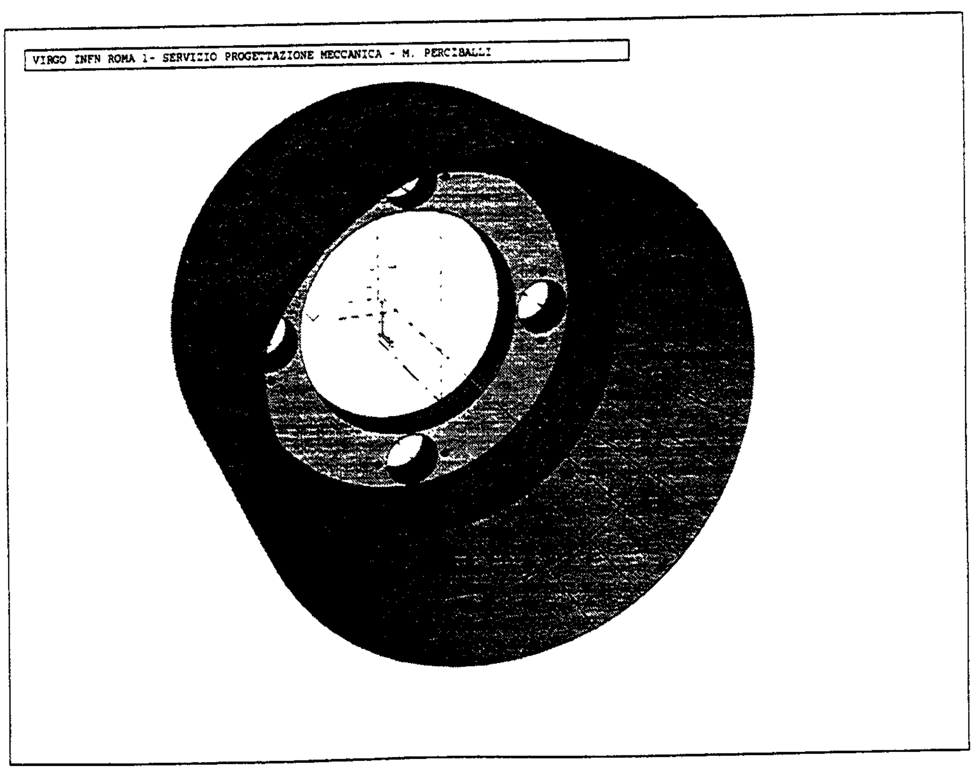
VIRGO INFN ROMA 1- SERVIZIO PROGETTAZIONE MECCANICA - M. PERCIBALLI

Super Attenuation filters

Principle of attenuation

Each super attenuator filter is a

5 + 1 Degrees of Freedom pendulum

with **resonant frequency below the Hertz**

The center of mass of a pendulum which suspension point is shaken at a frequency higher than its resonant frequency will move with amplitude proportional to the suspension point vibration amplitude times an attenuation factor $A_f = f_0^2/f^2$.

At 10 Hz $A_f = 10^{-2}$ per stage

With seven stages $A_f = 10^{-14}$

If seismic noise is $10^{-6}/f^2$ ==> @ 10 Hz 10-8 $m/Hz^{-1/2}$

Mirror will vibrates **less than 10^{-18} $m/Hz^{-1/2}$** @ 10 Hz as required

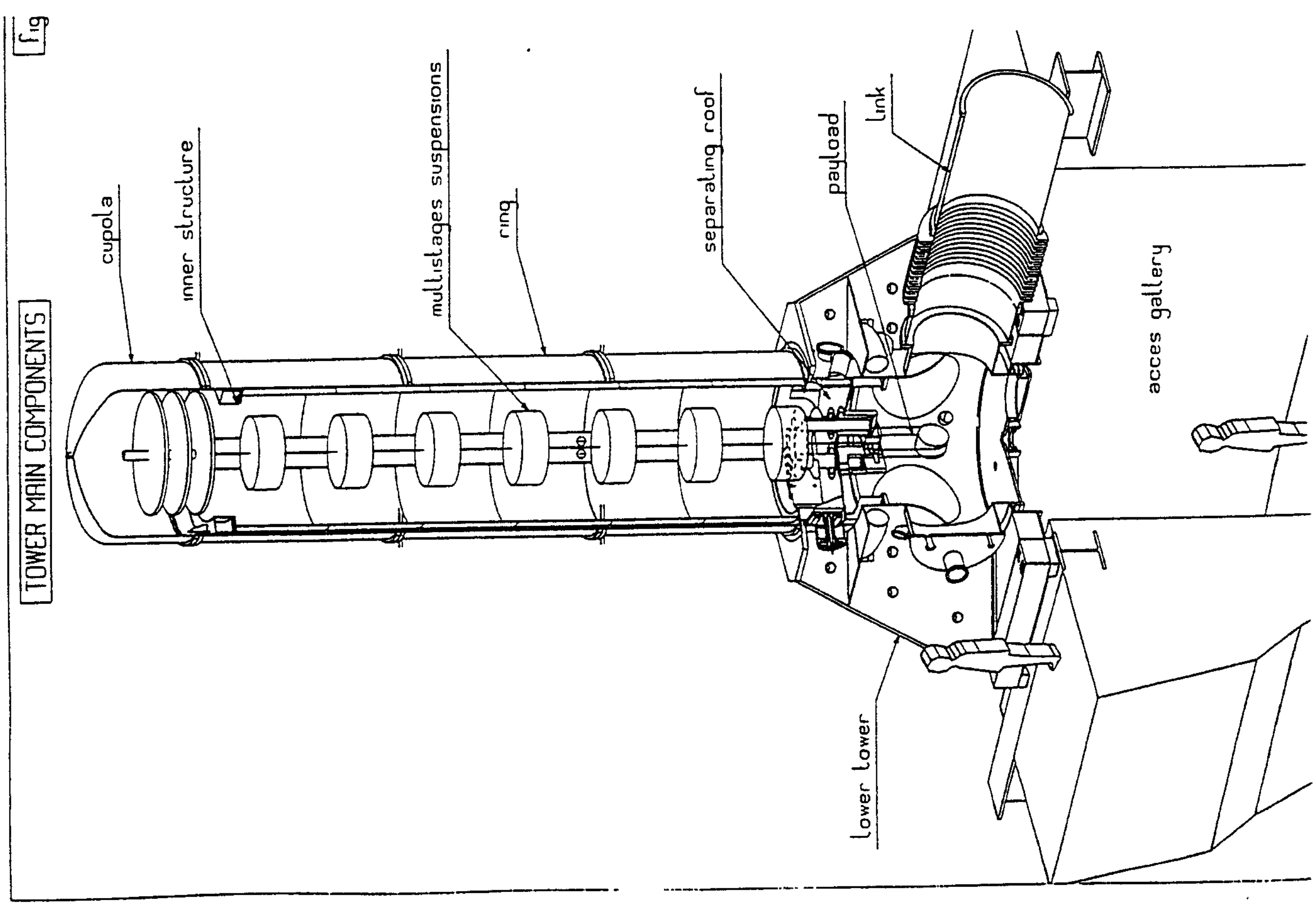

Super Attenuation filters

Characteristics

5 + 1 Degrees of Freedom pendulum below 1 Hz

x - y pendulum	OK
torsion pendulum	OK
x-y tilt pendulum	OK
z pendulum	a real MESS

very complex mechanics

a)

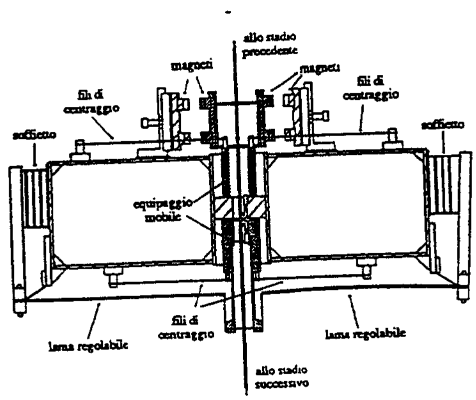

b)

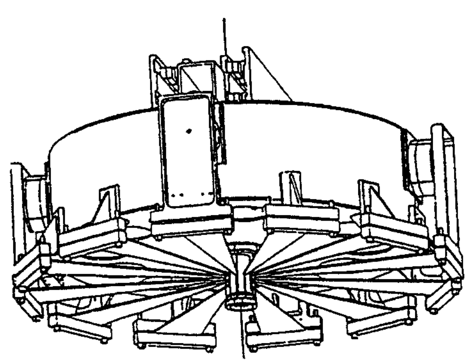

Super Attenuation filters

Mechanical design and construction

Prototypes under test

work on

final engineering

vacuum proofing

controls

characterisation

heat dissipation

connectivity

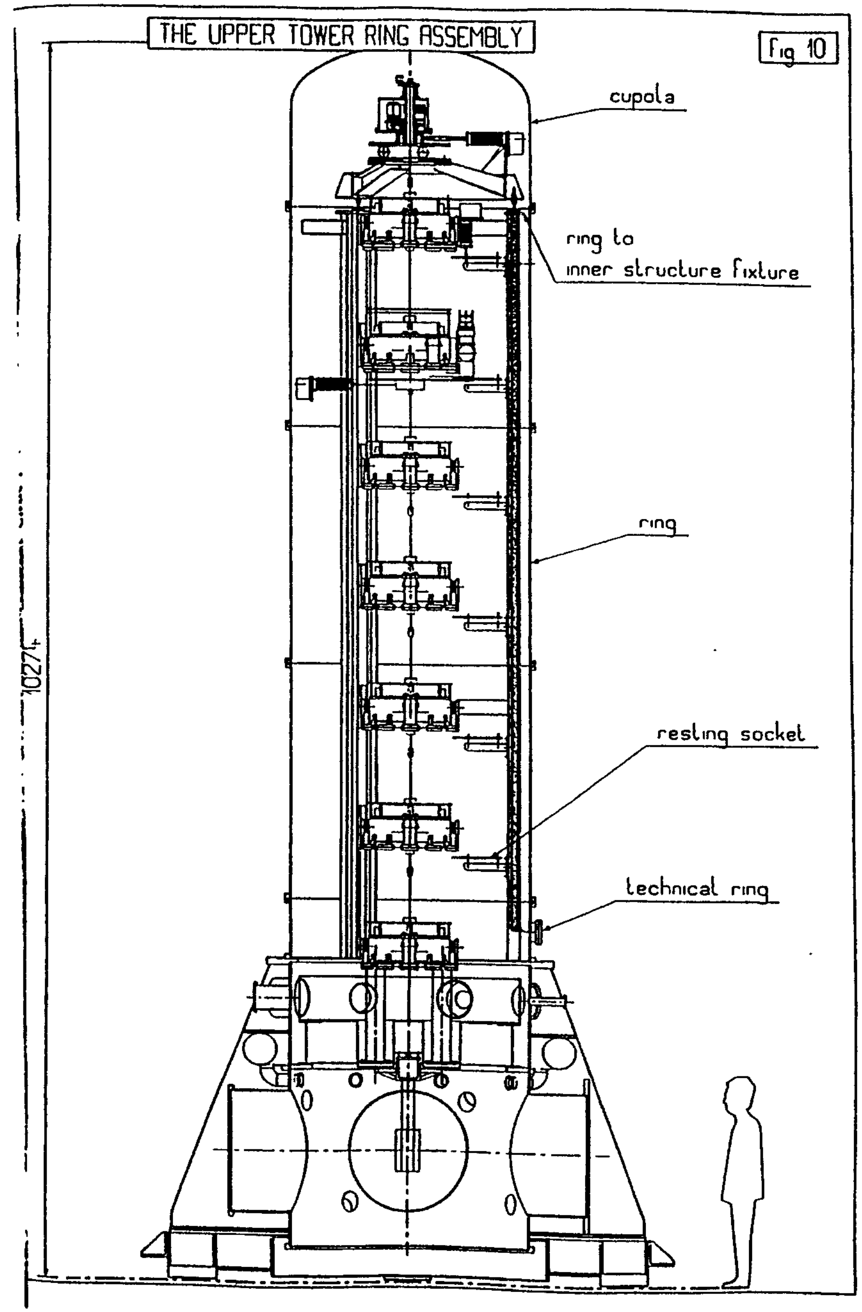

Phase 1: Measurements on the bare filter (conclüded)

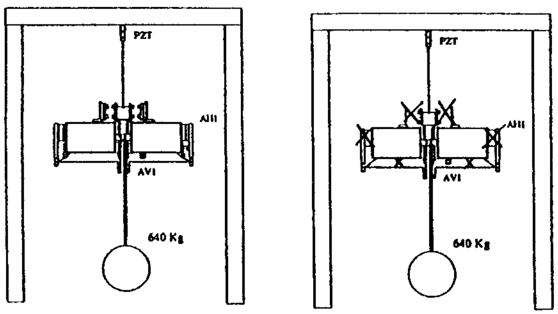

1.a) ==> Vertical Transfer Function

1.b) ==> Horizontal Transfer Functions

1.c) ==> Quality factor of the fundamental vertical resonance

1.d) ==> Anharmonic behaviors of the blades system

1.e) ==> Dependence of the fundamental frequency on the offset position

1.f) ==> Creep of the blades !!!! ==> the only bad surprise

Super Attenuation filters

Status of characterisation

Separate **measurement** of attenuation **characteristics** of

Bare filter

With **Resonant frequency reduction** Anti Spring System

With **tuning mechanisms**

With **internal resonances dampeners**

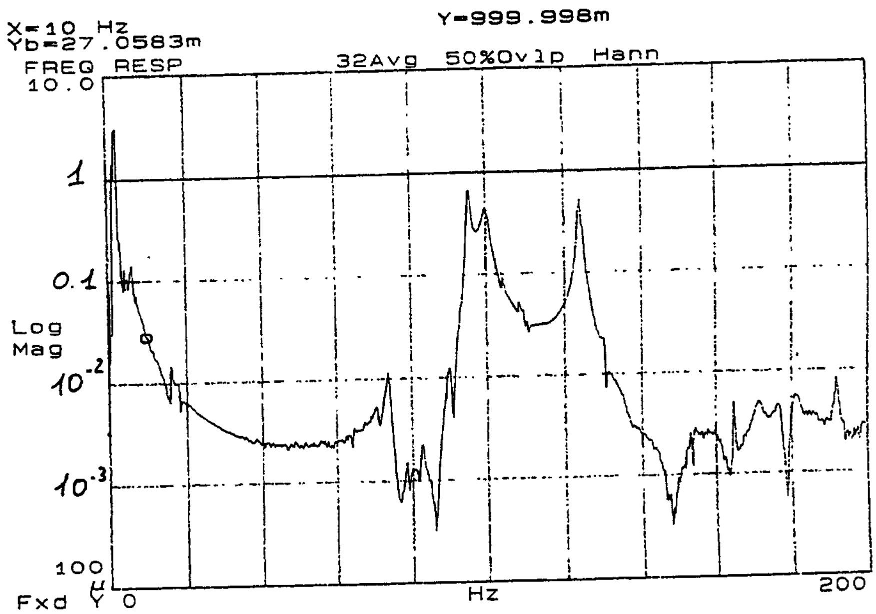

VERTICAL TRANSFER
FUNCTION

HORIZONTAL TRANSFER
FUNCTION OF THE BARE FILTER

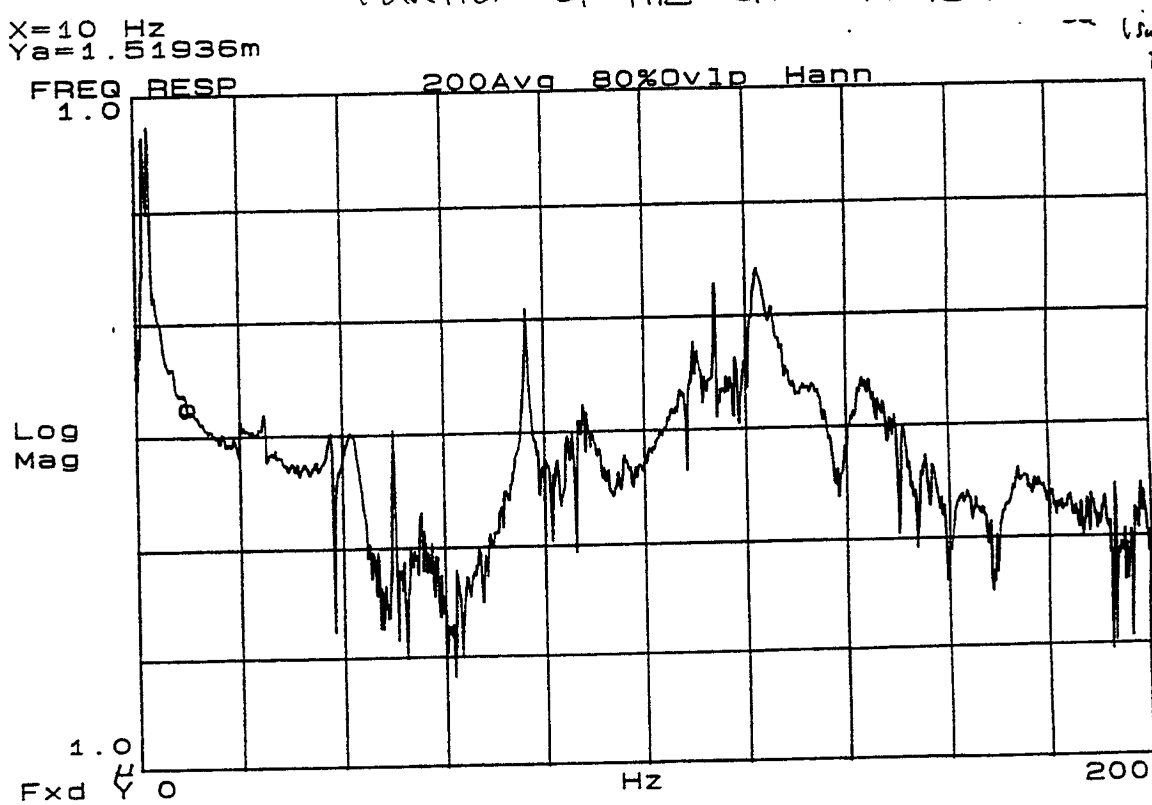

QUALITY FACTOR Vs.

OFFSET OF BLADES WORKING POSITION

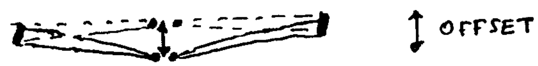

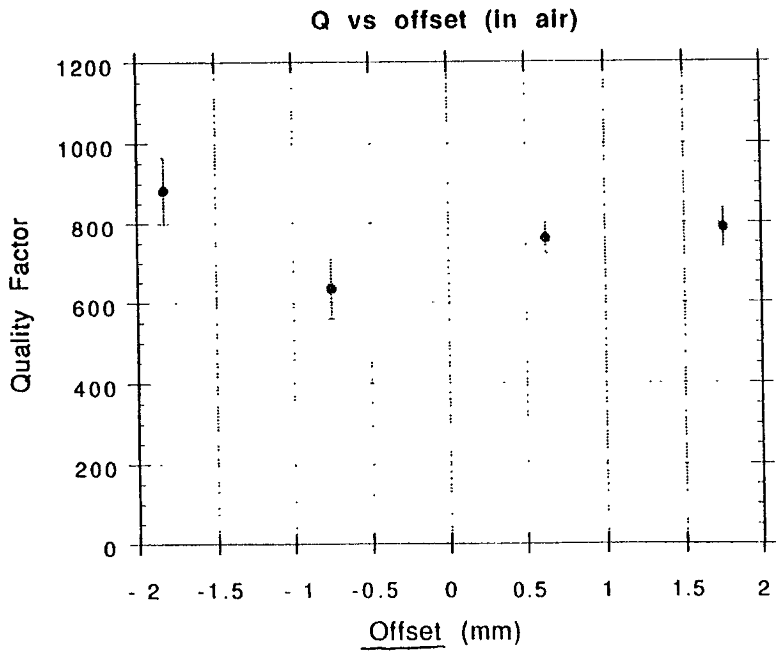

NO RUBBING EFFECT EVEN IF THE SYSTEM WORKS OUT OF ITS STANDARD POSITION

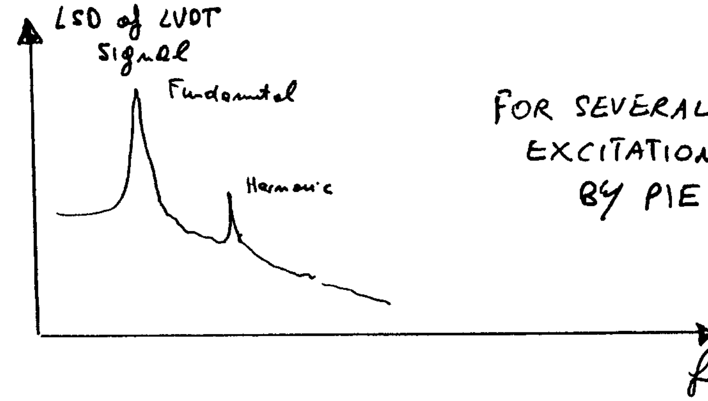

FOR SEVERAL EXCITATIONS BY PIEZO

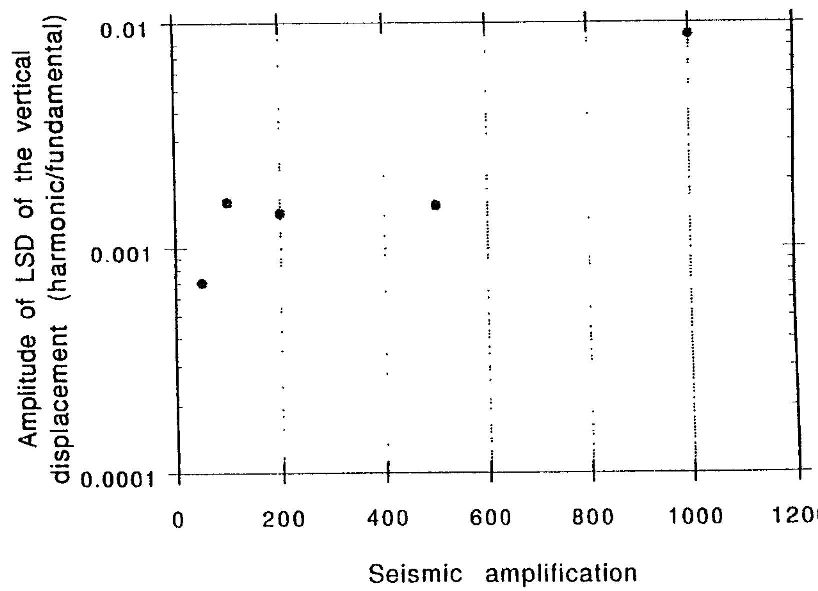

OFFSET = + 1.1 mm

NO UP CONVERSION!

PHASE 2: Antisprings

The following antisprings system has been mounted on the filter

3 lines of 7 magnets (6 x 2 x 1.5 cm) on each of the four supports in a repulsive configuration.

a)

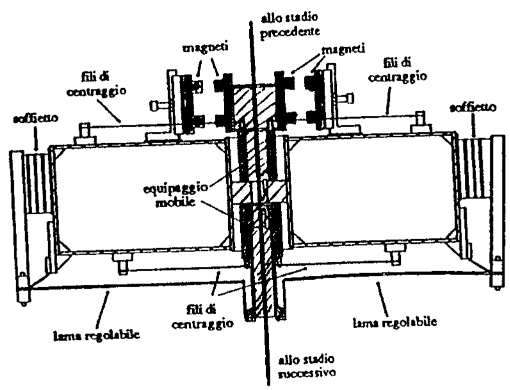

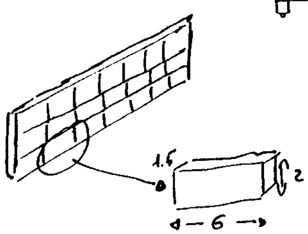

b)

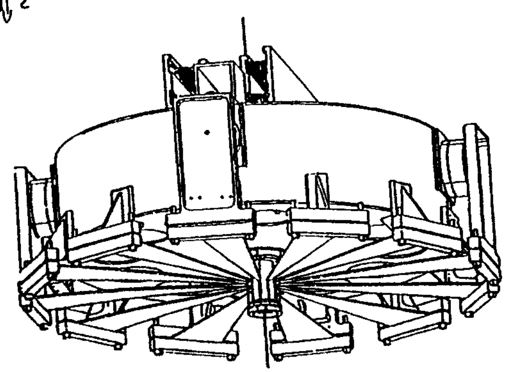

WORKING PRINCIPLE

REPULSIVE CONFIGURATION

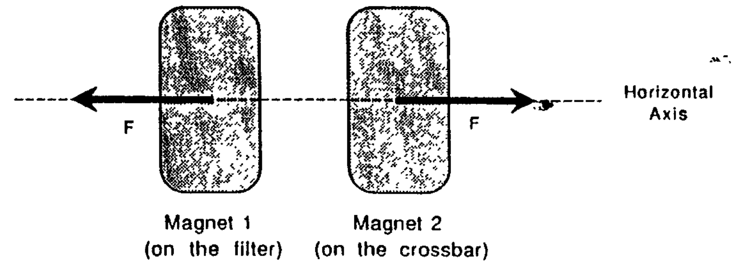

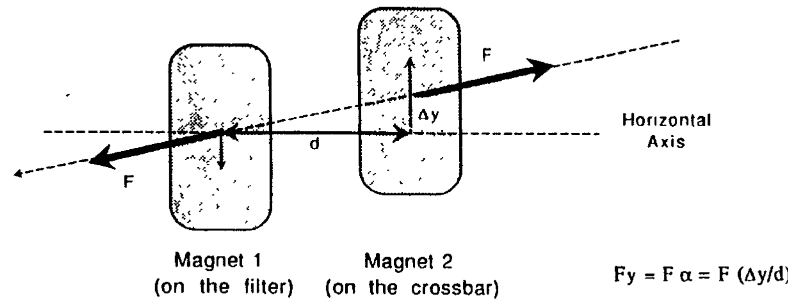

$F_y = F\,\alpha = F\,(\Delta y/d)$

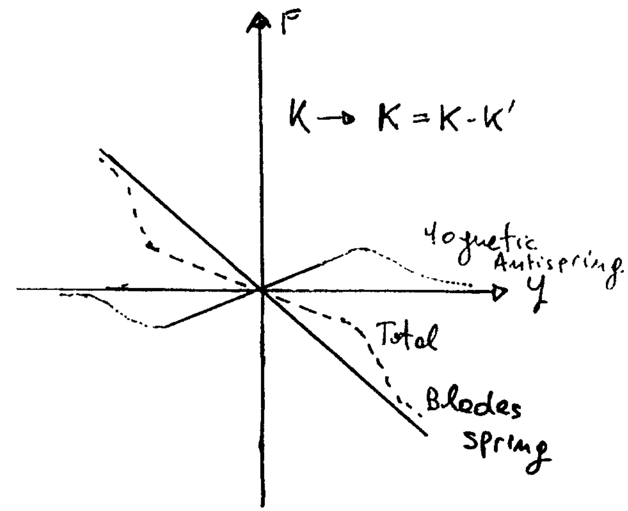

$\left(F_y \propto \frac{\Delta y}{d^2}\right)$

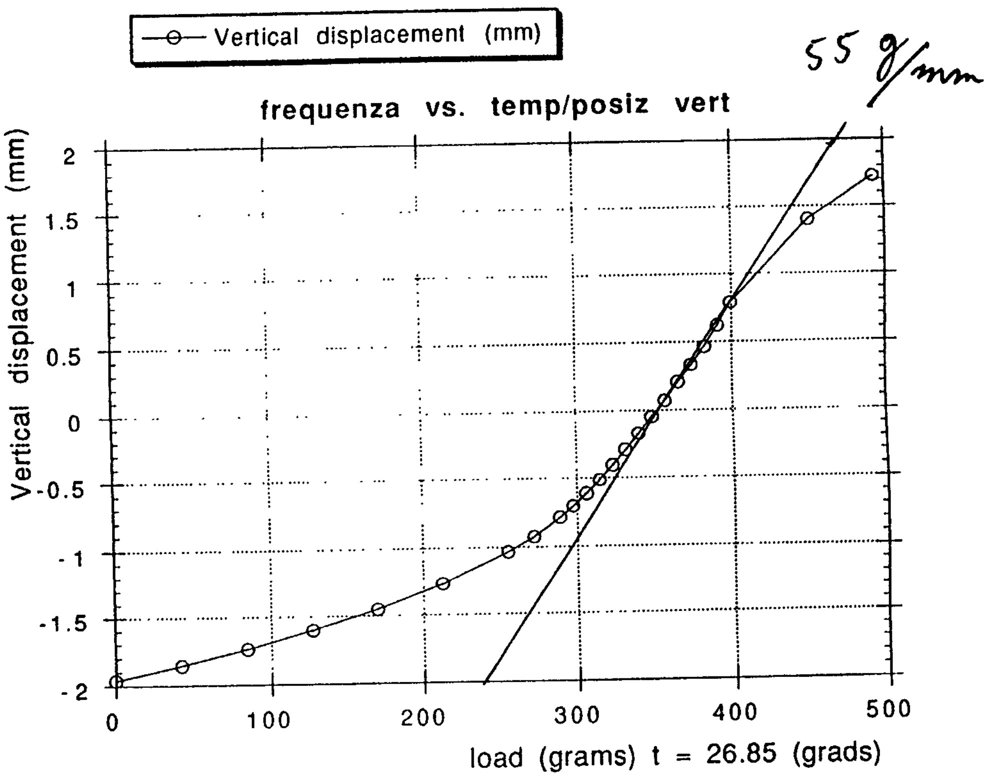

GOAL

TO MAKE THE VERTICAL FUNDAMENTAL RESONANCE FREQUENCY LOWER THAN THE HORIZONTAL ONE (Pendulum = 0.5 Hz) FOR EACH STAGE.

MEASUREMENT

1) Vertical transfer function

2) Vertical resonance frequency as a function of the system positioning (distance and offset)

3) Quality factors

4) Dependence on temperature of the system

In this way a complete characterisation of the system can be attained

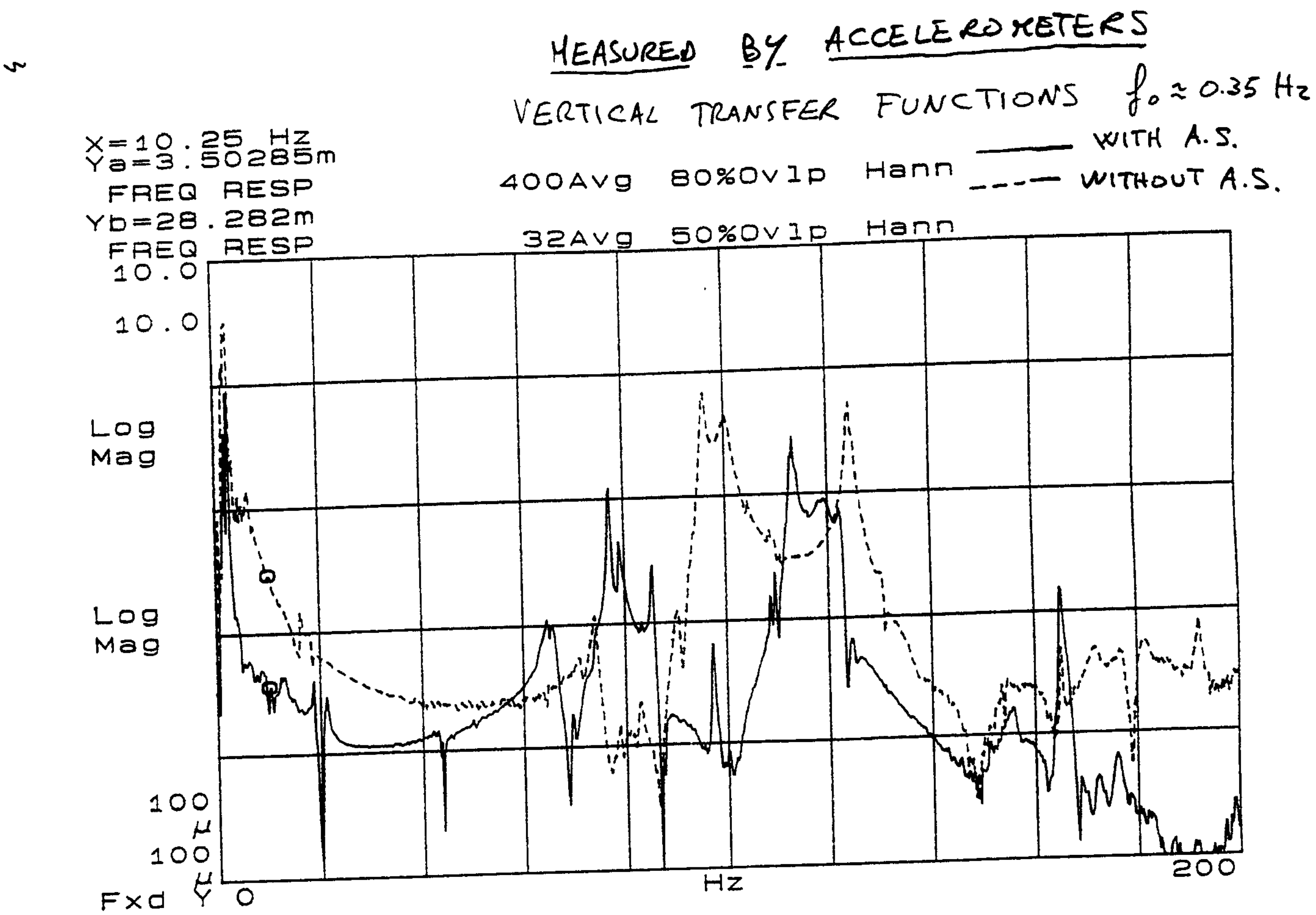

Measurement of

Vertical Resonance Frequence

of Super Attenuator filters

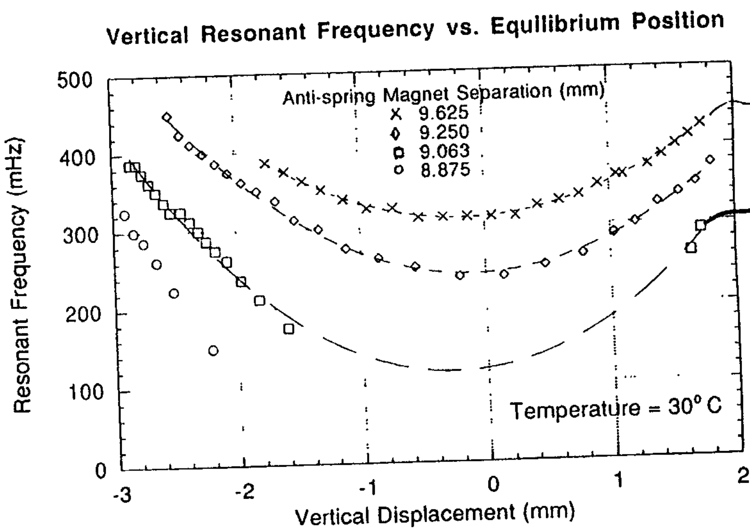

MAGNETS WELL SEPARATED

MAGNETS TOO CLOSE (BISTABILITY)

THE GOAL IS EASILY OBTAINED
(Large Tolerances)

EXPERIMENTAL SET-UP

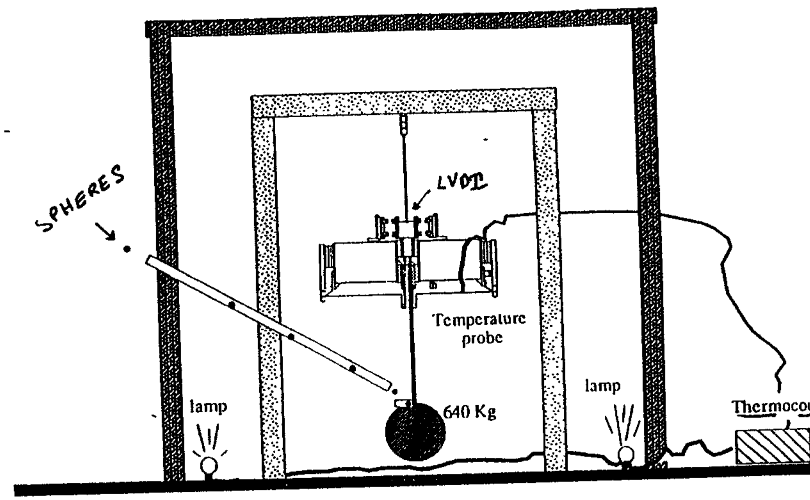

→ CHANGE OF THE RELATIVE VERTICAL POSITION BETWEEN THE MAGNETS

→ SHOCK ⇒ 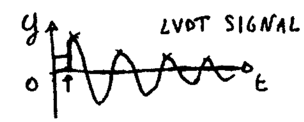 ⇒ $\underline{Q}$, $\underline{\omega}$

MEASUREMENT OF ω_0 (or K) AND Q AS A FUNCTION OF Δy.
(Can be done for several horizontal distances and for several Temperatures)

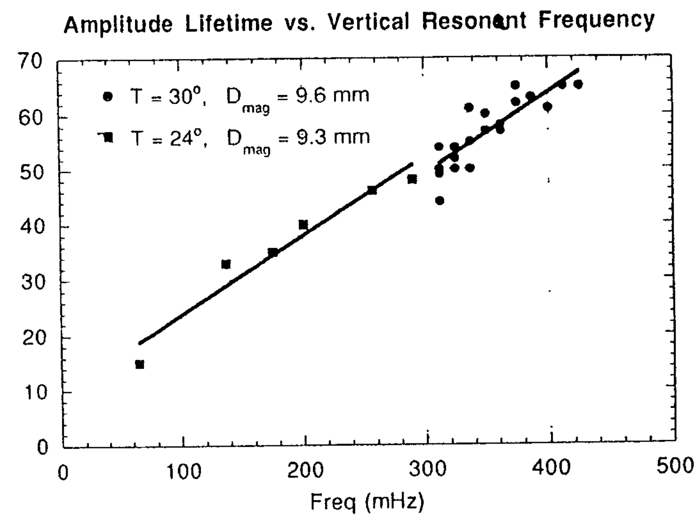

$Q = \omega_0 \tau/2$

$Q \propto \frac{\omega^2}{\omega_0^2} Q_0$

$\Rightarrow$ INTERNAL FRICTION DOMINATES.

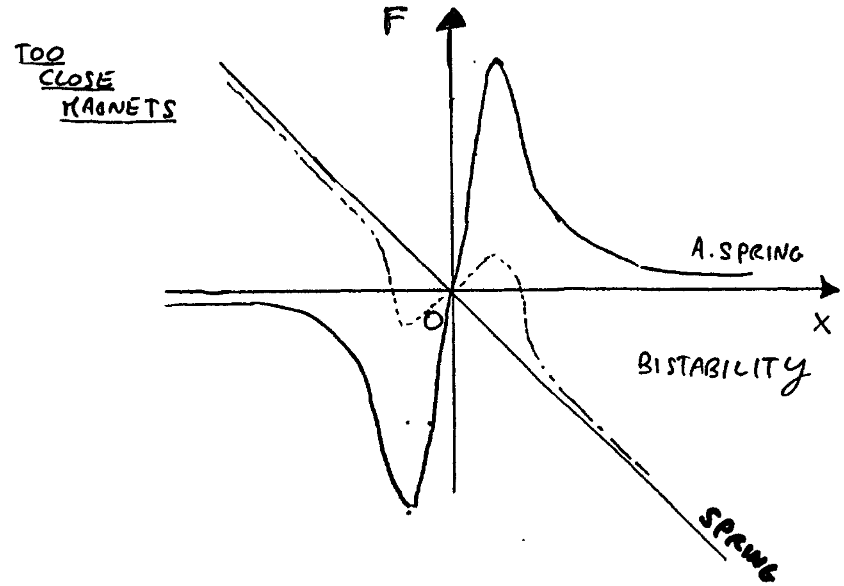

THE FORCE INDUCED BY THE MAGNETS DEPENDS ON TEMPERATURE

$$K_{TOT} = K_{SPRING} - K_{ASPRING} \approx 1.000\ N/\mu$$

$(30.000\ N/\mu)$ $(29.000\ N/\mu)$

A SMALL VARIATION IN K_{AS} CAN BE A LARGE VARIATION IN K_{TOT}

Super Attenuation filters

Working point determination and

Thermal stability

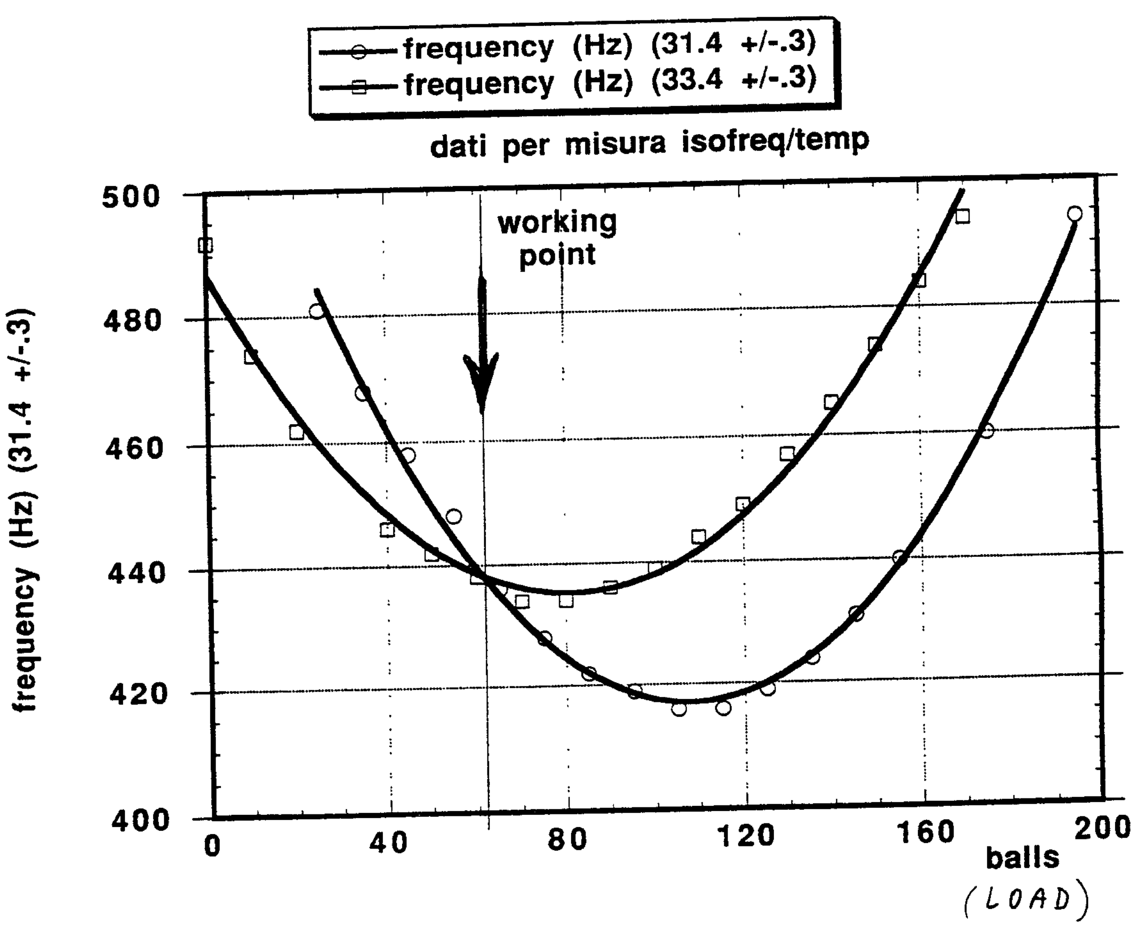

thermal stability
f/dy * dy/dt - df/dt

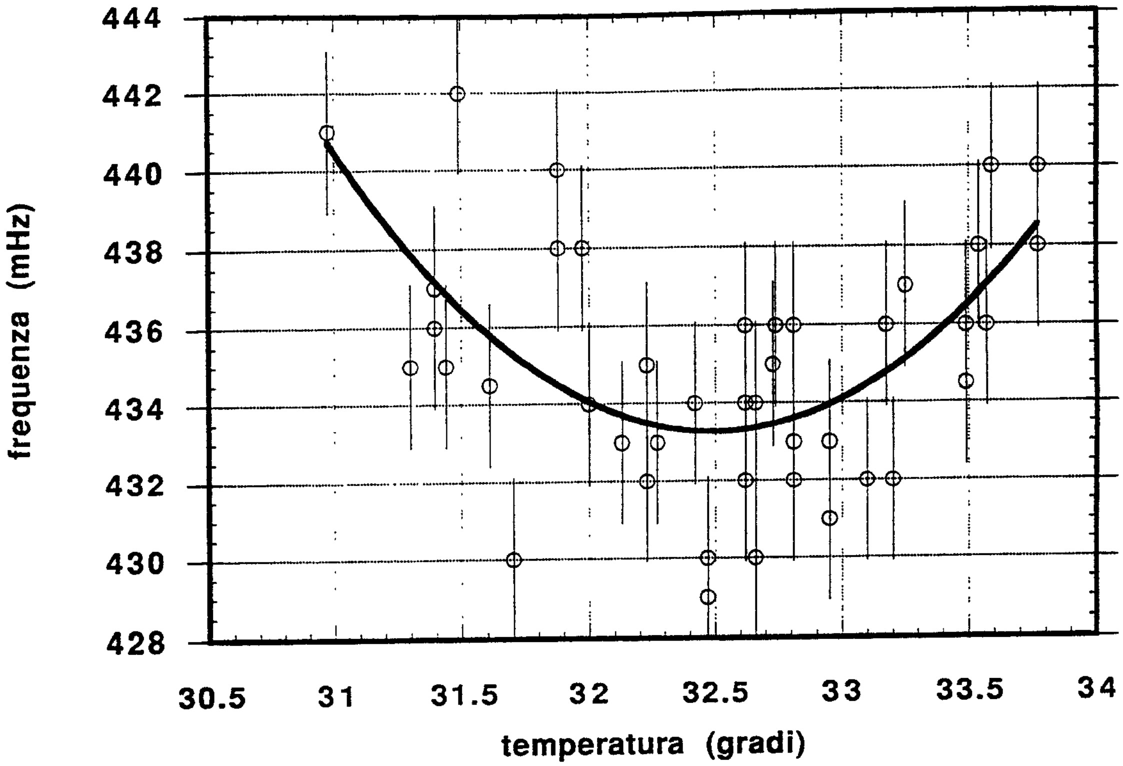

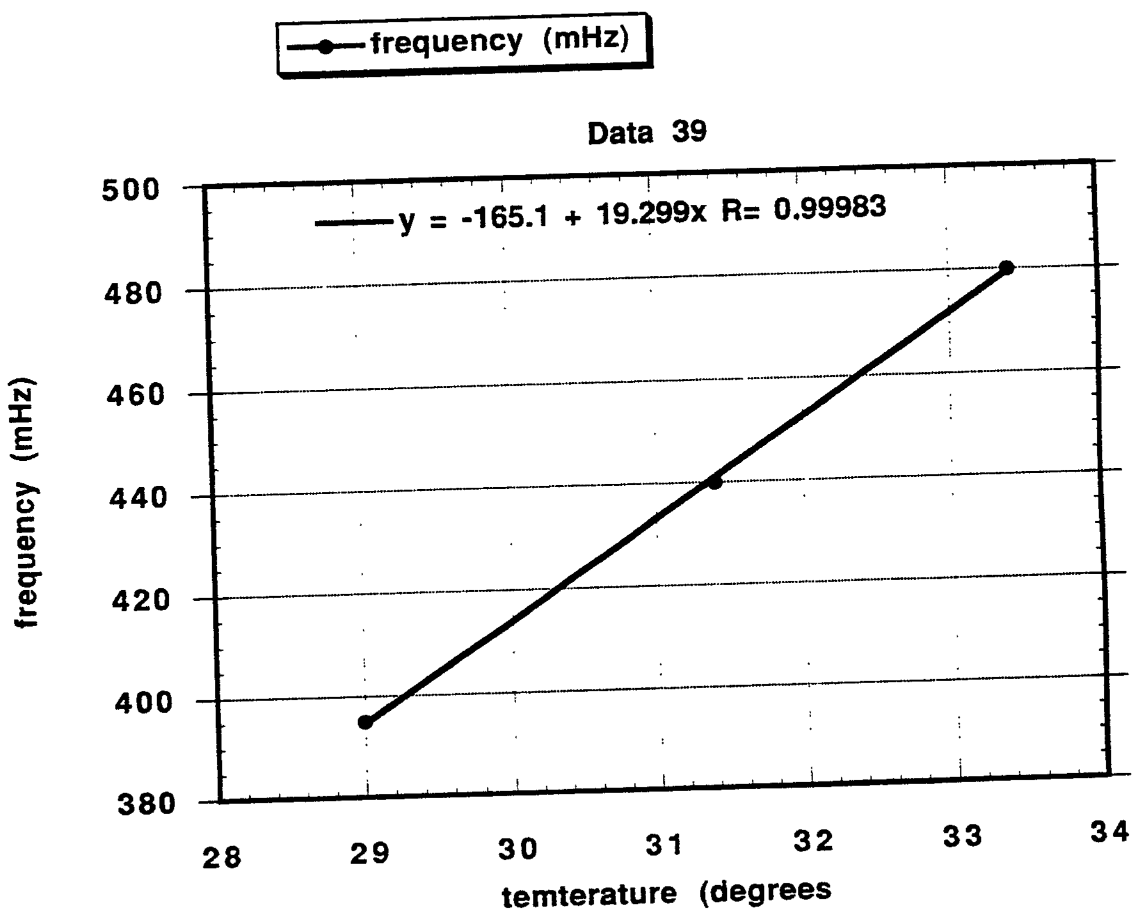

THERMAL DRIFT
FOR F FIXED

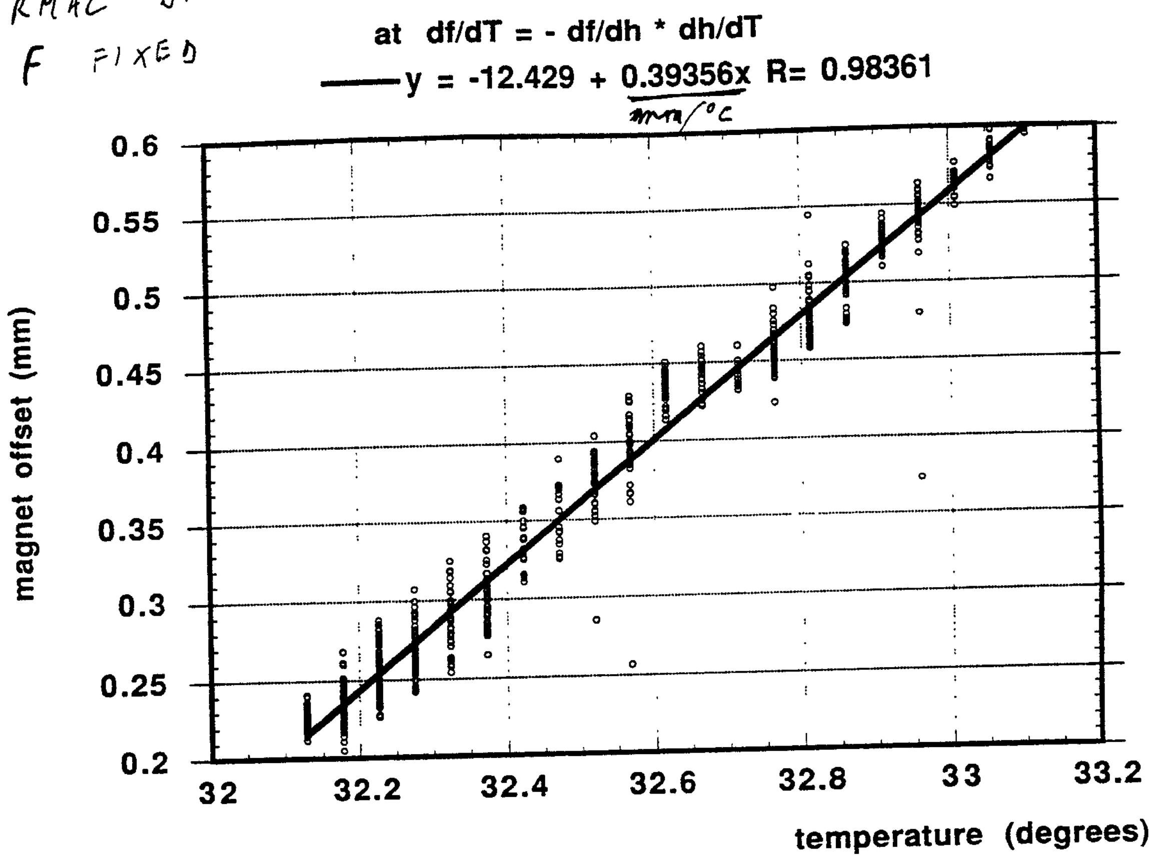

THERMAL DRIFT
FOR F MINIMIZED

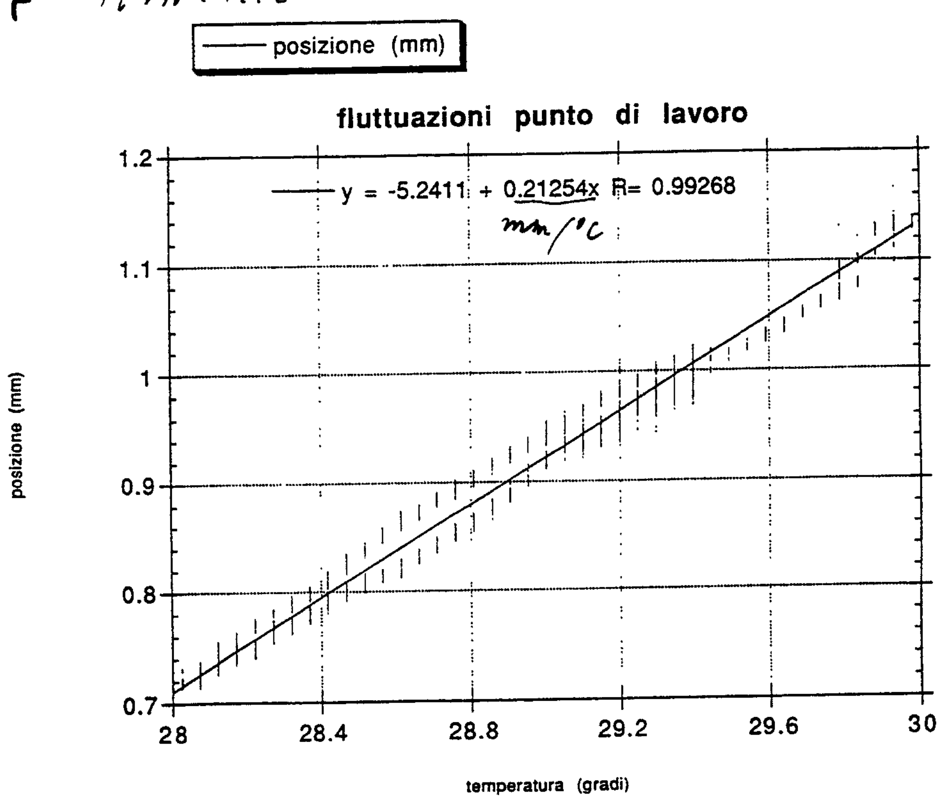

Super Attenuation filters

Creep

Observed abnormally high creep

Discrete process with **random steps** at random intervals

creep steps introduce **internal nanoseisms**

comparable to **attenuated seismic activity**

Must reduce creep induced noise below 10^{-18} m/Hz$^{-1/2}$

which requires **creep activity less than 10^{-4} μm/day** (not measurable)

14

DISPLACEMENT VS. TEMPERATURE

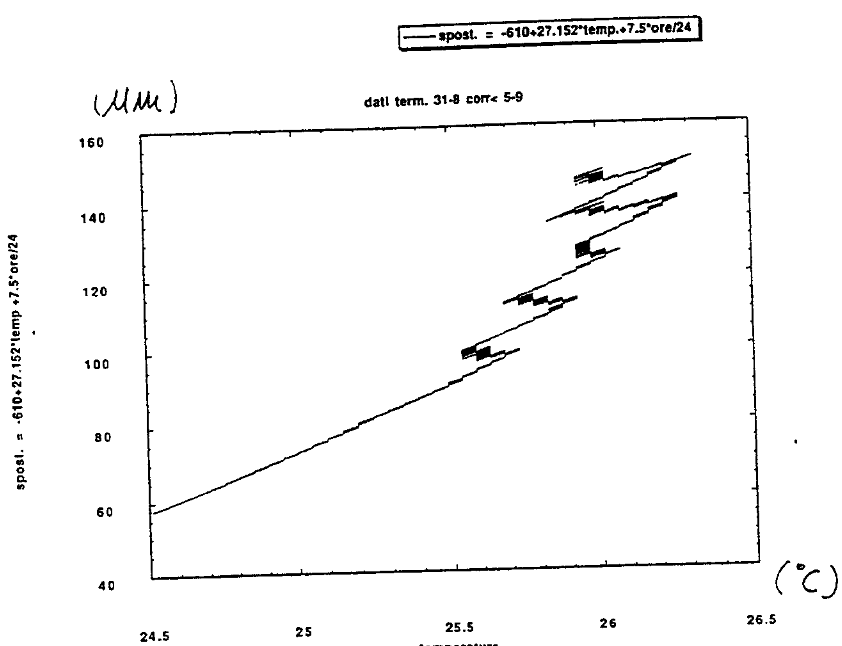

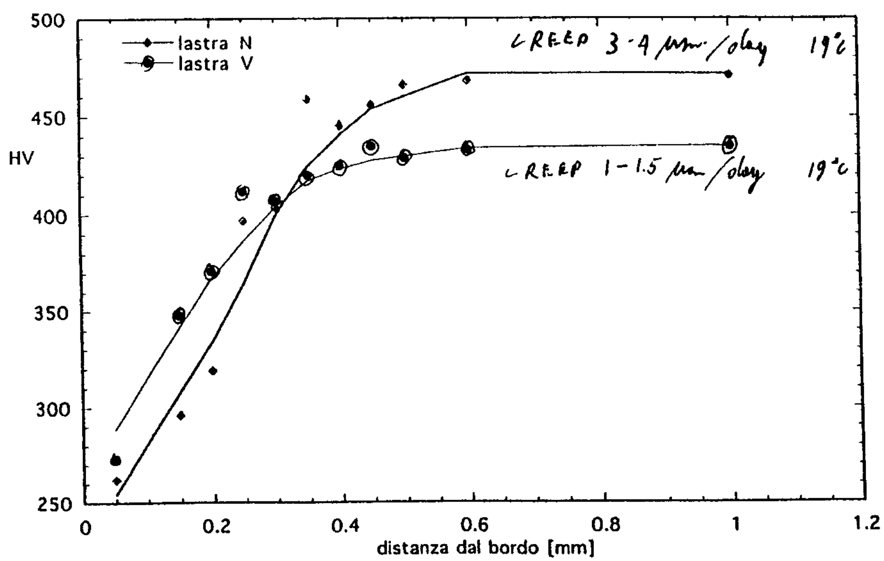

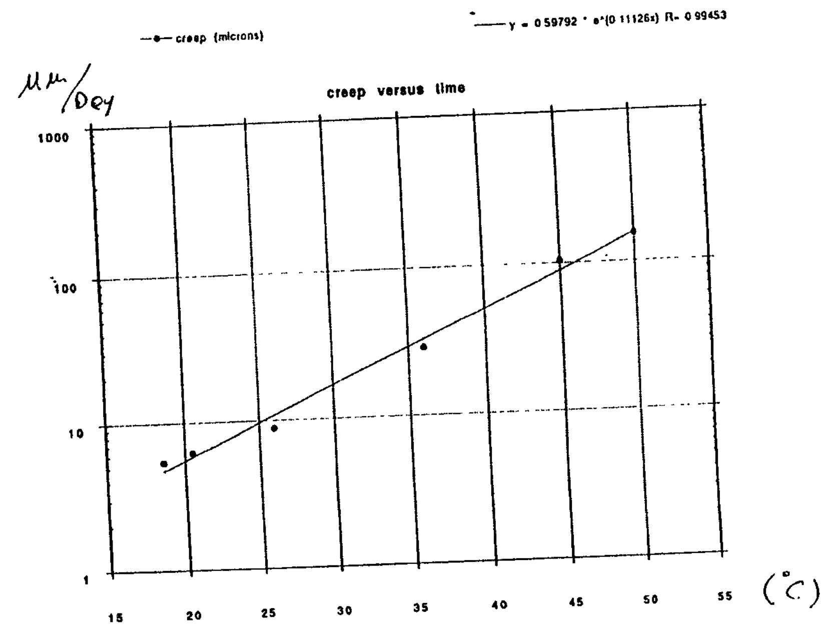

→ CREEP (μm/Day) VS. TEMPERATURE

Super Attenuation filters

Creep

Creep of 1 μm/day is measurable

Creep **step amplitude independant from temperature**

dependent on cristalline structure

Creep **event frequency** $f_{creep} = e^{-\Delta E/KT}$

Measured **creep activity reduction by a factor of 10 every 20° cooling**

Mequire **less than 1 μm/day creep activity 80° above operational temperature**

Test superattenuators at 80°C and operation at -10°C

(Good for outgassing)

VIRGO

INTERNATIONAL CONFERENCE ON GRAVITATIONAL WAVES: SOURCES AND DETECTORS

Cascina (Pisa), Italy March 19-23, 1996

VIRGO KICKOFF MEETING

APPLICATIONS AVAILABLE

PLEASE ENQUIRE AND APPLY A.S.A.P

January 15, 1996 Aspen, USA
1996 Aspen Winter Physics Conference

- Present Status of the Tokyo 300m FP Interferometer (TAMA300)

M. Fujimoto
National Astronomical Observatory (NAO), Japan

- Data Acquisition and Analysis for TENKO100 and TAMA300

Ei-ichi Mizuno
The Institute of Space and Astronautical Science (ISAS), Japan

---

Laser interferometer GW detectors in Japan
(Arm length > 10m)

- Technology
- Researchers

→ transfer

This talk

	ISAS	NAO	
	10m DL (TENKO10)		
1990	↓		U. Tokyo etc. (3m FP)
	100m DL (TENKO100)	20m FP	
1995	Data acquisition system 100 hours of data taking	300m FP (TAMA300) Data acquisition system	
		Future antenna	

Project Director

Yoshihide KOZAI

National Astronomical Observatory (NAO)

Institute for Cosmic Ray Research (ICRR)

National Laboratory for High Energy Physics (KEK)

Institute of Space and Astronautical Science (ISAS)

University of Tokyo

University of Electro-Communications

Kyoto University

300-m laser interferometer fundamental parameters

target sensitivity

$h=3\times10^{-21}$
@300Hz

arm-length

300m

detector type

recombined Fabry-Perot
type with power recycling

cavity finesse

520

laser

injection locked LD pumped Nd:YAG
output power 10W
wavelength 1064nm
recycling gain 10

vacuum

10^{-6}Pa

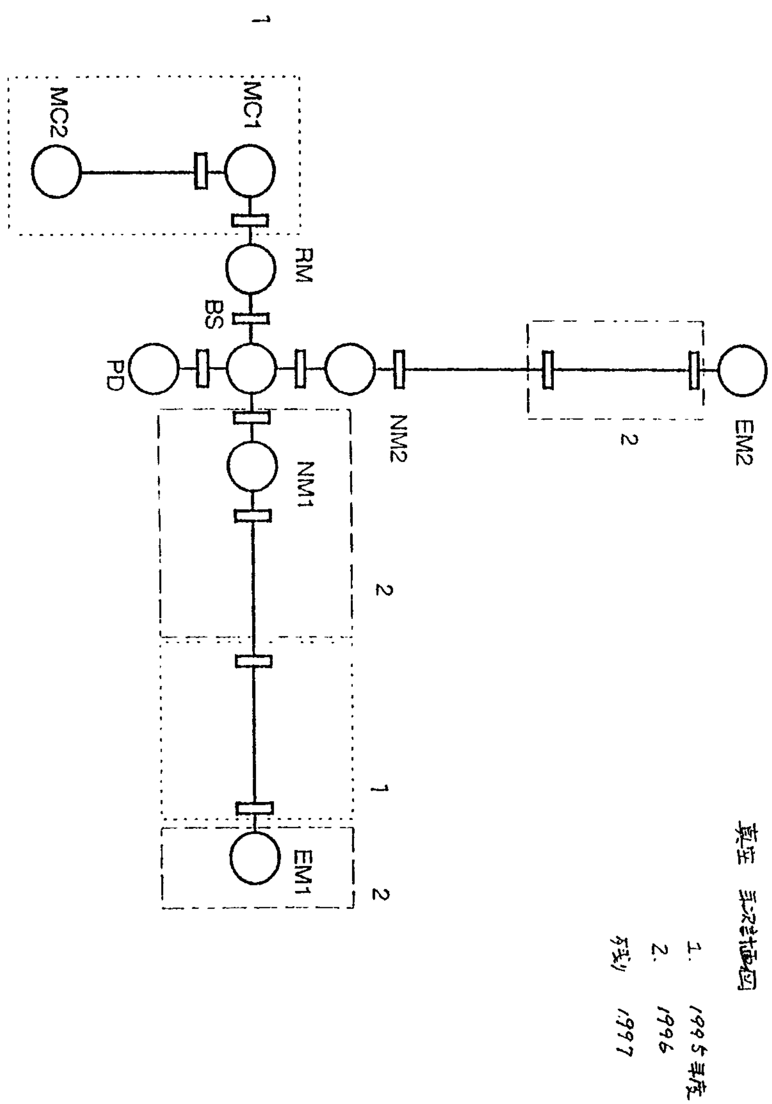

SCHEDULE OF THE LASER INTERFEROMETER GRAVITATIONAL WAVE DETECTORS

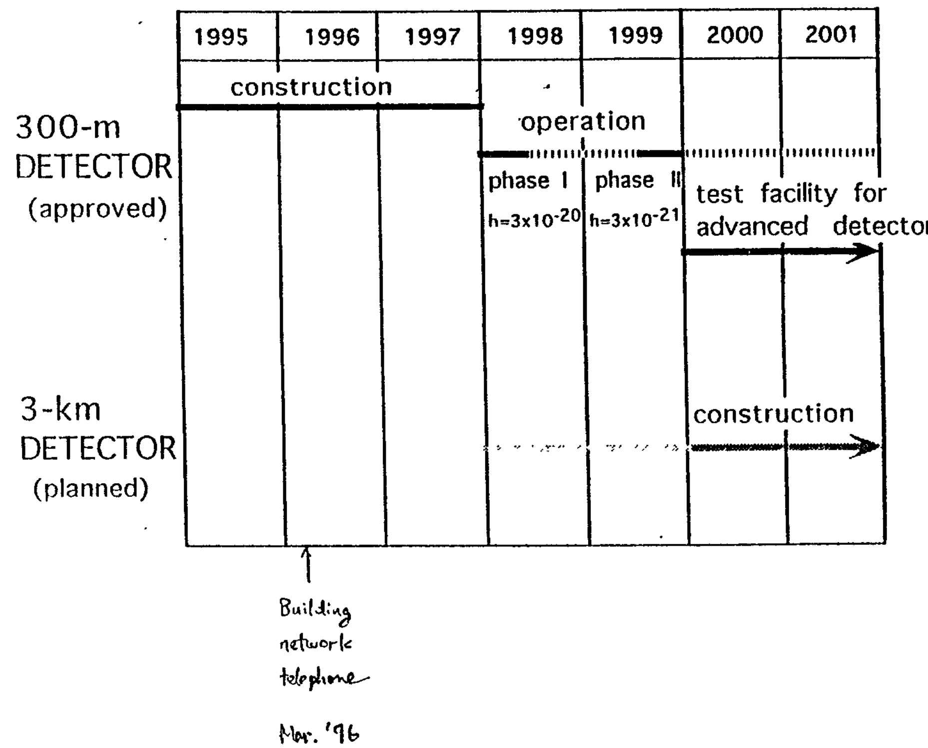

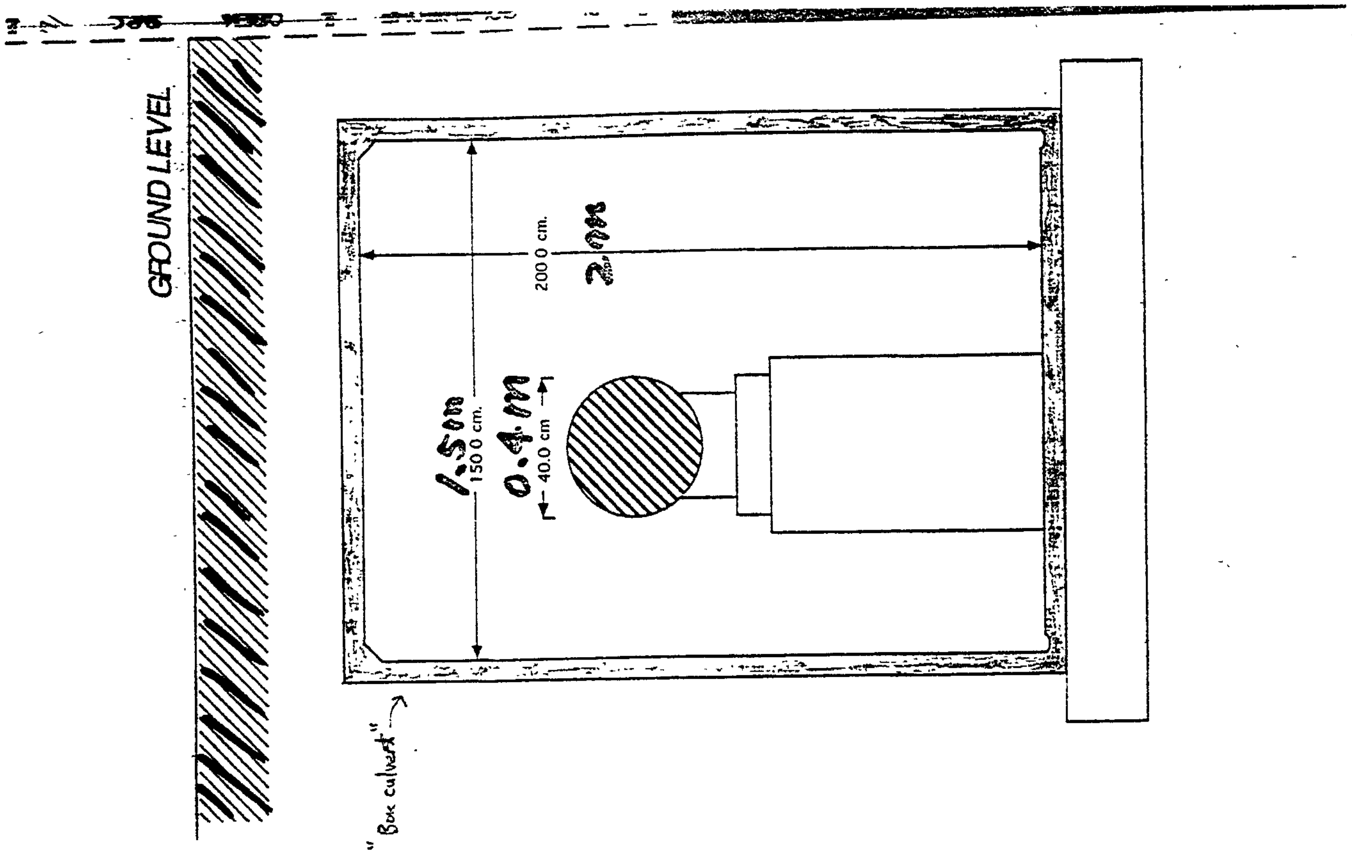

TAMA300 data management (d300)

Tasks

Data acquisition

High rate (600 kbytes/sec), 300 channels, A week of online data storage

Realtime monitoring of slow data

CRT, printers, through network

Realtime data reduction, triggering and analysis

Strain sensitivity (h), analysis triggering by h

Template matching, Data reduction (by channels and frequency bands)

Remote control of instruments

Vacuum system, Laser system, through EPICS

Feedback over 300m

End room -> Near mirror signal feedback through fiber optics

Database management

User interface, data format, internet services

TAMA300 data amount

High speed (20kHz)

- Interferometer signal
  - Low frequency (<700Hz)
  - High frequency (>500Hz)
- Feedback
  - Main mirror (X2)
  - Beam splitter
  - Recycling mirror
  - Mode cleaner
- Laser
  - Intensity
  - Frequency (X2)
- Realtime analysis
  - Strain sensitivity (h)
  - Various filters (X3)

20kHz * 14Ch. * 16bits
= 560 kbytes/sec

Medium speed (200Hz)

- Mirror angles, positions
- Beam positions
- Servo status
- Housekeeping
  - Ground motion
  - Accoustic noise
  - Powerline voltage
  - Magnetic field
- etc.

200Hz * 100Ch. * 16bits
= 40 kbytes/sec

Low speed (2Hz)

- Temperature
- Atmospheric pressure
- Laser status
- Vacuum pressure
- Vacuum instruments status
- GPS monitor
- etc.

2Hz * 200Ch. * 16bits
= 0.8 kbytes/sec

Total: 600 kbytes/sec

Policy

Networks-based system and interface

Fundamental network:	TCP/IP + Ethernet
User interface:	Unix + X-window + EPICS

Separation of several different kind of data by networks

High speed data:	Reflective memory - VXI
Low speed data:	VME - Ethernet - EPICS
Vacuum monitoring:	GPIB - Ethernet - EPICS
Analog data transfer:	TTL data transfer through fiber optics

Interface with other observations (other GW antennas, γ-ray, infrared, etc.)

Time keeping:	GPS / ntp

Establish an international standard data format
WWW information services

Collaboration with other groups (LIGO/VIRGO/GEO/etc.)

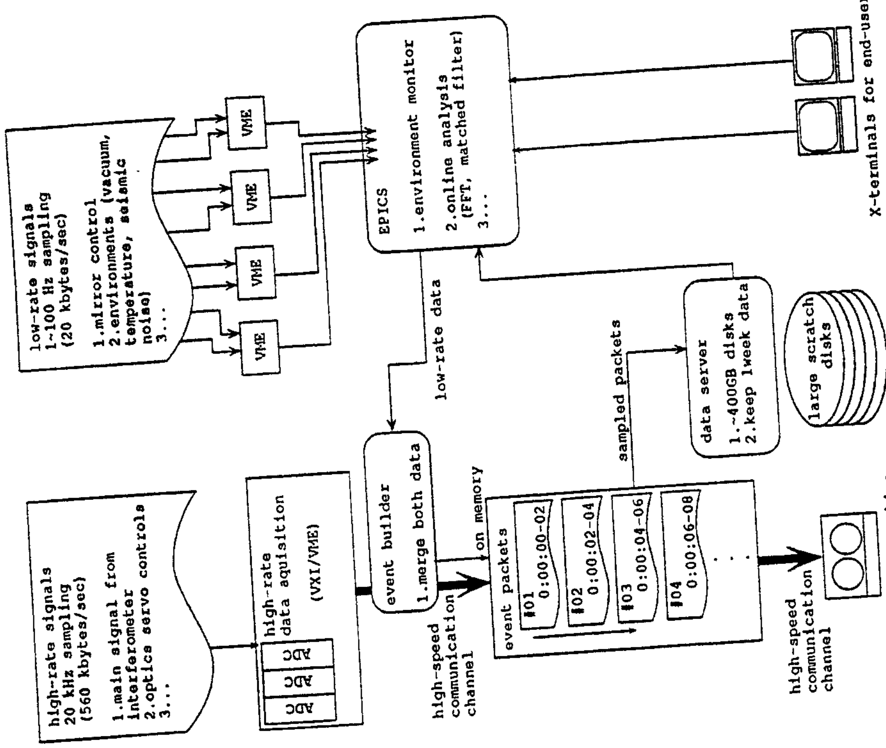

Figure 1: Schematic view of the data flows between the high-rate data-acquisition, the EPICS, the event builder, the data server, and the raw-data archiver.

TENKO100 long-term operation

Objectives:

- Study the reason why interferometer unlocks
- Correlations between various kind of signals
- Analysis of non-stationary noise, with long time scales
- Establishment of the data acquisition system and the realtime monitoring system
- Preparation of the TAMA300 data acquisition system

Period:

(1) July 24 - August 10, 1995

Operation: 100 hours, Data recording: 48 hours

Improvement of the system

(2) December 4 - 25, 1995

Operation: unknown, Data recording: 30 hours

12/19

TENKO100 recorded data

DL pockels cell feedback (300-2kHz)
Laser frequency (AC)
Laser intensity (AC)
Ground motion (5 channels)
Accoustic noise

High speed sampling

10 ksamples/sec * 2 bytes/sample * 9 channels
= 180 kbytes/sec

amplitude detection

amplitude detection

1 kHz sensitivity
500-2kHz sensitivity
Main loop gain monitor
DL dark fringe
Absolute control dark fringe
Laser frequency (DC)
Laser intensity (DC)
Ground motion (3 channels)
Accoustic noise (4 channels)
Vacuum pressure
Temperature
Atmospheric pressure
Mirror displacement

Low speed sampling

25 samples/sec * 2 bytes/sample * 30 channels
= 2.5 kbytes/sec

13/19

951220.PC.500Hz-2kHz

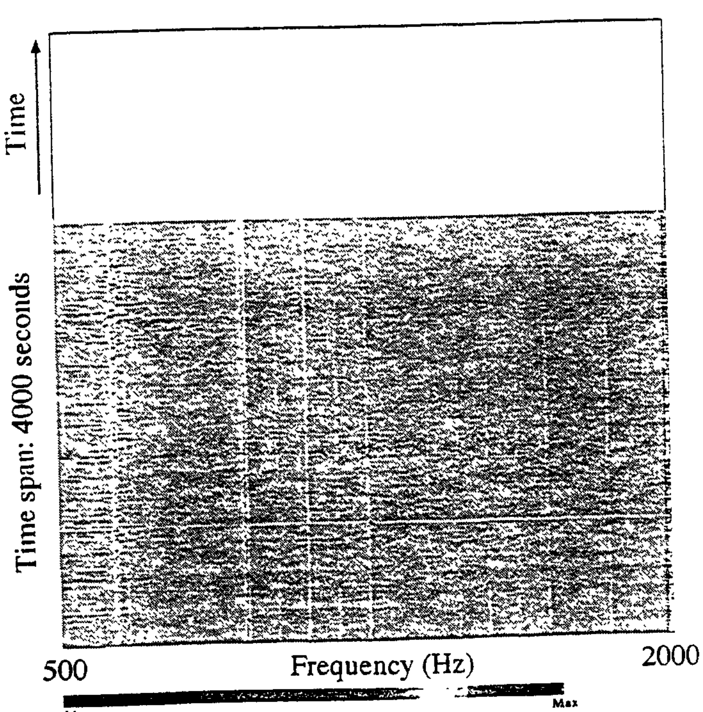

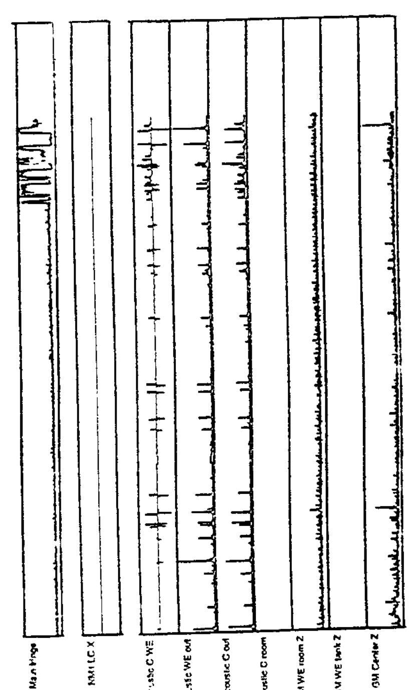

14/19

951219.MainPC

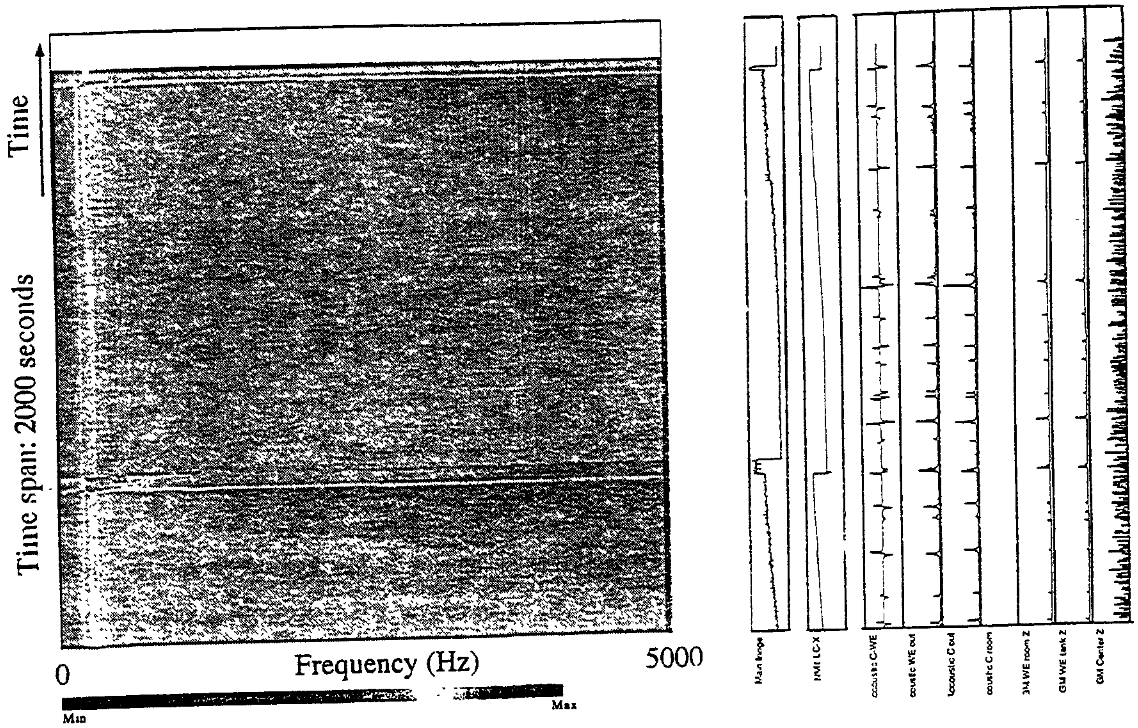

15/19

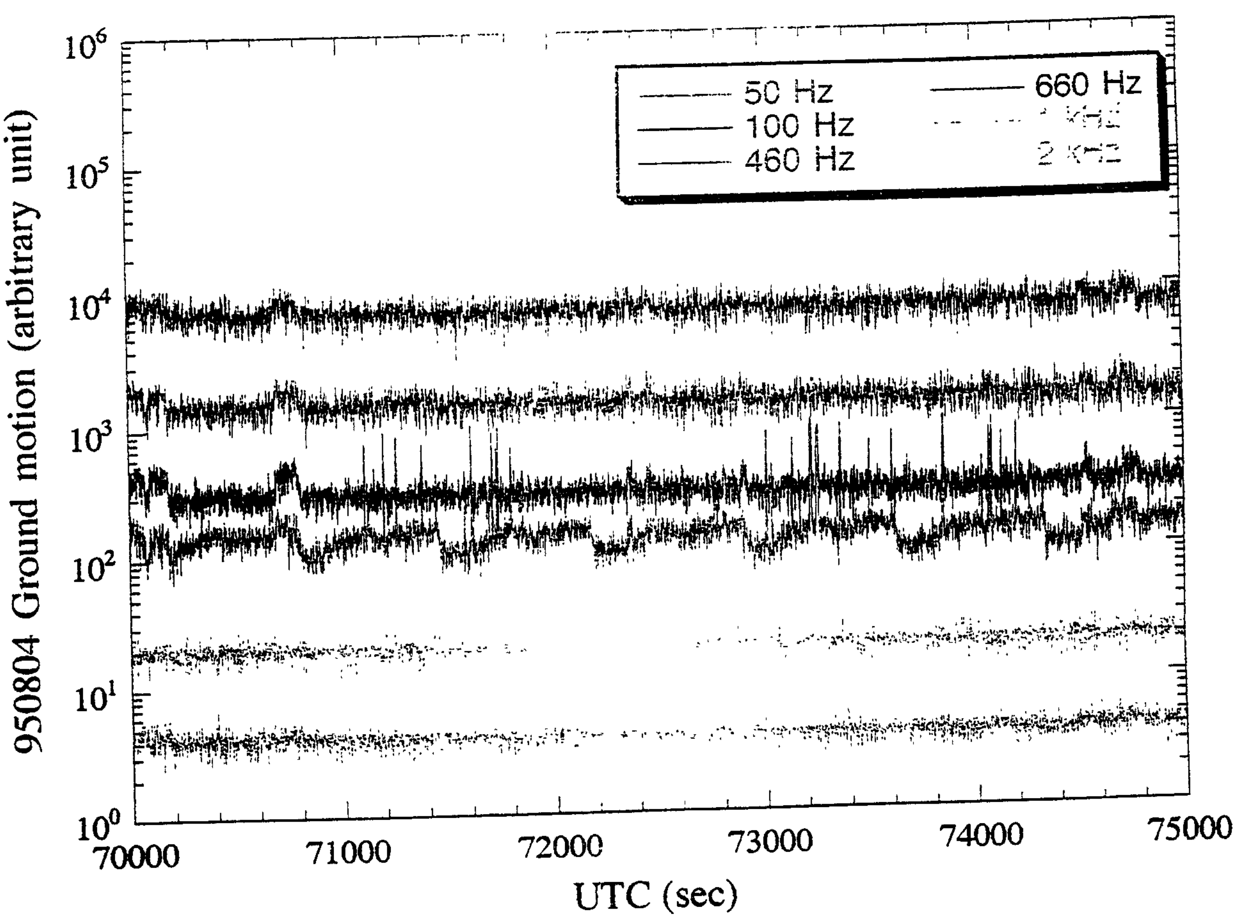

16/19

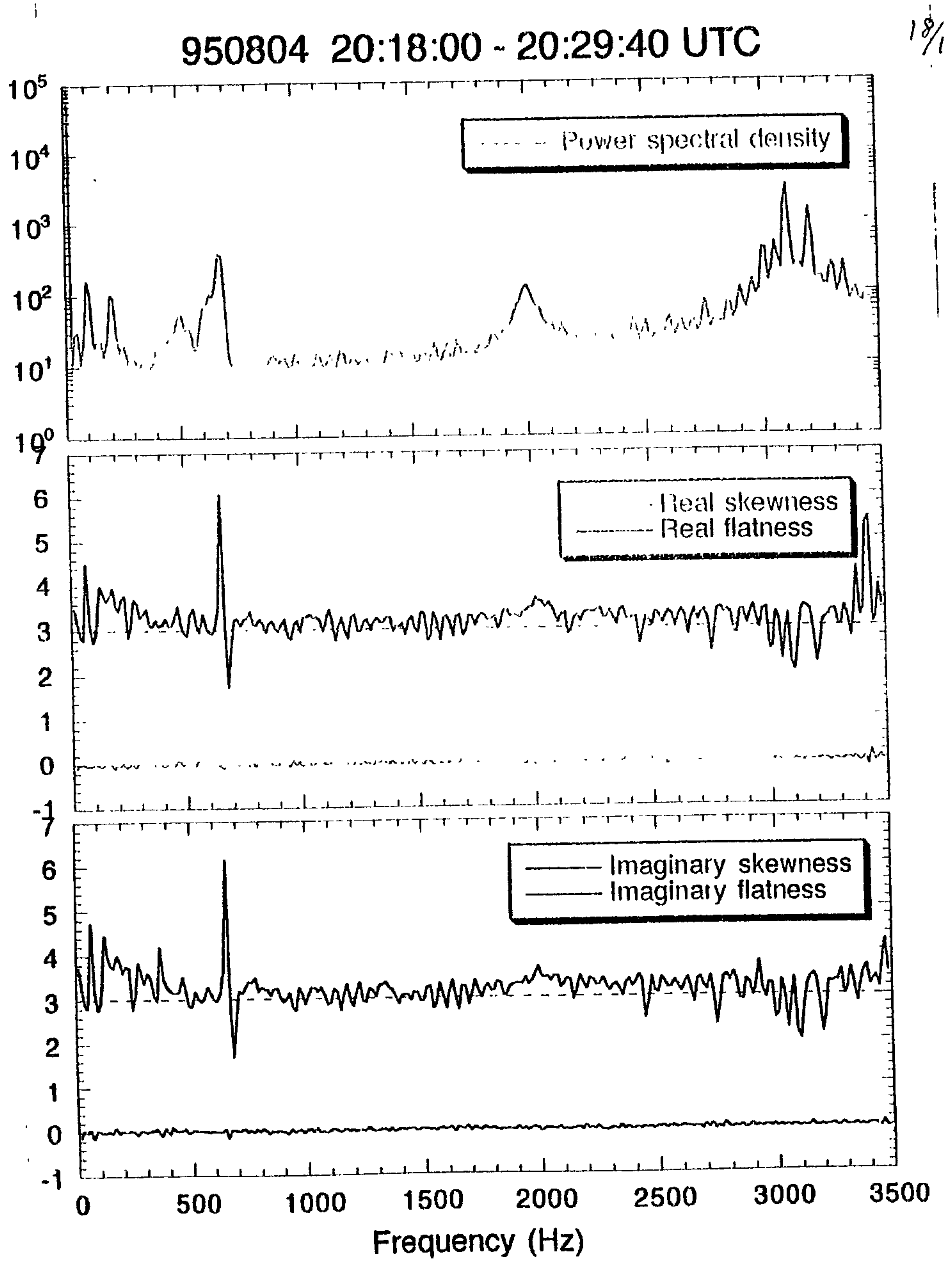

950804 20:18:00 - 20:29:40 UTC
Power spectral density
Real skewness
Real flatness
Imaginary skewness
Imaginary flatness
Frequency (Hz)

18/19

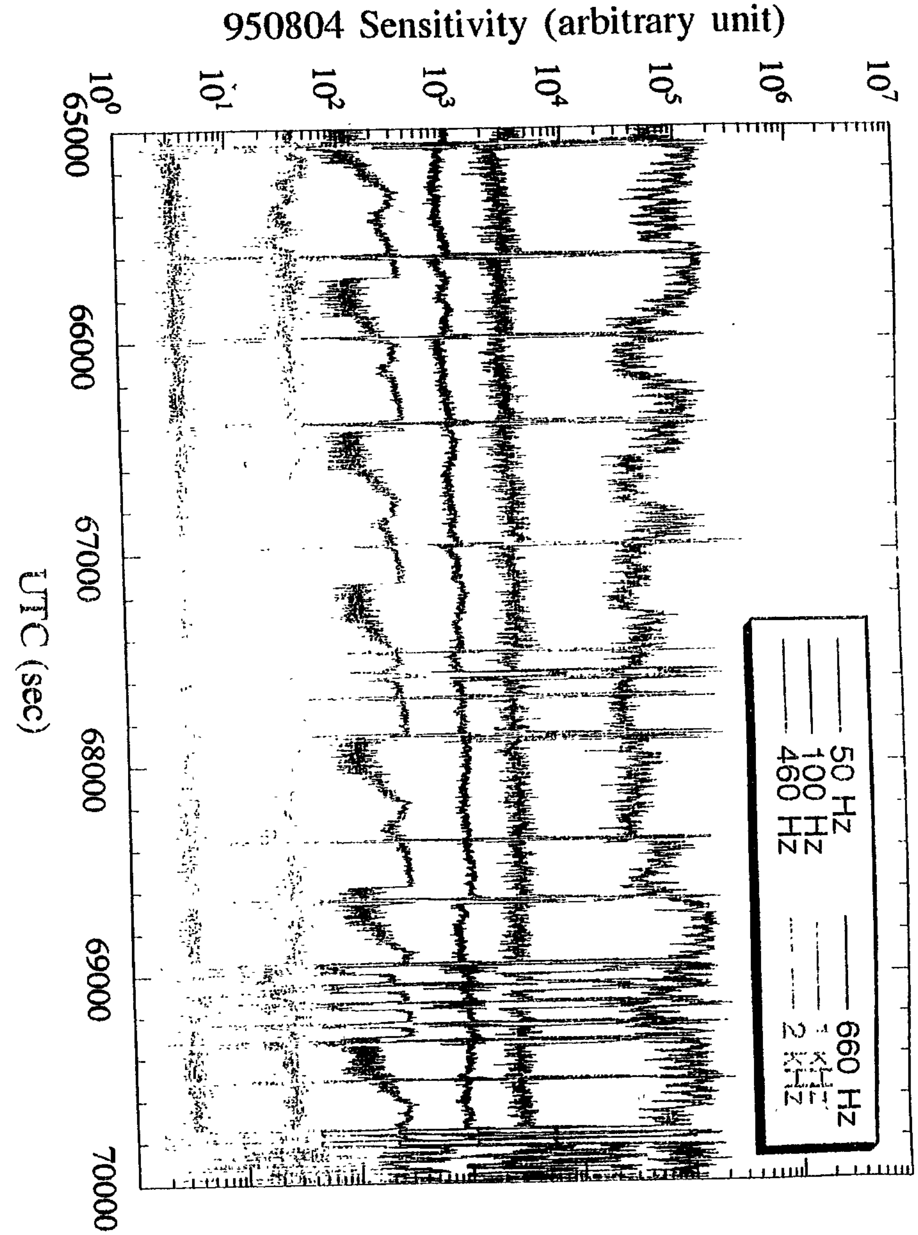

950804 Sensitivity (arbitrary unit)
UTC (sec)
50 Hz
100 Hz
460 Hz
660 Hz
1 kHz
2 kHz

What has become clear from the long-term operations?

- Interferometer signal and the unlocking of the system

  Sensitivity varies by factor of 10 (max) from day to day
  (especially below 600Hz)

  Slow motion of the DL mirror changes the dark fringe condition

  Dark fringe condition is highly correlated with the unlocking

  48Hz ground motion, due to an air conditioner, has a time scale
  of 10 minutes, and it also makes the system unlock.

  Car passing the street nearby, also makes the system unlock

- Data acquisition system and analysis

  Daily variation of the analog signal was difficult to handle
  with a small dynamic range (12 bit). Several days of data
  were lost. Choice of filter is important.

  Data compression at the analog stage simplified the data handling

- Future

  Realtime data compression

  Realtime data analysis

  A flag showing the validity of data

Revised manuscript submitted to *Physical Review Letters* on November 27, 1995

A Sagnac Interferometer for Gravitational Wave Detection

Ke-Xun Sun, M. M. Fejer, Eric Gustafson and Robert L. Byer

Edward L. Ginzton Laboratory, Stanford University, Stanford, CA 94305-4085

Abstract

We have investigated a zero-area Sagnac interferometer as a broadband gravitational wave detector. Frequency response measurements of a laboratory-scale interferometer are in excellent agreement with theory. The measured contrast ratio, 0.996, is insensitive to induced birefringence, laser-frequency variation, arm-reflectance imbalance, and DC mirror displacement. A near shot-noise-limited phase sensitivity of 3×10^{-9} rad/$\sqrt{\text{Hz}}$ was measured at the interferometer's maximum sensitivity frequency, 90.9 MHz.

PACS numbers: 04.80.Nn, 07.60.Ly, 42.25.Hz, 42.62.-b

POST DEADLINE
PAPER
MONDAY, JAN 15, 1996
Aspen WORKSHOP

Edward L. Ginzton Laboratory
Stanford University
Stanford, CA

Stanford Advanced Gravitational-Wave Laser Interferometer Program

GALILEO

Principal Investigator
Program Director of Galileo
Robert L. Byer
Robert L. Byer

Co Investigators
Daniel B. DeBra
Daniel B. DeBra

Martin M. Fejer
Martin M. Fejer

James S. Harris
James S. Harris

Peter F. Michelson
Associate Director of Galileo
Peter F. Michelson

Yoshihisa Yamamoto
Yoshi Yamamoto

Richard E. Taylor
Richard E. Taylor

October 19, 1995

p 3

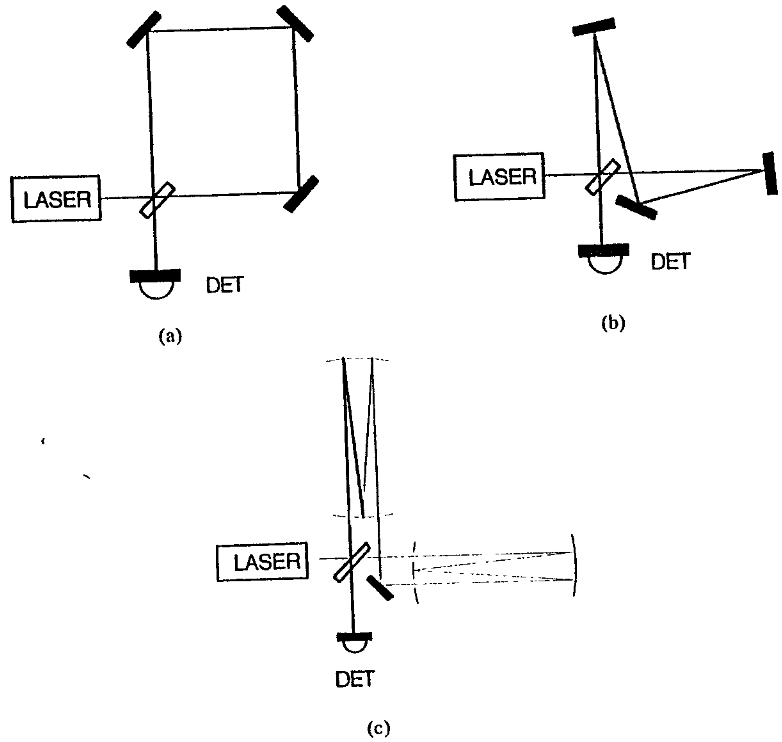

Figure C19 (a) Sagnac interferometer for rotational sensing (b) Sagnac interferometer for displacement sensing. Rotational sensitivity is suppressed by area cancellation. (c) Two-round trip Delay line Sagnac interferometer for gravitational wave detection.

I. The Sagnac Common Path Interferometer

The Sagnac interferometer, invented in 1910 for rotation sensing, is a common-path interferometer in which waves traveling in the opposite direction experience identical optical paths. In the original version of this interferometer, and the version most widely used today for laser gyro rotation sensing, the Sagnac interferometer is an open ring that encompasses an area A. The rotation sensitivity is increased as the product NA where N is the number of times that the laser beam traverses the perimeter of the enclosed area. Fiber optics is used today to increase N and yet maintain the rotation sensitivity in a

p 4

Co Investigators
Daniel B. DeBra
Martin M. Fejer
James S. Harris
Peter F. Michelson
Yoshihisa Yamamoto
Richard E. Taylor

Principal Investigator
Robert L. Byer
Ginzton Laboratory
Stanford University
94305-4085
tel (415) 723 0226
fax (415) 723 2666

The Null Area Sagnac Interferometer for Gravitational Wave Detection

The concept of the common-path, reciprocal-path interferometer

Calculated Response Function for a LIGO scale interferometer

Comparison with the Michelson Interferometer

Laboratory experimental measurements

Response function

Contrast Ratio

Phase sensitivity measurements

near quantum limited phase sensitivity at 90 MHz

Signal extraction and detector local oscillator p5

$$|\Delta\phi| = \frac{4 f_l h_g}{f_g} \sin^2(\pi \tau_s f_g), \qquad \textit{Sagnac interferometer.} \qquad (2)$$

The absolute magnitude of the differential phase for a Michelson interferometer which uses delay lines rather than Fabry-Perots in the arms can be calculated similarly [2],

$$|\Delta\phi_m| = \frac{2 f_l h_g}{f_g} |\sin(\pi \tau_s f_g)|, \qquad \textit{Michelson interferometer.} \qquad (3)$$

For both the Sagnac and the Michelson interferometers, the single arm storage time τ_s is defined as $\tau_s = \frac{2NL}{c}$, where L is their arm length, N is the number of bounces on one end mirror of the delay line, and c is the speed of light.

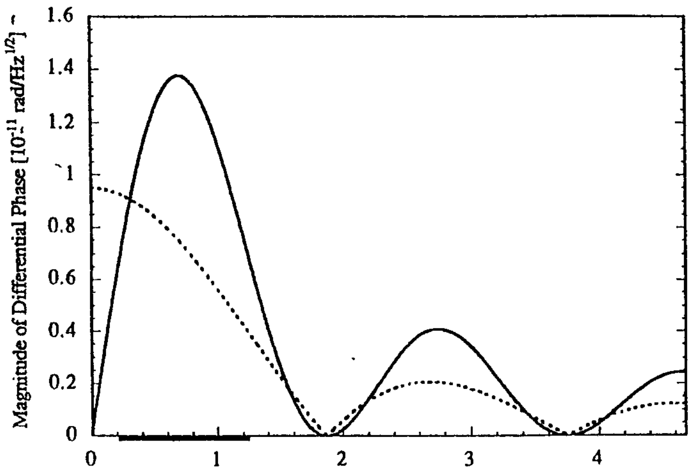

Figure 1(c) shows the response function for 4-km 20 bounce ($N = 20$) LIGO-scale interferometers. The Michelson interferometer has its peak response at DC and sub-peaks at frequencies determined by the transcendental equation $x = \tan x$, where $x = \pi \tau_s f_g$. The Sagnac interferometer has its peak and sub-peak responses at frequencies determined by $2x = \tan x$. The first and highest peak occurs at $f_{g,max} = 0.37/\tau_s = 0.74/\tau_{loop}$, where τ_{loop} is the loop time of the Sagnac interferometer. Setting τ_s allows the Sagnac peak frequency to be tuned to the gravitational wave band of interest, and for this LIGO example $f_{g,max} \approx 690\,\text{Hz}$. The first leaf of Sagnac interferometer responses has a 3-dB bandwidth of $0.54/\tau_s$, which for the LIGO example extends from 220 to 1250 Hz.

p 6

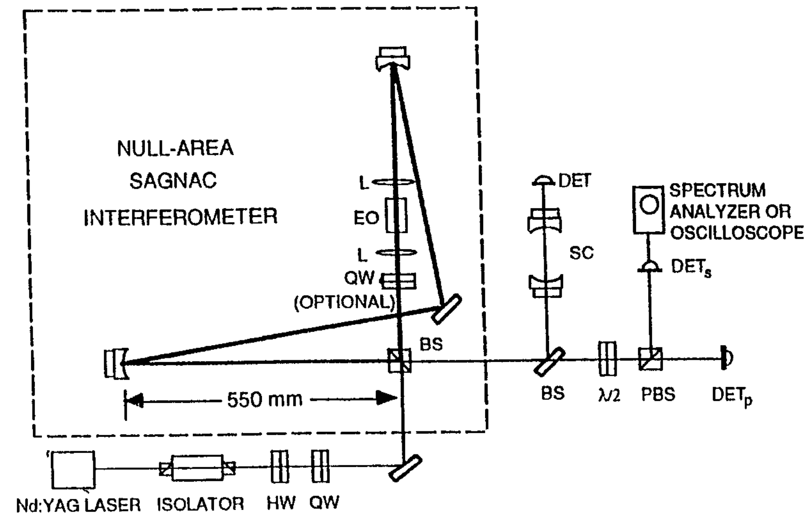

Figure 2 (a)

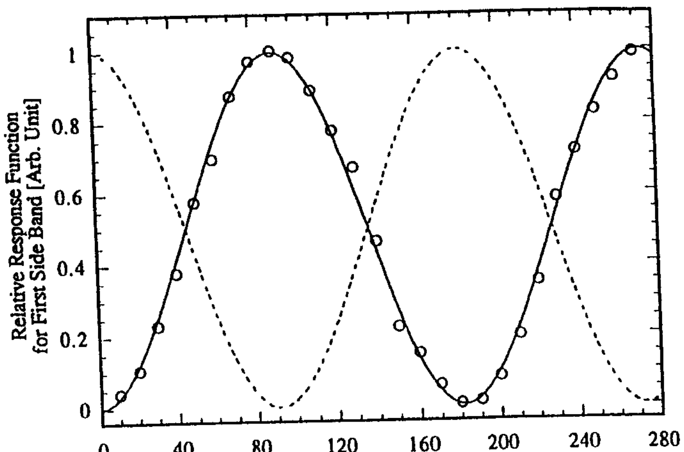

The frequency response of a Sagnac interferometer to a spatially lumped phase modulation is derived from Eq.(1) by replacing the integrandwith δ-functions, and expanding the field in a series of Bessel functions. With a 50/50 beam splitter, the first-side-band response function normalized to the input power for is given by

$$T_{1,s}(f_{\rm mod}) = \frac{I_1}{I_{\rm in}} = J_1^2(m)\sin^2[\pi f_{\rm mod}(\tau_a - \tau_b)] \quad , \tag{4}$$

The peak response is at the modulation frequency

$$f_{\max} = \frac{2}{|\tau_a - \tau_b|} \quad . \tag{5}$$

For small modulation ($m << 1$), Eq. (5) reduces to

$$T_{1,S}(f_{\rm mod}) \approx \frac{1}{4}m^2 \sin^2[\pi f_{\rm mod}(\tau_a - \tau_b)] \quad \textit{Sagnac interferometer}. \tag{6}$$

$$T_{1,M}(f_{\rm mod}) \approx \frac{1}{4}m^2 \cos^2[\pi f_{\rm mod}\tau_M] \quad \textit{Michelson..} \tag{8}$$

If $\tau_M = |\tau_a - \tau_b|/2$, this result is phase shifted by 90° with respect to the result in Eq.(6).

Contrast Ratio = 0.998
30dB below bright port!

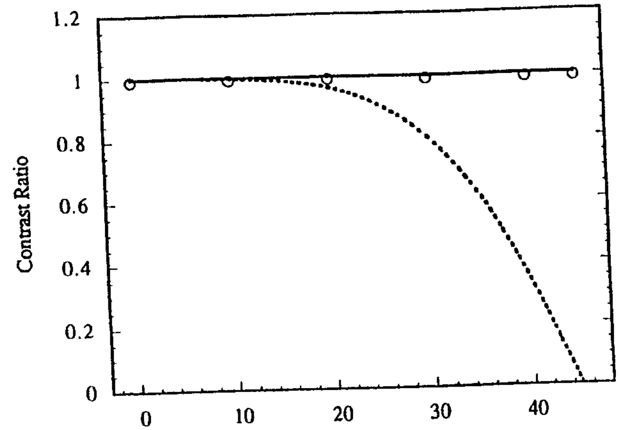

The shot-noise-limited phase sensitivity of a Sagnac interferometer assuming a homodyne detection scheme at the dark port is given by

$$|\Delta\phi| \approx \sqrt{\frac{2(I_{LO} + I_{\min})2\pi\hbar f_l}{I_{LO} I_{\rm in} \eta C^2}} \quad , \tag{9}$$

where I_{LO} is the local oscillator power, $I_{\min}$ is the leakage power from the dark port, $\hbar$ is the reduced Planck constant, $I_{\rm in}$ is the interferometer input power, η is the quantum efficiency of the photodetector, and C is the contrast ratio defined as

$$C = \frac{I_{\max} - I_{\min}}{I_{\max} + I_{\min}}, \tag{10}$$

where $I_{\max}$ is the maximum power out of the bright port. For less-than-unity contrast ratio, the power incident onto the detector is given by $I_{LO} + I_{\min}$. A near-unity contrast ratio is desirable in an interferometer for two reasons; first, the phase sensitivity reaches the quantum limit only if the contrast ratio approaches unity; second, the photo detector saturates if illuminated with too much leakage power, $I_{\min}$. Therefore, we paid particular attention to the measurement of the contrast ratio and the dark-port leakage power of the Sagnac interferometer.

p9

Insensitivity of Outputs to Low Frequency Mirror Displacement

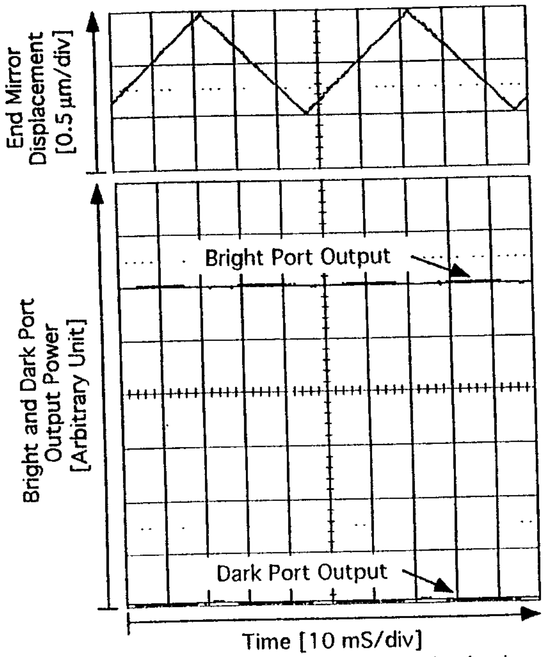

Figure C24 The outputs from the dark and bright ports when the mirror PZT was driven over 1 µm distance, a full wavelength of YAG laser. Both of the outputs stayed nearly constant during the scan, for which a Michelson interferometer would produce two periods of interference fringes. The small ripple was due to PZT tilt. The PZT was driven at 20 Hz, 400 V peak to peak.

We undertook to investigate the contrast ratio as a function of depolarization of the optical beam within the interferometer. This study simulates the impact of thermal induced birefringence in a optical element in a under high power illumination expected for an advanced interferometer. For this experiment we inserted a quarter wave plate into the Sagnac interferometer and measured the dark port power as a function of the angle of the axis of the wave plate. **Figure C25** shows the dark fringe contrast ratio vs quarter wave plate orientation angle and also shows the expected contrast ratio for a Michelson interferometer. As is well known, the Michelson interferometer has no fringes for

p10

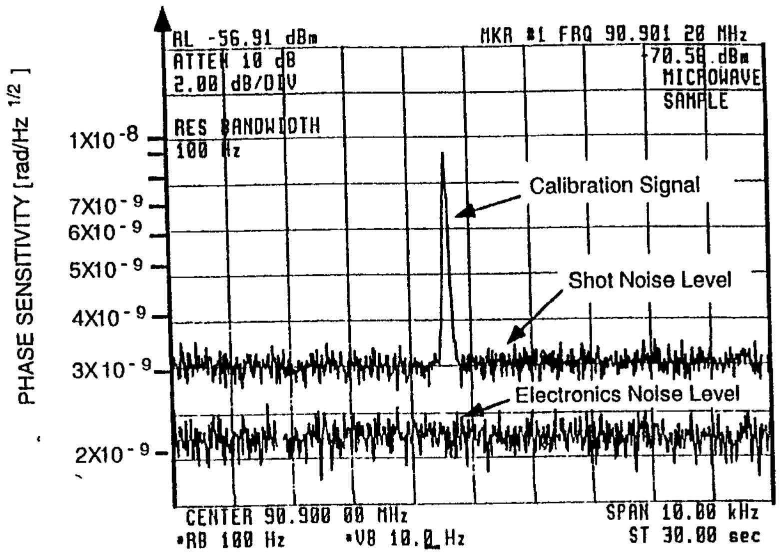

Figure 4

p 11

conductivity but which are absorbing at 1064 nm. As a final demonstration of the potential for these interferometers, and to attempt to determine limits to the performance of such a system we will make a suspended mass interferometer using a simple design and measure the phase noise as a function of the laser power.

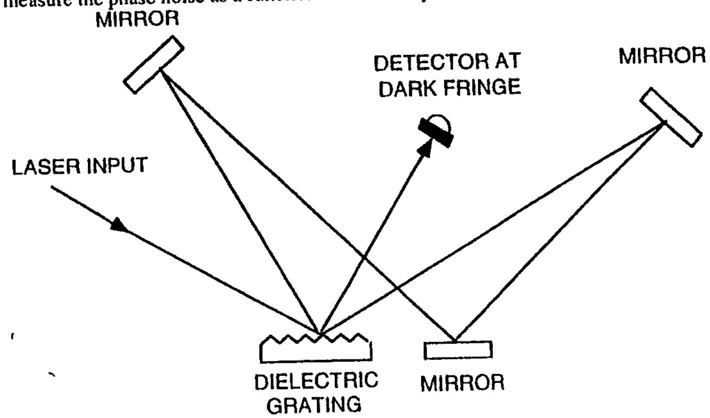

Figure C29. An all reflective Stanford Sagnac Interferometer using a grating beam splitter.

We have consulted with the team at LLNL regarding the design and the fabrication of high reflecting gratings on dielectric substrates. (Boyd 95) The LLNL group has indicated that they wish to cooperate to assist the LIGO effort. Further, they have demonstrated the capability to fabricate gratings using lithographic techniques with dimensions that exceed one meter. Thus this approach is appropriate to consider for an advanced LIGO interferometer. Combined with one dimensional face cooling technology, an all reflective element interferometer can be designed to accommodate kilowatts of laser power with minimum optical distortion and no induced birefringence.

iii. Reflective Beamsplitter

b. Thermal Noise and Materials Effects

i. Thermal Noise and Q in Test Masses and Suspensions

Thermal problems are of two types. The first type results from thermally-induced figure distortions in the optical components that produce spatial variations in the phase fronts, and also thermally-induced stresses that produce spatial variations in the polarizations of the optical beams which reduce the fringe contrast. The second type of problem is thermal noise in the test masses and test mass suspensions, the spectral densities of which

p 12

Co Investigators
Daniel B. DeBra
Martin M. Fejer
James S. Harris
Peter F. Michelson
Yoshihisa Yamamoto
Richard E Taylor

Principal Investigator
Robert L. Byer
Ginzton Laboratory
Stanford University
94305-4085
tel (415) 723 0226
fax (415) 723 2666

Summary

Next steps in the laboratory

The 10 meter interferometer

Tuesday AM   Space Based Detectors-LISA I
January 16   Chair: A. Ruediger

8:00	P. Bender(JILA)	Sources for LISA
8:25	Discussion	
8:35	H. Ward(Glasgow)	LISA Overview
9:00	Discussion	
9:10	Coffee Break	
9:25	H. Ward(Glasgow)	LISA Overview(continued)
9:50	Discussion	
10:00	D. Hils(JILA)	BH-SMBH Binaries
10:25	Discussion	

LISA Sensitivity

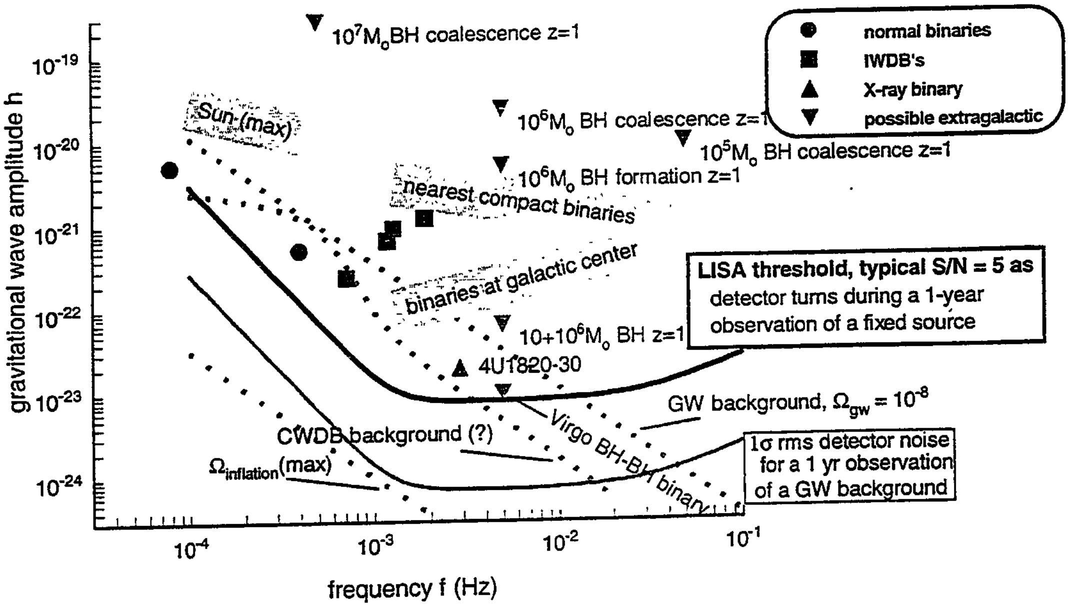

Extragalactic Astronomy

Objective: To detect and study gravitational wave signals from sources involving massive black holes (MBHs) with masses of 10^3 to 10^8 M⊙.

- 5 or 10 M⊙ black holes (BHs) or compact stars orbiting 10^5 to 10^7 M⊙ MBHs.
- MBH-MBH binaries resulting from formation of multiple MBHs in many galaxies plus their sinking to the center by dynamical friction.
- MBH-MBH binaries formed by mergers of galaxies or pre-galactic structures that already contain MBHs.
- MBH-MBH binaries formed by growth of several seed BHs in the same galactic nucleus.
- Sudden formation of MBHs.

It appears plausible, or even likely, that at least one of these types of binaries can be detected and studied by LISA.

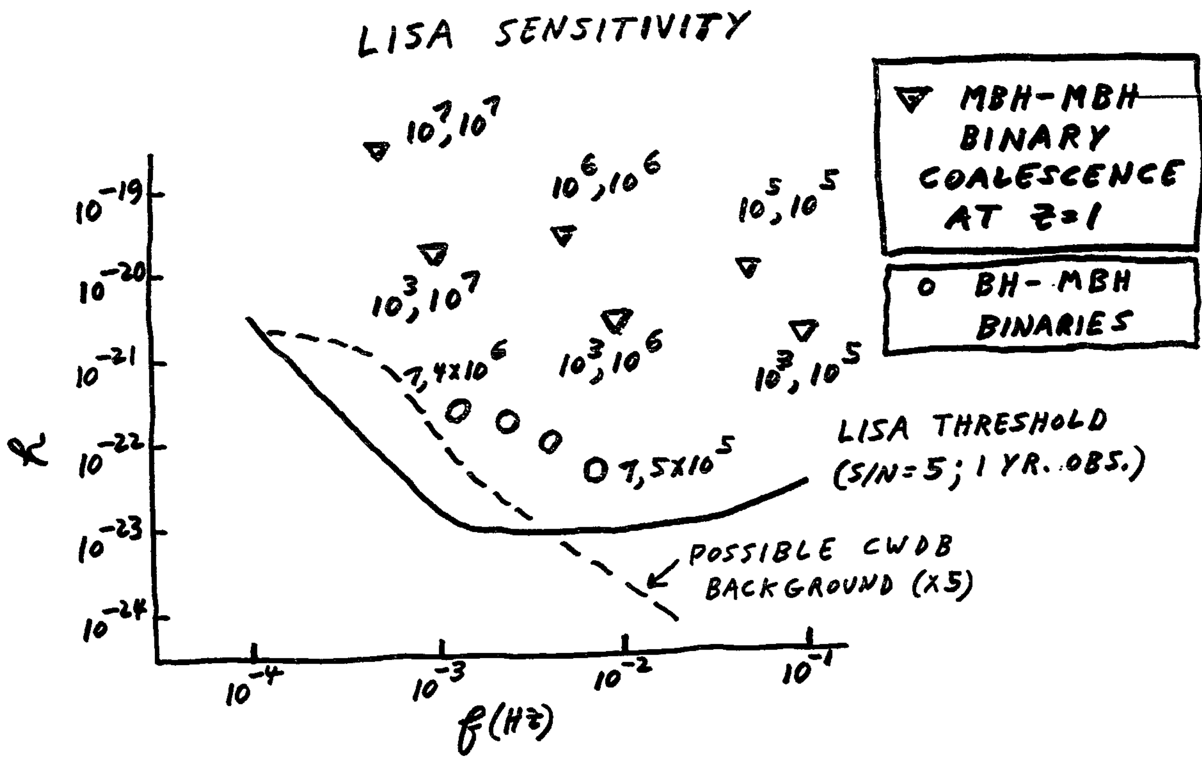

Fundamental Physics and Cosmology

Objective: To test general relativity in the high field limit, and to search for cosmological information on gravitational background radiation and possibly on the expansion parameter q_0.

- If BH-MBH or MBH-MBH coalescence signals are seen, they will provide a unique test of general relativity at extremely high fields. Even slight deviations from the dynamical predictions of the theory would be detectable.
- Cosmological background radiation could be detected near 10 mHz with a sensitivity of 10^{-10} to 10^{-11} of the closure density.
- If several MBH-MBH coalescences with both masses $\geq 10^5$ M$_\odot$ occur, the S/N will be high even at cosmological distances, and very accurate luminosity distances can be obtained. If the event directions are measured and can be associated with clusters of galaxies with known redshifts, it appears possible to determine the cosmological expansion parameter q_0.

BACKGROUND SIGNALS
+LISA SENSITIVITY

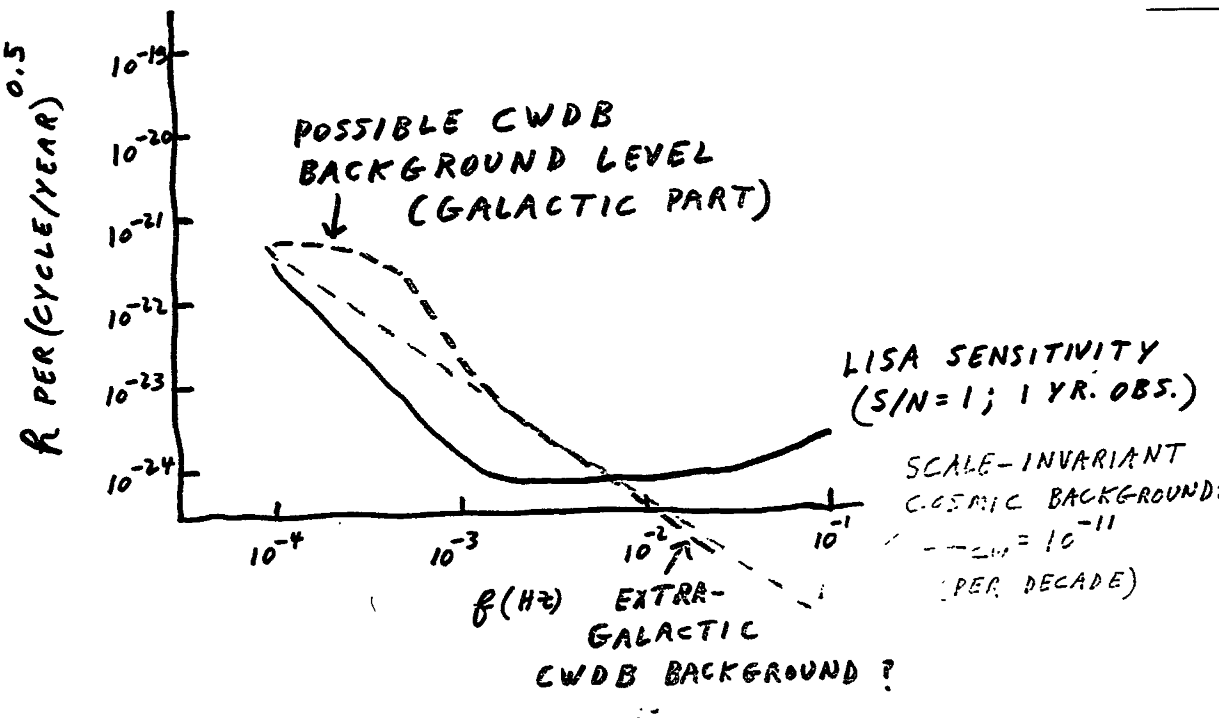

Galactic Astronomy

<u>Objective:</u> To investigate the number and distribution of different types of short period binaries in our galaxy.

- Neutron star binaries: hundreds will be detectable and their locations can be determined throughout the galaxy.
- Close white dwarf binaries (CWDBs): thousands above about 1 mHz are expected to be resolvable.
- Known sources: a few will be detectable, including i Boo (normal binary), WZ Sge (cataclysmic variable) and 4U1820-30 (x-ray binary).
- Interacting white dwarf binaries (IWDBs): many will be observable, GP Com is known, and several others are known except for possible frequency ambiguities.
- Other compact binaries: BH-neutron star and BH-BH binaries are expected to be detectable.
- CWDB background: below about 1 mHz, the very large number of CWDBs will give a confusion-limited background.

LISA SENSITIVITY

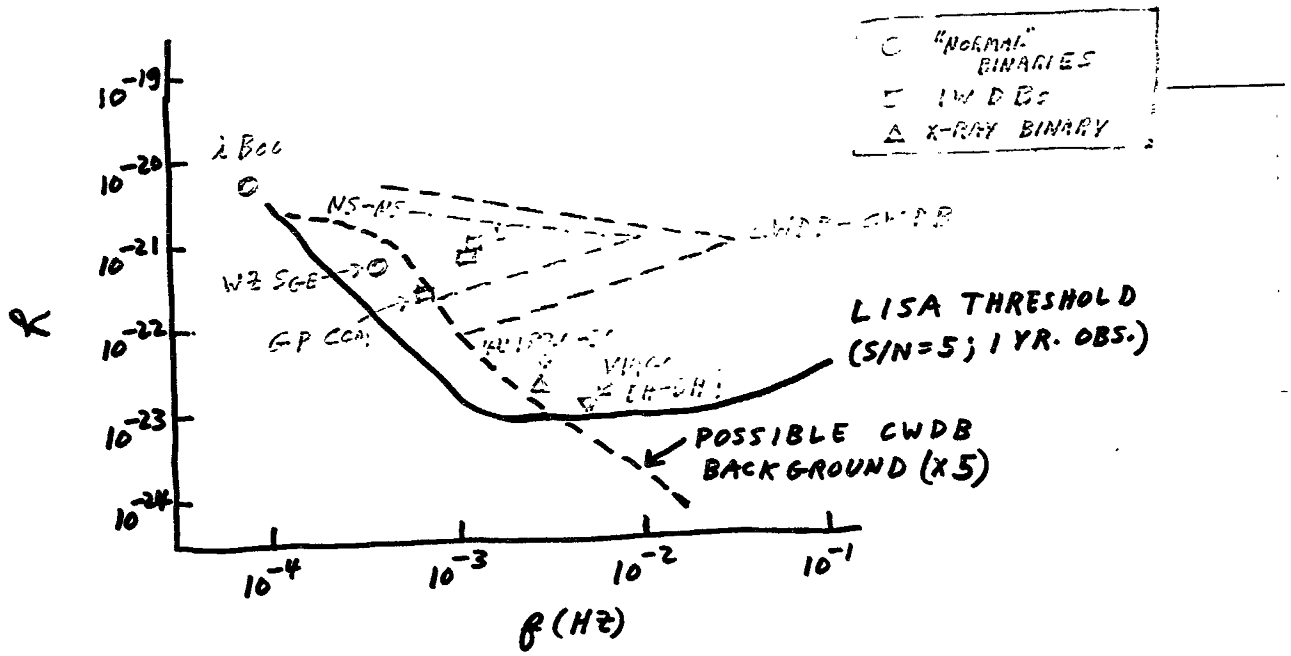

LISA

Laser Interferometer Space Antenna

– a gravitational wave detector
for low frequency signals

H. Ward, Aspen, January 1996

LISA Science Team

- P. Bender, JILA
- K. Danzmann, Uni Hannover
- J. Hough, Uni Glasgow
- A. Rudiger, MPQ
- R. Schilling, MPQ
- R. Stebbins, JILA
- P. Touboul, ONERA
- W. Winkler, MPQ
- I. Ciufolini, CNR
- W.M. Folkner, JPL
- D. Robertson, Uni Glasgow
- M. Sandford, RAL
- B. Schutz, AEI
- T.J. Sumner, Imperial Coll.
- H. Ward, Uni Glasgow

- J. Cornelisse, Study Manager, ESTEC
- Y. Jafry, Study Scientist, ESTEC

Spaceborne Detectors

- Space-based detectors are sensitive in the low-frequency range
  - long baseline
  - no gravity-gradient wall
- Two-arm interferometers are much more sensitive then spacecraft tracking

Complementary to other Detectors

- Ground-based (VIRGO / LIGO / GEO) “blind” below 1 Hz
- Space-based frequency range extends down to 10^{-4} Hz
- LISA detects local precursors of stellar coalescing binaries
- LISA + ground-based detectors could provide spectrum of cosmological background

Measurement Technique

- Laser interferometry between inertial masses
- Long baseline : 5×10^9 m
- High measurement sensitivity :
  - $\delta x < 25$ pm $/\sqrt{Hz}$ from 10^{-3} to 10^{-1} Hz
  - $\delta a < 10^{-15}$ ms$^{-2}/\sqrt{Hz}$ from 10^{-4} to 10^{-3} Hz

Spacecraft Orbits

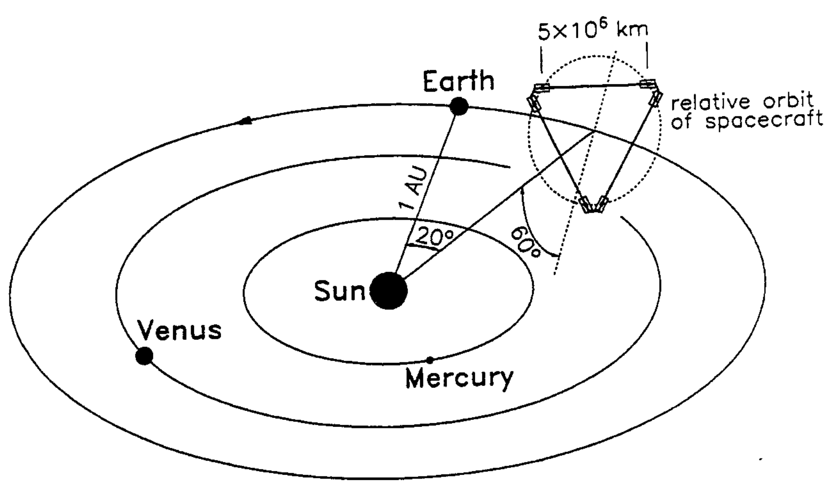

LISA – Interferometry

- Effectively a Michelson interferometer
- Phase-locked laser transponders at arm ends
- Lasers in central spacecraft phase-locked

Outline Layout of LISA (2 arms)

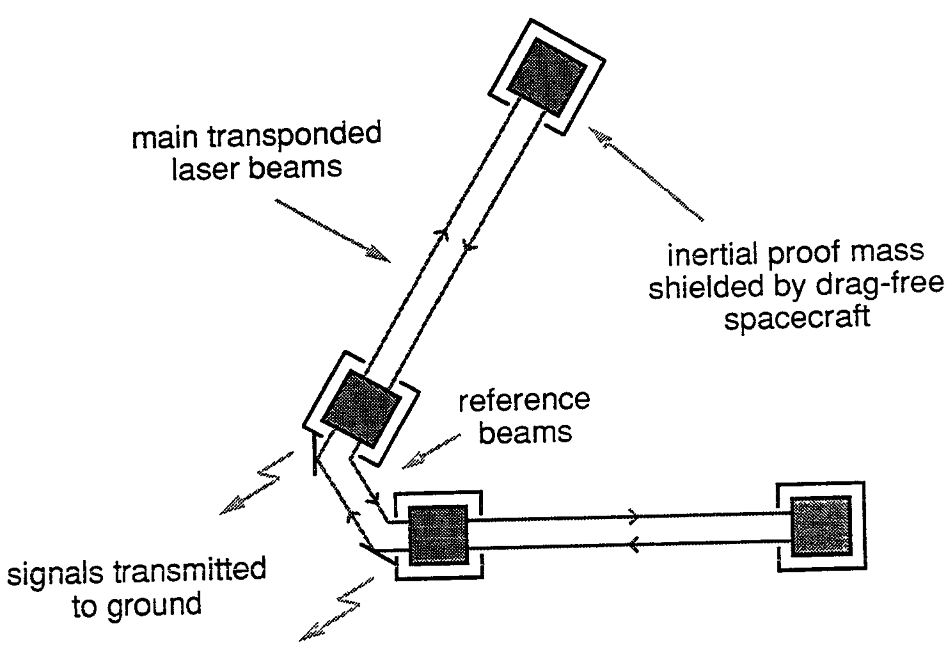

LISA Science Payload

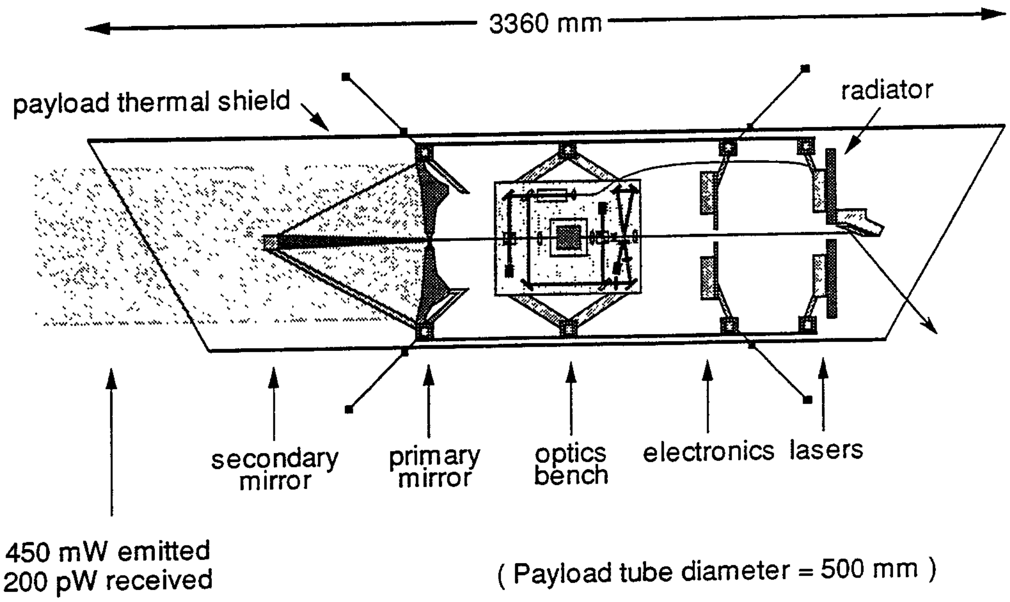

Drag - free Control – 1

- Objective
  - To obtain at the centre of each spacecraft a proof-mass free of spurious accelerations in order to define the intereferometer arms
- Concepts
  - Accelerometer based on a cubic proof-mass (highly accurate geometry, 1.3 kg of Au-Pt alloy)
  - Capacitive position sensing of the 6 degrees of freedom
  - Electrostatic servo control of the proof-mass position and attitude with respect to the ULE accelerometer cage
  - Spacecraft driven by FEEP thrusters to nullify the electrostatic feedback forces on the proof-mass

SENSOR PERFORMANCE OBJECTIVES

● PROOF-MASS POSITION SENSING :

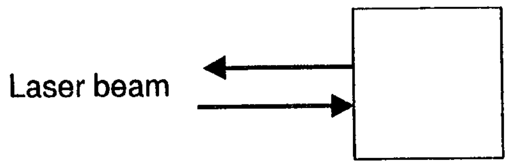

Since the laser beam is reflected on the proof-mass :

- a resolution of 10^{-9} m/$\sqrt{Hz}$ is sufficient to limit the variations of proof-mass disturbances (S/C gravity gradient in particular).
- but the electrostatic stiffness induced by the sensing must be very weak ($<10^{-6}$ N/m).

● PROOF-MASS FREE MOTION :

- All accelerometric disturbances must be less than 10^{-15} ms^{-2}/$\sqrt{Hz}$ in [10^{-4} Hz; 5×10^{-3} Hz]
  - ➡ optimization of geometrical and electrical configurations
  - ➡ high thermal stability.
- Sensor output kept at null
  - ➡ no stringent requirement on scale factor accuracy, stability and linearity.

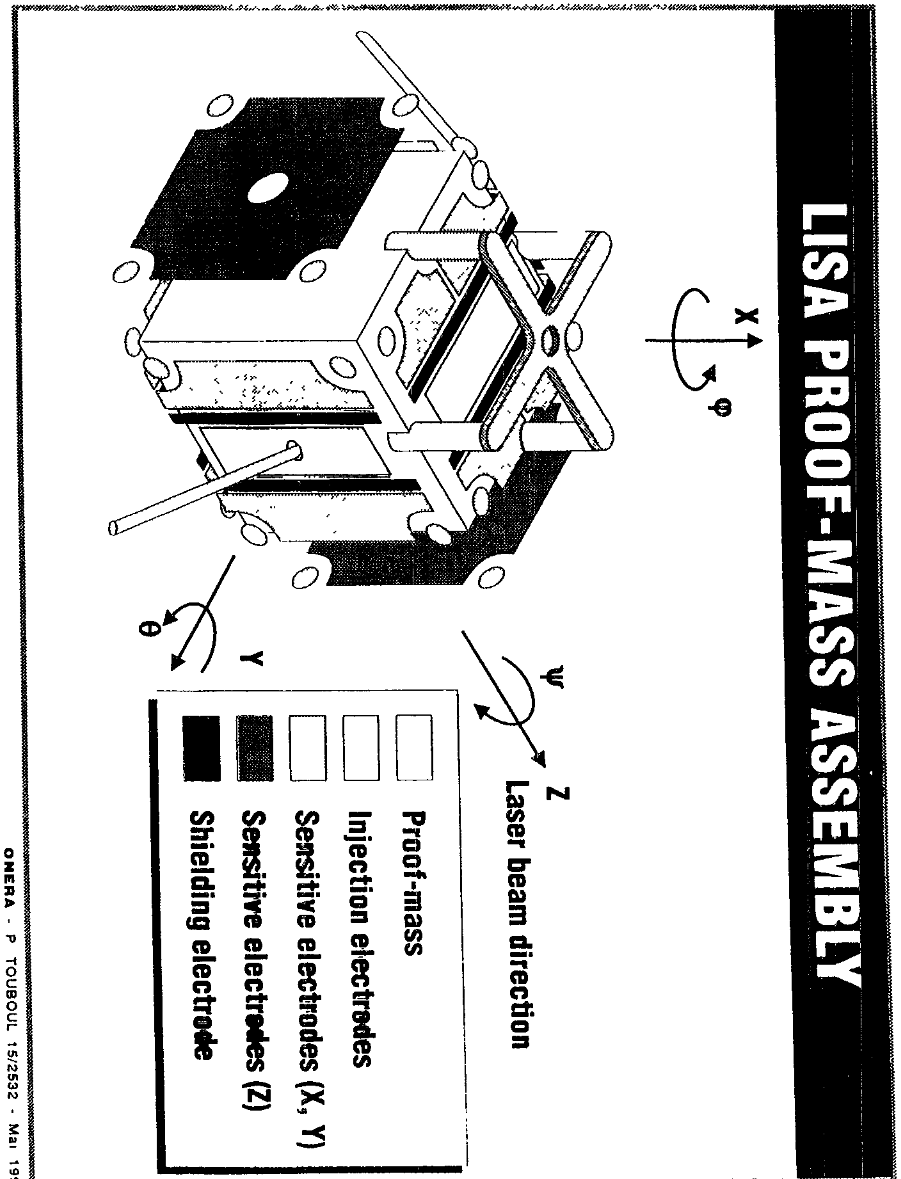

PROOF-MASS DISTURBANCES DUE TO ENVIRONMENT (cn'd)

■ PROOF-MASS CHARGE Q :

variations due to flux of particles from cosmic rays and solar flares

evaluated to ~ 10^{-17} C/s - 10^{-18} C/s

■ DISTURBANCES :

due to
- Lorentz force
- electrical forces when asymmetry of the geometry

⟶ $Q < 3 \times 10^{-14}$ C   corresponding to 1 mV

$\delta Q < 10^{-12}$ C / $\sqrt{\text{Hz}}$

Q to be deduced from the measurement of the effect of a sine wave exciting voltage on the electrostatic suspension.

Q to be controlled by use of U.V. lights.

PROOF-MASS DISTURBANCES DUE TO ENVIRONMENT

■ MAGNETIC :

- Lorentz force :
  - ⟶ control of the proof-mass charge
- Magnetic moment of the proof-mass
  - ⟶ Au Pt alloy : $\chi = 10^{-6}$

■ RESIDUAL GAS :

- radiometer effect
- damping
- acoustic tranfer
- statiscal fluctuations
  - ⟶ $P_0 < 10^{-6}$ Pa
  - ⟶ internal core opened to space vacuum use of low outgassing parts and baked sensor core

■ RADIATION PRESSURE

■ GEOMETRICAL STABILITY :

- U.L.E. accelerometer cage
- suspended proof-mass
  - ⟶ expected thermal stability better than 10^{-6} K / $\sqrt{\text{Hz}}$

FEEP Thrusters

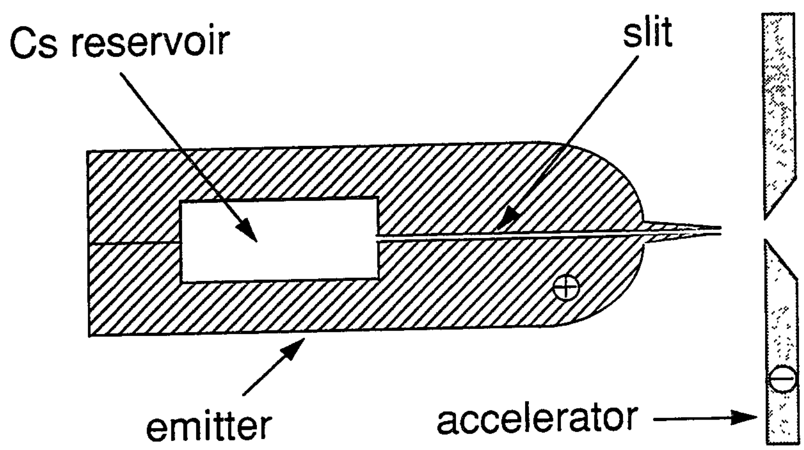

Force range : 1 – 25 μN   Response time : 10 – 30 ms

LISA Science Payload

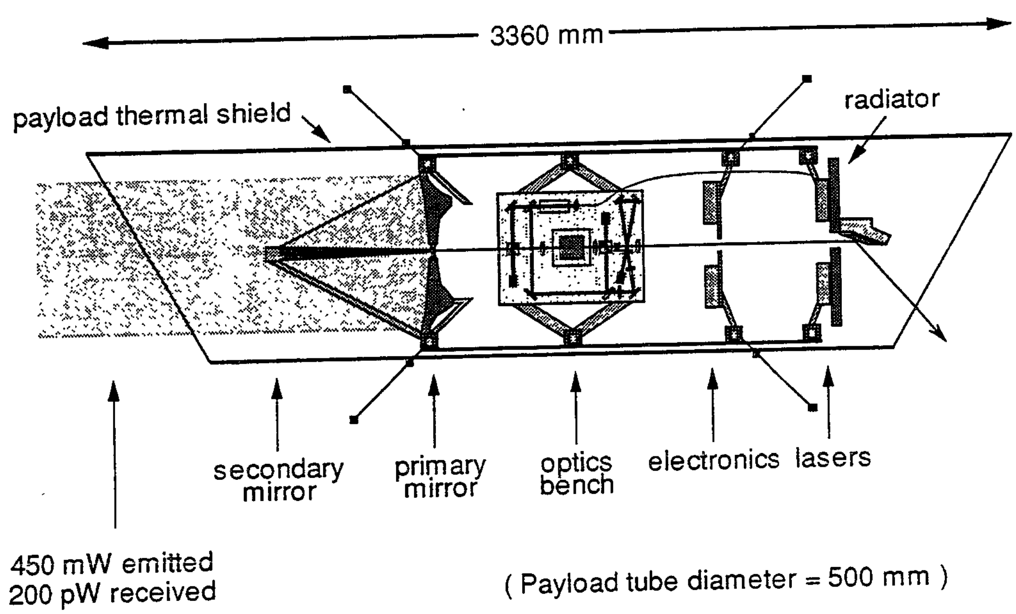

(Payload tube diameter = 500 mm)

Optical Layout

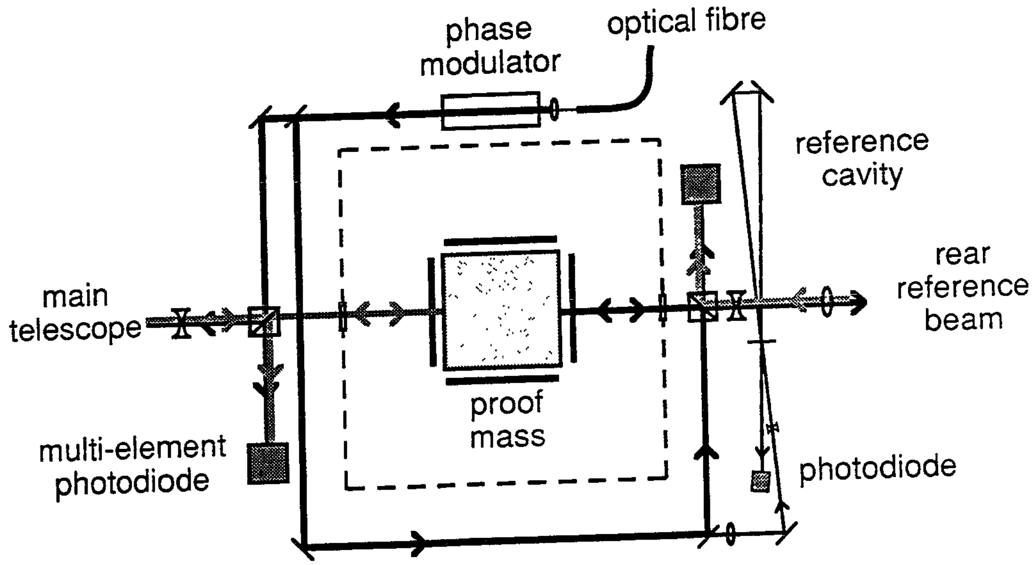

Photon Noise

- Want photo-electron shot noise to contribute a measurement noise less than 5 pm $/\sqrt{\text{Hz}}$ for a single traverse of one arm
- For a given laser power and arm length this requirement sets the mirror diameter needed
- For 1.06 μm light, effective power 300 mW, and an arm length of 5×10^9 m, a telescope output mirror diameter of 38 cm is required

Lasers for LISA

- High output power (~ 1 W)
- Low noise
- Good reliability
- High efficiency
- Compact size

➡ Diode pumped Nd:YAG lasers

Laser Power Fluctuations

- Power fluctuations cause acceleration noise since light is reflected from the proof mass
- Require any component of spurious acceleration noise to be $< 10^{-16}\,\mathrm{m\,s^{-2}}$
- For proof mass of 1.3 kg and 10 mW reflected power this sets a tolerable limit to laser power fluctuations of

$$\delta P/P < 2 \times 10^{-6} /\sqrt{\mathrm{Hz}}$$

Laser Frequency Noise

- Couples in through difference (Δx) in arm length
- Fractional laser frequency noise ($\delta\nu/\nu$) translates to apparent displacement noise $\delta x = \Delta x.(\delta\nu/\nu)$
  - For arm length 5×10^9 m, Δx could be 10^9 m, so for $\delta x < 2$ pm $/\sqrt{\text{Hz}}$ we need $\delta\nu < 6\ \mu\text{Hz}/\sqrt{\text{Hz}}$
- Stabilisation to a ULE cavity with thermal stability $\Delta T < 6\ \mu\text{Hz}/\sqrt{\text{Hz}}$ could only give $\delta\nu < 10\ \text{Hz}/\sqrt{\text{Hz}}$
  - Not good enough, so further correction algorithm needed

Frequency Correction Algorithm

- Provided by comparing the mean phase of the light returning in two adjacent arms with the phase of the transmitted light
  - Since $\phi = (4\pi/c).\nu.L$, $\delta\phi = (4\pi/c)(\nu.\delta L + L.\delta\nu)$ and since δL is small, $\delta\phi \sim (4\pi/c).L.\delta\nu$. So if $\delta\phi$ is measured, $\delta\nu$ can be calculated
  - Now the gravity wave signal is found from the phase difference between adjacent arms; the measured phase difference can now be corrected for the effect of $\delta\nu$

Doppler Effect – 1

- Relative velocity between craft leads to Doppler beat signals in the phase comparisons
- Possible velocity of 8 m/s gives a beat in one return arm of 16 MHz
- Need to reduce this to manageable rate (few Hz) for later signal processing and transmission
  - Done by beating with a stable on-board reference clock
  - Clock noise must allow measurement precision of $\delta x < 2$ pm $/\sqrt{\mathrm{Hz}}$ or $\delta\phi < 2.5 \times 10^{-5}$ rad $/\sqrt{\mathrm{Hz}}$

HW 2/96

Doppler Effect – 2

- Required frequency stability of clock = measurement frequency / clock frequency * measurement phase noise limit
  - Thus for observations at 10^{-3} Hz and a beating frequency of 16 MHz, a clock frequency stability of 1.6×10^{-15} $/\sqrt{\mathrm{Hz}}$ is required
  - This is equivalent to an Allan standard deviation of $\sigma_{Allan} \sim 4 \times 10^{-17}$ over 1000 second timescales
  - Typical USO has $\sigma_{Allan} \sim 2 \times 10^{-13}$ so clock stabilisation technique is required

HW 2/96

Doppler Effect – 3

- Stabilisation of clock frequency done analogously to the scheme for laser frequency stabilisation – essentially by using the stable arm length as a reference against which to measure the frequency
  - Clock signal is phase modulated on to the laser light at a high modulation frequency (~ 1GHz)
  - Carrier and sideband signals monitored and their frequency fluctuations deduced from knowledge of approximate common mode and differential arm lengths

Spacecraft – 1

- Drag-free
  - $10^{-15}\,\mathrm{m\,s^{-2}}$ (rms) in the band 10^{-4} to 10^{-1} Hz using Caesium FEEP thrusters for control
- Pointing
  - few nrad/$\sqrt{\mathrm{Hz}}$ in above band
- Payload (each spacecraft)
  - mass : 67 kg
  - power : 48 W
  - size : cylinder 0.5 m diameter by 3.3 m long

Spacecraft – 2

- Spacecraft - 3 axis stabilised (6 S/C in total)
  - Mass : 290 kg each spacecraft in orbit
  - Power : 183 W each spacecraft in orbit
- Propulsion module
  - Mass : 216 kg, 2 spacecraft per module
  - Propellant : 240 – 920 kg, depending on launch date, for 2 spacecraft
- Total launch mass : 6200 kg

Spacecraft – 3

- Telemetry
  - 560 bps continuous total
  - Ground stations : Villafranca and Perth
- Mission life
  - Specification : 2 years
  - Feasible life : 3 to 10 years

Spacecraft with Payload

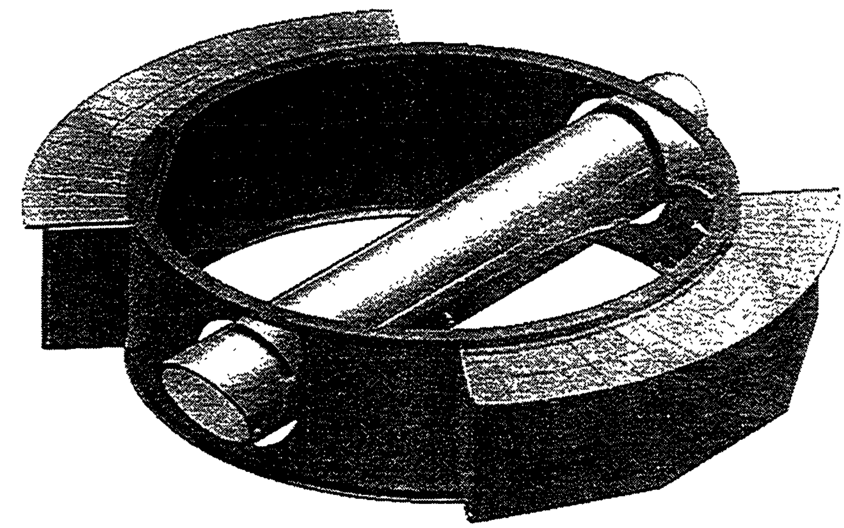

Propulsion Module + 2 Spacecraft

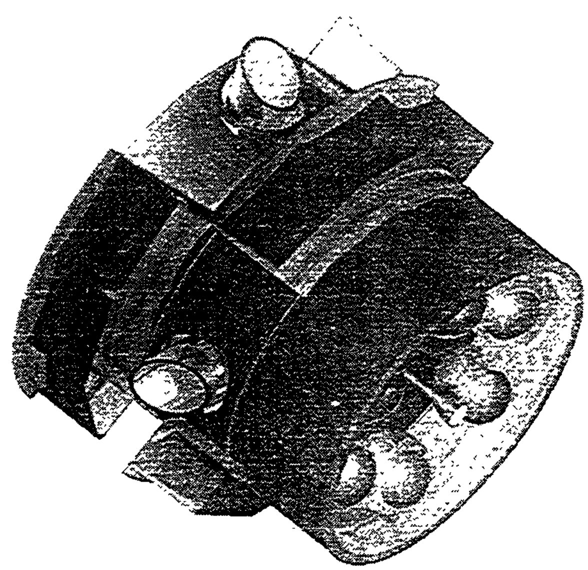

Launcher

- ARIANE 5, dual launch configuration
  - two pairs of spacecraft in the lower compartment
  - one pair in the upper under the short fairing
- Each pair of spacecraft has its own jettisonable propulsion module
  - provides a ΔV of 1000 m/s for final orbit injection

Conclusion

- LISA will probe the gravitational wave spectrum in a region not accessible to ground-based detectors
- LISA is complementary to the ground-based experiments and should detect a range of exciting sources
- LISA's technology is demanding but no breakthroughs are required

BH- MBH BINARIES

P.L. BENDER + D. HILS

LISA IS EXPECTED TO SEE MANY

'GUARANTIED SOURCES'

- NOT ALL ARE AP EXCITING
- COMPACT STAR - MBH BINARIES ARE NOT CERTAIN TO EXIST
- BUT OF GREAT INTEREST TO AP + P

COMPACT ✡ : WD OR NS

$m_c = 1.4\ M_\odot$

RECENTLY

COMPACT STAR : BH

$m_c = 7\ M_\odot$

ADVANTAGE : LARGER SIGNAL

WORRY : ARE THERE ENOUGH BH's

DIFFERENCE : $m_c \gg m_f = M_\odot$

MASS SEGREGATION

1. NEED NEAR RADIAL ORBITS

ΔE_{GR} ΔL_{GR}

2. EFFECT OF CLUSTER FIELD ✡'s :

- DISPERSION ΔL_{RMS}
- FATAL IF $L < L_{crit}$ AT PERICENTER
- SHORT DURATION ORBITS

MORE TIGHTLY BOUND ✡

HAS SMALLER ΔL_{RMS}

BETTER CHANCE TO RADIATE

ENERGY GRADUALLY BY GR

ΔE : FEW %

LISA CANDIDATE

Expected Signals from BH-SMBH Binaries

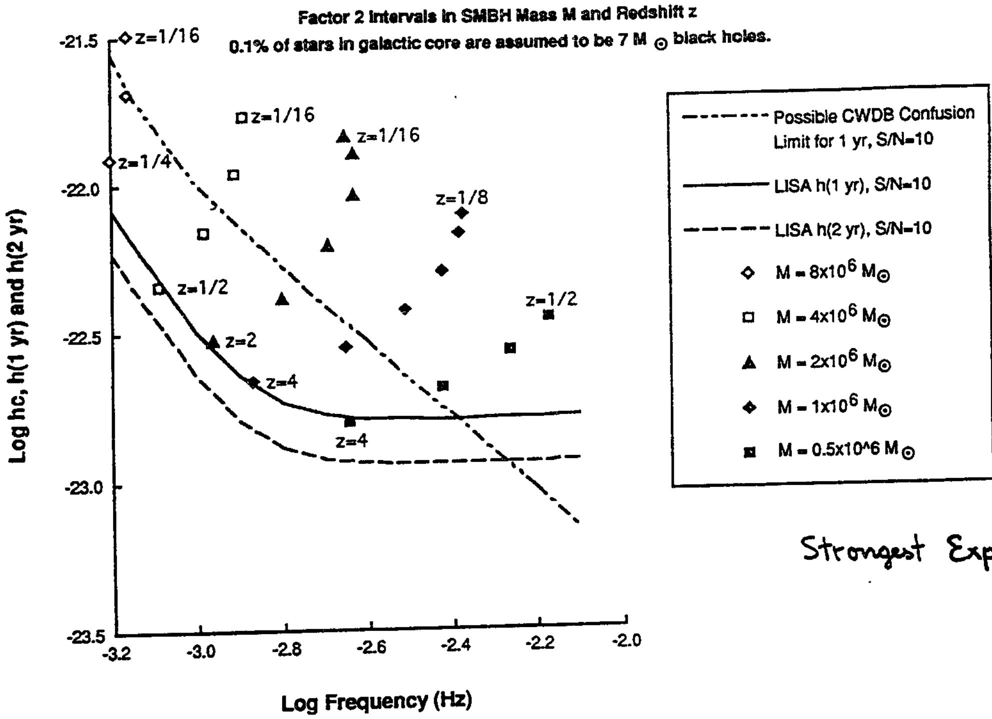

Strongest Expected Sources

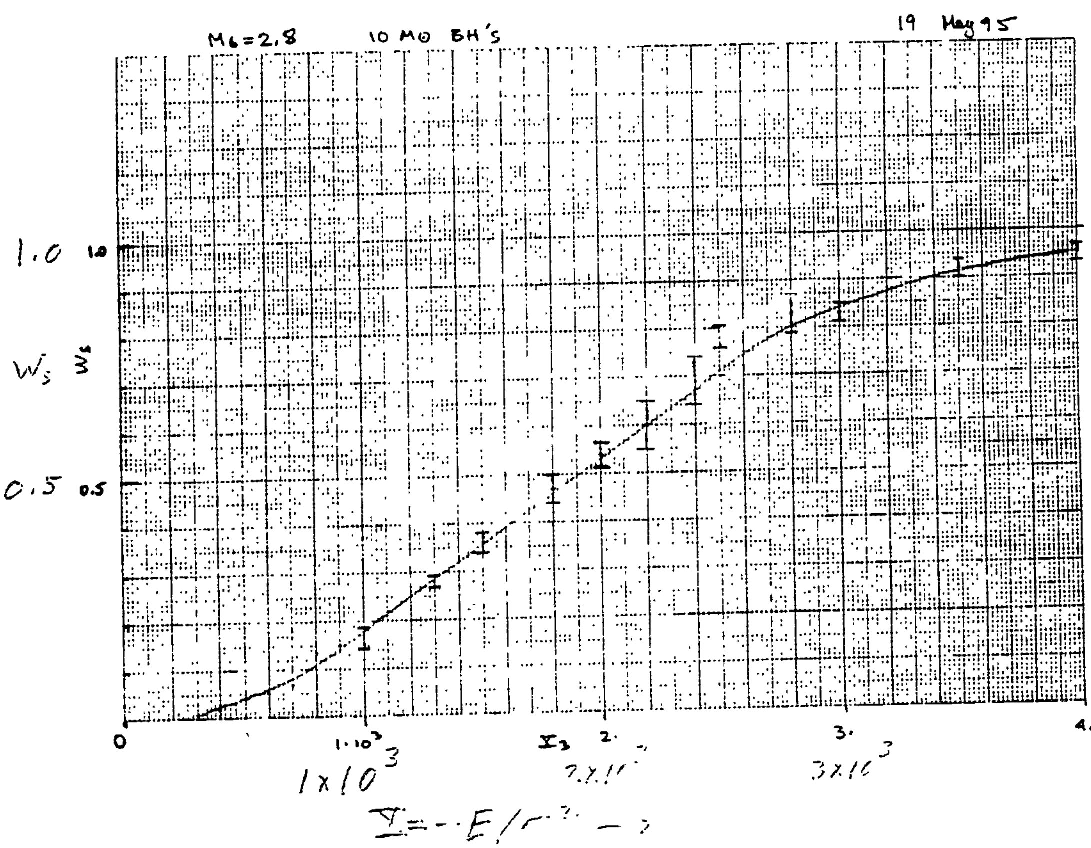

Expected Signals from BH-SMBH Binaries

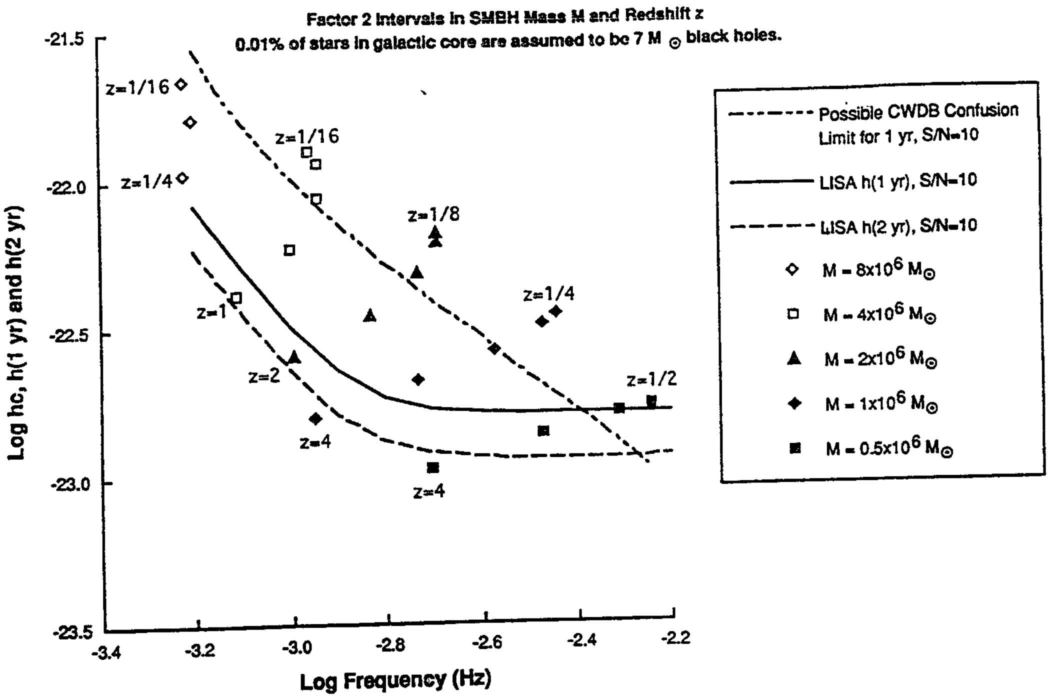

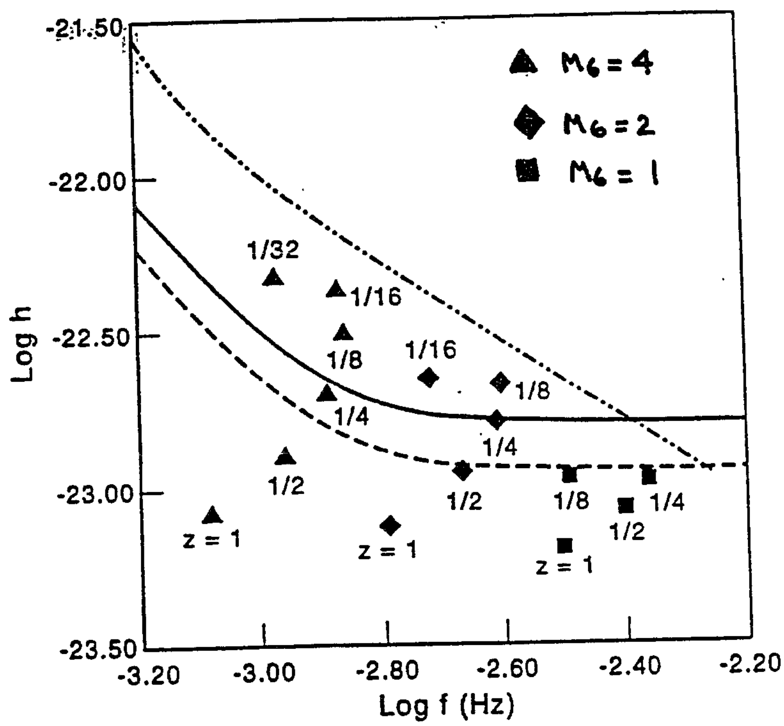

Hills + Bender : ApJ 445, L7 (1995)

Figure 1

10% compact stars

$m_c = 1.4\ M_\odot$

Strongest Expected Sources

0.1 % of stars in core are in 7 $M_\odot$ BH's

Estimated BH-MBH Coalescence
Event Rate
(per year)

	M_6				
Z	0.5	1	2	4	8
1/16	.010	.014	.024	.040	.065
1/ 8	.056	.093	.16	.26	.42
1/4	.30	.50	.83	1.4	2.2
1/2	1.2	2.0	3.3	5.4	8.8
1	3.0	5.0	8.3	14	22
2	4.1	6.8	11	19	30

Observable Duration of BH-MBH
Coalescence Events for LISA
(years)

	M_6				
Z	0.5	1	2	4	8
1/16	18	71	280	590	390
1/ 8	10	39	150	260	65
1/4	5.2	21	73	82	3.0
1/2	2.5	10	30	11	
1	1.1	4.5	6.0	0	
2	0	1.7	0		

Estimated Number of Events Above LISA Instrumental Threshold (S/N = 10; 1 year)

	M_6				
Z	0.5	1	2	4	8
1/16	0.2	1.0	7	24	26
1/ 8	0.6	3.6	23	67	27
1/4	1.5	10	60	110	7
1/2	2.9	22	97	61	
1	3.2	20	49	0	
2	0	7	0		

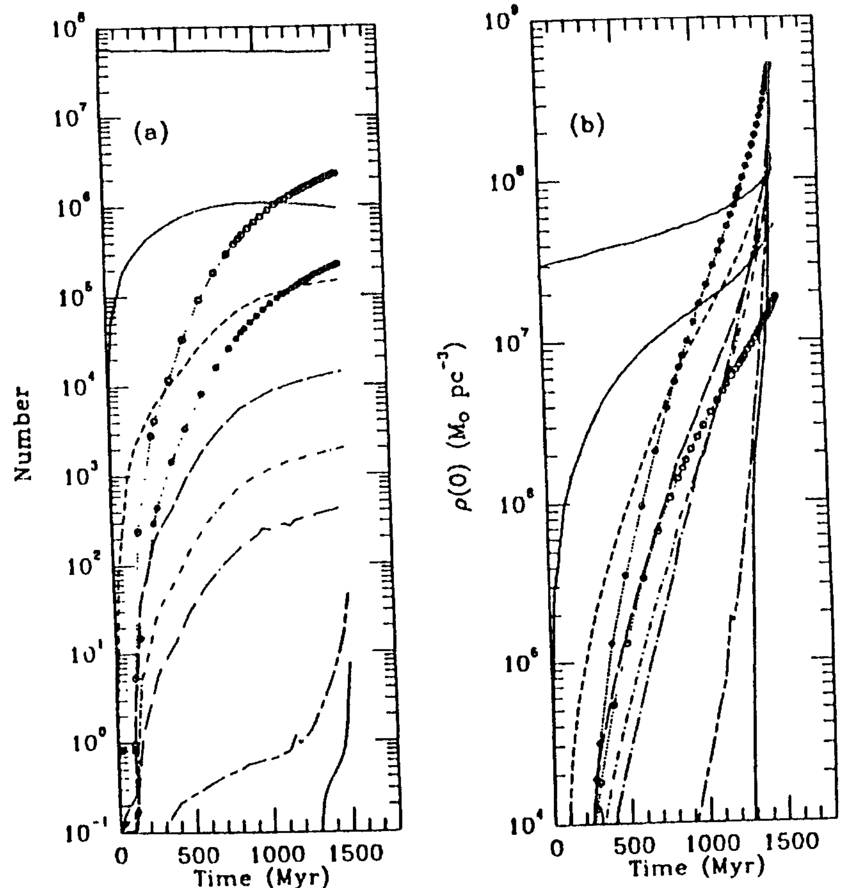

QUINLAN + SHAPIRO 1990, ApJ, 356, 483

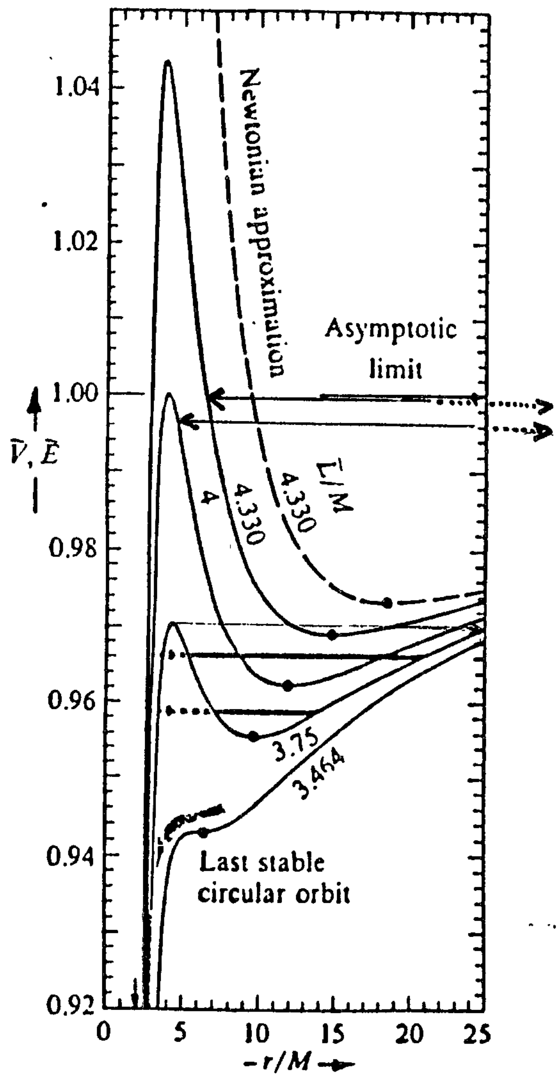

1.04
1.02
1.00
0.98
0.96
0.94
0.92
$\tilde{V}, \tilde{E}$
Newtonian approximation
Asymptotic limit
$\tilde{L}/M$
4.330
4.330
4
3.75
3.464
Last stable circular orbit
0
5
10
15
20
25
r/M

Tuesday PM	Space Based Detectors-LISA II	
January 16	Chair: R. Schilling	
4:30	B. Willke (Hannover)	Lasers for LISA
5:00	Discussion	
5:10	D. Robertson (Glasgow)	Spacecraft Pointing
5:40	Discussion	
5:50	R. Stebbins (JILA)	LISA Error Budgets
6:20	Discussion	
6:30	Coffee Break	
6:45	D. Robertson (Glasgow)	GEO 600 Developments
7:15	Discussion	
7:25	D. Schnier (Hannover)	Power Recycling
7:40	Discussion	

Lasers for LISA

Benno Willke
University of Hanover

results of the LISA study team
reported in the Pre-Phase A Report

Aspen Winter Conference 96

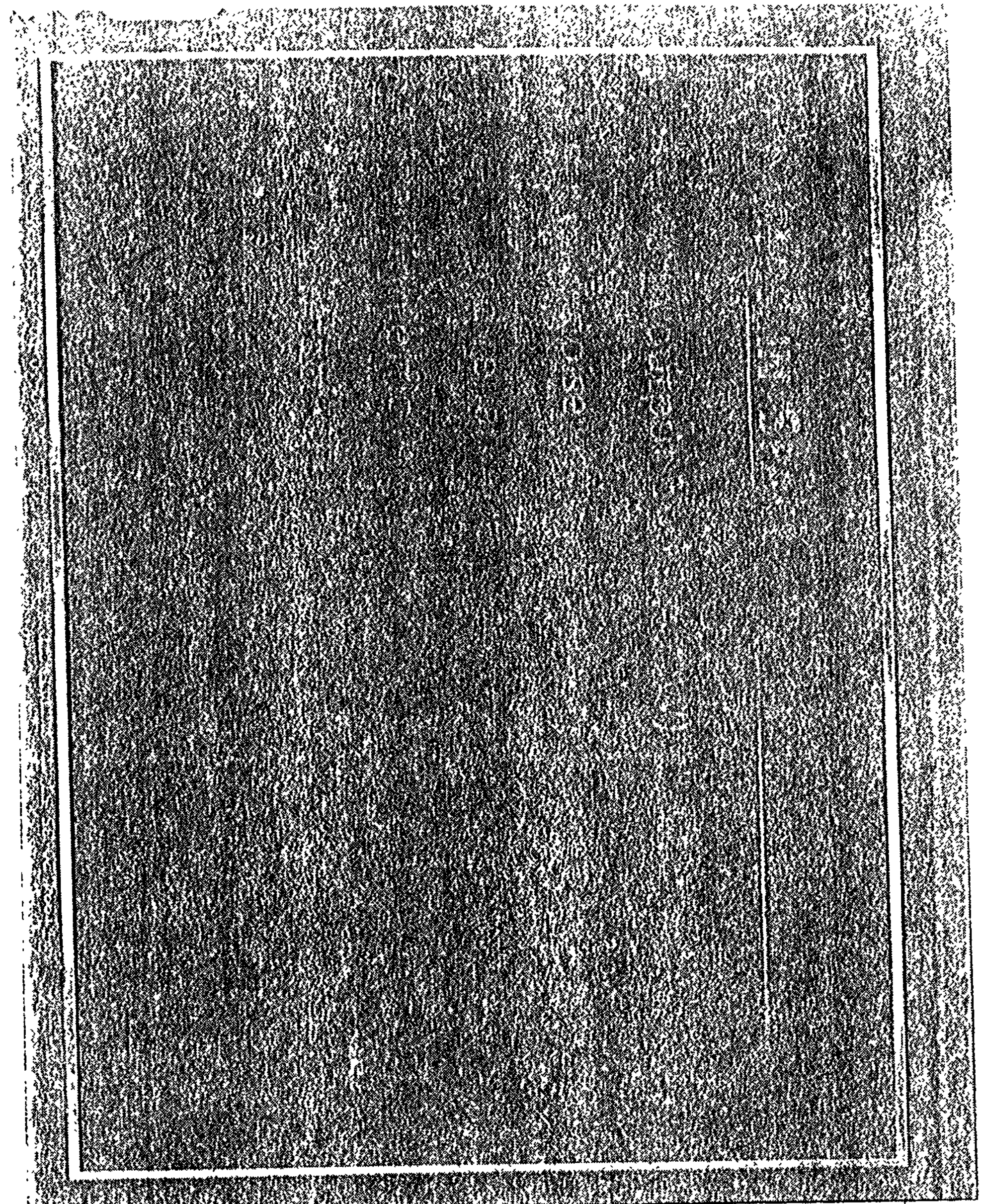

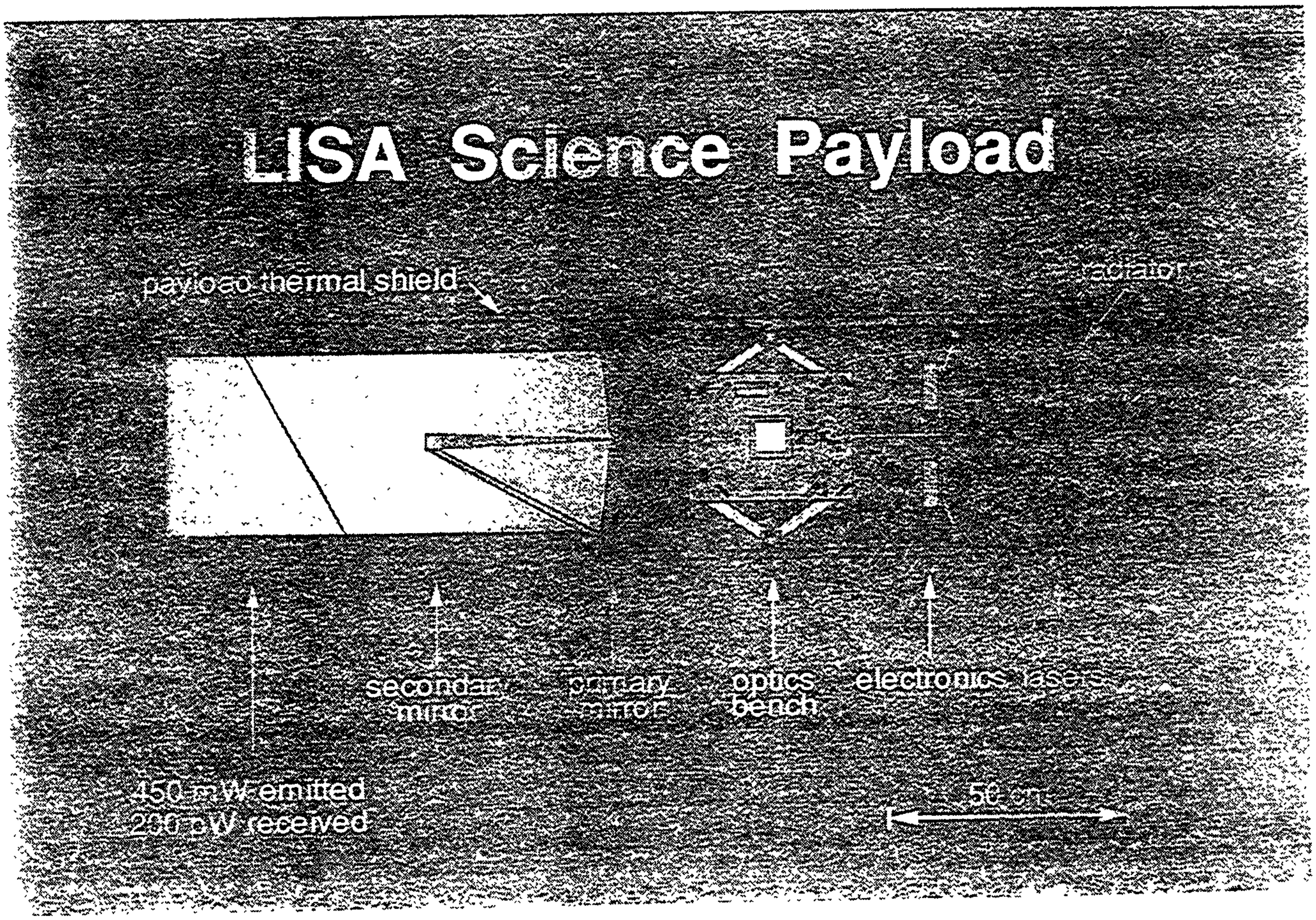
LISA Science Payload
payload thermal shield
radiator
secondary mirror
primary mirror
optics bench
electronics
lasers
450 mW emitted
200 pW received
50 cm

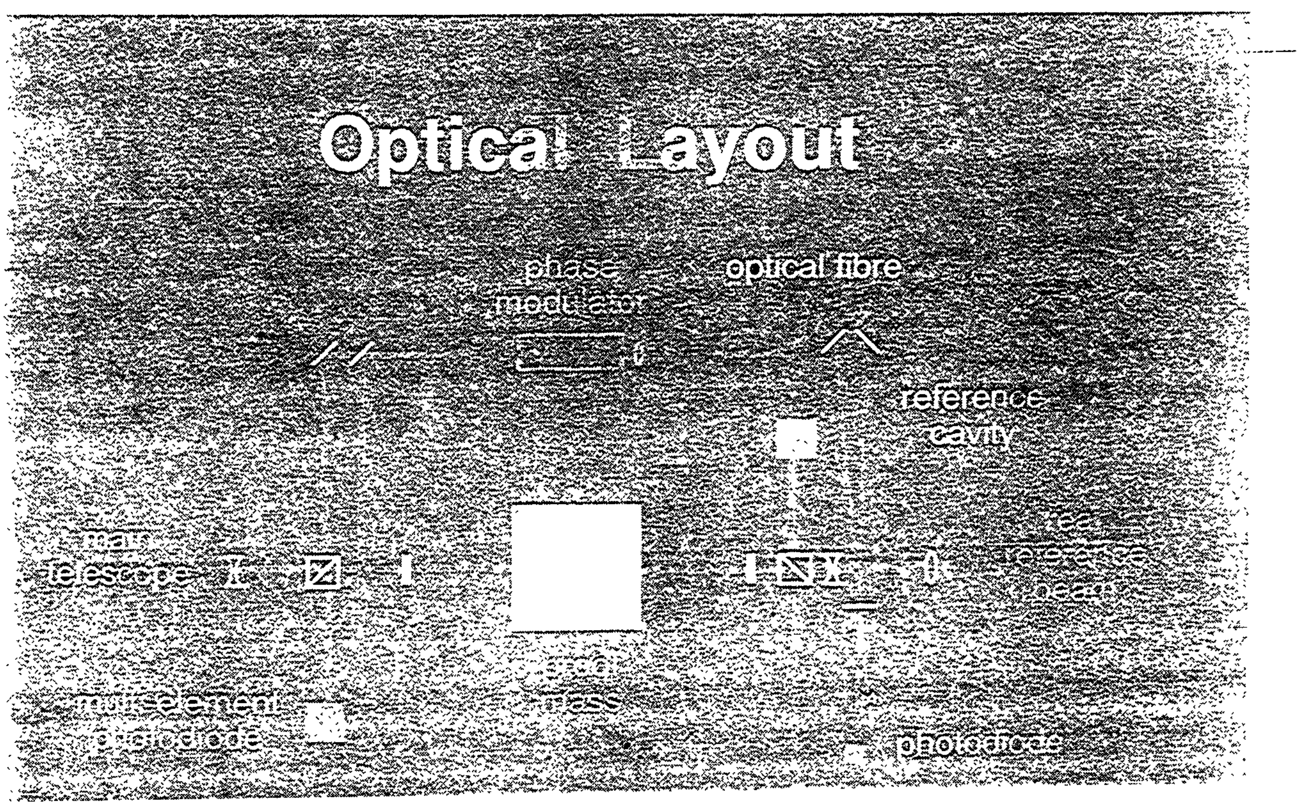
Optical Layout
phase modulator
optical fibre
reference cavity
main telescope
reference beam
proof mass
multi-element photodiode
photodiode

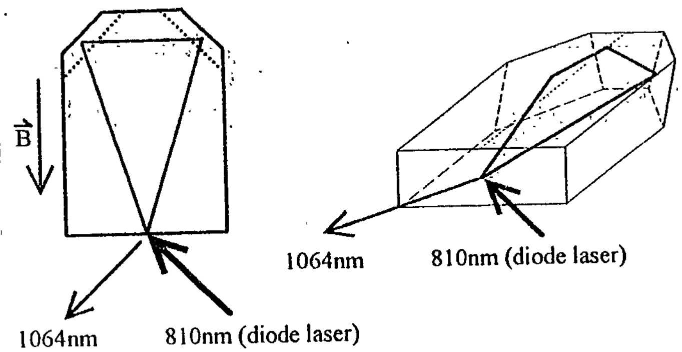

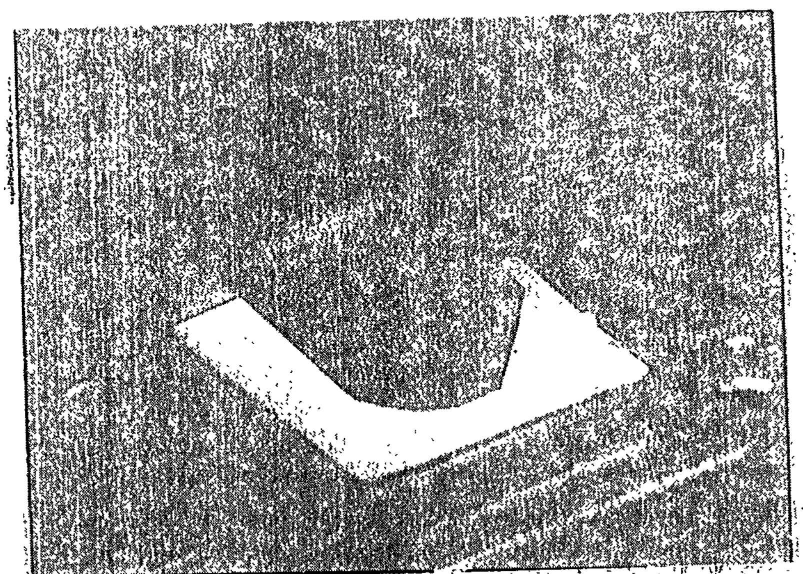

Monolithic Nd:YAG ring laser

Pump Scheme

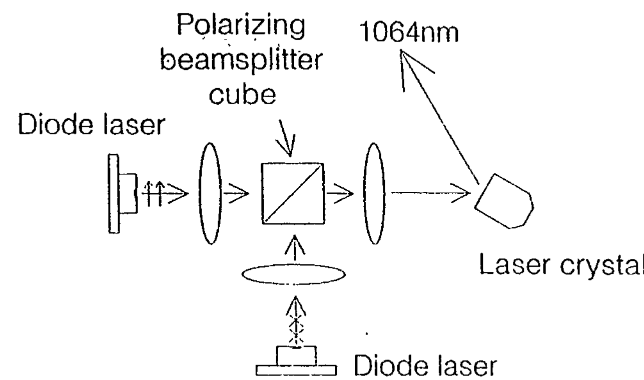

Diode lasers:
Siemens SFH 487401
emitting aperture 1x200um
output power 1W cw

Maximum pump power:	2.0W
Maximum output power:	1.1W
Slope Efficiency:	60%
Electrical/optical	
Conversion efficiency:	>15%

Pump scheme

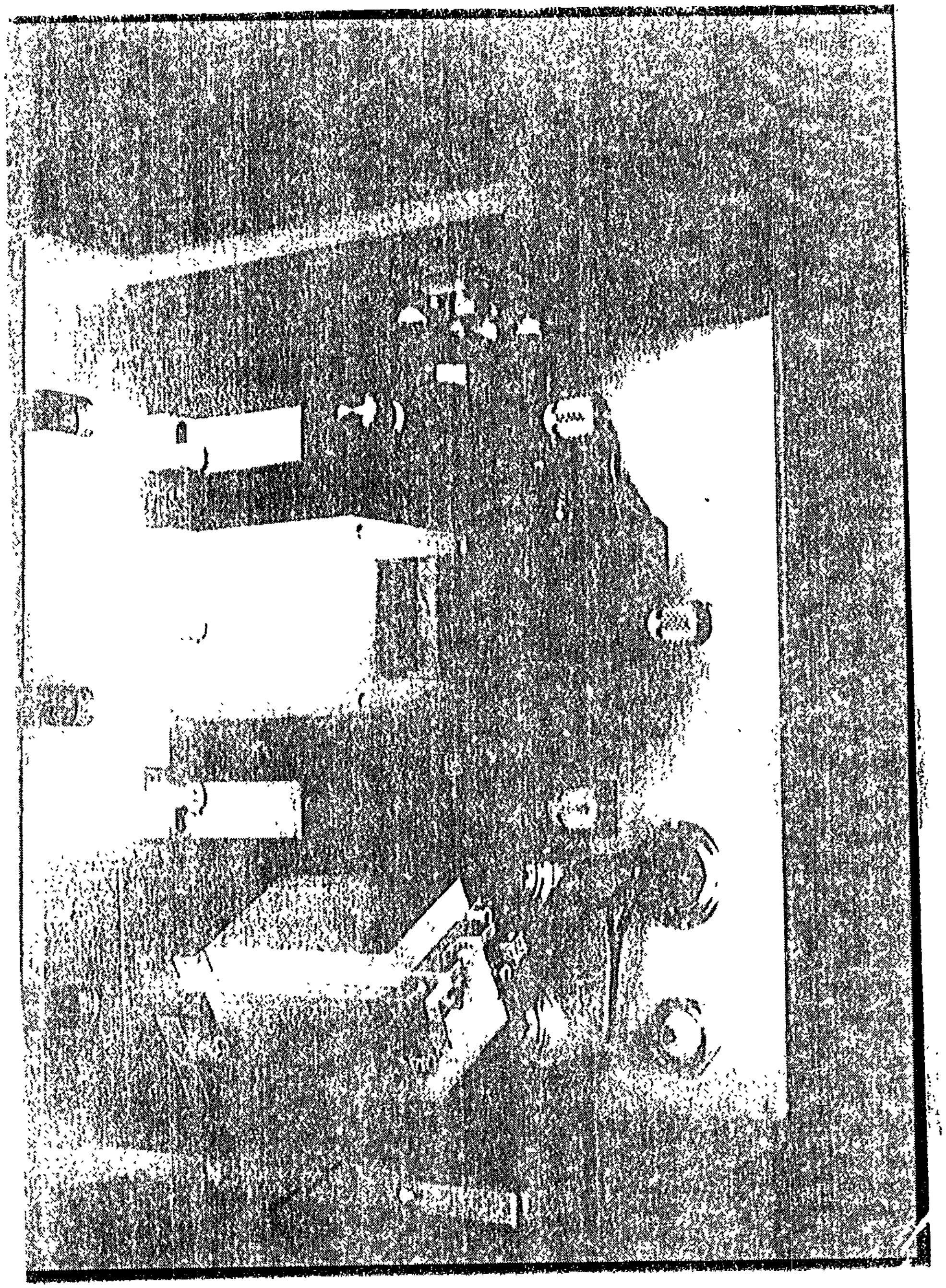

required frequency stability

phase of light $\phi = \frac{2\pi\nu}{c}\,\ell$

interference $\Delta\phi = \frac{2\pi\nu}{c}\,\Delta\ell$

frequency noise $\Rightarrow$ $d(\Delta\phi) = \frac{2\pi}{c}\,\Delta\ell\cdot d\nu$

displacement $\Rightarrow$ $d(\Delta\phi) = \frac{2\pi}{c}\,\nu\cdot d(\Delta\ell)$

GOAL : $d(\Delta\tilde{\ell})_{noise} < 2\cdot10^{-12}\,\frac{m}{\sqrt{Hz}}$

$\sim\ d\nu = 1\cdot10^{-6}\left[\frac{5\cdot10^{8}\,m}{\Delta\ell}\right]\frac{Hz}{\sqrt{Hz}}$

Noboru Uehara and Ken-ichi Ueda

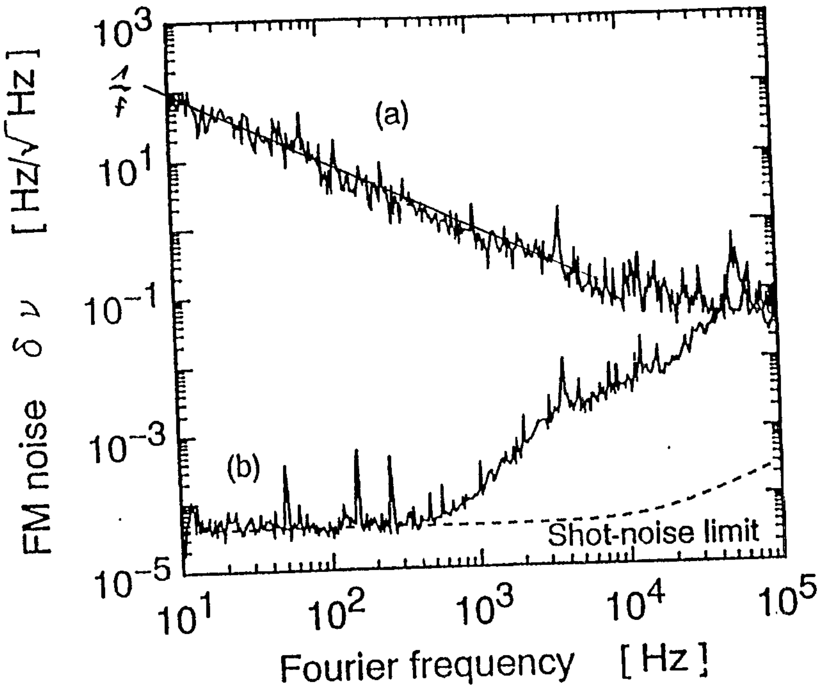

Fig. 3. Relative FM noise spectra at the error signal at a free-running state [curve (a)] at a stabilized state [curve (b)]. The calculated shot-noise limit is 4.2×10^{-5} asuming a $\frac{1}{f}$ dependency

$\sim \quad \delta\nu = 1\ \text{MHz}/\sqrt{\text{Hz}} \quad @\ 1\ \text{mHz}$

frequncy stabilisation

stabilization on a cavity mounted to an ULE platform

$$\frac{d\nu}{\nu} = \frac{d\ell}{\ell}$$

thermal expansion of the platform

$$\frac{d\ell}{\ell} = \alpha \cdot dT$$

$$\sim \quad d\nu = \nu \cdot \alpha \cdot dT$$

linear spectral density of frequency noise

$$d\nu = 8 \cdot \left[\frac{\alpha}{3 \cdot 10^{-8}\ \frac{1}{K}}\right] \cdot \left[\frac{dT}{10^{-6}\ K/\sqrt{\text{Hz}}}\right] \frac{\text{Hz}}{\sqrt{\text{Hz}}}$$

required amplitude stability

radiation pressure of 10 mW causes

i) steady acceleration $a = 6 \cdot 10^{-11} \frac{m}{s^2}$

ii) fluctuating acceleration

$$\hat{a} = 6 \cdot 10^{-11} \frac{m}{s^2} \cdot \frac{\widetilde{\delta P}}{P}$$

to keep $\hat{a} \leq 10^{-16} \frac{m}{s^2} \cdot \frac{1}{\sqrt{Hz}}$ we need

$$\frac{\widetilde{\delta P}}{P} \leq 2 \cdot 10^{-6} \frac{1}{\sqrt{Hz}}$$

Suppression of Intensity Noise by Electronic Feedback to the Diode Laser *

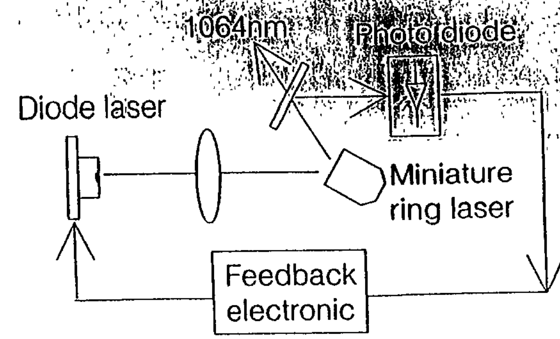

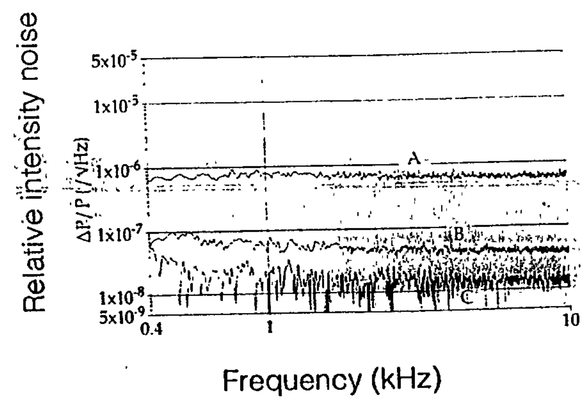

* Collaboration with the Australian National University
C.C. Harb, T.C. Ralph, M. B. Gray, H.-A. Bachor
published in IEEE J. of Quantum Electron. (1994).

2 04031-72 if

Intensity noise suppression

LZH

High power miniature ring laser

Diode lasers:
Siemens SFH 487401
emitting aperture 1x200um
output power 1W cw
internal cylindrical lens
to compensate astigmatism

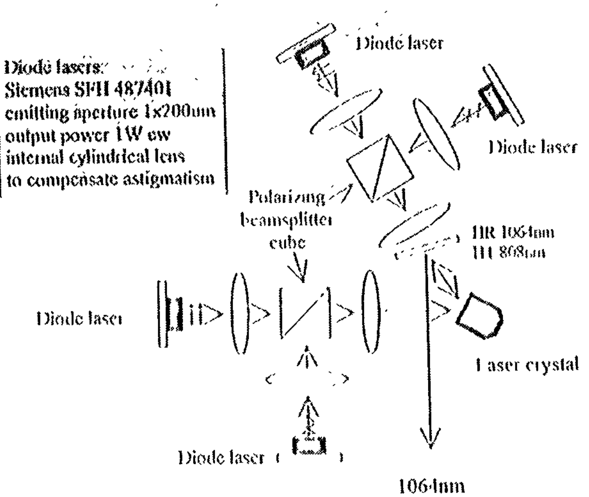

Maximum pump power:	4.0W
Maximum output power:	2.1W multimode
	1.8W single-frequency
Conversion Efficiency:	15%

Emitted radiation has low amplitude noise and a small spectral linewidth less than 1kHz.

High power miniature ring laser

Laser Design for LISA

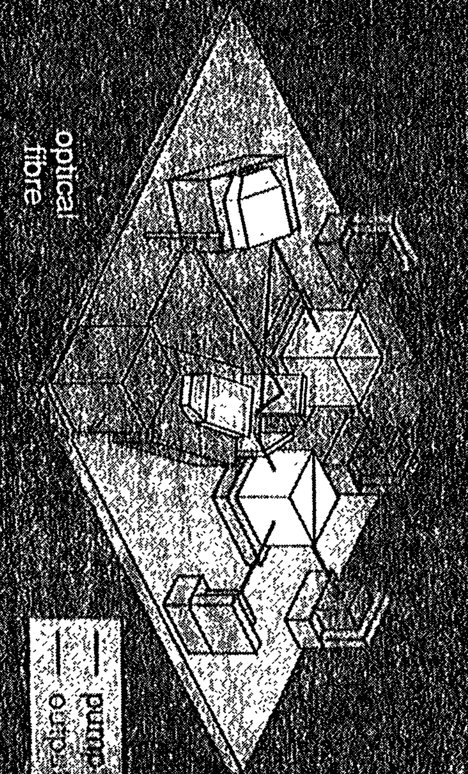

work to be done :

- one directional operation without or with low magnetic field
- injection-locked concept or single Nd-YAG laser
- reduction of intensity noise due to pointing of the laser at the fiber coupler
- investigation and stabilisation at low frequency
- test of new pump concepts (MOPA)
- longtime test of laser diodes :
  - lifetime
  - wavelength
- space qualification

OPTICAL ALIGNMENT FOR LISA

- ACQUISITION
- REQUIRED ACCURACY
- SENSING
- MODELLING

DAVID ROBERTSON
U. OF GLASGOW

POINTING ACQUISITION

LASER BEAM WIDTH 4×10^{-6} R

STAR TRACKER ACCURACY 10^{-4} R

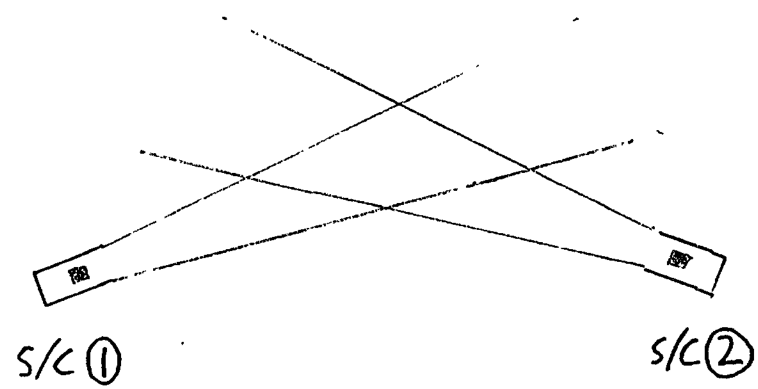

POINTING ACQUISITION

STAR TRACKER 10^{-4} RAD

EXPAND BEAMS *3 1.2×10^{-5} R

SCAN S/C 2 10×10 GRID 10^{-5} RAD
- PROOF MASS AS REFERENCE

ALIGN S/C 1 TO RECEIVED WAVEFRONT

ALIGN S/C 2 TO RECEIVED WAVEFRONT

WAVEFRONT DISTORTION

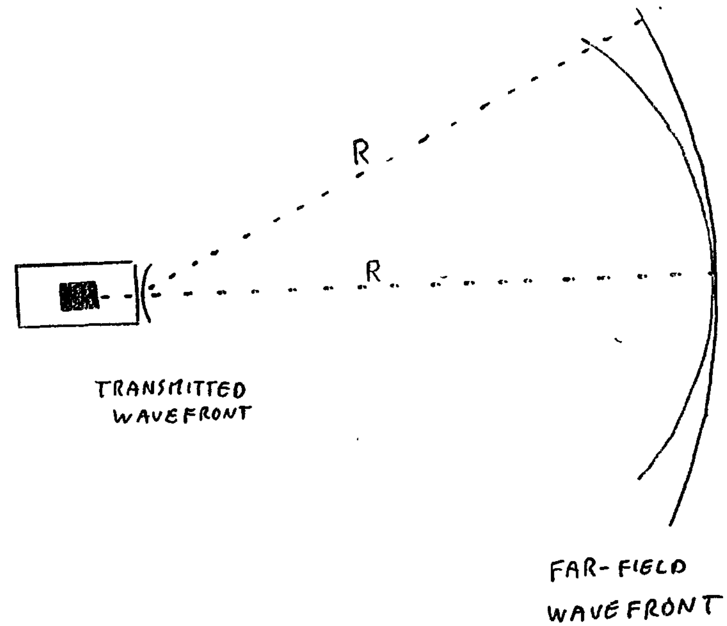

DEFOCUS ERROR

— STRONGEST COUPLING

$$\delta x = \frac{1}{32}\left(\frac{2\pi}{\lambda}\right)^2 D^2 \, \underline{d} \; \underline{\theta_{oc}} \; \underline{\delta\theta}$$

D - MIRROR DIAMETER [38 cm]
d - CURVATURE ERROR [TRANSMITTED WAVE FRONT]

REQUIREMENTS

$\delta x \lesssim 10^{-12}$ m/$\sqrt{Hz}$

$d \simeq \frac{\lambda}{15}$

$\rightarrow \theta_{oc}\,\delta\theta \lesssim 90 \times 10^{-18}$ rad^2/$\sqrt{Hz}$

E.G. $\theta_{oc} \simeq 15$ nrad

$\delta\theta \sim 6$ nrad/$\sqrt{Hz}$

WAVEFRONT SENSING

- DIFFERENTIAL PHASE SENSING WITH SPLIT PHOTODIODE

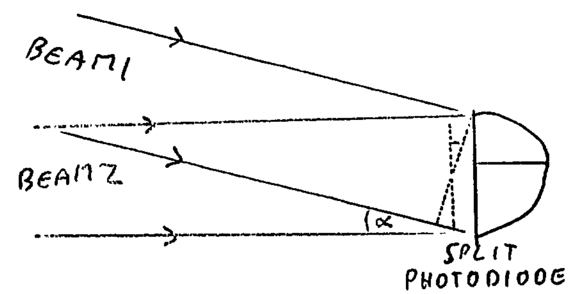

$\phi_1 = \phi_0 + \delta\phi$

$\phi_2 = \phi_0 - \delta\phi$

$\phi_1 + \phi_2 \rightarrow \phi_0$

$\phi_1 - \phi_2 \rightarrow \delta\phi \rightarrow \alpha$

FINE FOCUS

LOCK INTERFEROMETER

MODULATE POINTING θ, ω_θ

"GW" SIGNAL AT ω_θ

- ADJUST FOCUS TO MINIMISE

OPTICAL MODELLING

PAUL McNAMARA - GLASGOW

MARTIN CALDWELL - R.A.L.

A.S.A.P - RAY ANALYSIS

CODE V - TOLERANCING

Field after spider and secondary mirror have been cut out

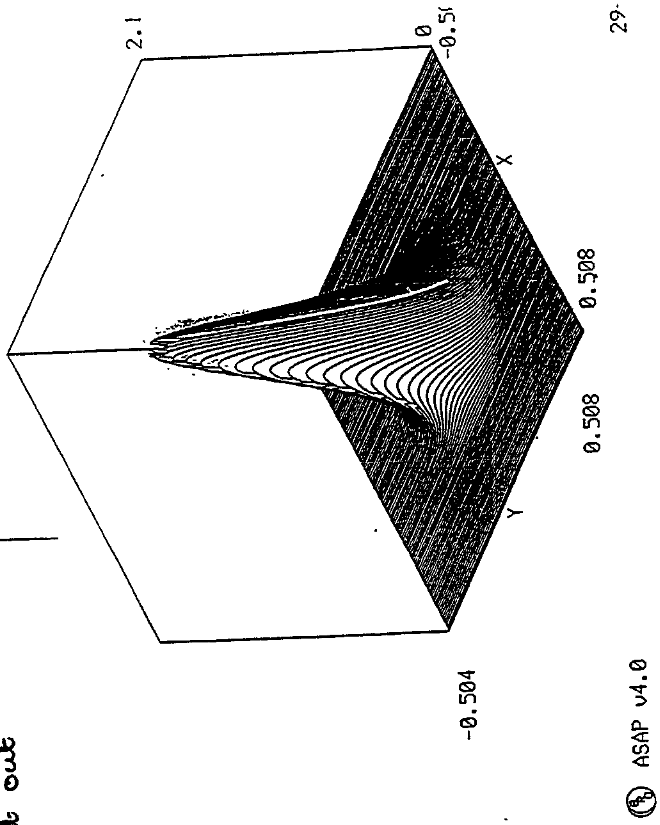

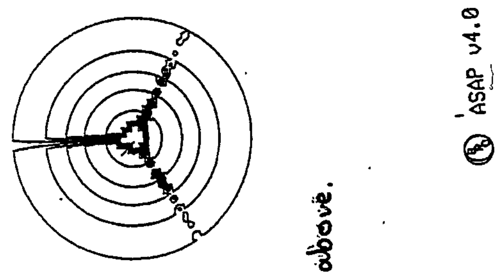

Contour plot of above.

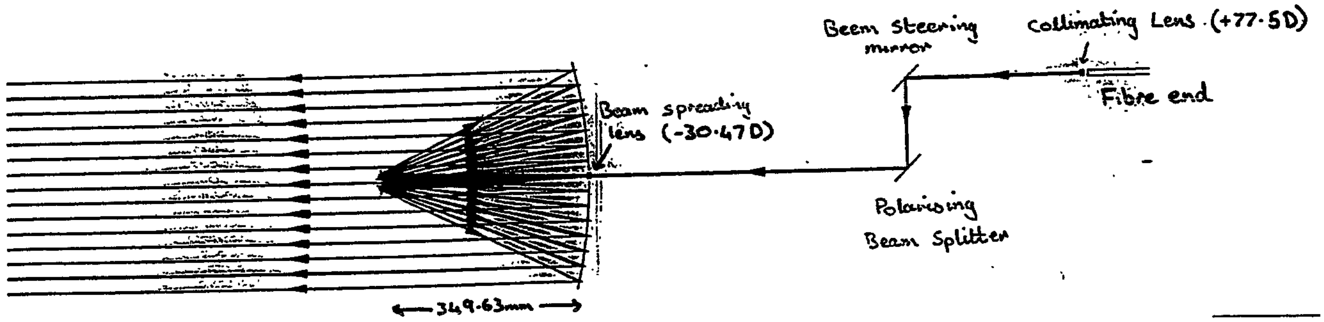

Primary : Diameter = 380mm
Focal Length = 380mm

Secondary : Diameter = 40mm
Focal length = 33mm

Z
7203,-.1000E-2

Contour plot of wavefront error, showing signs of spider obsceration

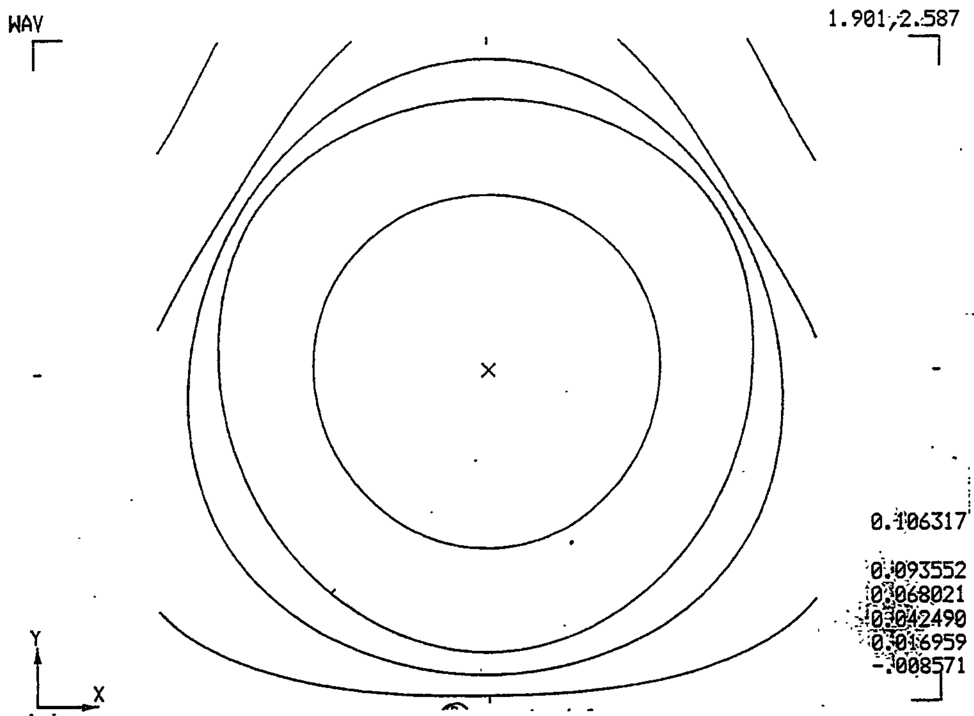

Field after propogation (at 5x Confocal Distance)

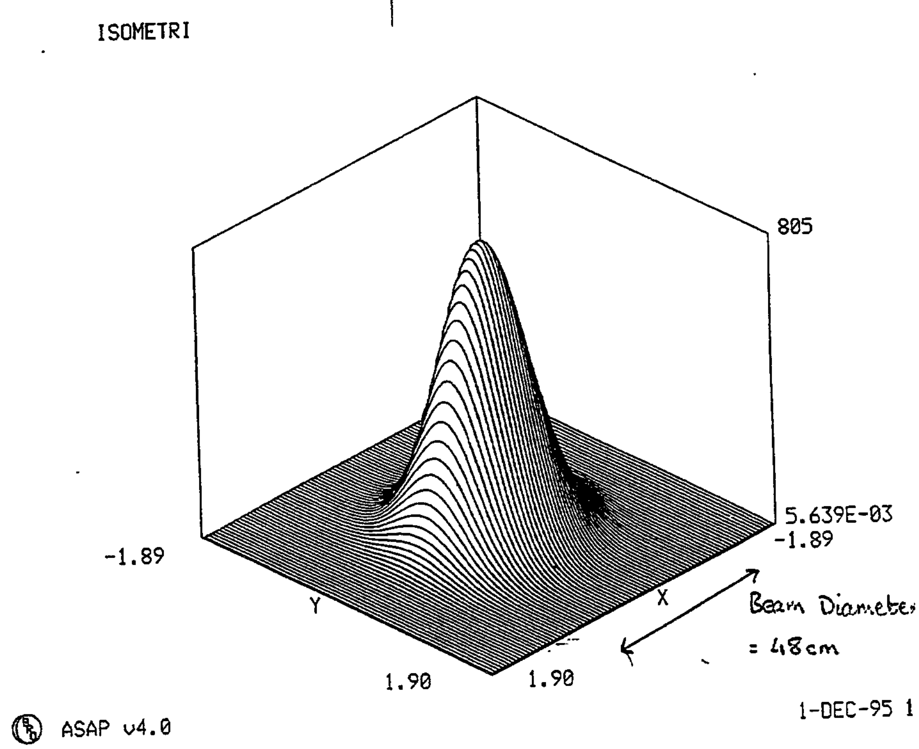

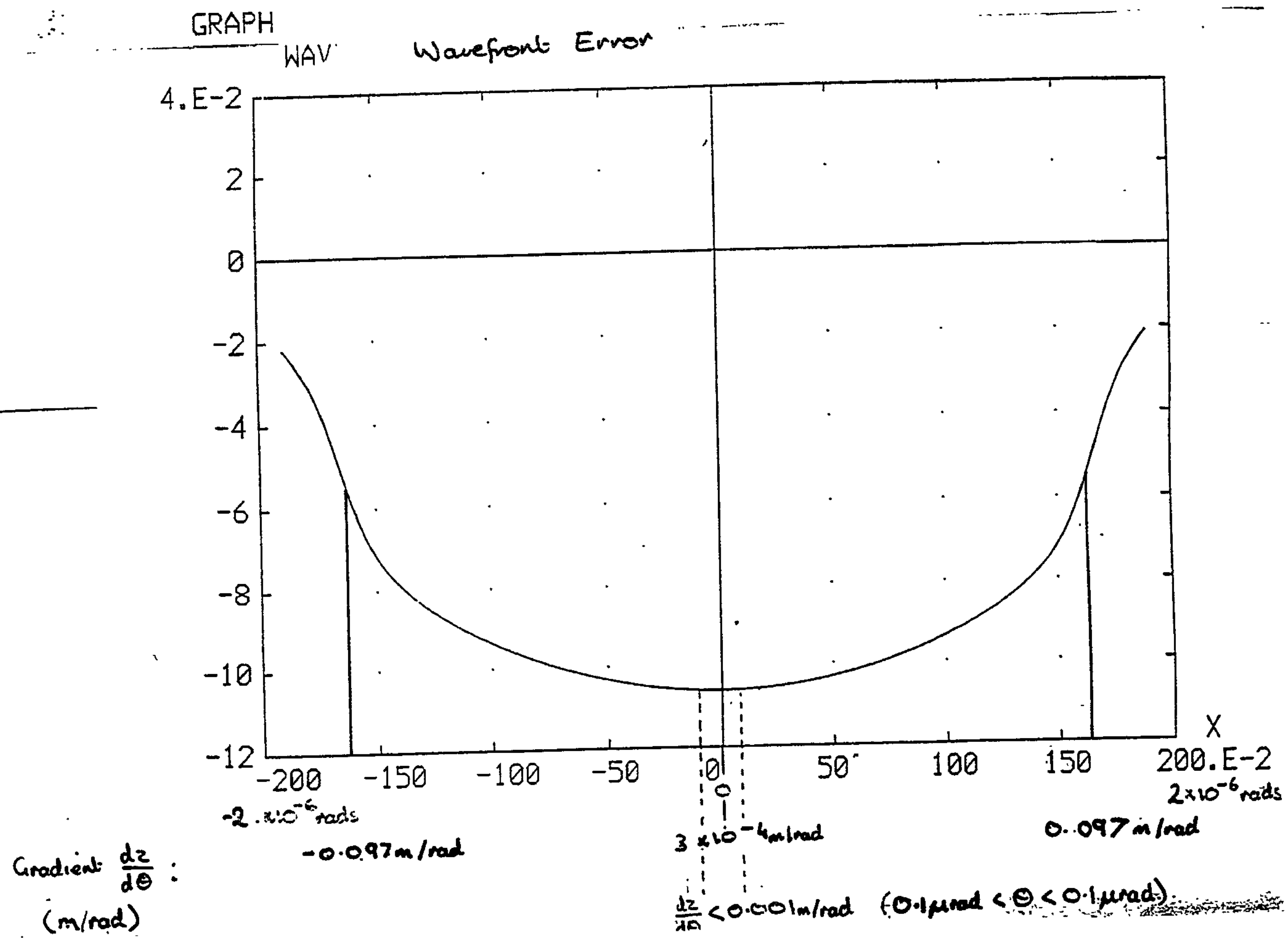

GRAPH
WAV
Wavefront Error
4.E-2
2
0
-2
-4
-6
-8
-10
-12
-200
-150
-100
-50
0
50
100
150
200.E-2
X
-2 x10^-6 rads
2x10^-6 rads
-0.097 m/rad
0.097 m/rad
3 x10^-4 m/rad
Gradient dz/dθ :
(m/rad)
dz/dθ < 0.001 m/rad (0.1 μrad < θ < 0.1 μrad)

LISA Error Budgets

Robin T. Stebbins
JILA/University of Colorado

Aspen Winter Conference on Gravitational
Waves and Their Detection
Aspen Center for Physics

Aspen, Colorado
16 January 1996

Outline

- LISA - A different kind of interferometer
- Noise types, error allocation and combination
  - Optical-path noise
  - Acceleration-like noise
  - Allocation, budget and all that
  - Combining error allocations
- Optical-path noise
  - Detector shot noise
  - Master clock noise
  - Residual laser phase noise
  - Laser beam-pointing noise
  - Scattered-light effects
- Acceleration noise
  - Thermal distortion of spacecraft
  - Thermal distortion of payload
  - Payload gravity noise
  - Thermal gradients in test mass cavity
  - Electrical force from charging and patch fields
  - Lorentz force from charging and interplanetary fields
  - Residual gas impacts
  - Telescope thermal expansion
  - Magnetic force on test mass from fluctuating interplanetary field
  - Other substantial effects
  - Other insubstantial effects

A Different Interferometer

- Test masses are in free fall.
- The solar orbit is a very benign environment.
- The drag-free system further reduces external disturbances.
- LISA has a comparatively simple optical system.

Noise Types, Error Allocation and Combination

- Optical-path noise: unwanted effects that make the apparent optical path change. These generally have a white spectrum.
- Acceleration noise: unwanted effects that are, or look like, forces on the test masses, i.e., that have $1/f^2$ frequency dependence when displayed as a displacement. Warning: Those which are driven by solar insolation are different by a small fractional power of f.
- We have constructed a budget by identifying the major sources of errors, picking an error allocation that appears sufficient - or even generous - and making an allocation for other smaller effects, known and unknown.
- We have adopted a noise combination procedure that was recommended to us by Dan Debra as one that worked well in other precision measurement satellites at Stanford.
  - Simply add the five largest errors, which are not know to be uncorrelated
  - Add the remainder quadratically.

This is an attempt to be conservative and reflect our ignorance.

Major Sources of Optical-Path Noise

Source	Error 10^{-12} m/$\sqrt{\text{Hz}}$	Number
Detector shot noise (random)	7	×4
Master clock noise (random)	10	×1
Residual laser phase noise after correction	4	×1
Laser beam pointing instability	4	×4
Laser phase measurements and offset lock	2	×4
Scattered light effects	2	×4
Other substantial effects	2	×60
Total Error Allocation for L_2-L_1	**31×10^{-12} m/$\sqrt{\text{Hz}}$**	

Major Sources of Acceleration Noise

Source	Error $10^{-16} \cdot (10^{-4}\text{ Hz}/f)^{1/3}$	Number
Thermal distortion of outer layer	5	×4
Thermal distortion of payload (internal)	2.5	×4
Payload gravity noise, plus spacecraft displacement	2.5	×4
Temperature difference variations across cavity	2.5	×4
Electrical force on charged proof mass	2.5	×4
Lorentz force on charged proof mass from fluctuating interplanetary field	2.5	×4
Residual gas impacts on proof mass	2.5	×4
Telescope thermal expansion	2.5	×4
Magnetic force on test mass	1	×4
Other substantial effects	2.5	×20
Other smaller effects	1	×100
Total Error Allocation for Second Time Derivative of L_2-L_1	**$3 \times 10^{-15} \cdot (10^{-4}\text{ Hz}/f)^{1/3}$ m/s^2/$\sqrt{\text{Hz}}$**	

Conclusions

- We have made a fairly extensive, initial survey of possible error sources.
- The major contributors have been estimated.
- There are no insurmountable obstacles.
- These conservative budgets give a very rewarding sensitivity.

Glasgow Group

Jim Hough
Gavin Newton
Norna Robertson
Harry Ward

David Robertson
Sheila Rowan
Ken Skeldon
Ken Strain
Alison McLaren - M. PLISSI

Morag Casey
Paul McNamara
Stuart Killbourn
Sharon Twyford

Colin Craig
Allan Latta
Angus McKellar

PROTOTYPE DETECTOR *

- THERMAL NOISE
- TEST GEO600 ITEMS + STRATEGIE

SUSPENSION DEVELOPMENT

- MODELLING
- BUILDING
- MONOLITHIC, HIGH Q *

OPTICAL MODECLEANER *

LASER AMPLIFIER

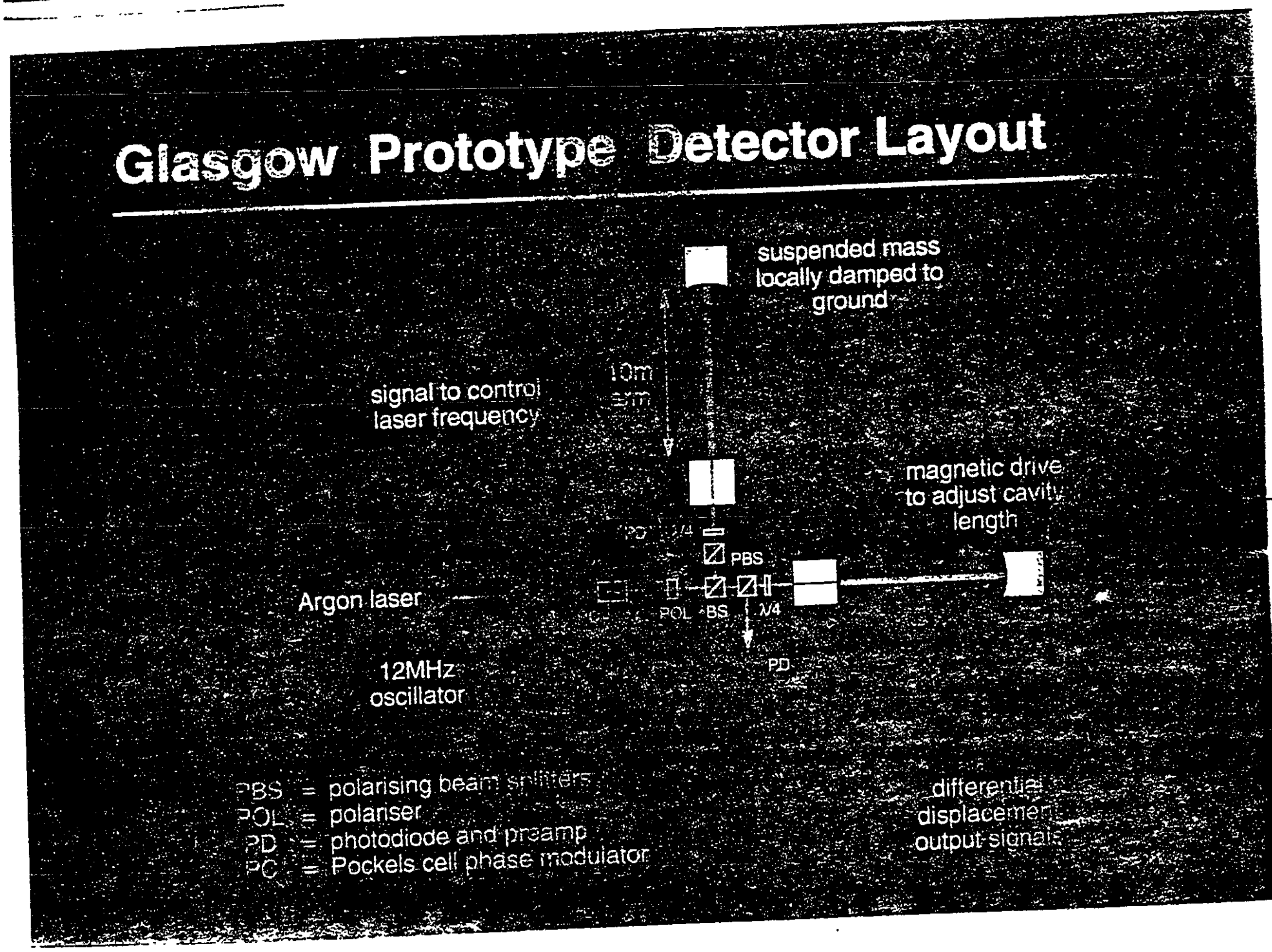

CALIBRATION CROSS-CHECK

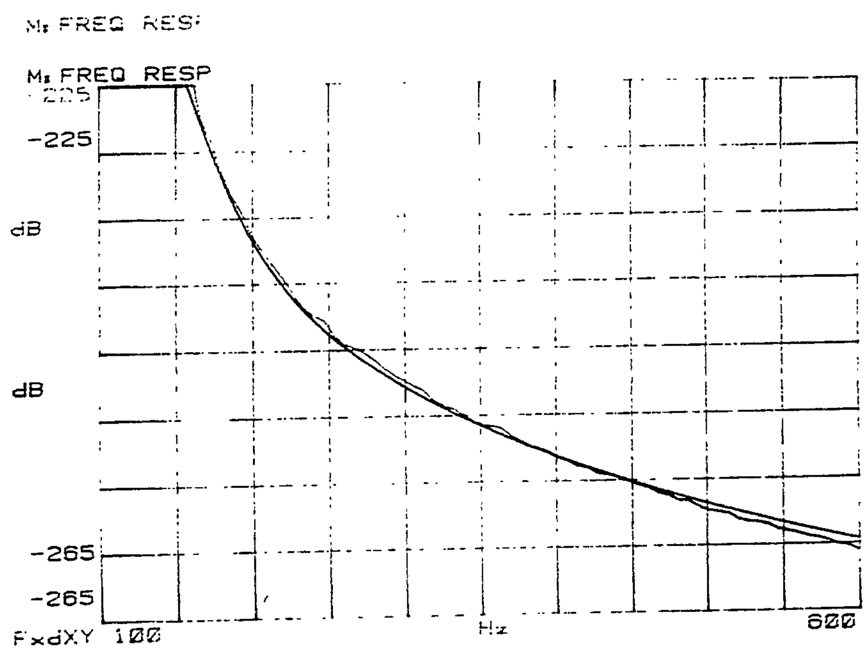

Displacement Noise

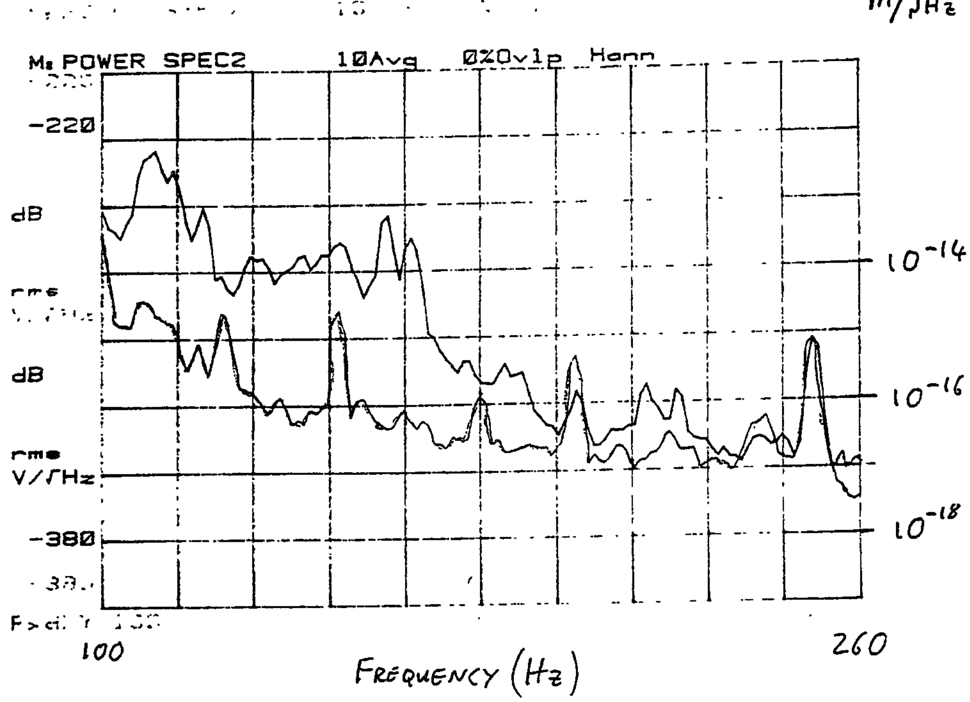

Displacement Noise

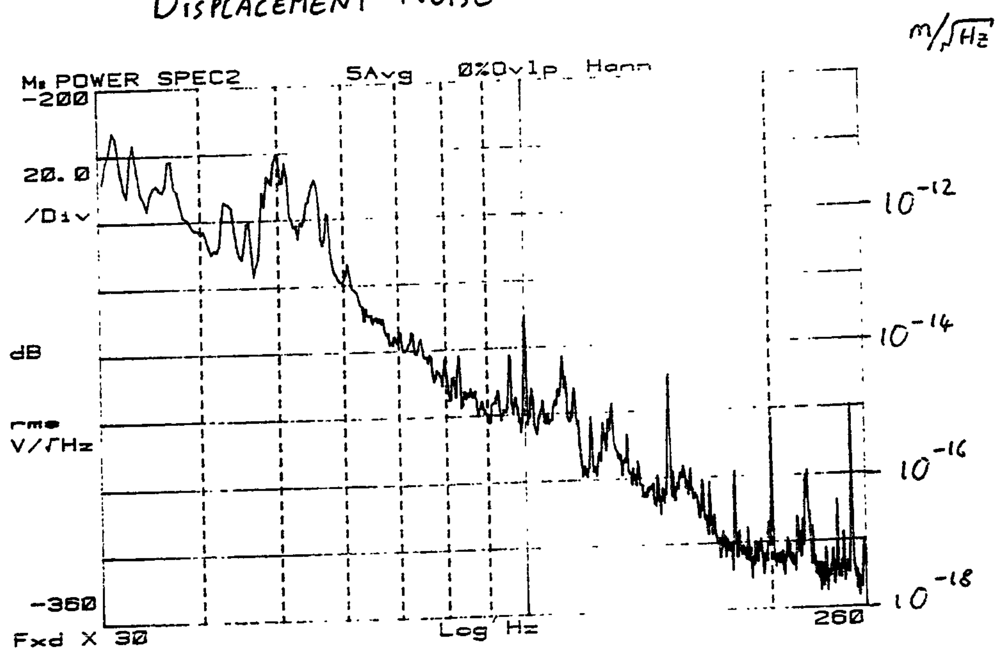

Glasgow Prototype Modecleaner

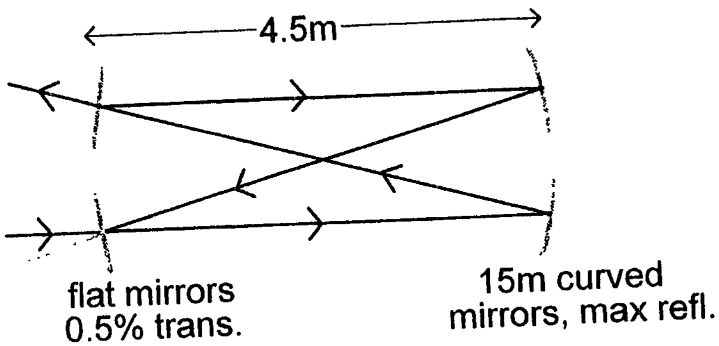

finesse = 600
FSR/2 = 8.3 MHz
effective cavity length = 9 m
optical path length = 18 m
TEM10 suppression = 350
TEM20 suppression = 300

Glasgow Modecleaner

Progress Report
December 1995

K. Skeldon

Acknowledgments

K. Strain
A. Grant
H. Ward
J. Hough
A. Latta
D. Edwards
et al...

Coupling of Beam Jitter through Beam Splitter Misalignment

Require!

$$\frac{\Delta x}{w} < 10^{-10} / \sqrt{\text{Hz}}$$

Implies 4 orders of magnitude suppression

Coupling of Beam Width Pulsation through Mirror Curvature Mismatch or Effects of Scattered Light

Require!

$$\frac{\Delta w}{w} < 10^{-11} / \sqrt{\text{Hz}}$$

Implies about five orders of magnitude suppression

Typical Nd:YAG Laser Beam Jitter Noise

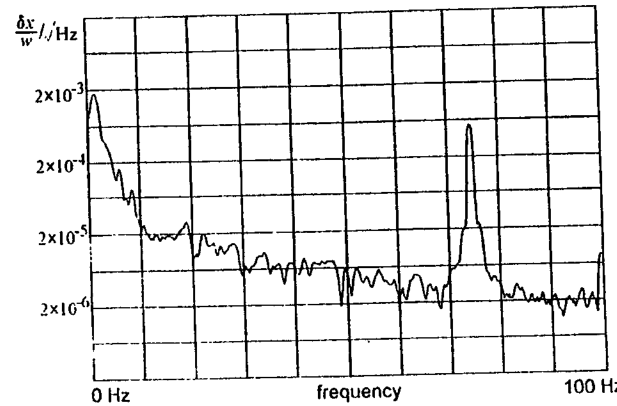

Typical Nd:YAG Laser Beam Width Pulsation Noise

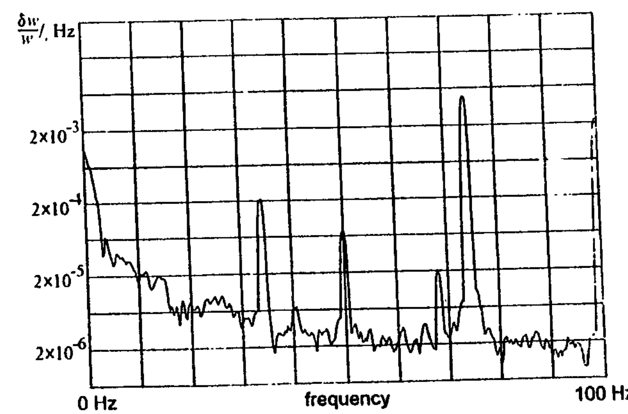

Spatial Filtering Action

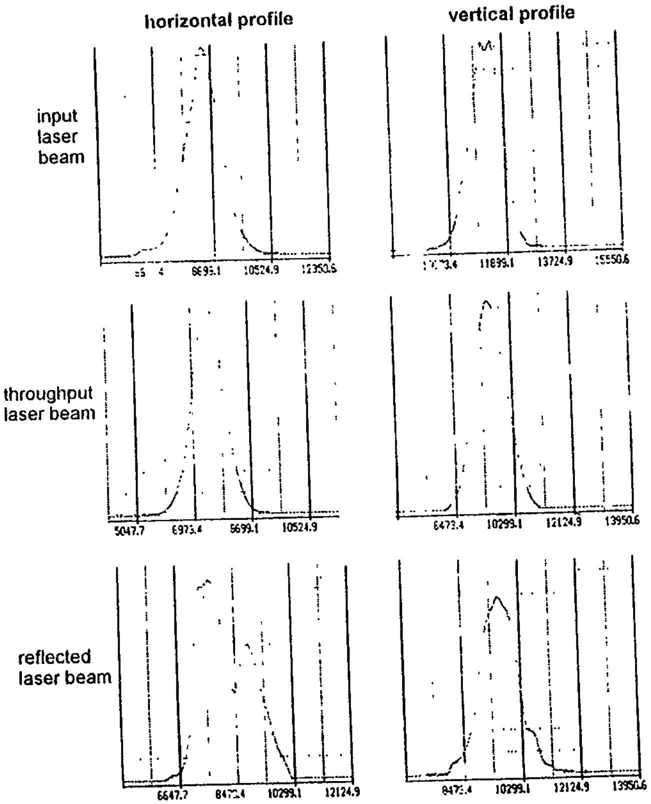

Reduction of Applied Jitter Peak

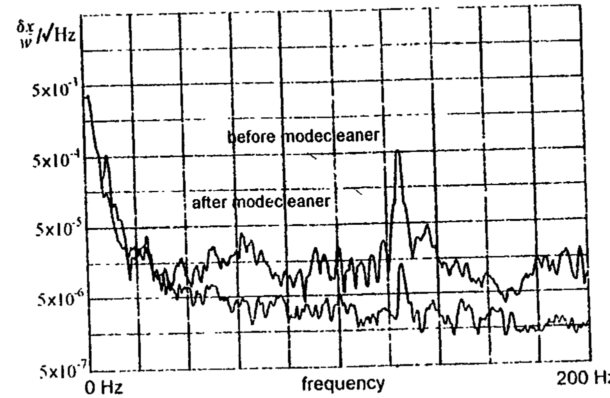

Reduction of Applied Jitter Peak (Intensity Servo after Modecleaner)

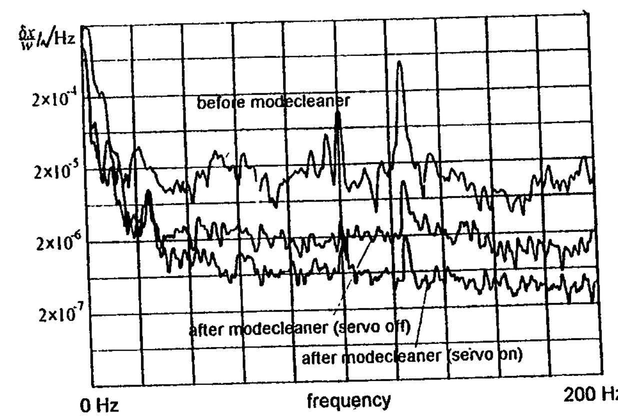

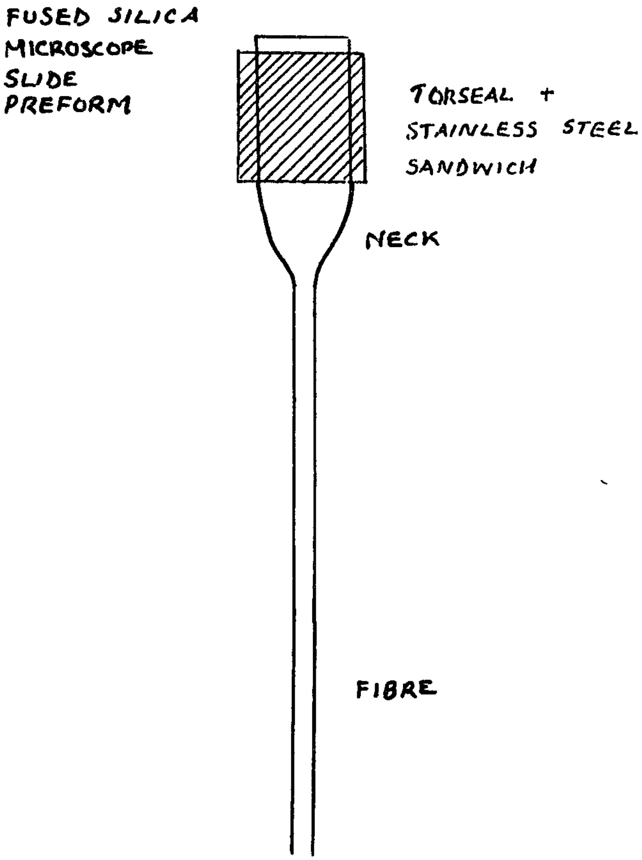

DIRECT MEASUREMENT OF MATERIAL Q FOR FUSED SILICA RIBBON FIBRES

S.M. TWYFORD
A.C. MCLAREN

R. HUTCHINS
J. HOUGH
N.A. ROBERTSON

J. FALLER.

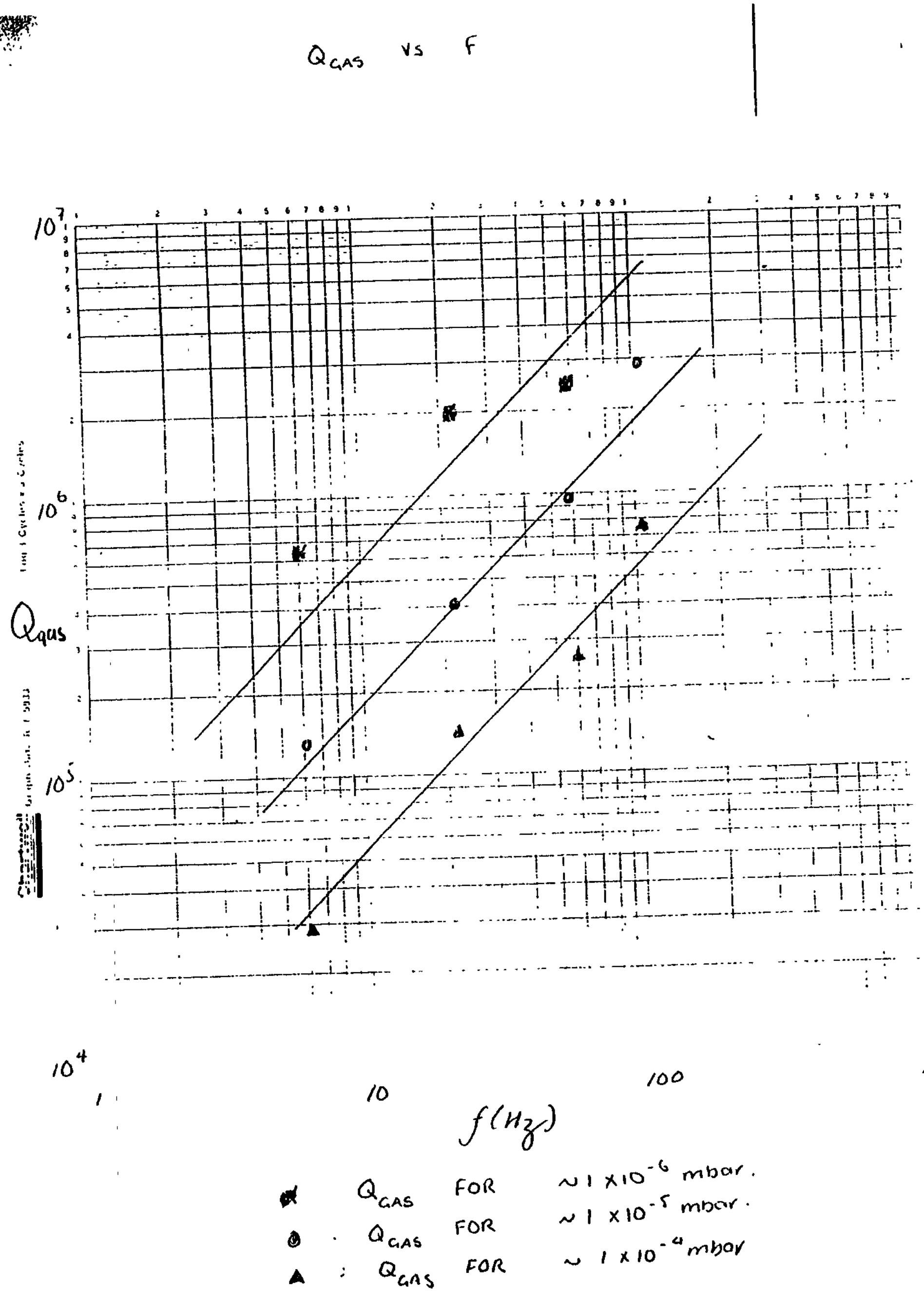

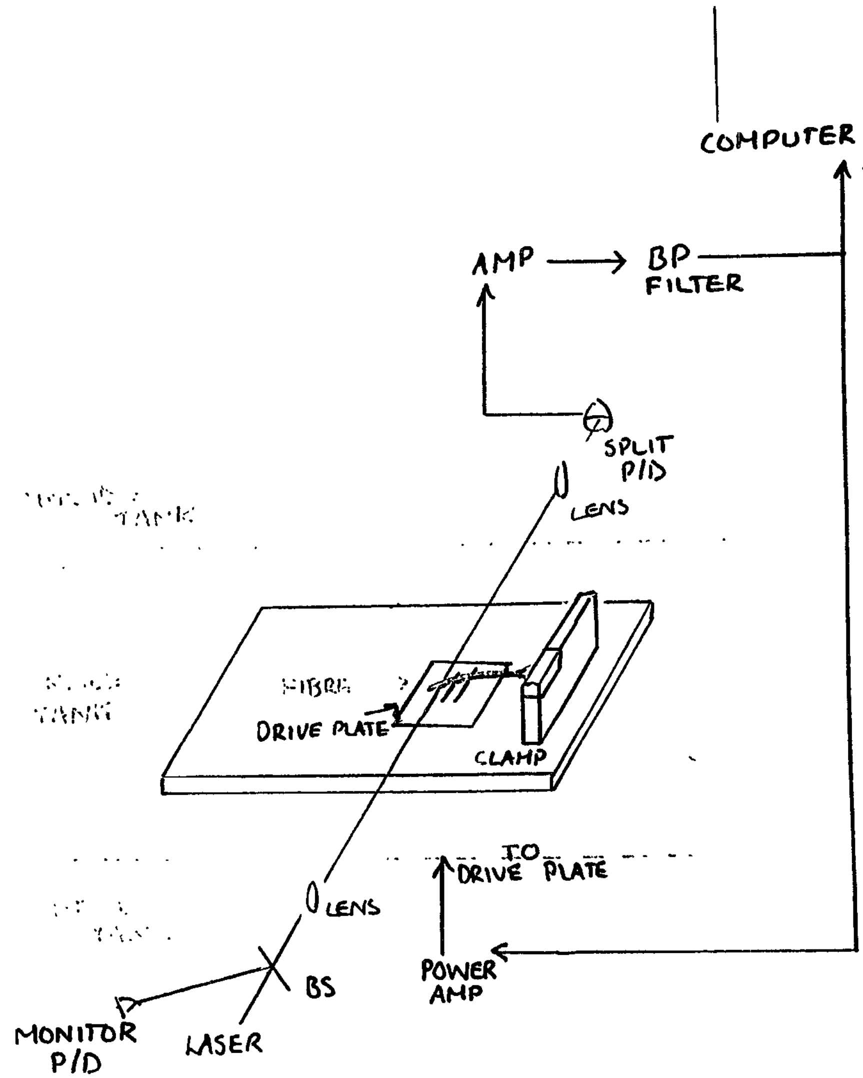

+ SEISMOMETER TO MONITOR GROUND VIBRATIONS

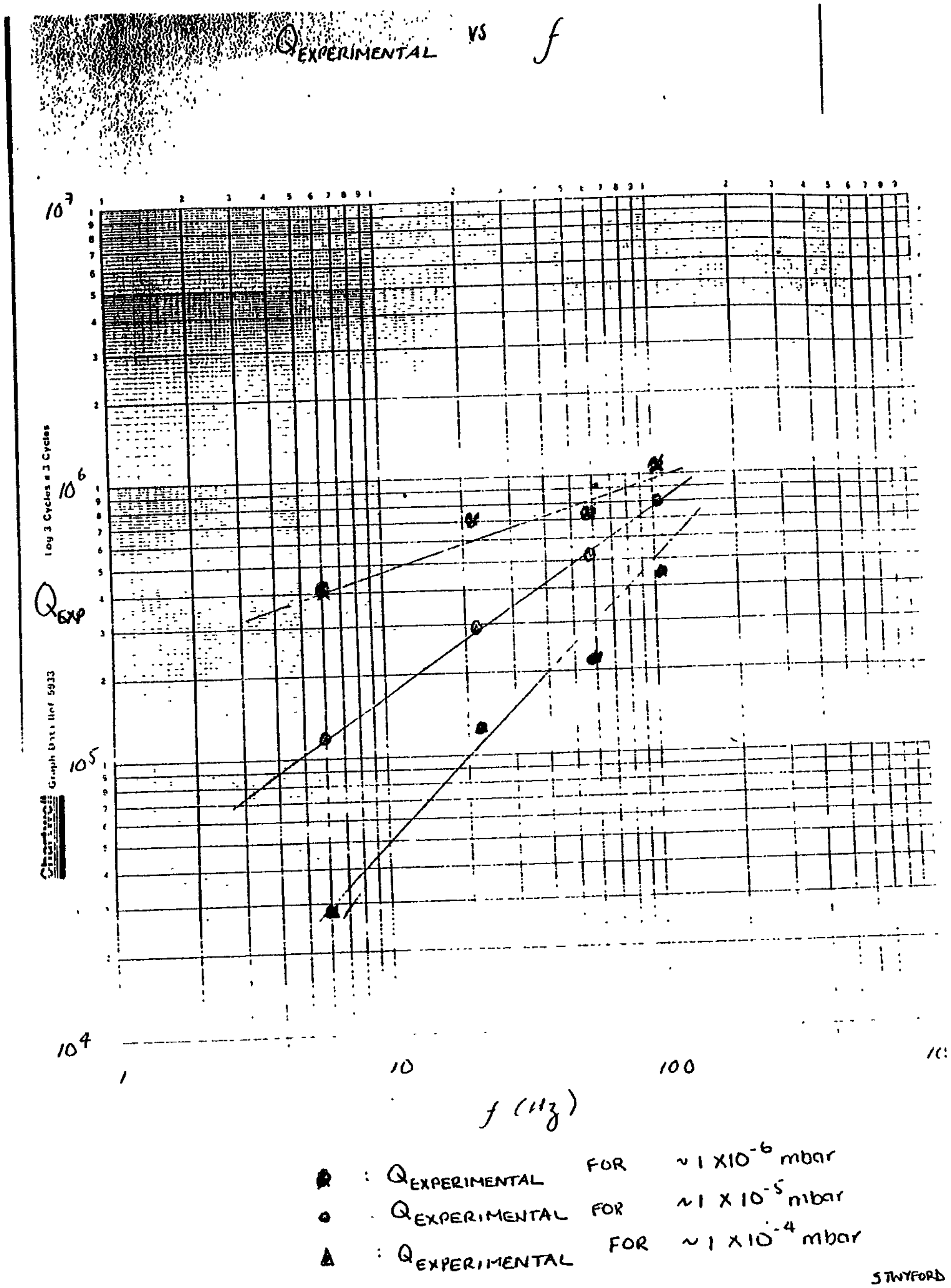

$$\frac{1}{Q_{gas}} = \frac{1}{Q_{experiment}} - \frac{1}{Q_{material}}$$

Q_{gas} = Q UPPER LIMIT ASSUMING GAS DAMPING (FOR A GIVEN FREQ. AT A GIVEN PRESSURE).

$Q_{experiment}$ = Q OBTAINED FROM EXPERIMENT

$Q_{material}$ = ASSUMED MATERIAL $Q = 1 \cdot 1 \times 10^6$ OBTAINED FROM BEST EXPERIMENTAL RESULT.

Q_{gas} VS P

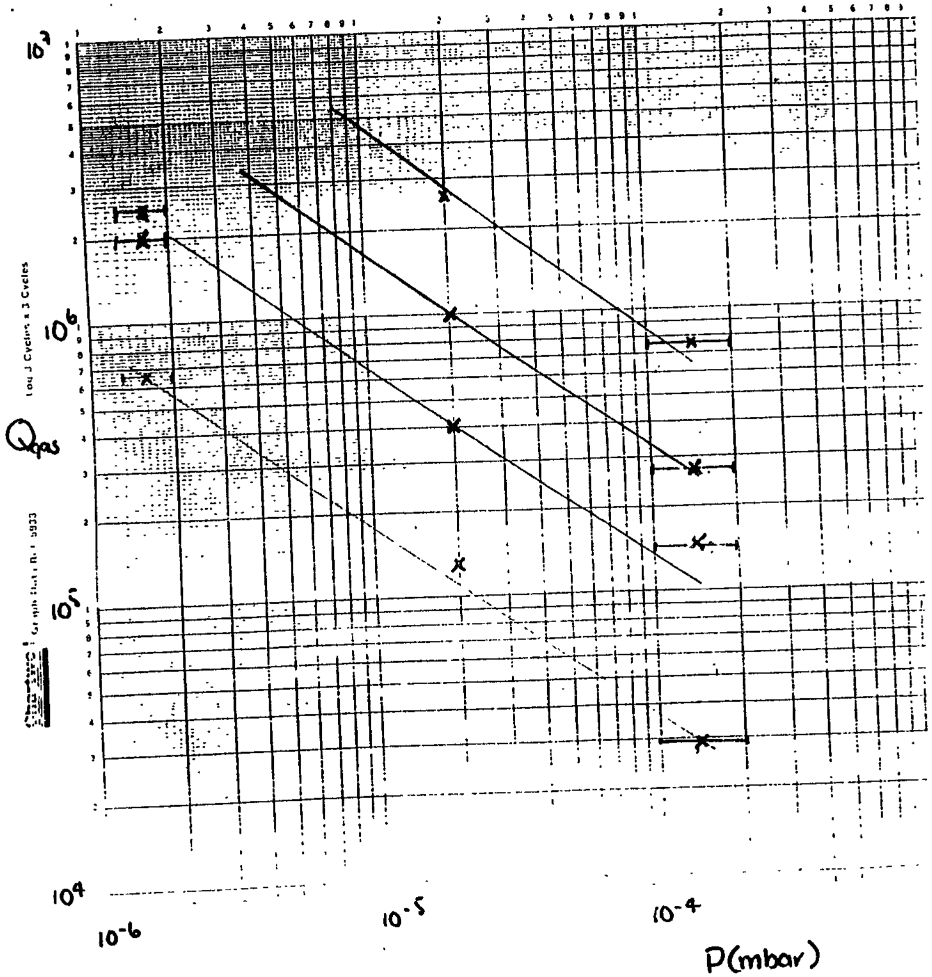

X : 6·06 Hz
X : 22·8 Hz
X : 59·6 Hz
X : 106 Hz

RESULTS SHOW

$$Q_{gas} \propto F$$

AGREEMENT WITH SIMPLIFIED STATIST GAS DAMPING MODEL

$$Q_{gas} = \frac{\omega_n m}{2PA}\sqrt{\frac{RT}{M}}$$

ω_n = MODE FREQUENCY

m : FIBRE MASS

P : TANK PRESSURE

A : SURFACE AREA.

T : TEMP.

M : MOLECULAR MASS OF GAS PRESENT IN TANK

THERMOELASTIC DAMPING

FREQ. OF MAX. DAMPING GIVEN BY :-

$$f_{char} = \frac{\pi}{2} \frac{K}{\rho C t^2} \qquad \text{(RIBBON)}$$

f_{char} = CHARACTERISTIC FREQ

K = 1·38 W/mK (AT 20°C)

ρ = 2·2 x10^3 Kg/m^3

C = 772 J/Kg.K

t = 100μm :- ESTIMATE

Q AT f_{char} GIVEN BY :-

$$\phi(\omega) = \frac{\Delta}{2}$$

$$Q = \frac{1}{\phi(\omega)}$$

$\phi(\omega)$: LOSS ANGLE

Δ = RELAXATION STRENGTH

$$= \frac{E\alpha^2 T}{\rho C}$$

$E = 7 \times 10^{10}$ N/m^2

$\alpha = 5·1 \times 10^{-7}$ /K

FROM SIMPLE GAS DAMPING, EXPECT :

$$Q_{gas} \propto \frac{1}{P}$$

EXPERIMENTAL RESULTS SHOW :

$$Q_{gas} \propto P^{-2/3}$$

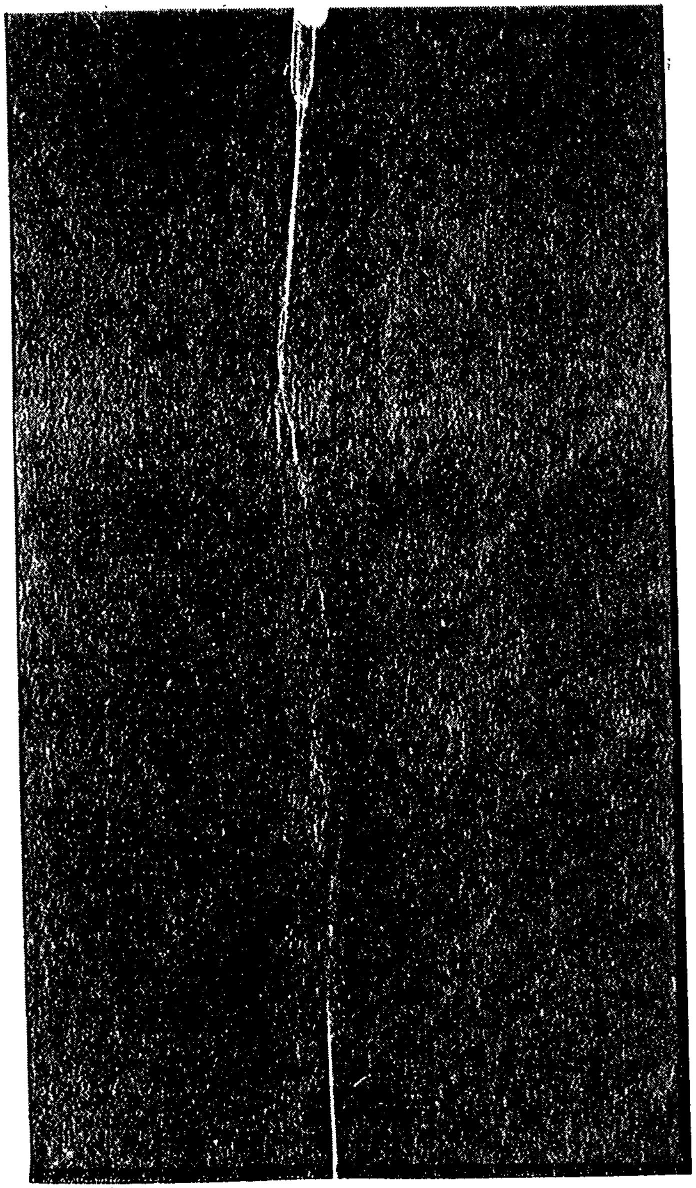

THE RELAXATION TIME, τ, FOLLOWS FROM f_{char}

$$\tau = \frac{1}{2\pi f_{char}}$$

FOR REMAINING PTS. ON THERMOELASTI DAMPING CURVE :-

$$\phi = \frac{\Delta \omega \tau}{1 + \omega^2 \tau^2}$$

$$Q = \frac{1}{\phi}$$

Power Recycling at the 30m Prototype Detector in Garching

Dietmar Schnier

Mathias Schrempel
Harald Lück

Karsten Danzmann
Walter Winkler
Roland Schilling

Jun Mizuno
Gerhard Heinzel

30m-Prototype Setup

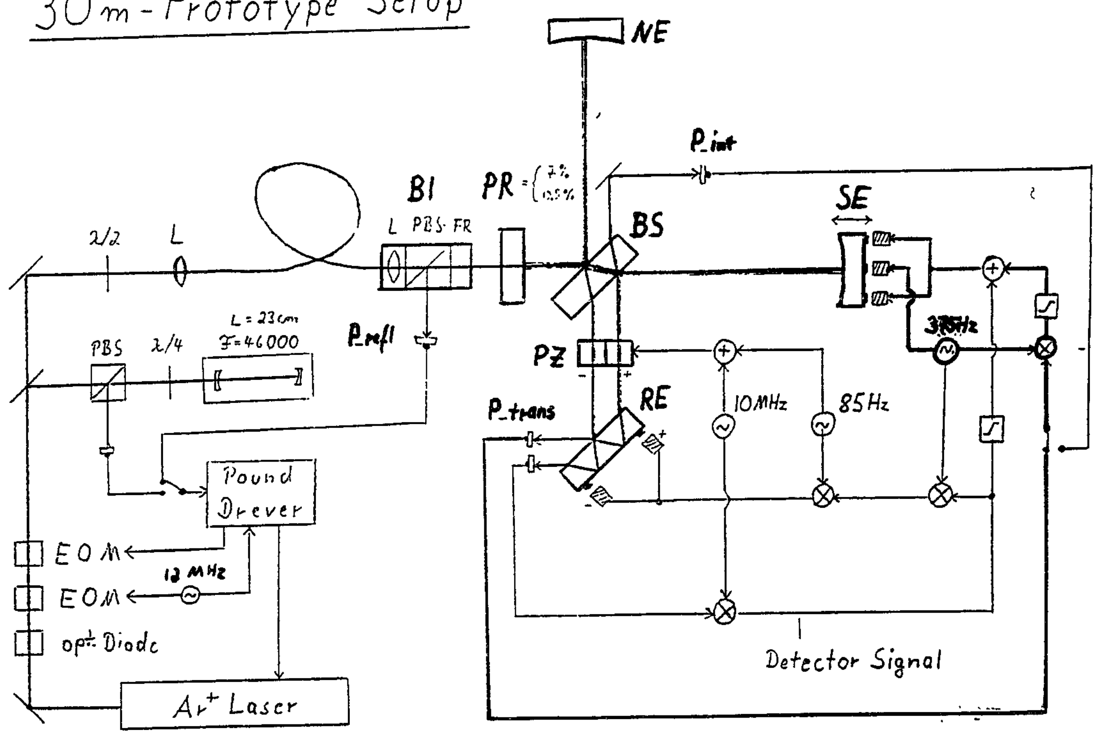

50% Beamsplitter, T_PR=7%, Losses=.3%

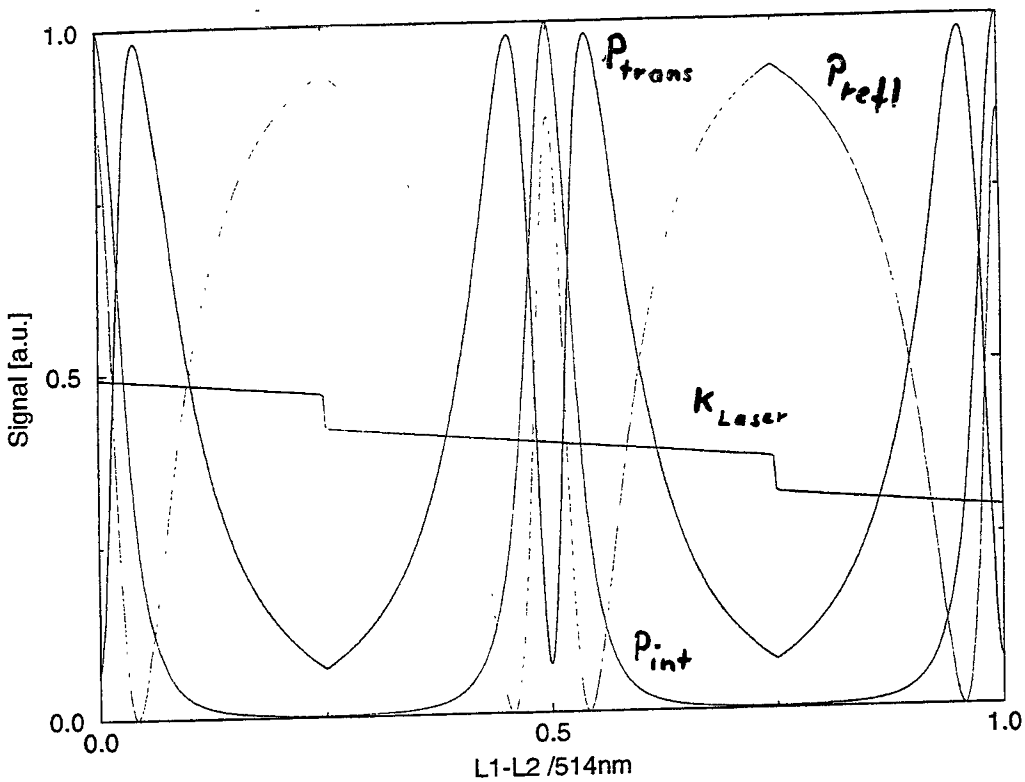

T_BS = 54% , T_PR = 7% , L = 0.3%

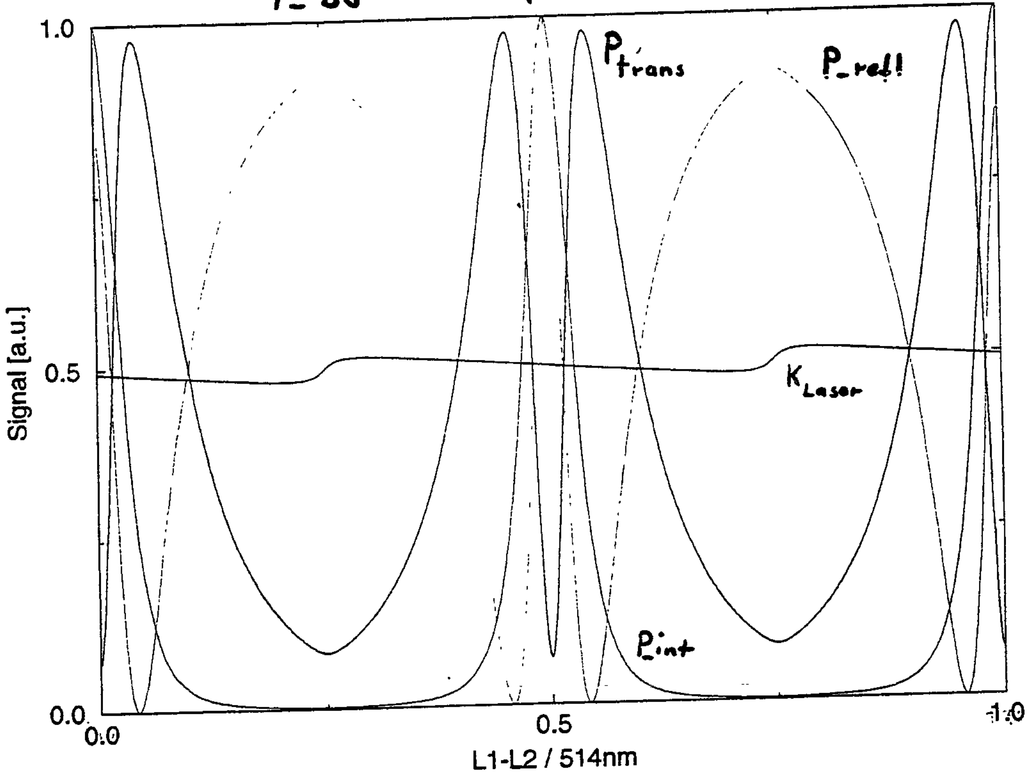

T_PR = 7%

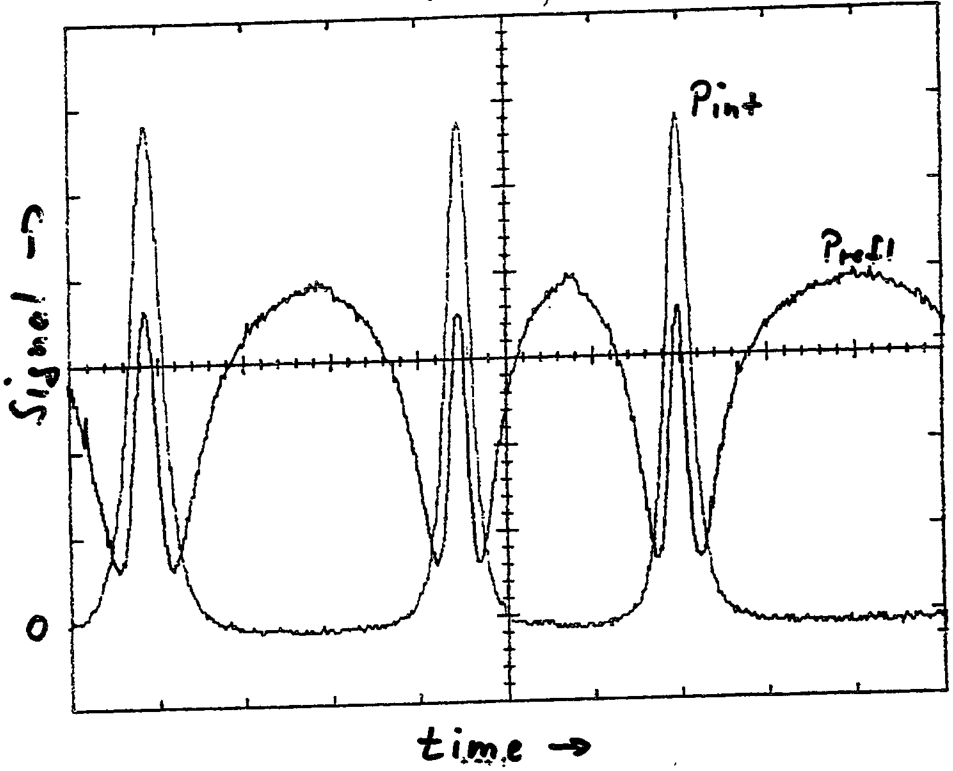

T_PR = 7%

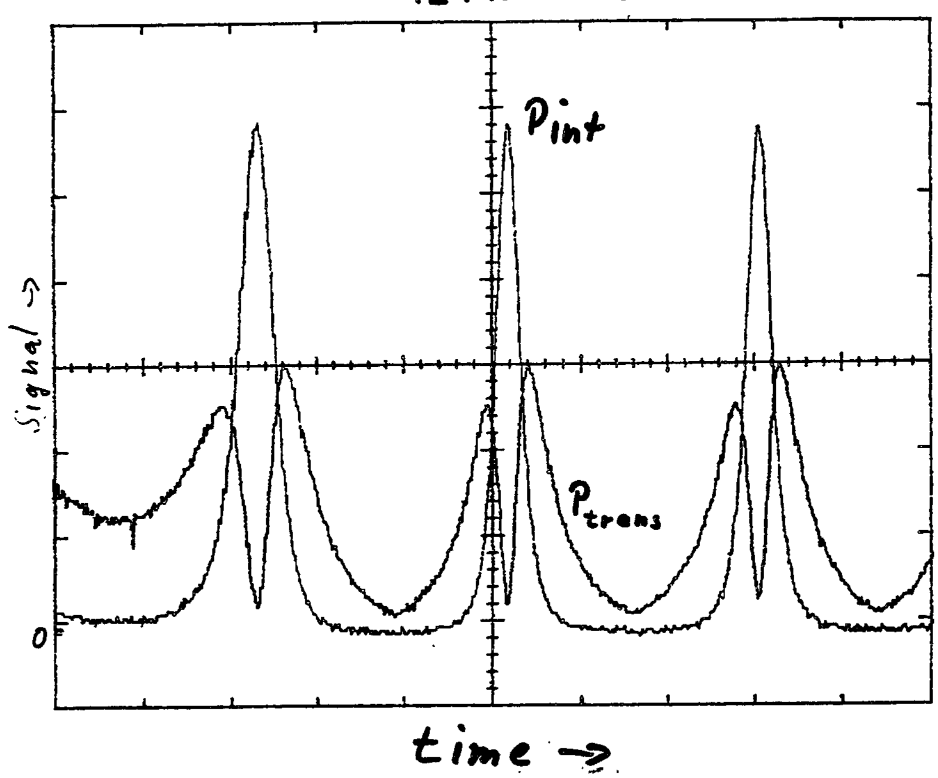

T_PR = 7%

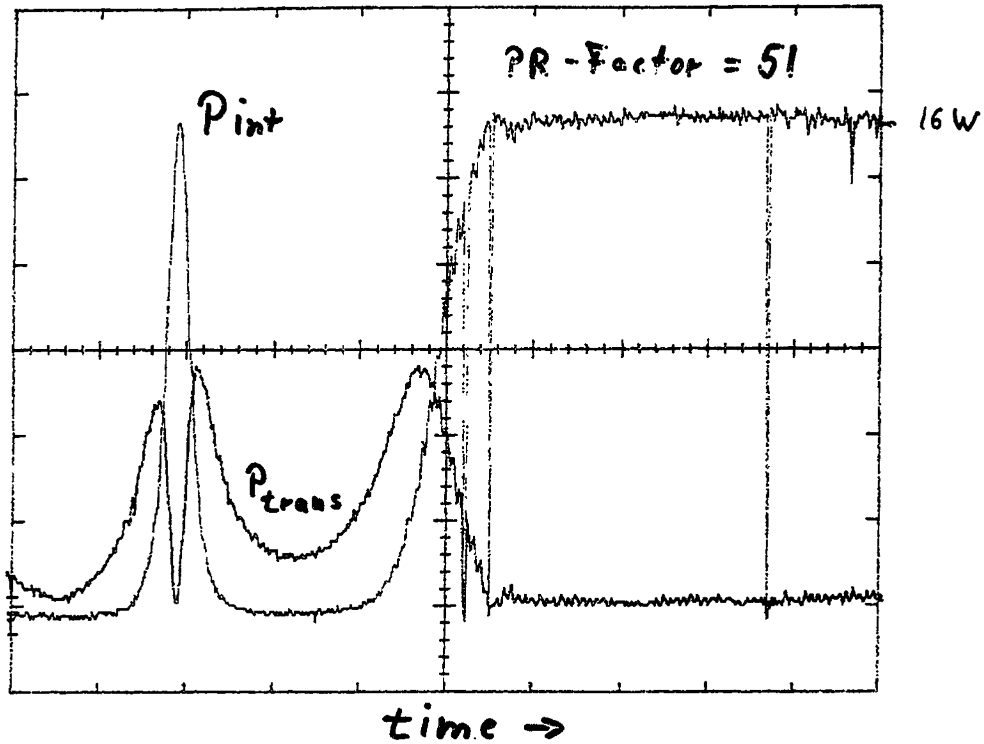

Transmission PR-Mirror = 0.5%

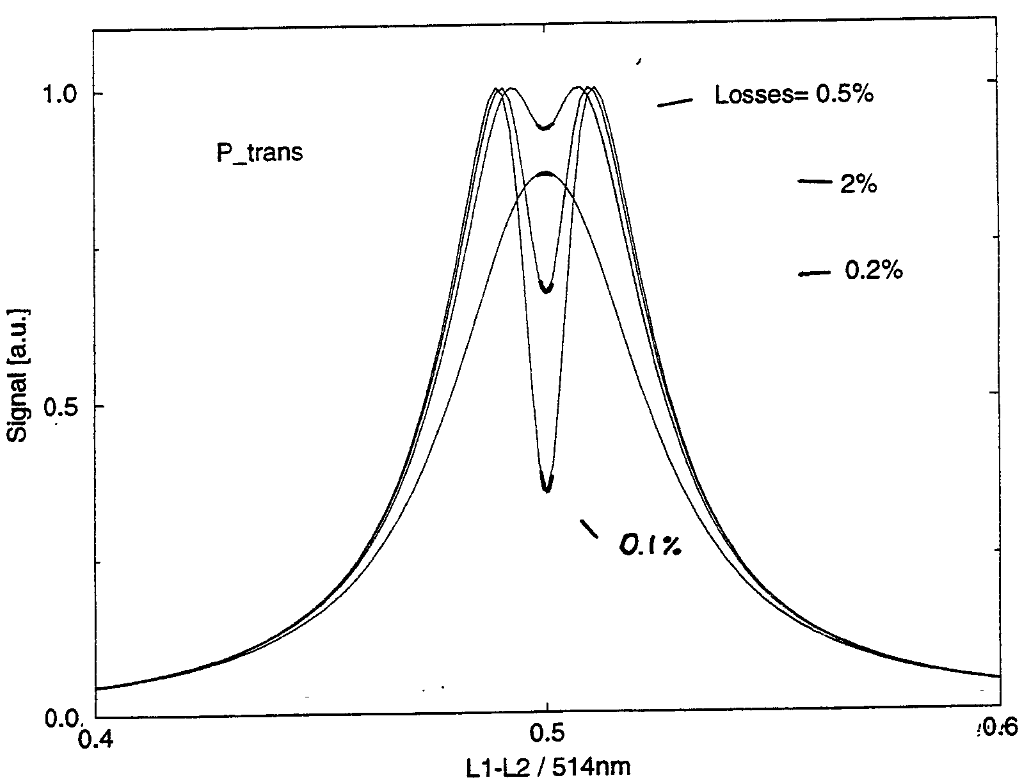

⊕

Cross Section P_{trans} at dark fringe

T_PR=0.5%, T_BS=54%, Losses=0.3%

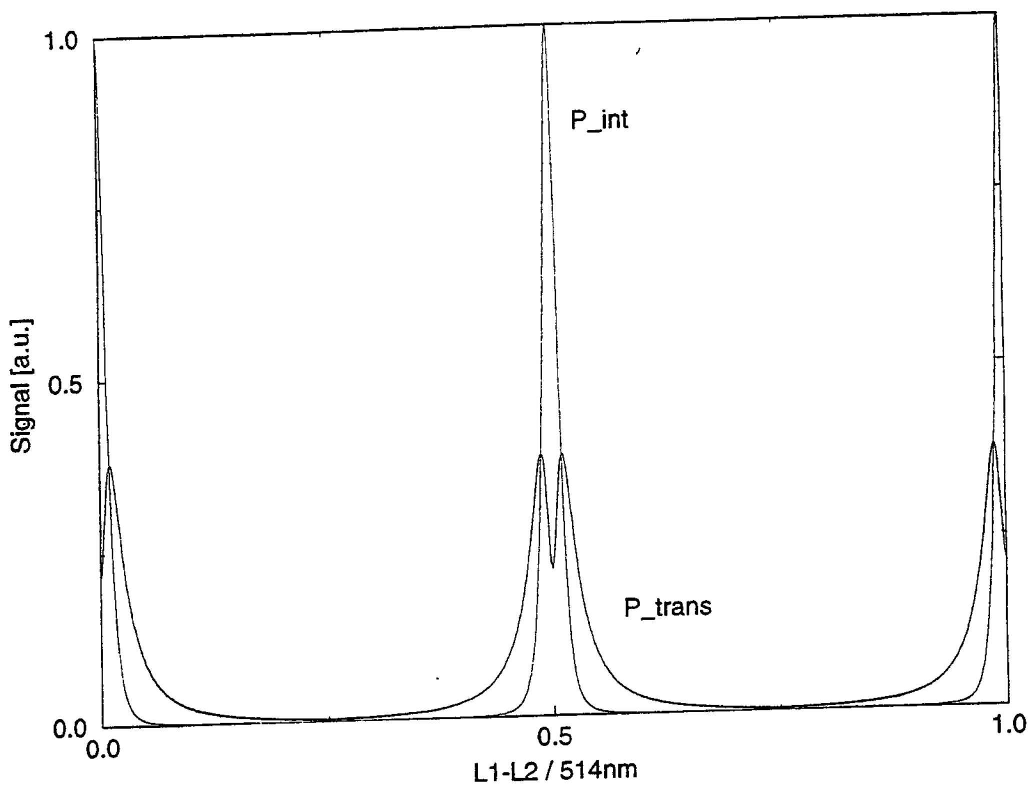

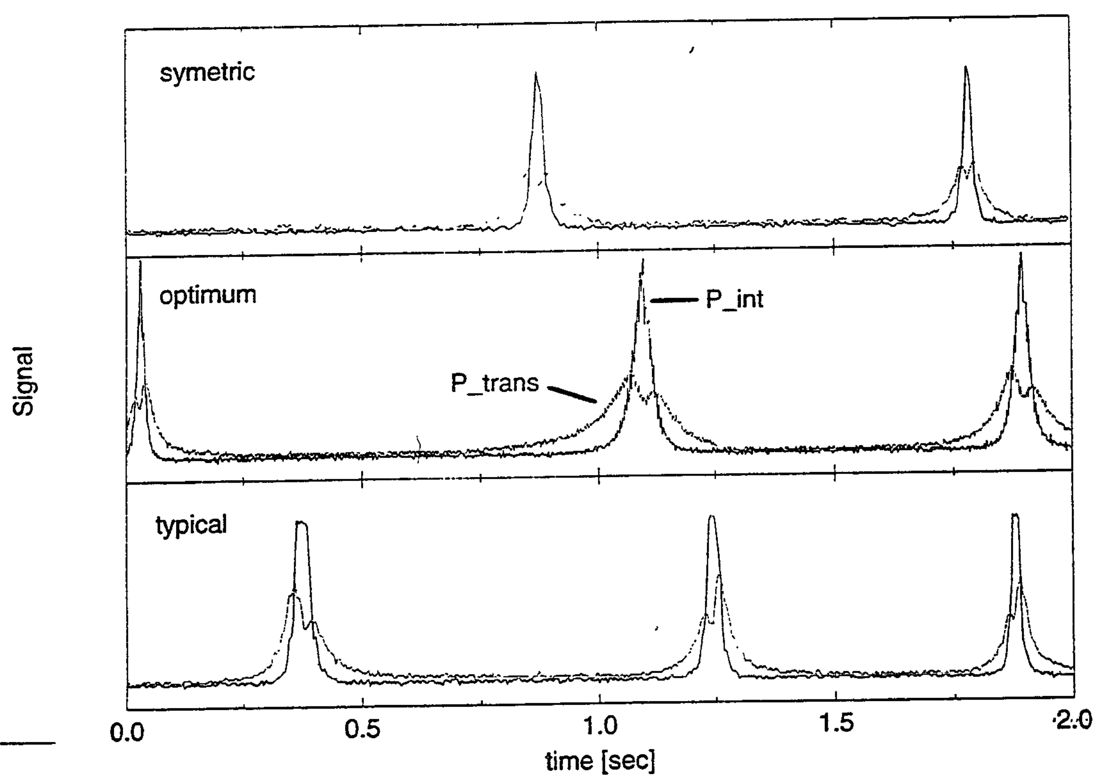

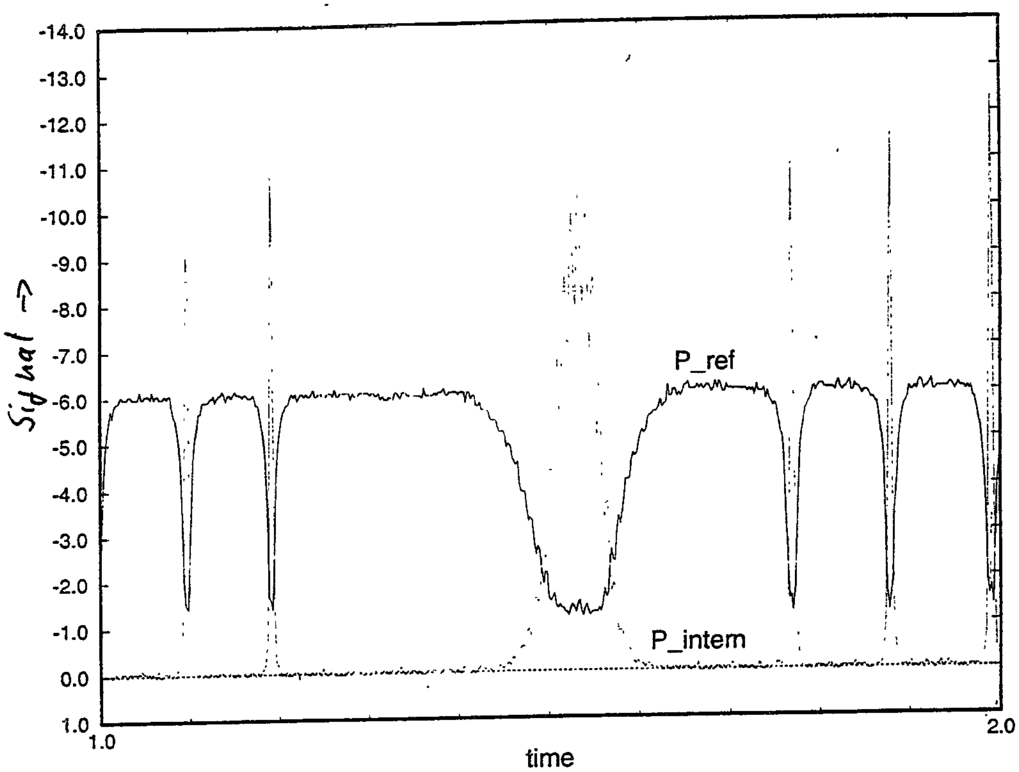

PR–Mirror T=0.5%, Prelock with P_int

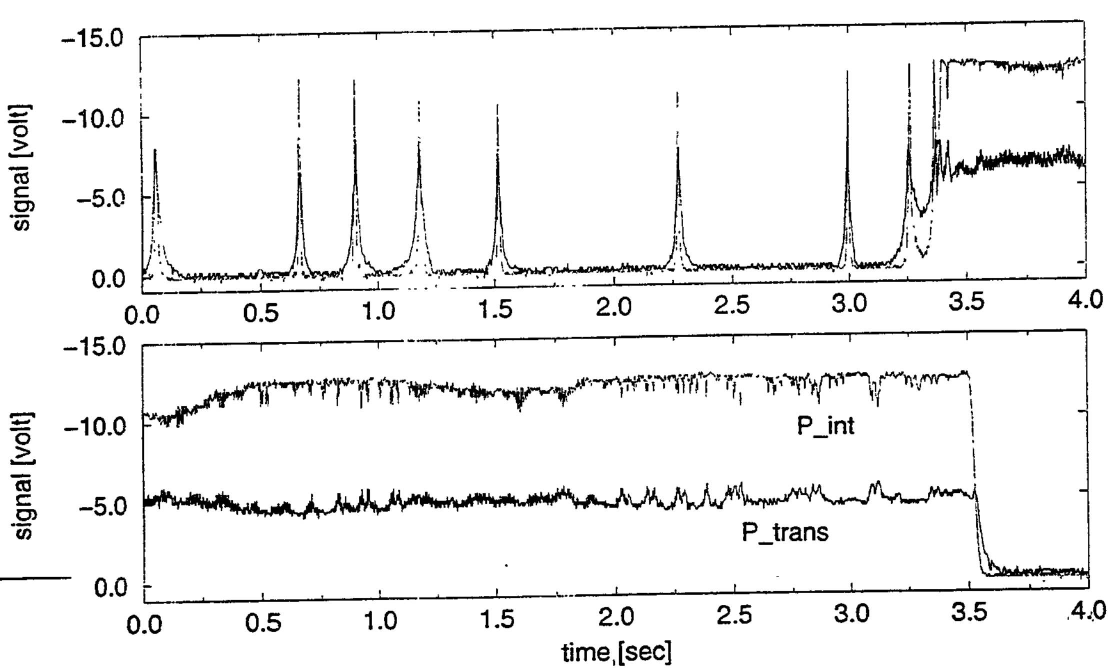

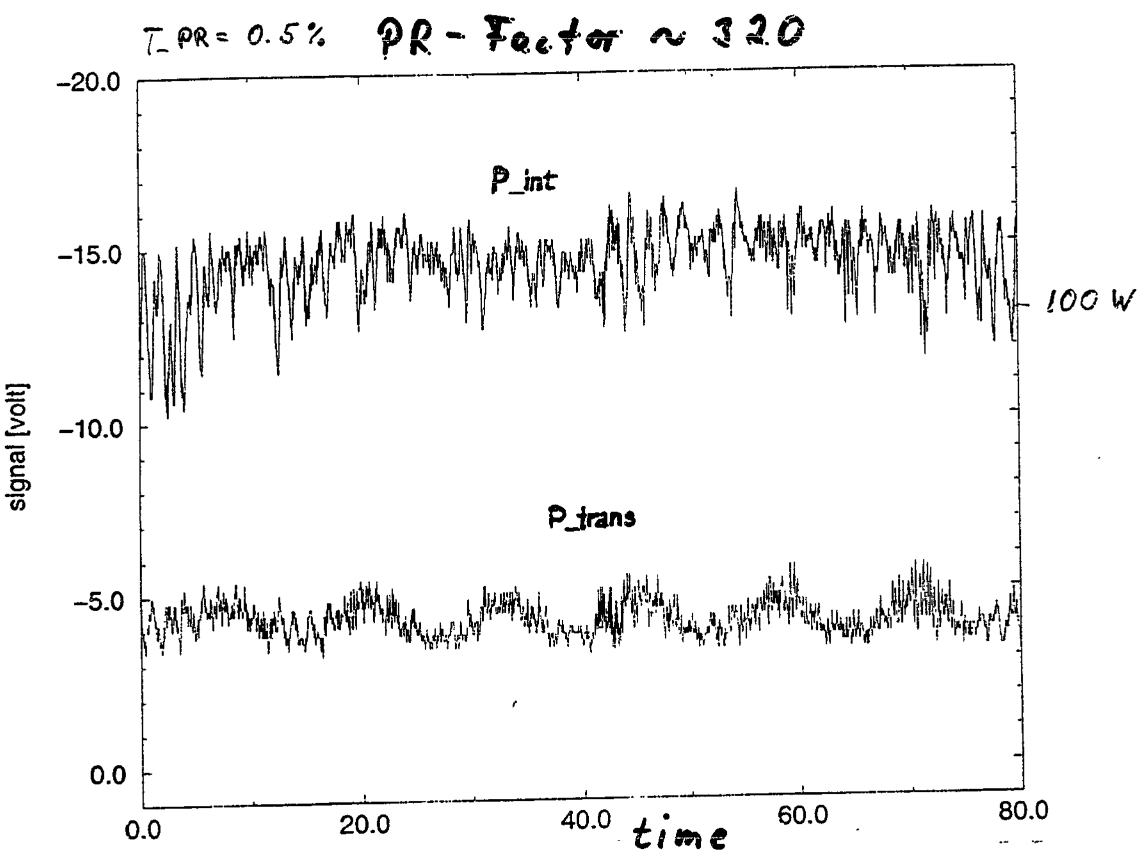

Open Questions

- Cross Section of P_{trans} at dark fringe : ⊕ = ?
- ⊕ <=> Mirror Deformation
- Asymmetry of P_{trans}

⋮

Future Work

- Laser Power Stabilization
- External Modulation with P. R.
- Auto Beam Aligment

⋮

Wednesday AM   LIGO Research Community(LRC)
January 17   Chair: H. Ward

8:00   G. Sanders(Caltech)   The View From LIGO
8:20   Discussion
8:30   Meeting of LIGO Research Community and Discussion

1:30   Meeting of LIGO Research Community(continued)

LIGO Research Community: The View From LIGO

Gary Sanders

Aspen Workshop

January, 1996

LIGO Users Community

Gary H. Sanders

California Institute of Technology

Aspen Winter Conference on Gravitational Waves and Their Detection

January 24, 1995

LIGO-G950002-A-MAA

Traditional "Users" Models

- High Energy and Nuclear Physics
  - » Accelerators
    - – CERN, FNAL, TRIUMF, SIN, Frascati, Saclay
  - » Reactors
    - – Grenoble
- Astronomy
  - » Telescopes
    - – Palomar, Arecibo, Submillimeter, Owens Valley, Hubble
- Magnetic Fusion Machines
  - » TFTR, MFTF, ITER
- Materials Science
  - » Light Sources
  - » Spallation Sources

"User" Models (recited by a high energy physicist)

- Facility capabilities supported by in-house team
- Access to facility generally open to international community
- Research can be collaboration between in-house and community scientists or can be completely independent
- Research proposals are collaborative and submitted to peer review
- Review includes scientific/technical review and agency funding review
  - » Scientific review generally held by facility Director/Principal Investigator
  - » Agency holds funding review
- Facility creates a Program Advisory Committee
- Users organize a Users Group with elected leadership and charter
  - » Users Group becomes the "customers" voice

Immediate User Issues

- User requirements for facilities
  - » Visitor accommodations - offices, labs, food, sleeping quarters
  - » Clean room storage and work areas for test and assembly - "staging" areas and labs
  - » Computing
  - » Intellectual climate
- Computing infrastructure
  - » hardware environment
  - » software tools
    - – AVS vs. Khoros
- Review of proposals
  - » Early LIGO program
  - » Advanced detectors

National/International

- US groups
  - » NSF funding proposals
  - » LIGO project deliverables funded by LIGO
- International Gravity Wave Network
  - » Interlaboratory agreements to share data for combined results
  - » Share in technology development
- International joint projects
  - » Government to government

AVS 5 vs. Khoros 2

- Price
  - » AVS is $7K - $25K/user
  - » Khoros is "free"
- Support
  - » AVS offers commercial type support
  - » Khoros is informal and unpredictable
    - – LIGO may have to hire support staff
- Distribution licenses
  - » AVS run-time modules cost $
  - » Khoros executable modules free

LIGO considering selection within 1995

(LIGO has negotiated "community" price 40% lower)

Aspen Discussions

- "Users Group Charter" strawman (Berley/BNL model) discussed
  - » "Users" changed to "Research Community"
  - » Changes made to Executive Committee and nominating process
  - » Revised draft charter agreed to at end of day
- Communique sent internationally by Syd Meshkov
  - » Conference proceedings and communique (L950365) available
  - » comments on role of LIGO Research Community
  - » comments on nominating process
  - » comments on composition, membership, and organization
  - » names submitted for Nominating Committee and LIGO Pre Program Advisory Committee
- Response was very supportive and constructive

LIGO

LIGO Research Community

The LIGO Research Community(LRC) is currently in an early stage of existence. The first steps towards its organization were made at the Aspen Winter Conference on Gravitational Waves and Their Detection, Jan. 22-28, 1995. A communique (postscript) describing what happened at the meeting was circulated shortly thereafter. As a result of the views expressed at the meeting, a LIGO Pre-Program Advisory Committee(LPPAC) was formed recently. News items that affect the LIGO Research Community will be posted in this part of the LIGO Home Page as they occur. The next major meeting of the LRC will be at the 1996 Aspen Winter Conference on Gravitational Waves, Jan. 15-21, 1996. A preliminary program for the meeting will also be posted here when it is formulated.

News:

- We are currently gathering information for the LIGO Research Community database. NEW
- Executive Committee: Election results
- The Aspen Center for Physics announces the Aspen Winter Conference on Gravitational Waves and Their Detection
- Invitation to Join the LIGO Research Community
- Charter of the LIGO Research Community
- LPPAC Formation Announcement

Return to the LIGO Home page

Last modified 12 Dec 95

For problems or suggestions about Web material, contact webmaster@ligo.caltech.edu

For information about LIGO, contact info@ligo.caltech.edu

External Users and Advisors

- LIGO involvement with the scientific community
  - All who are interested in exploiting the scientific opportunities offered by LIGO
  - Nominating Committee
  - Executive Committee
- Pre Program Advisory Committee
- Program Advisory Committee
- External Advisory Committee

LIGO Decided to ask Pre-Program Advisory Committee to facilitate formation of EAC, PAC, LRC Ex. Comm.

LPPAC Formation Announcement

At the Aspen Winter Conference on Gravitational Waves and their Detection in January, it was the sense of the meeting that a LIGO Pre-Program Advisory Committee (LPPAC) should be formed. Taking into account the many suggestions that have been received, this committee has been constituted with the following membership:

- P. Saulson (Syracuse) - Chair
- S. Finn (Northwestern)
- A. Giazotto (Pisa)
- J. Hall (JILA)
- W. Hamilton (LSU)
- C. Prescott (SLAC)
- A. Ruediger (MPI-Garching)

The LPPAC will exist only for a year or two. During its brief life it will act as both a LIGO Program Advisory Committee (LPAC) and as an External Advisory Committee (EAC). Before it goes out of existence it will help design a final LPAC and EAC. We hope to convene the first meeting some time in the fall.

At Aspen, it was also agreed that a Nominating Committee be formed to finalize a charter and organize the initial leadership for the LIGO Research Community, consisting of all scientists interested in LIGO's scientific opportunities. We propose that the LPPAC should play this role as well. This makes efficient use of the time of the members, and reflects the strong overlap in suggestions of members made to us by the research community contacted after the Aspen meeting. In the interim it will concern itself with:

1. Initial interferometer design technical advice
2. Commissioning Plan
3. Community Research Proposals
4. Establishing a LIGO Visitors Program, as well as a Users Program

As soon as the LPPAC meets, you will be informed about its deliberations, as well as about other activities.

We plan to hold another Aspen Winter Conference on Gravitational Waves from Jan. 15-21, 1996. The subject has not been finalized and we welcome your suggestions.

Return to the LIGO Research Community page
Return to the LIGO Home Page

webmaster@ligo.caltech.edu / 15 Jul 95

Executive Committee: election results

The ballots for election to the Executive Committee of the LIGO Research Community have been tabulated. The Executive Committee has the following membership, listed in a ranked order by the number of votes received:

1. David Shoemaker
2. Sam Finn
3. Bill Hamilton
4. Harry Ward
5. Joan Centrella
6. Eric Gustafson
7. Bruce Allen

Thus Shoemaker, Finn, and Hamilton have won terms on the Executive Committee of three sessions; Ward and Centrella terms of two sessions; and Gustafson and Allen single session terms.

At a teleconference meeting of these seven members, they elected Sam Finn to be the Chair of the Executive Committee.

The next general meeting the LIGO Research Community and of the Executive Committee will be held at the Aspen Center for Physics Winter Conference on Gravitational Waves and Their Detection, Jan. 14-20, 1996, Aspen Colorado.

Return to the LIGO Home Page
Return to the Research Community Home Page

last modified 28 Nov 95

For problems or suggestions about Web materials, contact webmaster@ligo.caltech.edu

For information about LIGO, contact info@ligo.caltech.edu

LIGO

Invitation to Join the LIGO Research Community

I am writing to invite you to join a new organization, called the LIGO Research Community, or LRC. It has two goals:

1. to facilitate communication between the Laser Interferometer Gravitational-Wave Observatory Project (LIGO) and the community of people interested in the field of gravitational wave detection, and
2. to serve as an advocacy group for the study of gravitational waves.

Membership in the LIGO Research Community is open to all persons interested in these goals. We expect this to include

1. experimental physicists and engineers working in any branch of gravitational wave detection, or who have an interest in the technology,
2. theoretical physicists, numerical relativists, and astronomers interested in astrophysical sources of gravitational waves or in what they may reveal about the ~~universe,~~
3. students interested in these areas, and
4. anyone else.

Membership is open to people from all countries, without regard to affiliation (or lack thereof) with any gravitational wave project.

The organization has the acronym "LIGO" in its name because we expect it to serve as a kind of users' group for the LIGO Project. But LIGO needs advice from the widest possible community of actual and potential "users" of all kinds. In addition, we hope that the LIGO Research Community will play an important role in promoting and fostering the study of gravitational waves.

The first work toward creating the LRC was carried out by the LIGO Project, culminating in a series of discussions at the January 1995 Aspen Winter Conference on Gravitational Waves and Their Detection. A communique and draft charter were circulated after that meeting for comments. Final work on organizing the LIGO Research Community was performed by the LIGO Pre-Program Advisory Committee, which met on September 8 and 9, 1995.

Joining the LIGO Research Community is simple -- just send a message to **lrc@ligo.caltech.edu**, indicating your interest. Or, if you prefer, send regular paper mail to LIGO Research Community, c/o LIGO Project, Mail Code 51-33, California Institute of Technology, Pasadena, CA 91125, USA.

When you join, you should also vote for members of the Executive Committee of the LIGO Research Community. This is the governing body of the LRC. For details on its role, and on other aspects of the functioning of the LRC, please see the LIGO Research Community Charter, in the LaTeX file attached to the end of this message.

The Executive Committee will have seven members. A slate of nine nominees, broadly representative of the gravitational wave community, has been prepared by LIGO's Pre-Program Advisory Committee. The nominees for seats on the LRC Executive Committee are:

- Bruce Allen, Wisconsin-Milwaukee
- Joan Centrella, Drexel
- L. Sam Finn, Northwestern
- Eric Gustafson, Stanford
- William Hamilton, LSU
- C. Nary Man, LAL Orsay
- Robin T. Stebbins, JILA
- Henry Ward, Glasgow.

Please cast your votes by giving the seven names from this list whom you would most like to have serve on the Executive Committee. Include your votes in your message to lrc@ligo.caltech.edu.

In order for your vote to count, please send it before Friday, November 3. The seven who receive the most votes will be named to the Executive Committee. For further details, please refer to the LRC Charter, especially to Section 6.

Each year there will be at least one general membership meeting of the LIGO Research Community. The first such meeting will be held in Aspen, Colorado, as part of the Aspen Winter Conference on Gravitational Wave Sources and their Detection, January 15-20, 1996. For more information on this meeting, please contact Syd Meshkov at syd@theory.caltech.edu.

I hope you will want to join the LIGO Research Community, and that you will cast your ballot soon. If you have any questions, please contact me at saulson@suhep.phy.syr.edu.

Please share this message with anyone else who may be interested in joining the LIGO Research Community. This message will also be posted on the World Wide Web, via a link from the LIGO Home Page, at the location http://ligo.caltech.edu.

Sincerely yours,
Peter Saulson
Chair, LIGO Pre-Program Advisory Committee
for the Committee:
Sam Finn, Adalberto Giazotto, John Hall, William Hamilton, Charles Prescott, and Albrecht Ruediger

Return to the Research Community Home Page
Return to the LIGO Home Page

17 Oct 95

LIGO

Charter of the LIGO Research Community

September 26, 1995

Contents:

1> Name and Goals

1. Name

The name of this organization is the **LIGO Research Community**. The LIGO Research Community is also referred to as the LRC.

2. Goals

The goals of the LIGO Research Community are to

1. provide an organized channel for the interchange of information between the LIGO management and those who utilize the scientific opportunities afforded by LIGO;
2. to serve as an advocacy body for the study of gravitational waves and related physics and astronomy.

2> Membership

Discussions with VIRGO

- Barish/Sanders meeting with Giazotto/Brillet in March
- Broad agreement on need for intimate collaboration to optimize physics output of LIGO/VIRGO
- Draft of Memorandum of Understanding underway
- Agreement to exchange personnel, information, technical advice, technology
- Plan to form working groups on data collection, data analysis protocols, observing/maintenance cycles
- Possibility to jointly form LIGO/VIRGO Research Community with rotating meetings

Memoranda of Understanding

- Standardized format
  - » MOU - broad areas of agreement, legal principles, description of general programs, no fixed term
  - » Attachments - written as needed with fixed terms and describing specific tasks, deliverables, dates and payments, if relevant. These may be rewritten and replaced without modifying the MOU
- NSF visibility/concurrence
  - » domestic, <$100K - NSF provided copies
  - » domestic, >$100K - NSF concurrence
  - » international, NSF concurrence

Plans

- LIGO Research Community
- MOU's
- LIGO/VIRGO working groups
- LIGO Visitor's Program
- Program Advisory Committee
- External Advisory Committee

Agenda: LIGO Research Community

Sam Finn

- What is the LRC?

  Aims / Goals
  Relationship to LIGO
  Members and membership

- Questions / Discussion

  What is LRC?
  How does it operate?

- Coffee Break
- Defining a Research Environment:
  LIGO and the Grav. Physics Research Community
- Questions / Discussion
- Adjourn

What is the LRC?

From Charter:

Provide an organized channel for the interchange of information btwn LIGO management and those individuals who utilize the scientific opportunities afforded by LIGO;

To serve as an advocacy body for the study of gravitational waves and related physics and astronomy

Examples:

Facilitate exchange within user community (hardware, data analysis, theory)

Two-way communication about design decisions today & science program decisions in future

To insure LIGO functions as part of an International community

The Voice of those who will "use" LIGO or are interested in its functioning!

Relationship with LIGO

- Independent & Separate

Members & Membership

- Who should want to be a member?

  Anyone who...

  Agrees with aims

  Is interested in keeping abreast of LIGO plans

  Wants to insure LIGO remains a healthy part of the international gravitational research community

- Who can be a member?

  Anyone. The LRC is an organization of individuals

- How do I join?

  E-Mail to: LRC@LIGO.CALTECH.EDU

Members & Membership

- Who is a member?

As of 6 November 1995

95	US Members
43	European
25	Asian
6	Canada / Mexico
3	South America
2	Africa
1	Australia

Officers

- Executive Comittee LRC_EXCOMM @ HOLMES.ASTRO.NWU.EDU

Bruce Allan   Joan Centrella

Sam Finn (Chair)   Eric Gustafson

Bill Hamilton   David Shoemaker

Harry Ward

- Executive Committee Secretary Syd Meshkov

Defining a Research Environment:

LIGO and the Gravitational Physics Research Community

- The grav. physics research environment

  Now
  Future

- Nine month goal:

  Identify how operating LIGO affects our Research environment.

  Decide what we want that environment to look like

  Recommend, to LIGO & NSF, what steps be taken to create that environment

- Today: Issue Identification Groups

  Canvas Membership; Report to Ex Comm 4/96

- May APS Meeting: Policy Study Committees

  Report to ExComm July (?)

- End Summer: White Paper to LIGO, NSF

Issue Identification Groups

- Sources, Data and Analysis

  Chair: Joan Centrella
  E-Mail: LRC_SDA@HOLMES.ASTRO.NWU.EDU

- Hardware Development/Installation/Operations

  Chair: Eric Gustafson
  E-Mail: LRC_HARDWARE@HOLMES.ASTRO.NWU.EDU

- People

  Chair: Harry Ward
  E-Mail: LRC_PEOPLE@HOLMES.ASTRO.NWU.EDU

- Chairs select group members from volunteers

  Charge: Canvas Members
  Assemble Contributions
  Report to Executive Committee

Wednesday PM	Shot Noise; Detector Improvement	
January 17	Chair: D. Shoemaker	
4:30	A. Ruediger (Garching)	History and Derivation of Shot Noise Equations
5:00	Discussion	
5:10	J. Hall (JILA)	Dynamic Light-induced Mirror Birefringence
5:40	Discussion	

Wednesday Evening: Public Lecture, Wheeler Opera House
Chair: S. Meshkov

8:00	L. Krauss (Case-Western Reserve)	The Physics of Star Trek

Rüdiger ①

Shot Noise Equation
History and Derivation

In laser-interferometric GW detectors
fundamental limit set by shot noise

Recognized by pioneers Forward, Weiss (71/72)
did first calculations

Since then, other authors
copied
interpreted
estimated
calculated anew.

Led to host of — sadly to say — spectrum of differing equations

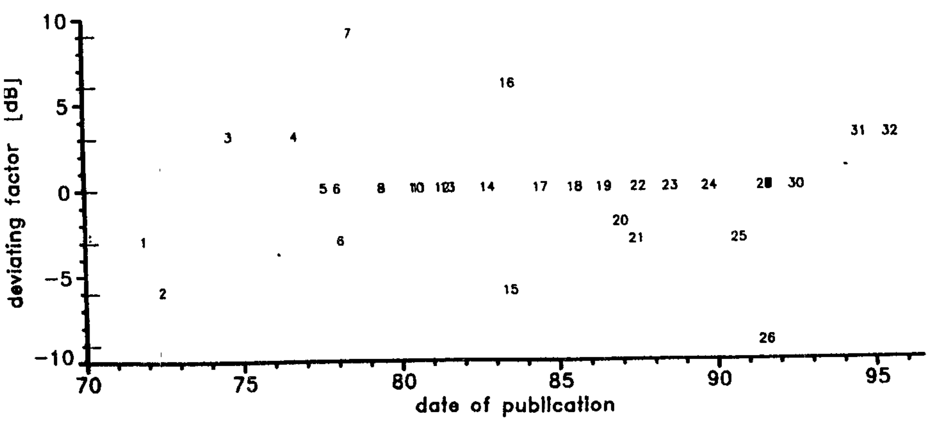

(2)

wide spread in numerical factors
started idea to derive, write up, publish "correct equation"

Shot Noise in Interferometers used for gravitational wave measurements

A. Rüdiger, J. Mizuno, R. Schilling, W. Winkler, and K. Danzmann*

Max-Planck-Institut für Quantenoptik, D-85748 Garching
(* *also Universität Hannover, D-30167 Hannover*)

Abstract

The phenomenon of shot noise sets a severe limitation to the sensitivity of (laser illuminated) Michelson-type interferometers, as used or proposed for the detection of gravitational waves. Despite the high significance of this noise source, and though the general scaling laws with light power P, wave length λ, detector efficiency η, etc., are generally agreed upon, there is a wide variety of different numerical factors used in describing the *precise magnitude* of the effect. This paper is intended to clarify the correct magnitude, once and for all. The result will be an apparent fluctuation δL in the path length difference $\Delta L = L_2 - L_1$ that is described by a single-sided (power) spectral density of

$$S_{\delta L}(f) = \left(\widetilde{\delta L}(f)\right)^2 = \frac{\hbar c}{\pi}\,\frac{\lambda}{\eta P}.$$

1 Introduction

1.1 A historical survey

In the many (almost 25) years since first publications on laser interferometers for the detection of gravitational waves, it has been recognized that *shot noise* would be one of the most fundamental and most stringent limitations to achieving the high sensitivities required to detect the astrophysical sources of interest.

It is quite natural that this shot noise limit has found appropriate attention in almost all of the early papers and proposals, and also later in textbooks, review articles, and proposals for large scale antennas.

plans for write-up on shot noise

Mentioned to Syd Meshkov
--- promptly recruited me for
talk at Aspen Winter Conference
--- and I agreed.
But then
[illegible]

Because:
more to it than just "write it up":
different derivations
different formulations
wide variety of different cases
much literature search

Yet:
usefulness of such a collection,
if only to save others time and pain in
deriving equations anew
working through conflicting sources
perhaps stumbling into pitfalls
before finding the true answer,
or answer to particular case.

Write-up :

Found no time [LISA !]
to tackle this ambitious program

Put before you only skeleton,
flesh to be added in next months:
careful derivations
discussion of different approaches
clear statements of validity
consistent nomenclature, notation

Request to all interested for assistance.

Nomenclature, notation important
to prevent misinterpretations

make lavish use of [illegible]

[illegible] = geometric arm length
[illegible] = total optical path = [illegible]
[illegible] = number of passes in DL
(elsewhere: $N =$ [illegible], $2N =$ [illegible]; $b = N$; $b = N-1$)

[illegible] = single-sided power spectral density of y

$\tilde{y}(f) = \sqrt{\cdot\ }$ = "linear" spectral density of [illegible]

$\Lambda = \frac{c}{f_{GW}}$ = wave length of GW

One simple derivation

Michelson interferometer (simple, DL)

Response to gravitational wave h

$$\delta\mathcal{L} = h \cdot \mathcal{L}.$$

Effect of path difference fluctuation $\delta\mathcal{L}$ on photo current:

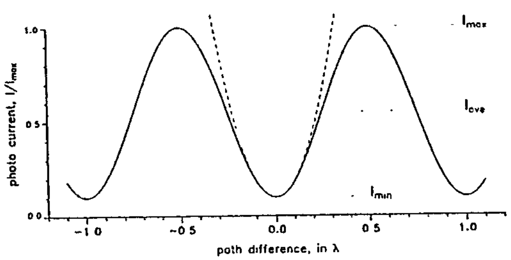

Fig. 3. *Output current of single photodiode, vs. phase difference* $\Delta\phi$.

mid-slope detection scheme:

$$\delta I = \frac{I_{max} - I_{min}}{2} \cdot \sin \delta\phi$$

$$\cong \frac{I_{max} - I_{min}}{2} \cdot \delta\mathcal{L} \cdot \frac{2\pi}{\lambda}$$

Schottky equation for (Poisson distributed) current I_{ave}

$$\delta\tilde{I}(f) = \sqrt{2 e I_{ave}} = \sqrt{2e \frac{I_{max} + I_{min}}{2}}.$$

by equating the δI, and with $I = \eta \cdot P \cdot \frac{e}{\hbar\omega}$:

$$\delta\tilde{\mathcal{L}}_1(f) = \sqrt{2 \frac{\hbar c}{\pi} \cdot \frac{\lambda}{\eta P}} \cdot \sqrt{\frac{1+\mu}{(1-\mu)^2}}$$

$I_{min} \sim 1$

Result was:

$$\delta\tilde{\mathcal{L}}_1(f) \cong \sqrt{2 \frac{\hbar c}{\pi} \cdot \frac{\lambda}{\eta P}} \cdot \sqrt{\frac{1+\mu}{(1-\mu)^2}}$$

Perfectly legal derivation, but result not yet complete:

Can do measurements at both output ports: take the difference of the two: signal response doubled

Shot noise contributions add only in quadrature.

slightly counter-intuitive, might expect anti-correlation

but Poissonian distribution is "robust"

By monitoring both output ports

$$\boxed{\delta\tilde{\mathcal{L}}(f) = \sqrt{\frac{\hbar c}{\pi} \cdot \frac{\lambda}{\eta P}}} \times \left(\begin{array}{l}\text{QI-dependent} \\ \text{correction}, \geq 1\end{array}\right)$$

$$\underbrace{\phantom{\sqrt{\frac{\hbar c}{\pi} \cdot \frac{\lambda}{\eta P}}}}_{\text{main concern}}$$

e.g. $= \sqrt{\frac{1+\mu}{(1-\mu)^2}}$ for mid-slope scheme

QI = quality of interference

have to consider

⑦

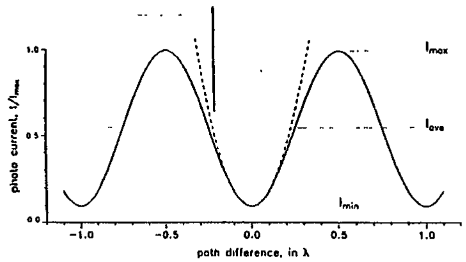

Fig. 3. Output current of single photodiode, vs. phase difference $\Delta\phi$.

dark-fringe scheme
prerequisite for power recycling

$$I(\delta\phi) = I_{min} + (I_{max} - I_{min}) \cdot \sin^2\left(\frac{\delta\Phi}{2}\right)$$

needs modulation to read out GW signal

simplest case: $I_{min} = 0$
then for purely quadratic function (parabola)
same as for mid-slope with $\mu = 0$.
for realistic sinusoidal response
same only for small modulation

With finite dark-fringe current I_{min}:
optimum modulation swing
is function of I_{min}

furthermore have to specify
method and wave shape of modulation

$$\varphi_{min} = \sqrt{\frac{2e}{(1-L)SI_L}} \cdot E \cdot F$$

General		Without Recycling: $F = 1$ for $M = 0$	With Recycling: $F = \sqrt{L}$ for $M = 0$
INTERNAL sine wave	$E = 1.0$	....	...
INTERNAL square wave	$E = \frac{\pi}{\sqrt{8}} = 1.111$	$F = \frac{\sqrt{1-M} + \sqrt{M}}{1-2M} = \frac{1}{\sqrt{1-M} - \sqrt{M}}$ $\sin\varphi_m = 2 \cdot \frac{\sqrt[4]{M(1-M)}}{\sqrt{1-M} + \sqrt{M}}$	---
EXTERNAL sine wave	$E = \frac{1}{\sqrt{2} \cdot J_{1\,max}} = 1{,}215$	$F = \frac{1 + \sqrt{M(1-L)S}}{\sqrt{1-2M}}$	$F = \frac{\sqrt{L + M(1-L)S} + \sqrt{M(1-L)S}}{\sqrt{1-2M}}$
EXTERNAL square wave	$E = \frac{\pi}{\sqrt{8}} = 1.111$		$r_{ext} = \frac{\sqrt{M(1-L)S}}{\sqrt{L + M(1-L)S} + \sqrt{M(1-L)S}}$
EXTERNAL SSB (A-O)	$E = \sqrt{2} = 1{,}414$	$r = \frac{\sqrt{M(1-L)S}}{1 + \sqrt{M(1-L)S}}$	$r_{int} = \frac{\sqrt{M(1-L)S[L + M(1-L)S]}}{1 - [L + M(1-L)S]}$

Gain in light power: $G_P = 10 \cdot \log \frac{P_I}{P_L}$

Gain in sensitivity: $G_S = 20 \cdot \log \frac{\sqrt{(1-L)S}}{E \cdot F}$

(9)

Get back to front factor

$$\boxed{S = \frac{\hbar c}{\pi} \cdot \frac{\lambda}{\eta P}}$$

In literature observe some diversity in numerical factor to it.

Why is that ?

Many pitfalls, particularly factors of 2 (in power representation) lurking

e.g.

- consider only one mid-slope photo detector
- $h = 2\delta\ell/\ell$ as opposed to $h = \delta\mathcal{L}/\mathcal{L}$
- in derivation via number of photons, $n = \frac{P \cdot \tau}{\hbar\omega}$: from measurement time τ to bandwidth: $\Delta f = 1/2\tau$
- number of bounces $b = N$, but also $b = N/2$
- simple Michelson: $N = 2$
- ... and many more

(10)

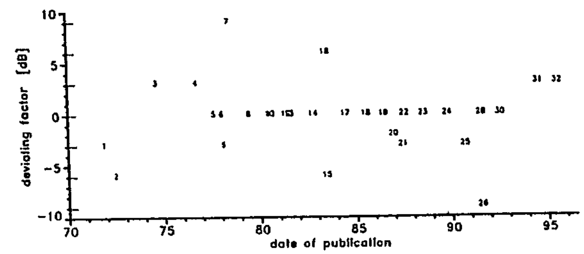

Fig. 1. *Semigraphical display of the deviating numerical factors in some selected publications, presented in logarithmic scale* (dB). *Owing to its definition, the presentation in these units of* dB *covers the comparison in "amplitude"* ($20 \cdot \log \frac{a}{a_0}$) *as well as in "power"* ($10 \cdot \log \frac{a^2}{a_0^2}$) *spectral densities. The ominous factors of 2 in power (or $\sqrt{2}$ in amplitude) correspond to a distance of* 3 dB. *With the exception of one reference,* [20], *this one having a deviation factor $\pi^2/16$ in power* (2.1 dB), *all factors are off by integer multiples of* 3 dB.

and truly enough:

nearly all deviations from true value are integer powers of 2 (in power) or integer powers of $\sqrt{2}$ (in amplitude)

but important

observe carefully what author meant

Important: quantum-mechanical approach (11)
(C. Caves)

Other topics to be discussed

⋮

3.3 Experimental evidence, for MP interferometers

... calibration with DC incandescent light
.. Shoemaker 88, calibration, 250 mW (?), measured 86

... very close. only a few dB off
... Niebauer: even closer ← Schnupp: Non-stationary shot noise
... would be in severe need of explanation

4 Fabry-Perot cavities in the arms

... not terribly different from DL,
.... requires phase response with $\mathcal{F}$

$$N_{\text{eff}} \simeq \frac{4}{\pi} \mathcal{F} \qquad \mathcal{F} = \text{finesse}$$

particularly for FP:
assistance from other groups required

(12)

5 Other Michelson configurations

5.1 Advanced interferometers (ground-based)

5.1.1 Power recycling

... assumed in several of the papers
... $(1 - R)$ perhaps oversimplified

5.1.2 Signal recycling

5.1.3 Resonant sideband extraction

5.2 Shot noise theorem ← Jun Mizuno

. not make this central part of this paper
... will be topic of further paper

5.3 Squeezed light

... discussed by Caves
... investigated ...
... no significant improvement expected
... Kimble (Aspen)

5.4 Interferometers in space

... also goes back to early proposals, [...]
... only recently coming within reach [...]

5.4.1 Space projects

... configuration, long distances,
... requires active transponders instead of mirrors
... extremely low light power

5.4.2 Shot noise in LISA

... David Robertson ?
... 60° ?

13

The "Shot Noise Theorem"
(Jun Mizuno)

$$\tilde{h} = \frac{\delta \mathcal{L}}{\mathcal{L}} = \frac{1}{\mathcal{N} \cdot \ell} \cdot \sqrt{\frac{\hbar c}{\pi} \cdot \frac{\lambda}{\eta P_{BS}}}$$

$$= \sqrt{\frac{\hbar c}{\pi} \cdot \frac{\lambda}{\eta P_{BS} \cdot (\mathcal{N} \ell)^2}}$$

$$\boxed{\tilde{h} = \sqrt{2 \frac{\hbar \lambda}{\pi c} \cdot \frac{\Delta f}{\eta \mathcal{E}}}}$$

$\mathcal{E}$ = stored energy

Δf = "bandwidth" $= \frac{c}{2 \mathcal{N} \cdot \ell}$

covers very wide variety of interferometer configurations

DL, FP

recycled (power, signal, RSE)

14

Question:

would such a write-up be useful?

does something already exist?

how far into details, cases should it go?

would take not only my time, but also that of others.

Is it worth that?

"Dynamic Photo-refractive Birefringence in Gyro/LIGO quality Mirrors"

Jun Ye
John Hall
JILA · NIST & University of Colorado

a Glitch on the long road to "Measurement of the Magnetically-Induced Birefringence of the Vacuum"

* S.A. Lee, W. M. Fairbank, Jr, W. H. Toki } Colorado State Univ

Tariq S. Jaffery - SSC

Frank Neznick, P. Colestock, H. Kautzky, V. Cupps, M. Kuchnir } Fermi Labs

— Hall   JILA

Magnetically-Induced Birefringence

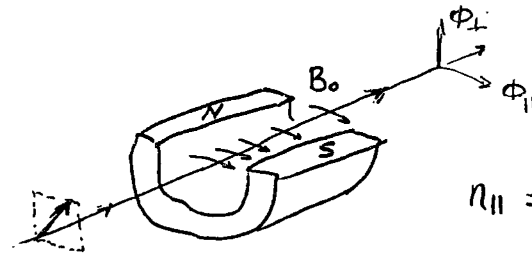

polarization-depend. phase delay

$$n_{\parallel} \neq n_{\perp}$$

$$\Delta n \equiv n_{\parallel} - n_{\perp} = \left(\frac{\alpha}{30\pi}\right)\left(\frac{B}{B_{cr}}\right)^2$$

where $B_{cr} = 4.4 \times 10^9$ T

$$\Psi_{QED} = \Phi_{\parallel} - \Phi_{\perp} = \left(\frac{\alpha}{30}\right)\left(\frac{B}{B_{cr}}\right)^2 \frac{\ell N}{\lambda}$$

for B = 6 Tesla

→ $\Delta n = 1.4 \times 10^{-22}$ ←

E. Zavatinni, A. Melisinos, F. Neznick ....
Phys Rev D 1994
"The Brookhaven Experiment"

E. Zavatinni, Carlo Rizzo ....
a new expt. in Legnaro - starts ~1997
(using rotating SC magnet)

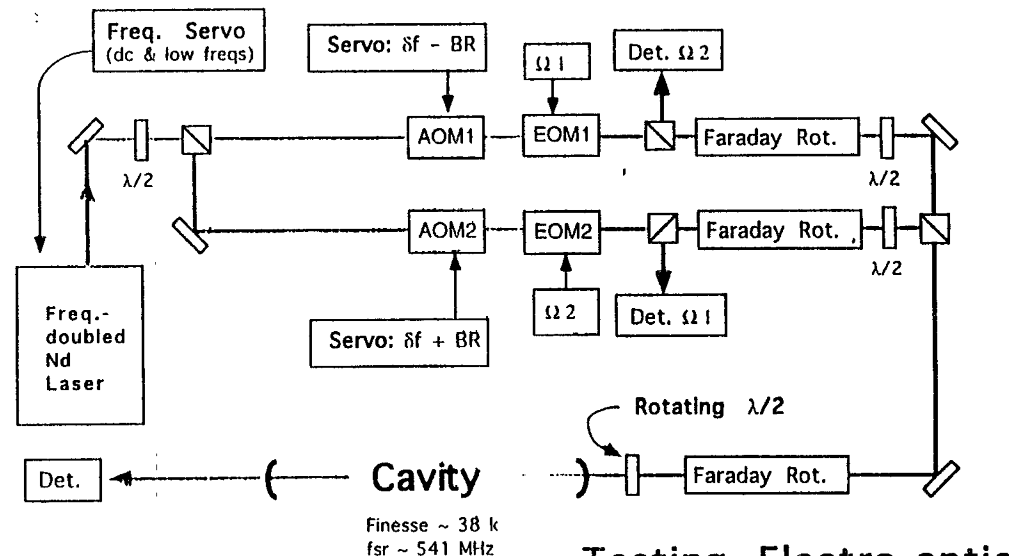

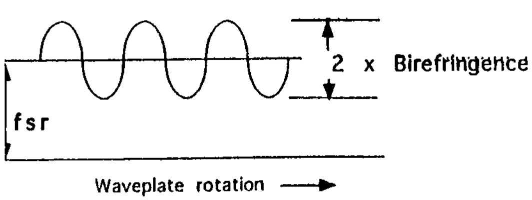

Testing Electro-optic measurement techniques for QED / Axion expt

Jun Ye & John Hall - JILA Oct 94

QED Origin of Magnetic Effect

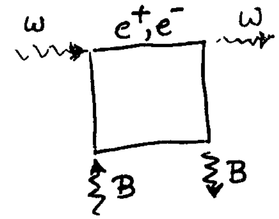

Dominant Term
"Light-by-light" scattering

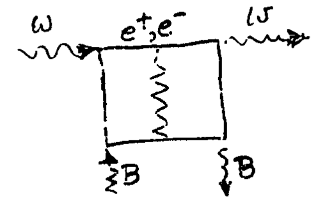

1.45% Radiative Correction

(1936) Euler-Heisenberg Lagrangian for EM field in Vac.

$$\mathcal{L}_{eff} = \frac{1}{2}(E^2 - B^2) + \underbrace{\left(\frac{2\alpha^2}{45\, m_e^4}\right)\left[(E^2 - B^2)^2 + 7(\vec{E}\cdot\vec{B})^2\right]}_{\text{lowest order QED term}}$$

Weisskopf 1936
Schwinger 1951

Circular polarization

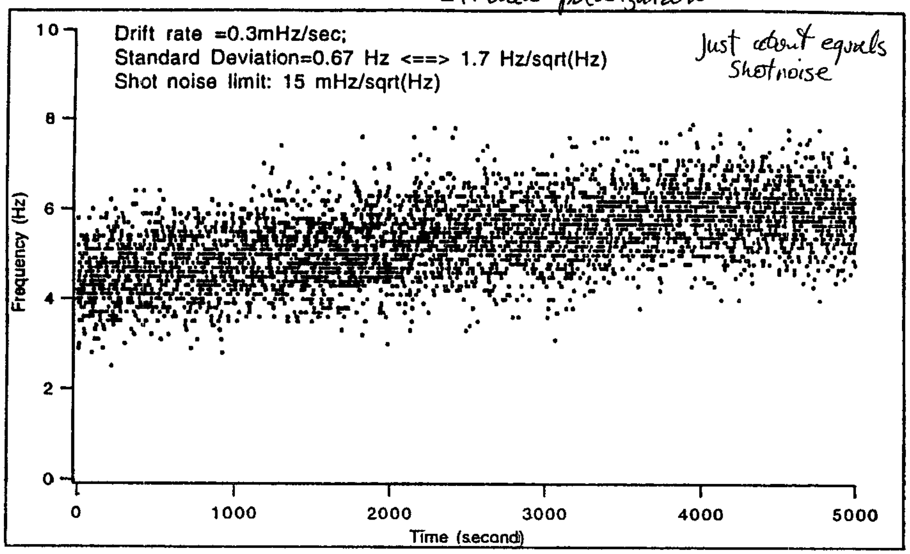

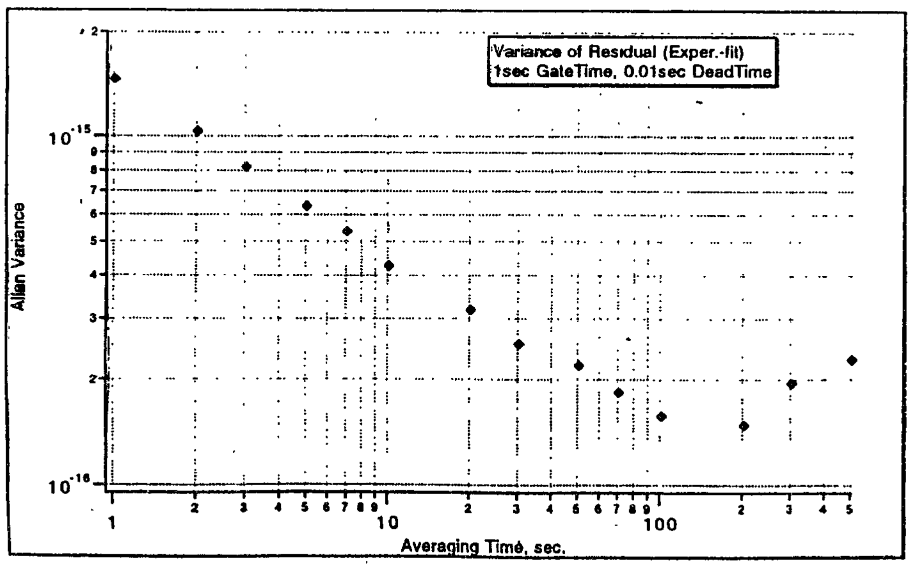

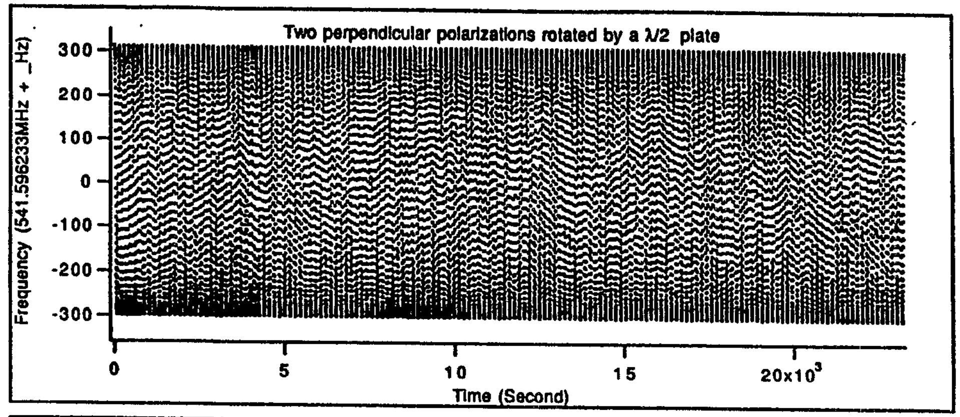

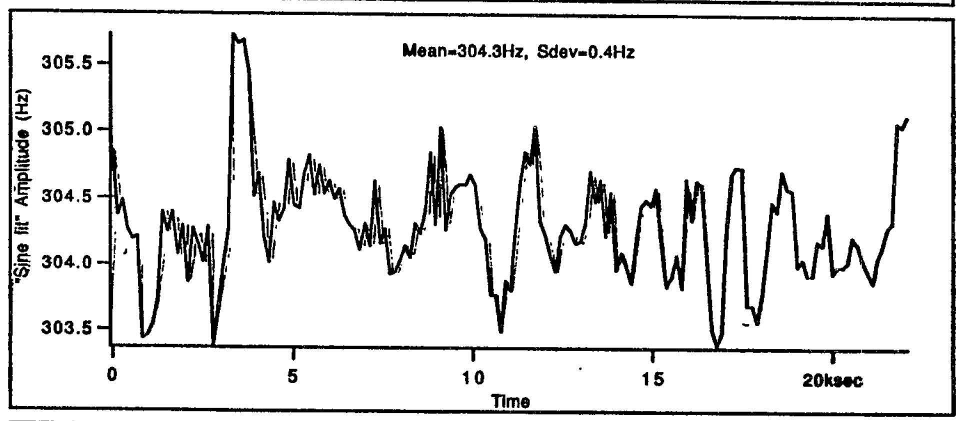

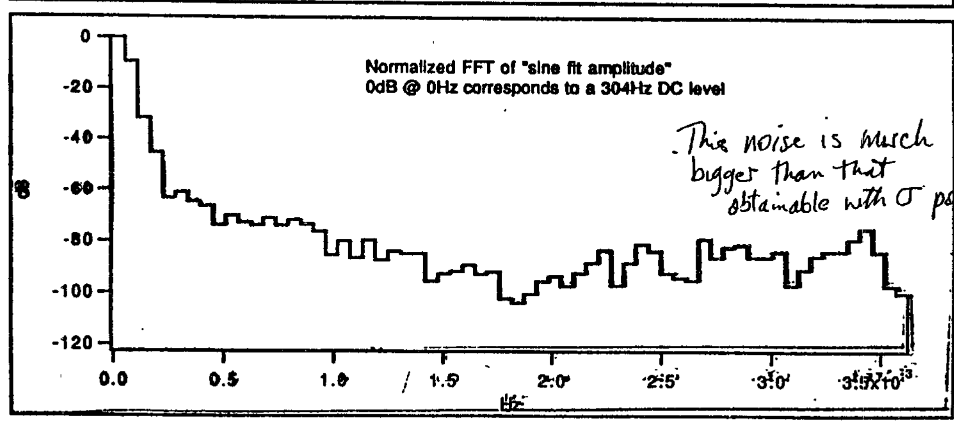

What does this mean?

Noise is bigger with linear polarization by ~5 fold. Why?

Static birefringence 300 Hz

fsr → 540 MHz

5.5 ppm of 1 order

~0.9 microradians phase diff/bounce

Noise of "static" birefringence: −100 dB

→ 9 picoradians phase noise

effective measurement time 2×10^4 sec

equiv 3 nanorads/$\sqrt{Hz}$

Freq Equivalents

Noise is ~ 3 milliHertz – This is shot noise at 1 sec NOT at 20,000 s

QED signal $\frac{\Delta f}{f} = \frac{\Delta n}{n} = 10^{-22} \times 1.4$

→ 80 NANO Hertz

PROBLEMS HERE

Time Dependence? Power Dependence?

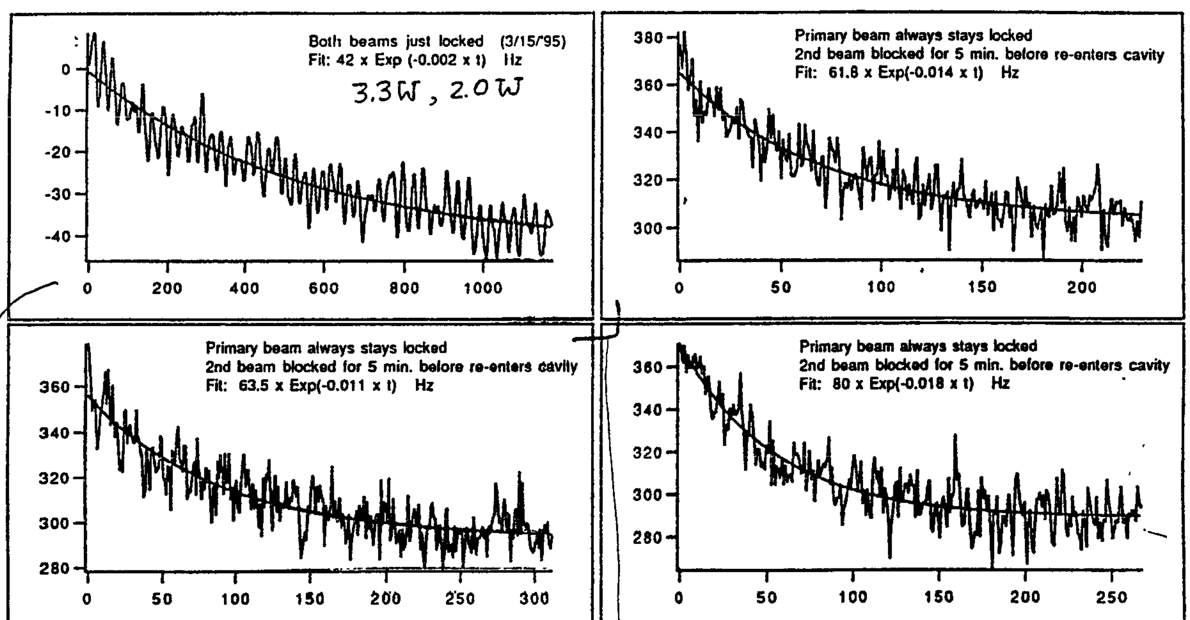

Both Beams Switched

jump ~40Hz

relax time ~ 500 sec

jump ~ 70Hz   0.4 μrads

relaxation rate ~ 0.014 s^{-1} (70sec)

One Beam Switched (~2W)

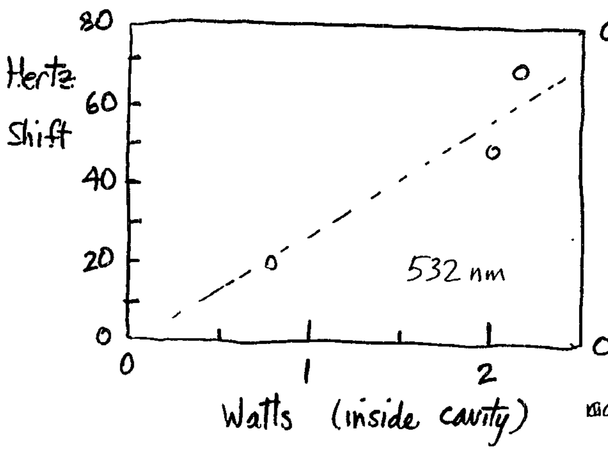

Slope ~ 30Hz/W

~ .17 $\frac{\mu rad}{Watt}$

<u>switch one</u>

cavity mirrors 1m R
separation 28cm

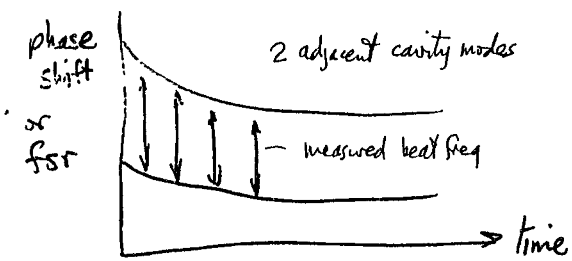

<u>switch both</u>

→ smaller step

- longer relaxation

Mirrors coated by Ojai Research ~ 1986

T ≃ 25 ppm A+S ≃ 50 ppm $\mathcal{F}$ ~ 42,000

Use σ-pol → UNDETECTABLE SMALL EFFECT

crossed linear polarization → dynamic BR

photorefractivity ; orientationally-aware traps

→ Need 2-sets of 2-level systems ?

Bottom Line

1. Mirrors know if they have been fluxed with linear polarized light.
2. Circular polarization can "erase".
3. Some evidence that relaxation time is power dependent
4. Weak depolarized component in LIGO may give non-thermal time-dependent contrast
5. May be possibility of mode coupling in high Q systems

Thursday AM   Data Analysis I. Search for Compact Object Binaries
January 18   Chair: S. Finn (Northwestern)

8:00	C. Will (Washington U)	Compact Binary Inspiral: A Post-Newtonian Playground
8:25	Discussion	
8:35	J. Wilson (LLNL)	Neutron Star Binaries Hydrodynamics
9:00	Discussion	
9:10	A. Wiseman (Caltech)	Final Wave Forms for Binary Inspiral
9:35	Discussion	
9:45	Coffee Break	
10:00	K. Thorne (Caltech)	The Final Merger of Compact Binaries: Information Content, Waveform Computations, and Data Analysis Changes
10:25	Discussion	
10:35	R. Matzner (UT-Austin)	Grand Challenge Update
11:00	Discussion	

COMPACT BINARY INSPIRAL: A POST-NEWTONIAN PLAYGROUND

Clifford M. Will

WUGRAV

WASHINGTON UNIVERSITY GRAVITATION GROUP

- The Challenge to Post-Newtonian Theorists
- An Extended Epstein-Wagoner Framework
  - *C. M. Will & A. G. Wiseman (Caltech)*
- The BDI post-Minkowskian Framework
  - *L. Blanchet, T. Damour & B. R. Iyer*
- The Struggle for Higher Orders
  - How convergent is the PN Series?

A Post-Newtonian Playground

Einstein's Equations

+

$\frac{v^2}{c^2} \ll 1$

$\Downarrow$

Post-Newtonian Expansion

Evolution of orbital frequency caused by gravitational radiation energy-loss

$$\frac{df}{dt} = \left(\frac{df}{dt}\right)_Q \left\{1 + O\left(\frac{v^2}{c^2}\right) + O\left(\frac{v^3}{c^3}\right) + O\left(\frac{v^4}{c^4}\right) \dots\right\}$$

1916
Einstein
Standard Texts
1993
Nobel Prize

1976
Wagoner & Will

1995
Blanchet, Damour, Iyer, Will & Wiseman

THE RELAXED EINSTEIN EQUATIONS

Field Definition:

$$h^{\alpha\beta} = \eta^{\alpha\beta} - \sqrt{-g}g^{\alpha\beta}$$

Harmonic Coordinate Condition:

$$\partial_\beta h^{\alpha\beta} = 0$$

"Reduced" Field Equations:

$$\Box h^{\alpha\beta} = -16\pi(-g)T^{\alpha\beta} - \Lambda^{\alpha\beta}(h) \equiv -16\pi\tau^{\alpha\beta}$$

$$\partial_\beta \tau^{\alpha\beta} = 0$$

Formal Solution:

$$h^{\alpha\beta} = 4\int_C \frac{\tau^{\alpha\beta}(t', \mathbf{x}')}{|\mathbf{x} - \mathbf{x}'|}\delta(t' - t + |\mathbf{x} - \mathbf{x}'|)d^4x'$$

Divide into Inner ($\mathcal{N} = \{|\mathbf{x}'| < \mathcal{R}\}$) and Outer ($\mathcal{C} - \mathcal{N} = \{|\mathbf{x}'| > \mathcal{R}\}$) integrals, where $\mathcal{R} \sim \lambda$.

Characteristics of Inspiralling Binaries

Type of Binary	$2 \times 1.4M_\odot$	$10M_\odot + 1.4M_\odot$	$2 \times 10M_\odot$
r/m when f=10Hz	180	70	47
v/c when f=10Hz	0.07	0.12	0.15
r/m when f=1000Hz	8	–	–
v/c when f=1000Hz	0.3	–	–
f at coalescence (Hz)	1,400	360	190
Time to coalescence (s)	1,030	270	40
Number of GW cycles to coalescence	16,500	3,520	600

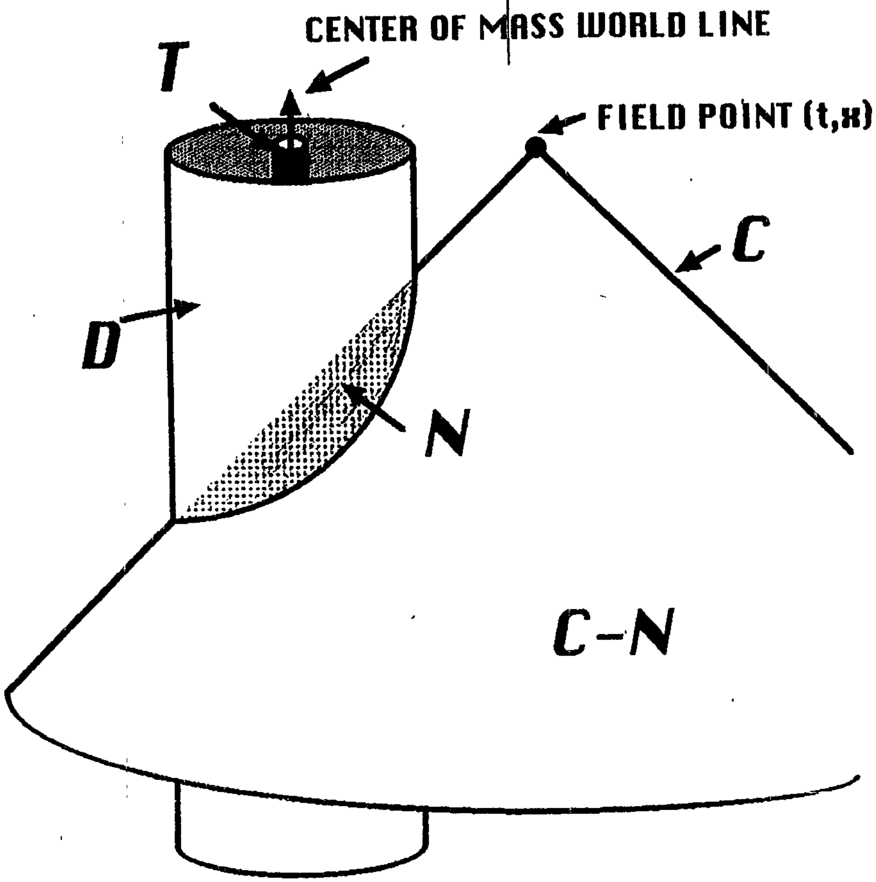
CENTER OF MASS WORLD LINE
T
FIELD POINT (t,x)
C
D
N
C–N

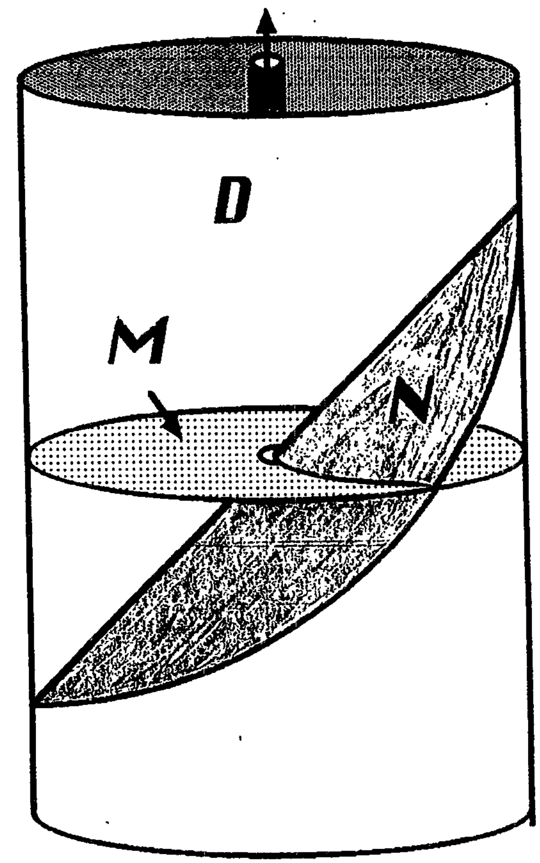
D
M
N

RADIATION ZONE SOLUTION: NEAR ZONE INTEGRAL

$$R >> \mathcal{R}$$

Radiative Field:

$$h^{ij}_{\mathcal{N}}(t,\mathbf{x}) = \frac{4}{R}\sum_{m=0}^{\infty}\frac{1}{m!}\frac{\partial^m}{\partial t^m}\int_{\mathcal{M}}\tau^{ij}(u,\mathbf{x}')(\hat{\mathbf{N}}\cdot\mathbf{x}')^m d^3x' + O(R^{-2})$$

$$u \equiv t - R$$

Harmonic Identities ($\tau^{\alpha\beta}{}_{,\beta} = 0$):

$$\tau^{ij} = \frac{1}{2}(\tau^{00}x^ix^j)_{,00} + 2(\tau^{k(i}x^{j)})_{,k} - \frac{1}{2}(\tau^{kl}x^ix^j)_{,kl}$$

$$\tau^{ij}x^k = \frac{1}{2}(2\tau^{0(i}x^{j)}x^k - \tau^{0k}x^ix^j)_{,0} + (\tau^{l(i}x^{j)}x^k - \frac{1}{2}\tau^{lk}x^ix^j)_{,l}$$

Multipole Expansion of Radiative Field:

$$\boxed{h^{ij}_{\mathcal{N}} = \frac{2}{R}\frac{d^2}{dt^2}\sum_{m=0}^{\infty}\hat{N}_{k_1}\ldots\hat{N}_{k_m}I^{ijk_1\ldots k_m}_{EW}(u)}$$

Epstein-Wagoner Moments:

$$I^{ij}_{EW} = \int_{\mathcal{M}}\tau^{00}x^ix^jd^3x + I^{ij}_{SURF}$$

$$I^{ijk}_{EW} = \int_{\mathcal{M}}(2\tau^{0(i}x^{j)}x^k - \tau^{0k}x^ix^j)d^3x + I^{ijk}_{SURF}$$

$$I^{ijkl}_{EW} = \int_{\mathcal{M}}\tau^{ij}x^kx^ld^3x$$

$$I^{ijk_1\ldots k_m}_{EW} = \frac{2}{m!}\frac{d^{m-2}}{dt^{m-2}}\int_{\mathcal{M}}\tau^{ij}x^{k_1}\ldots x^{k_m}d^3x$$

RADIATION ZONE SOLUTION: RADIATION ZONE INTEGRAL

Change Variables:

$$u' \equiv t' - r'$$

Radiative Field:

$$h^{ij}_{TT} = 4\int_{-\infty}^{u}du'\int\frac{\tau^{ij}(u'+r',\mathbf{x}')}{t-u'-\mathbf{n}'\cdot\mathbf{x}}[r'(u',\Omega')]^2d^2\Omega'$$

where

$$t - u' = r' + |\mathbf{x}-\mathbf{x}'|$$

$$r'(u',\Omega') = \frac{r^2-(t-u')^2}{2(\mathbf{n}'\cdot\mathbf{x}-t+u')}$$

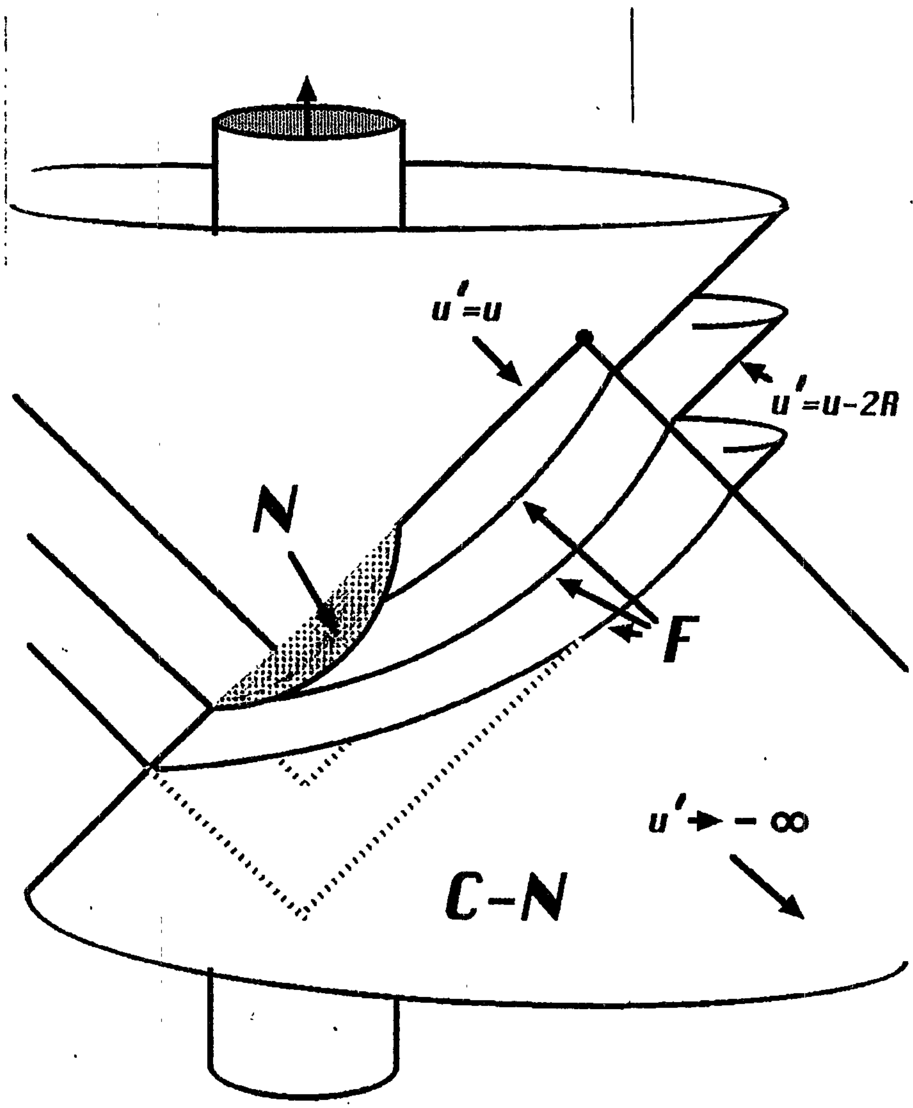

u'=u
u'=u-2R
N
F
u'→−∞
C-N

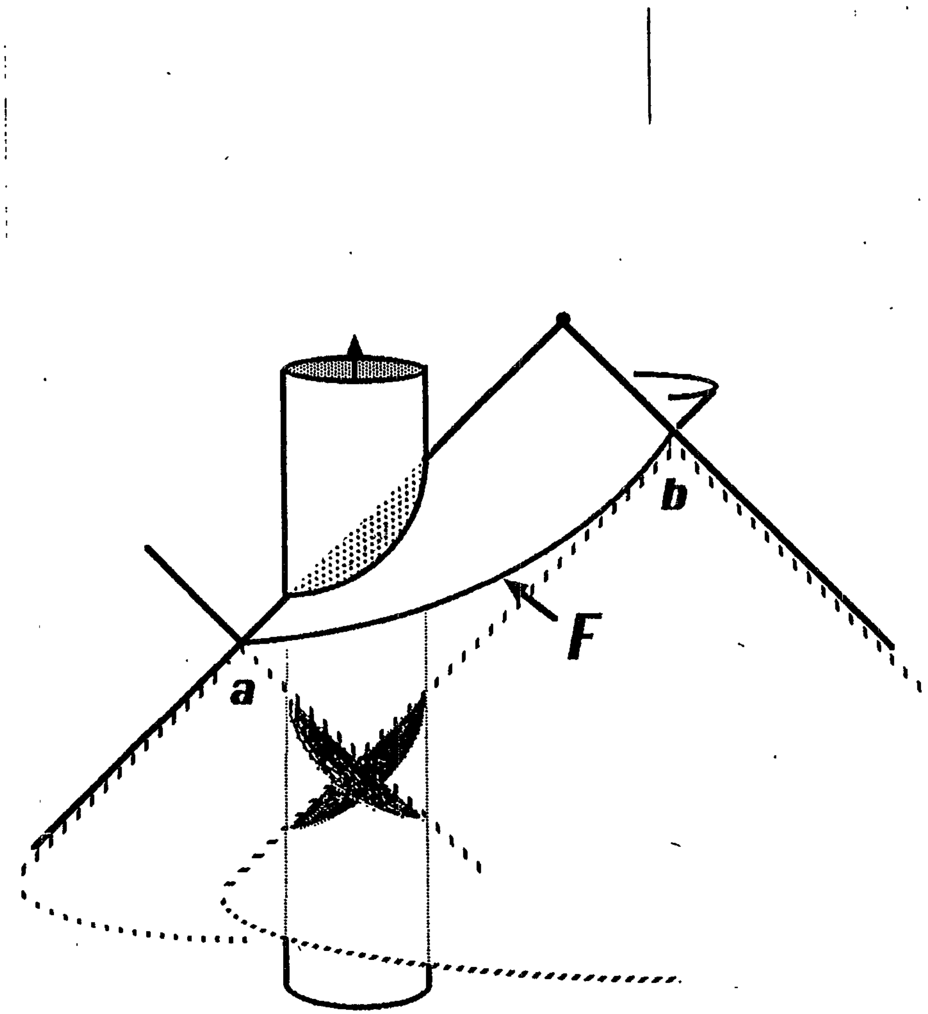

b
F
a

NEAR ZONE SOLUTION

$$|\mathbf{x}| < \mathcal{R}$$

Source Densities:

$$\sigma = T^{00} + \sum_i T^{ii}$$

$$\sigma_i = T^{0i}$$

$$\sigma_{ij} = T^{ij}$$

Expansion Parameter:

$$\epsilon \sim v^2 \sim (m/r)$$

Retarded Potentials:

$$V(t,\mathbf{x}) \equiv \int_{\mathcal{C}} \frac{d^3x'}{|\mathbf{x}-\mathbf{x}'|}\sigma(t-|\mathbf{x}-\mathbf{x}'|,\mathbf{x}')$$
$$V_i(t,\mathbf{x}) \equiv \int_{\mathcal{C}} \frac{d^3x'}{|\mathbf{x}-\mathbf{x}'|}\sigma_i(t-|\mathbf{x}-\mathbf{x}'|,\mathbf{x}')$$
$$W_{ij}(t,\mathbf{x}) \equiv \int_{\mathcal{C}} \frac{d^3x'}{|\mathbf{x}-\mathbf{x}'|}\left[\sigma_{ij} + \frac{1}{4\pi}(V_{,i}V_{,j} - \frac{1}{2}\delta_{ij}V_{,k}V_{,k})\right](t-|\mathbf{x}-\mathbf{x}'|,\mathbf{x}')$$

Near Zone Field

$$h^{00} = -4V + 4(W_{ii} - 2V^2) + O(3)$$

$$h^{0i} = -4V_i + O(5/2)$$

$$h^{ij} = -4W_{ij} + O(3)$$

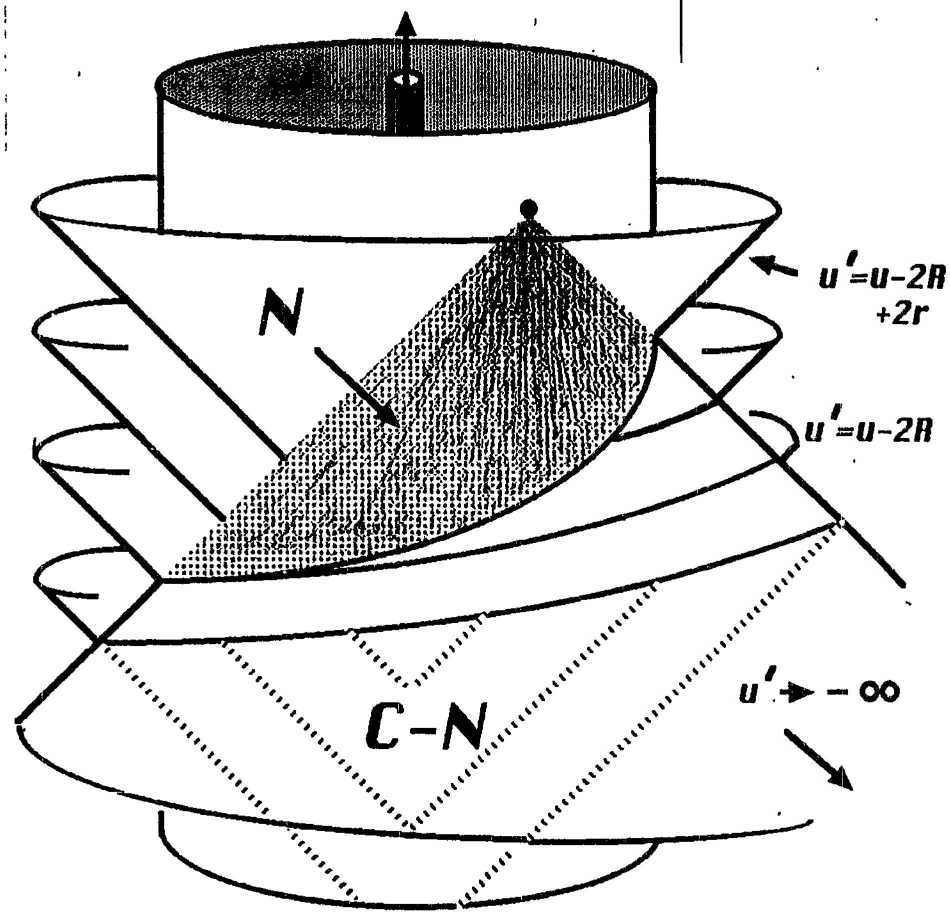

RESULTS OF EXTENDED EW FRAMEWORK

- **Finite and Well-defined**
  - ⋆ Outer integrals convergent
  - ⋆ No infinite or ill-defined terms

$$
\begin{aligned}
h^{ij}_{\mathcal{N}}(t,\mathrm{x}) =& \text{finite EW terms} + 1/\mathcal{R} \text{ terms} \\
& - \frac{1912}{315}\frac{m}{R}\,{}^{(4)}Q^{ij}(u)\mathcal{R} \\
h^{ij}_{C-\mathcal{N}}(t,\mathrm{x}) =& \frac{4m}{R}\int_0^\infty ds\,{}^{(4)}Q^{ij}(u-s)\left[\ln\left(\frac{s}{2R+s}\right)+\frac{11}{12}\right] \\
& + \frac{4m}{3R}\hat{N}^k\int_0^\infty ds\,{}^{(5)}Q^{ijk}(u-s)\left[\ln\left(\frac{s}{2R+s}\right)+\frac{97}{60}\right] \\
& - \frac{16m}{3R}\epsilon^{(i|ka}\hat{N}^k\int_0^\infty ds\,{}^{(4)}J^{a|j)}(u-s)\left[\ln\left(\frac{s}{2R+s}\right)+\frac{7}{6}\right] \\
& + \frac{1912}{315}\frac{m}{R}\,{}^{(4)}Q^{ij}(u)\mathcal{R}
\end{aligned}
$$

- **3/2PN and 2PN tail terms**
  - ⋆ Correct constants in harmonic coordinates
  - ⋆ No dependence on "matching" radius
- **Propagation along "true" null cones**
  - ⋆ R dependence in tail integral gives circular orbit waveform phase

$$\psi = \omega\{t - R - 2m\ln R - 2m[\gamma + \ln(4\omega e^{-11/12})]\}$$

- **2PN results for general systems**

Energy Loss Formula:

$$
\begin{aligned}
\frac{dE}{dt} = \frac{1}{5}\Big\{ & {}^{(3)}\mathcal{I}^{ij}_{STF}\,{}^{(3)}\mathcal{I}^{ij}_{STF} + \frac{5}{189}\,{}^{(4)}\mathcal{I}^{ijk}_{STF}\,{}^{(4)}\mathcal{I}^{ijk}_{STF} + \frac{5}{9072}\,{}^{(5)}\mathcal{I}^{ijkl}_{STF}\,{}^{(5)}\mathcal{I}^{ijkl}_{STF} \\
& + \frac{16}{9}\,{}^{(3)}\mathcal{J}^{ij}_{STF}\,{}^{(3)}\mathcal{J}^{ij}_{STF} + \frac{5}{84}\,{}^{(4)}\mathcal{J}^{ijk}_{STF}\,{}^{(4)}\mathcal{J}^{ijk}_{STF}\Big\}
\end{aligned}
$$

Relation between STF Moments and EW moments:

$$
\begin{aligned}
\mathcal{I}^{ij}_{STF} =& [I^{ij}_{EW} + \frac{1}{21}(11I^{ijkk}_{EW} - 12I^{k(ij)k}_{EW} + 4I^{kkij}_{EW}) \\
& + \frac{1}{63}(23I^{ijkkll}_{EW} - 32I^{k(ij)kll}_{EW} + 10I^{kkijll}_{EW} + 2I^{klklij}_{EW})]_{STF} \\
& + \mathcal{I}^{ij}_{TAIL} \\
\dot{\mathcal{I}}^{ijk}_{STF} =& [3I^{ijk}_{EW} + 3I^{ijkll}_{EW} - 3I^{illjk}_{EW} + I^{llijk}_{EW}]_{STF} + \mathcal{I}^{ijk}_{TAIL} \\
\ddot{\mathcal{I}}^{ijkl}_{STF} =& [12I^{ijkl}_{EW} + \frac{72}{55}(13I^{ijklmm}_{EW} - 12I^{immjkl}_{EW} + 4I^{mmijkl}_{EW})]_{STF} \\
{}^{(3)}\mathcal{I}^{ijklm}_{STF} =& [60I^{ijklm}_{EW}]_{STF} \\
{}^{(4)}\mathcal{I}^{ijklmn}_{STF} =& [360I^{ijklmn}_{EW}]_{STF} \\
\mathcal{J}^{ij}_{STF} =& [\epsilon_{ipq}(\frac{1}{2}I^{jqp}_{EW} + \frac{9}{28}I^{jqpmm}_{EW} - \frac{3}{28}I^{qmmjp}_{EW})]_{STF} + \mathcal{J}^{ij}_{TAIL} \\
\dot{\mathcal{J}}^{ijk}_{STF} =& [\epsilon_{ipq}(2I^{jqpk}_{EW} + \frac{28}{15}I^{jqpkmm}_{EW} - \frac{8}{15}I^{qmmpjk}_{EW})]_{STF} \\
\ddot{\mathcal{J}}^{ijkl}_{STF} =& [9\epsilon_{ipq}I^{jqpkl}_{EW}]_{STF} \\
{}^{(3)}\mathcal{J}^{ijklm}_{STF} =& [48\epsilon_{ipq}I^{jqpklm}_{EW}]_{STF}
\end{aligned}
$$

THE STF MOMENTS TO 2PN ORDER

$$
\begin{aligned}
\mathcal{I}^{ij}_{STF} = \mu r^2 \Big\{ & \hat{n}^i\hat{n}^j + \frac{1}{42}\Big[\hat{n}^i\hat{n}^j\left(29(1-3\eta)v^2 - 6(5-8\eta)\frac{m}{r}\right) \\
& -24(1-3\eta)\dot{r}\hat{n}^{(i}v^{j)} + 22(1-3\eta)v^iv^j\Big] \\
& + \frac{1}{1512}\hat{n}^i\hat{n}^j\Big[3(253-1835\eta+3545\eta^2)v^4 - 6(355+1906\eta-337\eta^2)\left(\frac{m}{r}\right)^2 \\
& +2(2021-5947\eta-4883\eta^2)\frac{m}{r}v^2 - 2(131-907\eta+1273\eta^2)\frac{m}{r}\dot{r}^2\Big] \\
& + \frac{1}{378}v^iv^j\Big[2(742-335\eta-985\eta^2)\frac{m}{r} \\
& +3(41-337\eta+733\eta^2)v^2 + 30(1-5\eta+5\eta^2)\dot{r}^2\Big] \\
& - \frac{1}{378}\hat{n}^{(i}v^{j)}\dot{r}\left[(1085-4057\eta-1463\eta^2)\frac{m}{r} + 12(13-101\eta+209\eta^2)v^2\right]\Big\}_{STF} \\
& + \mathcal{I}^{ij}_{TAIL} \,,
\end{aligned}
$$

$$
\begin{aligned}
\mathcal{I}^{ijk}_{STF} = -\mu\frac{\delta m}{m}r^3\Big\{ & \hat{n}^i\hat{n}^j\hat{n}^k\Big[1 + \frac{1}{6}(5-19\eta)v^2 - \frac{1}{6}(5-13\eta)\frac{m}{r}\Big] \\
& +(1-2\eta)(v^iv^j\hat{n}^k - \dot{r}v^i\hat{n}^j\hat{n}^k)\Big\}_{STF} + \mathcal{I}^{ijk}_{TAIL} \,,
\end{aligned}
$$

$$
\begin{aligned}
\mathcal{I}^{ijkl}_{STF} = \mu r^4\Big\{ & \hat{n}^i\hat{n}^j\hat{n}^k\hat{n}^l\Big[(1-3\eta) \\
& + \frac{1}{110}(103-735\eta+1395\eta^2)v^2 - \frac{1}{11}(10-61\eta+105\eta^2)\frac{m}{r}\Big] \\
& + \frac{6}{55}(1-5\eta+5\eta^2)(13v^iv^j\hat{n}^k\hat{n}^l - 12\dot{r}v^i\hat{n}^j\hat{n}^k\hat{n}^l)\Big\}_{STF} \,,
\end{aligned}
$$

$$
\mathcal{I}^{ijklm}_{STF} = -\mu\frac{\delta m}{m}r^5\Big\{(1-2\eta)\hat{n}^i\hat{n}^j\hat{n}^k\hat{n}^l\hat{n}^m\Big\}_{STF} \,,
$$

$$
\mathcal{I}^{ijklmn}_{STF} = \mu r^6\Big\{(1-5\eta+5\eta^2)\hat{n}^i\hat{n}^j\hat{n}^k\hat{n}^l\hat{n}^m\hat{n}^n\Big\}_{STF} \,,
$$

$$
\begin{aligned}
\mathcal{J}^{ij}_{STF} = -\mu\frac{\delta m}{m}r\Big\{ & (\mathrm{x}\times\mathrm{v})^i\Big[\hat{n}^j\left(1 + \frac{1}{28}(13-68\eta)v^2 + \frac{3}{14}(9+10\eta)\frac{m}{r}\right) \\
& + \frac{5}{28}(1-2\eta)\dot{r}v^j\Big]\Big\}_{STF} + \mathcal{J}^{ij}_{TAIL} \,,
\end{aligned}
$$

$$
\begin{aligned}
\mathcal{J}^{ijk}_{STF} = \mu r^2\Big\{ & (\mathrm{x}\times\mathrm{v})^i\Big[\hat{n}^j\hat{n}^k\Big(1-3\eta \\
& + \frac{1}{90}(41-385\eta+925\eta^2)v^2 + \frac{2}{9}(7-8\eta-43\eta^2)\frac{m}{r}\Big) \\
& + \frac{1}{45}(1-5\eta+5\eta^2)(10\dot{r}v^j\hat{n}^k + 7v^jv^k)\Big]\Big\}_{STF} \,,
\end{aligned}
$$

$$
\mathcal{J}^{ijkl}_{STF} = -\mu\frac{\delta m}{m}r^3(1-2\eta)\Big\{(\mathrm{x}\times\mathrm{v})^i\hat{n}^j\hat{n}^k\hat{n}^l\Big\}_{STF} \,,
$$

$$
\mathcal{J}^{ijklm}_{STF} = \mu r^4(1-5\eta+5\eta^2)\Big\{(\mathrm{x}\times\mathrm{v})^i\hat{n}^j\hat{n}^k\hat{n}^l\hat{n}^m\Big\}_{STF} \,,
$$

EVOLUTION OF GRAVITY-WAVE FREQUENCY

$$
\begin{aligned}
\frac{df}{dt} = \frac{96}{5\pi\mathcal{M}^2}(\pi\mathcal{M}f)^{11/3}\Big[& 1 \\
& - \left(\frac{753}{336} + \frac{11}{4}\eta\right)(\pi M f)^{2/3} \\
& + (4\pi - \text{[redacted]})(\pi M f) \\
& + \left(\frac{34103}{18144} + \frac{13661}{2016}\eta + \frac{59}{18}\eta^2 + \text{[redacted]}\right)(\pi M f)^{4/3} \\
& + O[(\pi M f)^{5/3}]\Big]
\end{aligned}
$$

(Wagoner & Will '76)

(Poisson '93, Wiseman '93)

(Blanchet, Damour, Iyer, Will, Wiseman '95)

$$
M \equiv m_1 + m_2 \quad , \qquad \eta \equiv m_1 m_2 / M
$$

$$
\mathcal{M} \equiv \eta^{3/5} M
$$

$$
\text{[redacted]} \equiv \frac{1}{12}\sum_{i=1}^{2}\left(113\frac{m_i^2}{m^2} + 75\eta\right)\hat{\mathbf{L}}\cdot\chi_i
$$

$$
\text{[redacted]} \equiv -\frac{\eta}{48}\left(247\chi_1\cdot\chi_2 - 721\hat{\mathbf{L}}\cdot\chi_1\hat{\mathbf{L}}\cdot\chi_2\right)
$$

(Kidder, Wiseman & Will '93)

The post-Newtonian Playground

Multipole moments (I^L, J^L)

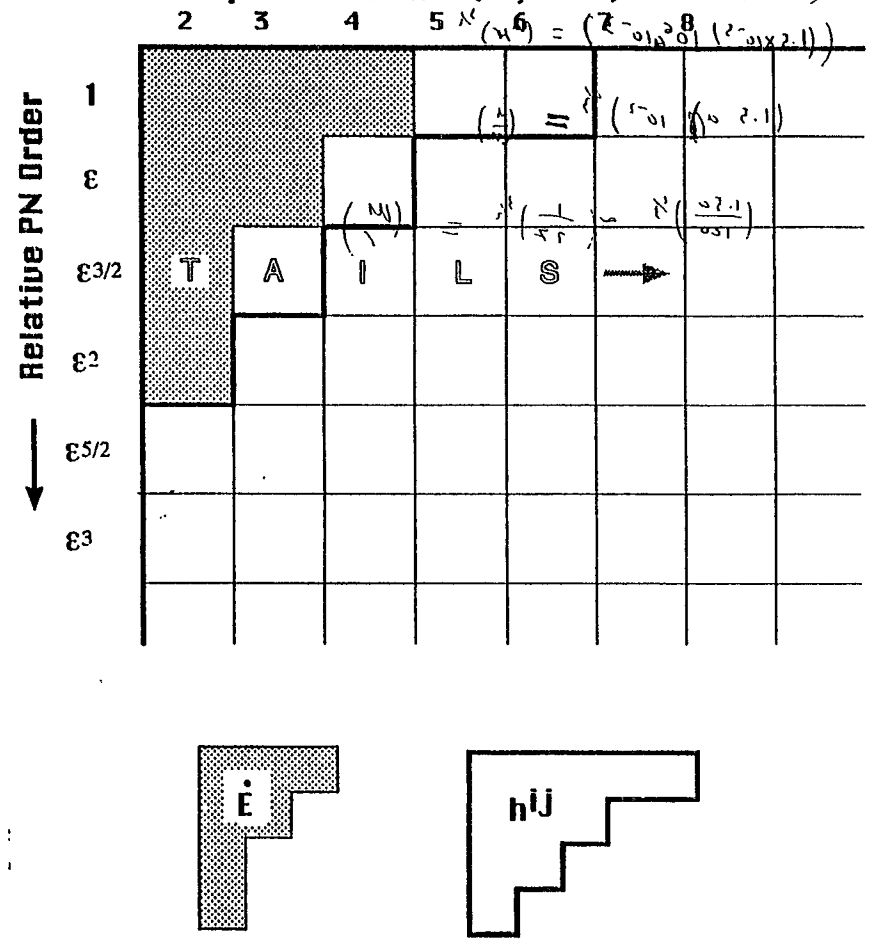

Simone & Poisson (1996)

Convergence (test body) if $\boxed{\frac{v}{c} < \sqrt{\frac{2}{e}}}$

NEUTRON STAR BINARIES HYDRODYNAMICS I

WILSON
MATHEWS
MARRONETTI } N.D.

FIELD EQUATIONS

$$ds^2 = -(\alpha^2 - \beta_i\beta^i)dt^2 + 2\beta_i dx^i dt + \varphi^4 \delta_{ij} dx^i dx^j$$

$$K_{ij} = (D_i\beta_j + D_j\beta_i - \tfrac{2}{3}\varphi^4\delta_{ij} D_k\beta^k)/2\alpha$$

$\mathrm{tr}\,K = 0$ $\qquad \dfrac{\dot\varphi}{\varphi} = \dfrac{1}{6} D_k\beta^k$

ASSUMPTIONS { CONFORMAL FLATNESS, STATIONARITY

HAMILTONIAN EQ.

$$\nabla^2\varphi = -2\pi\varphi^5\left(\rho W + \rho\epsilon W\left(\Gamma W - \frac{(\Gamma-1)}{W}\right) + \frac{K_{ij}K^{ij}}{16\pi}\right)$$

$$K \Rightarrow \nabla^2(\alpha\varphi) = 2\pi\alpha\varphi^5\left(\rho(3W^2-2) + \rho\epsilon(3\Gamma(W^2-1)+5) + \frac{7}{16\pi}K_{ij}K^{ij}\right)$$

MOMENTUM CONSTRAINT

$$\nabla^2\beta^j = \frac{\partial}{\partial x^j}\left(\frac{D_k\beta^k}{3}\right) + 16\pi\alpha\varphi^4 S^j + \frac{\partial}{\partial x^i}\log A\left[\partial_i\beta^j + \partial_j\beta^i - \tfrac{2}{3}\delta_{ij}\partial_k\beta^k\right]$$

$A = \alpha/\varphi^6$
$W = \alpha U^t$

GIVEN ρ, ϵ, S^j solve these eqs. for α, φ, β^i

EQUATIONS II

PERFECT FLUID

$$T_{\mu\nu} = (\rho + \epsilon\rho + P)U_\mu U_\nu + P g_{\mu\nu}$$

$D = W\rho$
$E = W\rho\epsilon$ $\qquad \Gamma = 1 + \dfrac{P}{\rho\epsilon}$
$S_i = (D + \Gamma E)U_i$

THEN:

$$\frac{\partial D}{\partial t} = -6D\frac{\partial \log\varphi}{\partial t} - \frac{1}{\varphi^6}\frac{\partial}{\partial x^i}(\varphi^6 D V^i)$$

$$\frac{\partial E}{\partial t} = -6\Gamma E\frac{\partial\log\varphi}{\partial t} - \frac{1}{\varphi^6}\frac{\partial}{\partial x^i}(\varphi^6 E V^i) - P\left(\frac{\partial W}{\partial t} + \frac{1}{\varphi^6}\frac{\partial}{\partial x^i}(\varphi^6 W V^i)\right)$$

$$\frac{\partial S_i}{\partial t} = -6S_i\frac{\partial\log\varphi}{\partial t} - \frac{1}{\varphi^6}\frac{\partial}{\partial x^j}(\varphi^6 S_i V^j) - \alpha\frac{\partial P}{\partial x^i}$$
$$+ 2\alpha(D+\Gamma E)\left(\frac{W^2-1}{W}\right)\frac{\partial\log\varphi}{\partial x^i} - W(D+\Gamma E)\frac{\partial\alpha}{\partial x^i} + S_j\frac{\partial\beta^j}{\partial x^i}$$

CHOOSE $\vec\beta_{r\to\infty}$ such that V^i is minimized.

Or said $\vec\beta = \vec R \times \vec\omega + \vec\beta_d$

ω is coordinate rotation speed

DESCRETIZE THESE EQUATIONS AND INSERT INTO COMPUTOR.
FOR PRESENT FIND STATIONARY SOLUTIONS ONLY.

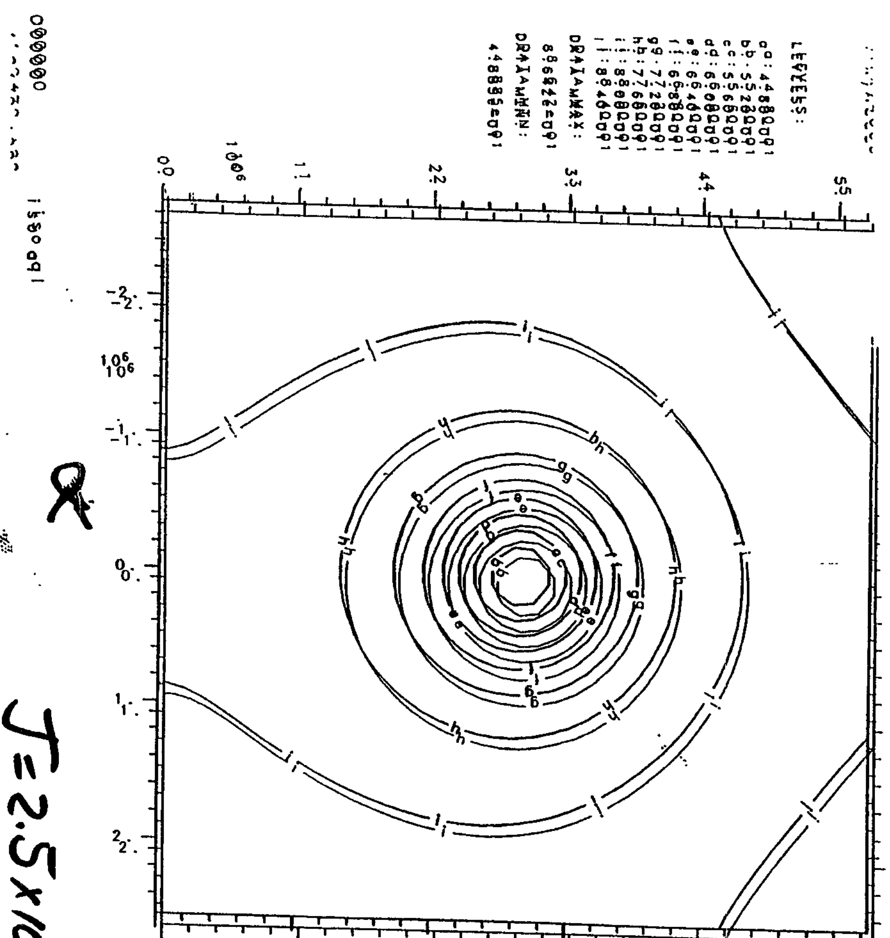

J=2.5x10^11 cm^2

RESULTS

WE HAVE SELECTED 3 VALUES OF ANGULAR MOMENTUM AND SEEN WHAT HAPPENS.

$M_G^0 = 1.45 M_\odot$

EOS SUCH THAT $M_G^{CRIT} = 1.59 M_\odot$

PUT STARS ON GRID. EVOLVE UNTIL STARS SETTLE DOWN.

$J = 2.2 \times 10^{11}\ cm^2$ $(G=c=1)$

ORBIT UNSTABLE.
STARS START TO SPIRAL IN.

$\frac{d_p}{m} = 9.2$ $m = 2M_G^0$ INSIDE LAST STABLE ORBIT.

$\frac{J}{M^2} = 1.26$

$J = 2.3 \times 10^{11}\ cm^2$

ORBIT STABLE.
BUT CENTRAL DENSITY HAS RISEN TO 2.7×10^{15} gm/cc (CRITICAL DENSITY FOR THIS EOS)

FREQUENCY GW 310 Hz

$J = 2.7 \times 10^{11}\ cm^2$

ORBIT STABLE
CENTRAL DENSITY $= 2 \times 10^{15}$

(INITIAL CENTRAL DENSITY $= 1.4 \times 10^{15}$ gm/cc)

$\dot{J}/\omega J \approx 10^{-4}$

2

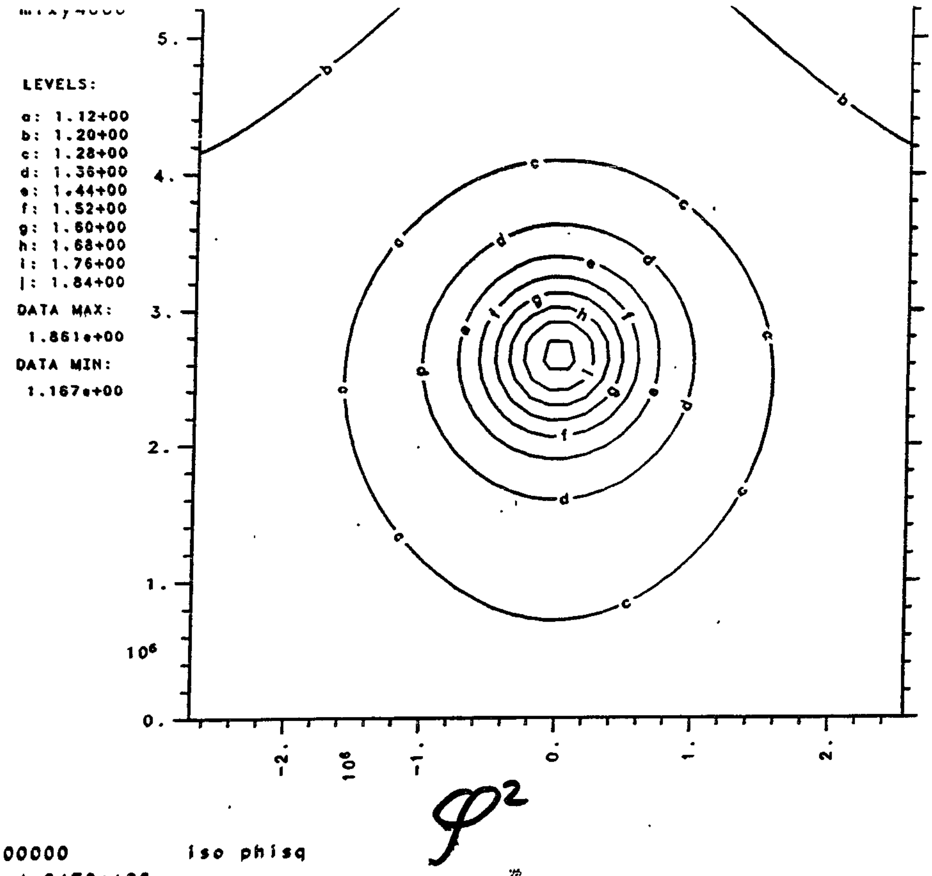

φ^2

3

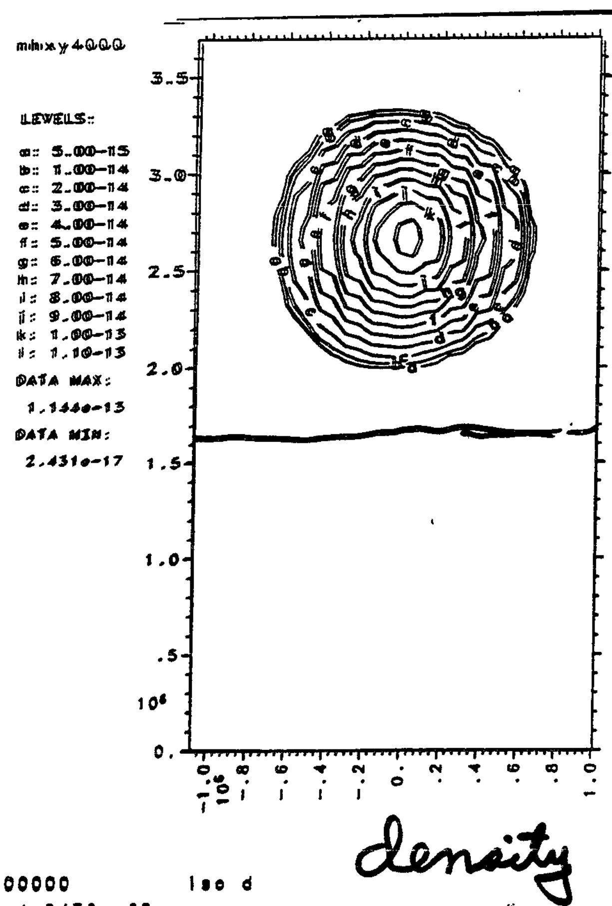

density

5

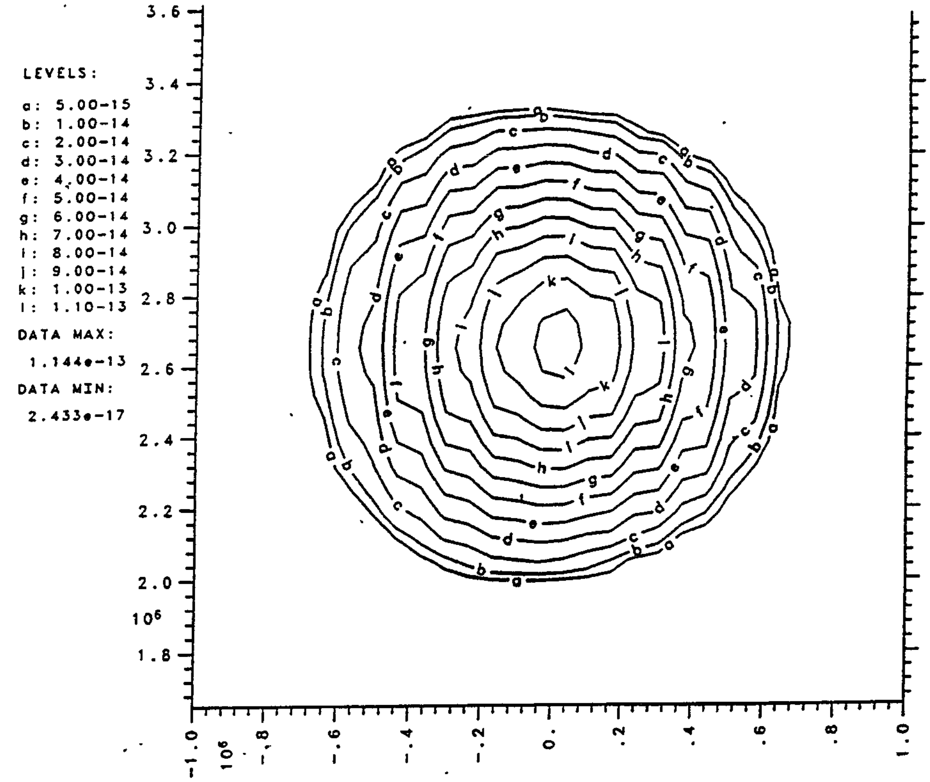

density

00000 iso d

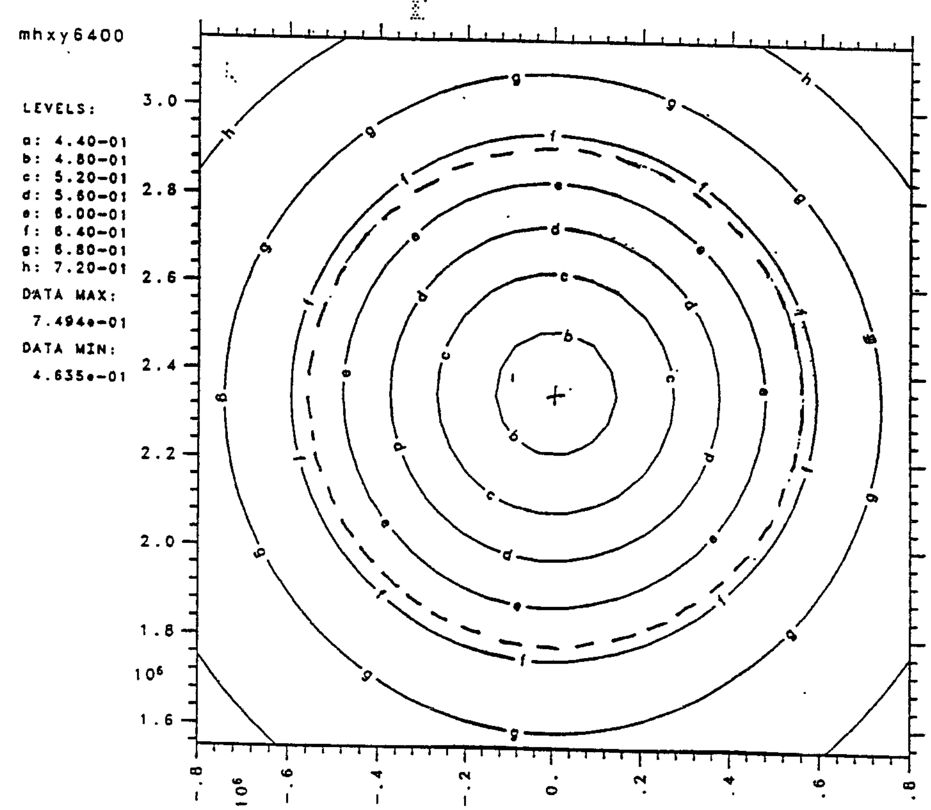

T

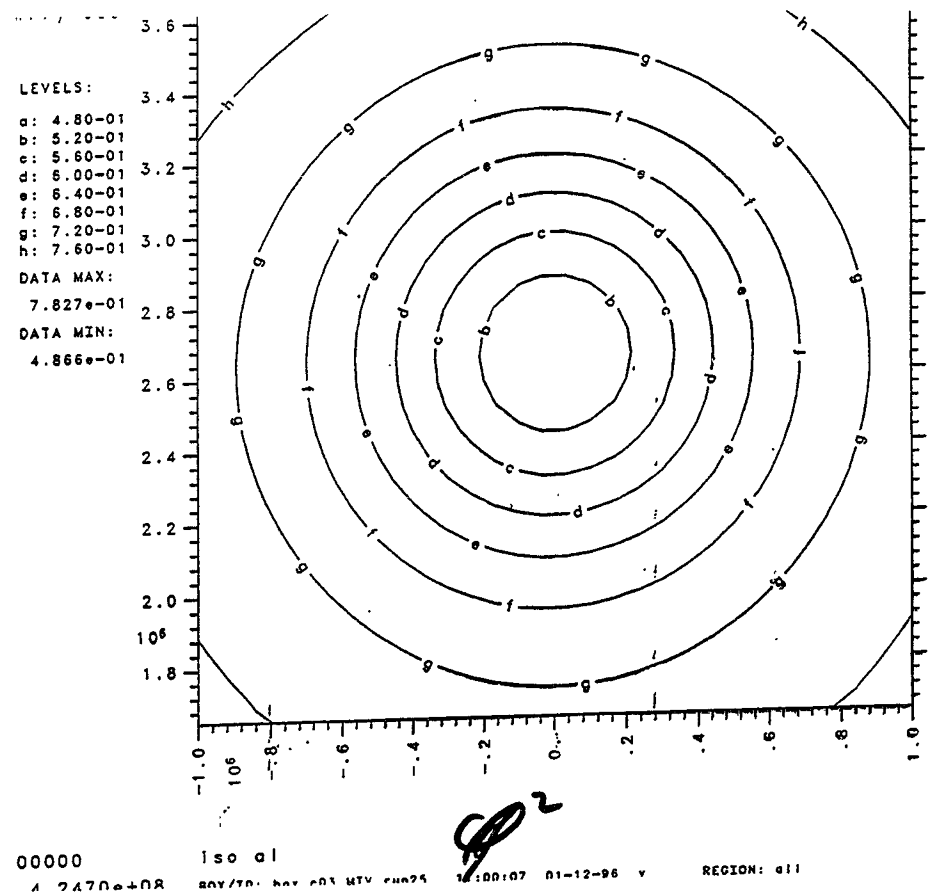

φ^2

6

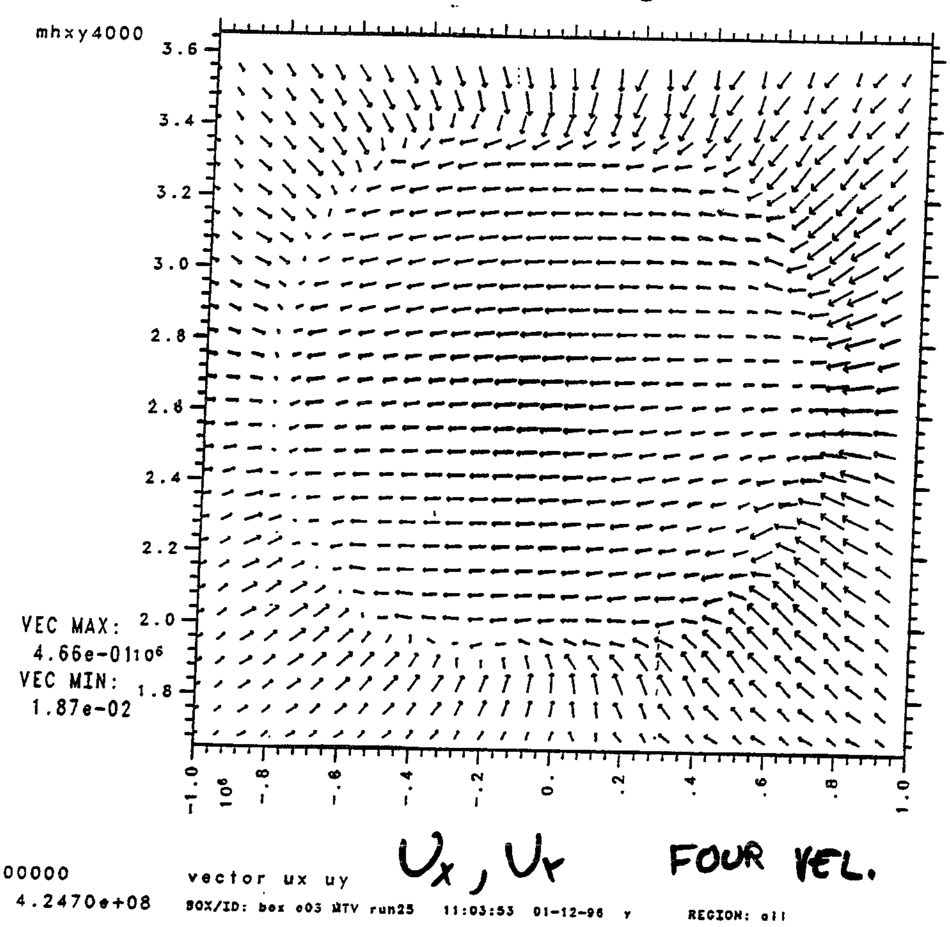

U_x, U_y FOUR VEL.

IN STAR $|U| \approx .3$

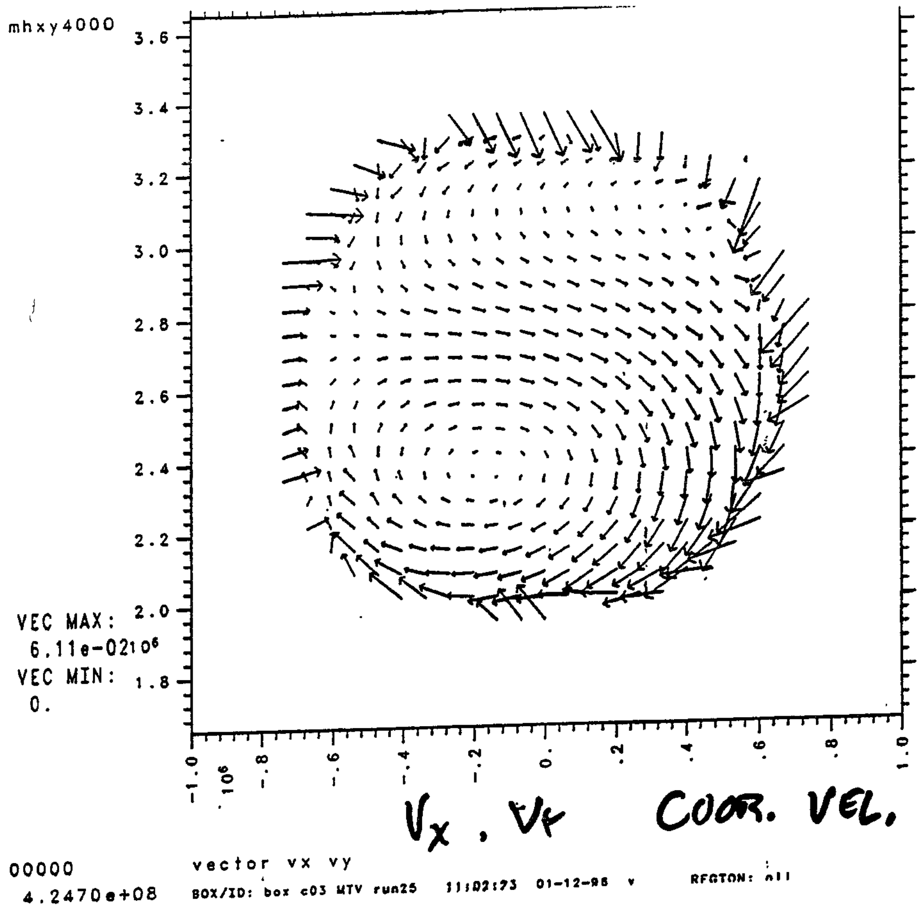
mhxy4000
VEC MAX:
6.11e-02
VEC MIN:
0.
10^6
Vx, Vf COOR. VEL.
00000
4.2470e+08
vector vx vy
BOX/ID: box c03 MTV run25 11:02:23 01-12-96 v REGION: all

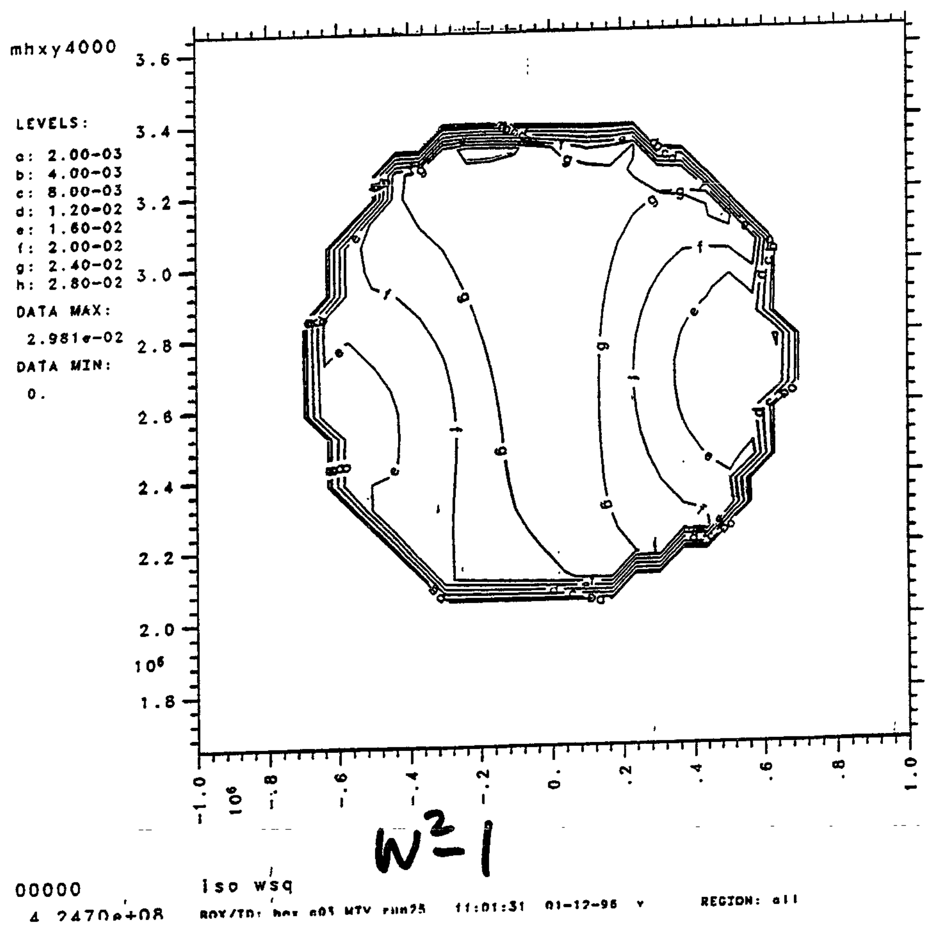
mhxy4000
LEVELS:
a: 2.00-03
b: 4.00-03
c: 8.00-03
d: 1.20-02
e: 1.60-02
f: 2.00-02
g: 2.40-02
h: 2.80-02
DATA MAX:
2.981e-02
DATA MIN:
0.
10^6
W²-1
00000
4.2470e+08
iso wsq
BOX/ID: box c03 MTV run25 11:01:31 01-12-96 v REGION: all

CONCLUSIONS. IV

ORBITS UNSTABLE AT
PERHAPS AT LARGE RADIUS.

STARS ARE UNSTABLE IF
EQUATION OF STATE NOT STIFF
ENOUGH.

ORBITAL FREQUENCY PERHAPS
LOW.

OUR EQUATION OF STATE IS
FROM WILSON MAYLE SUPERNOVA MODELING
$M^{CRIT.} = 1.59\ M_\odot$
BUT
RECENT WORK FAVORS A LOWER MASS

BETHE BROWN
$M^{CRIT.} = 1.50 - 1.56\ M_\odot$
OBSERVED N.S. MASSES CONSISTANT
WITH $M^{CRIT} = 1.5$ S. FINN

WHY DENSITY INCREASES. V

REWRITE FIELD SOURCES:

FOR φ

$$\rho = \rho + \rho\epsilon + (W^2-1)(\rho + \Gamma\rho\epsilon)$$

For $\alpha\varphi$

$$\cancel{\rho = \rho + \rho\epsilon + (W^2-1)(3\rho + \Gamma\rho\epsilon)}$$

$$\rho = \rho + \rho\epsilon(6\Gamma-5) + (W^2-1)(3\rho + 3\Gamma\rho\epsilon)$$

MOMENTUM EQUATION HYDRO STATICS

$$\frac{\partial P}{\partial x^i} = -(\rho + \rho\epsilon\Gamma)\frac{\partial \log \alpha}{\partial x^i}$$
$$+ (W^2-1)(\rho + \rho\epsilon\Gamma)\left[2\frac{\partial \log \varphi}{\partial x^i} - \frac{\partial \log \alpha}{\partial x^i}\right]$$

AS WE SAW IN FIGURES
W^2-1 IS SOMEWHAT CONSTANT
OVER THE STARS.

VI

TO STUDY FURTHER THE DENSITY ENHANCEMENT EFFECT. WE WROTE 1D SPHERICAL CODE WITH W^2-1 PUT INTO SOURCES AND FORCES.

RESULTS:

EOS $\quad M^{CRIT} = 1.57 M_\odot$

IF $M_g^0 = 1.40 M_\odot$

$W^2-1 > .035$ UNSTALBEE

$M_g^0 : 1.45 M_\odot$ $\quad$ at $\rho = 1.8 \times 10^{15} \frac{gm}{cc}$

$W^2-1 > .020$ UNSTABLE

EXAMPLE 3D

$J = 2.5 \times 10^{11}\, cm^2$

$W^2-1 \approx .024 - .030$

IF EOS SOFT GET BLACK HOLES

CAVEAT. IN 3D CALCULATIONS WE HAVE TAKEN ZERO TEMPERATURE BY EDICT.

VII

LOTS OF ENERGY MUST BE DISSAPATED.

ESTIMATE $\approx 6 \times 10^{52}$ ergs.

ENOUGH TO POWER γ-ray source.

or at least produce high velocity wind.

$$\frac{1}{\sqrt{1-v^2}} \approx 10$$

QUESTION: HOW IS or IS ENERGY DISSAPATED?

VISCOSITY, SHOCKS $\Rightarrow$ NEUTRINO EMISSION

IS CONNECTION OF NEUTRON STAR BINARIES AND γ-ray BURSTS IMPORTANT FOR G.W.s?

VIII

FUTURE
WHAT NEXT?

I IMPROVE NUMERICS SO MORE
QUANTATIVE. RESULTS.

II STUDY COLLAPSE IN 1D and 3D

III PERSUE γ-RAY MODELING

IV CONNECT TO P.N. CALCULATIONS

VI DEVELOP 3D G-R SUPERNOVA
COMPUTER PROGRAM

VII STUDY EOS ~~PAR~~

2^{nd} Post-Newtonian Waveforms

What are they?
What are they good for?

Alan Wiseman (Caltech
Cliff Will (Wash U. St. L
Luc Blanchet (Meudon)
Thibault Damour (Meudon)
Bala Iyer (RRI,

Wiseman

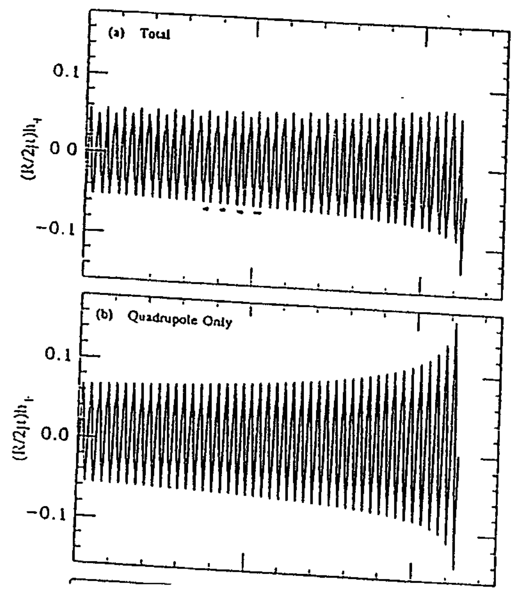

- $m_1/m_2 = 10$
- circular orbit
- Note true waveform does not grow as fast as Quad.

Wiseman

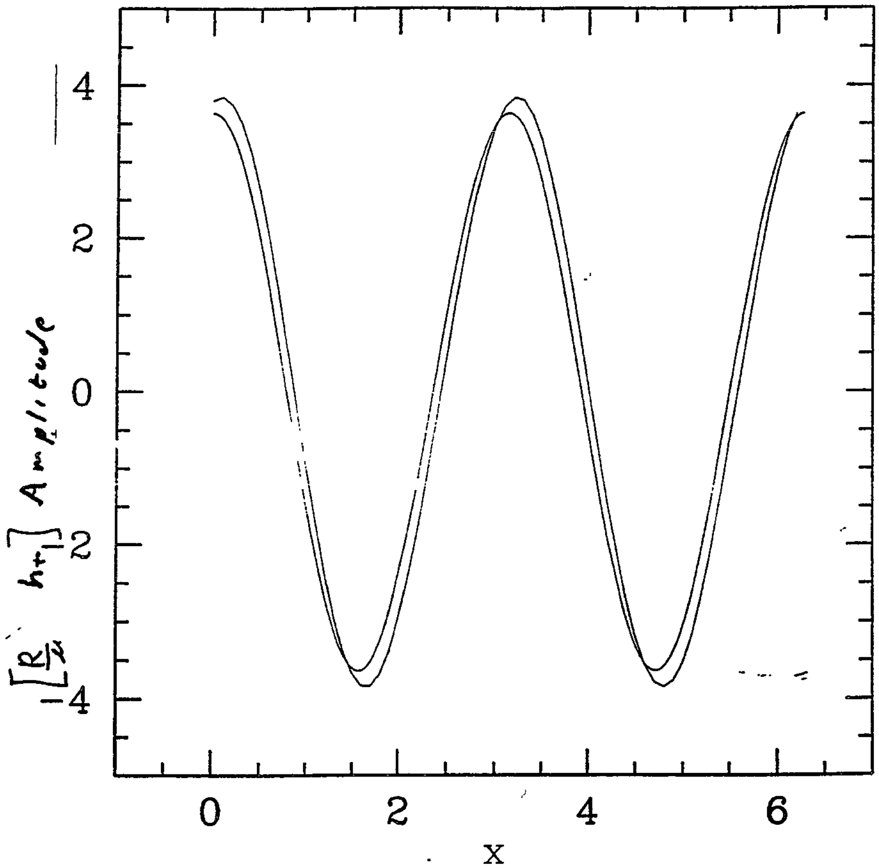

Phase

.8 $M_\odot$ $\qquad f_{GW} \approx 200$ Hz

2. $M_\odot$

wiseman

$$h_{+,\times} = \frac{2Gm\eta}{c_0^2 R}\left(\frac{Gm\omega}{c_0^3}\right)^{2/3}\left\{H^{(0)}_{+,\times} + x^{1/2}H^{(1/2)}_{+,\times} + xH^{(1)}_{+,\times} + x^{3/2}H^{(3/2)}_{+,\times} + x^2 H^{(2)}_{+,\times} + O(x^{5/2})\right\} \tag{2}$$

[illegible]
From BIWW

1 $$H^{(0)}_{+} = (1+c^2)\cos 2\psi \tag{3a}$$

2 $$H^{(1/2)}_{+} = \frac{s}{8}\frac{\delta m}{m}\left[(5+c^2)\sin\psi + 9(1+c^2)\sin 3\psi\right] \tag{3b}$$

3 $$H^{(1)}_{+} = \frac{1}{6}\left[-19-9c^2+2c^4+\eta(19-11c^2-6c^4)\right]\cos 2\psi - \frac{4}{3}s^2(1+c^2)(1-3\eta)\cos 4\psi \tag{3c}$$

4 $$H^{(3/2)}_{+} = \frac{s}{192}\frac{\delta m}{m}\left\{\left[-57-60c^2+c^4+2\eta(49-12c^2-c^4)\right]\sin\psi + \frac{27}{4}\left[-73-40c^2+9c^4+2\eta(25-8c^2-9c^4)\right]\sin 3\psi - \frac{625}{2}(1-2\eta)s^2(1+c^2)\sin 5\psi\right\} + 2\pi(1+c^2)\cos 2\psi \tag{3d}$$

5 $$\begin{aligned}H^{(2)}_{+} = {} & \frac{1}{120}\left[-22-396c^2-145c^4+5c^6+\frac{5}{3}\eta(-706+216c^2+251c^4-15c^6) + 5\eta^2(98-108c^2+7c^4+5c^6)\right]\cos 2\psi \\ & + \frac{2}{15}s^2\left[59+35c^2-8c^4+\frac{5}{3}\eta(-131-59c^2+24c^4) + 5\eta^2(21-3c^2-8c^4)\right]\cos 4\psi \\ & + \frac{81}{40}(1-5\eta+5\eta^2)s^4(1+c^2)\cos 6\psi \\ & + \frac{s}{40}\frac{\delta m}{m}\left\{\left[11+7c^2+10(5+c^2)\ln 2\right]\cos\psi + 5\pi(5+c^2)\sin\psi \right. \\ & \left. + 27\left[7-10\ln(3/2)\right](1+c^2)\cos 3\psi + 135(1+c^2)\sin 3\psi\right\}\end{aligned} \tag{3e}$$

$$H^{(0)}_{\times} = 2c\sin 2\psi$$

$$H^{(1/2)}_{\times} = -\frac{3}{4}sc\frac{\delta m}{m}\left[\cos\psi + 3\cos 3\psi\right]$$

$$H^{(1)}_{\times} = \frac{c}{3}\left[-17+4c^2+\eta(13-12c^2)\right]\sin 2\psi - \frac{8}{3}(1-3\eta)cs^2\sin 4\psi$$

$$H^{(3/2)}_{\times} = \frac{sc}{96}\frac{\delta m}{m}\left\{\left[63-5c^2+2\eta(-23+5c^2)\right]\cos\psi + \frac{27}{2}\left[67-15c^2+2\eta(-19+15c^2)\right]\cos 3\psi + \frac{625}{2}(1-2\eta)s^2\cos 5\psi\right\} + 4\pi c\sin 2\psi$$

$$\begin{aligned}H^{(2)}_{\times} = {} & \frac{c}{60}\left[-68-226c^2+15c^4+\frac{5}{3}\eta(-572+490c^2-45c^4) + 5\eta^2(56-70c^2+15c^4)\right]\sin 2\psi \\ & + \frac{4}{15}cs^2\left[55-12c^2+\frac{5}{3}\eta(-119+36c^2) + 5\eta^2(17-12c^2)\right]\sin 4\psi \\ & + \frac{81}{20}(1-5\eta+5\eta^2)cs^4\sin 6\psi \\ & + \frac{3}{20}sc\frac{\delta m}{m}\left\{\left[3+10\ln 2\right]\sin\psi - 5\pi\cos\psi + 9\left[7-10\ln(3/2)\right]\sin 3\psi - 45\pi\cos 3\psi\right\}\end{aligned}$$

... and c is shorthand for ...

$$\phi = \phi_0 - \frac{1}{\eta}\left\{\Theta^{5/8} + \left(\frac{3715}{8064}+\frac{55}{96}\eta\right)\Theta^{3/8} - \frac{3\pi}{4}\Theta^{1/4} + \left(\frac{9275495}{14450688}+\frac{284875}{258048}\eta + \frac{1855}{2048}\eta^2\right)\Theta^{1/8} + O(\ln\Theta)\right\} . \tag{6}$$

$$\psi = \varphi_{orbit} - \frac{2Gm\omega}{c_0^3}\ln(\omega/\omega_0)$$

and the frequency (satisfying $\omega = d\phi/dt$)

$$\omega = \frac{c_0^3}{8Gm}\left\{\Theta^{-3/8} + \left(\frac{743}{2688}+\frac{11}{32}\eta\right)\Theta^{-5/8} - \frac{3\pi}{10}\Theta^{-3/4} + \left(\frac{1855099}{14450688}+\frac{56975}{258048}\eta + \frac{371}{2048}\eta^2\right)\Theta^{-7/8} + O(\Theta^{-1})\right\} . \tag{7}$$

We use in these expressions the dimensionless time variable defined by

wiseman

Contributions to G.W. Phase

Relativistic Ord.	# of GW Cycles	Harmonic that carry Power	"Physical" Origin
Leading Ord.	16050	2	Simple Quad.
$(v/c)^2$	439	1, 2, 3	Current, Quadrpl.
$(v/c)^3$	-208	2	Tail !
$(v/c)^4$	9	1, 2, 3, 4	....
	≈ 17		Spin Orbit
	≈ 2		Spin - Spin

- Two N.S. $1.4\ M_\odot$
- Spiraling from $f_{orb} = 5\,Hz$ to $500\,Hz$

  $f_{GW} = 10\,Hz$ to $1000\,Hz$

? What about convergence properties of the Post-Newtonian Expansion?

Wiseman

Higher Harmonics Carry off (orbital) Energy

$\Rightarrow$ Orbital Radius Shrinks

$\Rightarrow$ Orbital Frequency Rises (Hence G.W. Freq. Rises)

∴ Tracking G.W. phase (or orbital phase) over many cycles (a long time) requires accurate knowledge of the energy-loss rate

∴ Need to know the harmonic structure of the emitted wave!

Wiseman

Wiseman

Higher Harmonics don't just carry energy - They carry <u>Information</u>.

Quad. Sig. Analysis.	Restricted P.N. Sig. Analysis	Signal Analysis
$h = A_1 \cos^{5/3} 2\Phi_{Quad}$	$h = A_1 \cos^{5/3} 2\Phi_{PN}$	$h = \sum_{n,m,p} A_{nmp} \cos m\Phi$
$\Phi_c \longrightarrow$	$\Phi_c \longrightarrow$	Φ_c
$T_c \longrightarrow$	$T_c \longrightarrow$	T_c
$m_{chirp} \longrightarrow$	$m_c \longrightarrow$	m_c
$\searrow$	$\mu/m \longrightarrow$	μ/m
$A \longrightarrow$	$A \longrightarrow$	F_+/R
	$\searrow$	F_x/R
	$\searrow$	$\cos(i)$ } *
Finn + Chernoff	Cutler + Flanagan Krolak	In Progress {Allen, Brady, Finn, AGW.}

* Weakly, but still determined harmonics 1, 2, 3, 4

Wiseman

$M_{total} = 2.8\ M_\odot$

$m_1/m_2 = 10$

inclination $= 90°$

f_{orb} 20 Hz – 250 Hz

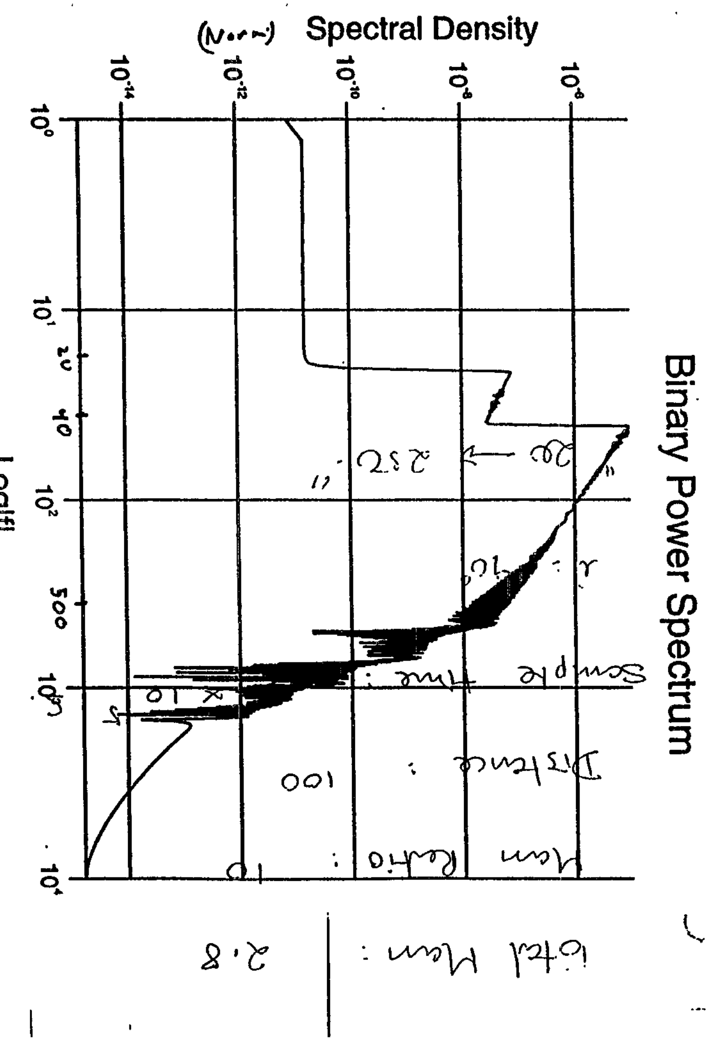

Kip Thorne

"The Final Merger of Compact Binaries: Information Content, Waveform Computations, and Data Analysis Issues

BLACK-HOLE COALESCENCE

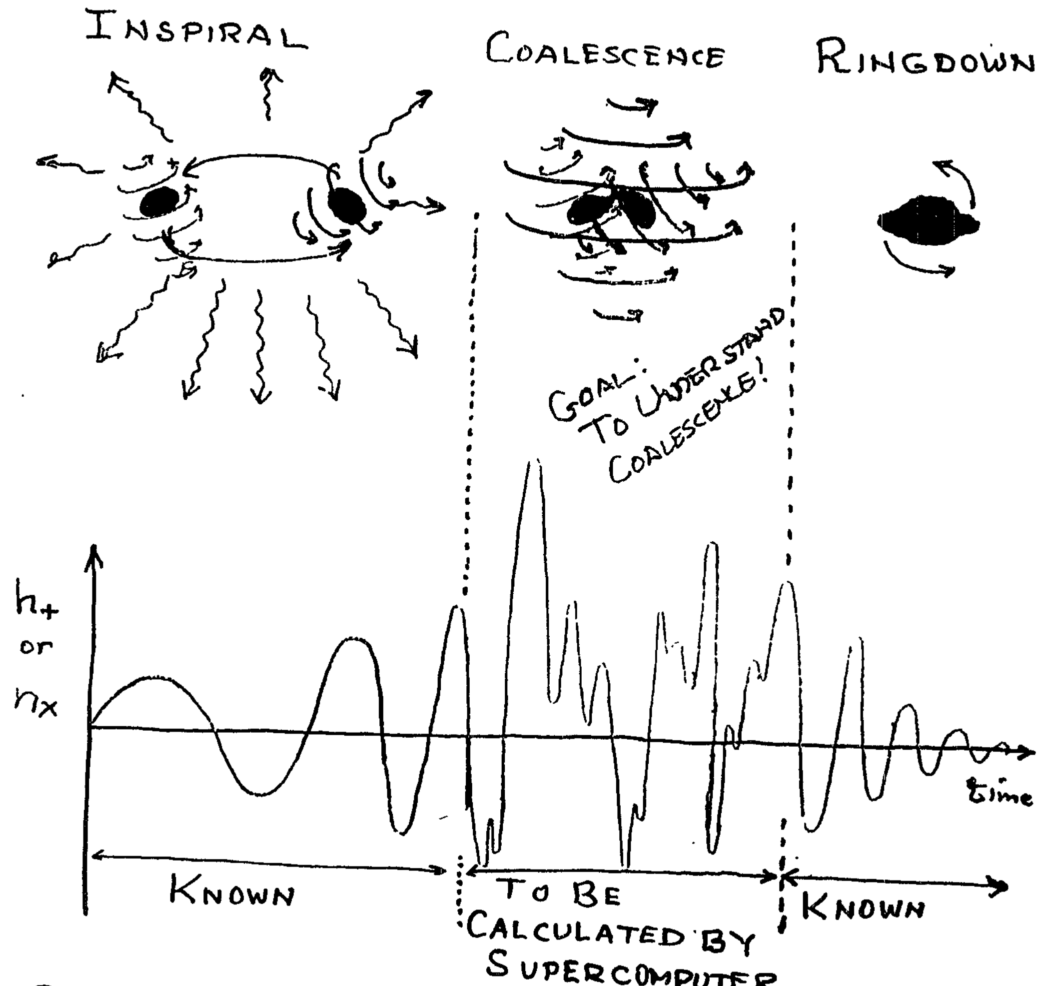

• Detectable throughout the Universe

$\boxed{\text{LIGO/VIRGO}}$: for $M_1 \sim M_2 \sim 15$ to $1000\, M_\odot$

$\boxed{\text{LISA}}$: for $M_1 \sim M_2 \sim 3\times10^4$ to $10^8\, M_\odot$

For First LIGO Interferometers

& Hughes

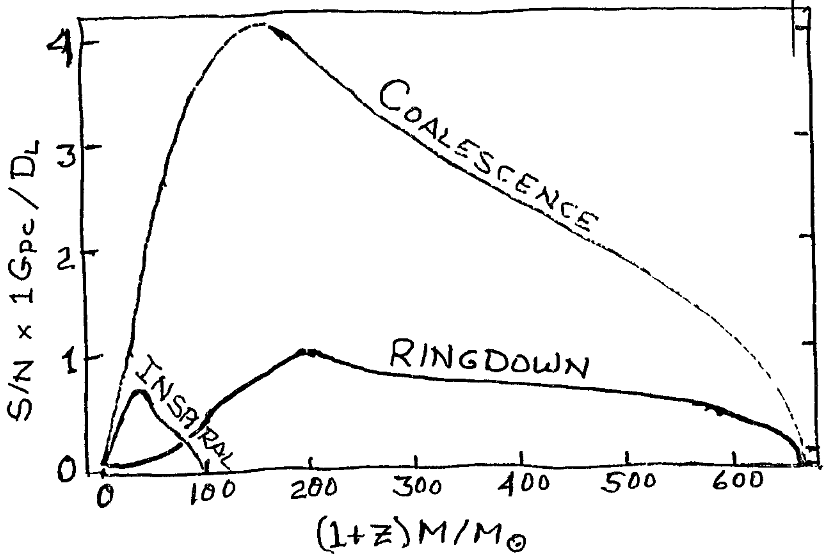

Number of bits of information in noise-contaminated) coalescence waveform $= \tau \int \log_2 \left(1 + \frac{1}{\tau} \frac{d(S/N)^2}{df}\right) df$

duration of coalescence

$\tau \Delta f \simeq$ Number of cycles in waveform (since $\Delta f \sim \bar{f}$)

$$\simeq N_{cyc} \log_2 \left[1 + \frac{(S/N)^2}{N_{cyc}}\right]$$

$$\simeq N_{cyc} \log_2 \left[\frac{(S/N)^2}{N_{cyc}}\right] \quad \text{for } N_{cyc} \ll (S/N)^2$$

$$\simeq 1.4\,(S/N)^2 \quad \text{for } N_{cyc} \gg (S/N)^2$$

S/N For Inspiral, Coalescence, Ringdown

[Eanna Flanagan & Scott Hughes]

[$M_1 = M_2 = M/2$; $(a/M)_{Final} = 0.98$; 10% efficiency]

"Advanced" Interferometers

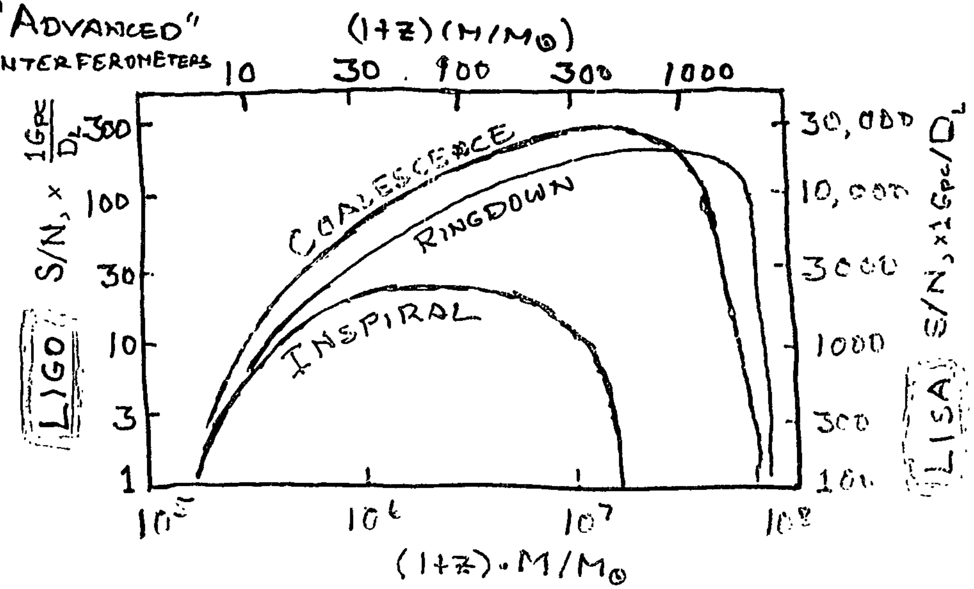

For LIGO/VIRGO: We need theoretical waveforms as aid in extracting coalescence information!! (BBH Grand Challenge)

If BBH Project fails to give us waveform information

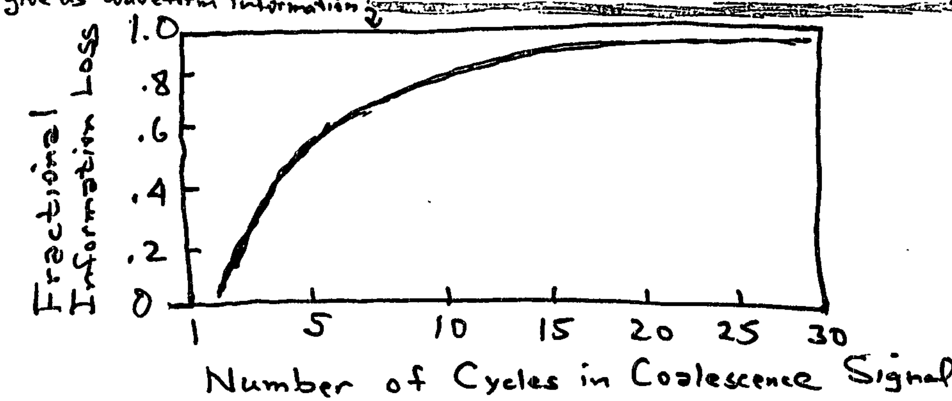

OTHER KINDS OF COMPACT OBJECTS

$R \lesssim 10\,GM/c^2$

Boson & Soliton Stars

- Condensates of (hypothetical) bosons, held together by gravity (& possibly also particle interactions) [cf. Liddle & Madsen, Int. J. Mod Phys, 1, 101 (1992)]
- Examples: Colpi, Shapiro, Wasserman, PRL, 57, 2485 (1986)

★ Complex scalar field ϕ, of mass m, $\lambda|\phi|^4$ coupling

$$M_{max} \simeq 0.06\,\lambda^{1/2}\,\frac{m_{PL}^3}{m^2} \simeq 0.1\,M_\odot\,\frac{\lambda^{1/2}}{(m/1\,GeV)^2}$$

– "Boson ★"

T. D. Lee, Y. Pang Phys. Reports, 221, 251 (1992)

★ Higgs type scalar field of mass m coupled to a complex scalar field or Fermion field

$$M_{max} \sim \frac{m_{PL}^4}{m^3} \sim \frac{10^{12}\,M_\odot}{(m/300\,GeV)^3}$$

– "Soliton ★"

Naked Singularities

- Conventional Wisdom: Cosmic Censorship [Penrose] – they don't exist
- But: "Choptuons" [Hawking vs Preskill & Thorne]

Horowitz's Inocuous Singularities

⋮

How Search for Exotic Compact Objects?

$\boxed{0.01 \text{ to } 0.2\,M_\odot}$ LIGO/VIRGO: Binary Inspiral

Note: for $\mathcal{M}_c \simeq 0.01\,M_\odot$

- Several months to sweep thru LIGO/VIRGO band
- verify radii $R \lesssim 10$ km
- "advanced" interferometers: search out to Virgo
- enormous computational task

$\boxed{\begin{array}{l} 30\text{-}300\,M_\odot \sim \text{LIGO/VIRGO} \\ 3\times10^5 - 3\times10^7\,M_\odot - \text{LISA} \end{array}}$ Watch a $\sim 1\,M_\odot$ WD, NS, BH spiral into the massive compact object

.... Map the massive object's spacetime geometry (measure its multipole moments)

... If it is a BH: "No Hair"

$$\underset{\Uparrow \atop M_0}{\text{Mass}} \;\&\; \underset{\Uparrow \atop S_1}{\text{Spin}} \Rightarrow \underset{\Uparrow \atop M_2, M_3, M_4, \ldots \atop S_2, S_3, S_4, \ldots}{\text{All Other Moments}}$$

IDEALIZED EXAMPLE [Fintan Ryan: Phys Rev D in press]

- Axisymmetric Central Object

  Moments $M_0, M_2, M_4, M_6, \ldots$

  $S_1, S_3, S_5, S_7, \ldots$

- Circular Orbit in Equatorial Plane

- Monitor Evolution of Orbital Phase

  [to accuracy $\sim 1/10^3$ for LIGO, $\sim 1/10^6$ for LISA]

  as WD, NS, or BH spirals from $r \sim 10M$ to $r \sim 1M$

$$v = (\pi M_0 f)^{1/3}$$

$$\frac{dN_{cycles}}{d\ln f} = \frac{5}{96\pi}\frac{1}{(\pi \underbrace{M_c}_{\mu^{2/5}M_0^{3/5}} f)^{5/3}}\left[1 + \frac{743}{336}v^2 + \left(\underbrace{-4\pi}_{\text{GW Tail - Poisson}} + \frac{113}{12}\frac{\boxed{S_1}}{M_0^2}\right)v^3\right.$$

$$+\left(\frac{3058673}{1016064} - \frac{1}{16}\frac{S_1^2}{M_0^4} + 5\frac{\boxed{M_2}}{M_0^3}\right)v^4$$

$$+(\ldots\ldots)v^5 + (\ldots\ldots)v^6$$

$$+\left(\ldots\ldots - 22\frac{\boxed{S_3}}{M_0^4}\right)v^7 + \left(\ldots\ldots - \frac{45}{4}\frac{\boxed{M_4}}{M_0^5}\right)v^8$$

...

TWO EXAMPLES

LIGO

$1 M_\odot$ NS / $300 M_\odot$ BH @ 1 Gpc

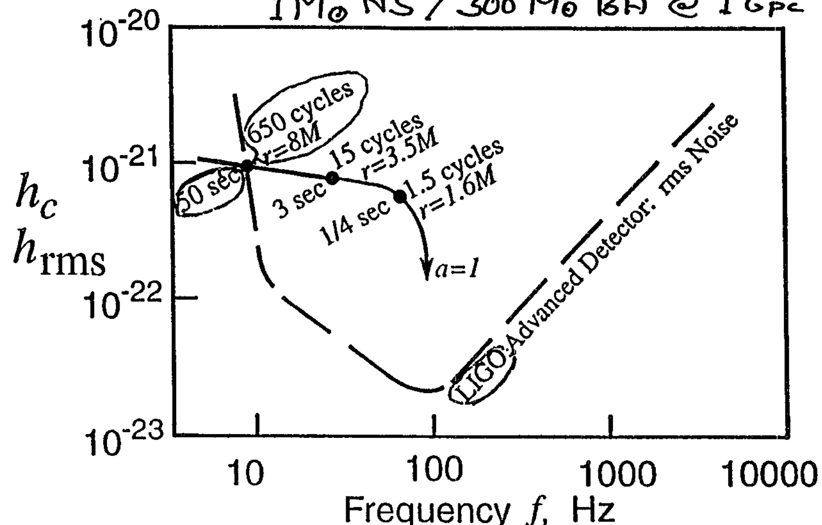

LISA

$1 M_\odot$ WD or NS / $10^6 M_\odot$ BH @ 1 Gpc

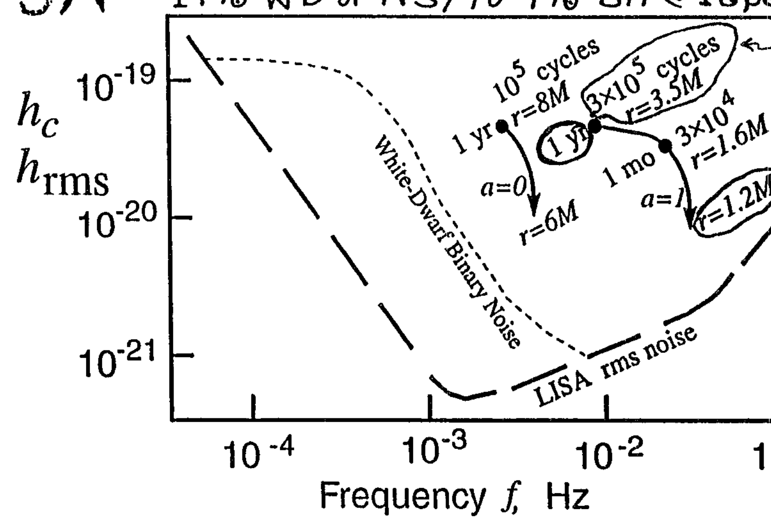

~10% of cycles due to mass quadrupole moment of BH

Can probably measure lowest few moments to very high accuracy

Complications:

Theoretical:

- To compute nonlinear terms in series extremely difficult:
  - Components of curvature/metric don't decouple
  - No separation of variables
- Series may not be accurate enough.

Astrophysical [especially for LISA]:

- Orbit should be nonequatorial & nonspherical
- Accretion disk will perturb orbit

$$\frac{\dot{L}_{Acc}}{\dot{L}_{GW}} \sim \frac{\begin{pmatrix}\text{Mass in disk}\\ \text{inside orbit}\end{pmatrix}}{M_0}\left(\frac{r}{M_0}\right)^{5/2}$$

↑ very roughly

will drive orbit into equatorial plane...

Comparison of Dual Recycled Interferometers & Spherical Bars or TIGAS [Daniel Kennefick & Dustin Laurence]

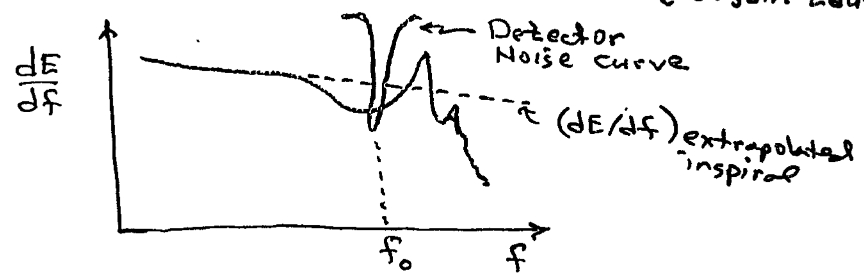

Interferometers:

$$\frac{S}{N} = \sqrt{\frac{(dE/df)_0}{(dE/df)_{\substack{\text{extrapolated}\\ \text{inspiral}}}}}\left(\frac{200\,\text{Mpc}}{r}\right)\left(\frac{1\,\text{kHz}}{f_0}\right) 0.7 \sqrt{\frac{\text{circulating power}}{100\,\text{kWatts}}}$$

Bars:

$$\frac{S}{N} = \sqrt{\frac{(dE/df)_0}{(dE/df)_{\substack{\text{extrapolated}\\ \text{inspiral}}}}}\left(\frac{200\,\text{Mpc}}{r}\right)\left(\frac{1\,\text{kHz}}{f_0}\right) 0.3 \sqrt{\frac{\hbar f_0}{k T_{noise}}}$$

Comparison of Dual Recycled Interferometers & Spherical Bars, or TIGAS [Daniel Kennefick & Dustin Laurence]

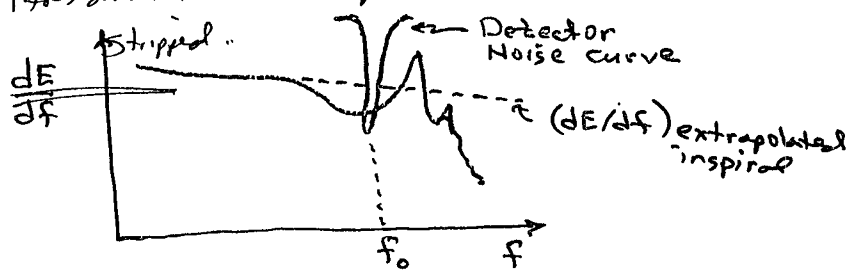

Interferometers:

$$\frac{S}{N} = \sqrt{\frac{(dE/df)_o}{(dE/df)_{\text{extrapolated inspiral}}}} \left(\frac{200\,\text{Mpc}}{r}\right)\left(\frac{1\,\text{kHz}}{f_o}\right) 0.7 \sqrt{\frac{\text{Circulating power}}{100\,\text{kWatts}}}$$

Bars:

$$\frac{S}{N} \doteq \sqrt{\frac{(dE/df)_o}{(dE/df)_{\text{extrapolated inspiral}}}} \left(\frac{200\,\text{Mpc}}{r}\right)\left(\frac{1\,\text{kHz}}{f_o}\right) 0.3 \sqrt{\frac{h f_o}{k T_{\text{noise}}}}$$

Comments: • NS explosion
– Nadezhin
To detect: Specialty detectors
– [illegible]
Nuzzy: $\Gamma = 1.1$

NS/NS Coalescence

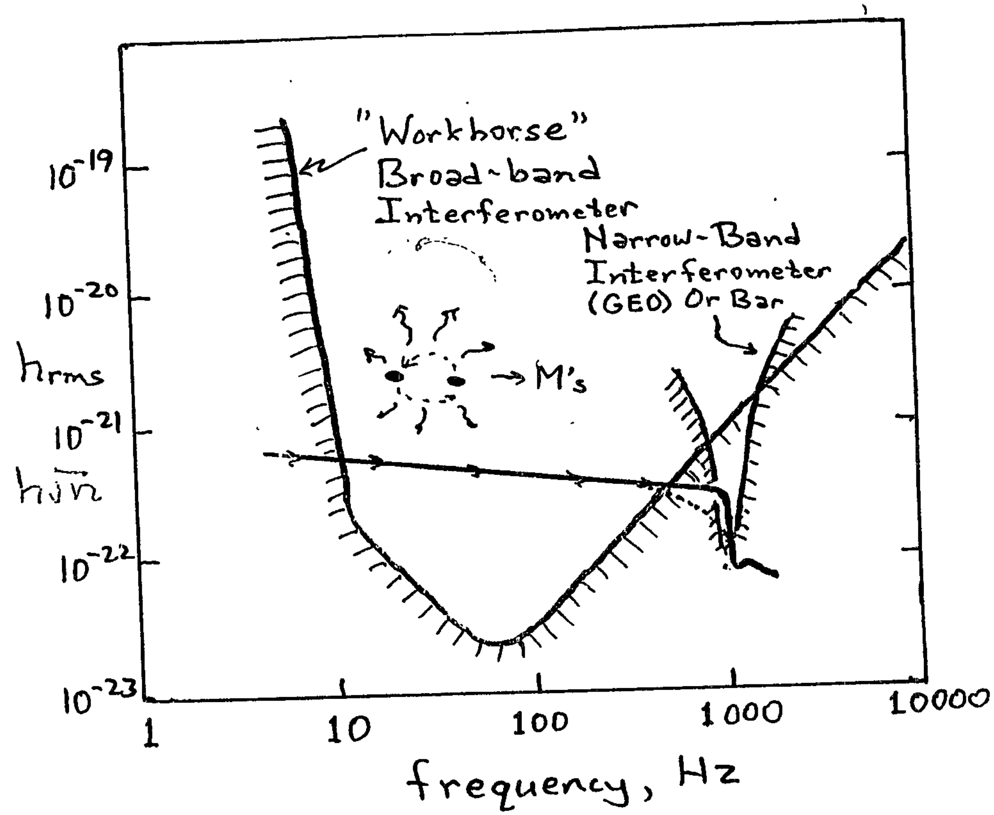

- **Objective:** Get information about NS Eqn of State from Coalescence Waves
- **Opposite Extreme From Inspiral**
  - can only get a few bits of information
  - must jointly design interferometer & data analysis to get stiffness of Eqn of State
  - For this need: $\boxed{\text{Numerical Simulations - Dependence of Waveforms on Eqn of State}}$

Comparison of Dual Recycled Interferometers & Spherical Bars or TIGAS

[Daniel Kennefick & Dustin Laurence]

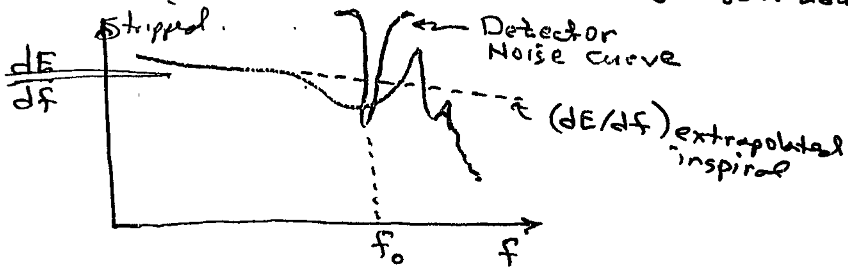

Interferometers:

$$\frac{S}{N} = \sqrt{\frac{(dE/df)_0}{(dE/df)_{\substack{\text{extrapolated}\\ \text{inspiral}}}}}\left(\frac{200\,\text{Mpc}}{r}\right)\left(\frac{1\,\text{kHz}}{f_0}\right)0.7\sqrt{\frac{\text{circulating power}}{100\,\text{kWatts}}}$$

Bars:

$$\frac{S}{N} = \sqrt{\frac{(dE/df)_0}{(dE/df)_{\substack{\text{extrapolated}\\ \text{inspiral}}}}}\left(\frac{200\,\text{Mpc}}{r}\right)\left(\frac{1\,\text{kHz}}{f_0}\right)0.3\sqrt{\frac{\hbar f_0}{k T_{\text{noise}}}}$$

Comments: • NS explosion
— Nadezhin

To detect: spherical detectors
— [illegible]

Nugzar: $\Gamma = 1.1$

"Black Hole Binaries: Coalescence and Gravitational Radiation" UPDATE - R MATZNER

Computational Grand Challengé Program NSF ASC/PHY 9318152
(ARPA Supplemented)

PI: Richard Matzner	The University of Texas at Austin, Austin, TX 78712
Co PIs:	
J. Browne	The University of Texas at Austin, Austin, TX 78712
L.L. Smarr, H.E. Seidel	National Center for SuperComputing Applications, University of Illinois, Urbana, IL
P.E. Saylor, F. Saied	University of Illinois, Urbana, IL
G. Fox	Northeast Parallel Architecture Center, Syracuse University, Syracuse, NY
S. Teukolsky	Center for Radio Physics and Space Research. Cornell University, Cornell, NY
S.L. Shapiro	Center for Astrophysics and Relativity, Cornell, NY
J.W. York, C.R. Evans	University of North Carolina. Chapel Hill, NC
L.S. Finn	Northwestern University. Evanston. IL
P. Laguna	Pennsylvania State University. University Park. PA
J. Winicour	University of Pittsburgh. Pittsburgh, PA

Binary Black Hole Grand Challenge

Purposes:

To develop a Problem Solving Environment [RNPL + Dynamic Adaptive Parallel infrastructure/PAMRSL]

To provide controllable convergent algorithms to compute gravitational waveforms from Black Hole encounters (relevant to detectors)

To provide representative examples of computational waveforms.

BLACK HOLE COALESCENCE

~ 1 TO 10 SOLAR MASS BLACK HOLES.

BINARIES FORMED IN SN?

VERY STRONG SOURCES OF GRAVITATIONAL RADIATION:

$\boldsymbol{\phi \sim 1}$

[NEUTRON STARS $\phi \sim 0.1$]

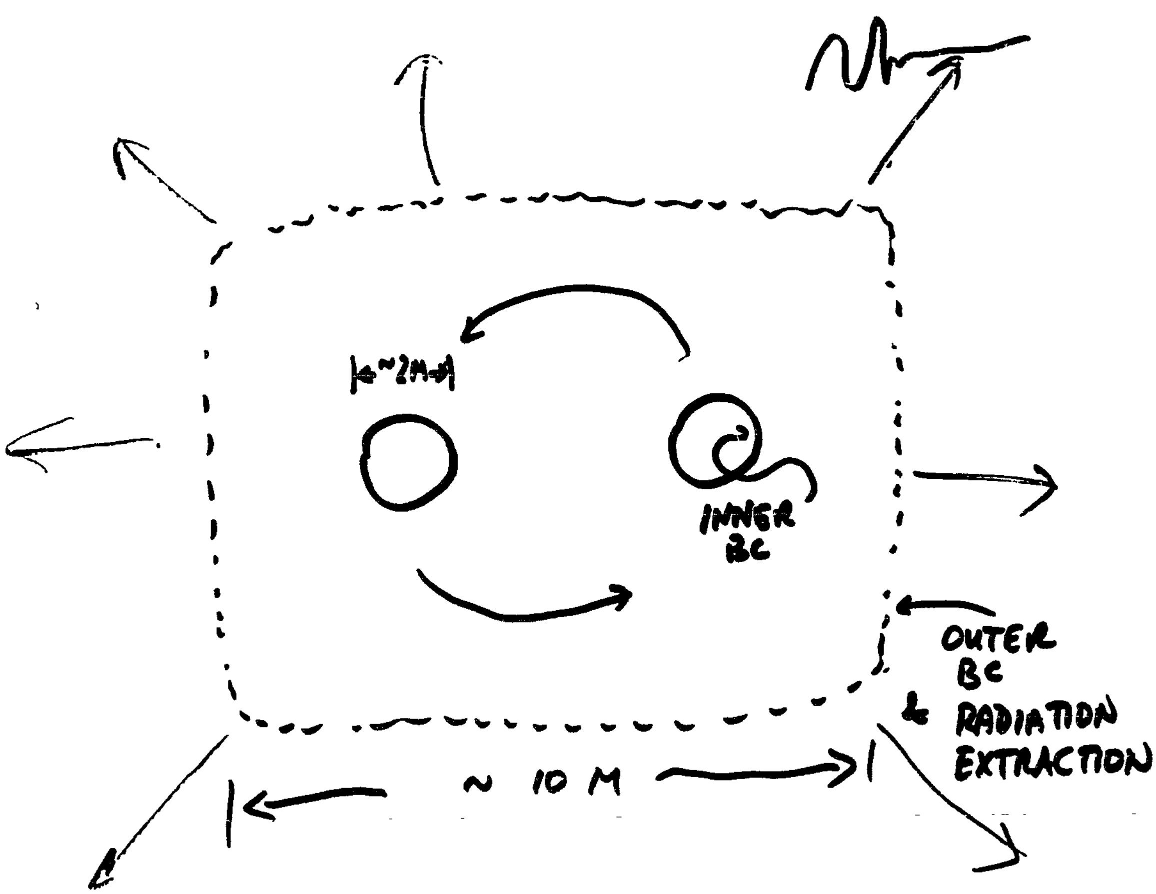

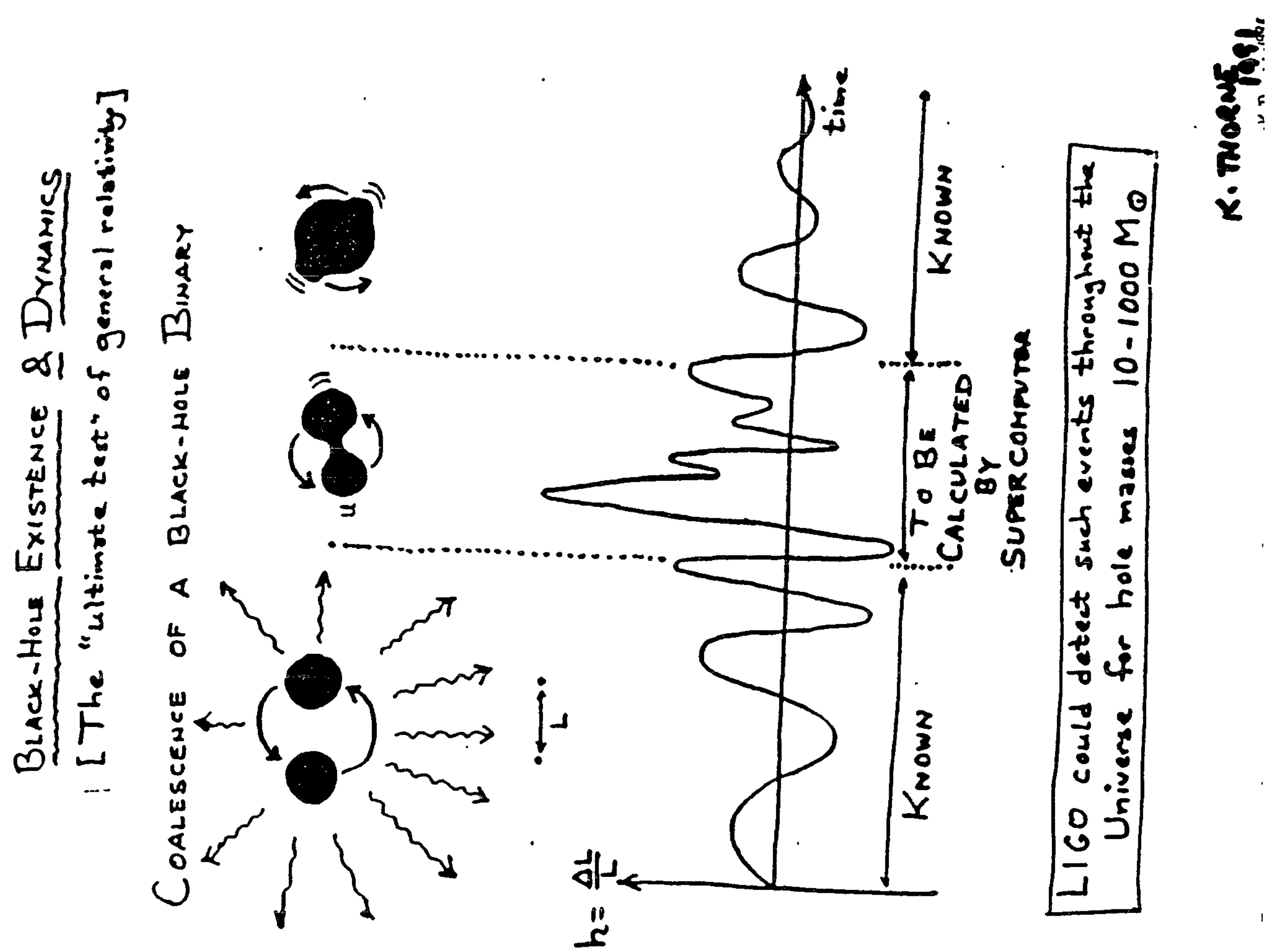

[The "ultimate test" of general relativity]

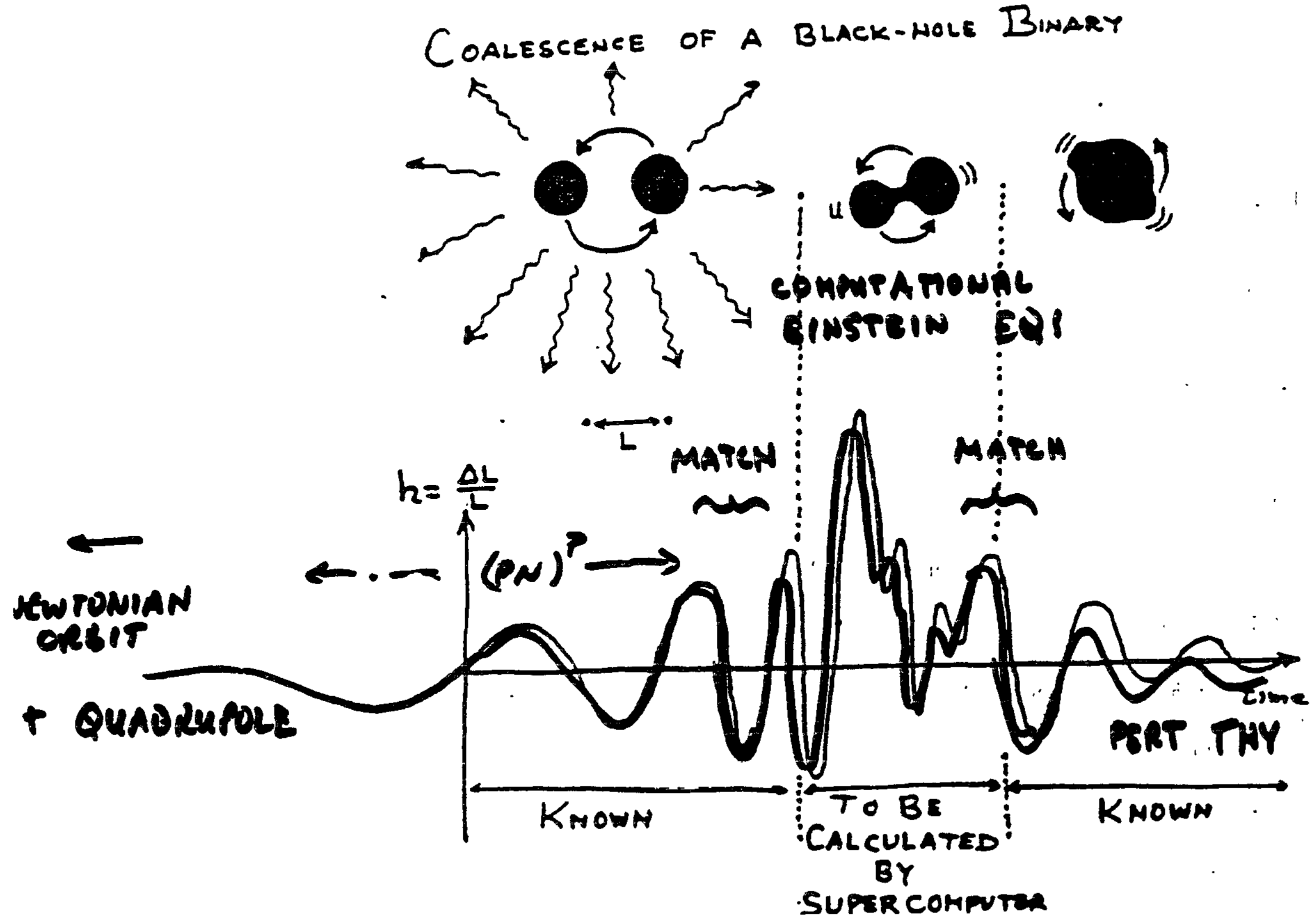

- CONTROLLABLE CONVERGENT ALGORITHMS.

DISCRETIZATION Δh

$$u_N = u_a + k(x,t)(\Delta h)^p + \cdots$$

$p = 2$ 2nd ORDER

$$u_h = u_a + k(\Delta h)^2 + \cdots$$

$$u_{2h} = u_a + 4k(\Delta h)^2 + \cdots$$

$$3u_a = 4u_h - u_{2h} + \cdots$$

RICHARDSON EXTRAPOLATION
(1911)

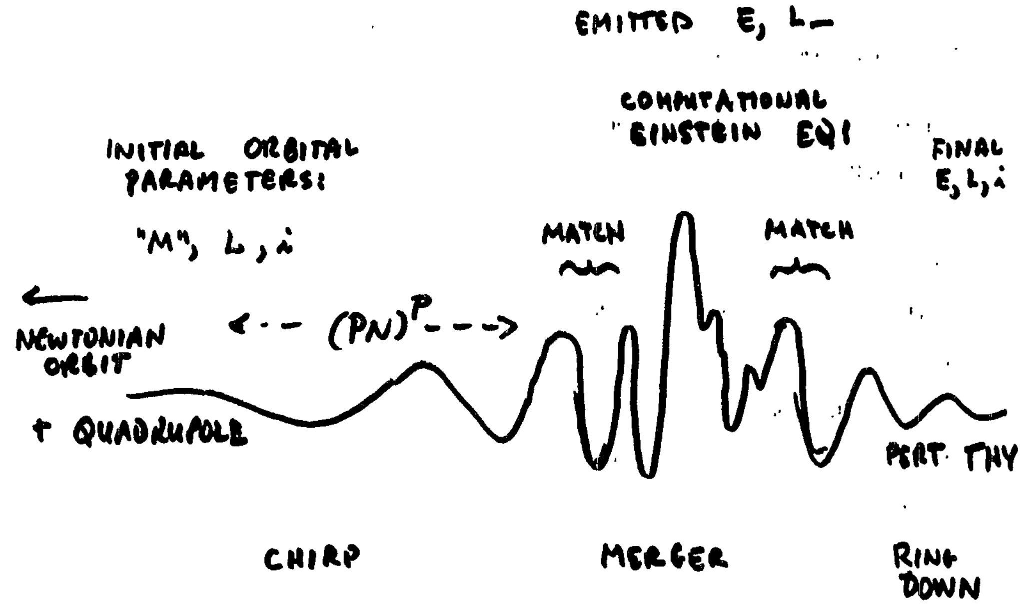

Distributed Adaptive Grid Hierarchy

- C, C++, MPI wrapper

- Recylces "dusty deck" FORTRAN, C

- Automatically (spacetime) refines/derefines. [Shadow Hierarchy].

- Efficient ~ 90%; better than hand coded in all cases checked.

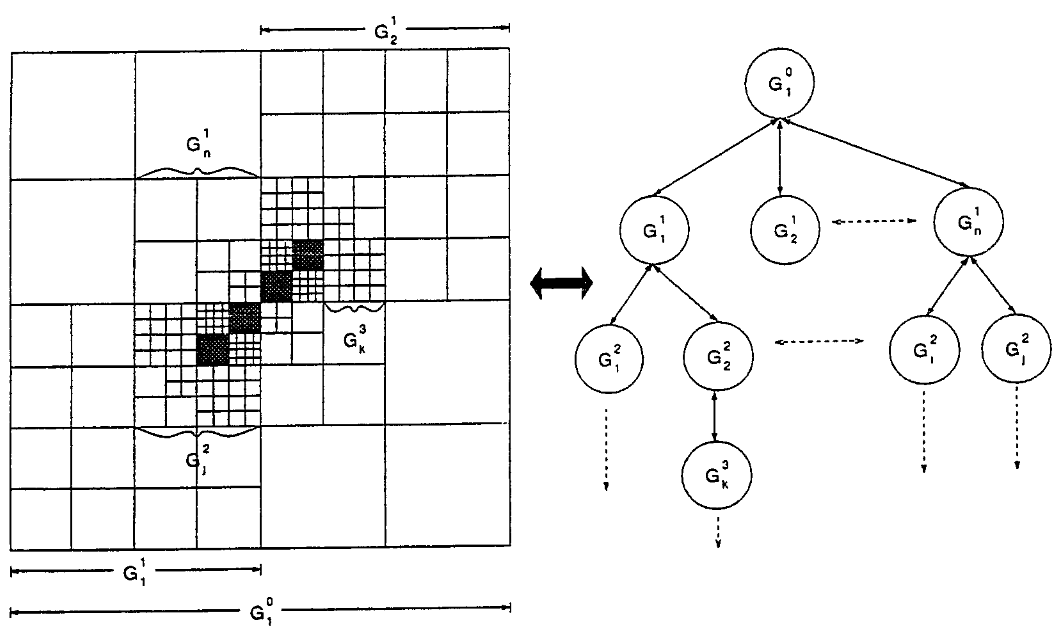

Figure 1: Adaptive Grid Hierarchy - (2D)

```
#include "DAGH.h"
#include "sorfortran.h"

#define DIM 3
#define MaxLev 1

void main(INTEGER argc, char *argv[])
 {

  MPI_Init( &argc, &argv );

  INTEGER nx, ny, nz;
  DOUBLE h, p, omega, epsilon;
  f_readinput(&nx, &ny, &nz, &h, &p, &omega, &epsilon);

  // Set up the Grid Structure
  INTEGER shape[DIM];
  DOUBLE bb[2*DIM];
  shape[0] = nx;
  bb[0] = 1.0;
  bb[1] = 1.0*(nx+1);
  shape[1] = ny;
  bb[2] = 1.0;
  bb[3] = 1.0*(ny+1);
  shape[2] = nz;
  bb[4] = 1.0;
  bb[5] = 1.0*(nz+1);

  INTEGER t = 0, l = 0;

  GridHierarchy GH(DIM,NON_CELL_CENTERED,MaxLev);
  SetBaseGrid (GH,bb,shape);
  ComposeHierarchy(GH);

  INTEGER t_sten = 0; INTEGER s_sten = 1;
  GridFunction(DIM)<DOUBLE> u("u",t_sten,s_sten,GH);
  GridFunction(DIM)<DOUBLE> rhs("rhs",t_sten,s_sten,GH);
  GridFunction(DIM)<DOUBLE> res("res",t_sten,s_sten,GH);

  while (norm2 > epsilon) {

      cnt++;

      Sync(u,t,l);

      pass = 1;
      forall(u,t,l,c)

        f_relax (
          FBA(u(t,l,c)), shape,
          FDA(u(t,l,c)), FDA(rhs(t,l,c)), FDA(res(t,l,c)),
          &h, &p, &omega, &epsilon, &norm, &pass);

      end_forall

      Sync(u,t,l);

      pass = 2;
      forall(u,t,l,c)

        f_relax (
          FBA(u(t,l,c)), shape,
          FDA(u(t,l,c)), FDA(rhs(t,l,c)), FDA(res(t,l,c)),
          &h, &p, &omega, &epsilon, &norm, &pass);

      end_forall

      norm2 = Norm2(res,t,l);
      maxval = MaxVal(u,t,l);
      minval = MinVal(u,t,l);

      if (me == 0) {
       cout << cnt << " " << norm2 << " " << norm << " ";
       cout << maxval << " " << minval << " ";
       cout << "\n" << flush;
      }
  }
```

```
/* Fortran Interfaces */

#define f_readinput FORTRAN_NAME(sor_readinput_, SOR_READINPUT, sor_readinput)
extern "C" {
void f_readinput(
            INTEGER *, INTEGER *, INTEGER *,
            DOUBLE *, DOUBLE *, DOUBLE *, DOUBLE *);
}

#define f_initial FORTRAN_NAME(sor_init_, SOR_INIT, sor_init)
extern "C" {
void f_initial(
            BI,
            DOUBLE *, DOUBLE *, DOUBLE *,
            FDI(DOUBLE), FDI(DOUBLE), FDI(DOUBLE),
            DOUBLE *, DOUBLE *, DOUBLE *, DOUBLE *);
}

#define f_relax FORTRAN_NAME(sor_relax_, SOR_RELAX, sor_relax)
extern "C" {
void f_relax(
            BI, INTEGER *,
            FDI(DOUBLE), FDI(DOUBLE), FDI(DOUBLE),
            DOUBLE *, DOUBLE *, DOUBLE *, DOUBLE *, DOUBLE *,
            INTEGER *);
}
```

```
C-----------------------------------------------------------------------
                subroutine sor_relax(lb,ub,shape,gshape,
     &              u,rhs,res,
     &              h, p, omega, epsilon, norm, pass)
                implicit none

      integer lb(3),ub(3),shape(3),gshape(3)
      real*8  u(shape(1),shape(2),shape(3))
      real*8  rhs(shape(1),shape(2),shape(3))
      real*8  res(shape(1),shape(2),shape(3))

      real*8 h, p, omega, epsilon, norm
      real*8 norm2
      integer pass


               call relaxc(lb,ub,shape,gshape,
     *              u,rhs,res,
     *              h, p, omega, pass)

               if (pass .eq. 2) then
                 norm = norm2( shape(1)*shape(2)*shape(3) , res )
               endif

                return
                end

C-----------------------------------------------------------------------
```

SYSTEM ARCHITECTURE

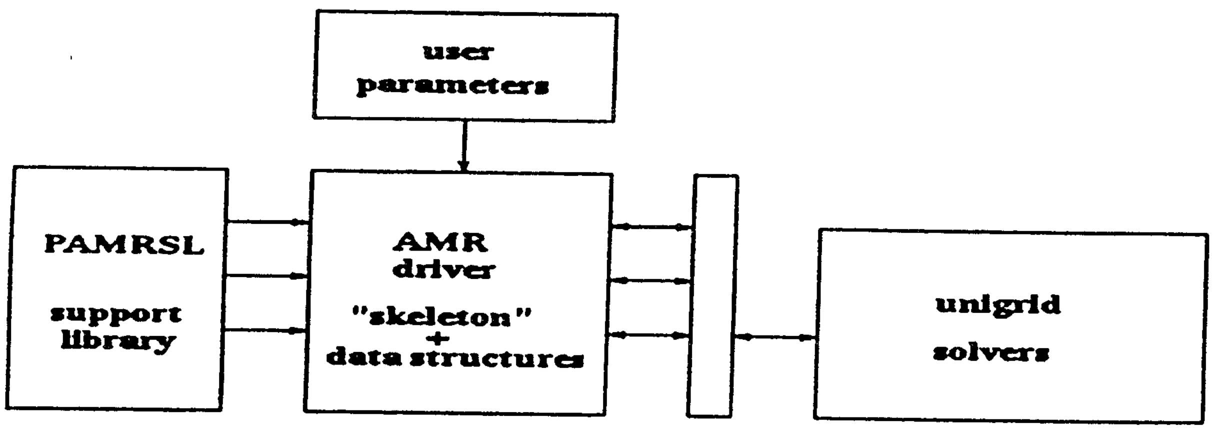

HPF/FORTRAN 90.

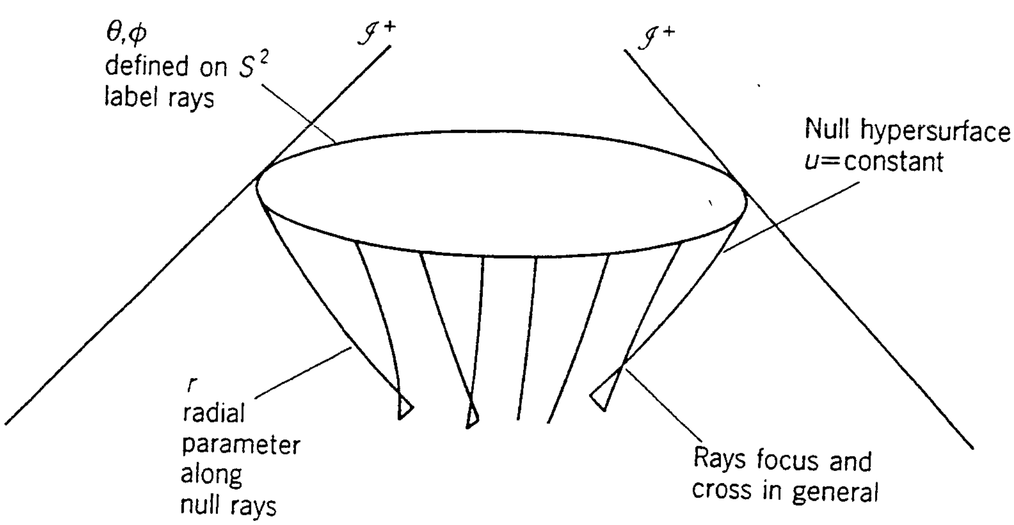

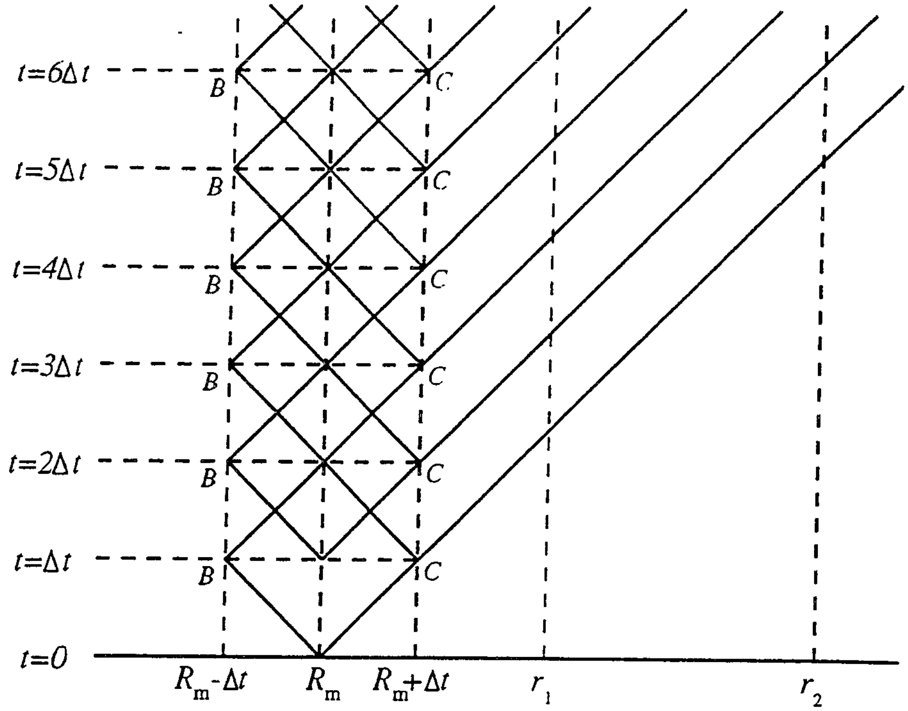

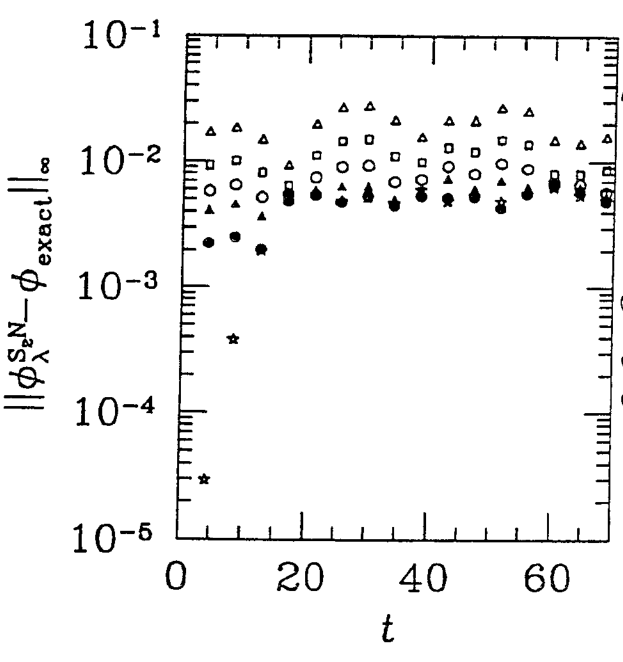

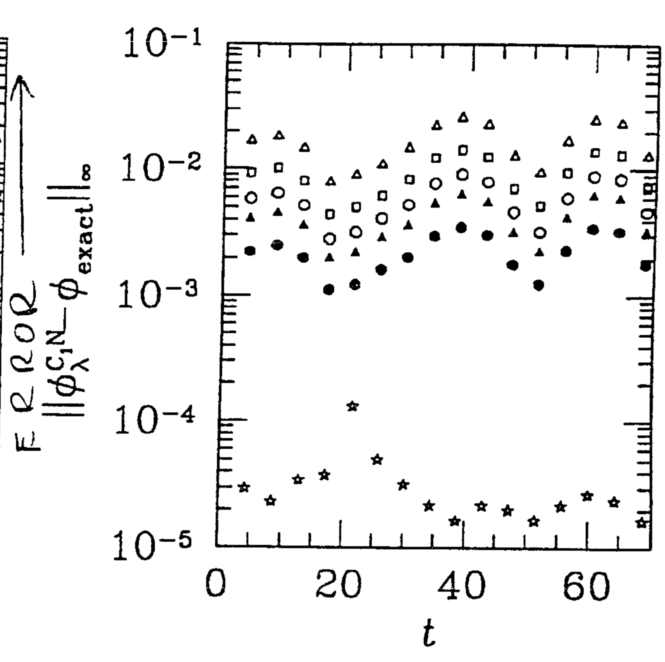

SUMMER FELD BOUNDARY

MATCHED BOUNDARIES

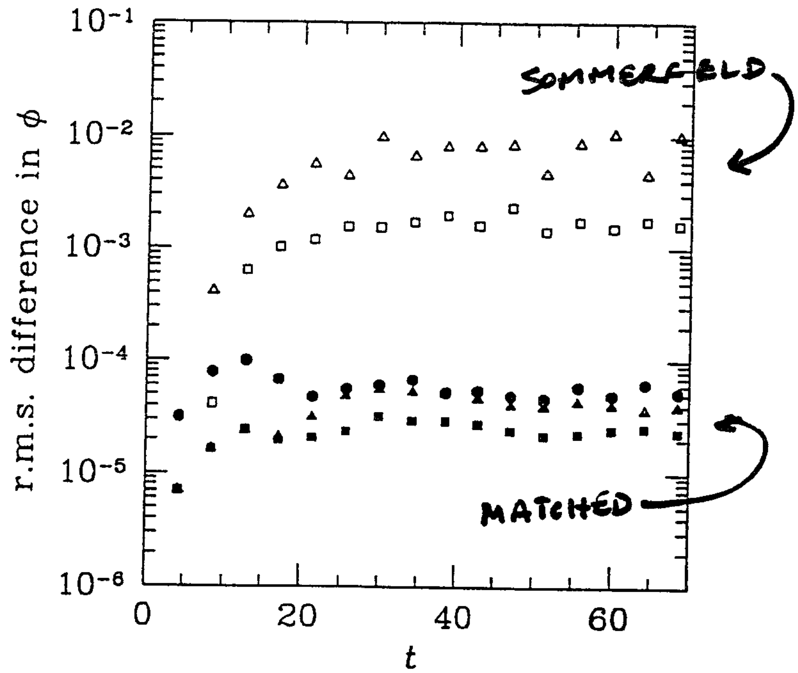

SENSITIVITY TO BOUNDARY POSITION: COMPARE AT 2 OUTER RADII

YORK/CHOQUET-BRUHAT HYPERBOLIC FORMULATION

MAXWELL EXAMPLE

$$\left.\begin{aligned}\partial_o E_i - (\nabla\times\mathbf{B})_i &= 0\\ \partial_o B_i + (\nabla\times\mathbf{E})_i &= 0\end{aligned}\right\}\text{ EVOLUTION EQS}$$

$$\left.\begin{aligned}\nabla\cdot\mathbf{E} &= 0\\ \nabla\cdot\mathbf{B} &= 0\end{aligned}\right\}\text{ CONSTRAINTS}$$

"OLD WAY":

$$\begin{aligned} E_i &= -\partial_o A_i - \nabla_i \phi \\ B_l &= (\nabla \times \mathbf{A})_l \end{aligned}$$

$$\begin{aligned} -\partial_o^2 A_i - \nabla_i \partial_o \phi &= (\nabla \times \nabla \times \mathbf{A})_i \\ &= -\nabla^2 A_i + \nabla_i (\nabla \cdot \mathbf{A}) \\ -\partial_o^2 A_i + \nabla^2 A_i &= \nabla_i \underbrace{(\partial_o \phi + \nabla \cdot \mathbf{A})} \end{aligned}$$

SPECIFY (eg. to zero) by gauge

CONSERVATION OF GAUGE MUST BE EXPLICITLY CHECKED

"NEW WAY":

$$\left.\begin{aligned} \mathcal{G}_{oi} &= \partial_o E_i \\ \mathcal{G}_{ij} &= \nabla_i E_j \end{aligned}\right\} \text{DEFINE } \mathcal{G}_{oi}, \mathcal{G}_{ij}$$

$$\begin{aligned} \partial \mathcal{G}_{oi} &= \partial_o \partial_o E_i = (\nabla \times \partial_o \mathbf{B})_i \\ &= -(\nabla \times (\nabla \times \mathbf{E}))_i \\ &= \nabla^2 E_i - \nabla_i (\nabla \cdot \mathbf{E}) \\ &= \nabla^j \nabla_j E_i \\ &= \nabla^i \mathcal{G}_{ij} \end{aligned}$$

zero by constraint

$$
\begin{aligned}
\partial_o \mathcal{G}_{oi} &= \nabla^j \mathcal{G}_{ij} \\
\partial_o \mathcal{G}_{ji} &= \partial_o \nabla_j E_i = \nabla_i \partial_o E_i \\
&= \nabla_j \mathcal{G}_{oi}
\end{aligned}
$$

∂_o

HYPER-BOLIC

$$
\begin{aligned}
\partial_o E_i &= \mathcal{G}_{oi} \leftarrow \text{time integration} \\
\partial_o \mathcal{G}_{oi} &= \nabla^j \mathcal{G}_{ji} \\
\partial_o \mathcal{G}_{ji} &= \nabla_j \mathcal{G}_{oi}
\end{aligned}
$$

$$
\partial_o \partial_o \mathcal{G}_{oi} = \nabla^j \nabla_j \mathcal{G}_{oi}
$$

CONSTRAINT IS ESSENTIAL.
GAUGE IS IRRELEVANT
- EVOLVE TIME DERIVATIVE.

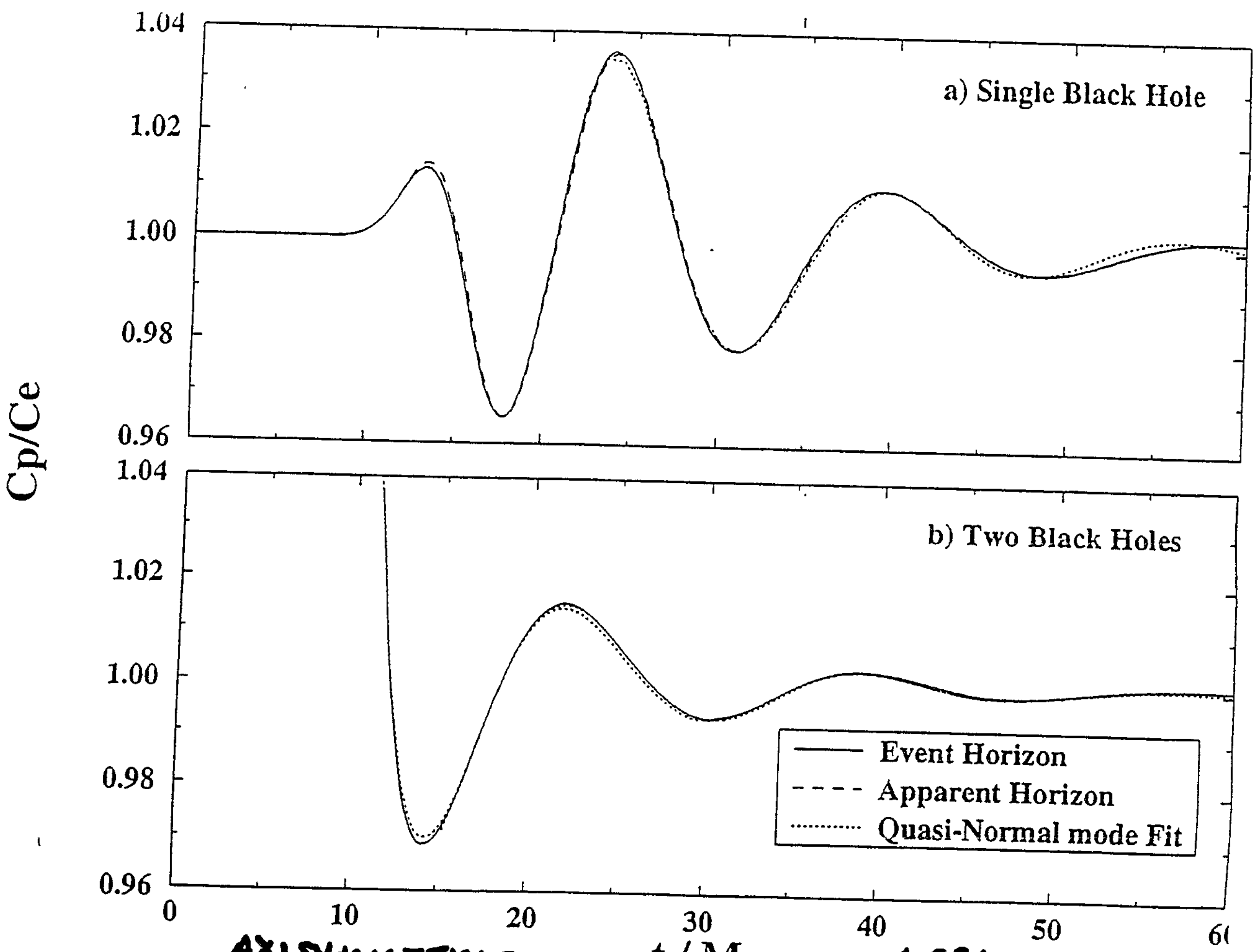

AXISYMMETRIC NCSA

Thursday PM
January 18

Data Analysis II. Time-Frequency Techniques and Other Issues
Chair: C. Will

4:30	B. Owen (Caltech)	Searching for Coalescing Binaries: Templates, Strategies, Computing Requirements
4:55	Discussion	
5:05	J. Centrella (Drexel)	Coalescence Wave Forms and Rotational Instabilities
5:30	Discussion	
5:40	A. Krolak (Warsaw)	Estimating Parameters of GW Signals Using Wavelet Analysis
6:05	Discussion	
6:15	Coffee Break	
6:30	A. Vecchio (Cardiff)	Why Realistic Errors in Parameter Extraction Don't Follow Cramer-Rao Bounds
6:55	Discussion	
7:05	H. Yamamoto (Caltech)	LIGO Simulation Environment
7:30	Discussion	

B. OWEN

Introduction

A. The gist.

This is a summary of current conventional wisdom.
I'll describe implementations of matched filtering, for 50 years known as the optimal linear technique — for well-known signals.
Recently unconventional wisdom has grown: neural nets, adaptive filtering algorithms, other nonlinear methods.
These are interesting but little quantitative analysis exists — yet.

B. Basics of matched filtering.

SNR is defined as the cross-correlation of whitened data stream with a template ~~the~~ expected signal.
This statistic is compared to a threshold to decide if a signal is there.
Threshold is set to control false alarms.

. Basics of mismatched filtering.

We don't know the two-body solution in GR but approximate it.
An imperfect template reduces the mean SNR as its cross-correlation with the actual signal. → So it's good to know how accurate templates need to be to keep a certain fraction of ~~cost~~ optimal event rate.

. Parameterized filtering.

Also: we expect many different signals; same functional form ~~waveforms~~ but different parameters.
∴ We need to construct many filters spanning parameter space, and use them all.
To detect most signals we space filters parameters very finely, but this means many filters and lots of computing power.
So it's worth some effort to find the optimum tradeoff between event rate and computing power, (i.e. fine grid and coarse grid).

Hierarchical search strategy.

We can combine the low CPU power of a coarse grid ~~set~~ of templates with the high event rate/low false alarm rate of a fine grid by making two passes.
The first pass, with a coarse grid selects likely candidates for an inspiral signal,
Candidates are then sent through a fine grid in the second pass, and more rigorously tested for false alarms.

1

II. Imperfection of Waveform Templates

3 transp. A. The post-Newtonian expansion, and others.
Cliff Will/Alan Wiseman have much more to say about this.
~3 lines PN is the workhorse for constructing templates — an approximation currently good to $O(v/c)^4$ beyond leading RR.
Test-mass perturbation of exact GR (extreme mass ratio) is up to $O(v/c)^{11}$ in some cases and rapidly getting higher — as Tagoshi said Tuesday.
This is a lot of PhD-hours for each order — how much is needed?
Cutler & Flanagan estimate $O(v/c)^6$ for parameter extraction — but search templates should be less finicky.

B. The fitting factor.

For search templates we don't want to use v/c as a criterion.
FF = max... Instead, Apostolatos introduced the fitting factor, which gives the fraction of optimal SNR obtained by an approximate family of templates.
ΔΨ graph The max appears because an approximate ~~imperfect~~ template with one set of parameters will in general have its greatest cross-correlation with an exact waveform which has a different set of parameters.
geometric graph That's bad for extraction — leads to systematic errors in parameters — but good for detection because ensures FF is (much) higher than the simple cross-correlation.

Harris' table C. Estimates of fitting factors

We don't really know FF because we don't know the signal — estimate FF by taking best approximate waveform for signal and seeing how lesser templates do.
Best estimate now is Apostolatos' manuscript using $O(v/c)^4$ PN templates as the signal — his results indicate that $O(v/c)^3$ is good enough to keep well over 90% of optimal ER (~ cube of FF).
As expected, search templates don't require as much accuracy as extraction templates.

2

: Parameterized Filtering

A. The goal.

We want to find an expression for $\mathcal{N}$ and $\mathcal{P}$ in terms of event rate – i.e. if 10% ER loss is acceptable, how much will that cost us?

B. The method. → Begun by Sathyaprakash & Dhurandhar, a couple years ago.

For each template shape u_{λ} we compute the following function... this SNR ~~takes~~ rules for all ~~into account~~ the ~~possibility of differ~~ various possible coalescence times and phases the signal might have.

Thus a single FFT tells us if a stretch of data exceeds threshold for a certain template shape, which is numerically efficient. goes as $N \log N$

In a brute-force search we do this for $\mathcal{N}$ different values of λ; so it's useful to define the match as....

The match is the fraction of optimal SNR we get by searching for u_{λ_1} with u_{λ_2} / vice versa.

We chose our filter spacing so that the match between neighbors is some fixed amount.

C. The minimal match.

Analogous to the FF, we define the MM to be the worst case match between signal and template (assuming our templates are good enough that $FF \simeq 1$). → $ER \sim MM^3$ — my ~~...~~ preprint

For a brute-force search, or 2nd pass of a hierarchical search, $MM \simeq 1$ in order to keep most of the event rate – so expand the match to get a metric defined on the intrinsic parameter space.

Thus ds^2 between nearby template parameters is fraction of optimal SNR lost due to parameter difference.

D. Achieving the goals.

Now getting $\mathcal{N}$ is a trivial ratio of volumes – lets us decide what part of parameter space, too.

For a two-parameter family of templates (PN, two masses) searching for signals from objects of mass M_{min} or greater, we get ...

This corresponds to a computing power of ...

We see that even a brute force search is possible for nonspinning binaries of minimum NS mass or greater.

Believe $\mathcal{N}$ and $\mathcal{P}$ to ~3: I used restricted PN to $\mathcal{O}(v/c)^2$, no ecc. no spin.

E. Precessing binaries.

Apostolatos' new manuscript ~~does~~ suggests that significant spin-orbit precession necessitates 3 more parameters – multiplies $\mathcal{N}, \mathcal{P}$ by 10^6!

Don't know yet what range of spins is a problem – too new & complicated.

Also don't know feasibility of considering spins only for the most common masses, e.g. ($1.4 M_{\odot}$).

or approximating simpler functions.

Too new to say – got the manuscript Monday – but warns of a possible major problem.

3

IV. Hierarchical Search Strategy (work in progress) Dhurandhar & Mohanty / Thorne & Owen

5) transp.

A. The method.

First the data are passed through a coarse grid of filters and compared to a relatively low threshold.

For every template shape that triggers on the first pass, a second pass is made in which all shapes on a finer grid around it are tested for some range of coalescence times including the range that triggered the first-pass template.

A detection is registered only if one of these second-pass templates achieves a SNR above a higher threshold – roughly that which would have been used for a brute force search, to control false alarms

B. Calculating $\mathcal{P}$.

) transp.

$\mathcal{P} = \mathcal{P}_1 - \mathcal{P}_2$

ρ, h

~~$\mathcal{P}$ depends on MM₁, MM₂ (of course), and ρ₁ (false alarms on 1st pass ... trigger for 2nd).~~

~~Fixing overall false alarm rate~~

We have four ind. variables $\rho_1, \rho_2, MM_1, MM_2$ characterizing the two passes' false rates.

Because the second pass is conditional on the results of the first, we lose one independent variable.

Setting overall false alarm and false dismissal rates reduces us to one independent variable, which is convenient to parameterize as roughly $\xi \simeq \frac{1-MM_1}{1-MM_2}$.

Find minimum $\mathcal{P}$ by setting $\frac{d\mathcal{P}}{d\xi} = 0$.

Gory details make it hard to do exactly, but a rough approximation (current best guess) indicates a savings of tenfold (1st LIGO) or less (advanced).

V. Conclusions

It is possible to achieve over 90 percent of ideal event rate well within the limits of end-of-the-decade computing technology.

Except... high-spin systems are a problem, and Kip now wants to look for objects down to $10^{-2} M_{\odot}$ for reasons he will tell you about.

Not only does my scaling law predict horrible computing requirements, but filters will need to last for months.

Thus we have Doppler shifts, sky patches, all the headaches of pulsar searches in addition to binary searches.

4

Searching for Inspiraling Binaries: Strategies, Templates, and Computing Requirements

Ben Owen
Caltech

atched filtering:

$$\rho = 4\,\mathrm{Re}\left[\int_0^\infty df\, \frac{\tilde{s}^*(f)\,[A\tilde{s}(f)+\tilde{n}(f)]}{S_n(f)}\right] \equiv \mathrm{Re}\left[(s, As+n)\right]$$

$(s,s)=1$; A = constant amplitude of signal

$$\bar{\rho} = A \text{ (optimal)}$$

ismatched filtering:

template u such that $(u,u)=1$

$$\bar{\rho} = \mathrm{Re}\left[(As,u)\right]$$

$$\bar{\rho}/\bar{\rho}_{opt} = \mathrm{Re}\left[(s,u)\right]$$

ameterized filtering:

u_{λ}: template with shape parameters λ

$$\rho = \max_k \mathrm{Re}\left[(As+n, u_{\lambda(k)})\right]$$

$$k = 1, 2, \ldots, N$$

Approximations to two-body GR:

Post-Newtonian known to $O(v/c)^4$

BH Perturbation subject to weekly changes!

How well do we need to know these approximations?

Cutler & Flanagan: less than $O(v/c)^6$

Fitting Factor: $FF(\theta) = \max_{\lambda} \max_{\Delta t_c} \left|(s_\theta, u_\lambda e^{i2\pi f \Delta t_c})\right|$

(Apostolatos)

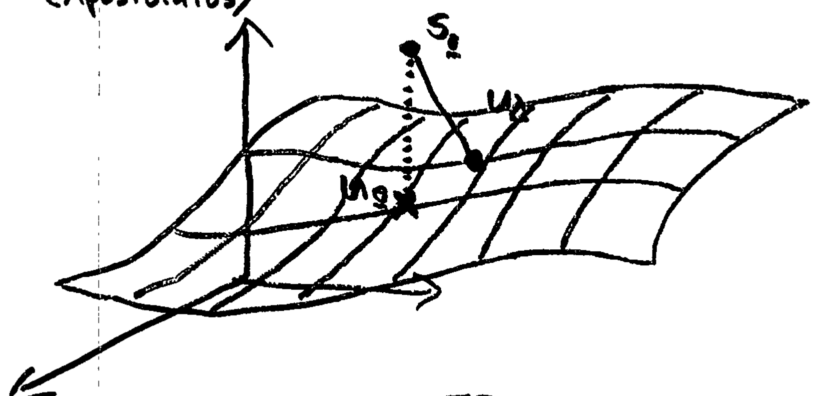

Template Family	FF with $O(v/c)^4$ NS/NS	BH/NS
"Newtonian"	.531	.669
$O(v/c)^2$	.620	.729
$O(v/c)^3$	.993	.990

mplate Counting

Sathyaprakash & Dhurandhar, Owen

$$\rho_{\lambda}(t) = \left| 4\int_0^\infty df \frac{[A\tilde{s}(f) + \tilde{n}(f)]^*}{S_n(f)} u_{\lambda}(f)\, e^{i2\pi ft} \right|$$

$$= \left|(As+n,\ u_{\lambda} e^{i2\pi ft})\right|$$

gle

T

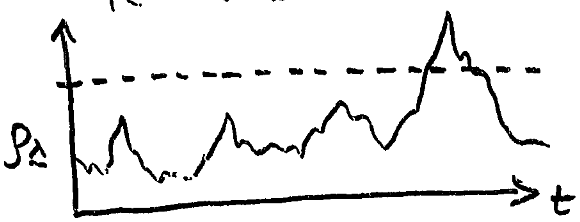

Match: $M(\lambda, \Lambda) = \max_t \left|(u_{\Lambda},\ u_{\lambda} e^{i2\pi ft})\right|$

- accounts for covariance between λ and time, phase

nimal Match fixes spacing, number of templates

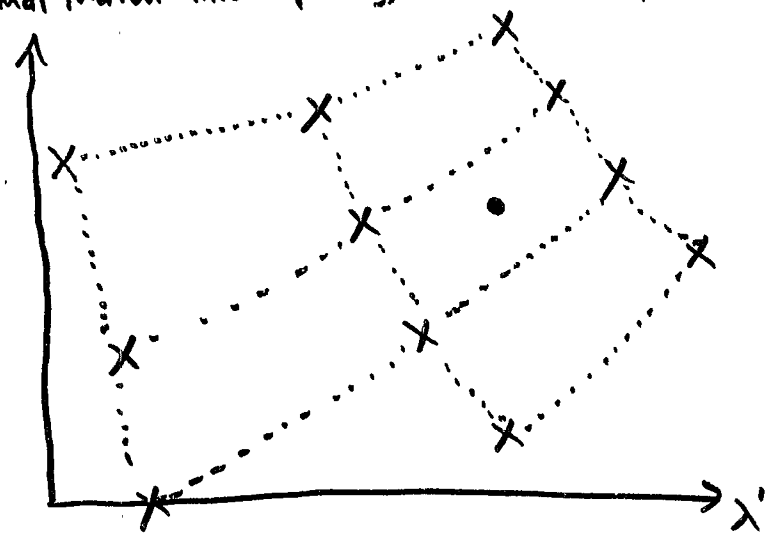

Fine grid approximation:

$$M(\lambda, \lambda+\Delta\lambda) \simeq 1 - \mathcal{O}(\Delta\lambda)^2$$

$$g_{ij} = -\frac{1}{2} \frac{\partial^2 M}{\partial\lambda^i \partial\lambda^j}\bigg|_{\Delta\lambda=0}$$

Differential geometry makes it easy:

$$\mathcal{N} = \frac{\text{total proper volume of parameter space}}{\text{proper volume per template}}$$

$$= \frac{\int d^n\lambda \sqrt{\det \|g_{ij}\|}}{\left(2\sqrt{(1-MM)/N}\right)^N}$$

Loss of event rate $\mathcal{L} \simeq 3(1-MM)$ for $MM \simeq 1$

Example templates:
- (two) mass parameters only
- restricted PN to $\mathcal{O}(v/c)^2$
- objects with mass $\geq M_{min}$

$$\mathcal{N} \simeq \left(\frac{0.1}{\mathcal{L}}\right)\left(\frac{0.2M_\odot}{M_{min}}\right)^{2.7} \times \begin{cases} 2\times10^5 & \text{first LIGO} \\ 8\times10^6 & \text{advanced LIGO} \end{cases}$$

$$\mathcal{P} \simeq \left(\frac{0.1}{\mathcal{L}}\right)\left(\frac{0.2M_\odot}{M_{min}}\right)^{2.7} \times \begin{cases} 30\text{ Gflops} & \text{first LIGO} \\ 400\text{ Gflops} & \text{advanced LIGO} \end{cases}$$

→ Heavy (but bearable) demands

ierarchical Search Strategy

In preparation: Dhurandhar; Mohanty, Thorne; Owen

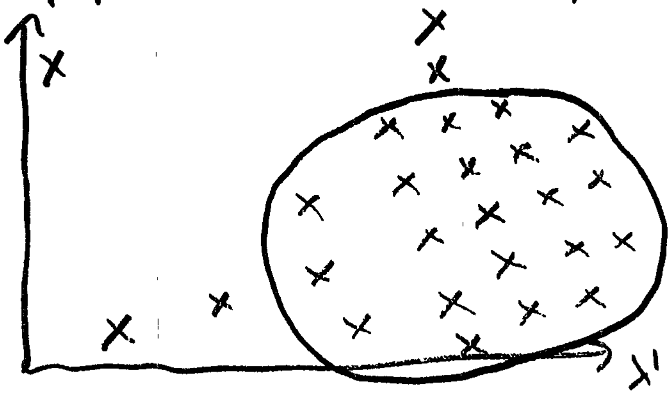

al computing power: $\mathcal{P} = \mathcal{P}_1 + \mathcal{P}_2$

Four parameters: $\rho_1, \rho_2, MM_1, MM_2$

- $\mathcal{P}_2 \propto$ false alarm rate in first pass
- Set fixed overall false alarm rate ... and false dismissal rate
- One remaining independent parameter: $$\xi \simeq \frac{1-MM_1}{1-MM_2}$$
- Minimize $\mathcal{P}(\xi)$: $d\mathcal{P}/d\xi = 0$

$\sim \frac{1}{10}$ of brute force $\mathcal{P}$ (first LIGO)

$\sim \frac{1}{3}$ for advanced LIGO

Conclusions:

- We can achieve over 90% of optimal event rate with end-of-decade computing technology for some common binary systems.
- Detecting rapidly spinning binaries may be more difficult.
- Kip's new suggestion – to search for $10^{-2} M_\odot$ objects – will be even more difficult.

Binary Coalescence and Rotational Instabilities

Joan Centrella

Drexel University

3-D numerical models of astrophysical GW sources

Use 2 different hydrodynamical codes:

Eulerian - grid

Lagrangian - particles - SPH

Current simulations use Newtonian gravity, with GW in quadrupole approximation

Coalescing Binary Neutron Stars

Zhuge, Centrella, McMillan 1994 PRD **50**, 6247;
" " " 1996, in preparation

- Model NS as spherical polytropes of mass M, radius R, EOS $P = K\rho^{\Gamma} = K\rho^{1+1/n}$
- Start out in point-mass limit at wide separation $\gtrsim 4R$ on circular orbit
- To cause inspiral, mimic grav. radiation reaction
  - add "frictional" terms to eqns of motion
  - removes energy from orbit at rate given by point-mass inspiral
  - turn frictional terms off when Newtonian tidal forces dominate $\rightarrow$ coalescence
- Simulations carried out using smoothed particle hydrodynamics - SPH
- Standard Run: $M_1 = M_2 = 1.4\ M_\odot$
  $R_1 = R_2 = 10$ km
  $\Gamma = 2$; no spin
- Vary: R, Γ, $\frac{M_2}{M_1}$, spin

N = 4096 particles/star

$= M_2 = 1.4\, M_\odot$

$= 2$

$= 10$ km

$t_D = \left(R^3/GM\right)^{1/2}$

$= .073$ ms

stars orbit counterclockwise

turn off "friction" term

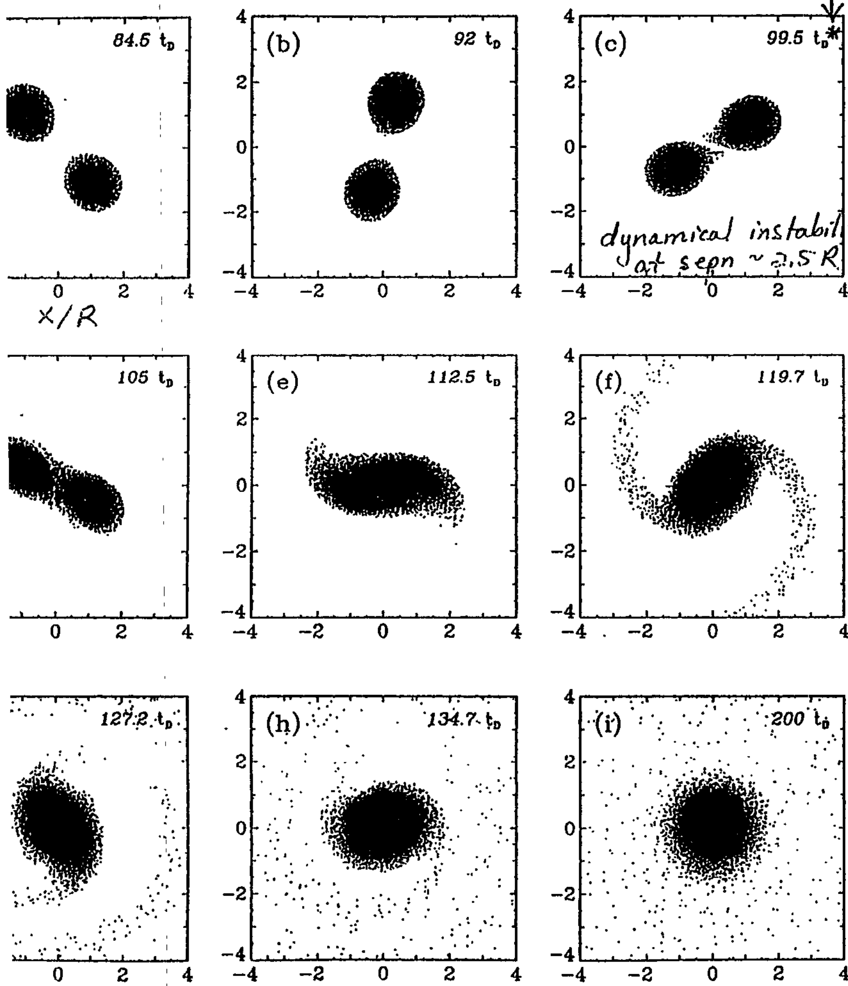

$M_1 = M_2 = 1.4\, M_\odot$

$\Gamma = 2$

$R = 10$ km

dynamical instability

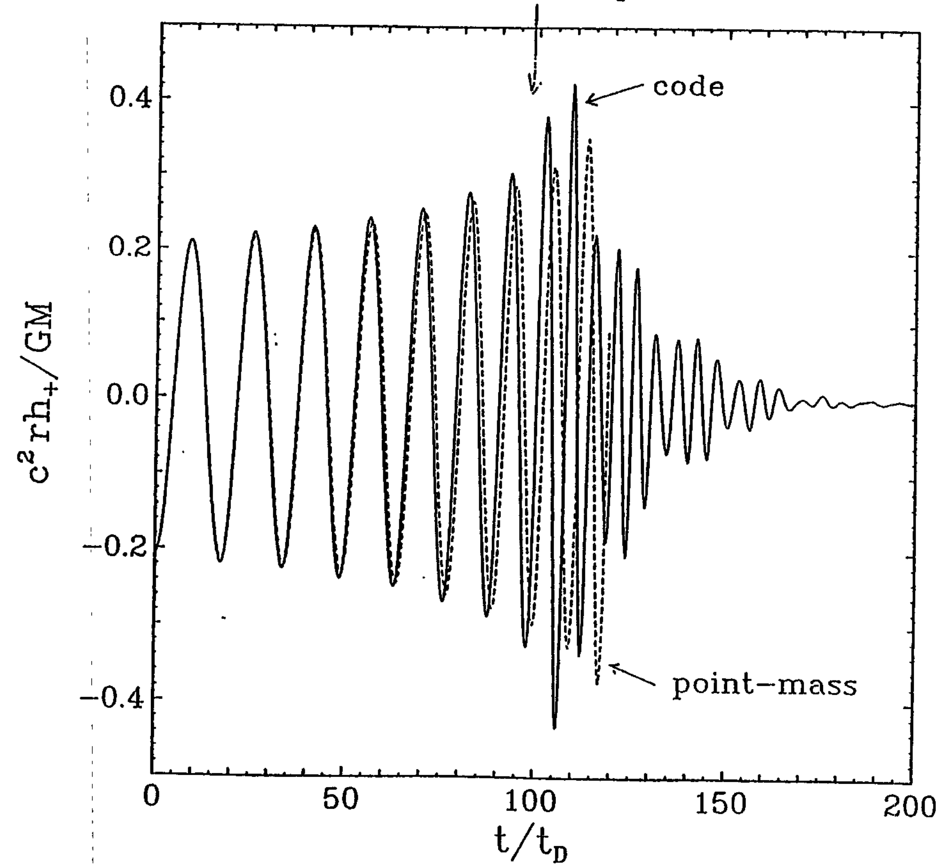

$M_1 = M_2 = 1.4\,M_\odot$

$\Gamma = 2$

$R = 10$ km

$M_1 = M_2 = 1.4\,M_\odot$

$\Gamma = 2$

$\boxed{R = 15\text{ km}}$

.. point mass inspiral + $\sim a^{-1/\alpha}$; a = separation

.. features in spectrum show this scaling:

$$\frac{f_{R=10km}}{f_{R=15km}} \sim \left(\frac{R=10km}{R=15km}\right)^{-3/2} \sim 1.8$$

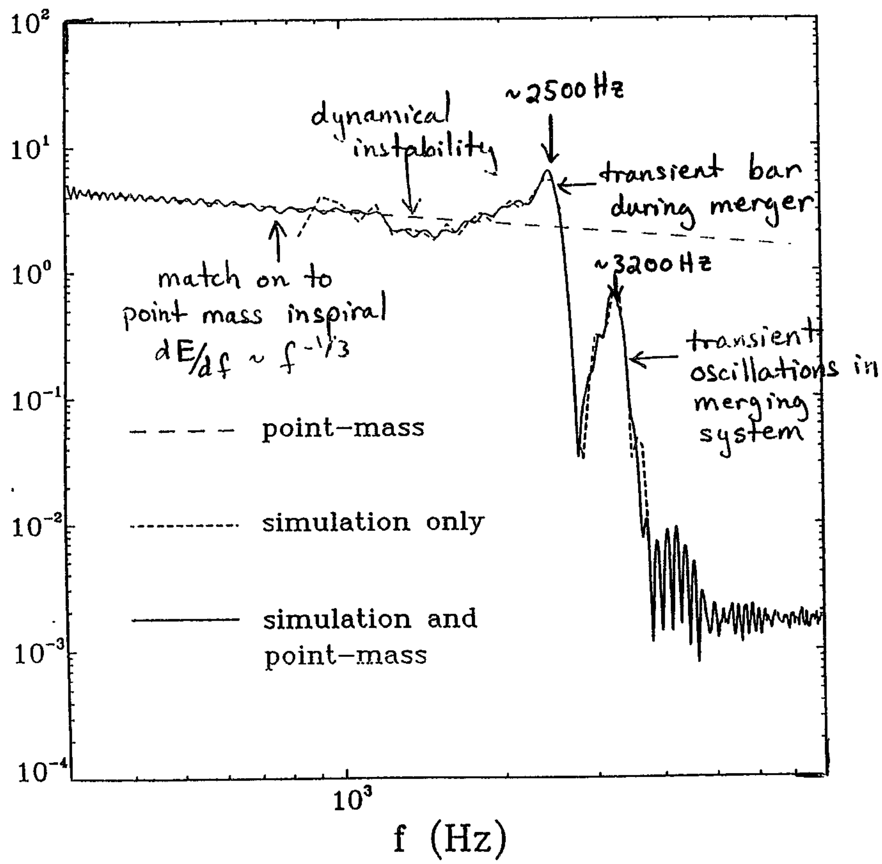

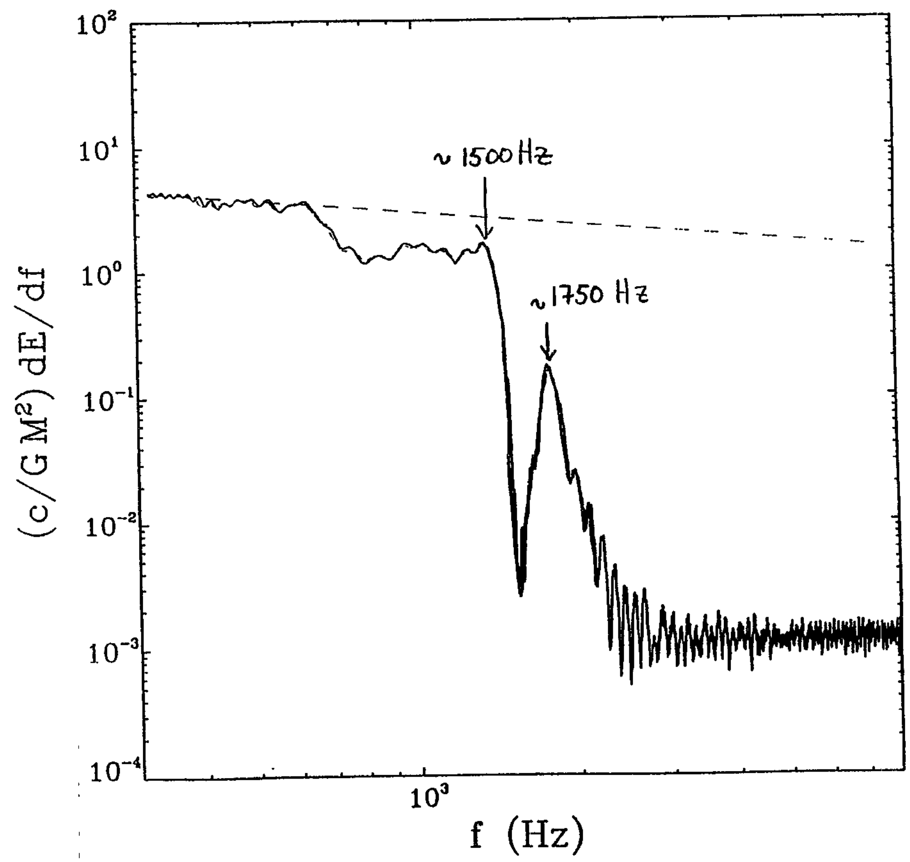

$M_1 = M_2 = 1.4\,M_\odot$

$R = 10$ km

$\boxed{\Gamma = 3}$

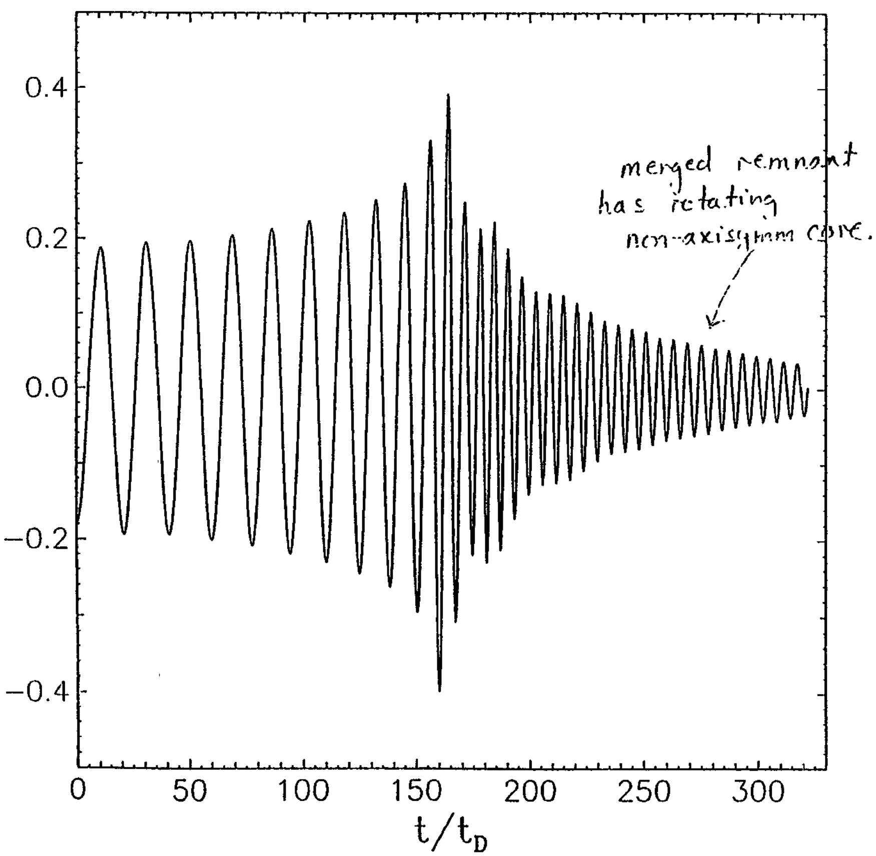

$M_1 = M_2 = 1.4\,M_\odot$

$R = 10$ km

$\boxed{\Gamma = 3}$

frequency scaling:

$$\frac{f_{\Gamma=2}}{f_{\Gamma=3}} \sim 1.2$$

cf. Lai, Rasio + Shapiro – freq scaling for onset of dynamical instab

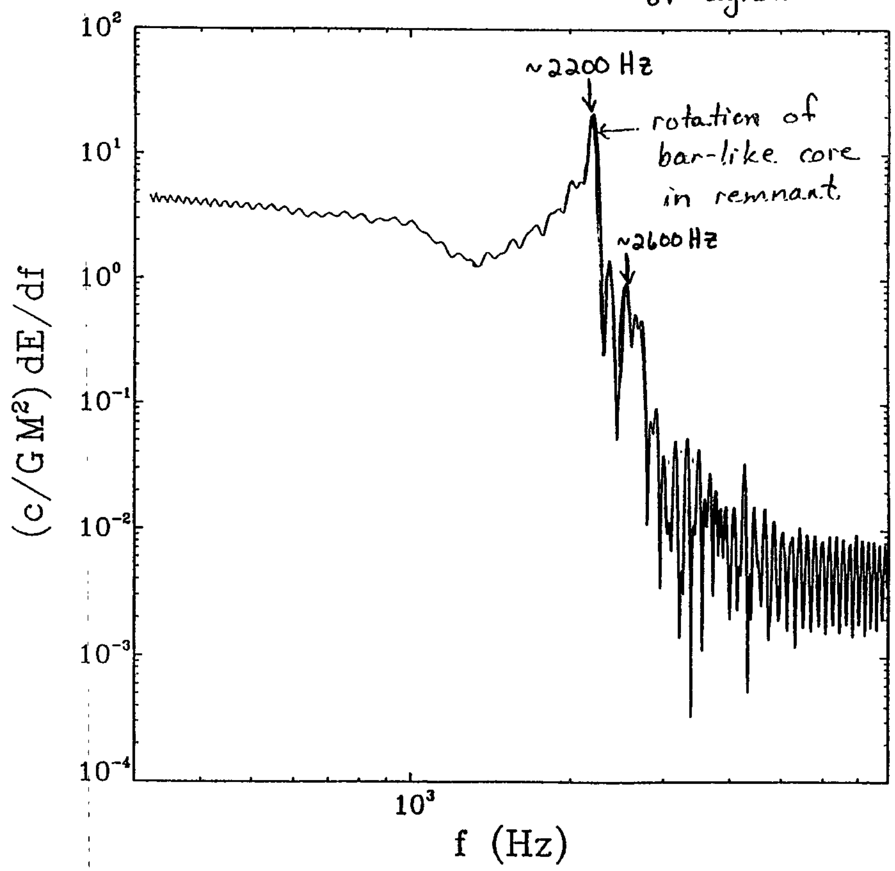

$N = 4096$ particles / star

$M_1 = 1.4\ M_\odot$

$\boxed{M_2 = \frac{1}{2} M_1 = 0.7\ M_\odot}$

$\Gamma = 2$

$\left.\begin{array}{l} R_1 = 10\,\text{km} \\ R_2 = 10\,\text{km} \end{array}\right\} K_1 = K_2$

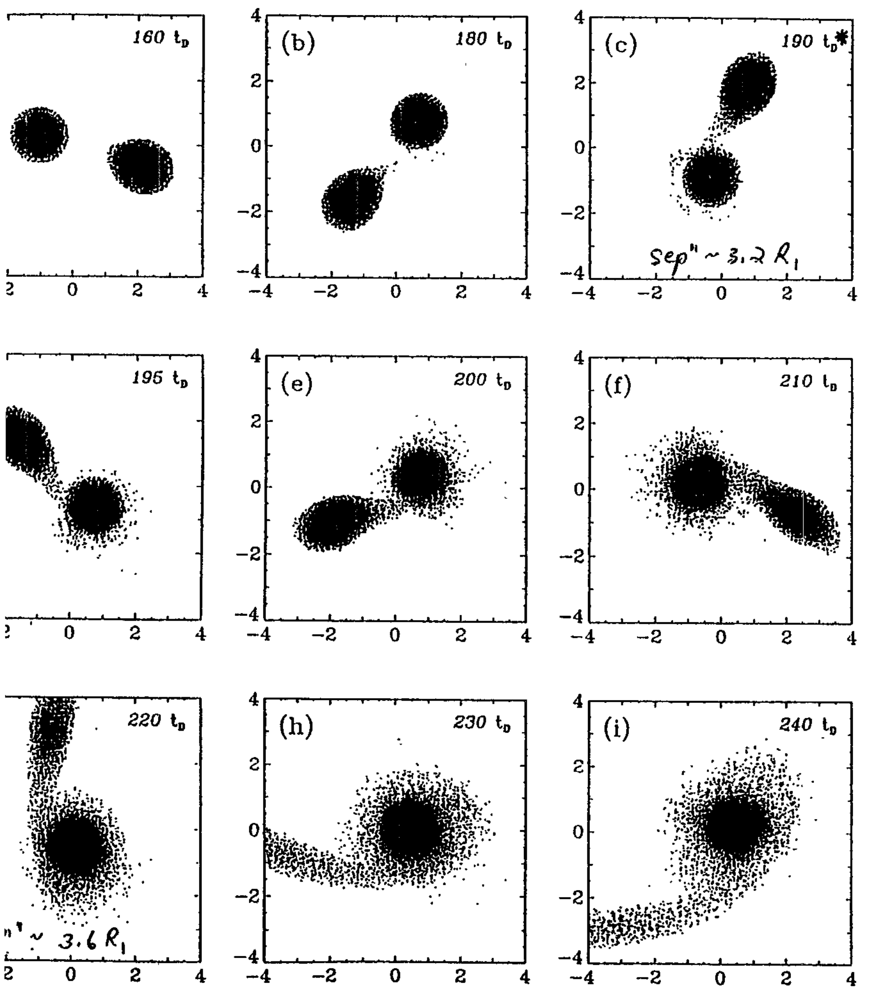

$M_1 = 1.4\ M_\odot$ $\qquad R_1 = 10\,\text{km}$

$\boxed{M_2 = \frac{1}{2} M_1 = 0.7\ M_\odot}$ $\qquad R_2 = 10\,\text{km}$

$\Gamma = 2$

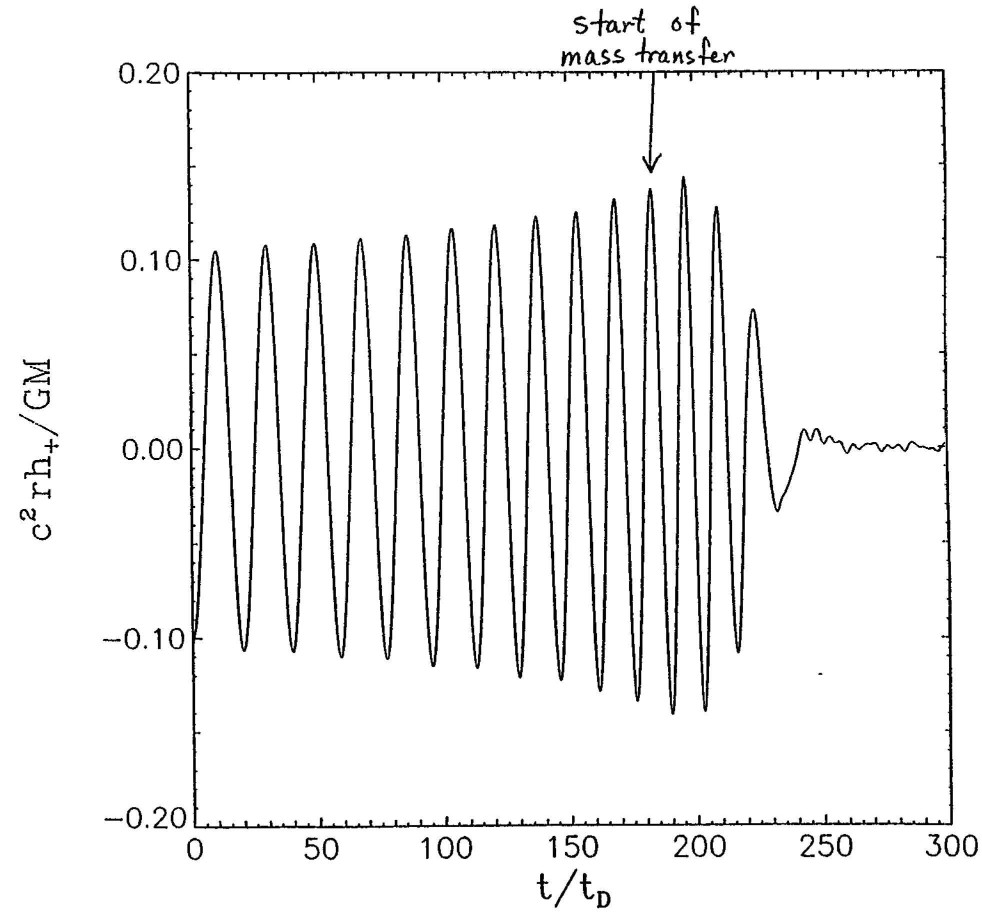

$N = 4096$ particles/star

$M_1 = 1.4\,M_\odot$ $R_1 = 10\,km$

$M_2 = \frac{1}{2} M_1 = 0.7\,M_\odot$ $R_2 = 8.7\,km$

$\Gamma = 3$

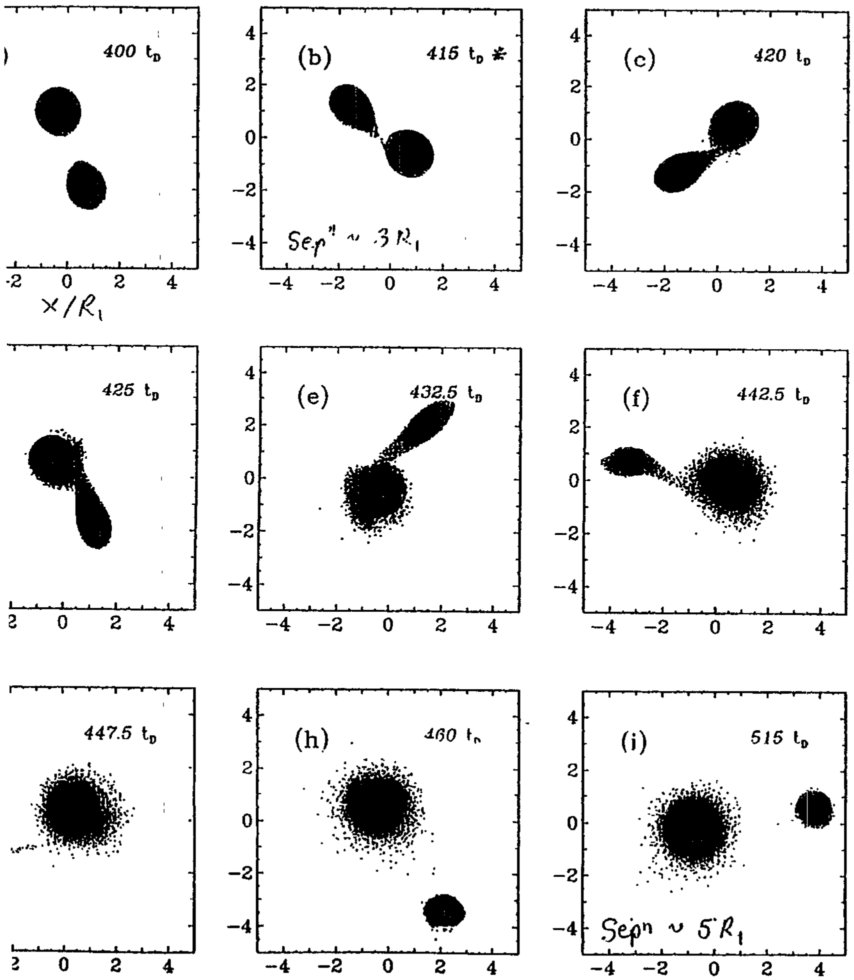

$M_1 = 1.4\,M_\odot$ $R_1 = 10\,km$

$M_2 = \frac{1}{2} M_1 = 0.7\,M_\odot$ $R_2 = 8.7\,km$

$\Gamma = 3$

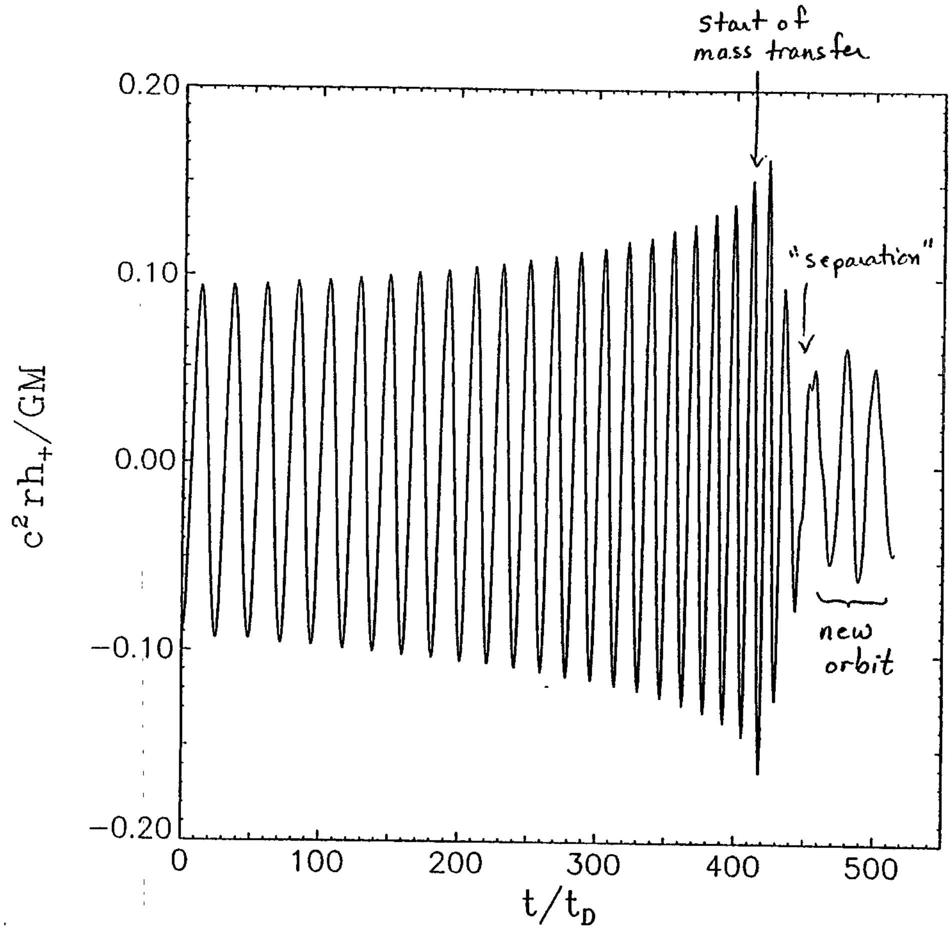

naxisymmetric Rotational Instabilities

louser, Centrella, + Smith 1994 PRL 72, 1314
imith, Houser, Centrella, 1996 ApJ (in press)

al rotational instabilities $e^{im\varphi}$

- arise in rapidly rotating axisymmetric fluids
- $\beta = \dfrac{\text{rotational KE}}{\text{grav PE}}$ sufficiently large
- m = 2 "bar mode"

narios:

- Rotating, collapsing stellar core - prevented from collapsing to NS by centrifugal forces - "centrifugal hang-up"
- Rotating stellar spun up by accretion

on axisymmetric instability occurs
$\longrightarrow$ burst of GW

ulations: start with axisymmetric quilibrium models, polytropes $P = K\rho^{\Gamma}$, mass M, equatorial radius R

dels run using Eulerian code + SPH

Models:

- $\Gamma = 5/3$, $\beta = .30$, run using SPH + Eulerian code

highly flattened:
polar radius $\sim .2\,R$

differential rotation

$N \approx 32{,}000$ particles

system rotates counterclockwise

Figure 10

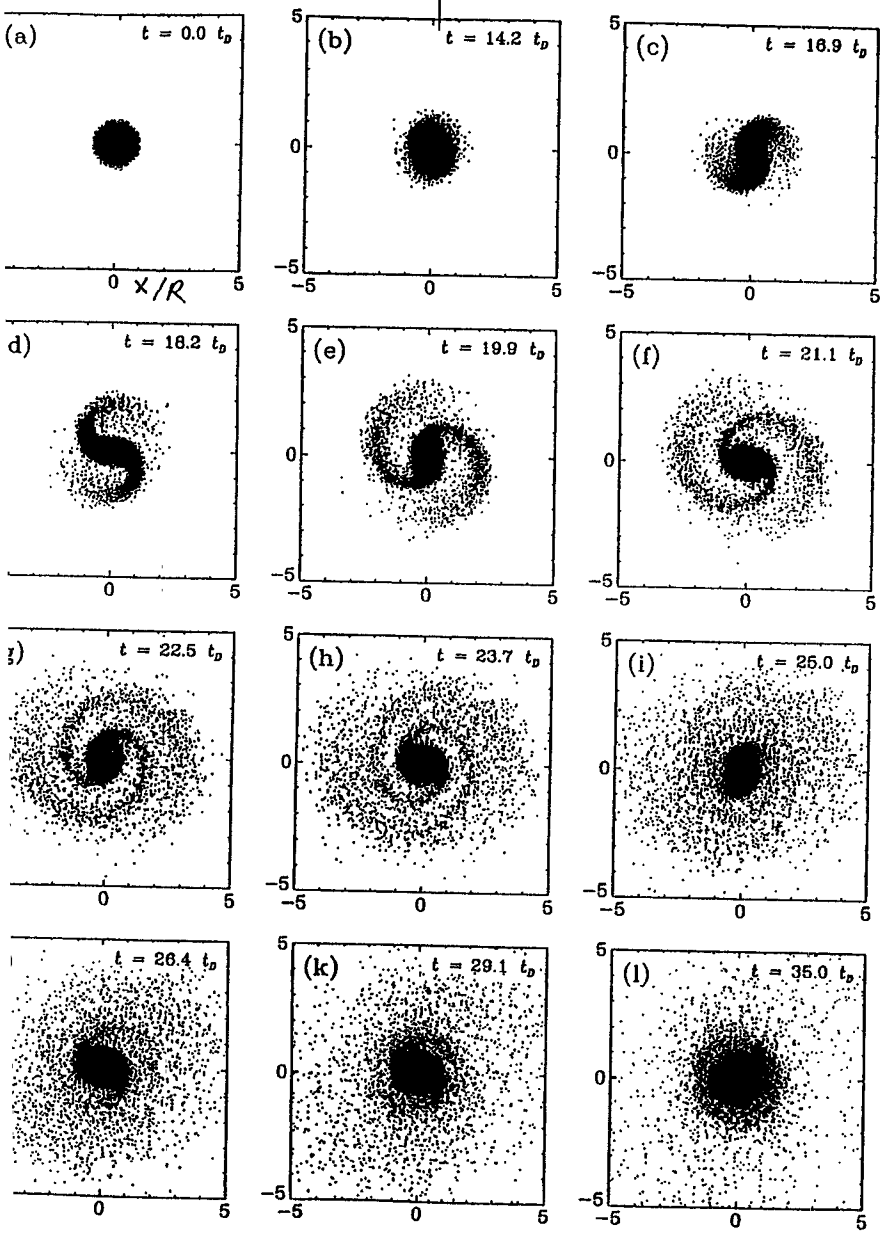

Figure 18

Grav Waves for observer on axis at $\theta = \varphi = 0$

$(c = G = 1)$

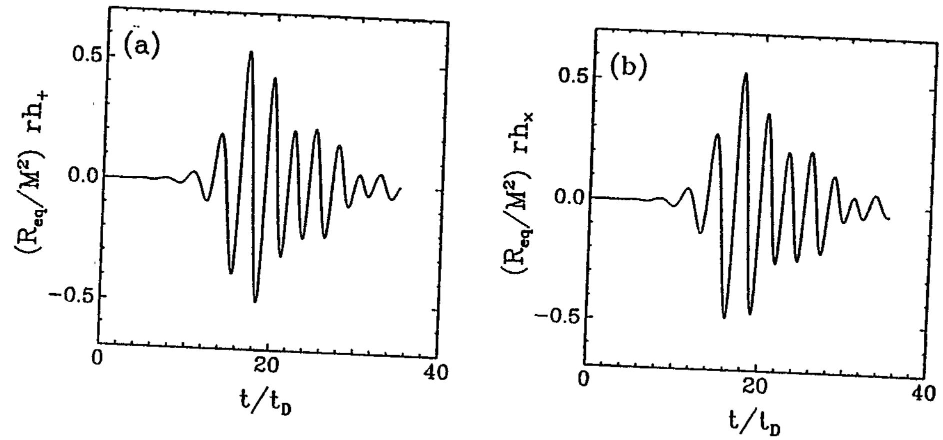

$T_{GW} \sim 3.5\ t_D$

$$t_D = \left[\frac{R^3}{GM}\right]^{1/2}$$

$N=3$

$N=3$

Gravitational Waveform ($c = G = 1$)

$T_{GW} \sim t_D$

$\Gamma = 4/3$, $\beta = .30$

run using Eulerian code

initial axisymm. equilibrium model

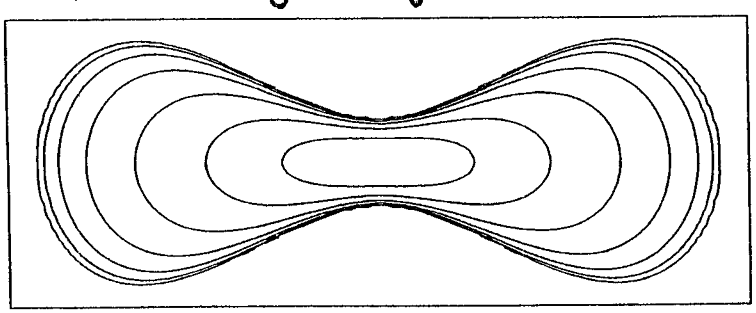

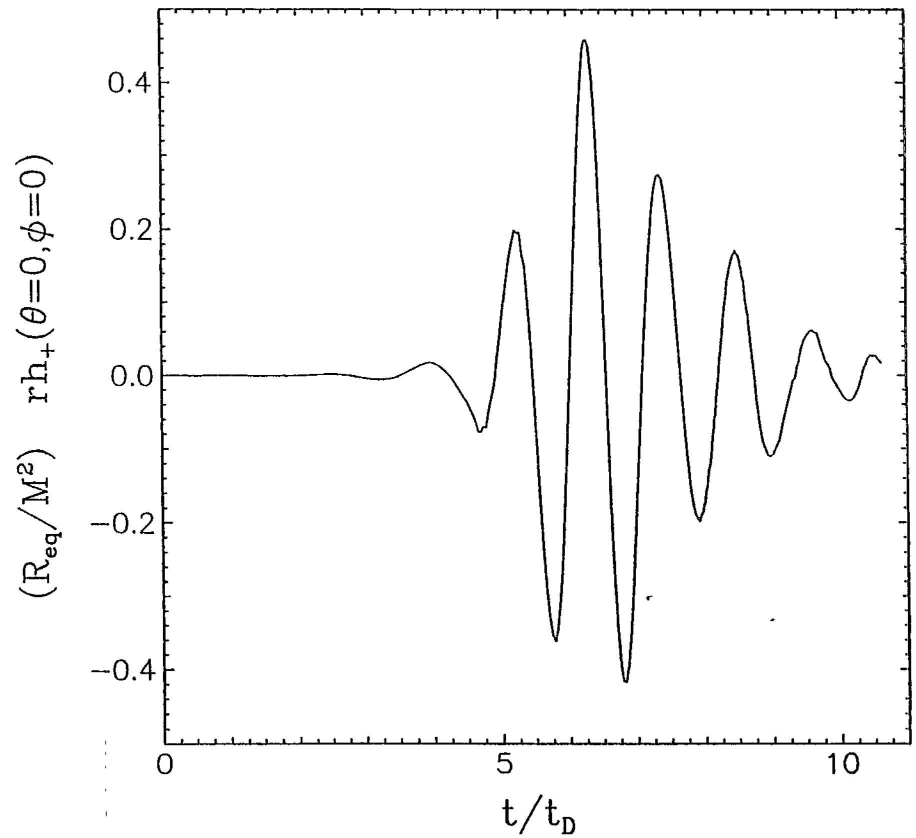

...ling - Amplitude + frequency of GW depend
...n physical parameters when instability occurs

$1.4 M_\odot$, $R = 10^3$ km
...t $r = 20$ Mpc, $h \sim 3 \times 10^{-24}$ $\quad f \sim 10$ Hz
...t $r = 10$ kpc, $h \sim 6 \times 10^{-21}$

$2 M_\odot$, $R = 4 \times 10^3$ km
...t $r = 20$ Mpc, $h \sim 1.5 \times 10^{-24}$ $\quad f \sim 1$ Hz
...t $r = 10$ kpc, $h \sim 3 \times 10^{-21}$

$1.4 M_\odot$, $R = 10^2$ km
...t $r = 20$ Mpc, $h \sim 3 \times 10^{-23}$ $\quad f \sim 300$ Hz
...t $r = 10$ kpc, $h \sim 6 \times 10^{-26}$

$1.4 M_\odot$, $R = 10$ km
...t $r = 20$ Mpc, $h \sim 3 \times 10^{-22}$ $\quad f \sim 4$ kHz $\longrightarrow$ Robust numerical codes able to carry out detailed astrophysical modeling in the "Golden Age" of Gravitational Wave Astronomy
...t $r = 10$ kpc, $h \sim 6 \times 10^{-19}$

irections ...

r rotational instabilities : effects of
different rotation laws + collapse

ore realistic modeling of EOS

eneral Relativistic effects :

- for binaries, more rapid plunge ?
- collapse to Black Hole
  - final remnant ?
  - earlier – cf. J. Wilson – ?
- rotational instabilities + collapse

⋮

Estimating parameters of gravitational wave signals using wavelet analysis

A. KRÓLAK

Aspen Winter Physics Conference – January 1996

A common way to analyse a signal $s(t)$ to decompose it with respect to a certain ts of functions $\psi(t,p)$

$$Tf(p) = \int_{-\infty}^{+\infty} s(t)\,\Psi^*(t,p)\,dt$$

$$= \int_{-\infty}^{+\infty} \hat{s}(\omega)\,\hat{\Psi}^*(\omega,p)\,d\omega$$

ncertainty principle : $\Delta t\, \Delta\omega \geq 1/2$

on sampling ! $\psi(t,t_0) = \delta(t-t_0)$ $\quad \hat{\psi}(\omega,t_0) = \frac{1}{\sqrt{2\pi}}\, e^{i\omega t_0}$

transform : $\psi(t,\omega_0) = \frac{1}{\sqrt{2\pi}}\, e^{-i\omega_0 t}$ $\quad \hat{\psi}(\omega,\omega_0) = \delta(\omega-\omega_0)$

transform : $\psi(t,t_0,\omega_0) = \frac{1}{\sqrt{2\pi}}\, e^{-i\omega_0 t}\, e^{-\frac{(t-t_0)^2}{2\sigma^2}}$

$$\hat{\psi}(\omega,t_0,\omega_0) = \sigma\, e^{-\frac{(\omega-\omega_0)^2\sigma^2}{2}}$$

transform : $\psi(t,t_0,a) = \frac{1}{\sqrt{2\pi}}\,\frac{1}{a}\, e^{-i\frac{2\pi(t-t_0)}{a}}\, e^{-\frac{(t-t_0)^2}{2a^2}}$

t wavelet)

$$\hat{\psi}(\omega,t_0,a) = e^{i\frac{2\pi t_0}{a}}\, e^{-\frac{(\omega-\omega_0)^2 a^2}{2}}$$

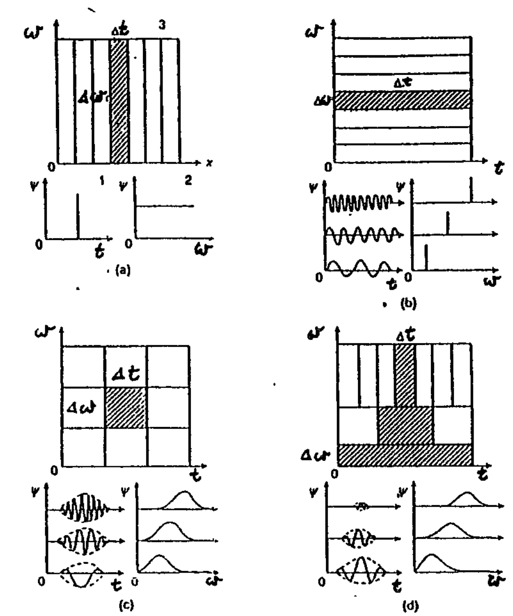

A comparison of the way different transforms balance physical- and wavenumber-space resolution. (a) Shannon transform. Perfect physical resolution, no wavenumber-space resolution. (b) Fourier transform. Perfect wavenumber-space resolution, no physical-space resolution. (c) Gabor transform. Balance between wavenumber- and physical-space resolution: the same at all length-scales. (d) Wavelet transform. Balance between wavenumber- and physical-space resolution varies with length-scale. Smaller length-scales are more finely resolved: mathematical microscope

...vitational wave signal from a binary in quadrupole approximation

$$h(t) = \frac{A}{(t_c - t)^{1/4}} \cos \phi(t) \quad , \; A = \text{const}$$

$$\phi(t) = -2\left(\frac{t_c - t}{5\mathcal{M}}\right)^{5/8}$$

$$t_c = \frac{5}{256} \frac{1}{(\pi f_i)^{8/3}} \frac{1}{\mathcal{M}^{5/3}} \qquad f_i = f(0)$$

...ntaneous frequency:

$$f(t) = \frac{1}{2\pi}\phi'(t) = \frac{1}{8\pi\mathcal{M}}\left(\frac{t_c - t}{5\mathcal{M}}\right)^{-3/8}$$

...important characteristic of the signal is ... - bandwidth product BT

$$BT = T_s \cdot B_s$$

$$= \frac{\int_{-\infty}^{+\infty} t^2 |h(t)|^2 dt}{\int_{-\infty}^{+\infty} |h(t)|^2 dt} \qquad B_s = \frac{\int_{-\infty}^{+\infty} f^2 |\hat{h}(f)|^2 dt}{\int_{-\infty}^{+\infty} |\hat{h}(f)|^2 df}$$

$$BT \approx \underbrace{581 \frac{1}{(\mathcal{M}_\odot f_{i\,100\,Hz})^{5/3}}}_{\text{NUMBER OF CYCLES}} \left(\frac{f_u}{f_i}\right)^{1/3}$$

...typical GW signal from a coalescing binary ...ved by laser interferometers will be ...acterized by a LARGE BT product.

A large time-bandwidth product allows application of the ridge extraction method from wavelet transform and consequently determination of the frequency modulation law of the signal.*

Phase of the wavelet transform (calculated by means of stationary phase approximation) and using the Morlet wavelet is given by

$$T(b, a) = \frac{1}{a}\int_{-\infty}^{+\infty} s(t)\, \overline{g\left(\frac{t-b}{a}\right)}\, dt$$

stationary point $f(t_s) = \frac{1}{a}$

$$\Psi_s(b, a) = \arg T(b, a) = \phi(t_s) - \omega_0 \frac{t_s - b}{a} + \frac{1}{2}(t_s - b)^2 \frac{\Phi''(t_s)}{1 + a^4 \Phi''^2(t_s)}$$

$$+ \frac{1}{2}\arctan[a^2 \Phi''(t_s)]$$

$$\Phi''(t_s) = 2\pi f'(t_s) = \frac{192\pi^2}{5} a^{-11/3} (\pi\mathcal{M})^{5/3}$$

$$t_s = \frac{5}{256\pi} \frac{1}{(\pi\mathcal{M})^{5/3}}\left[\frac{1}{f_i^{8/3}} - a^{8/3}\right]$$

* Delprat et al. IEEE Trans. Inform. Theory 38, 644 (1992).

General theory

Innocent e Vinet Cardiff workshop, April 1992

Application to GW signal from a binary

idge of the transform is defined by (5)

$$t_s(b,a) = b$$

$$\Rightarrow \quad \frac{1}{a_r(b)} = \frac{1}{8\pi \mathcal{M}} \left(\frac{t_c - b}{5\mathcal{M}}\right)^{-3/8} = f(b)$$

e ridge determines the frequency modulation

$$\frac{1}{a}\frac{d\Psi}{db}\Big|_{a=\mathrm{const}} = \frac{1}{a} + (t_s - b)\frac{\frac{1}{2\pi}\Phi''(t_s)}{(1+a^4\Phi''(t_s))^2}$$

On the ridge

$$\frac{1}{2\pi}\frac{d\Psi}{db}\Big|_{a=\mathrm{const},\,\mathrm{ridge}} = \frac{1}{a_r}$$

This provides a way to extract numerically ridge of the wavelet transform and the frequency modulation law.

Reconstruction of the signal

$$s(b) = \sqrt{\frac{2}{\pi}}\left(1 + a_r^4\,\Phi''(b)^2\right)^{1/4} \exp\left[-\frac{i}{2}\arctan(a_r^2\,\Phi''(b))\right] T(b, a_r)$$

skeleton of the wavelet transform

$$t) = \mathrm{Re}\, Z_s(t)$$

be used as a matched filter

Estimation of the chirp mass (6)

A numerical algorithm consisting of

1. Linearization $\quad \ell(t) = 1 - \left(\frac{f(t)}{100}\right)^{-8/3}$
2. Smoothing $\quad \ell(t) = \left(\frac{800\pi}{5}\right)^{8/3} \mathcal{M}^{5/3}\, t$
3. Linear regression

Estimation of the chirp mass from the frequency modulation extracted from the wavelet transform.

$m_1 = m_2 = 1.4\ M_\odot \qquad \mathcal{M}_\odot = 1.22$

50 runs for each signal-to-noise ratio

d_0	$\overline{\mathcal{M}_\odot}$	bias	$\sigma_{\mathcal{M}}$
84	1.2157	0.0031	0.0023
25	1.2155	0.0033	0.0087
8	1.2156	0.0032	0.021

$$\frac{\sigma_{\mathcal{M}}}{\mathcal{M}} \simeq \frac{20}{d_0}\ \%$$

Ridge of the wavelet transform $f_i = 100\,Hz$ $f_u = 200\,Hz$

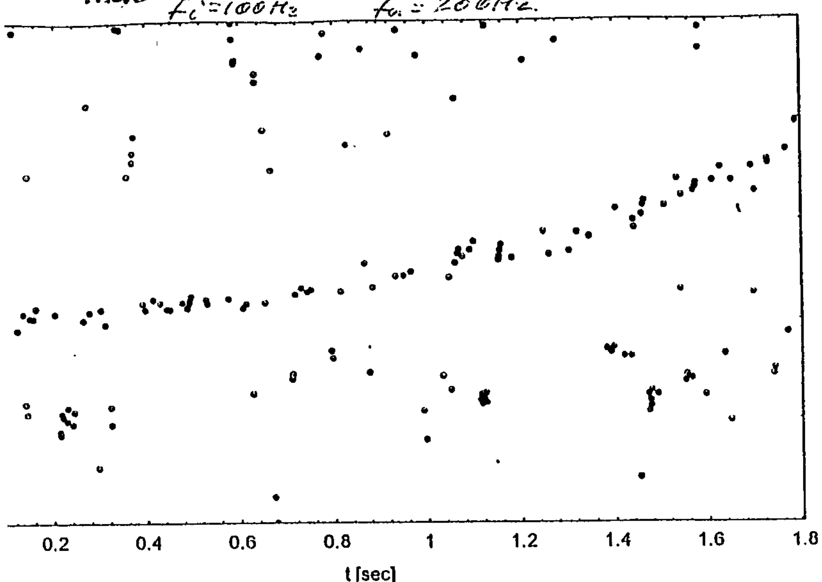

responding optimal signal-to-noise
tio $d_0 = 25$

Linearization and smoothing of the ridge

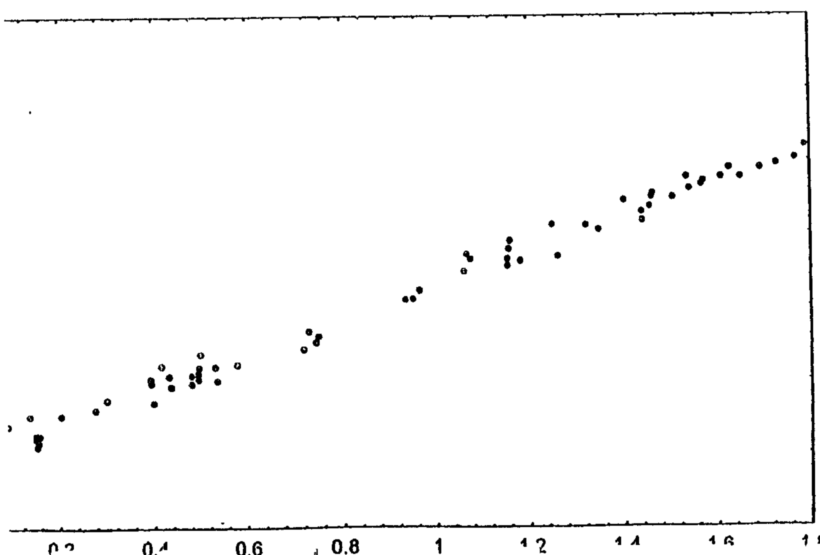

We have analyzed the signal with the 1st pN correction to see whether by wavelet analysis one can discriminate small corrections to the signal

Estimation of generalized chirp mass

d_0	$\overline{\mathcal{M}_{g0}}$	bias	$\sigma_{\mathcal{M}}$
84	1.1584	0.06042	0.002733
25	1.1584	0.06096	0.01298
8	1.1648	0.05397	0.02952

comparison with Newtonian filter analysis

Analytic formula for the generalized chirp mass:

$$\mathcal{M}_g = 1/k_{\equiv}^{3/5} \qquad k = \frac{1}{\mu m^{2/3}}$$

$$k_{\equiv} = k + k_1 (\pi f_0')^{2/3} \qquad k_1 = \frac{1}{\mu}\left(\frac{743}{336} + \frac{11}{4}\frac{\mu}{m}\right)$$

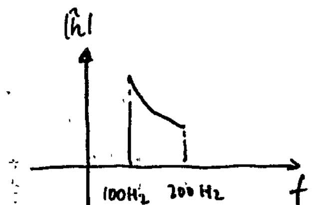

$f_0' = 100\,Hz$

$$d^2 = 4\int_0^\infty \frac{|\tilde{h}|^2}{S_h(f)}\,df = \text{const}\int_{f_i}^{f_u} \frac{df}{f^{7/3}}$$

$$\mathcal{M}_g = 1.1655$$

There now exist better numerical [illegible]orithms to extract the ridge of wavelet transform and reconstruct signal when the noise is high;

[illegible]g. simulated annealing algorithm.

R.A. Carmona, W.L. Hwang, B. Torrésani "[illegible]fication of ridges with continuous [illegible] transform" preprint [illegible]"

[illegible]cation of wavelet analysis to [illegible]ion of GW signals from coalescing [illegible]ries

([illegible] Flamino, L. Massonnet, B. Mours, S. Tissot, Verkindt, M. Yvert, Astroparticle Physics 2, 35 (1994))

③

Non-linear wavelet analysis ?

The idea is to generalize the wavelet analysis by introducing a non-linear dilation in the wavelets

$$g(b, a) = \frac{1}{a^n}\, g\left(\frac{t-b}{a^k}\right)$$

where n and k can be any real number.
(In the standard wavelet analysis $k = 1$.)

The motivation to consider such a generalization is that by suitably choosing the number k one can after application of the ridge extraction algorithm get the ridge a a LINEAR function of b

In our case we have

$$f(t) = \frac{1}{8\pi\mathcal{M}}\left(\frac{t_c - t}{5\mathcal{M}}\right)^{-3/8}$$

$$f(b) = \frac{1}{a_r{}^k}$$

choosing $k = 3/8$

$$a_r = \frac{(8\pi)^{8/3}}{5}\, \mathcal{M}^{5/3}\,(t_c - b)$$

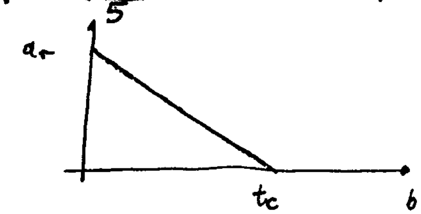

Generalized Morlet wavelets

(11)

$$\psi_k = e^{-\frac{t^2}{2a^k}} \cos \frac{2\pi t}{a^k}$$

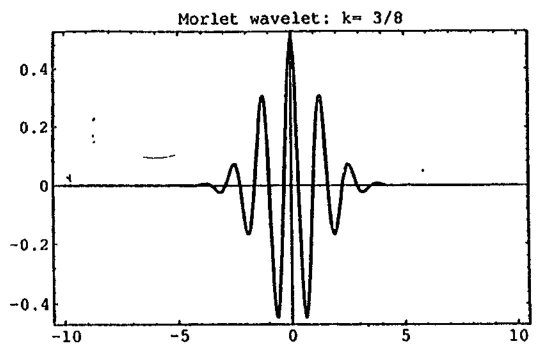

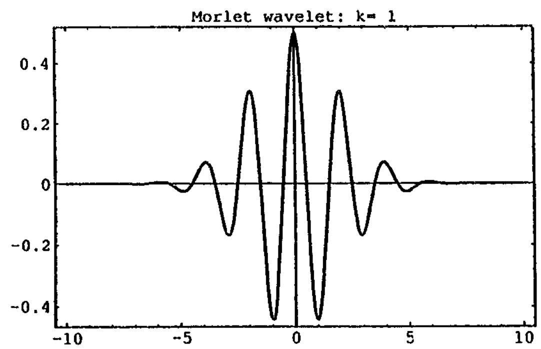

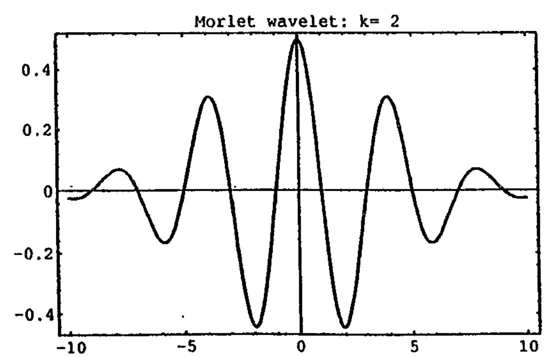

Modulus of the transforms

(12)

Gabor transform

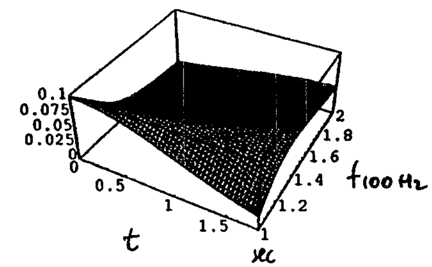

Wavelet transform

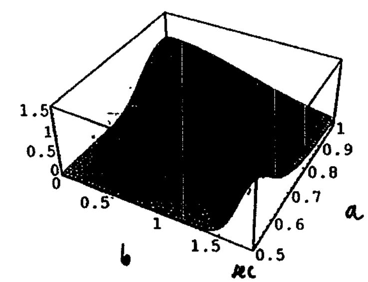

non-linear wavelet transform

$k = 3/8$

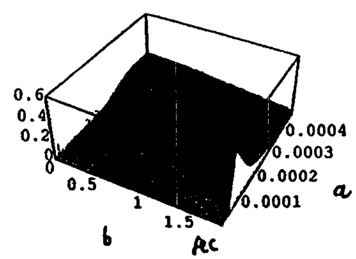

LOWER BOUNDS ON THE MINIMUM MEAN SQUARE ERROR

David Nicholson & Alberto Vecchio

Department of Physics and Astronomy
University of Wales - College of Cardiff

Gravitational wave observations:

$$s(t) = h(t;\ \theta) + n(t)$$

where θ is a M-dimensional vector parameter.

Error on the estimation of θ ?

For any estimator $\hat{\theta}$ the estimator error is $\epsilon = \hat{\theta} - \theta$ and the error correlation matrix is given by:

$$R_\epsilon = \langle \epsilon \epsilon^T \rangle$$

THE GOAL:
We are interested in lower bounding $a\, R_\epsilon\, a^T$ for any M-dimensional vector a. If a unit vector $\longrightarrow$ bound on the MSE of θ

The **minimum MSE estimator** is the conditional mean estimator:

$$\hat{\theta} = \langle \theta | x \rangle = \int \theta p(\theta | x) d\theta$$

Its MSE is the greatest lower bound

MSE behaviour in non linear estimation problems

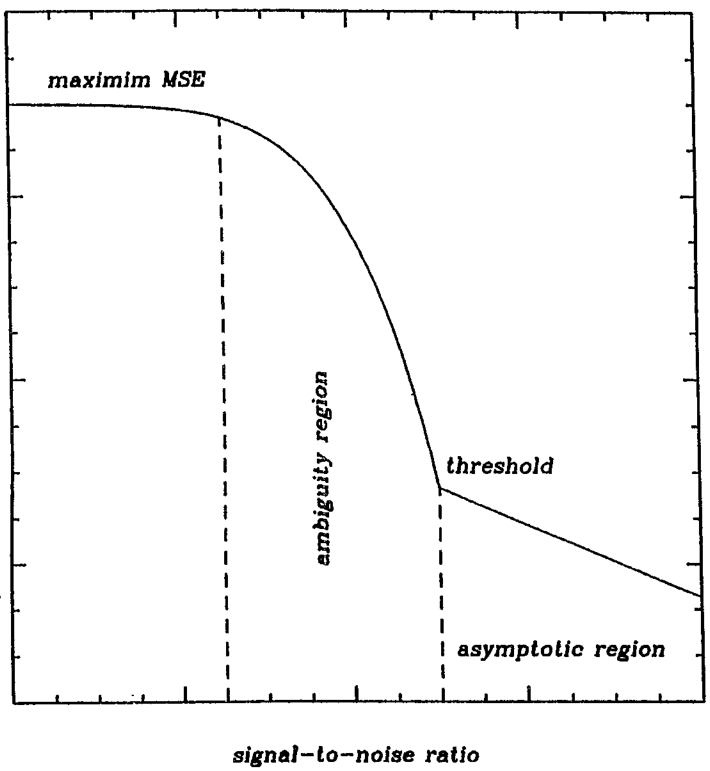

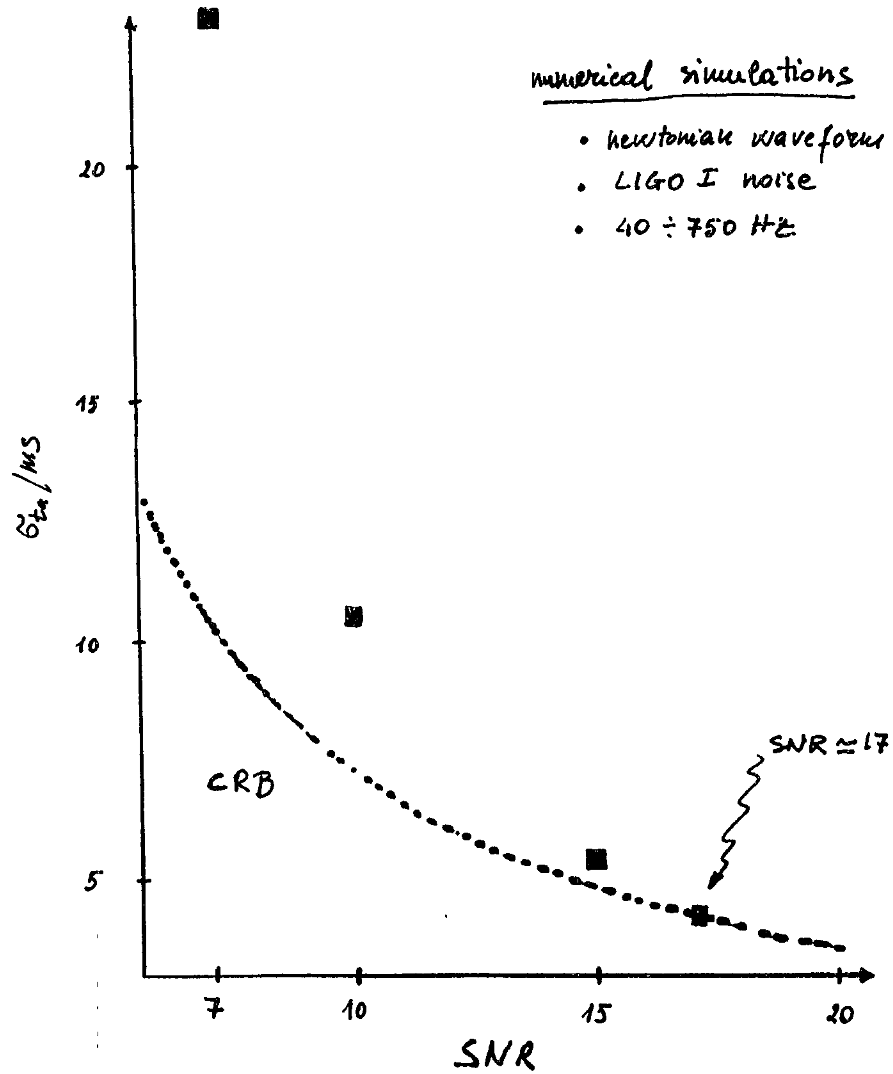

evaluation of the exact minimum MSE is often difficult or even ossible $\rightsquigarrow$ good computable bounds:

local

- Cramer-Rao (Cramer 1945; Rao 1946)
- Barankin (Barankin 1949)

global

- Weiss-Weinstein (Weiss & Weinstein 1985a, 1985b, 1986)
- Ziv-Zakai (Ziv & Zakai 1969; Chazan, Zakai & Ziv 1975; Bellini & Tartara 1974; Bell 1995)

iss-Weinstein and Ziv-Zakai bounds (GB):

- ayesian
- lobal
- dependent on the estimation process
- ree from regularity conditions
- hey can incorporate **any** *a priori* information
- the limit SNR $\gg$ 1:

$$\left.\begin{array}{l}\text{WWB}\\ \text{ZZB}\end{array}\right\} \longrightarrow \text{CRB}$$

- the limit SNR $\ll$ 1:

$$\left.\begin{array}{l}\text{WWB}\\ \text{ZZB}\end{array}\right\} \longrightarrow \text{a priori information}$$

Used so far $\Longrightarrow$ **Cramer-Rao's bounds:**

- Theoretical problems:
  1. local estimate
  2. they can not incorporate general *a priori* information
- Results of numerical simulations (Balasubramanian, Sathyaprakash & Dhurandhar 1995)

$\Downarrow$

New bounds:

- Good performance in the whole SNR region
- Accurate prediction of the location of the threshold
- Useful to compare numerical simulations and to test *information extraction algorithms*

$$\psi(\underline{x},\theta)\, p(\underline{x},\theta)\, d\theta = 0$$

$$\boxed{\epsilon^2 \geq \frac{\langle \theta\, \psi(\underline{x},\theta)\rangle^2}{\langle \psi^2(\underline{x},\theta)\rangle}}$$

WWB

$$\ldots,\theta) = L^{r}(\underline{x};\theta+\delta,\theta) - L^{1-r}(\underline{x};\theta-\delta,\theta)$$

$\forall \delta,\ 0<r<1$

$$(\underline{x};\theta,\theta') = \frac{p(\underline{x},\theta)}{p(\underline{x},\theta')}$$

$$_{WW} \geq \frac{\delta^2\, e^{2\mu(r,\delta)}}{e^{\mu(2r,\delta)} + e^{\mu(2-2r,-\delta)} - e^{\mu(1-r,-2\delta)}}$$

$$(r,\delta) = \ln \langle L^{r}(\underline{x};\theta+\delta,\theta)\rangle$$

: TEST POINT

(displacement from the true parameter value)

$$\underline{\theta} = (\theta_1, \theta_2, \ldots, \theta_M)$$ M parameters

$$\langle \underline{\epsilon}\, \underline{\epsilon}^T \rangle \geq \Delta Q^{-1} \Delta^T$$

test points

$$\Delta = [\underline{\delta}_1, \underline{\delta}_2, \ldots, \underline{\delta}_M] \qquad (M \times P)$$

$$Q_{ij} = 2\, \frac{e^{\mu(\frac{1}{2},\, \underline{\delta}_i - \underline{\delta}_j)} - e^{\mu(\frac{1}{2},\, \underline{\delta}_i + \underline{\delta}_j)}}{e^{\mu(\frac{1}{2},\, \underline{\delta}_i)}\; e^{\mu(\frac{1}{2},\, \underline{\delta}_j)}} \qquad (P \times P)$$

$$\mu(\tfrac{1}{2}, \underline{\delta}) = -\frac{1}{4}\rho^2 [1 - \gamma(\underline{\delta})] + \ln \int_{-\infty}^{+\infty} d\underline{\theta}\, [p(\underline{\theta}+\underline{\delta})\, p(\underline{\theta})]^{1/2}$$

$$\gamma(\underline{\delta}) = \frac{(h(\underline{\theta}+\underline{\delta}) \,|\, h(\underline{\theta}))}{(h(\underline{\theta}) \,|\, h(\underline{\theta}))}$$

$(\cdot|\cdot)$: inner product

Simple example

Preliminary results:

. Newtonian waveforms:

2D problem (t_a, τ)

3D problem (t_a, τ, ϕ_a)

. LIGO I noise

. range of parameters

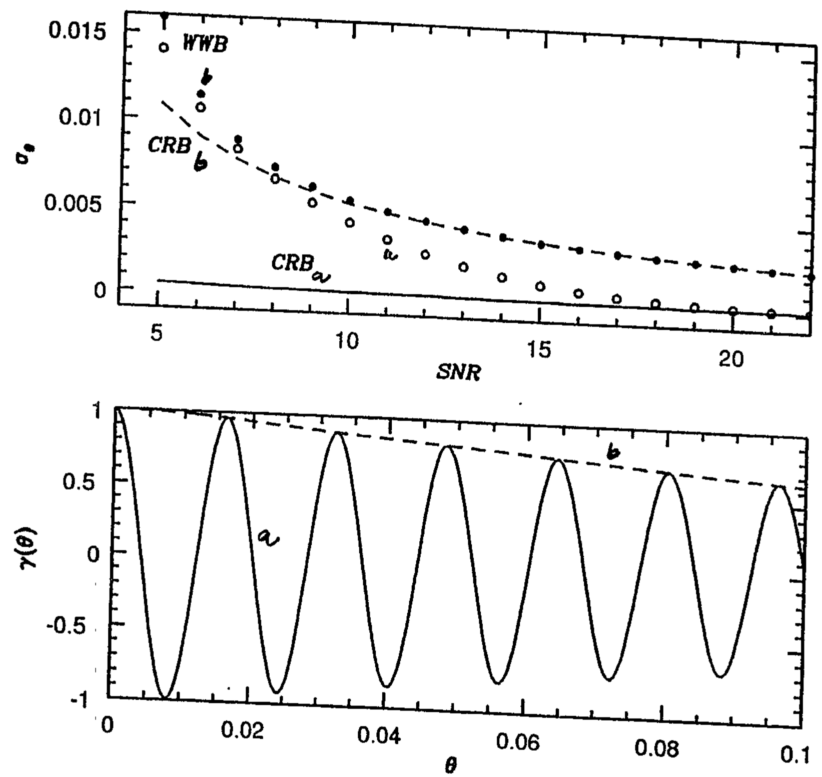

LIGO I noise
40÷750 Hz

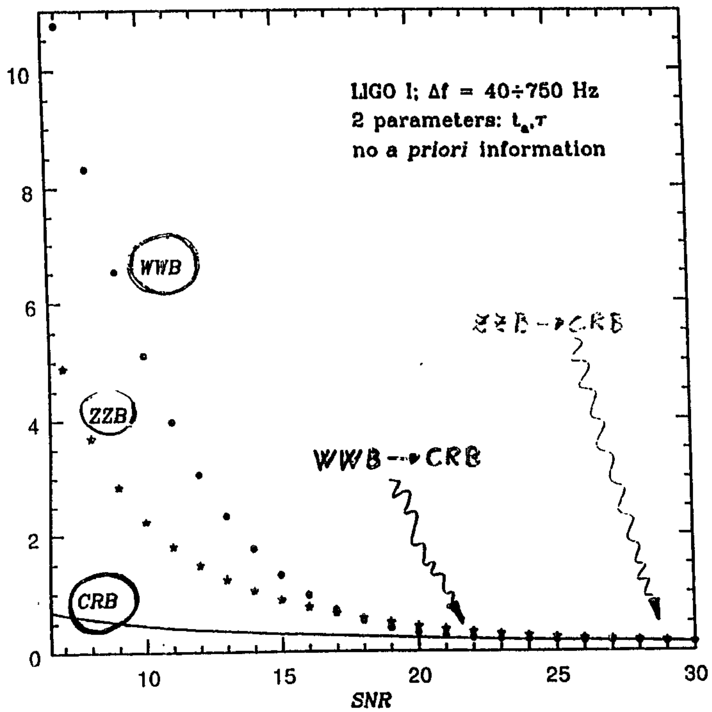

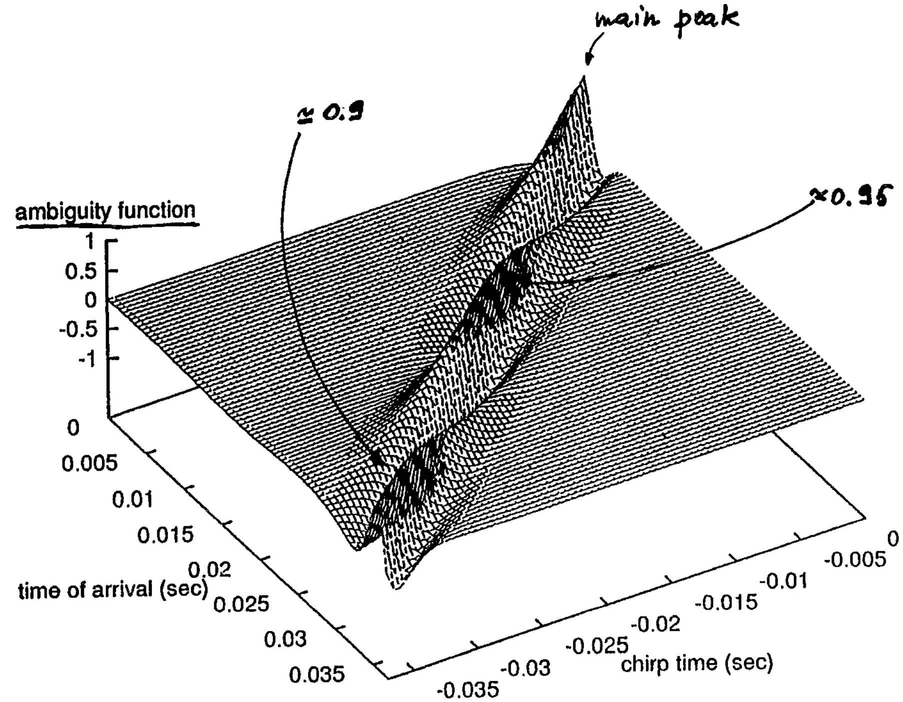

Newtonian signal
(t_a, τ, ϕ_a)

LIGO I noise
40÷750 Hz

$\phi_a = \phi_a^{(max)}$

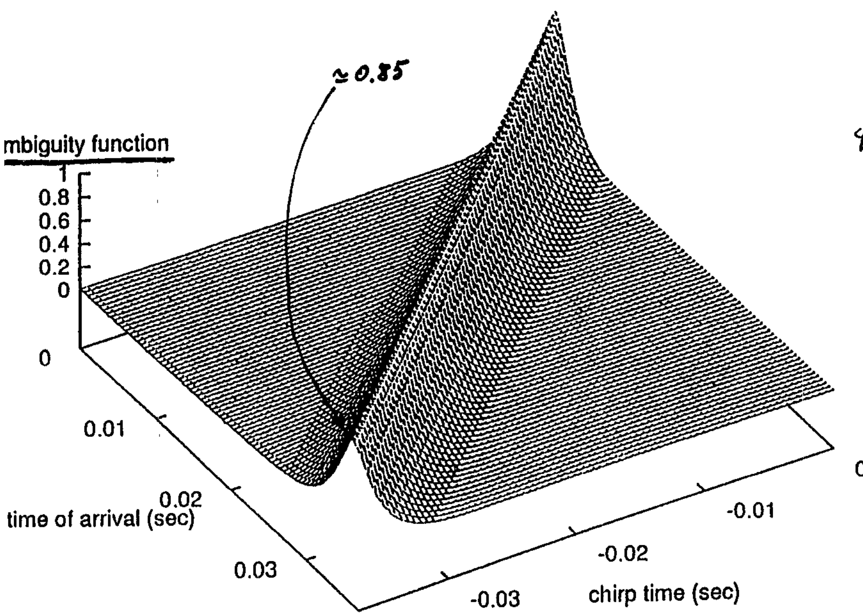

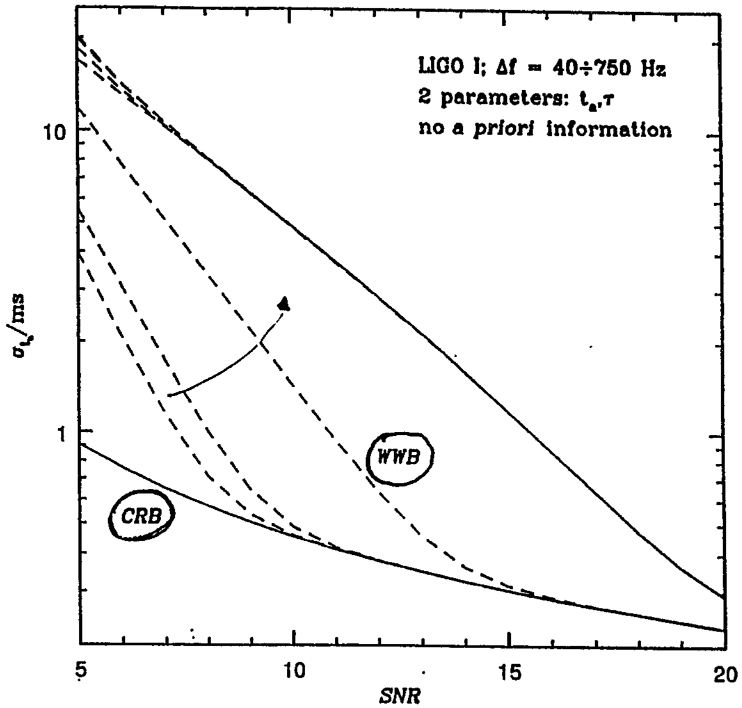

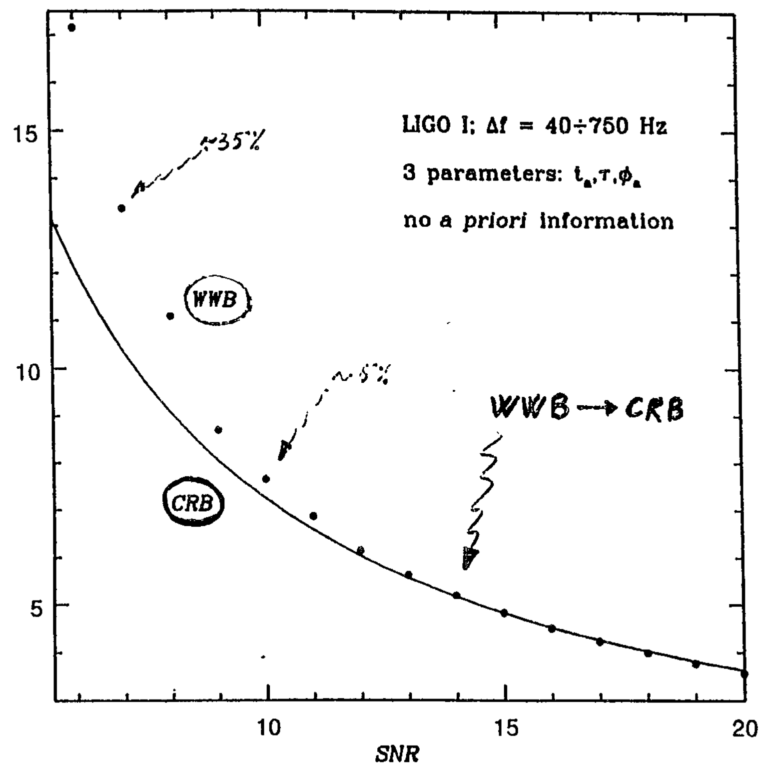

LIGO I; Δf = 40÷750 Hz
3 parameters: t_a, τ, ϕ_a
no a *priori* information
~35%
WWB
~5%
WWB → CRB
CRB
15
10
5
10
15
20
SNR

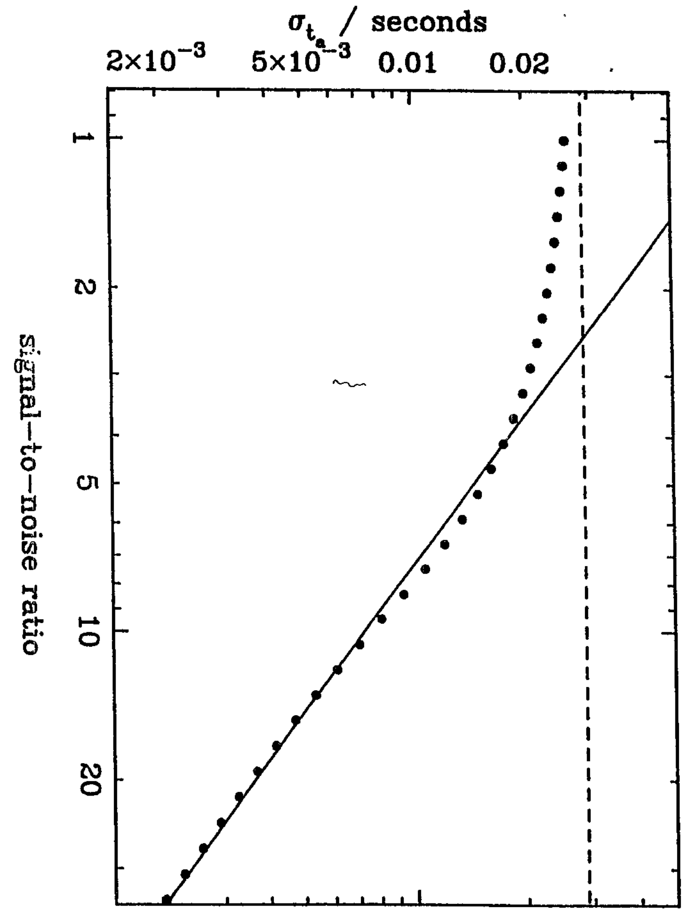

σ_{t_a} / seconds
2×10^{-3}
5×10^{-3}
0.01
0.02
signal-to-noise ratio
1
2
5
10
20

CONCLUSIONS

The general behaviour of WWB and ZZB applied to gravitational wave observations of coalescing binaries is in agreement with the results obtained in other fields

The discrepancy between CRB and GB depends on the shape of the ambiguity function

The knowledge of the parameter range before the estimation problem is important to reduce the errors

Numerical simulations predict greater errors and thresholds

FUTURE WORK

- Thorough study of the ambiguity function
- Extension to all the parameters
- Ligo II noise
- A priori probability
- Optimal bandwidth
- Coincidence experiments
- Comparison with numerical simulations

LIGO Simulation Environment

Jan. 18, 1996 Hiroaki Yamamoto / Caltech

- LIGO End-to-End model
  - >>We are developing integrated modular environment
    - — SIESTA of VIRGO or GRID of GEO
- Physics models
  - >>Building blocks - Interferometer(IFO) and Noise sources
- AVS
  - >>Software framework of LIGO simulation environment
- Environment
  - >>Modeling and Simulation Environment using AVS

LIGO End-to-End model - Why do we need it ? -

- Understand apparatus behavior
- Design trade study
  - >>Predict performance
  - >>Try different models
- Easy integration of work in LIGO
  - >>Work going on using different flavors - c/fortran/ MatLab/Mathematica
  - >>Use same environment to reuse work
- Data analysis
  - >>Compare models' predictions and data
  - >>On-line preselection algorithm
  - >>off-line search algorithm
- Make life easier
  - >>Friendlier interface
  - >>Data visualization

LIGO End-to-End model = IFO + Noise

$$\Delta\phi(P_{in}, 1\text{-}c, G\ldots) \oplus t_1 \otimes \Delta x_1 \oplus t_2 \otimes \Delta x_2$$

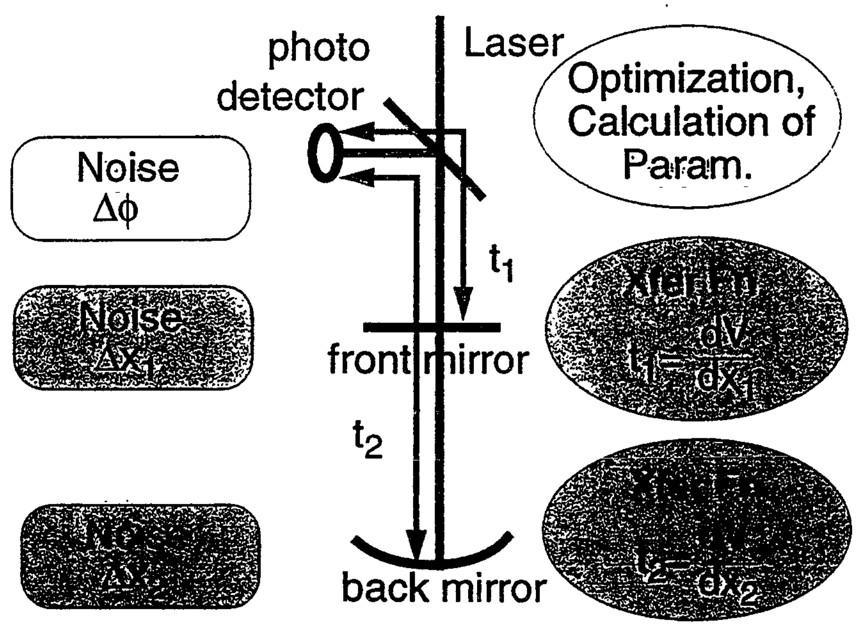

Physics models
- Interferometer -

Static model		InLock model	Lock acquisition model	
FFT model	Modal model	Twiddle	Single mode	Spacial multi mode
		frequency dom.	time domain	
J.Y.Vinet etc (VIR-GO) and Y.Hefetz etc (MIT/LIGO)	N.Mavalvala and Y.Hefetz (MIT)	Martin M. Regehr (CIT grad)	D. Reding (JPL)	D. Reding (JPL) and R. Beausoleil (CYG-NUS Laser Corp)
FFT(128,256), Paraxial apprx.	Hermit Gauss (00,01,10), small misalignm	Single mode steady state linear apprx.	Convergence in time space (*3)	Small/Large amplitude misalignment
all static quanti-ties, realistically deformed/tilted mirrors	low frequency alignment control design	Transfer function	Lock acquisition control design	Alignment control design
CPU/Memory demanding, 1 day w/ SS20 (*1)		base of End-to-End model (*2)	FP, CC, Recom-bined IFO done, Recycled IFO Feb~Mar	just starting

Physics models
- Super Computers -

- CSCC (Concurrent Supercomputing Consortium) hardware at Center for Advanced Computing Research of Caltech
  - ›› Massively Parallel Processors (MPP)
  - ›› effectively x 10 ~ 100 times faster than SPARC20

FEATURES	DELTA	TREX	RAPTOR	JPL CRAY
MODEL	PROTOTYPE	XPS L38	XPS A4	T3D
GFLOPS	30.7	38.4	4.3	38.4
NODES, PE'S PER NODE	513, 1PE	512, 1 PE & 1 Comms Procsr	57, 1 PE & 1 Comms Procsr	128, 2 PE's
CPU	i860 XR	i860 XP	i860 XP	DEC 21064
SPEED	40 MHZ	50 MHZ	50 MHZ	150 MHZ
MFLOPS/CPU	60	75	75	150
MB/NODE	16	32	32	64
TOTAL GB	8.2	16.4	1.8	16.4
DISKS IN GB'S	93 (RAID0)	67.2 (RAID3)	14.4 (RAID3)	103
TOPOLOGY	2D (16X36)	2D (16X36)	2D (16X4)	3D TORUS

Twiddle

ngle mode InLock state model in freq. domain

abry-Perot, example

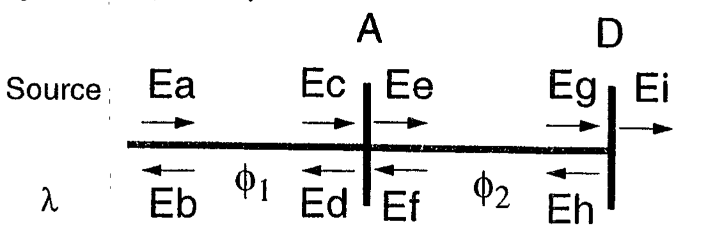

$Ee = t_A Ec + r_A Ef, \ldots \quad x_D(t) = X \cos\omega t$

quations

$$M_{DC}(r, t, \phi(\lambda)) \begin{bmatrix} Ea \\ Eb \\ \ldots \\ Ei \end{bmatrix} = \begin{bmatrix} 1 \\ 0 \\ \ldots \\ 0 \end{bmatrix} \Rightarrow M_{AF}(r, t, \phi(\lambda, \omega)) \begin{bmatrix} Ea \\ \ldots \\ Eh \\ Ei \end{bmatrix} = \begin{bmatrix} 0 \\ \ldots \\ S \\ 0 \end{bmatrix} \qquad S \sim \frac{X}{\lambda} E_0$$

pproximation

›› $\frac{X}{\lambda} \ll 1$

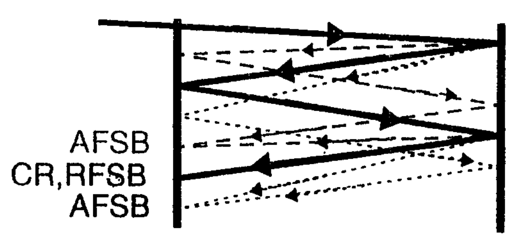

Implementation of Twiddle in Mathematica and AVS

- Mathematica code for FP

```
s1 = source[gamma]
m1 = mirror[r1,t1]
m2 = endmirror[r2,t2]
connect[s1,1,m1,1,length1,phase1]
connect[m1,2,m2,1,length2,phase2]
shake[m2]
findfields[ omega ]
```

- Nice feature of Twiddle
  - ››Automatic construction of the matrix M
  - ››Easy to build various IFO configurations
- AVS version of Twiddle
  - ››Twiddle Mathematica code is ported to Fortran
  - ››Grag optics elements and link to construct IFO
  - ››GUI parameter specification

Overview of Lock Acquisition Modeling Program: Building Block Approach

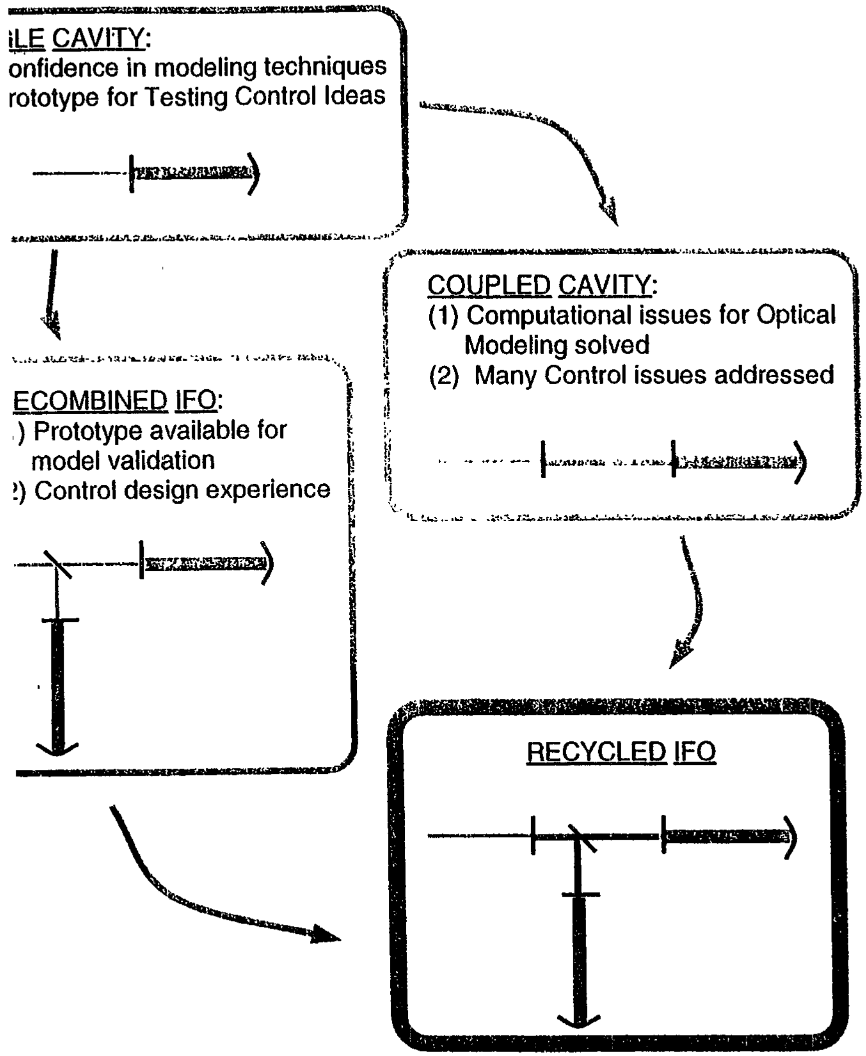

Method for Calculating Optical Response (Single Cavity)

E field in cavity at τ: $E(\tau) = E_1 + tE_s$

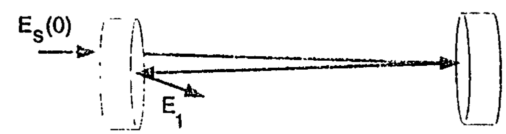

E field in cavity at 2τ: $E(2\tau) = E_2 + E_3 + tE_s$

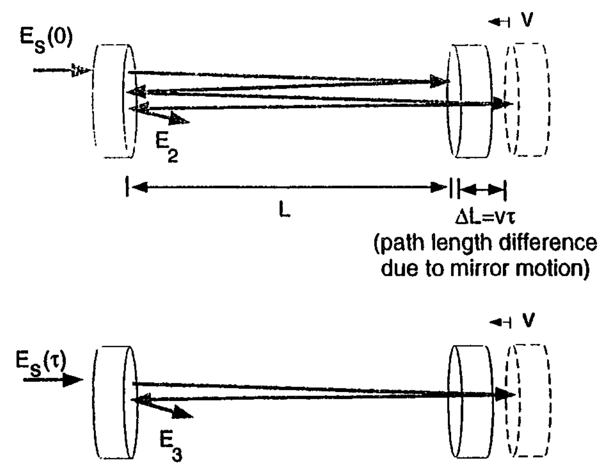

- Want to calculate E field in cavity as mirrors move.
- Sum contribution of E field due to light entering cavity at discrete intervals $t, t-\tau, t-2\tau, \ldots$

Physics models
- Noise -

Seismic Noise	Model to use either the LIGO standard spectrum or optional data from sites along with the transfer function of the seismic isolation stacks. Issues such as possible correlations between different testmasses to be studied for inclusion in model.
Thermal Noise	Model developed out of code written J.R. Hutchinson to calculate frequencies of modes of a solid cylinder and code by A. Gillespie to calculate effective mass coefficients for these modes. Together the frequencies and coefficients determine the thermal noise of the internal modes of the test mass. Model for thermal noise for the violin and pendulum resonances based on calculations and code by A. Gillespie and F. Raab.
Shot Noise	Model based on calculation for Recycled Unbalanced Fabry Perot LIGO IFO by Torrey Lyons and Martin Regehr.
*** Radiation Pressure and Quantum Noise,** *** Residual Gas Noise, * Laser Noise,** *** Phase Noise Due to Scattering and Stray Beams,** *** Magnetic and Electric Field Noise,** *** Technical Noise**	Rainer Weiss gravnoise program

AVS
- software framework -

(*4)-

1) Object Oriented
2) Visual Program
3) Open/Extensible
4) Application Framework
5) GUI builder
6) Library 2D/3D

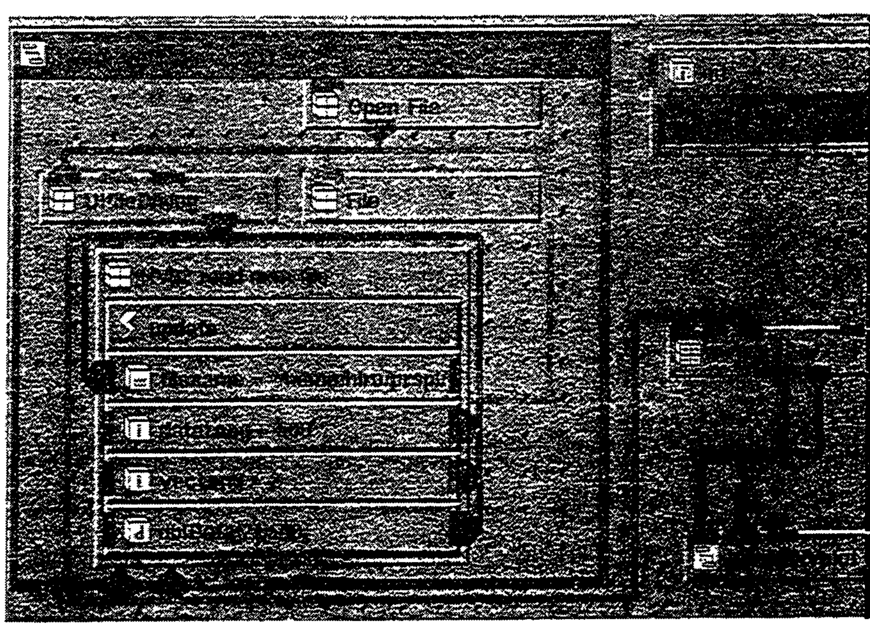

Modules are like

Subroutines because
1) various kinds of data can be passed between modules
2) the data flow can be arbitrarily defined

Processes linked by pipe in unix shell because
1) module can be any compless / big
2) does not need to link together
3) man pages are available

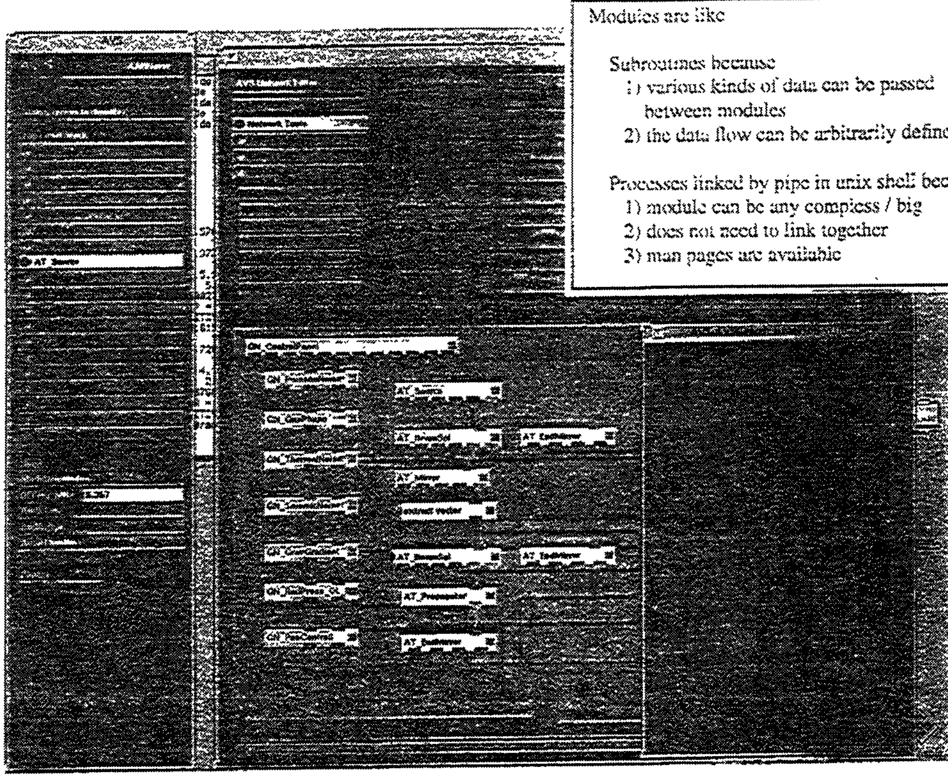

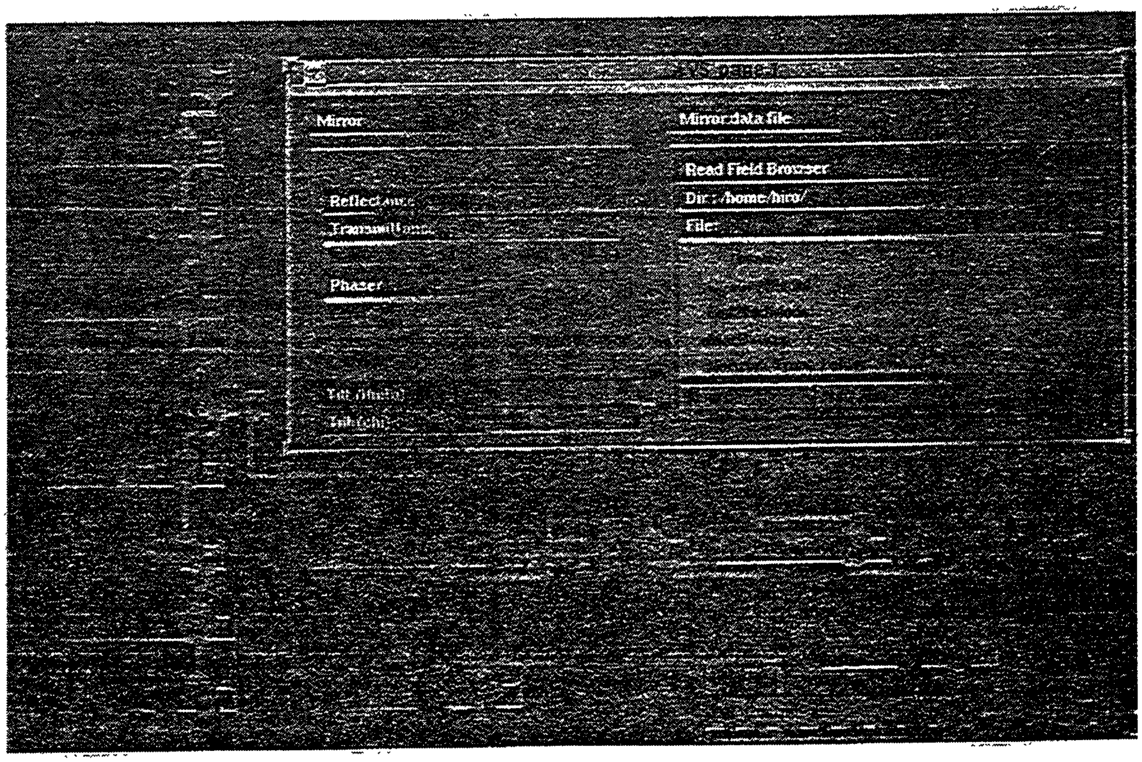

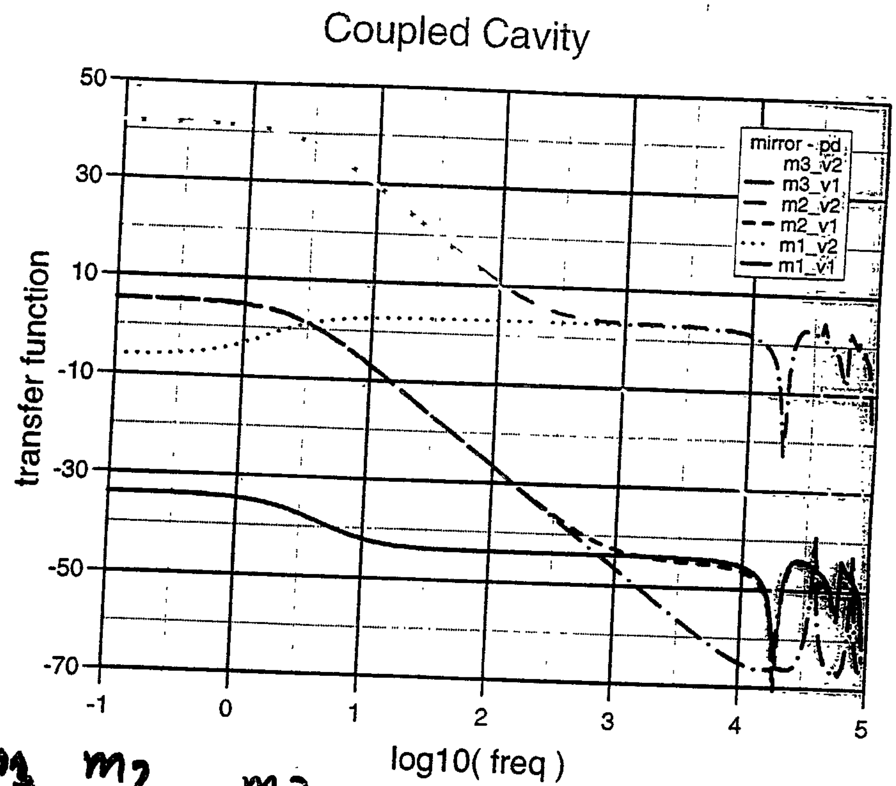

Coupled Cavity
transfer function
log10(freq)
50
30
10
-10
-30
-50
-70
-1
0
1
2
3
4
5
mirror - pd
m3_v2
m3_v1
m2_v2
m2_v1
m1_v2
m1_v1

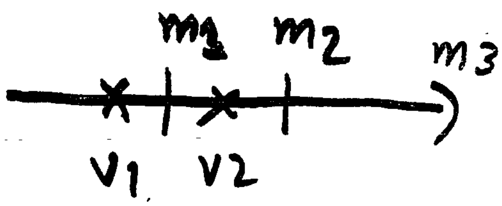

m1
m2
m3
v1
v2

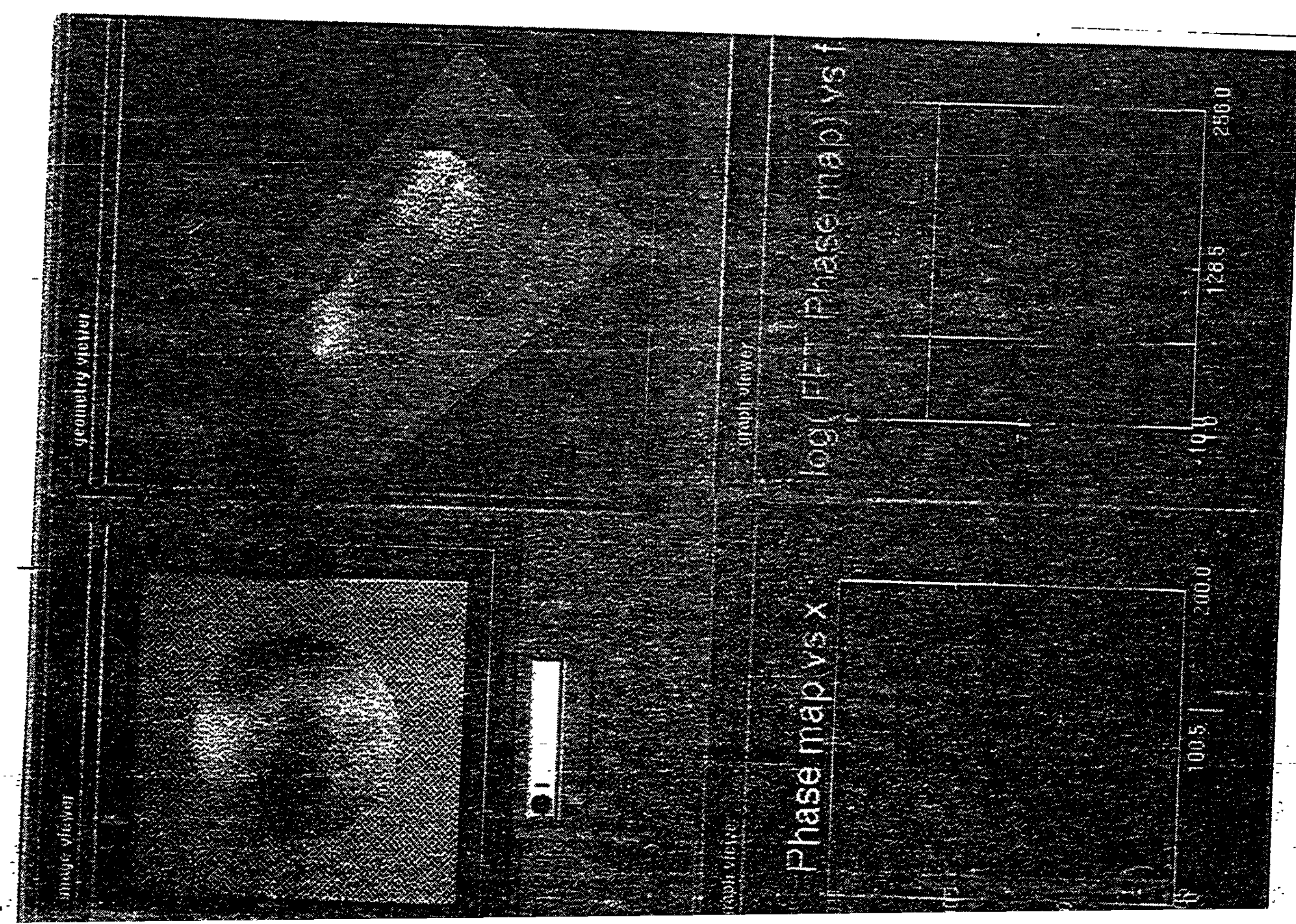

Phase map vs x
log(FFT Phase map) vs f
geometry viewer
graph viewer
256.0
128.5
200.0
100.5

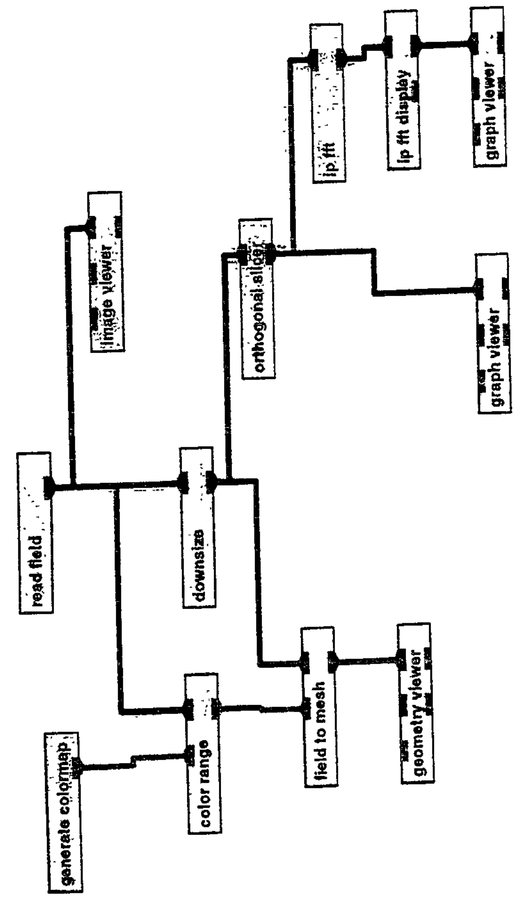

AVS
- how to use -

- End user
  - >>Use AVS module without modification
  - >>Custom-made interface - easy to use
- Network programmer
  - >>Use network editor to build network and use
  - >>Object Oriented feature allows very flexible programming
  - >>Build IFO using Twiddle, define what to measure
- Low level programmer
  - >>Extend/create modules using C/C++/Fortran
  - >>Object Oriented Application Framework makes it easy to combine work done independently
  - >>Build IFO model, implement noise, then build End-to-End model

Modeling and simulation environment using AVS

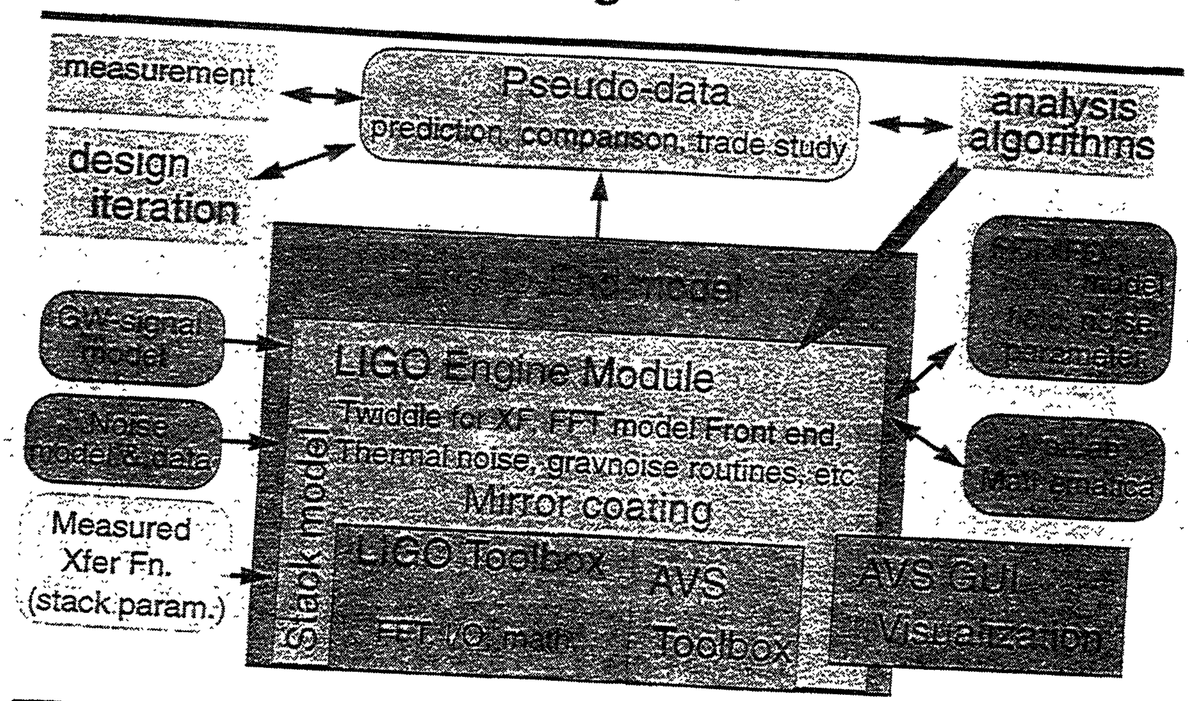

Friday AM Data Analysis III. Pulsar and Other Periodic Source Searches
Stochastic Background Searches

January 19 Chair: F. Raab

8:00	D. Nicholson (Cardiff)	Realistic Search of One Year's Data
8:30	Discussion	
8:40	G. Jones (Cardiff)	Results of a Practical Search of a Large Patch of Sky for a Pulsar-type Signal
9:10	Discussion	
9:20	Coffee Break	
9:30	B. Allen (Milwaukee)	Stochastic Background Searches
10:00	Discussion	
10:10	R. Fakir (UBC)	The GAP Concept
10:15	Discussion	

D. Nicholson, Aspen Jan 14-21 1996

ANALYSING INTERFEROMETER DATA (~1yr) FOR CONTINUOUS WAVE SOURCES

B. Schutz, G. Jones, DN

University of Wales, Cardiff, UK

- targetted searches
- wideband search across the sky
- open issues

TARGETTED SEARCHES

① Selected radio pulsars (Crab, J0437-4715)

- f_{gw}, (θ, φ) known
- analysis is 'straightforward'

— data compression] complex heterodyning
— Doppler demodulation] (MPQ group)
— Fourier transform
— statistical peak search

- no severe computational demands

② Massive X-ray binary systems

- f_{gw} unknown, (θ, φ) known
- analysis significantly more difficult !

— Doppler demodulation
— wideband FFT of very long time-series
— statistical peak search

- enormous computational demand on memory

Options:

→ slice time-series into $M \times L$ $(= N)$ chunks
operation count : $M \cdot N \log_2 N$ (slow !)
→ incoherent FT (loss in sensitivity)
→ process data on a parallel machine
operation count : $N \log_2 N + N$] v. efficient !
+ 1 communications burst

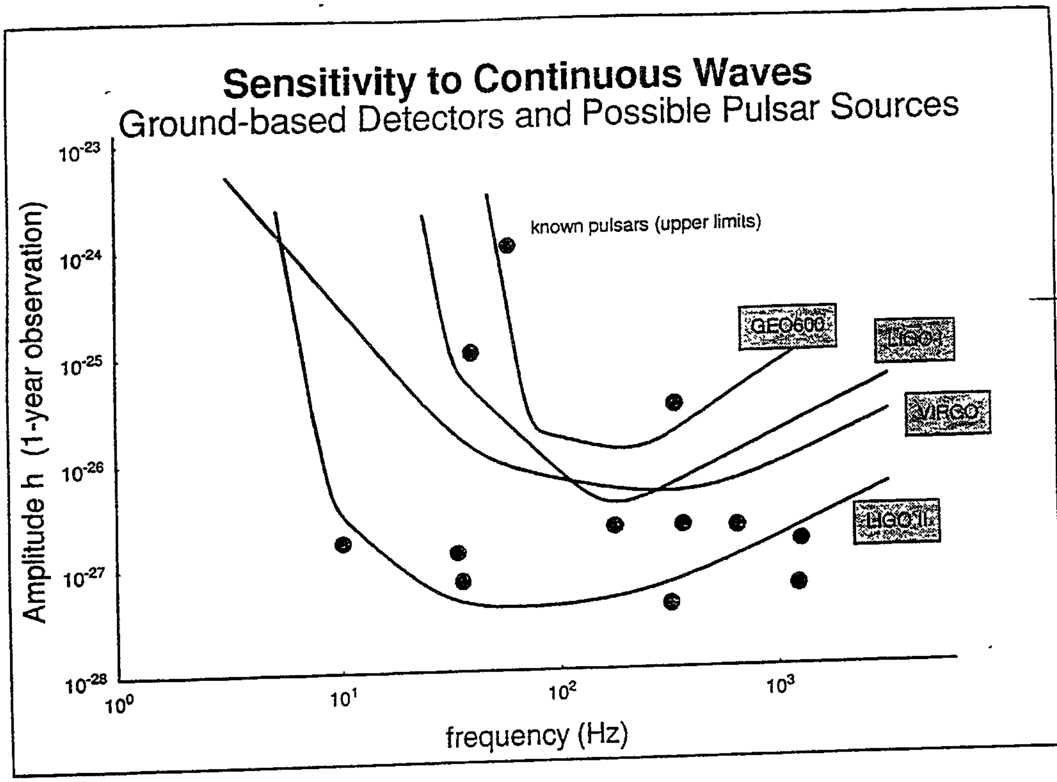
Sensitivity to Continuous Waves
Ground-based Detectors and Possible Pulsar Sources
known pulsars (upper limits)
GEO600
LIGO I
VIRGO
LIGO II
Amplitude h (1-year observation)
frequency (Hz)

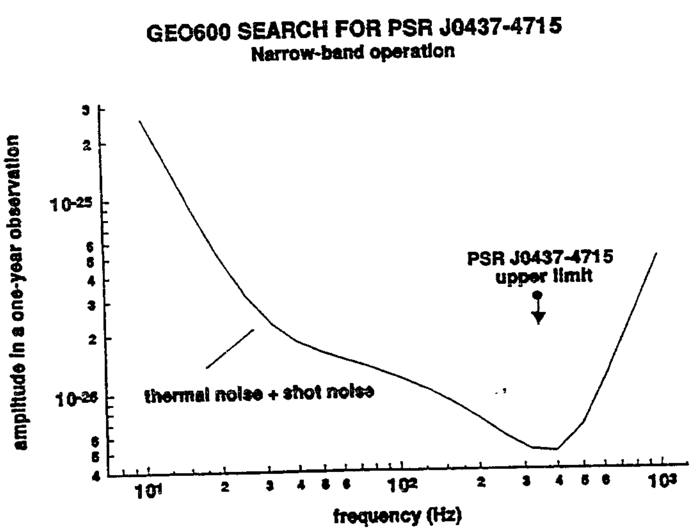
GEO600 SEARCH FOR PSR J0437-4715
Narrow-band operation
PSR J0437-4715
upper limit
thermal noise + shot noise
amplitude in a one-year observation
frequency (Hz)

ALL SKY/FREQUENCY SEARCH

- f_{gw}, (θ, φ) unknown
- analysis looks outrageously difficult

— no symmetry in Doppler motions

Angular resolution: ($T_{obs} \gtrsim$ 2 days)

$$\Delta\theta = 1 \times 10^{-6} \left(\frac{f}{1\,\mathrm{kHz}}\right)^{-1} \left(\frac{T_{obs}}{10^7\,\mathrm{s}}\right)^{-2}$$

$$N_{patch} = \frac{4\pi}{(\Delta\theta)^2} \sim 10^{13} \left(\frac{f}{1\,\mathrm{kHz}}\right)^{2} \left(\frac{T_{obs}}{10^7\,\mathrm{s}}\right)^{4}$$

Computational costs:

- search patches by 'stepping around the sky' (Schutz)

$$\tilde{S}_b(f_b', \theta', \varphi') = \int_{-\infty}^{\infty} \tilde{S}_b(f_b, \theta, \varphi)\, q(\theta', \varphi', f_b'; \theta, \varphi, f_b)\, df_b$$

→ q is a peaked function → sets angular resolution

- assume 'stepping' operation count = 10/data point

→ analysis time $T' = 2.5 \times 10^{16} \left(\frac{f}{1\,\mathrm{kHz}}\right)^{3} \left(\frac{T_{obs}}{10^7\,\mathrm{s}}\right)^{5} \left(\frac{S}{100\,\mathrm{MFlop}}\right)^{-1}$

$\sim \frac{1}{10} H_0^{-1}$!!

→ observation time allowed $= 4.4 \times 10^4 \left(\frac{f}{1\,\mathrm{kHz}}\right)^{-3/4} \left(\frac{S}{100\,\mathrm{MFlop}}\right)^{1/4}$ s.

HIERARCHIAL SEARCH

or chase the signal

- N Gaussian samples of data @ 2kHz, N_{patch}
  Allow 1 false-alarm in the full, wideband search

→ $\tilde{h}$ threshold ~ 11

- Break long time-series into M chunks

  — Doppler demodulations on chunk data
  $N_{patch} \rightarrow N_{patch}/M^4$

  — compute power spectra
  — form incoherent average
  — set $\tilde{h}$ threshold at $\tilde{h}_T/M^{1/4}$
  — statistical peak search
  → candidate f_{gw}, (θ, φ)

- Search full data around f_{gw}, (θ, φ) candidates
- Select M to trade off sky patch size against # false-alarms

  M ~ 35 appears optimal

  allowed observation time ~ 3 months

- possibly we can develop more hierarchial stages
  statistical analysis will not be easy

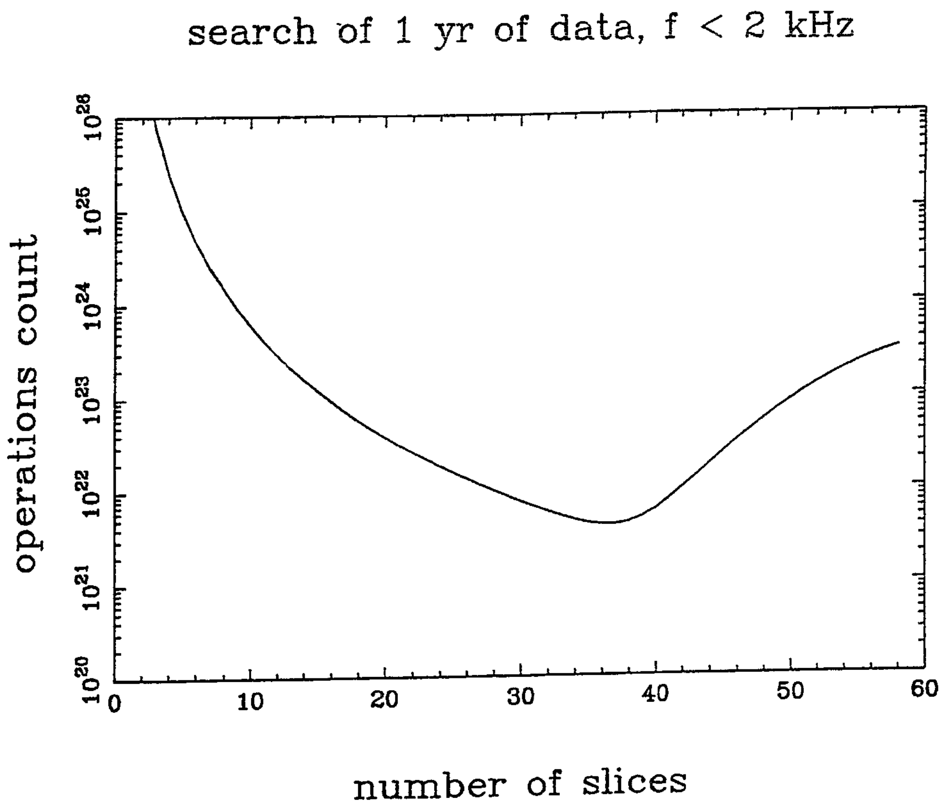
search of 1 yr of data, f < 2 kHz
operations count
number of slices
0
10
20
30
40
50
60

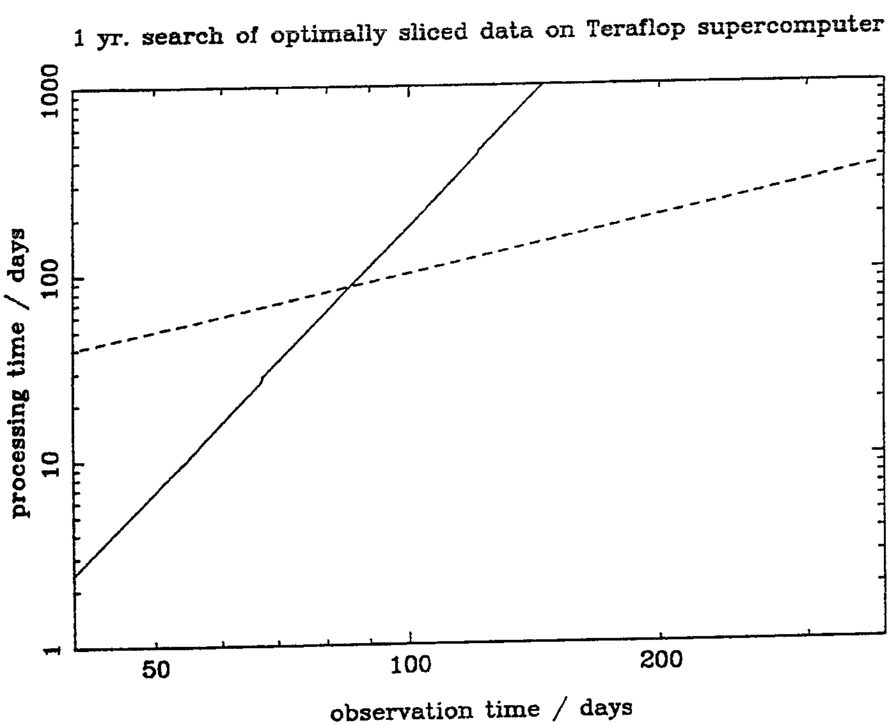
1 yr. search of optimally sliced data on Teraflop supercomputer
processing time / days
observation time / days
1
10
100
1000
50
100
200

OPTIMIZING LONG FT EFFICIENCY

- FT's of very long time-series underpin our analysis.
- LIGO, VIRGO may archive short FT's from on-line analysis
- would these improve efficiency of pulsar searches?

Arrange N samples of data in a matrix:

$$
\begin{array}{c} \\ \downarrow \\ m \end{array}
\overset{\rightarrow n}{\begin{pmatrix} x_0 & x_1 & \cdots & x_{n-1} \\ x_n & x_{n+1} & \cdots & x_{2n-1} \\ \vdots & \vdots & & \vdots \\ x_{n(m-1)} & & & \end{pmatrix}}
\qquad nm = N
$$

1. FT on <u>rows</u> → short FT's forming our start point
2. FT on <u>columns</u> → $C_{b\beta}$ $\quad b \in (0, \ldots n-1)$, $\beta \in (0, \ldots m-1)$

We can show,

$$C_{b\beta} = \sum_c \tilde{X}_{\beta + cm} S_{c-b,\beta} \qquad c \in (0, \ldots n-1)$$

$$\text{where, } S_{c-b,\beta} = \frac{1}{n}\left[\frac{1 - e^{2\pi i (c-b-\beta/m)}}{1 - e^{2\pi i (c-b-\beta/m)/n}}\right]$$

+ <u>suspect</u> 90% accuracy for $0 < \beta < m/4$, $3m/4 < \beta < m-1$

→ half the long FT approximately right

→ big savings: $\log_2 m / \log_2 (mn)$

REALISTIC SEARCH OF ONE YEAR OF DATA (?)

- start with short (archived) FT's aligned along <u>rows</u> of a data matrix
- assign <u>columns</u> to parallel processors
- optimally slice column data
- Doppler demodulate for some (θ, φ)
- FT's on processors
- implement stepping algorithm
- weed out candidate f_{gw}, (θ, φ)'s
- refine search

For $T_{obs} \sim 3 \times 10^7$ s

$T_{analyze} \sim T_{obs}$?

Looks possible with a Teraflop parallel supercomputer

QUESTION – for LRC (SDA)

- A state-of-the-art parallel machine seems essential for pulsar data analysis

- Should LIGO, VIRGO, GEO600 have proprietary machines? Purchase when?

- Long FT's underpin the data analysis

  - special chips can be configured for efficient computation of FT's

  → dedicated pulsar search computers

  → are these preferable

Topics for LRC (SDA)
special interest group ?

Results of a practical search of a large patch of sky for a pulsar-type signal

G.S. Jones, D. Nicholson, B.F.Schutz
Department of Physics and Astronomy, University of Wales College Cardiff
PO BOX 913
CARDIFF

January 13, 1996

Abstract

A method for a search for continuous gravitational waves in data produced by laser interferometers is presented in this talk. An algorithm is shown that can be used to correct for the Doppler shifts introduced by the Earth's accelerations, and that can 'search' many separate positions in the sky without the need of more costly techniques. How this algorithm is implemented is presented.

A new method of compressing data to a heterodyned narrow frequency bandwidth time series is described. This method, called Fourier domain sampling, reconstructs an effectively re-sampled and filtered time series from short period Fourier transforms. As these short period Fourier transforms are produced from the data taken by detectors for other research, then this method is much more efficient than other ways of producing heterodyned narrow frequency bandwidth time series.

These procedures were applied to 100 hours of data taken with the Glasgow gravitational wave detector to search the Large Magellanic Cloud (an area 52 degrees in R.A. and 10 degrees in declination with 171 individual 'patches') and the SN1987A remnant, over a 5Hz bandwidth centred around 934Hz for sources of continuous gravitational waves. No significant evidence was found for sources of gravitational waves of strain amplitudes greater than of order 2×10^{-21} for all the patches searched and no significant evidence was found for sources of strain amplitudes greater than of order 2×10^{-21} for the region about SN1987A taking into account the spin down rate of a pulsar claimed to have been observed.

These results have been presented in Phd thesis 'Search for continuous gravitational wave sources' by Gareth S. Jones

G.JONES@ASTRO.CF.AC.UK
URL: WWW.ASTRO.CF.AC.UK/~Gareth.Jones/

Search for Continuous Gravitational Wave Sources

Talk Plan

- 'pulsar' search
- q kernel
- Data compression
- Application to real data
- Problems to be solved in future

'STEPPING' AROUND THE SKY

1. Correct data for Doppler broadening for a particular region in the sky
2. Fourier transform data
3. Calculate q kernel for step
4. Convolve q with Fourier domain
5. repeat steps 3 and 4

CONVENTIONAL SEARCH TECHNIQUE

1. Correct data for Doppler broadening for a particular region in the sky
2. Fourier transform data
3. Repeat steps 1 and 2

Stepping in Fourier Space

$$\hat{S}_b[f_b', \theta', \phi'] = \int_{-\infty}^{\infty} \hat{S}_b[f_b, \theta, \phi] q(\theta', \phi', f_b'; \theta, \phi, f_b) df_b$$

$$q(\theta', \phi', f'; \theta, \phi, f) =$$
$$exp\left(2\pi i f \tfrac{R_\oplus}{c} \cos\psi(\cos\theta - \cos\theta') + 2\pi i(f - f')(t_o + T_{obs}/2)\right) S$$

$$S = 2 \sum_{k=-\infty}^{\infty} J_k(B) exp\left(-ik\alpha - ik\Omega t_o - ik\Omega T_{obs}/2\right) \frac{\sin(T_{obs}(2\pi(f - f') - k\Omega)/2)}{(2\pi(f - f') - k\Omega)}$$

$$\begin{aligned} A^2 &= \sin^2\theta' + \sin^2\theta - 2\sin\theta\sin\theta'\cos[\phi' - \phi] \\ B &= 2\pi f \frac{R_\oplus}{c} A \sin\psi \\ \alpha' &= \tan^{-1}\left[\frac{\sin\theta''\cos\phi'' - \sin\theta\cos\phi}{\sin\theta''\sin\phi'' - \sin\theta\sin\phi}\right] \end{aligned}$$

FOURIER DOMAIN SAMPLING

1. Fourier transform short periods of data (For coalescing binaries search)
2. Take region of Fourier transform
3. Inverse Fourier transform region
4. Re-combine sections of data, applying phase corrections

COMPLEX HETERODYNE TECHNIQUE

1. Heterodyne data
2. Filter and resample

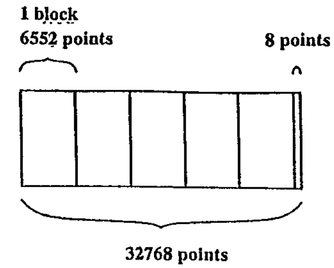

Figure 4.3: Diagram of block structure in a group of data with padded zeros

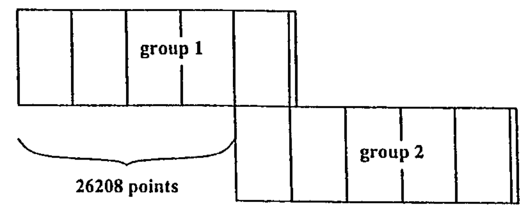

Figure 4.4: Diagram of how consecutive groups contain data from previous group

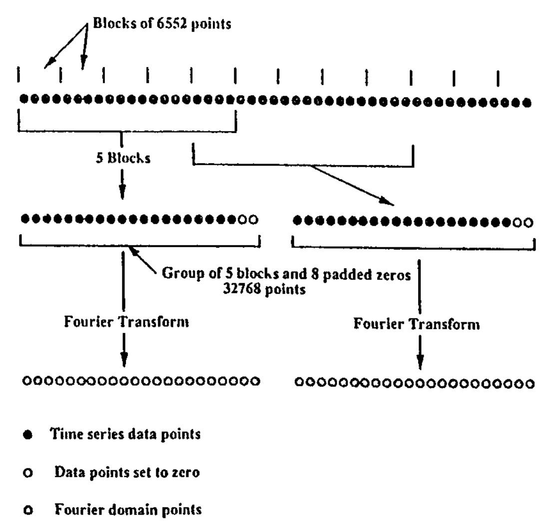

Figure 4.5: Diagram of how Fourier transforms are obtained from the data stream

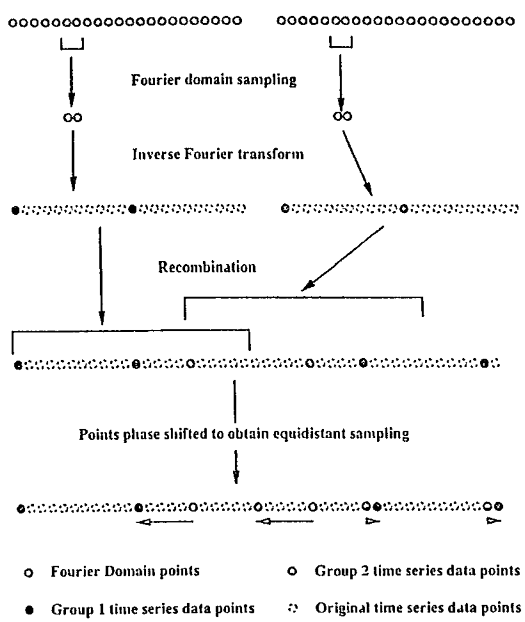

Figure 4.10: Fourier domain sampling and re combination:*a somewhat idealised diagram of how any number of Fourier domain sampling can be used with phase shifts*

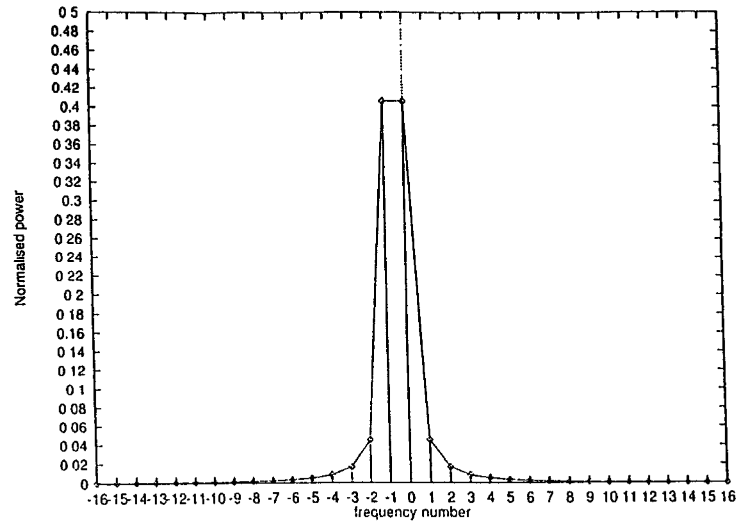

Figure 4.11: Discrete Fourier transform of example signal:*Plot of 32 sample points taken from a Fourier transform sample with a signal present at frequency index of $k_s = -0.5$.*

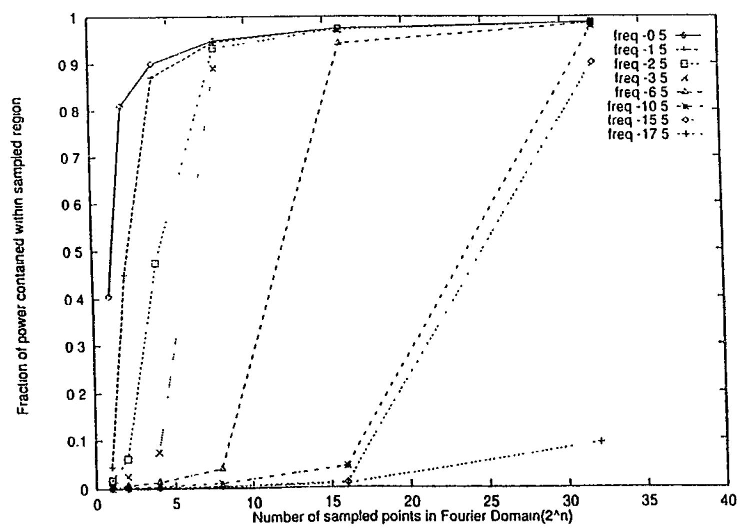

Figure 4.12: Comparison of different compression schemes:*Plot of the amount of power within the sampled region caused by different frequency signals. A signal with frequency outside the region would ideally have no power within it and vice versa.*

GLASGOW 100 HOUR DATA RUN

- DATA TAKEN BETWEEN

2nd MARCH 1989 $22^h\ 51^m\ 41.971^s$
to 6th MARCH 1989 $19^h\ 04^m\ 03.34^s$

SAMPLED AT 20KHz
+ HOUSEKEEPING DATA

SEARCH OF LARGE MAGELLANIC CLOUD

- Data corrected for signals coming from region of SN1987A
- 'Stepping' with q kernel 10 steps away from central patch
- Total of 171 patches examined

SEARCH FOR SN1987A 'PULSAR' SIGNAL

- Data corrected for signals coming from region of SN1987A
- Data corrected for assumed spin-down rate of pulsar frequency
- PREDICTED STRAIN $h \sim 10^{-26}$ (UPPER LIMIT)

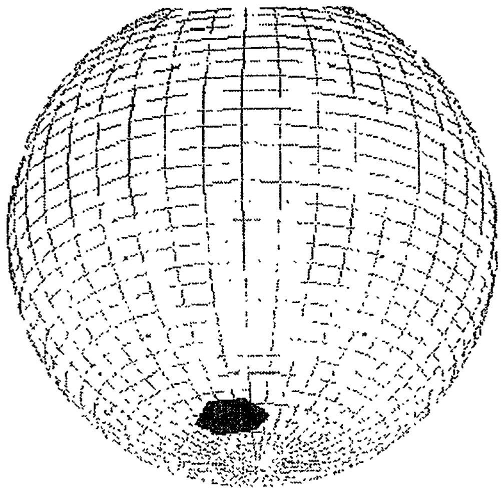

Celestial sphere with area being searched superimposed over it.

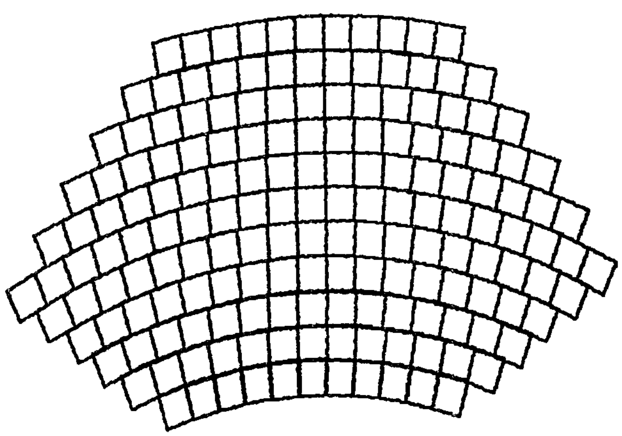

Graphical representation of patches being searched

RESULTS

SN1987A remnant search

- A frequency range of ± 2.5Hz around 934Hz was searched
- Data Doppler corrected for SN1987A
- Data corrected for 'measured' spin-down of 'pulsar'
- The characteristics of the noise about 934Hz was noted
- No significant evidence was found for sources of strain amplitudes greater than a strain amplitude of 2×10^{-21}

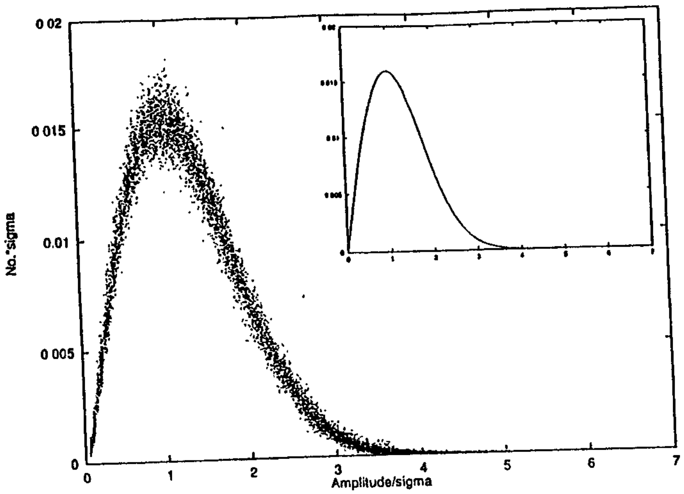

Figure 6.12: Histogram of data from central patch with all corrections for pulsar. *The predicted Rayleigh distribution is shown as the insert.*

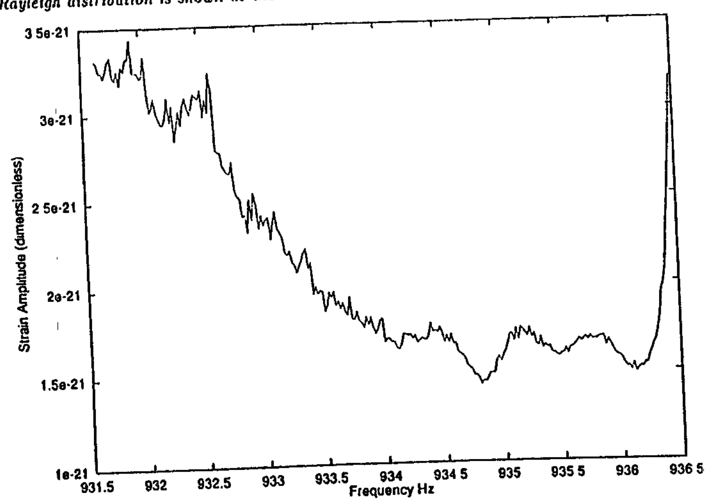

Figure 6.13: Upper limit for non-observed Gravitational waves. *Upper limit for a source of gravitational wave for it not to be detected at a 99% confidence level, corrected fot the SN1987A pulsar.*

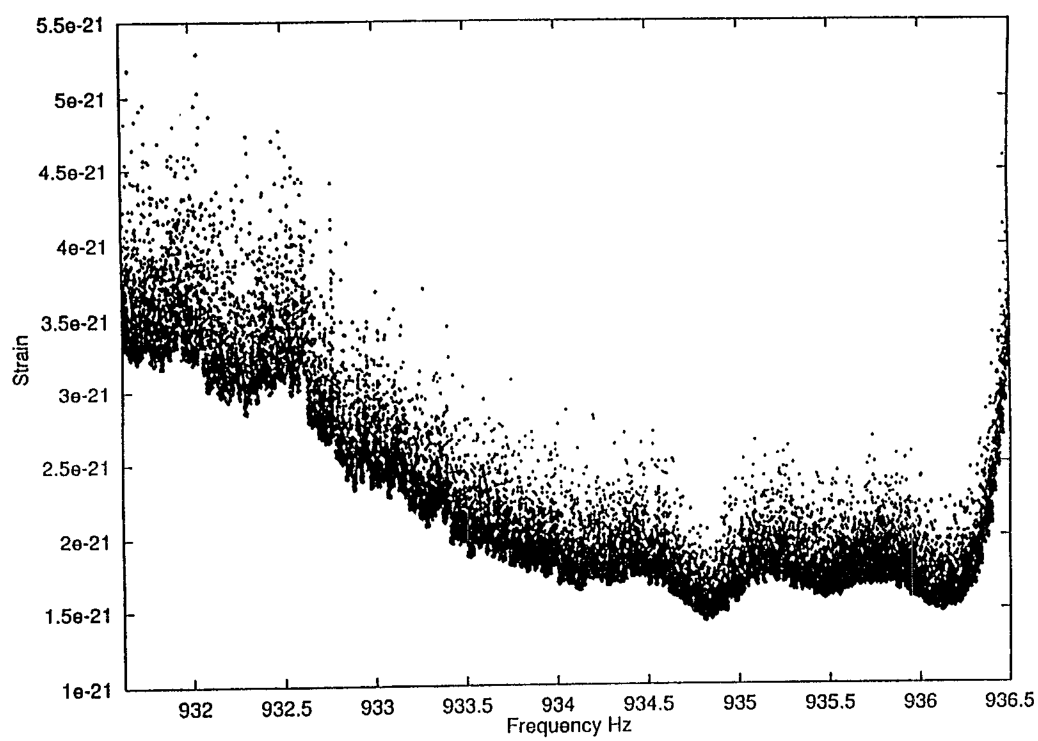

Figure 6.10: Fourier spectrum of data from central patch with all corrections for pulsar.

RESULTS

Large Magellanic Cloud Search

- A frequency range of ± 2.5Hz around 934Hz was searched
- 171 patches were examined covering the entire LMC
- The characteristics of the noise about 934Hz was noted
- No significant evidence was found for sources of strain amplitudes greater than a strain amplitude of 2×10^{-21}

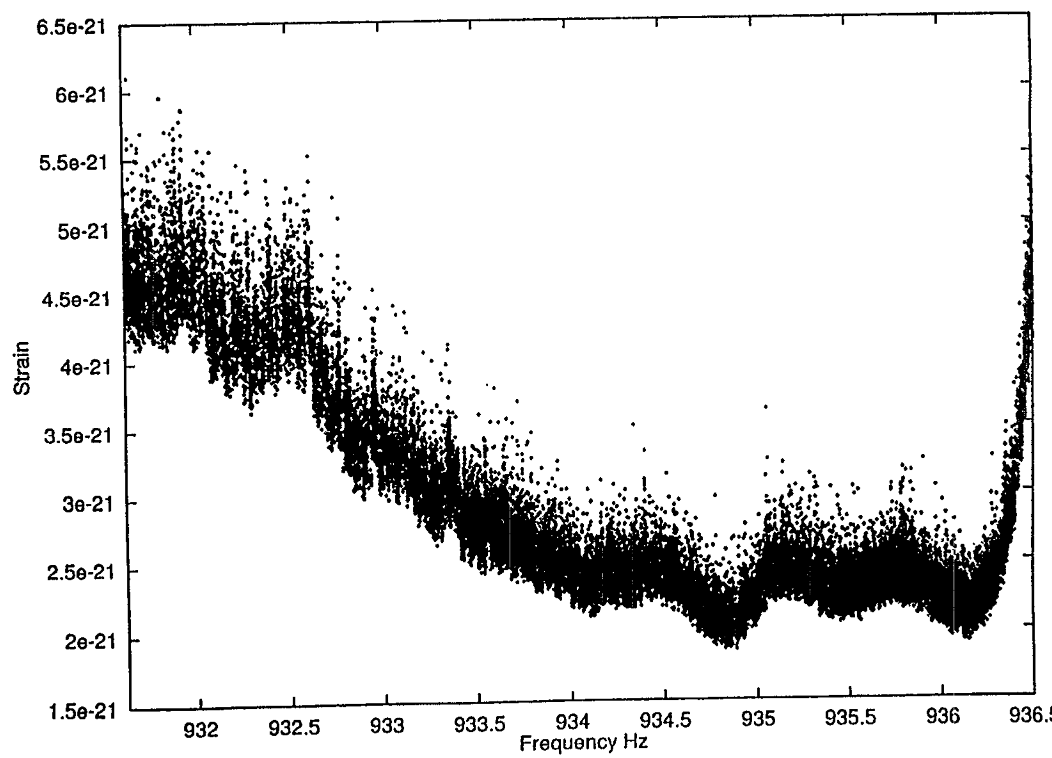

Figure 6.16: Fourier spectrum of data from ALL patches.

Future work

- Current q kernel only valid for times < 100 hours

Searching for unknown sources

- Pulsar spin-down
- Binary system
- Proper motion

Data handling

- Fourier transform averaging
- Use of parallel machines

Aspen
1/19/96

STOCHASTIC BACKGROUND SEARCHES

Bruce Allen
U. Wisconsin - Milwaukee

1. Define Ω_{gw}
2. Some Sources (brief)

---

3. How to detect
4. Optimal Filtering
5. A Data Analysis Pipeline
   What next?

Aspen
1/19/96

STOCHASTIC BACKGROUND SEARCHES

Bruce Allen
U. Wisconsin - Milwaukee

1. Define Ω_{gw}
2. Some Sources (brief)

3. How to detect
4. Optimal Filtering
5. A Data Analysis Pipeline
   What next?

Stochastic Background

Assumed: isotropic, stationary, Gaussian
(isotropic: not essential)

$$\Omega_{gw}(f) = \frac{1}{\rho_{\text{close-universe}}} \frac{d\rho_{gw}}{d\ln f} \quad \text{(dimensionless)}$$

$$h_c(f) = 1.3 \times 10^{-20}\, h \sqrt{\Omega_{gw}(f)} \left(\frac{100\,\text{Hz}}{f}\right)$$

h: Hubble, 100 km sec^{-1} Mpc^{-1}

For comparison consider electromagnetic background (CMBR)

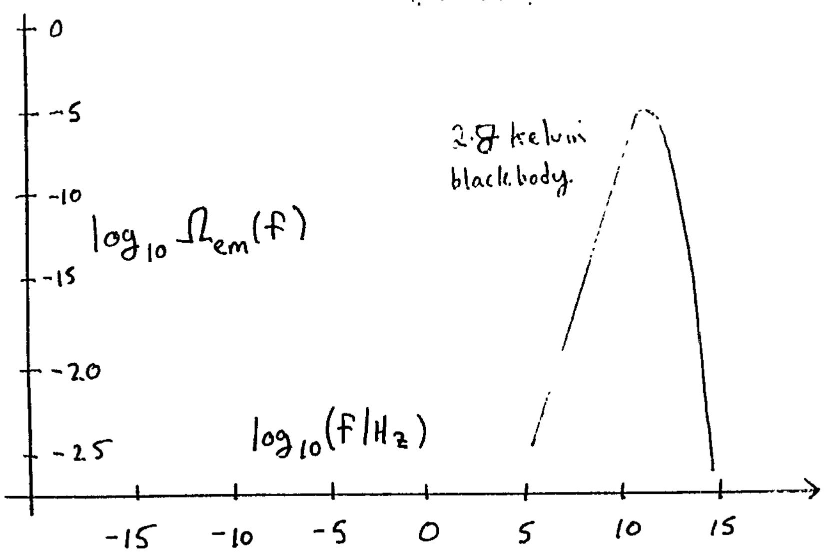

Observational Limits on $\Omega(f)$

nucleo-synthesis: $\frac{\rho_{gw}}{\rho_c} < 10^{-5} \Rightarrow \int_{-\infty}^{\infty} \Omega(f)\, d(\ln f) < 10^{-5}$

pulsar timing: $\Omega\left(f = \frac{1}{10\,\text{yr}}\right) < 6 \times 10^{-8}$

CMBR + COBE: $\Omega < 7 \times 10^{-11} \left(\frac{10^{-18}\,\text{Hz}}{f}\right)^2 \quad 10^{-18}\,\text{Hz} < f < 3 \times 10^{-17}\,\text{Hz}$

Possible Early Universe Sources

"standard" inflation $\Omega \lesssim 10^{-14}$ wide freq. band

cosmic strings: $\Omega < 10^{-9}$ in LIGO band. $\Omega \propto f^{\gamma}$ $\gamma < 0$

First order phase transition: $\Omega < 10^{-6}$, bump in spectrum

"stringy" inflation: $\Omega < 10^{-5}$, slope $\Omega \propto f^3$ in LIGO band

HOW TO DETECT STOCHASTIC BACKGROUND

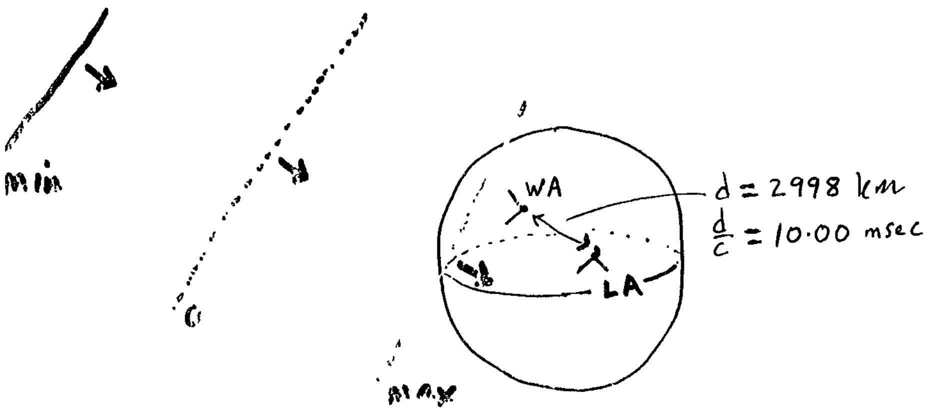

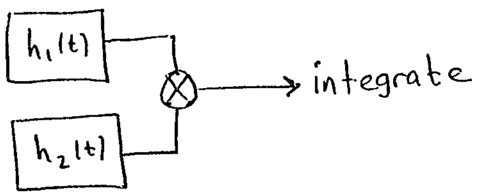

For waves with $\frac{\lambda}{2} > 3000$ km $(f \lesssim 50$ Hz$)$ detector arms move in phase (together) so average product $h_1(t)\, h_2(t) > 0$

In absence of background (and other signals) average product $h_1(t)\, h_2(t) \to 0$.

Michelson, Mon. Not. Roy. Astron. Soc. 227 (1987) 933.
Christensen, Phys. Rev. D46 (1992) 5250.
Flanagan, Phys. Rev. D48 (1993) 2389.

Overlap Reduction Function $\gamma(f)$

Sensitivity reduced by factor γ

(1) non-parallel alignment

(2) separation time delay $\Rightarrow$ signals out of phase

$$\gamma(f) = \frac{5}{8\pi}\int d^2\Omega\, e^{2\pi i f \hat{\Omega}\cdot\Delta\vec{x}} \left(F_1^{+} F_2^{+} + F_1^{\times} F_2^{\times}\right)$$

unit vector — detector separation

$$F_1^{+,\times} = \left(X_1^a X_1^b - Y_1^a Y_1^b\right) e_{ab}^{+,\times}(\Omega)$$

defines $\perp$ arms of detector — spin 2 polarization tensor

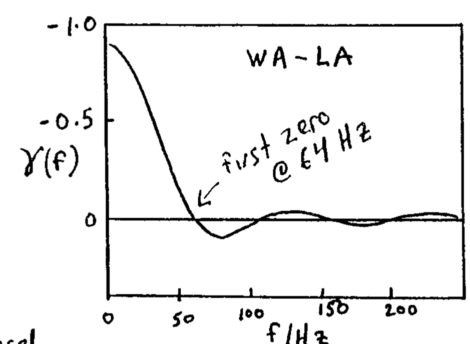

Bessel — detector separation

$$\gamma(f) = A\, J_0(\alpha) + B\,\frac{J_1(\alpha)}{\alpha} + C\,\frac{J_2(\alpha)}{\alpha^2} \qquad \alpha = 2\pi f|\Delta\vec{x}|$$

A, B, C depend upon arm orientations, constant.

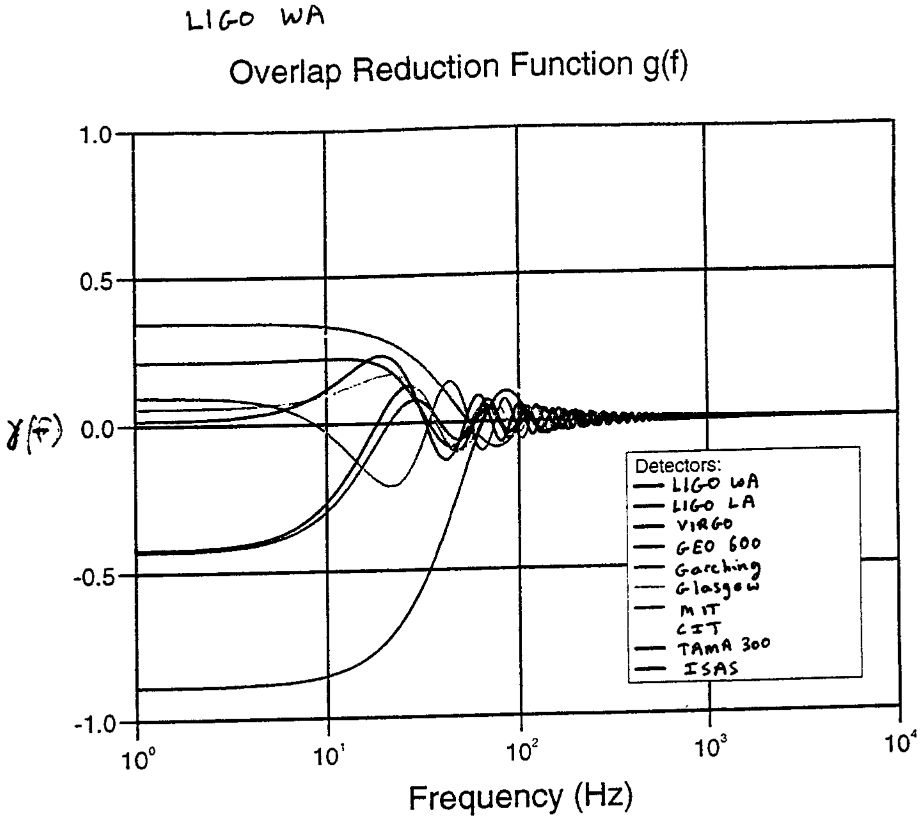
LIGO WA
Overlap Reduction Function g(f)
1.0
0.5
0.0
-0.5
-1.0
γ(f)
10^0
10^1
10^2
10^3
10^4
Frequency (Hz)
Detectors:
LIGO WA
LIGO LA
VIRGO
GEO 600
Garching
Glasgow
MIT
CIT
TAMA 300
ISAS

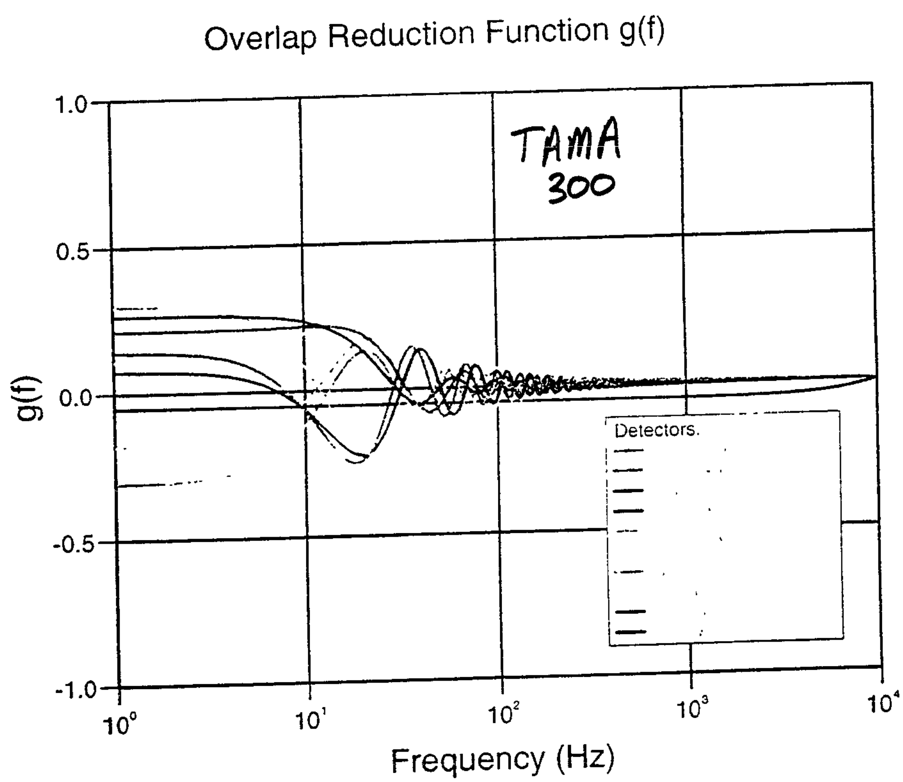
Overlap Reduction Function g(f)
TAMA 300
1.0
0.5
0.0
-0.5
-1.0
g(f)
10^0
10^1
10^2
10^3
10^4
Frequency (Hz)
Detectors.

OPTIMAL FILTERING (Sorry, Sam Frequentist!)

Signal: $S = \int_0^T dt \int_0^T dt' \, h_1(t) h_2(t') Q(t-t')$

WA LA Optimal Filter

Typically $Q(\Delta t) \to 0$ for $\Delta t \gtrsim d/c = 10^{-2}$ sec

Freq Domain $S = \int_{-\infty}^{\infty} df \, \tilde{h}_1(f) \tilde{h}_2^*(f) \tilde{Q}(f)$

Fourier Transform is $\tilde{g}(f) = \int_{-\infty}^{\infty} e^{2\pi i f t} g(t) \, dt$

To find optimal $\tilde{Q}(f)$: assume isotropic + unpolarized source.

Spectral properties of stochastic background, detector noise:

$$\langle \tilde{h}_1(f) \tilde{h}_2^*(f') \rangle = \delta(f-f') \frac{3H_0^2}{10\pi^2} f^{-3} \Omega_{gw}(f) \gamma(f)$$

overlap reduction fn

$$\langle \tilde{n}_i(f) \tilde{n}_j^*(f') \rangle = \delta(f-f') \delta_{ij} S_i(f)$$

label sites: 1 = WA, 2 = LA

detector noise power spectrum

Expected Signal: $\langle S \rangle = \frac{3H_0^2}{10\pi^2} T \int_{-\infty}^{\infty} df \, \gamma(f) f^{-3} \Omega_{gw}(f) \tilde{Q}(f)$

Expected Noise: $\langle N \rangle = 0$

Noise^2: $\langle N^2 \rangle = T \int_{-\infty}^{\infty} df \, S_1(f) S_2(f) |\tilde{Q}(f)|^2$

HOW DO WE CHOOSE $\tilde{Q}$ FOR LARGEST S/N?

OPTIMAL FILTERING (CONT)

Define $(A,B) \equiv \int_{-\infty}^{\infty} df \, A(f) B^*(f) S_1(f) S_2(f)$

Signal $= \langle S \rangle = \frac{3H_0^2}{10\pi^2} \left(\tilde{Q}, \frac{\gamma \Omega_{gw}}{f^3 S_1 S_2} \right) T$

$\langle N^2 \rangle = (\tilde{Q}, \tilde{Q}) T$

Extremize $\langle S \rangle^2 / \langle N^2 \rangle = \left(\frac{3H_0^2}{10\pi^2} \right)^2 T \frac{\left(\tilde{Q}, \frac{\gamma \Omega_{gw}}{f^3 S_1 S_2} \right)^2}{(\tilde{Q}, \tilde{Q})}$

Solution (Optimal Filter) $\boxed{\tilde{Q} = \frac{\gamma \Omega_{gw}}{f^3 S_1 S_2}}$

$$\left(S/N \right)^2 = \frac{9H_0^4}{100\pi^4} T \int_{-\infty}^{\infty} df \frac{\gamma^2(f) \Omega_{gw}^2(f)}{f^6 S_1(f) S_2(f)}$$

H_0 = Hubble expansion rate, sec^{-1}
T = integration time, sec
$\gamma(f)$ = overlap reduction function
$\Omega_{gw}(f)$ = fractional energy-density in GW
$S_i(f)$ = noise power, Hz^{-1} = sec

$T = 4$ month, $S(f)$ = Science '92

$\Omega_{gw\,min} = \frac{5.1 \times 10^{-6}}{h^2}$ (initial) $\frac{5 \times 10^{-11}}{h^2}$ (advanced)

OPTIMAL FILTER (INITIAL LIGO)

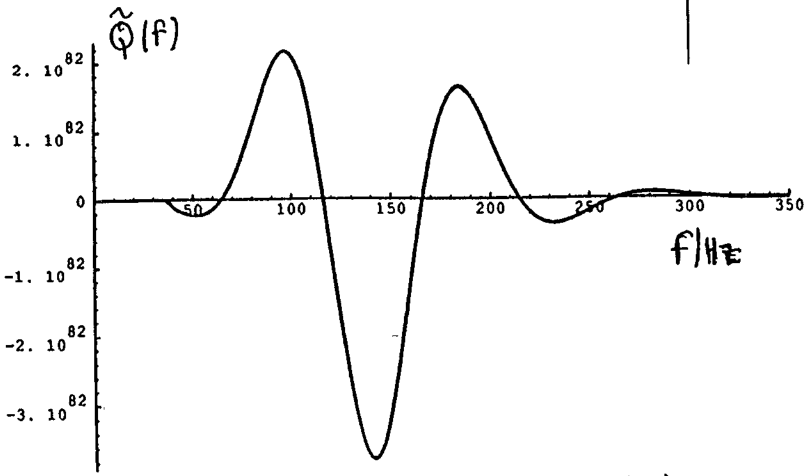

Initial LIGO optimal filter $\tilde{Q}(f) = \dfrac{\gamma(f)}{f^3 S_1(f) S_2(f)}$

Expected signal $\tilde{S}(f) = \dfrac{\gamma^2(f)}{f^6 S_1(f) S_2(f)}$

For $\Omega \sim f^0$

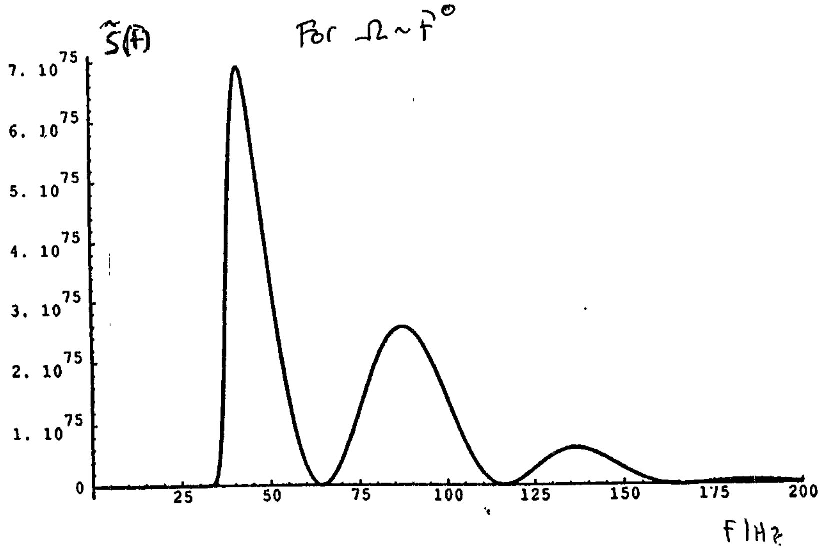

OPTIMAL FILTER (ADVANCED LIGO)

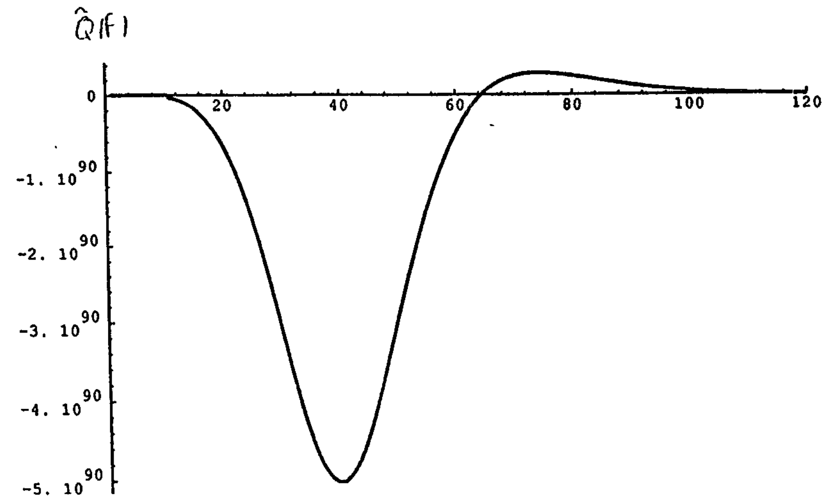

Advanced LIGO optimal filter $\tilde{Q}(f) = \dfrac{\gamma(f)}{f^3 S_1(f) S_2(f)}$

Expected signal $\tilde{S}(f) = \dfrac{\gamma^2(f)}{f^6 S_1(f) S_2(f)}$ for $\Omega \sim f^0$

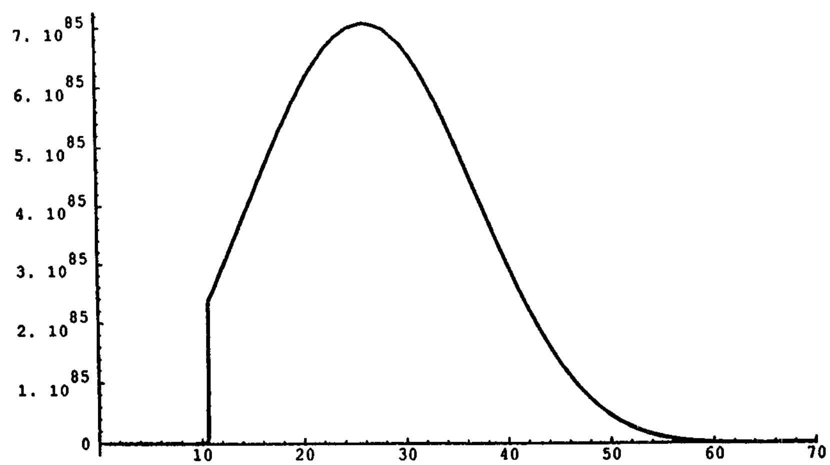

OPTIMAL FILTER (ADVANCED LIGO)

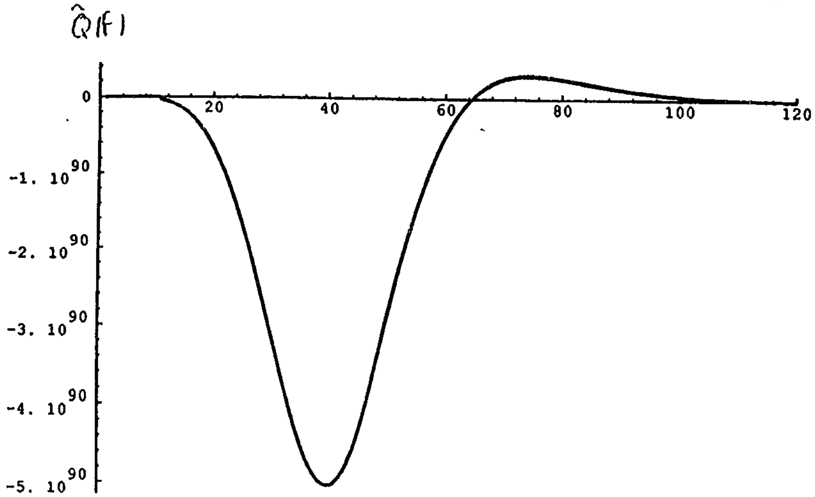

Advanced LIGO optimal filter $\tilde{Q}(f) = \dfrac{\gamma(f)}{f^3 S_1(f) S_2(f)}$

Expected signal $\tilde{S}(f) = \dfrac{\gamma^2(f)}{f^6 S_1(f) S_2(f)}$ for $\Omega \sim f^0$

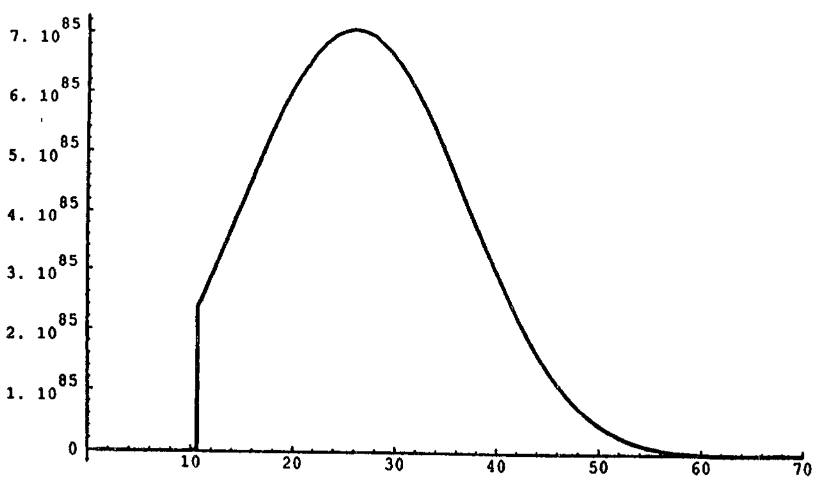

Data Analysis Pipeline (+ simulated data)

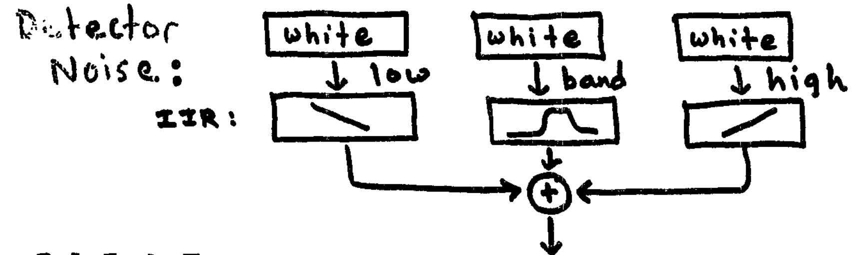

Stochastic Background:

(1) choose random sources on celestial sphere.
(2) generate time domain signals $h_+, h_\times$
(3) find time delay Δt between detectors
(4) add $h_+ F_+ + h_\times F_\times$ into output data streams

ANALYSIS:

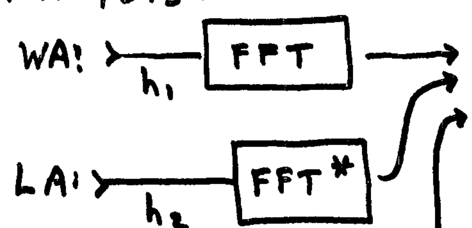

Signal $= \sum_i \tilde{h}_1(f_i)\tilde{h}_2^*(f_i)\tilde{Q}(f_i)$

$\downarrow$

Statistical Analysis of Signals

Filter: $\tilde{Q} = \dfrac{\Omega(f)\gamma(f)}{f^3 S_1(f) S_2(f)}$

Note: 3.28 sec = 65,536 samples
filters: predicted vs. on-the-fly
Simulate + Analyze at 1/3 real-time rate

WHAT NEXT:

1. TESTING
2. REDUCED BANDWIDTH
3. USE 40-m NOISE
4. 100 hours Garching/Glasgow data
5. "systematic" corruption, correlated $\overline{B}$
6. ANISOTROPIC stochastic BG
7. NetworKS OF $N > 2$ DETECTORS
8. OPTIMAL SLOPE DETERMINATION
   $\Omega(f) \propto f^{p}$
9. WEIGHTING/REJECTION OF "BAD" DATA

min

The GAP concept

Redouane Fakir

emails and comments → fakir@physics.ubc.ca

Goal: direct, low cost, timely detection of gravity waves at frequency $\lesssim 10^{-2}$ Hz

Limited ambition: individual, galactic, periodic sources only (e.g. not aiming at LISA targets)

Strategy: ∃ excellent, very high precision experiments (already designed or up and running) in astronomy ⟶ turn one or more of these into gravity wave detectors

HOW? →

→ Need to find new effects linking strongly gravity waves to these experiments

Findings:

3 different g.w. detection schemes with (equivalent) sensitivities of 10^{-21} for binary stars and 10^{-26} for neutron stars

(degree of interest ① < ② < ③ below)

① Based on new version of time delay effect (R.F. Phys. Rev. D)

→ could see neutron star waves of $h \sim 10^{-26}$ and $f < 10^{2}$ Hz

Experiment:

- Using existing pulsar timing experiments and possibly existing data sets
- Sensitivity evaluation (precise): awaiting response of pulsar timing experimentalists

(2) New astrometric effect of gw's :
(R.F. Ap.J.)

Periodic shifts in apparent stellar positions of amplitude $\underline{5 \times 10^{-9} \text{ to } 5 \times 10^{-8} \text{ arcsec}}$

- Astrometric experiments :
  - Hipparcos (ESA, completed 1994)
    sensitivity 10^{-4} arcsec for 100 sec integr.
    → potential 10^{-7} arcsec for 3 years
    (fell only 1 order of mag. short of g.w.)
  - GAIA (ESA, approved, partially designed)
    Sensitivity 5×10^{-6} arcsec for 100 sec integr.
    → Potential 5×10^{-9} arcsec for 3 years (Projected 5 years)
    Design to be modified for g.w. detection
  - POINT (NASA, status?)
    Sensitivity 10^{-6} arcsec for 100 sec integrati
    Potential 10^{-9} arcsec for 3 years integrati
    could work as g.w. detector as is

(3) New interstellar scintillation effect of gravity waves :

g.w. modulation of pulsar-interstellar-scintillation-pattern velocities. (Heavily studied since 1970's)

g.w. displacement of pattern : up to 100 km ! → macroscopic effect of gravity waves !

Amplitude of g.w. modulation of pattern speed $\underline{0.1 \text{ to } 1.0 \text{ m/sec}}$

Experiment : measurement of pattern speed mastered and carried out since 1970

Hardware → two radio antennae on the ground.

e.g. Penticton-Jodrell Bank Experiment (1973)

Sensitivity : 100 m/sec for 1000 sec

→ Potential $\underline{0.3 \text{ m/sec for 3 years}}$

5

→ Possible detection of gravity waves with 10^{-5} Hz < f < 10^{-2} Hz from the ground!

→ Not affected by seismic noise in same way)

N.B. Galactic background does not limit detectability of individual sources as it does for LISA.

Epilogue

Several observational astronomy techniques become relevant to gravity wave detection

→ Astronomers to be involved in GAP could become members of L.R.C.

By the way: G.A.P. concept → Gravity wave detection using Astronomical Phenomena

6

From "A macroscopic gravity wave effect" by Redouane FAKIR.. (available upon request fakir@physics.ubc.ca

Figure captions

Figure 1.- Blowup of the double trigger mechanism of scheme 1 leading from the phase modulated intensity $\tilde{I}(t)$ to the amplitude modulated intensity-peak duration $\tau(t)$ to the pulse train $p(t)$, which is to be spectrally analyzed.

Figure 2.- As predicted by eq (2)*, the detection (through scheme 2) of a gravity wave signal of amplitude v_{gw} and angular frequency ω_{gw} buried in random noise of loudness σ is successful all the way up to the realistic range $\sigma \sim 100 v_{gw}$. No period folding or periodigram variance reduction were used.

* eq. (2): $SNR = \frac{1}{\sqrt{3}} \frac{\Delta t}{t_c} \frac{s^2}{\sigma^2} \frac{\tau_0^2}{\sigma^2} \exp\left(-\frac{\tau_0^2}{2\sigma^2}\right)$

Δt: duration of experiment
t_c: $\sim \frac{1}{\text{Nyquist frequency}}$
s: amplitude of signal
σ: r.m.s. size of noise
τ_0: threshold of amplitude modulated data (velocity v_{gw} in scheme 2, peak duration τ in scheme 1).

New gravity wave data processing technique (periodic waves), here applied to toy model of Gaussian white noise.

Seems to perform better than non linear adaptive filtering at least for toy case.

Figure 1

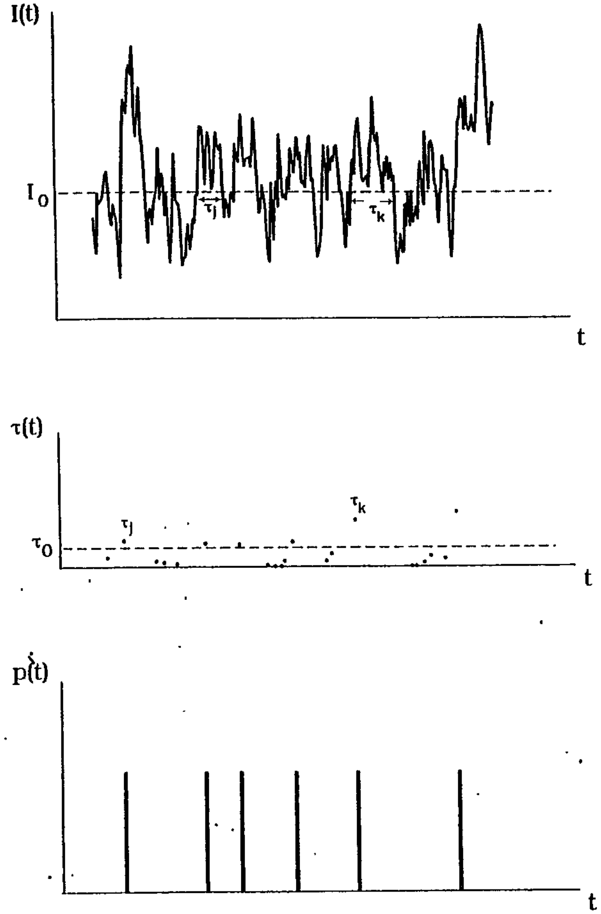

Figure 2

← SNR≈ predicted SNR = $\sqrt{10}$

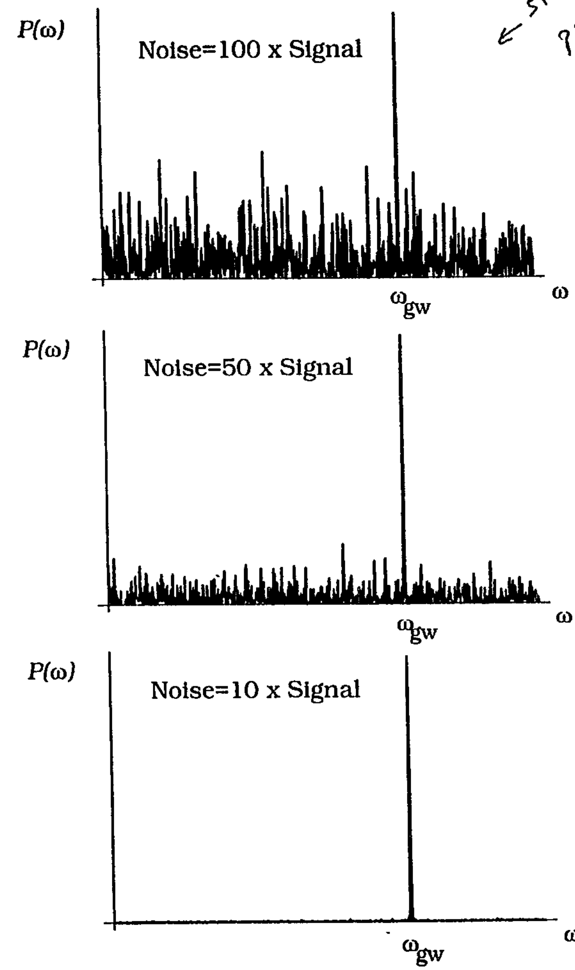

Friday PM January 19	Data Analysis IV. Analysis of Existing and Future Data Chair: N. Robertson	
4:30	D. Nicholson (Cardiff)	Overview of Data Analysis for 100 hour Glasgow-Garching Run **(NO TRANSPARENCY COPIES)**
5:00	Discussion	
5:10	R. Schilling (Garching)	Time Domain Analysis of 100hr Glasgow-Garching Run
5:40	Discussion	
5:50	Coffee Break	
6:05	S. Finn (Northwestern)	Data Analysis for A Network of Interferometers
6:35	Discussion	
6:45	B. Mours (LAPP-Annecy)	Plans for Organizing Data Analysis for Virgo
7:15	Discussion	

Saturday AM January 20	Impulsive Signal Searches, Round Table Chair: K. Thorne	
8:00	D. Nicholson (Cardiff)	Nonlinear Adaptive Filters **(NO TRANSPARENCY COPIES)**
8:30	Discussion	
8:45	Coffee Break	
9:00	S. Finn, W. Johnson A. Krolak, B. Mours, D. Nicholson. D. Shoemaker, R. Stebbins K. Thorne	Round Table on Waveforms and Data Analysis for Stellar Core Collapse and Other Sources
11:00	Conference Adjourns	

(1.)

100 Hour Test Run

2 – 6 March 1989

The main objectives for an extended test run have been:

- to prove that continuous operation of interferometric detectors are possible,
- to test the requirements on the stability of the adjustments and other hardware components,
- to provide long term data that can be analysed for various (non-gaussian) noise contributions,
- to rehearse the logistics of data acquisition, data exchange and archiving,
- and only as an extremly faint possibility the idea of finding some gravitational waves, or some other hidden correlations between the data of distant detectors.

(2)

100 Hour Test Run

2 – 6 March 1989

Total run time	100 hours
Data on tape	**91.34** hours $\mathrel{\widehat{=}}$ $\mathbf{91^h\,20^m\,36^s}$
Total amount of data	**14.5** G bytes in 657 672 records of 22048 bytes each, written on 94 reels of tape (6250 bpi), each tape storing 7200 records (158.7 MB), corresponding to one hour of run time.

Each record represents $^1/_2$ second of data, containing

- 5000 samples of interferometer data,
- 2500 samples of accelerometer data from laser table,
- 1250 samples of accelerometer data from central tank,
- 1250 samples of low frequency interferometer data,
- plus 8 different kinds of housekeeping data, sampled once per each $^1/_2$ second record.

(4)

Housekeeping data

Each 1/2 second record contains the following housekeeping data:

- The actual time from DCF 77,
- A logical signal indicating that the three main servo loops are in lock,
- A signal corresponding to the laser power,
- The low frequency correction signal from the frequency stabilization,
- A signal corresponding to the photocurrent in the diode for the abolute arm length control,
- The low frequency correction signal from the absolute arm length control,
- A signal corresponding to the photocurrent in the diode for the main interferometer output,
- The low frequency correction signal from the armlength difference control.

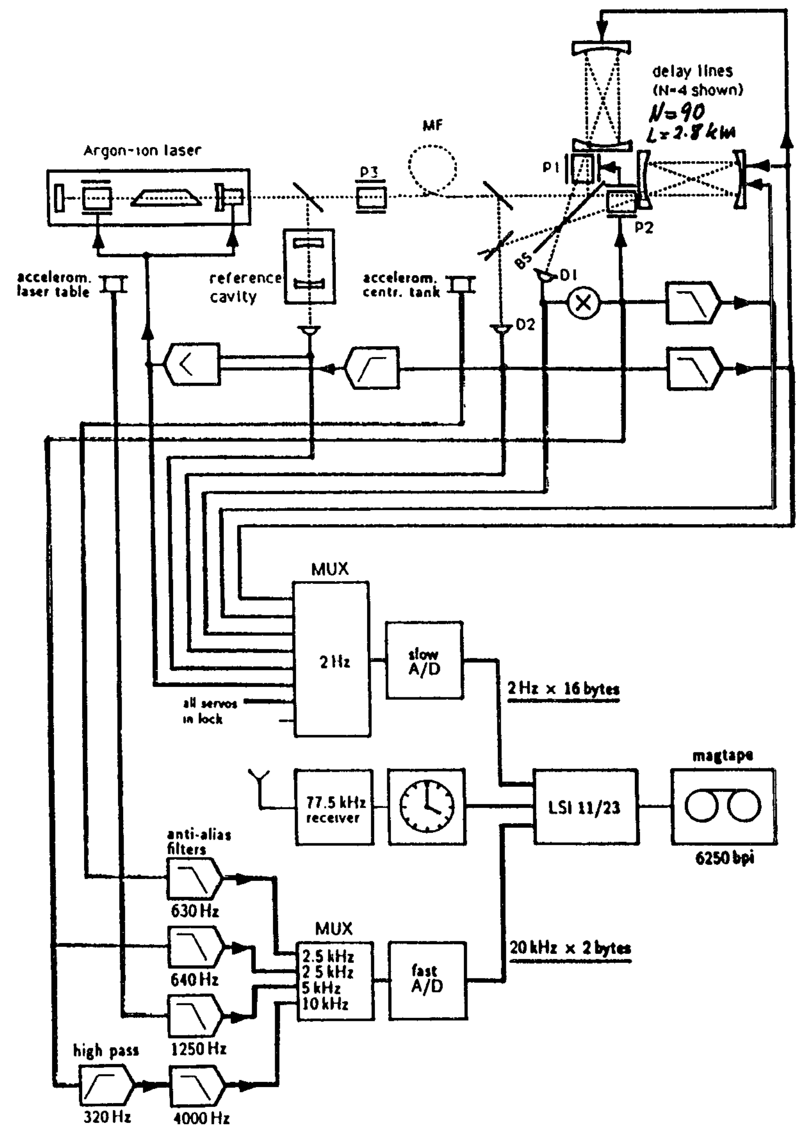

25.04.89 9.25:02

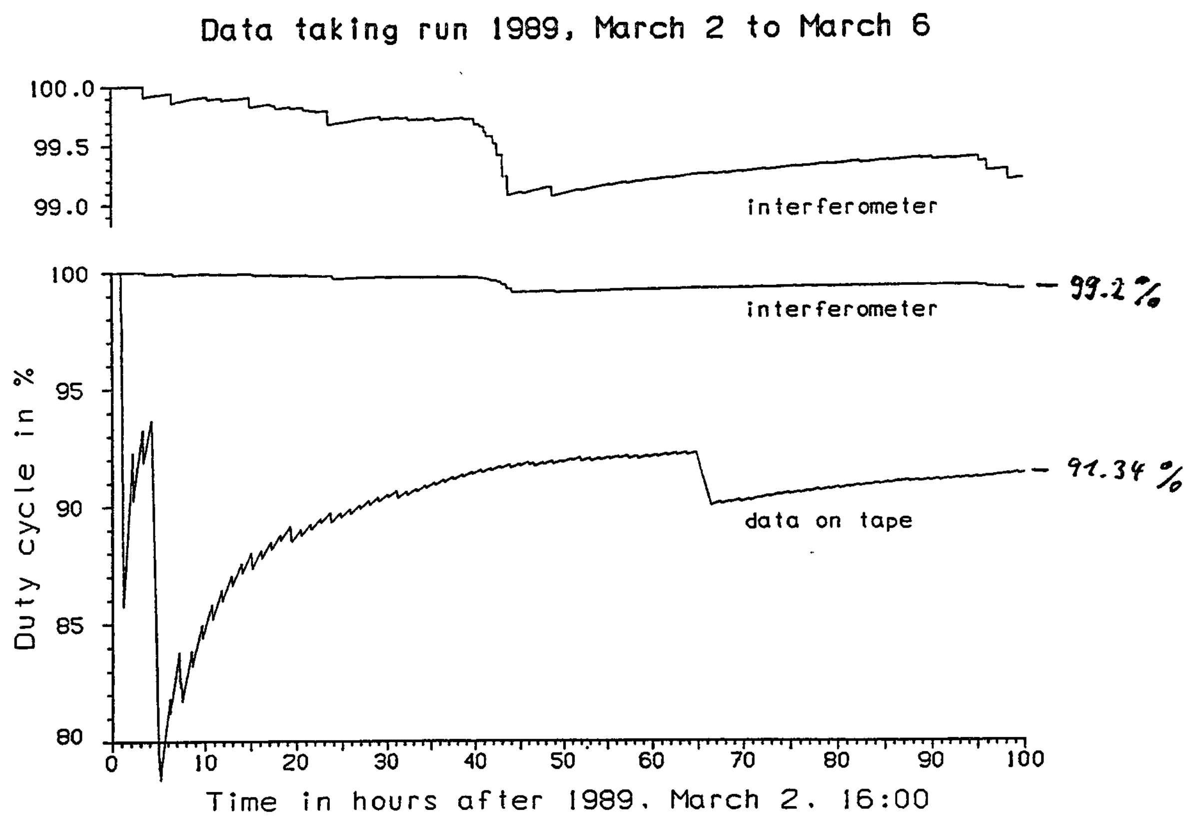

Roland Schilling, MPQ Garching, 12. 1. 1996 – 13:56

6

Investigations of recorded data

We looked at:

- Housekeeping data,
- Noise spectra for selected time slices,
- 1-minute *rms* averages,
- 0.1-second *rms* values of selected time slices,
- Amplitude statistics for selected time slices.

IPP--CMS RUS 2/0001 H1-05 21.04.89 17.25:52

21.04.89 17.24:02

Data taking run 1989, March 2 to March 6 sheet 1

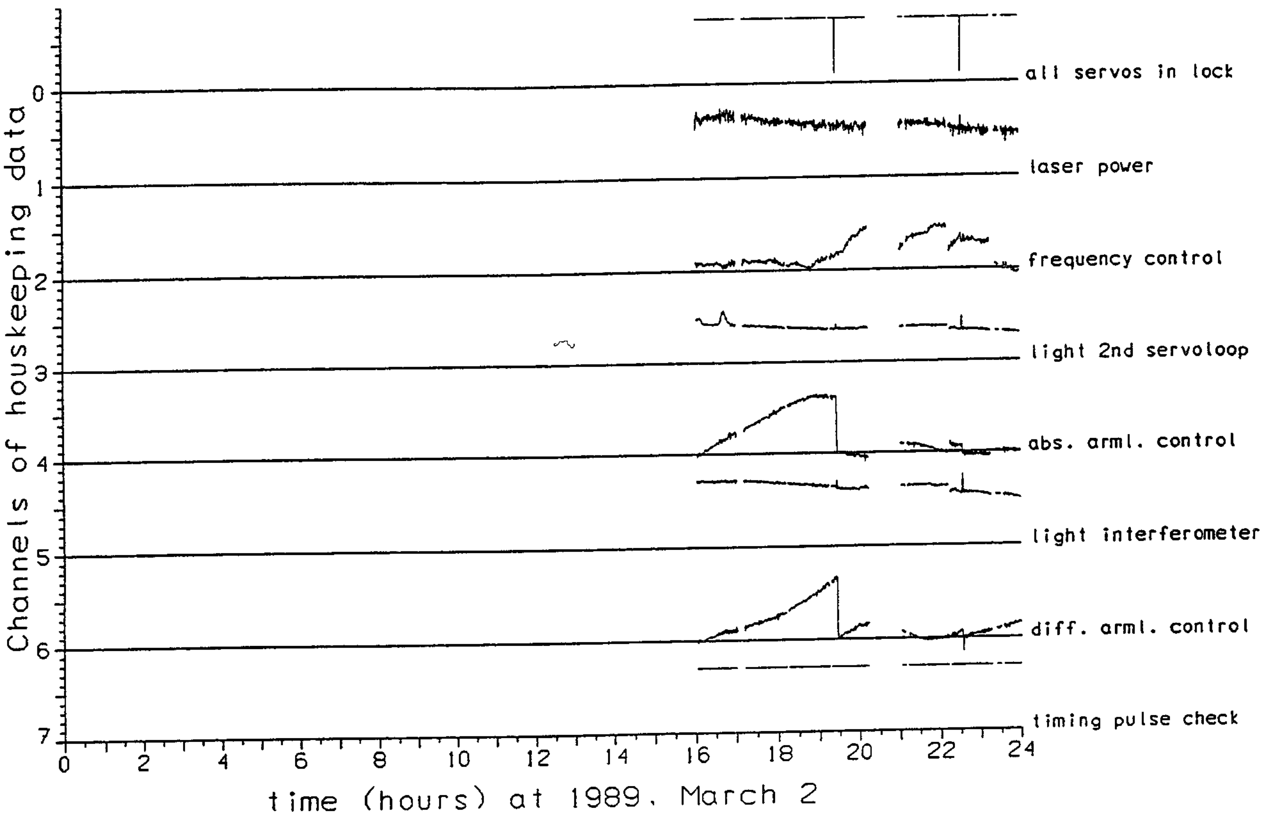

IPP--CMS RUS 3/0002 H1-05 21.04.89 17.26:03

21.04.89 17.24:22

Data taking run 1989, March 2 to March 6 sheet 2

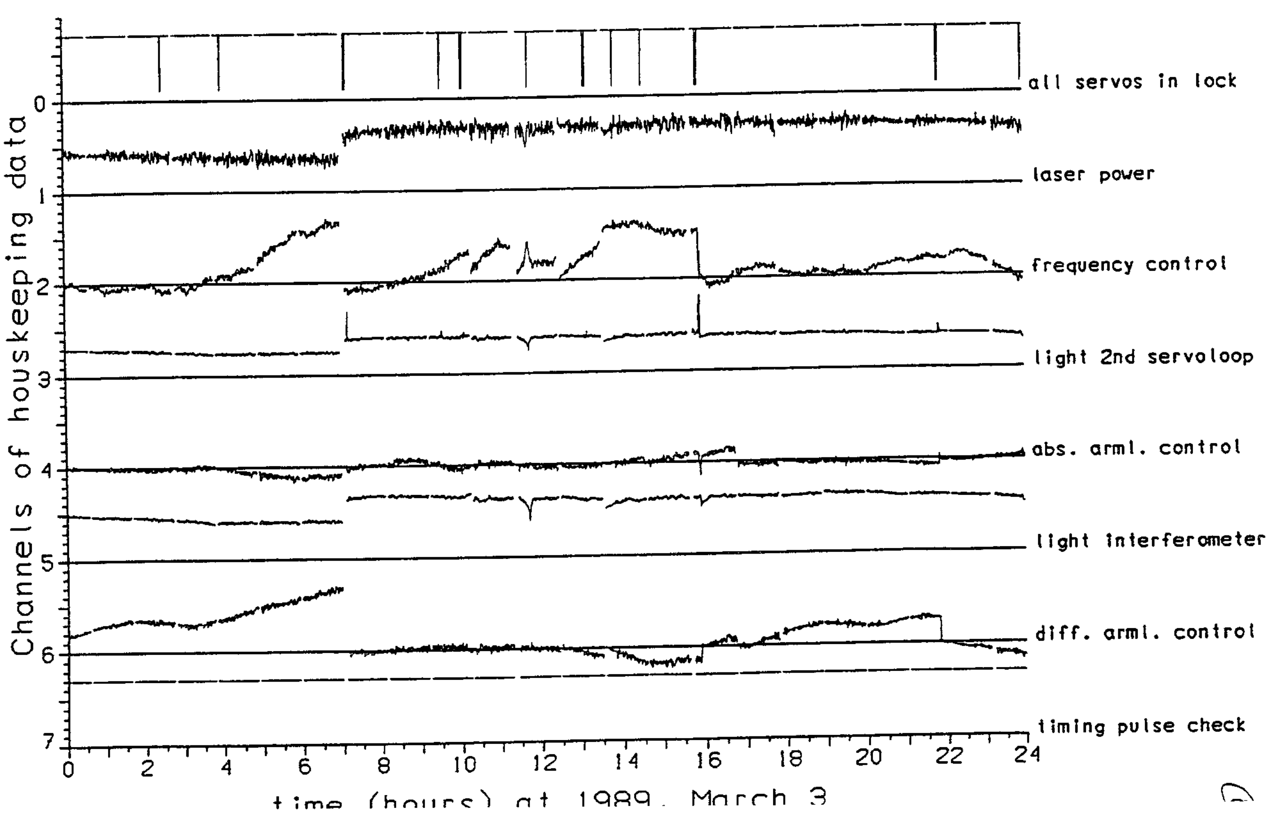

IPP--CMS ROS 4/0003 H1-05 21.04.89 17.26:15
21.04.89 17.24:48

Data taking run 1989, March 2 to March 6 sheet 3

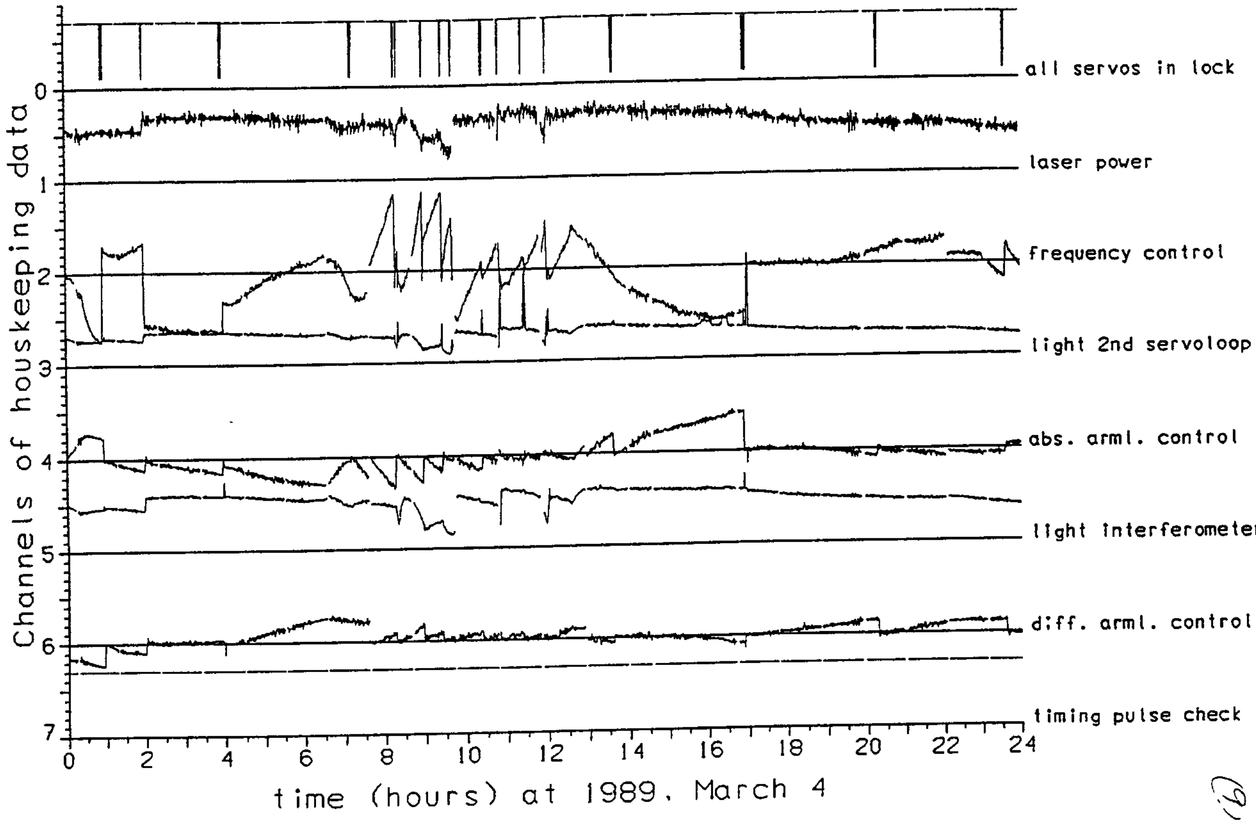

(9)

ROS--CMS SPHOD 1/0001 H1-05 27.03.90 9.06:25
27.03.90 9.05:14

Interferometer Spectrum

Data taking run 1989, March 2 to March 6

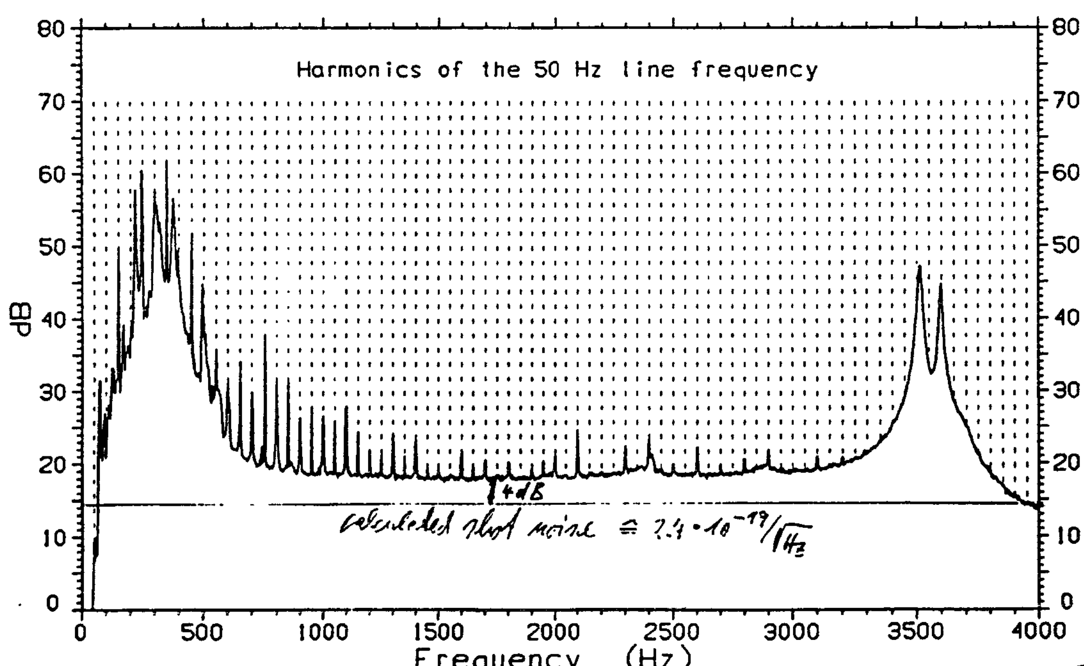

5 min after start

5000 point FFT, averaged over 600 records, starting at tinhs = 1440

IPP--CMS RUS 2/0002 H1-05 31.05.89 12.28:48
31.05.89 12.28:24

Interferometer Spectrum

Data taking run 1989, March 2 to March 6

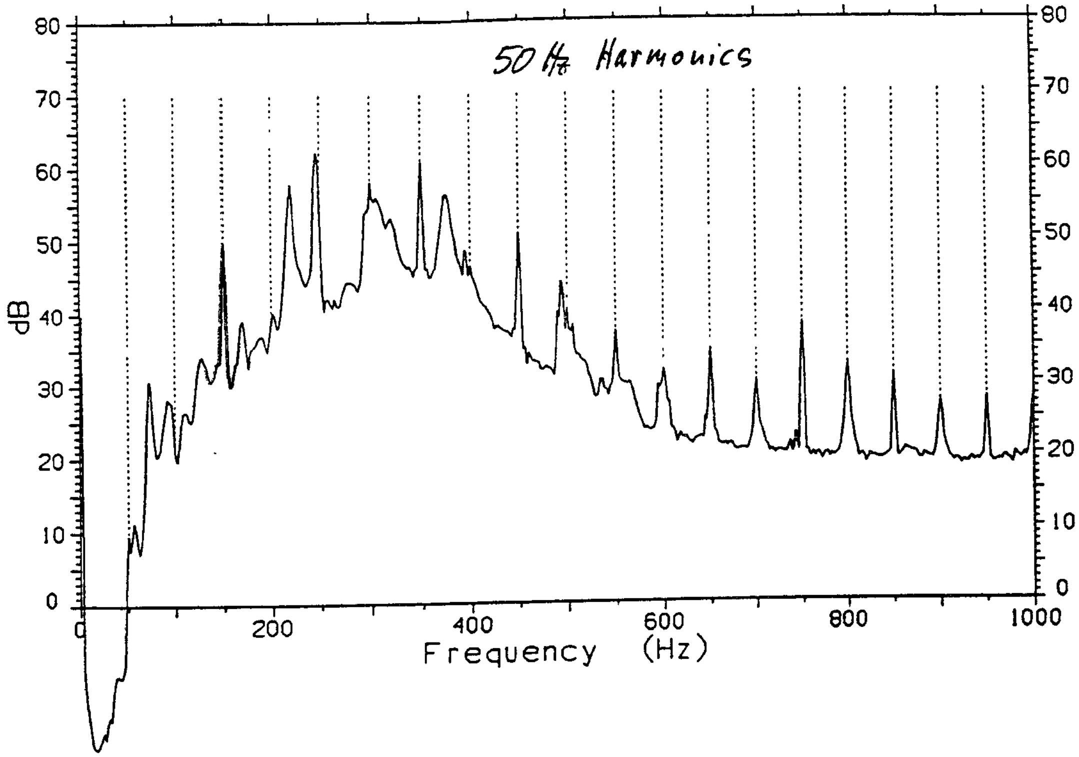

RUS--CMS SPHV 1/0001 H1-05 23.03.90 16.11:37
23.03.90 16.08:13

Data taking run 1989, March 2 to March 6

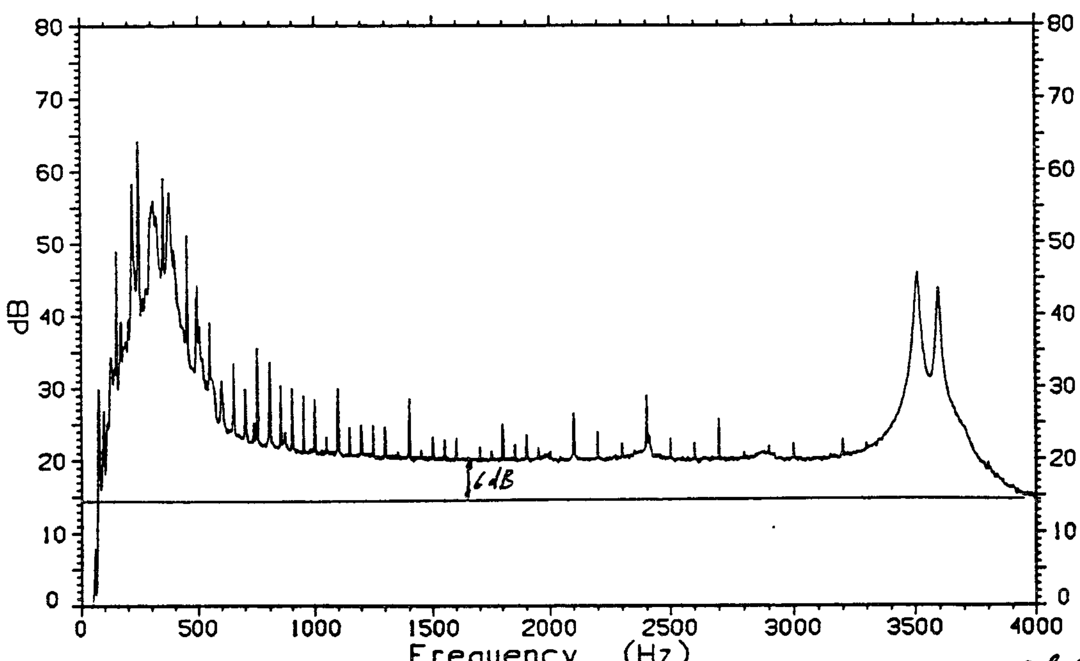

5 h 15 min after start

5000 point FFT, averaged over 600 records, starting at tinhs = 38040

RUS--CMS SPHU 1/0001 H1-05 23.03.90 14.57:48
23.03.90 14.54:07

Data taking run 1989, March 2 to March 6

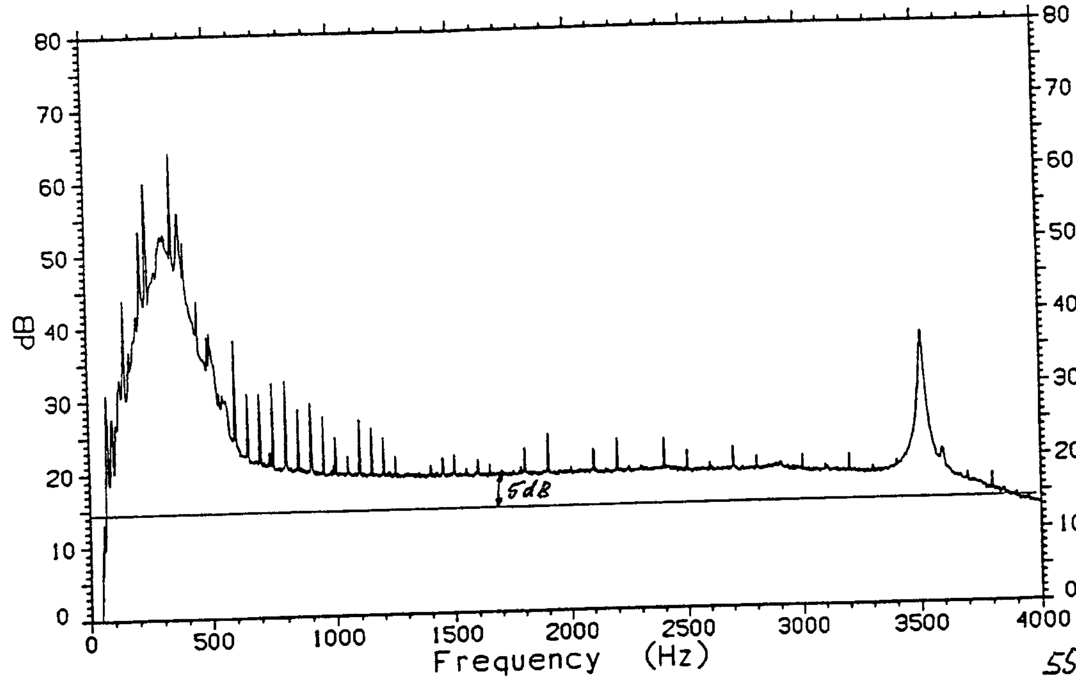

55 h 38 min after start

5000 point FFT, averaged over 600 records, starting at tinhs = 400800

17332?

RUS--CMS SPHU 1/0001 H1-05 23.03.90 15.07:36
23.03.90 15.00:29

Data taking run 1989, March 2 to March 6

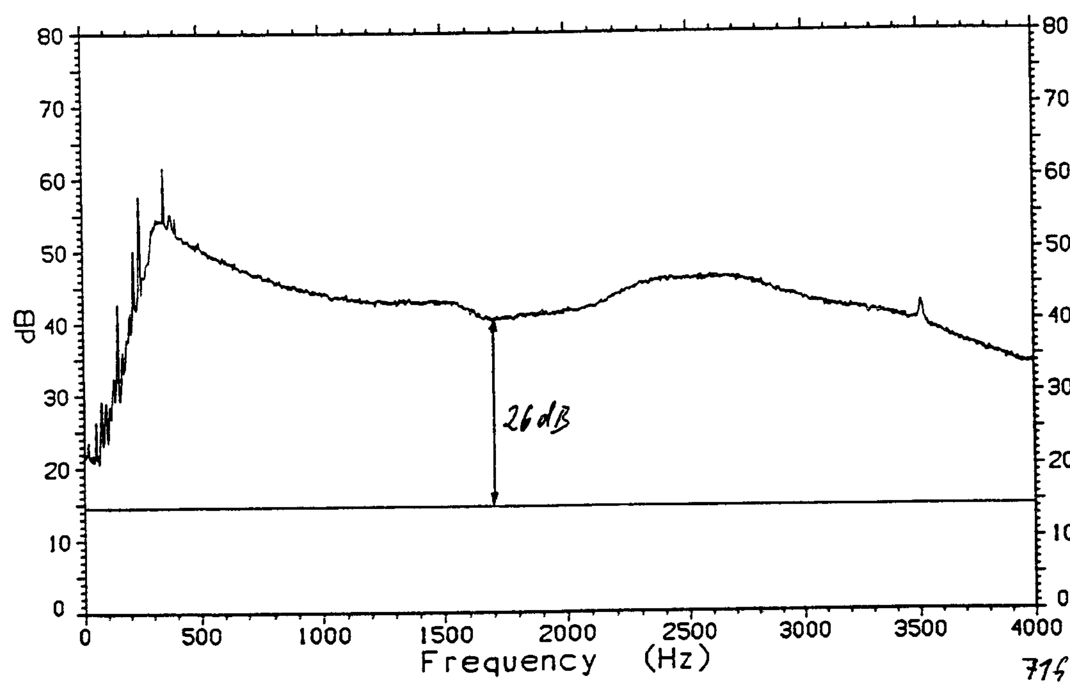

71 h 49 min after start

5000 point FFT, averaged over 600 records, starting at tinhs = 517320

Accelerometer Spectra

Data taking run 1989, March 2 to March 6

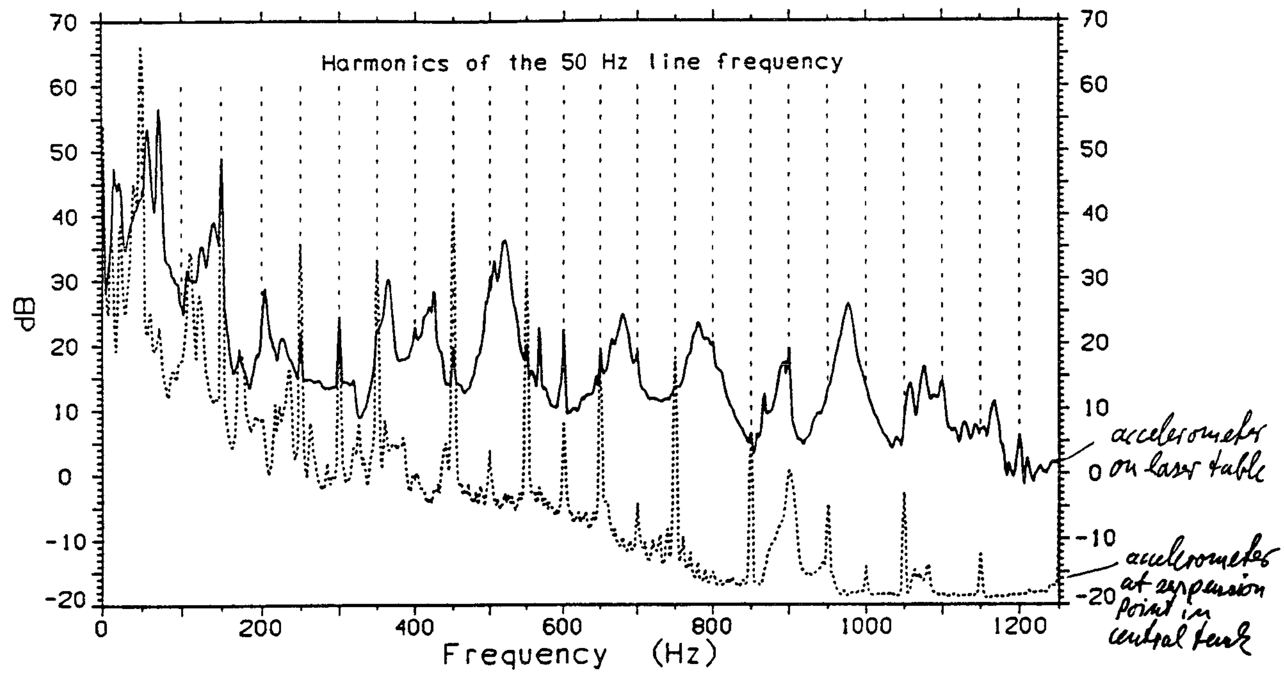

2500 point FFT, averaged over 600 records, starting at tinhs = 1440

08.05.89 14.42:14

Data taking run 1989, March 2 to March 6

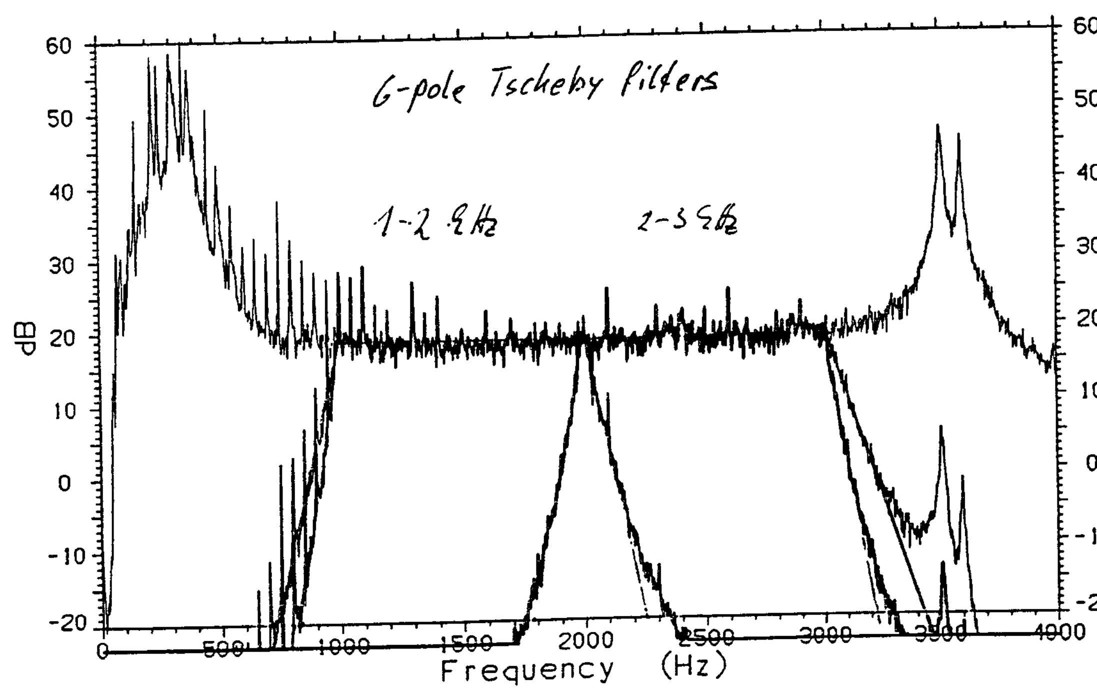

5000 point FFT, averaged from nrec = 1000 to nrec = 1020

ROS--CMS PRMSHV 1/0001 H1-05 30.03.90 17.42:12
30.03.90 17.40:23

Data taking run 1989, March 2 to March 6

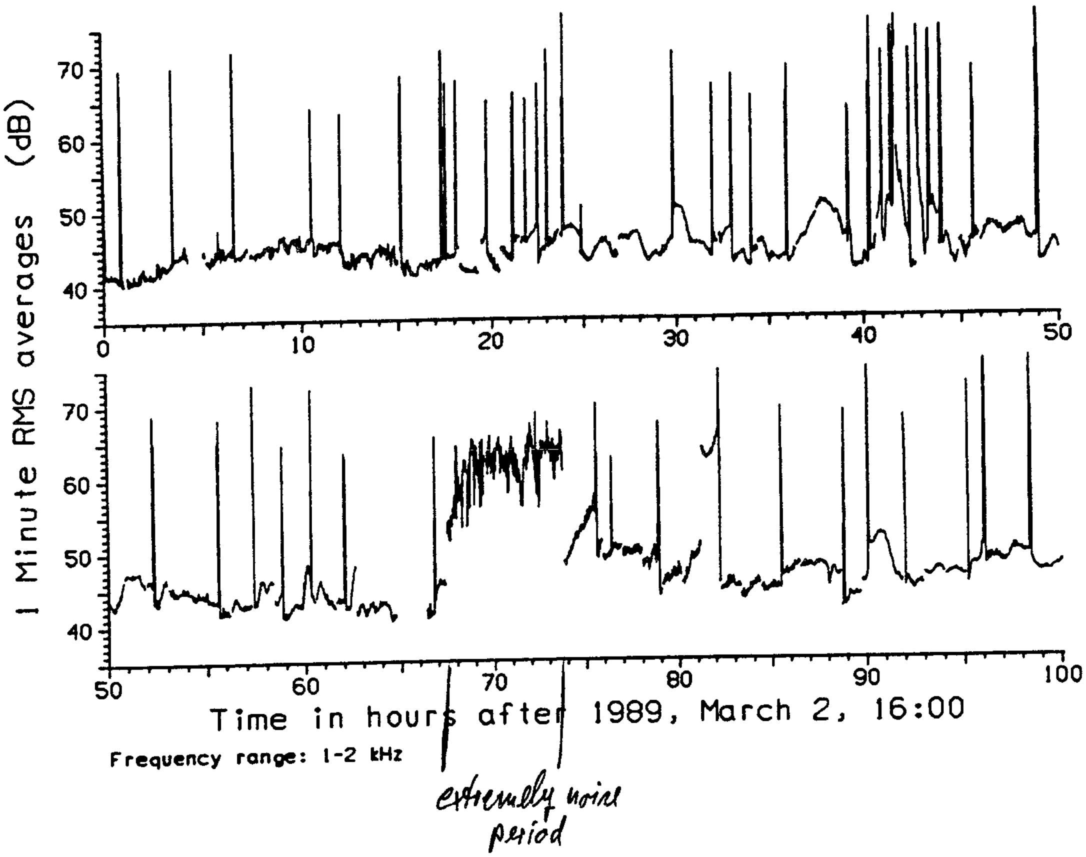

Frequency range: 1-2 kHz

IPP--CMS ROS 5/0004 H1-05 21.04.89 17.26:25
21.04.89 17.25:18

Data taking run 1989, March 2 to March 6 sheet 4

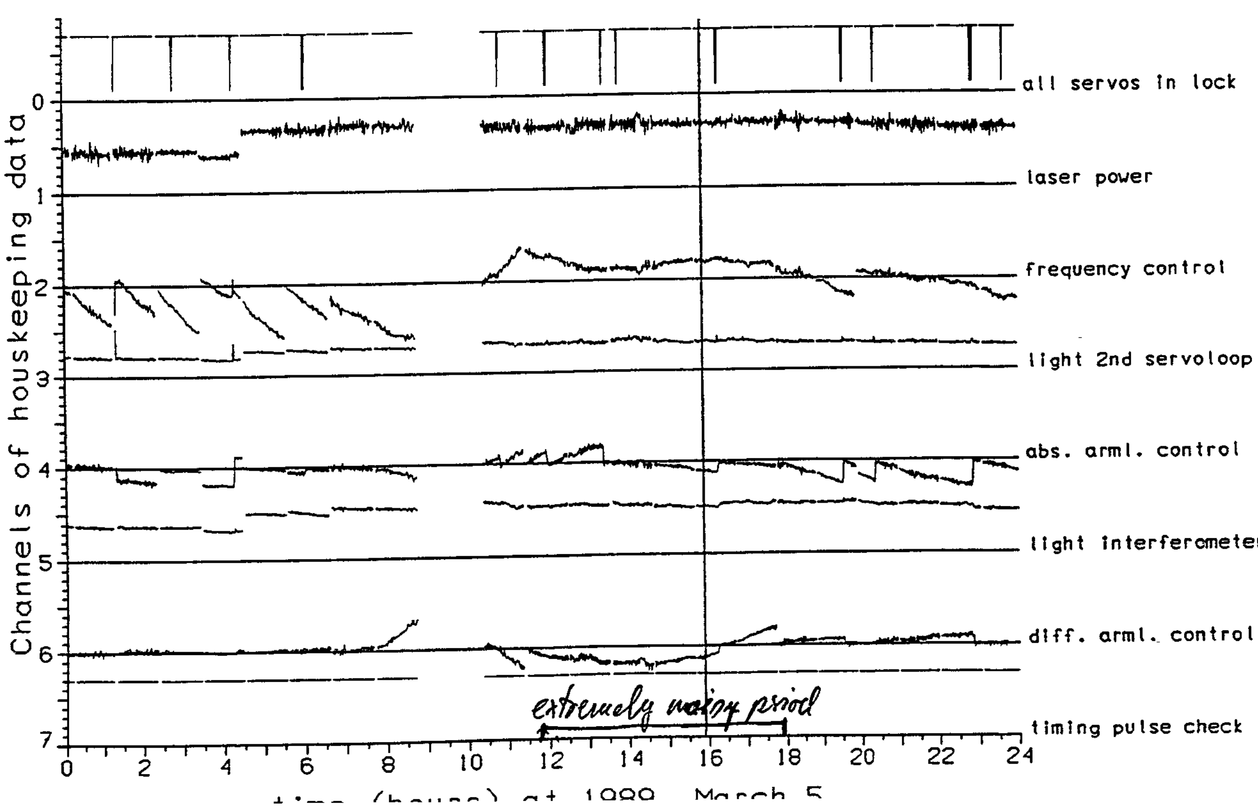

KUS--CMS PRMS 1/0001 H1-05 30.03.90 18.57:35
30.03.90 18.56:00

Data taking run 1989, March 2 to March 6

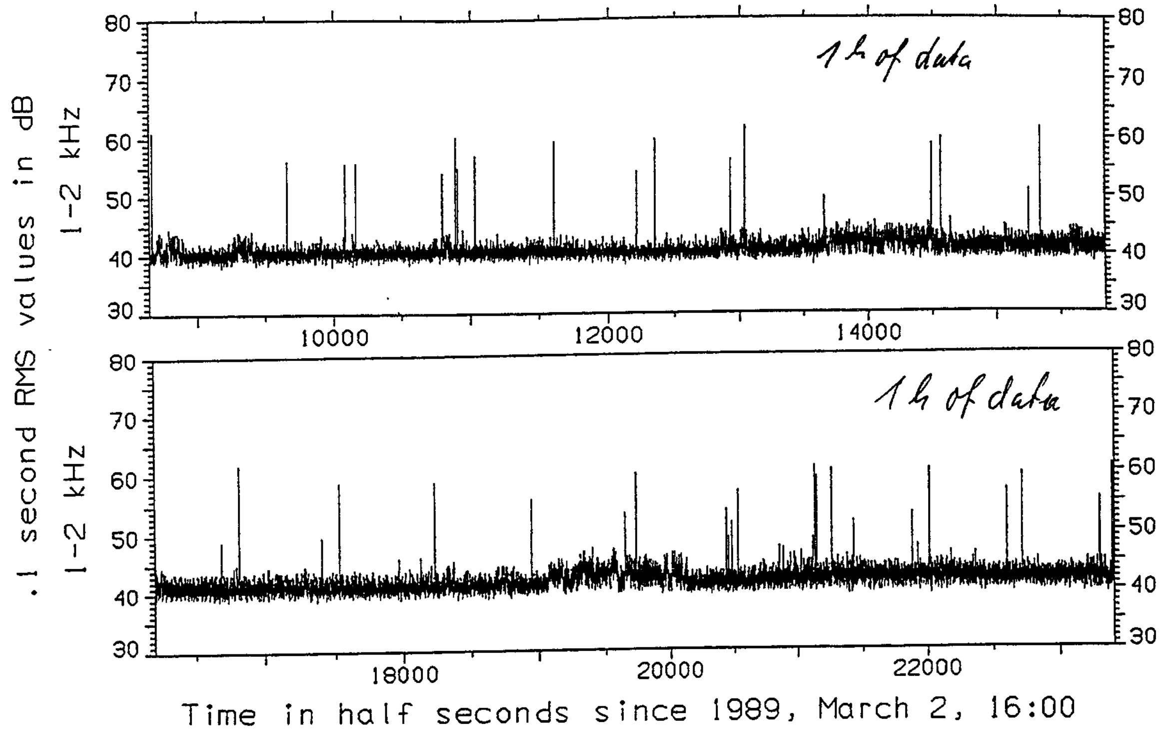

KUS--CMS PRMS 2/0002 H1-05 28.03.90 17.07:57
28.03.90 17.02:50

Data taking run 1989, March 2 to March 6

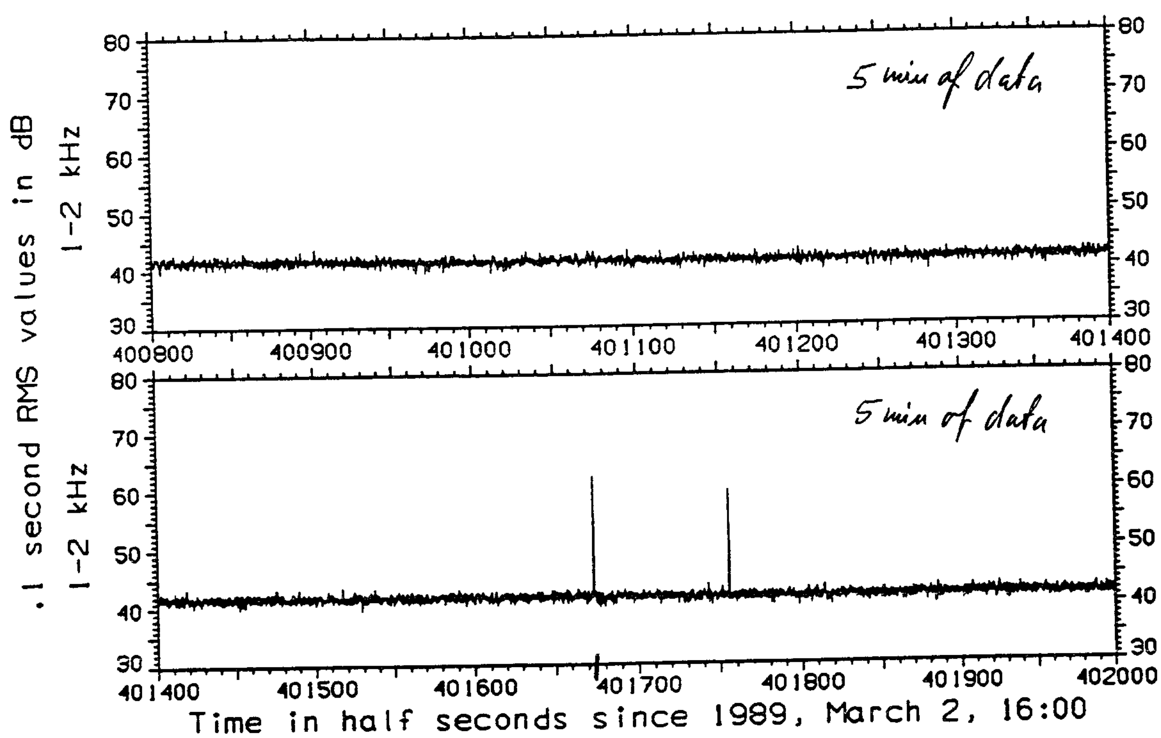

Original Data

Data taking run 1989, March 2 to March 6

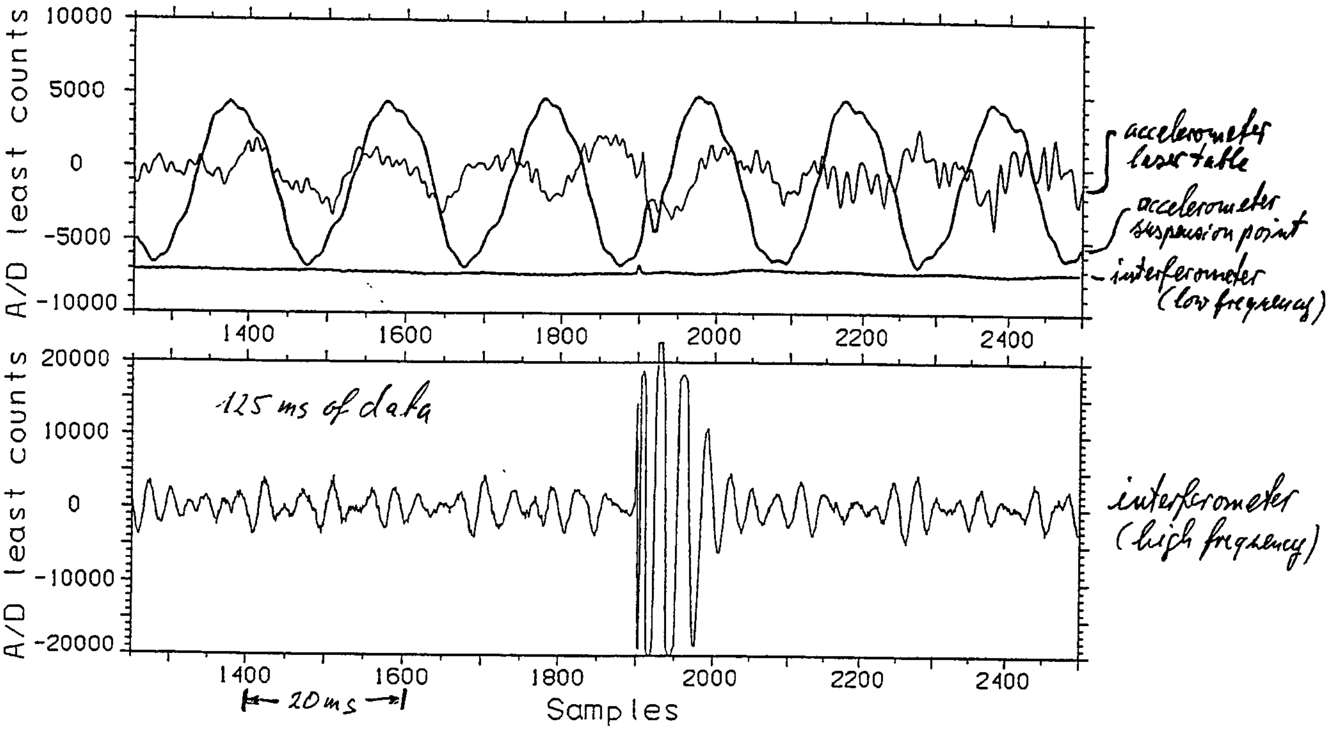

Cassette B00088, GW-file 310, record 874, tinhs = 401673

27

Data taking run 1989, March 2 to March 6

Histogram of separation of isolated spikes

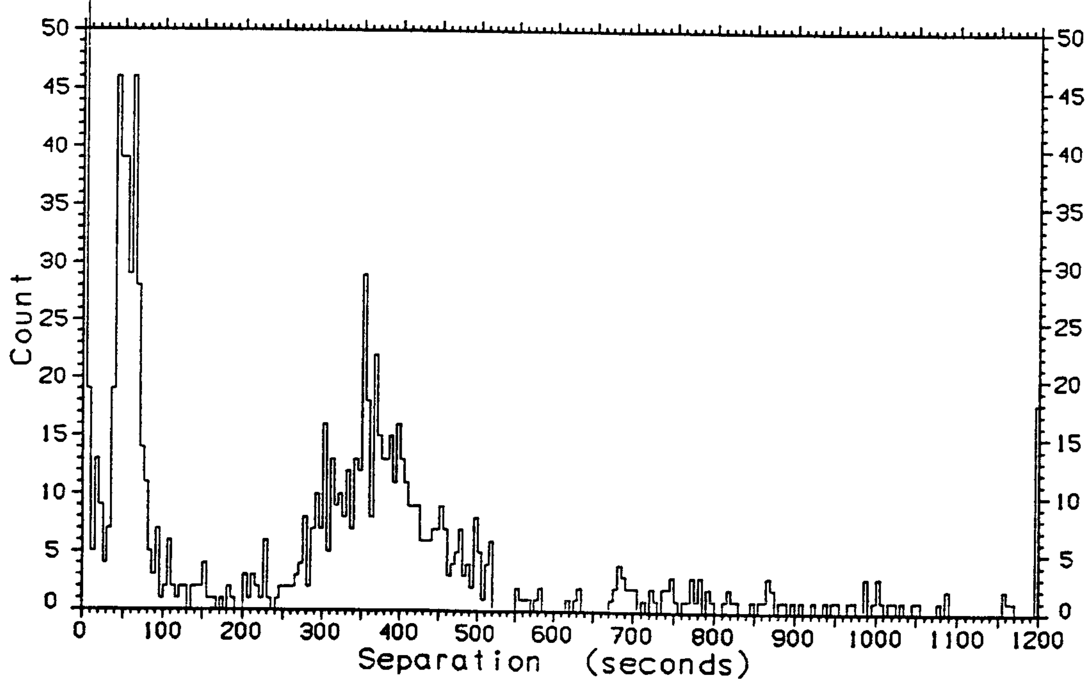

Bin width 5.0 seconds.

RUS--CMS PHST 1/0001 H1-05 16.03.90 17.37:19
16.03.90 17.33:50

Data taking run 1989, March 2 to March 6

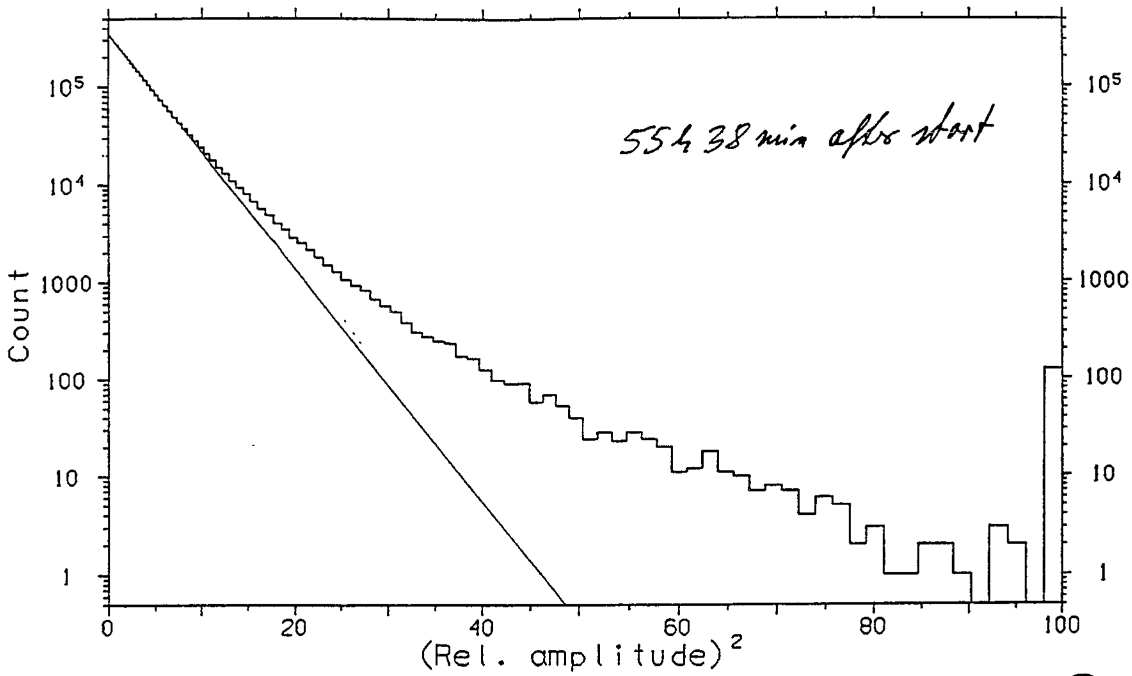

Amplitude statistic of 3 million data points ~ 5 min of data

Fitted RMS value = 42.6 dB
Record no. = 1235 1-2 Hz
Deviation from Gaussian: 59.

23

RUS--CMS PHST 3/0003 H1-05 16.03.90 17.37:21
16.03.90 17.33:51

Data taking run 1989, March 2 to March 6

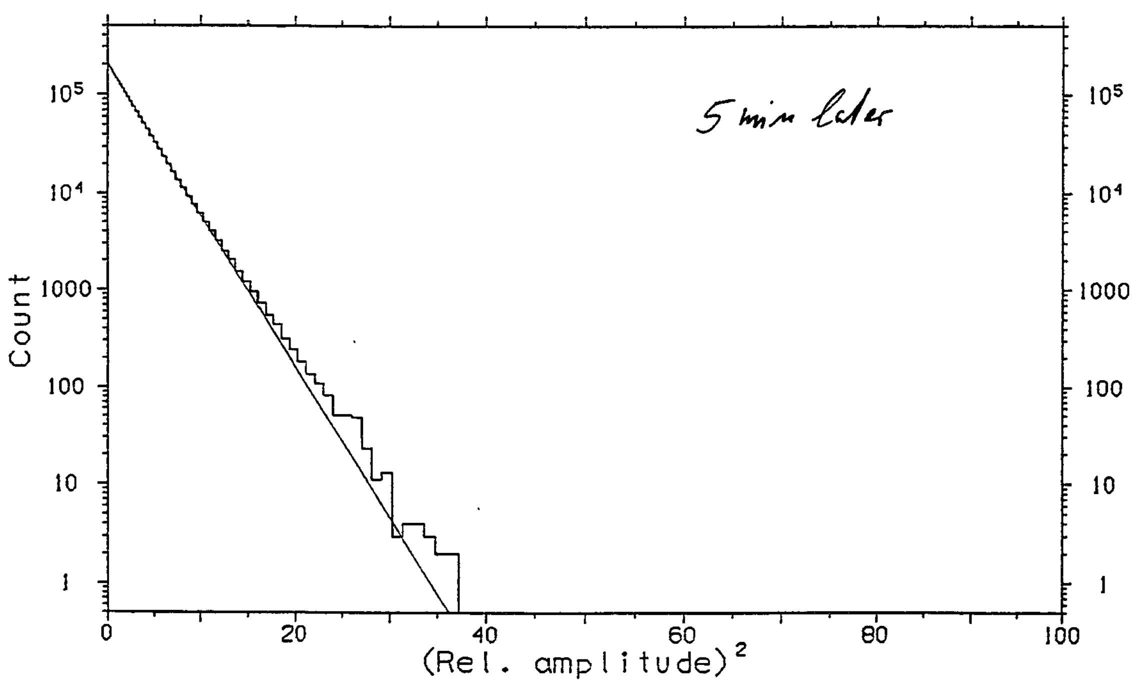

Amplitude statistic of 3 million data points

Fitted RMS value = 41.5 dB
Record no. = 1237 ≙ start of finish = 400800 1-2 Hz
Deviation from Gaussian: 27

RUS--CMS PHST 5/0005 H1-05 16.03.90 17.37:23
16.03.90 17.33:51

Data taking run 1989, March 2 to March 6

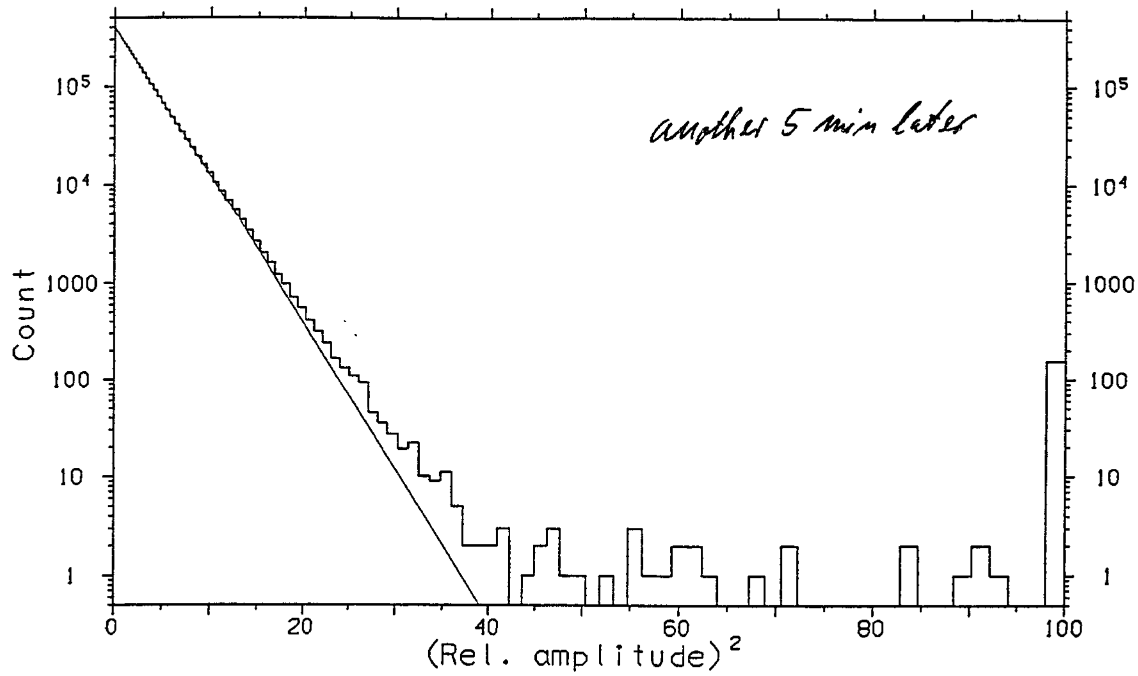

Amplitude statistic of 3 million data points

Fitted RMS value = 41.6 dB
Record no. = 1239
Deviation from Gaussian: 47.

1-2 kHz

25

BHT--CMS PRMAVPK 2/0002 H1-05 27.02.90 10.50:23
27.02.90 10.29:51

Data taking run 1989, March 2 to March 6 sheet 1

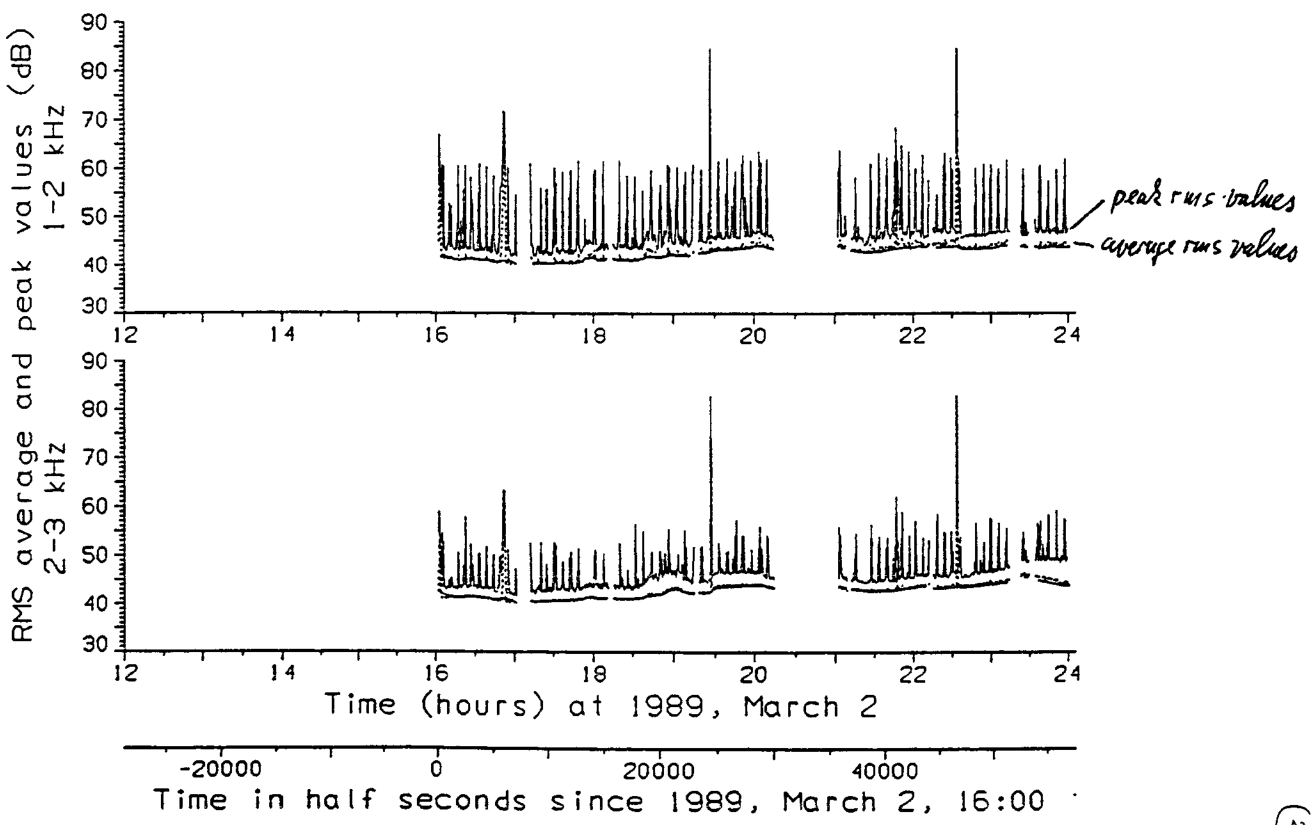

Data taking run 1989, March 2 to March 6 sheet 7

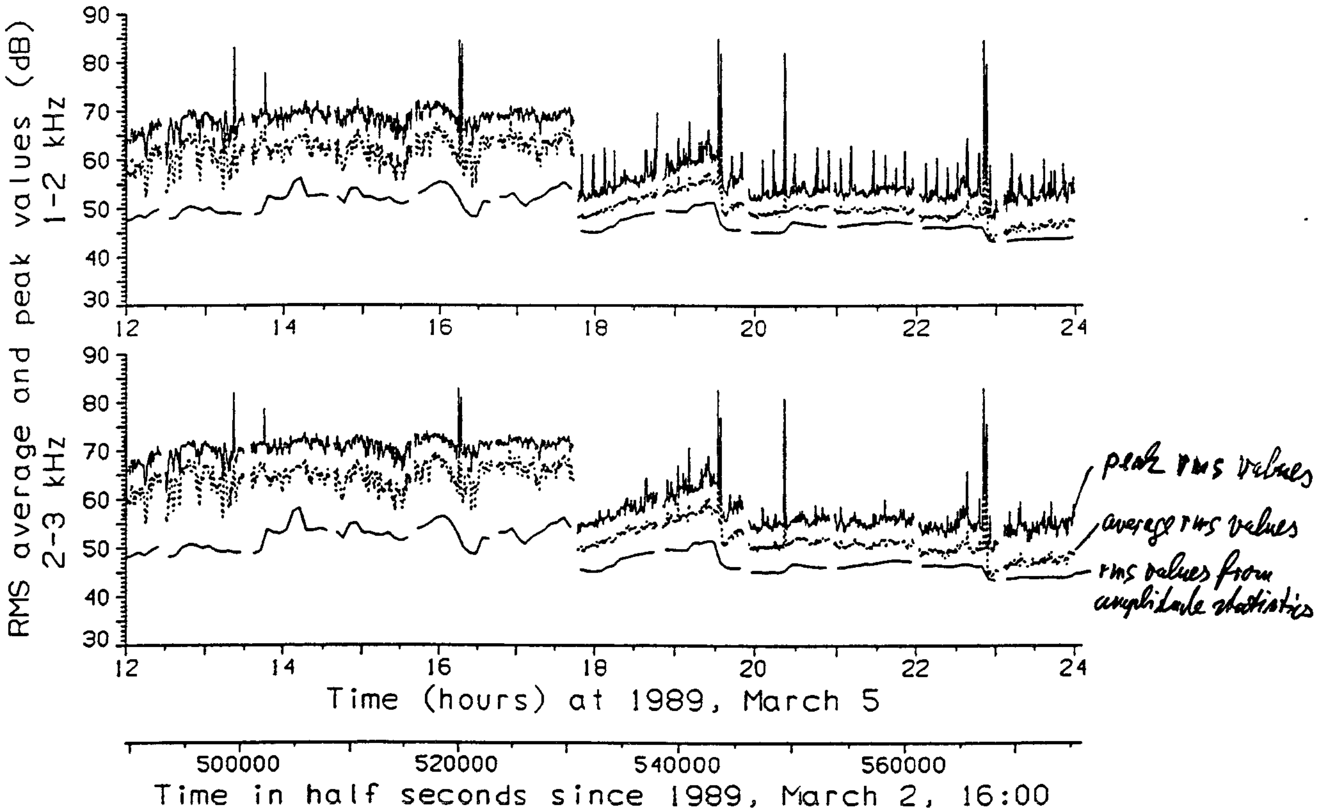

(27)

Data Analysis with Multiple Data Streams

Sam Finn
Northwestern

Multiple Cryogenic Resonant Instruments

Multiple Interferometers

Correlated Noise
- Multiple transducers & TIGA
- LISA
- Hanford 4 & 2 Km Interferometers

Heterogeneous Data Streams
- Resonant & interferometric instruments
- Delay-line vs. Fabry-Perot
- Signal recycling vs. broadband

I Single data stream data analysis

II Multiple detector data analysis

III Comments

IV Multiple data stream, single detector DA

V Conclusions / Exhortation

Single Data Stream Data Analysis

$$C_n(\tau) \equiv \lim_{T\to\infty} \frac{1}{T}\int_0^T dt\, n(t)\, n(t+\tau)$$

Detector Output
$$g(t) = \begin{cases} n(t) \\ n(t) + s(t,\vec{\mu}) \end{cases}$$

$$S_n(f) \xleftrightarrow{\text{F.T.}} C_n(\tau)$$

Probability $g(t)$ includes $s(\vec{\mu})$

$$P(\vec{\mu},s|g) = \frac{\Lambda(\vec{\mu})}{\Lambda + P(0)/1-P(0)}$$

$P(s|g) = \int d^N\mu\, P(\vec{\mu},s|g)$

CIs: $P(\vec{\mu},s|g) > \gamma$

$\hat{\mu}$ maximizes $P(\vec{\mu},s/g)$

$$\Lambda(\vec{\mu}) \equiv P(\vec{\mu}|s)\,\frac{P(g-s(\vec{\mu})|0)}{P(g|0)}$$

Discrete Sampling

$$P[g(t_0)|0] = \exp\left[-\frac{1}{2}\frac{g(t_0)^2}{C_n(0)}\right] \Big/ \left[2\pi C_n(0)\right]^{1/2}$$

$$P[g(t_1),g(t_2),\ldots|0] = \exp\left[-\frac{1}{2}C^{-1}_{ij}\, g(t_i)g(t_j)\right] \Big/ \left[(2\pi)^N \det\|C_{ij}\|\right]^{\frac{1}{2}}$$

$$C_{ij} \equiv C_n(t_j - t_i)$$

Continuum Limit

$$P(g|0) \propto \exp\left[-\langle g,g\rangle\right]$$

$$\langle g,h\rangle \equiv \int_{-\infty}^{\infty} \frac{\tilde{g}(f)\,\tilde{h}^*(f)}{S_n(|f|)}\,df$$

one-sided

$$\Lambda(\vec{\mu}) = P(\vec{\mu}|s)\,\underbrace{\exp\left[2\langle g,s(\vec{\mu})\rangle - \langle s(\vec{\mu}),s(\vec{\mu})\rangle\right]}$$

Frequentist $\Lambda(\mu)$ for thresholding

Multiple Detector Data Analysis

$${}^{\alpha}\hat{\mu}_i \equiv \begin{pmatrix} \text{Maximum Likelihood} \\ \text{estimator of } \mu_i \text{ in} \\ \text{detector } \alpha \end{pmatrix} \qquad \text{Source } \vec{\nu},\ \vec{\mu} = \vec{\mu}(\vec{\nu})$$

Different detectors, different noise: ${}^{\alpha}\hat{\mu} \neq {}^{\beta}\hat{\mu}$ $(\{{}^{\alpha}\nu\} \neq \{{}^{\beta}\nu\})$ if $\alpha \neq \beta$

Find "Best fit" $\hat{\mu}$ to $\{{}^{\alpha}\hat{\mu}\}$ (or $\hat{\nu}$ to $\{{}^{\alpha}\hat{\mu}(\nu)\}$)

Example: Binary Inspiral in several intfs [Jaranowski; Krolak]

$${}^{\alpha}\mathcal{M}$$

$${}^{\alpha}p \propto \frac{\Theta(\overbrace{\theta, \varphi, i, \psi}^{\text{orientation angles}})}{d_L} \leftarrow \text{Luminosity distance}$$

$${}^{\alpha}\phi = {}^{\alpha}\phi(\theta, \varphi, i, \psi, \Phi)$$

Φ: orbital phase at coalescence

$${}^{\alpha}T = {}^{\alpha}T(\theta, \varphi, T_0)$$

T_0: coalescence time at S.S. Barycenter

If # detectors ≥ 3, $\mathcal{M}, d_L, T_0, \theta, \varphi, i, \psi, \Phi$ over-determined

Find "best fit" in "least squares" sense

Comments

"Best fit" is ad hoc prescription

Least squares gives different μ than "Least quartic", or L_1, or ...

Detection probability? Confidence intervals?

Meaningless since "best fit" is ad hoc

Correlated detector noise?

What if $\tilde{\mu} - {}^{\alpha}\hat{\mu}$ correlated with $\tilde{\mu} - {}^{\beta}\hat{\mu}$?

Separate analysis,
Separate "sources"

Single analysis,
Single source

Multiple Data Streams, Single Detector Data Analysis

Detector Output

$$\vec{g}(t) = \begin{cases} \begin{pmatrix} {}^1n \\ {}^2n \\ \vdots \end{pmatrix}(t) \\ \begin{pmatrix} {}^1n \\ {}^2n \\ \vdots \end{pmatrix}(t) + \begin{pmatrix} {}^1s \\ {}^2s \\ \vdots \end{pmatrix}(t, \vec{\nu}) \end{cases}$$

$$P[\vec{g}(t_0) | 0] = \exp\left[-\tfrac{1}{2}\, {}^{\alpha\beta}C_n^{-1}(0)\, {}^{\alpha}g(t_0)\, {}^{\beta}g(t_0)\right] \Big/ \left[(2\pi)^N \det\|{}^{\alpha\beta}C_n(0)\|\right]^{\frac{1}{2}}$$

iscrete ampling

$${}^{\alpha\beta}C_n(\tau) \equiv \lim_{T\to\infty} \frac{1}{T}\int_0^T {}^{\alpha}n(t)\, {}^{\beta}n(t+\tau)\, dt$$

Note: ${}^{\alpha\beta}C_n(\tau) = {}^{\beta\alpha}C_n(-\tau)$

$$P[\vec{g}(t_1), \vec{g}(t_2), \dots | 0] = \exp\left[-\tfrac{1}{2}\, {}^{\alpha\beta}C_{ij}^{-1}\, {}^{\alpha}g(t_i)\, {}^{\beta}g(t_j)\right] \Big/ \left[(2\pi)^{NM} \det\|{}^{\alpha\beta}C_{ij}\|\right]^{\frac{1}{2}}$$

$${}^{\alpha\beta}C_{ij} \equiv {}^{\alpha\beta}C_n(t_j - t_i)$$

xample rrelation latrix"

$${}^{\alpha\beta}C_{ij} = \begin{pmatrix} {}^{11}C_{ij} & {}^{12}C_{ij} & \cdots & \cdots \\ {}^{21}C_{ij} & {}^{22}C_{ij} & \cdots & \cdots \\ \cdots & \cdots & {}^{33}C_{ij} & \cdots \\ \cdots & \cdots & \cdots & {}^{44}C_{ij} \end{pmatrix}$$

1 Hanford 2 Km
2 Hanford 4 Km
3 Livingston
4 Pisa

tinuum imit

$$P(\vec{g}|0) \propto \exp[-\langle \vec{g}, \vec{g} \rangle]$$

$$\langle \vec{g}, \vec{h} \rangle \equiv \int_{-\infty}^{\infty} {}^{\alpha\beta}S_n^{-1}(f)\; {}^{\alpha}\tilde{g}(f)\, {}^{\beta}\tilde{h}^*(f)$$

$${}^{\alpha\beta}S_n(f) \equiv 2\int_{-\infty}^{\infty} d\tau\, e^{2\pi i f\tau}\, {}^{\alpha\beta}C_n(\tau)$$

↑ Two-sided, Complex, Hermitian

Probability density

$$P(\vec{\mu}, s | \vec{g}) = \frac{\Lambda(\mu)}{\Lambda + P(0)/1-P(0)}$$

$$\Lambda(\vec{\mu}) = P(\vec{\mu}|s) \exp\left[2\langle \vec{g}, \vec{s}(\vec{\mu})\rangle - \langle \vec{s}(\vec{\mu}), \vec{s}(\vec{\mu})\rangle\right]$$

$$\Lambda = \int d^N\mu\; \Lambda(\mu)$$

Example : Independent noise ${}^{\alpha\beta}C_n(\tau) = 0$ if $\alpha \neq \beta$

$${}^{\alpha\beta}S_n(f) = \begin{pmatrix} {}^1S_n(f) & & 0 \\ 0 & {}^2S_n(f) & \\ & & \ddots \end{pmatrix}$$

$${}^{\alpha\beta}S_n^{-1}(f) = \begin{pmatrix} {}^1S_n^{-1}(f) & & 0 \\ 0 & {}^2S_n^{-1}(f) & \\ & & \ddots \end{pmatrix}$$

$$\Lambda(\vec{\mu}) = P(\vec{\mu}|s) \prod_{\alpha} \exp\Big[2\langle {}^{\alpha}g, {}^{\alpha}s(\vec{\mu})\rangle - \underbrace{\langle {}^{\alpha}s(\vec{\mu}), {}^{\alpha}s(\vec{\mu})\rangle}_{\frac{1}{2}\,{}^{\alpha}\rho^2(\vec{\mu})}\Big]$$

$\hat{\mu}$ maximizes $\Lambda(\mu)$ $[P(\vec{\mu}, \vec{s} | \vec{g})]$

$$\rho^2 = \sum_{\alpha} {}^{\alpha}\rho^2(\hat{\mu}) \le \sum_{\alpha} {}^{\alpha}\rho^2({}^{\alpha}\hat{\mu})$$

Conclusions

Treat Multiple Instruments as Single Detector!

Probability density $P(\vec{\mu}, s | \vec{g})$

No ad hoc estimators or prescriptions

Heterogeneous instruments/data streams

Correlated instrument noise

$$^{\alpha\beta}C_n(\tau) = \lim_{T\to\infty} \int_0^T dt\, {}^{\alpha}n(t)\, {}^{\beta}n(t+\tau)$$

$$^{\alpha\beta}S_n(f) = 2\int_{-\infty}^{\infty} d\tau\, e^{2\pi i f \tau}\, {}^{\alpha\beta}C_n(\tau)$$

Treat Multiple Instruments as Single Detector!

January 1996
B. Mours- LAPP (Annecy)
ASPEN

Data Analysis Preparation for

VIRGO

INFN - CNRS

(Annecy, Frascati, Lyon, Napoli, Orsay, ESPCI-Paris, Pisa, Perugia, Roma)

- The Experiment and the constraints
- The Online System
- The Calibration
- The Simulation
- Pulsar search

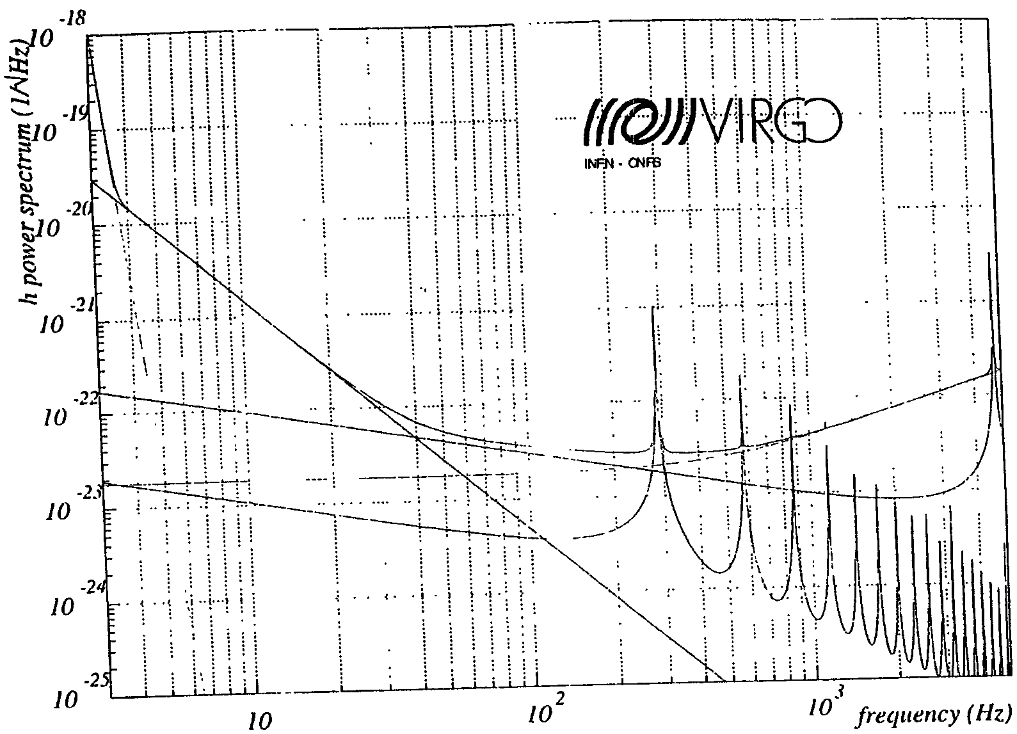

Real life

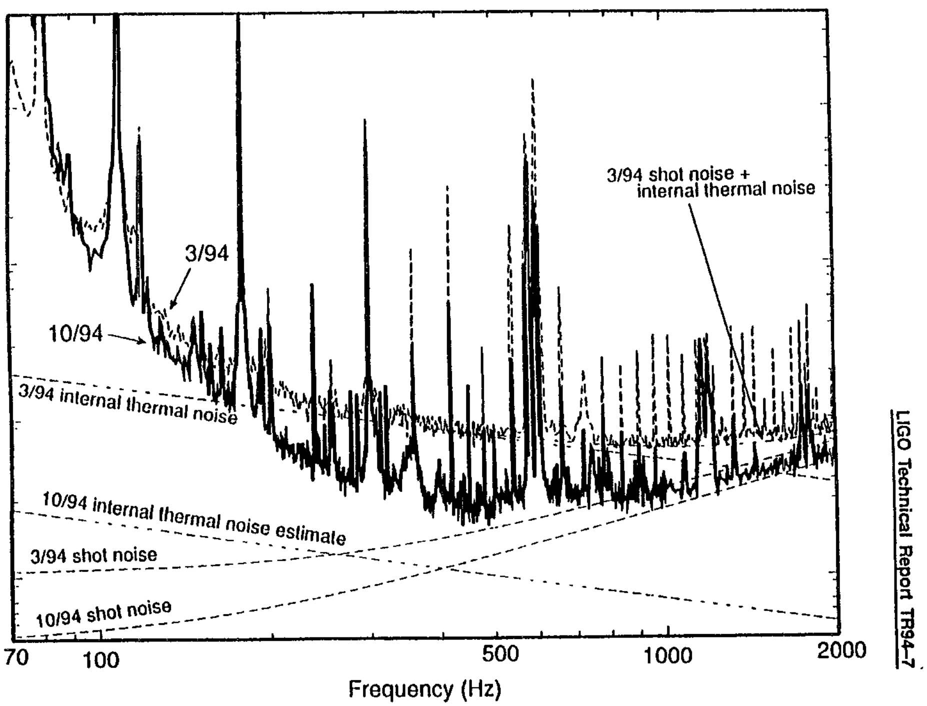

Constraints

Main signal sampling: up to 20 kHz

⇒ lot of data

Need to record additional monitoring signals

⇒ more data

Raw data rate: 1-5 Mbytes/sec

Online system:

- Robust
- Flexible
- Data reduction : Trigger
- Data organisation : The Frame structure (online/ offline compatibility)

Data analysis will need a very good understanding/modelling of the detector noise

⇒ Calibration

⇒ Simulation

VIRGO Controls

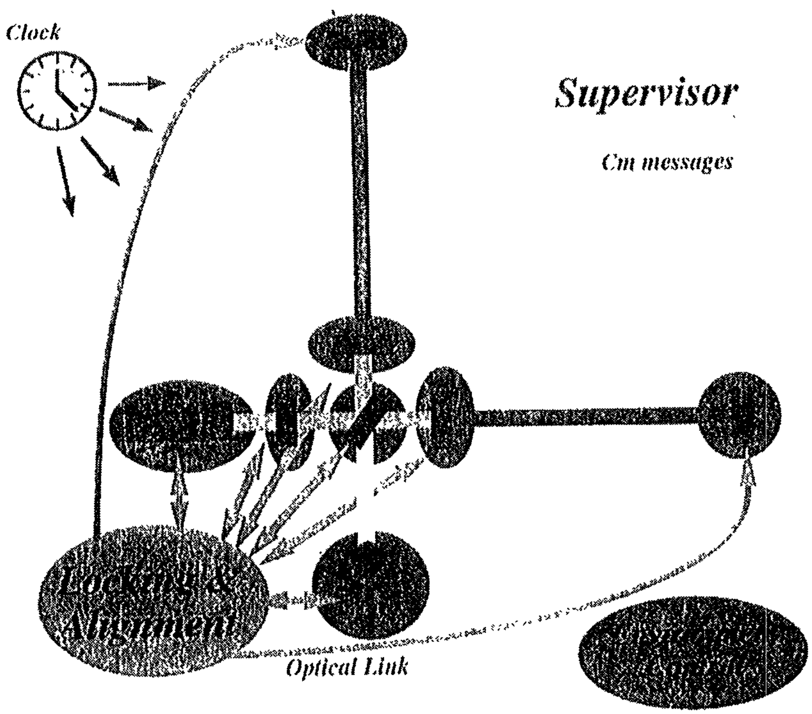

- Digital controls
- Local controls + global controls
- Digital Optical Link
- Clock
- Coordination by the Supervisor
- Slow monitoring by standalone stations

Virgo DAQ

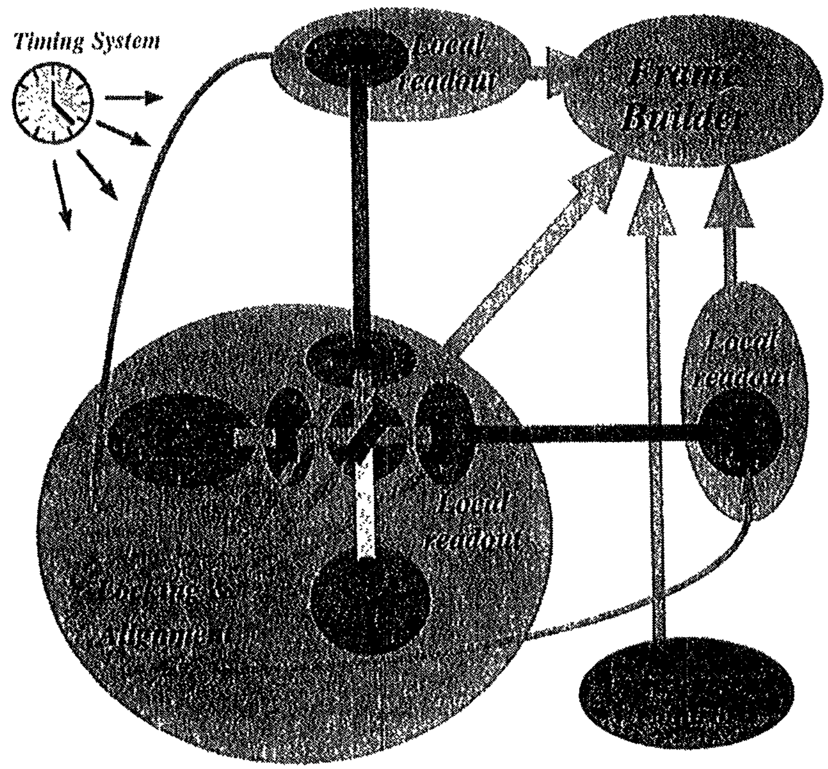

A Frame = a few seconds of organized data

Data Format

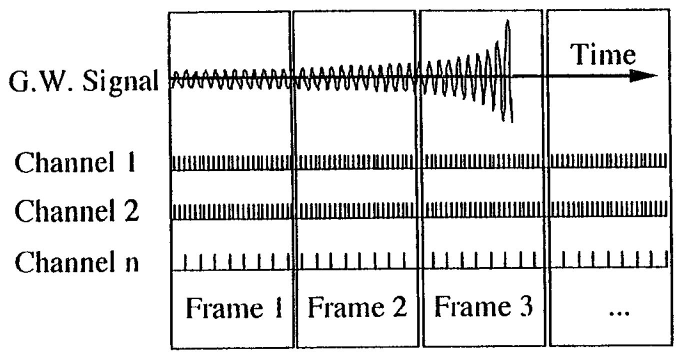

Data taking is a continuous process
Channels are sampled at different frequencies
⇒ Use a 'Frame' structure

A Frame is an organised data set
of few seconds length

One G.W. event correspond to several Frames

The Frame Structure

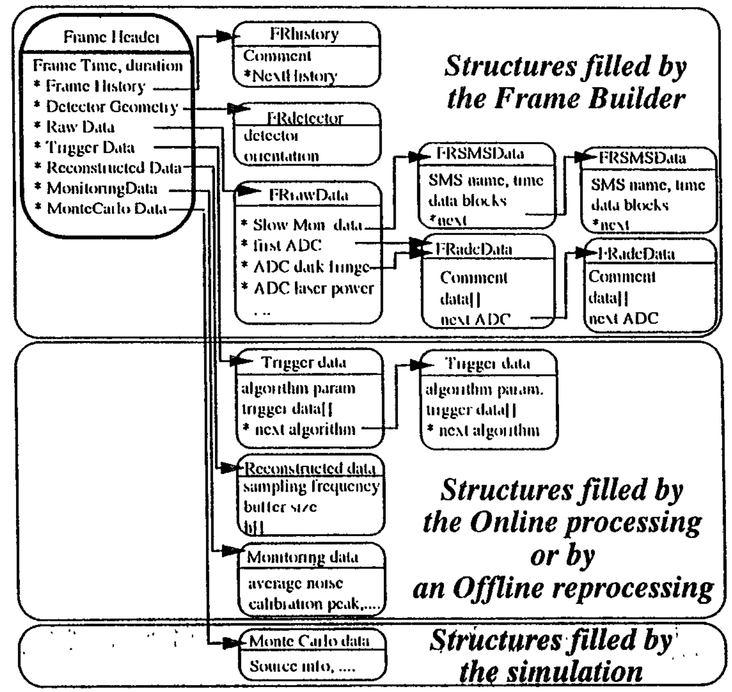

A Frame has a tree structure:

- Individual blocks are C structures
- Possible add/drop structure
- Used from online to offline

Online Processing

Frame Builder

Typical data flow = 1-5 Mbyte/s

Full Raw Data Archiving

Online Data Quality

Online Trigger

about 20 kbytes/s
or
1 Mbyte/s for burst candidates

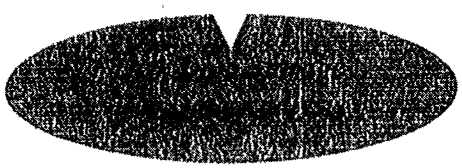

Online Trigger

Data flow: 1-500 Gbytes/day
⇒ Overflow any data analysis
⇒ Need Online data reduction : trigger

Algorithms will work on reconstructed 'h'
'h' reconstruction: convert raw data (i.e. ADC counts) to physical quantities (h)

Trigger algorithms will search for burst events.
⇒ select 'time windows'

keep:
- all the raw data for selected frames
- 'h' for the others (pulsars searches).

Algorithms
- simple
- robust
- multiples
- upgrades ⇒ data reprocessing

(D. Verkindt et al. Astroparticle physics 2 (1994) 235-248)

Calibration

Goal:
- Convert the ADC values to h
- Study of the Virgo sensitivity
  - ⇒ temporary signals
- Permanent monitoring of the interferometer
  - check the interferometer
  - check the data acquisition system
  - ⇒ few permanent sine waves

How:

Move a mirror by a well known amplitude

Need to know:
- the force applied on the mirror,
- the mechanical transfer function

Forces:
- Magnets (locking actuators)
- Radiation pressure from an additional laser

The calibration signal will be provided by an external and independent signal generator.

Simulation

Goals:
- Design of the detector
- Detector commissioning
- Data analysis

Tool: SIESTA

(Simulation of Interferometric Experiment Sensitive To grAvitational waves)

Integrated, general purpose program:
- Time dependent simulation
- Metric, Mechanic, Optic, Electronic
- Various levels of accuracy

Object Oriented Programming: Modularity

Mechanical simulation

Ex. simulation of mirror motion due to seismic and thermal noise
(in time domain)

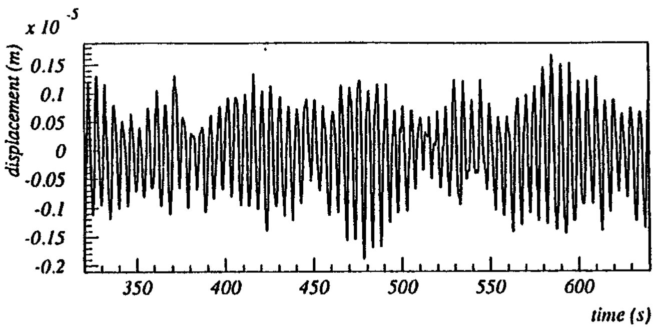

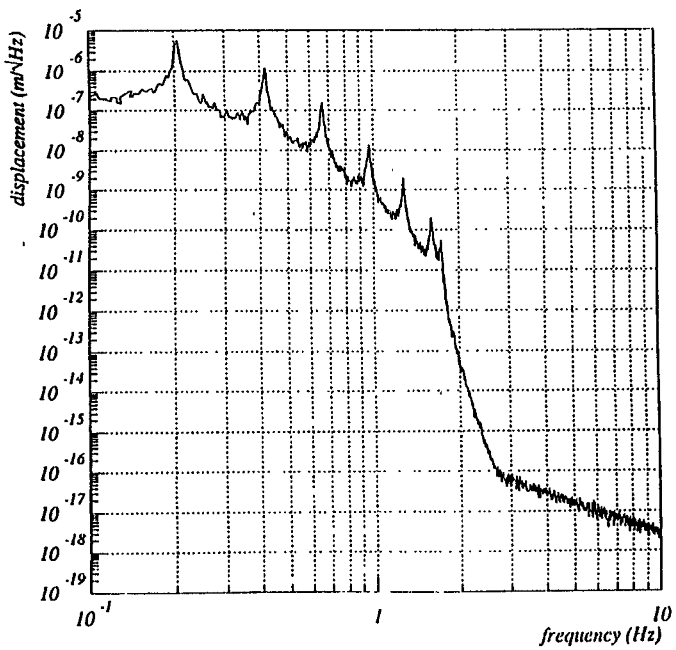

Optical response

- Detailed simulation: wavefront propagation computation; sensitive to surface defects
- Modal expansion of beam transversal structure; sensitive to misalignments
- Fast simulation: matrix relationship between detected signals and mirror translations, in the linear regime

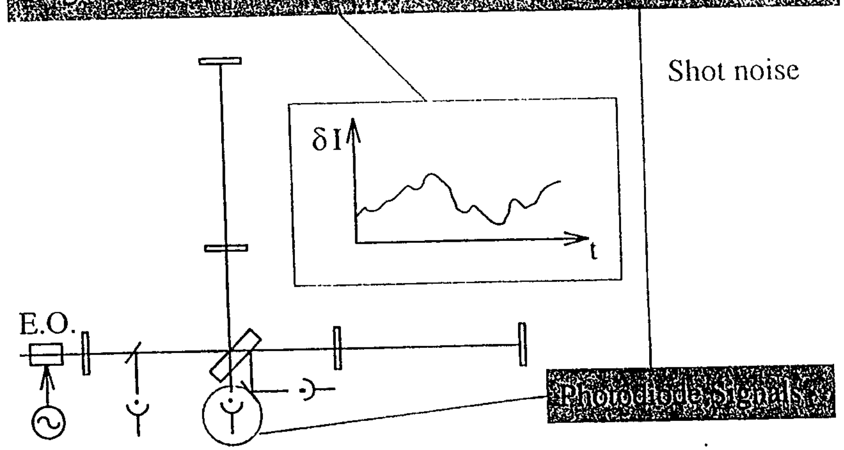

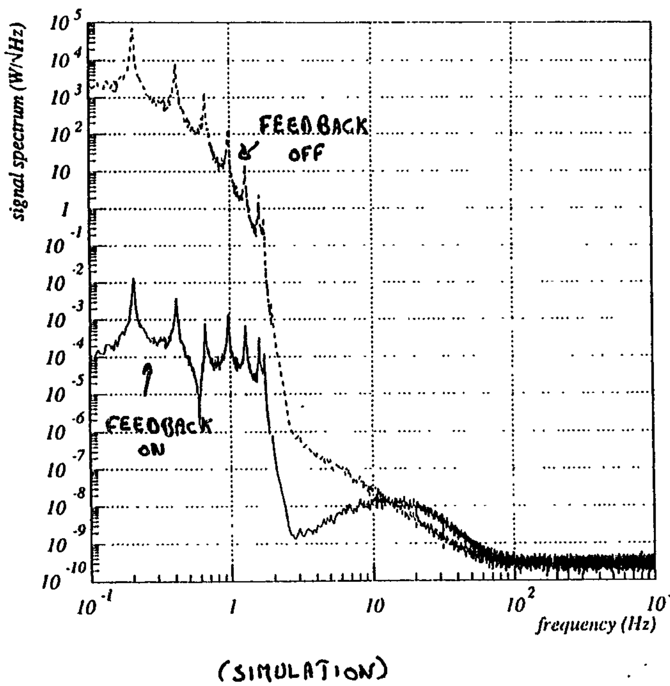

Feedback Simulation

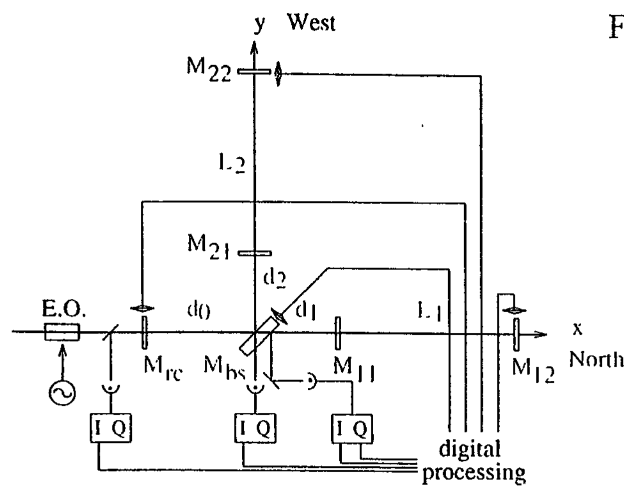

Feedback system:

- high gain ($\sim 10^5, 10^6$) at low frequency ($<\sim 1 Hz$)
- no noise introduced in the VIRGO frequency range ($10\ Hz\ -\ 1\ kHz$)

Fast Data Simulation

(Example)

This includes:
- Thermal noise (4 mirrors)
- Shot noise

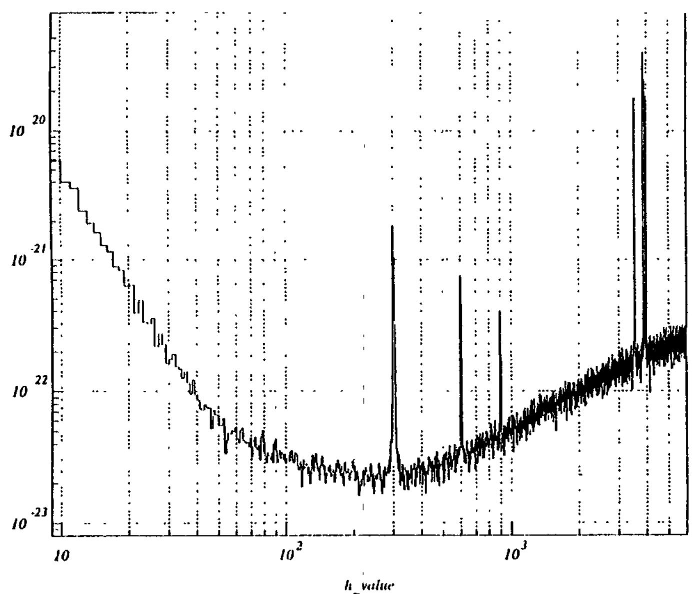

(1 sec of Data @ 20KHz= 6 sec real time)

Pulsar search

Doppler effect

⇒Need earth position
precision: 15km(1kHz/frequency)
(5% losses)

⇒Need some care

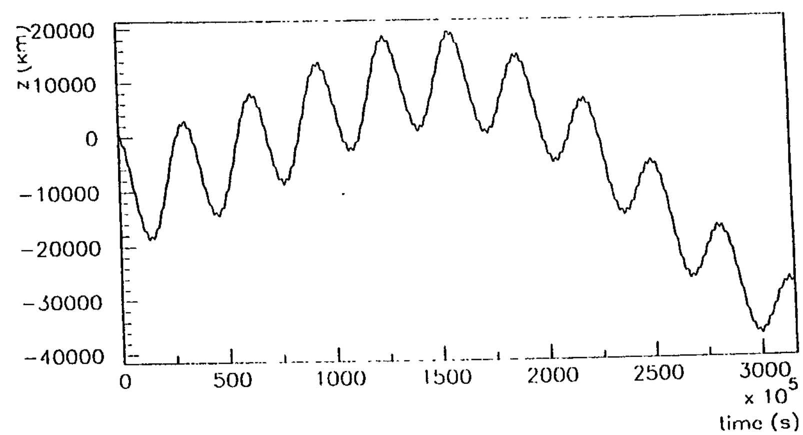

Earth position out of the ecliptic plan (10 years)

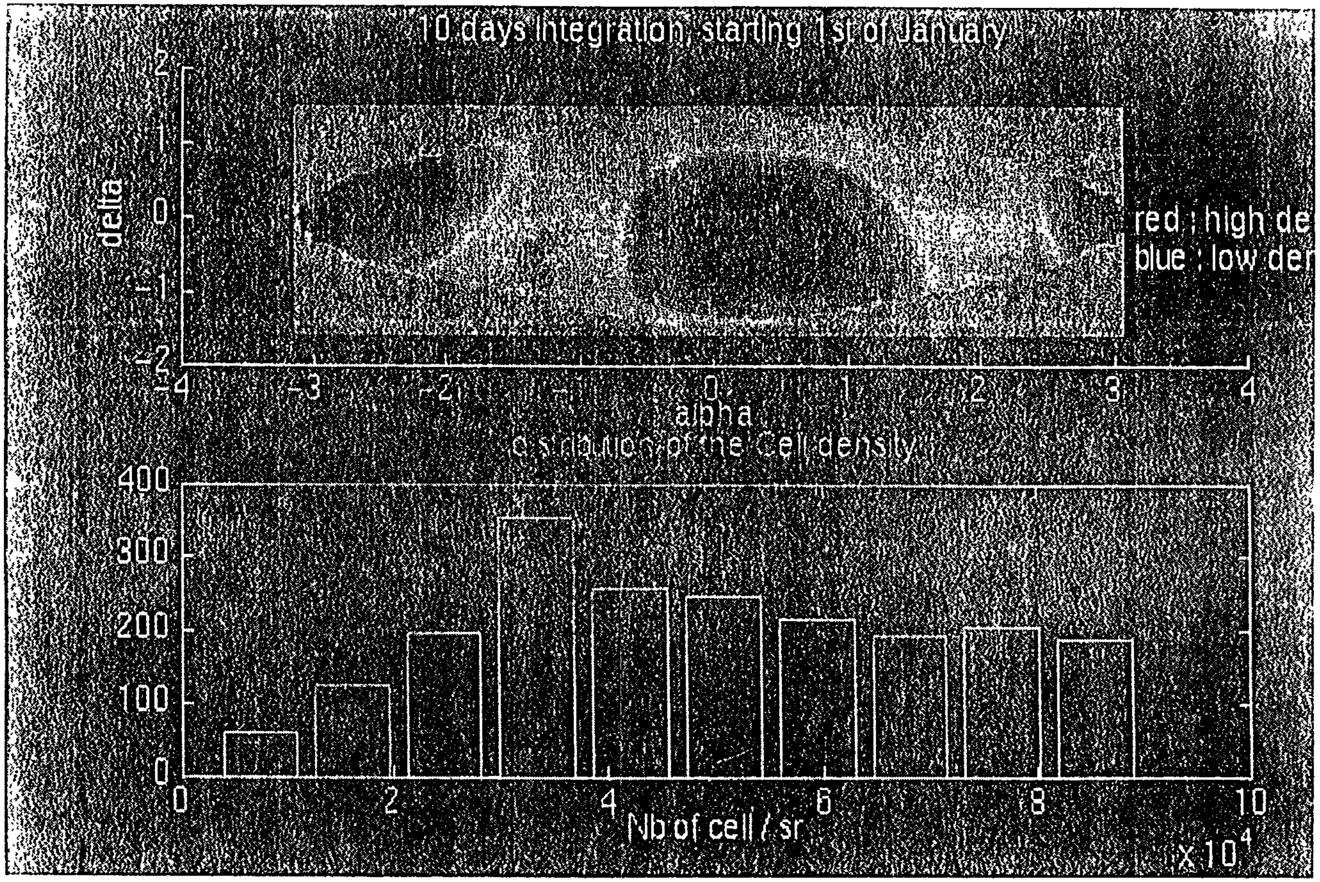
10 days integration, starting 1st of January
delta
alpha
red : high de
blue : low de
distribution of the Cell density
Nb of cell / sr
x 10^4

Pulsar search

Doppler effect

⇒Need source direction

Example:

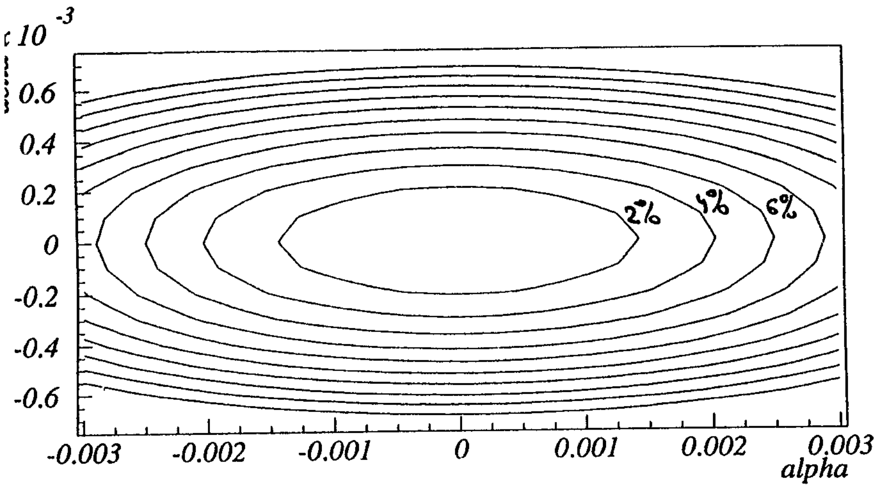

- 10 days of integration
- contour lines = 2% losses

# of Search Directions